# RARE ENDOCRINE TUMORS

EDITED BY: Barbara Altieri, Antongiulio Faggiano and Enzo Lalli
PUBLISHED IN: Frontiers in Endocrinology

frontiers Research Topics

ISSN 1664-8714
ISBN 978-2-88976-623-9
DOI 10.3389/978-2-88976-623-9

## About Frontiers

Frontiers is more than just an open-access publisher of scholarly articles: it is a pioneering approach to the world of academia, radically improving the way scholarly research is managed. The grand vision of Frontiers is a world where all people have an equal opportunity to seek, share and generate knowledge. Frontiers provides immediate and permanent online open access to all its publications, but this alone is not enough to realize our grand goals.

## Frontiers Journal Series

The Frontiers Journal Series is a multi-tier and interdisciplinary set of open-access, online journals, promising a paradigm shift from the current review, selection and dissemination processes in academic publishing. All Frontiers journals are driven by researchers for researchers; therefore, they constitute a service to the scholarly community. At the same time, the Frontiers Journal Series operates on a revolutionary invention, the tiered publishing system, initially addressing specific communities of scholars, and gradually climbing up to broader public understanding, thus serving the interests of the lay society, too.

## Dedication to Quality

Each Frontiers article is a landmark of the highest quality, thanks to genuinely collaborative interactions between authors and review editors, who include some of the world's best academicians. Research must be certified by peers before entering a stream of knowledge that may eventually reach the public - and shape society; therefore, Frontiers only applies the most rigorous and unbiased reviews.
Frontiers revolutionizes research publishing by freely delivering the most outstanding research, evaluated with no bias from both the academic and social point of view. By applying the most advanced information technologies, Frontiers is catapulting scholarly publishing into a new generation.

## What are Frontiers Research Topics?

Frontiers Research Topics are very popular trademarks of the Frontiers Journals Series: they are collections of at least ten articles, all centered on a particular subject. With their unique mix of varied contributions from Original Research to Review Articles, Frontiers Research Topics unify the most influential researchers, the latest key findings and historical advances in a hot research area! Find out more on how to host your own Frontiers Research Topic or contribute to one as an author by contacting the Frontiers Editorial Office: frontiersin.org/about/contact

# RARE ENDOCRINE TUMORS

Topic Editors:
**Barbara Altieri,** University Hospital of Wuerzburg, Germany
**Antongiulio Faggiano,** Sapienza University of Rome, Italy
**Enzo Lalli,** UMR7275 Institut de Pharmacologie Moléculaire et Cellulaire (IPMC), France

**Citation:** Altieri, B., Faggiano, A., Lalli, E., eds. (2022). Rare Endocrine Tumors. Lausanne: Frontiers Media SA. doi: 10.3389/978-2-88976-623-9

# Table of Contents


06 ***A Case Report of Sequential Use of a Yeast-CEA Therapeutic Cancer Vaccine and Anti-PD-L1 Inhibitor in Metastatic Medullary Thyroid Cancer***
Jaydira Del Rivero, Renee N. Donahue, Jennifer L. Marté, Ann W. Gramza, Marijo Bilusic, Myrna Rauckhorst, Lisa Cordes, Maria J. Merino, William L. Dahut, Jeffrey Schlom, James L. Gulley and Ravi A. Madan

13 ***Prevalence of Parathyroid Carcinoma and Atypical Parathyroid Neoplasms in 153 Patients With Multiple Endocrine Neoplasia Type 1: Case Series and Literature Review***
An Song, Yi Yang, Shuzhong Liu, Min Nie, Yan Jiang, Mei Li, Weibo Xia, Ou Wang and Xiaoping Xing

23 ***Clinical Prognostic Factors in Patients With Metastatic Adrenocortical Carcinoma Treated With Second Line Gemcitabine Plus Capecitabine Chemotherapy***
Salvatore Grisanti, Deborah Cosentini, Marta Laganà, Alessandra Morandi, Barbara Lazzari, Laura Ferrari, Alberto Dalla Volta, Roberta Ambrosini, Vittorio Domenico Ferrari, Sandra Sigala and Alfredo Berruti

32 ***Case Report: Irreversible Watery Diarrhea, Severe Metabolic Acidosis, Hypokalemia and Achloridria Syndrome Related to Vasoactive Intestinal Peptide Secreting Malignant Pheochromocytoma***
Aurelio Negro, Ignazio Verzicco, Stefano Tedeschi, Nicoletta Campanini, Magda Zanelli, Emanuele Negri, Enrico Farnetti, Davide Nicoli, Barbara Palladini, Rosaria Santi, Davide Cunzi, Anna Calvi, Pietro Coghi, Luigi Gerra, Riccardo Volpi, Gallia Graiani and Aderville Cabassi

38 ***Case Report: Ectopic Adrenocortical Carcinoma in the Ovary***
Wen-Hsuan Tsai, Tze-Chien Chen, Shuen-Han Dai and Yi-Hong Zeng

44 ***Case Report: Abdominal Lymph Node Metastases of Parathyroid Carcinoma: Diagnostic Workup, Molecular Diagnosis, and Clinical Management***
Christina Lenschow, Carmina Teresa Fuss, Stefan Kircher, Andreas Buck, Ralph Kickuth, Joachim Reibetanz, Armin Wiegering, Albrecht Stenzinger, Daniel Hübschmann, Christoph Thomas Germer, Martin Fassnacht, Stefan Fröhling, Nicolas Schlegel and Matthias Kroiss

51 ***Commentary: Case Report: Abdominal Lymph Node Metastases of Parathyroid Carcinoma: Diagnostic Workup, Molecular Diagnosis, and Clinical Management***
Giuseppe Fanciulli, Sergio Di Molfetta, Andrea Dotto, Tullio Florio, Tiziana Feola, Annamaria Colao, Antongiulio Faggiano and NIKE Group

54 ***Case Report: Metastatic Bronchopulmonary Carcinoid Tumor to the Pineal Region***
Joshua A. Cuoco, Michael W. Kortz, Edwin McCray, Evin L. Guilliams, Christopher M. Busch, Cara M. Rogers, Robert W. Jarrett and Sandeep Mittal

61 ***Case Report: A New Entity: Multiple Differentiated Variant of Papillary Thyroid Carcinoma With Advanced Clinical Behavior***
Jing Yang, Rixiang Gong, Yu Ma, Jun Gao, Zhihui Li, Jingqiang Zhu and Yanping Gong

67 ***Case Report: Exceptional Response to Second Line Temozolomide Therapy in a Patient With Metastatic Adrenocortical Carcinoma***
Deborah Cosentini, Antonella Turla, Ornella Carminati, Salvatore Grisanti, Vittorio Domenico Ferrari, Marta Laganà, Giovanni Rosti, Sandra Sigala and Alfredo Berruti

72 ***Carney Triad, Carney-Stratakis Syndrome, 3PAS and Other Tumors Due to SDH Deficiency***
Georgia Pitsava, Nikolaos Settas, Fabio R. Faucz and Constantine A. Stratakis

83 ***Case Report: Three Rare Cases of Ectopic ACTH Syndrome Caused by Adrenal Medullary Hyperplasia***
Yu Cheng, Jie Li, Jingtao Dou, Jianming Ba, Jin Du, Saichun Zhang, Yiming Mu, Zhaohui Lv and Weijun Gu

91 ***Highly Symptomatic Progressing Cardiac Paraganglioma With Intracardiac Extension Treated With $^{177}$Lu-DOTATATE: A Case Report***
Alexis Huot Daneault, Mélanie Desaulniers, Jean-Mathieu Beauregard, Alexis Beaulieu, Frédéric Arsenault, Geneviève April, Éric Turcotte and François-Alexandre Buteau

97 ***Parathyroid Adenoma With Respiratory-Like Epithelium: Case Report of a Potential Mimic With Unknown Etiology***
C. Christofer Juhlin and Jan Zedenius

101 ***Case Report: Consecutive Adrenal Cushing's Syndrome and Cushing's Disease in a Patient With Somatic* CTNNB1*,* USP8*, and* NR3C1 *Mutations***
Mario Detomas, Barbara Altieri, Wiebke Schlötelburg, Silke Appenzeller, Sven Schlaffer, Roland Coras, Andreas Schirbel, Vanessa Wild, Matthias Kroiss, Silviu Sbiera, Martin Fassnacht and Timo Deutschbein

110 ***Comparison of 68Ga-DOTANOC and 18F-FDG PET-CT Scans in the Evaluation of Primary Tumors and Lymph Node Metastasis in Patients With Rectal Neuroendocrine Tumors***
Zhihao Zhou, Zhixiong Wang, Bing Zhang, Yanzhang Wu, Guanghua Li and Zhao Wang

119 ***Catecholaminergic Crisis After a Bleeding Complication of COVID-19 Infection: A Case Report***
Angel Rebollo-Román, Maria R. Alhambra-Expósito, Yiraldine Herrera-Martínez, F. Leiva-Cepas, Carlos Alzas, Concepcion Muñoz-Jiménez, R. Ortega-Salas, María J. Molina-Puertas, Maria A. Gálvez-Moreno and Aura D. Herrera-Martínez

125 ***Spontaneous Remission After a Hypercalcemic Crisis Caused by an Intracystic Hemorrhage of Bilateral Parathyroid Adenomas: A Case Report and Literature Review***
Yaoxia Liu, Jianwei Li, Hui Liu, Han Yang, Jingtao Qiao, Tao Wei, Tao Wang and Yerong Yu

135 ***Adrenocortical Tumors in Children With Constitutive Chromosome 11p15 Paternal Uniparental Disomy: Implications for Diagnosis and Treatment***
Emilia Modolo Pinto, Carlos Rodriguez-Galindo, Catherine G. Lam, Robert E. Ruiz, Gerard P. Zambetti and Raul C. Ribeiro

145 ***Aggressive Pituitary Macroadenoma Treated With Capecitabine and Temozolomide Chemotherapy Combination in a Patient With Nelson's Syndrome: A Case Report***
Oriol Mirallas, Francesca Filippi-Arriaga, Irene Hernandez Hernandez, Anton Aubanell, Anas Chaachou, Alejandro Garcia-Alvarez, Jorge Hernando, Elena Martínez-Saez, Betina Biagetti and Jaume Capdevila

152 ***Role of FGF Receptors and Their Pathways in Adrenocortical Tumors and Possible Therapeutic Implications***
Iuliu Sbiera, Stefan Kircher, Barbara Altieri, Kerstin Lenz, Constanze Hantel, Martin Fassnacht, Silviu Sbiera and Matthias Kroiss

164 ***Case Report and Systematic Review: Sarcomatoid Parathyroid Carcinoma—A Rare, Highly Malignant Subtype***
Yongchao Yu, Yue Wang, Qingcheng Wu, Xuzi Zhao, Deshun Liu, Yongfu Zhao, Yuguo Li, Guangzhi Wang, Jingchao Xu, Junzhu Chen, Ning Zhang and Xiaofeng Tian

173 ***A Silent Corticotroph Pituitary Carcinoma: Lessons From an Exceptional Case Report***
Pablo Remón-Ruiz, Eva Venegas-Moreno, Elena Dios-Fuentes, Juan Manuel Canelo Moreno, Ignacio Fernandez Peña, Miriam Alonso Garcia, Miguel Angel Japón-Rodriguez, Florinda Roldán, Elena Fajardo, Ariel Kaen, Eugenio Cardenas Ruiz-Valdepeñas, David Cano and Alfonso Soto-Moreno

182 ***Adrenal Hemorrhage in a Cortisol-Secreting Adenoma Caused by Antiphospholipid Syndrome Revealed by Clinical and Pathological Investigations: A Case Report***
Kentaro Ochi, Ichiro Abe, Yuto Yamazaki, Mai Nagata, Yuki Senda, Kaori Takeshita, Midori Koga, Yuka Yamao, Toru Shigeoka, Tadachika Kudo, Yuichiro Fukuhara, Shigero Miyajima, Hiroshi Taira, Shoji Haraoka, Tatsu Ishii, Yuichi Takashi, Alfred K. Lam, Hironobu Sasano and Kunihisa Kobayashi

189 ***Recent Trends in the Incidence of Clear Cell Adenocarcinoma and Survival Outcomes: A SEER Analysis***
Yadong Guo, Anil Shrestha, Niraj Maskey, Xiaohui Dong, Zongtai Zheng, Fuhan Yang, Ruiliang Wang, Wenchao Ma, Ji Liu, Cheng Li, Wentao Zhang, Shiyu Mao, Aihong Zhang, Shenghua Liu and Xudong Yao

200 ***Tailored Approach in Adrenal Surgery: Retroperitoneoscopic Partial Adrenalectomy***
Pier Francesco Alesina, Polina Knyazeva, Jakob Hinrichs and Martin K. Walz

208 ***Case Report: Giant Paraganglioma of the Skull Base With Two Somatic Mutations in* SDHB *and* PTEN *Genes***
Ailsa Maria Main, Götz Benndorf, Ulla Feldt-Rasmussen, Kåre Fugleholm, Thomas Kistorp, Anand C. Loya, Lars Poulsgaard, Åse Krogh Rasmussen, Maria Rossing, Christine Sølling and Marianne Christina Klose

frontiers in Endocrinology

CASE REPORT
published: 07 August 2020
doi: 10.3389/fendo.2020.00490

# A Case Report of Sequential Use of a Yeast-CEA Therapeutic Cancer Vaccine and Anti-PD-L1 Inhibitor in Metastatic Medullary Thyroid Cancer

*Jaydira Del Rivero*[1,2]*, *Renee N. Donahue*[3], *Jennifer L. Marté*[1], *Ann W. Gramza*[4], *Marijo Bilusic*[1], *Myrna Rauckhorst*[1], *Lisa Cordes*[1], *Maria J. Merino*[5], *William L. Dahut*[1], *Jeffrey Schlom*[3], *James L. Gulley*[1] *and Ravi A. Madan*[1]

[1] Genitourinary Malignancies Branch, Center for Cancer Research, National Cancer Institute, Bethesda, MD, United States, [2] Developmental Therapeutics Branch, Center for Cancer Research, National Cancer Institute, Bethesda, MD, United States, [3] Laboratory of Tumor Immunology and Biology, Center for Cancer Research, National Cancer Institute, Bethesda, MD, United States, [4] Medstar Georgetown Lombardi Comprehensive Cancer Center, Georgetown University Medical Center, Washington, DC, United States, [5] Laboratory of Pathology, National Cancer Institute, Bethesda, MD, United States

OPEN ACCESS

**Edited by:**
Enzo Lalli,
UMR7275 Institut de Pharmacologie Moléculaire et Cellulaire (IPMC), France

**Reviewed by:**
Matthias Kroiss,
Julius Maximilian University of Würzburg, Germany
Mouhammed Amir Habra,
University of Texas MD Anderson Cancer Center, United States

***Correspondence:**
Jaydira Del Rivero
jaydira.delrivero@nih.gov

**Specialty section:**
This article was submitted to Cancer Endocrinology, a section of the journal Frontiers in Endocrinology

**Received:** 23 April 2020
**Accepted:** 22 June 2020
**Published:** 07 August 2020

**Citation:**
Del Rivero J, Donahue RN, Marté JL, Gramza AW, Bilusic M, Rauckhorst M, Cordes L, Merino MJ, Dahut WL, Schlom J, Gulley JL and Madan RA (2020) A Case Report of Sequential Use of a Yeast-CEA Therapeutic Cancer Vaccine and Anti-PD-L1 Inhibitor in Metastatic Medullary Thyroid Cancer. Front. Endocrinol. 11:490. doi: 10.3389/fendo.2020.00490

Medullary thyroid cancer (MTC) accounts for ∼4% of all thyroid malignancies. MTC derives from the neural crest and secretes calcitonin (CTN) and carcinoembryonic antigen (CEA). Unlike differentiated thyroid cancer, MTC does not uptake iodine and I-131 RAI (radioactive iodine) treatment is ineffective. Patients with metastatic disease are candidates for FDA-approved agents with either vandetanib or cabozantinib; however, adverse effects limit their use. There are ongoing trials exploring the role of less toxic immunotherapies in patients with MTC. We present a 61-year-old male with the diagnosis of MTC and persistent local recurrence despite multiple surgeries. He was started on sunitinib, but ultimately its use was limited by toxicity. He then presented to the National Cancer Institute (NCI) and was enrolled on a clinical trial with heat-killed yeast-CEA vaccine (NCT01856920) and his calcitonin doubling time improved in 3 months. He then came off vaccine for elective surgery. After surgery, his calcitonin was rising and he enrolled on a phase I trial of avelumab, a programmed death-ligand 1 (PD-L1) inhibitor (NCT01772004). Thereafter, his calcitonin decreased > 40% on 5 consecutive evaluations. His tumor was subsequently found to express PD-L1. CEA-specific T cells were increased following vaccination, and a number of potential immune-enhancing changes were noted in the peripheral immunome over the course of sequential immunotherapy treatment. Although calcitonin declines do not always directly correlate with clinical responses, this response is noteworthy and highlights the potential for immunotherapy or sequential immunotherapy in metastatic or unresectable MTC.

**Keywords: medullary thyroid cancer, CEA, calcitonin, immunotherapy, PD-L1 inhibitor**

## INTRODUCTION

Medullary thyroid cancer (MTC) accounts for ∼4% of all thyroid malignancies. It is a neuroendocrine tumor deriving from the neural crest-derived parafollicular or C cells of the thyroid gland (1). About 75% of MTC cases are sporadic and the remaining 25% present as part of an autosomal dominant inherited disorder. Activating mutations of the *RET* (Rearranged during

Transfection) proto-oncogene are characteristic, with germline activating RET mutations seen in fMTC (familial MTC) and MEN (multiple endocrine neoplasia) 2a/MEN2b (2–4). MTC most often produces both immunoreactive calcitonin (CTN) and carcinoembryonic antigen (CEA), which are used as tumor markers (5). The growth rate of MTC is estimated by using RECIST v.1.1 (Response Evaluation Criteria in Solid Tumors); however, it can also be determined by measuring serum levels of CTN and CEA over multiple time points to determine doubling time, which play an important role in the follow-up and management of MTC. Calcitonin doubling times of >2 years seem to be associated with a better long-term prognosis than those of <6 months (6, 7).

The role of immunotherapy in MTC is not fully studied. However, previous studies have identified evidence of T-cell infiltration on MTC (8). Dendritic cell (DC)-based immunotherapy was also given in patients with solid tumors including MTC and it was reported that vaccination with autologous tumor-pulsed DCs generated from peripheral blood was safe and can induce tumor-specific cellular cytotoxicity (9). Schott et al. (10) reported that subcutaneous injection of calcitonin and CEA loaded DC vaccine in patients with metastatic medullary thyroid cancer showed clinical benefit. Calcitonin and CEA decreased in 3 of 7 patients and one of these patients had complete regression of detectable liver metastasis and reduction of pulmonary lesions. A phase I study using the heat-killed yeast-CEA vaccine (GI-6207) was performed at the National Cancer Institute (NCI) (11). A total of 25 patients were enrolled in a classic phase I design at 3 dose levels. One patient with MTC had a significant inflammatory response at the sites of her tumors and a substantial and sustained antigen-specific immune response. Furthermore, the relatively low toxicity profile of therapeutic cancer vaccines could be advantageous compared to approved tyrosine kinase inhibitors (TKIs) for some patients with indolent recurrent or metastatic MTC. Here we present a case of a patient with recurrent MTC who was enrolled on a clinical trial with yeast-based vaccine targeting CEA. Upon surgical resection after vaccine, his tumor was found to express programmed death-ligand 1 (PD-L1), which may explain the patient's subsequent reponse to a PD-L1 inhibitor.

## CASE PRESENTATION

We report a 61-year-old male who initially presented with an enlarging anterior neck mass that was biopsied and found to be consistent with the diagnosis of MTC (no known somatic or germline mutation of the *RET* proto-oncogene). Subsequently, he underwent a total thyroidectomy with bilateral neck lymph node dissection. He then had multiple local recurrences, resulting in a total of five neck surgeries, the last one occurring 12 years after diagnosis. Based on the elevated CTN levels and persistent local recurrence, he then started systemic treatment with off-label sunitinib 13 years after diagnosis (12). While on sunitinib his CTN levels nadired to 199 pg/ml (reference <10 pg/ml), down from 461 pg/ml 6 months after starting treatment. He continued for 5 years and then stopped due to side effects. His CTN levels after discontinuing sunitinib rose to 2,243 pg/ml.

On follow-up imaging studies, there was no evidence of distant metastases and he presented to the NCI with disease involving his thyroid bed and cervical nodes, most of which were not amenable to resection. He then enrolled on a clinical trial with yeast-based therapeutic cancer vaccine targeting CEA (a phase 2 study of GI-6207 in patients with recurrent medullary thyroid cancer; NCT01856920) (8, 13). During a 6-month protocol–mandated surveillance, he had a CTN of 2,225 pg/mL and CEA of 11.9 ng/mL (reference 0.8–3.4 ng/mL) that increased to 5,964 pg/mL and CEA of 20.6 ng/mL (CTN doubling time of 135 days). During the subsequent 3-month vaccine period, his doubling time improved to 530 days (nadir CTN was 4,503 pg/mL and CEA 19 ng/mL). He then chose to have elective surgery to remove a neck lymph node and, per protocol, the vaccine was discontinued.

Approximately 3 months after surgery, his calcitonin had risen to 9,765 pg/ml and CEA 17.1 ng/mL and the patient was enrolled on a phase I trial of avelumab, a PD-L1 inhibitor (phase I, open-label, multiple-ascending dose trial to investigate the safety, tolerability, pharmacokinetics, biological, and clinical activity of avelumab (MSB0010718C), a monoclonal anti-PD-L1 antibody, in subjects with metastatic or locally advanced solid tumors (NCT01772004)) (14). He then had five consecutive declines in his calcitonin to 5,732 pg/ml and CEA levels remained overall stable at 22.0 ng/mL while on the immune checkpoint inhibitor avelumab, a > 40% decline not previously seen in his NCI clinical course (**Figure 1A**). Response assessment by RECIST v1.1 reported stable disease (**Figure 2**).

These findings coincided with an immune-related adverse event (asymptomatic rise in grade 3 lipase) that led to protocol-mandated treatment discontinuation. A subsequent analysis of the patient's lymph node resected post-vaccination revealed that the tumor was PD-L1 positive (**Figure 1B**). No baseline sample was available for evaluation given that the patient was diagnosed over 15 years prior to the latest surgery (15).

## Immune-Analysis

Sufficient cryopreserved peripheral blood mononuclear cells (PBMCs) were available from this patient to analyze CEA-specific $CD4^+$ and $CD8^+$ T cell responses before vaccination, and after six and seven vaccinations with yeast-CEA, corresponding to 3 and 4 months, respectively; PBMCs were also examined 15 days following one cycle (administered every 2 weeks for 30 days) of avelumab (**Figure 3A**). This assay involves intracellular cytokine staining (ICS) following a period of *in vitro* stimulation (IVS) with overlapping 15-mer peptide pools encoding the tumor-associated antigen CEA or the negative control pool HLA, as previously described (16, 17). The patient did not have pre-existing CEA-specific T cells, but displayed a notable increase in CEA-specific T cells 3 months following yeast-CEA vaccination; following subtraction of background and any value obtained prior to vaccination, there were 488 $CD4^+$ cells producing IFN$\gamma$ and 438 $CD4^+$ cells producing TNF per $1 \times 10^6$ cells plated at the start of the stimulation assay. As visualized in the dot plots of **Figure 3B**, the $CD4^+$ CEA-specific cells included multifunctional cells, or cells producing >1 cytokine. The increase in CEA-specific T cells was not seen at the two later time points evaluated.

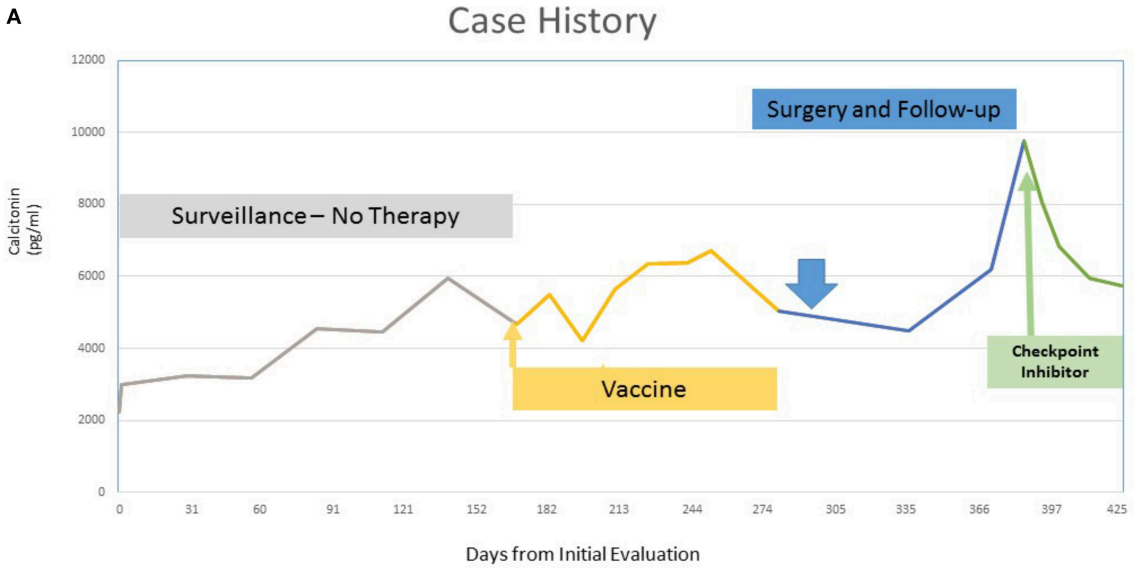


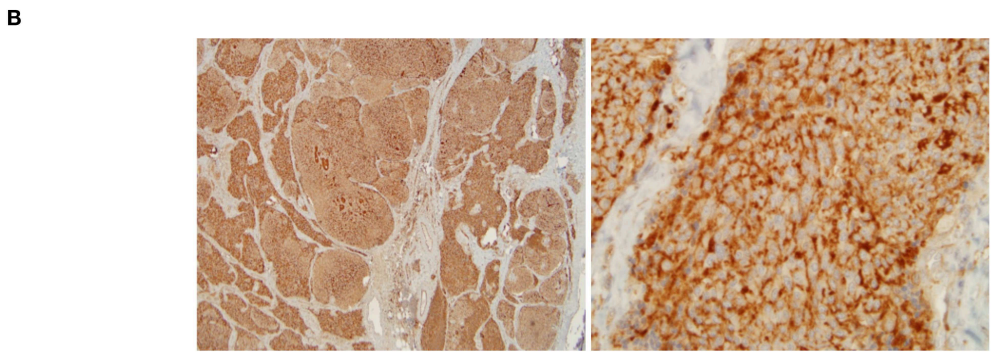


**FIGURE 1 | (A)** Five consecutive declines in the patient's calcitonin levels while on the immune checkpoint inhibitor, a > 40% decline. **(B)** Robustly positive PD-L1 staining after surgical resection of a neck lymph node after vaccine (higher power on the right).

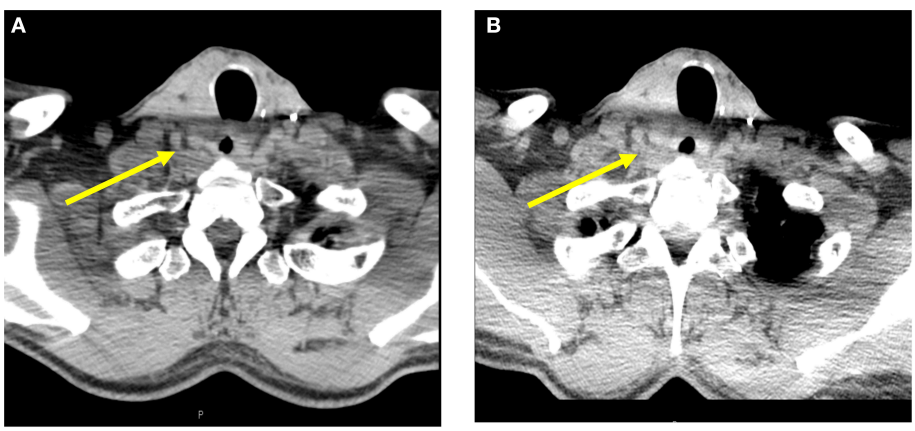


**FIGURE 2 |** Cross sectional imaging studies with computed tomography of the neck **(A)** prior to PD-L1 administration and **(B)** after a 40% decrease in calcitonin, showing stable thyroid bed recurrence.

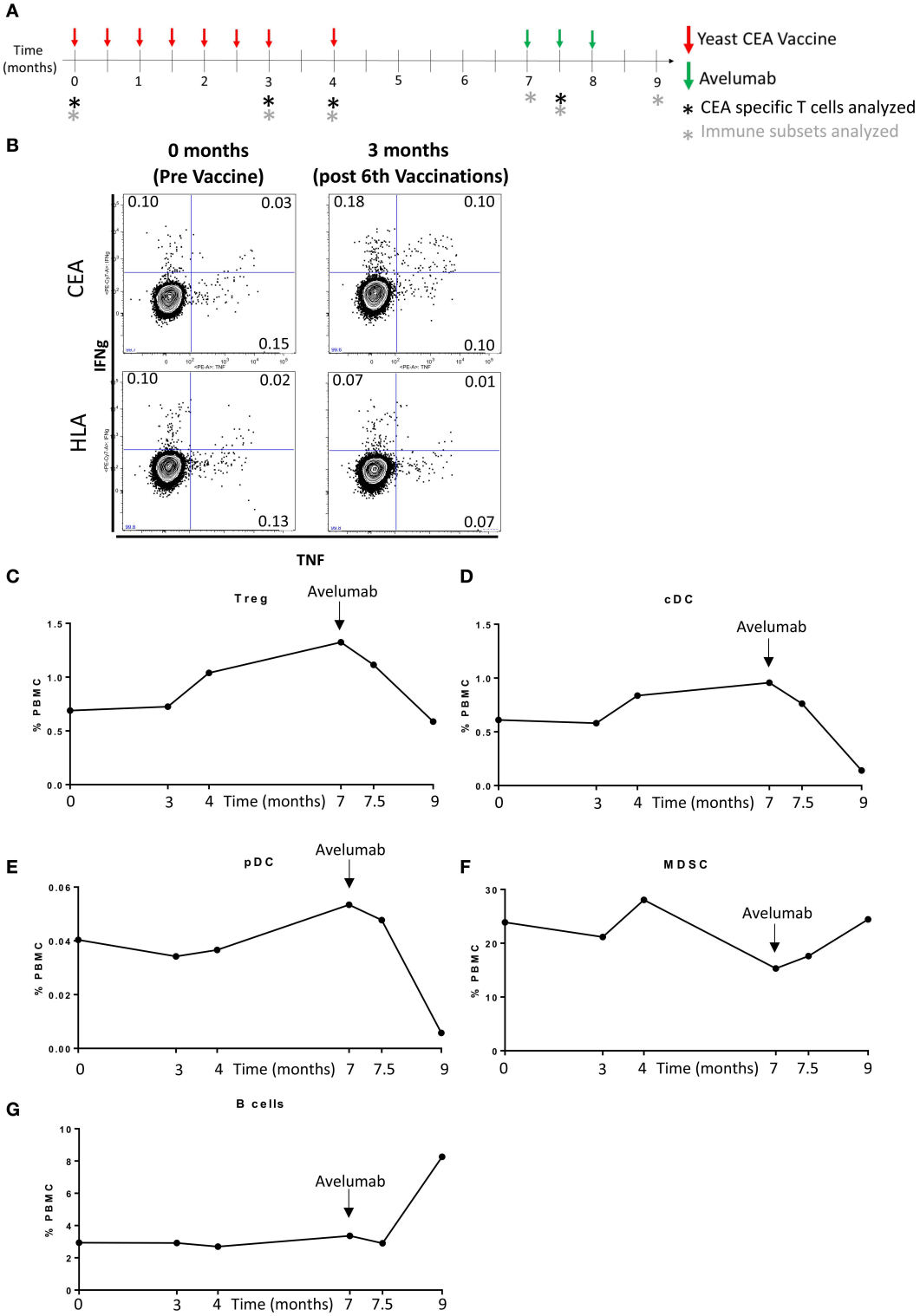


**FIGURE 3 |** Induction of CEA-specific T cells and changes in peripheral immune cell subsets. **(A)** Schema showing the timing of sequential immunotherapies and immune assays. **(B)** CEA-specific T cells were identified in PBMCs by intracellular cytokine staining following a period of *in vitro* stimulation with overlapping 15-mer peptide pools encoding for the tumor-associated antigen CEA or the negative control peptide pool HLA. Dot plots of IFNγ and TNF production by $CD4^+$ T cells showing induction of multifunctional CEA-specific T cells (producing >1 cytokine) at 3 months. **(C–G)** PBMCs were assessed for the frequency of 123 immune cell subsets over the course of immunotherapy. The most notable fluctuations were observed after initiation of avelumab (indicated by black arrow). The frequency over time of Tregs **(C)**, cDC **(D)**, pDC **(E)**, MDSC **(F)**, and B cells **(G)**, indicated as a percentage of total PBMCs.

The frequency of 123 PBMC subsets was also evaluated in this patient over his course of treatment at the National Cancer Institute using 11-color flow cytometry on cryopreserved PBMC as previously described (**Supplemental Table 1**) (18, 19). PBMCs were assayed prior to vaccination, 3 and 4 months following yeast-CEA vaccine, as well as at time points pre and post (15 and 42 days) avelumab (**Figure 3A**). Using 50% change as a cutoff, the first fluctuation in immune cell subsets was observed 4 months following vaccination with yeast-CEA, and included an increase in regulatory T-cells (Tregs) (51%), an inhibitory immune subset, compared to pre-vaccine levels (**Figure 3C**). After the patient completed vaccine and underwent surgery and prior to the initiation of avelumab, the patient had 92% more Tregs (**Figure 3C**) and 57% more conventional dendritic cells (cDC) (**Figure 3D**), a subset that is involved in antigen presentation, compared to pre-vaccine levels. The most dramatic fluctuations in immune subsets were noted at the time point after 6 weeks of avelumab, and included decreases in Tregs (**Figure 3C**), cDC (**Figure 3D**), and plasmacytoid DC (pDC, **Figure 3E**) compared to pre-avelumab therapy levels. pDC are tolerogenic DC, exhibiting poor immunostimulatory ability, and their interaction with T cells often favors the generation of Tregs (20). Increases in myeloid derived suppressor cells (MDSCs) (**Figure 3F**), another immune suppressive subset, and B cells (**Figure 3G**) were also noted after avelumab, compared to pre-avelumab levels. There were no alterations in the $CD4^+$, $CD8^+$, natural killer (NK) or NK-T compartments noted at any time point examined.

## DISCUSSION

For many years, doxorubicin was the only US Food and Drug Administration (FDA)–approved treatment for patients with advanced thyroid cancer; however, response rate in patients with MTC is up to 20% with significant toxicity (21–23). Recently, in advanced MTC, several TKIs, such as axitinib, cabozantinib, gefitinib, lenvatinib, imatinib, motesanib, sorafenib, pazopanib, sunitinib, and vandetanib, have been studied in phase I, II, and III clinical trials. Vandetanib, an oral inhibitor of VEGFR (vascular endothelial growth factor receptor), RET, and EGFR (epidermal growth factor receptor) (24, 25) was approved by the FDA in April 2011 after a phase III trial demonstrated improved median progression-free survival (PFS) compared to placebo (hazard ratio 0.45, 95% CI 0.30–0.69) and overall response rate of 45% (26). Cabozantinib, an inhibitor of hepatocyte growth factor receptor (MET), VEGFR2, and RET, was approved by the FDA in 2012 after a phase III trial demonstrated improved median PFS of 11.2 months relative to 4 months in the placebo group (5, 27, 28). The impact of toxicity on patients was clearly indicated and for cabozantinib 70% of patients required dose reductions and 65% required dosing delays (27). Therefore, toxicity of FDA-approved TKI agents limits their use in patients with small volume, asymptomatic, or indolent disease (26). Furthermore, no clear data exist from these studies that either agent impacts overall survival. In addition, RET-specific TKIs in development are Selpercatinib (previously LOXO-292) and Blue-667 with more specific RET-targeting activity. These agents have demonstrated evidence of efficacy in early trial results (29, 30); however, further treatments are warranted with less toxicity.

Evidence for cell-mediated immunity to tumor-specific antigens has been found in medullary thyroid cancer (31) and early studies suggested that MTC-specific T cells exist (32, 33). Emerging data suggest that the immune system may be relevant in the treatment of MTC (34–36). Furthermore, immune-based treatments have been studied. Dentritic cell–based immunotherapy was given in patients with solid tumors, including MTC, and it was reported that vaccination with autologous tumor-pulsed DCs generated from peripheral blood was safe and can induce tumor-specific cellular cytotoxicity (9).

This case report may demonstrate the potential for therapeutic cancer vaccines to synergize with immune checkpoint inhibition sequentially in MTC and that principle could be applied as well to other cancers that may have tumor microenvironments (TMEs) devoid of baseline immune recognition. The therapeutic cancer vaccine in this trial was a heat-killed yeast-based vaccine designed to stimulate an immune response against CEA. After a phase I trial demonstrated safety (transient injection site reaction was the most common adverse event) and preliminary evidence of immunologic and clinical activity, a phase II study was developed in MTC (NCT01856920) (11). The phase I study included a patient with MTC who had substantial inflammation at sites of disease that followed 3 months of the vaccine (11). It is also possible that the patient's previous sunitinib is relevant in this case report. In a model using CEA-transgenic mice bearing CEA tumors, continuous sunitinib followed by vaccine increased intratumoral infiltration of antigen-specific T lymphocytes, decreased immunosuppressant Tregs and MDSCs, reduced tumor volumes and increased survival. The immunomodulatory activity of continuous sunitinib administration can create a more immune-permissive environment (37).

Despite the significant recent advances of anti-PD-1 and anti-PD-L1 therapy, they still impact only a minority of patients whose TMEs express those molecules at baseline. One hypothesis is that sequential use of vaccine can drive immune cells to the TME, resulting in an adaptive reaction by tumor cells (potentially from the presence of cytokines produced by active immune cells in the TME); upregulating PD-L1 and perhaps defining a role for anti-PD-L1/PD-1 therapies in patients who may not have otherwise benefited from such immunotherapies (38, 39). Based on this perspective, combining or sequencing vaccines with anti-PD-L1/PD-1 therapies could broaden the clinical benefit for all patients with immunologically "cold tumor microenvironments" (devoid of reactive immune cells) to enhance the clinical efficacy among cancer patients with a variety of tumor types. This case may provide an example of how increasing peripheral T-cell activation with vaccines can enable immune cells to then migrate to the TME and improve response rates to anti-PD-L1/PD-1 therapies (8, 13). Indeed, existing data with the FDA-approved therapeutic cancer vaccine for prostate cancer, sipuleucel-T, indicate that vaccine did increase T cells in the TME after treatment (40).

Induction of CEA-specific T cells was noted in the peripheral blood of this patient following vaccination with yeast-CEA, but not at later time points. It is possible the CEA-specific cells homed in on the TME inducing PD-L1 expression subsequently

seen on the tumor. In addition, fluctuations in the peripheral immunome were noted in this patient over the course of therapy with yeast-CEA vaccine and subsequent avelumab therapy; these changes included both immune-potentiating and immune-suppressive alterations, with the most notable fluctuations occurring after several administrations of avelumab. The increase in suppressive elements may be a compensatory mechanism induced to tamper down the immune activation induced by the different immunotherapy treatments. However, as this patient had metastatic disease, it is unknown whether the changes in the peripheral immunome were directly induced by the sequential immunotherapy regimens or potentially related to disease progression.

As with all case reports, these presentations have limitations: the fact that the patient did not have a biopsy at baseline, prior to starting the vaccine, limits understanding of the baseline TME. Thus, it is unclear if the vaccine drove PD-L1 expression or if it was pre-existing in this patient. Little data exist for the presence of PD-L1 expression on MTC tumor cells. To further complicate this case's assessment, the patient was previously treated with sunitinib, which has been able to deplete Tregs, which alone or in combination with vaccine could have impacted the PD-L1 status of this patient (37). Nonetheless, data gleaned from using immunotherapy in such a rare disease are worth greater examination.

Although a decline in calcitonin does not directly correlate with clinical responses in this case or in MTC in general, the magnitude and consistency of the decline are noteworthy amidst data that suggest the predictive value of calcitonin doubling time and disease progression (41). Also, many patients with MTC have disease recurrence solely defined by serum tumor markers. In these patients, the opportunity to impact calcitonin kinetics with immunotherapy may decrease the pace of the disease and delay progression to overt metastasis requiring systemic therapies (TKIs) that are associated with toxicity or ultimately metastatic disease-related morbidity. Despite the effectiveness of TKIs in MTC, opportunities for immunotherapy clinical development may provide patients with additional treatment options that are less toxic and could thus be used earlier in the disease process.

## ETHICS STATEMENT

Written informed consent for publication of clinical details and/or clinical images was obtained from the patient.

## AUTHOR CONTRIBUTIONS

JD, RD, and RM were responsible for study concept and design. JD and RD acquired the data from the study and prepared the manuscript. RD was responsible for the immune analysis and interpretation. RM reviewed the manuscript. JM, AG, MB, MR, LC, MM, WD, JS, and JG read and approved the final version of the manuscript. All authors contributed to the article and approved the submitted version.

## FUNDING

This work was supported by National Cancer Institute, National Institutes of Health, Intramural Research Program. This research was financially supported by Merck KGaA, Darmstadt, Germany as part of an alliance between Merck KGaA and Pfizer given that JAVELIN Solid Tumor is an alliance-sponsored trial.

## ACKNOWLEDGMENTS

This work was selected for poster presentation at The Endocrine Society 99th Annual Meeting, Orlando, FL in 2017. We are thankful for the support of the National Institutes of Health Clinical Center staff including nurses, clinical and research fellows. Merck KGaA, Darmstadt, Germany, and Pfizer reviewed the manuscript for medical accuracy only before journal submission. The authors are fully responsible for the content of this manuscript, and the views and opinions described in the publication reflect solely those of the authors.

## SUPPLEMENTARY MATERIAL

The Supplementary Material for this article can be found online at: https://www.frontiersin.org/articles/10.3389/fendo.2020.00490/full#supplementary-material

## REFERENCES

1. Saad MF, Ordonez NG, Rashid RK, Guido JJ, Hill CS Jr, Hickey RC, et al. Medullary carcinoma of the thyroid. A study of the clinical features and prognostic factors in 161 patients. *Medicine.* (1984) 63:319–42. doi: 10.1097/00005792-198411000-00001
2. Kouvaraki MA, Shapiro SE, Perrier ND, Cote GJ, Gagel RF, Hoff AO, et al. RET proto-oncogene: a review and update of genotype-phenotype correlations in hereditary medullary thyroid cancer and associated endocrine tumors. *Thyroid.* (2005) 15:531–44. doi: 10.1089/thy.2005.15.531
3. Brandi ML, Gagel RF, Angeli A, Bilezikian JP, Beck-Peccoz P, Bordi C, et al. Guidelines for diagnosis and therapy of MEN type 1 and type 2. *J Clin Endocrinol Metab.* (2001) 86:5658–71. doi: 10.1210/jcem.86.12.8070
4. Eng C, Mulligan LM, Healey CS, Houghton C, Frilling A, Raue F, et al. Heterogeneous mutation of the RET proto-oncogene in subpopulations of medullary thyroid carcinoma. *Cancer Res.* (1996) 56:2167–70.
5. Del Rivero J, Edgerly M, Ward J, Madan RA, Balasubramaniam S, Fojo T, et al. Phase I/II trial of vandetanib and bortezomib in adults with locally advanced or metastatic medullary thyroid cancer. *Oncologist.* (2019) 24:16–e4. doi: 10.1634/theoncologist.2018-0452
6. Saad MF, Fritsche HA Jr, Samaan NA. Diagnostic and prognostic values of carcinoembryonic antigen in medullary carcinoma of the thyroid. *J Clin Endocrinol Metab.* (1984) 58:889–94. doi: 10.1210/jcem-58-5-889
7. Saad MF, Ordonez NG, Guido JJ, Samaan NA. The prognostic value of calcitonin immunostaining in medullary carcinoma of the thyroid. *J Clin Endocrinol Metab.* (1984) 59:850–6. doi: 10.1210/jcem-59-5-850
8. French JD, Bible K, Spitzweg C, Haugen BR, Ryder M. Leveraging the immune system to treat advanced thyroid cancers. *Lancet Diabetes Endocrinol.* (2017) 5:469–81. doi: 10.1016/S2213-8587(16)30277-7
9. Stift A, Friedl J, Dubsky P, Bachleitner-Hofmann T, Schueller G, Zontsich T, et al. Dendritic cell-based vaccination in solid cancer. *J Clin Oncol.* (2003) 21:135–42. doi: 10.1200/JCO.2003.02.135

10. Schott M, Seissler J, Lettmann M, Fouxon V, Scherbaum WA, Feldkamp J. Immunotherapy for medullary thyroid carcinoma by dendritic cell vaccination. *J Clin Endocrinol Metab.* (2001) 86:4965–9. doi: 10.1210/jcem.86.10.7949
11. Bilusic M, Heery CR, Arlen PM, Rauckhorst M, Apelian D, Tsang KY, et al. Phase I trial of a recombinant yeast-CEA vaccine (GI-6207) in adults with metastatic CEA-expressing carcinoma. *Cancer Immunol Immunother.* (2014) 63:225–34. doi: 10.1007/s00262-013-1505-8
12. Ravaud A, de la Fouchardiere C, Caron P, Doussau A, Do Cao C, Asselineau J, et al. A multicenter phase II study of sunitinib in patients with locally advanced or metastatic differentiated, anaplastic or medullary thyroid carcinomas: mature data from the THYSU study. *Eur J Cancer.* (2017) 76:110–7. doi: 10.1016/j.ejca.2017.01.029
13. Bastman JJ, Serracino HS, Zhu Y, Koenig MR, Mateescu V, Sams SB, et al. Tumor-Infiltrating T cells and the PD-1 checkpoint pathway in advanced differentiated and anaplastic thyroid cancer. *J Clin Endocrinol Metab.* (2016) 101:2863–73. doi: 10.1210/jc.2015-4227
14. Heery CR, O'Sullivan-Coyne G, Madan RA, Cordes L, Rajan A, Rauckhorst M, et al. Avelumab for metastatic or locally advanced previously treated solid tumours (JAVELIN Solid Tumor): a phase 1a, multicohort, dose-escalation trial. *Lancet Oncol.* (2017) 18:587–98. doi: 10.1016/S1470-2045(17)30239-5
15. Del Rivero JGA, Bilusic M, Rauckhorsts M, Cordes L, Karzai F, Strauss J, et al. Calcitonin response following sequential use of a yeast-CEA therapeutic cancer vaccine and avelumab, a monoclonal anti-PD-L1 inhibitor, in metastatic medullary thyroid cancer. *Poster 184, 99th Annual Meeting of the Endocrine Society 2017*. Orlando, FL (2017).
16. Heery CR, Ibrahim NK, Arlen PM, Mohebtash M, Murray JL, Koenig K, et al. Docetaxel alone or in combination with a therapeutic cancer vaccine (PANVAC) in patients with metastatic breast cancer: a randomized clinical trial. *JAMA Oncol.* (2015) 1:1087–95. doi: 10.1001/jamaoncol.2015.2736
17. Heery CR, Singh BH, Rauckhorst M, Marte JL, Donahue RN, Grenga I, et al. Phase I trial of a yeast-based therapeutic cancer vaccine (GI-6301) targeting the transcription factor brachyury. *Cancer Immunol Res.* (2015) 3:1248–56. doi: 10.1158/2326-6066.CIR-15-0119
18. Donahue RN, Lepone LM, Grenga I, Jochems C, Fantini M, Madan RA, et al. Analyses of the peripheral immunome following multiple administrations of avelumab, a human IgG1 anti-PD-L1 monoclonal antibody. *J Immunother Cancer.* (2017) 5:20. doi: 10.1186/s40425-017-0220-y
19. Lepone LM, Donahue RN, Grenga I, Metenou S, Richards J, Heery CR, et al. Analyses of 123 peripheral human immune cell subsets: defining differences with age and between healthy donors and cancer patients not detected in analysis of standard immune cell types. *J Circ Biomark.* (2016) 5:5. doi: 10.5772/62322
20. Matta BM, Castellaneta A, Thomson AW. Tolerogenic plasmacytoid DC. *Eur J Immunol.* (2010) 40:2667–76. doi: 10.1002/eji.201040839
21. Sculier J, Thiriaux J, Bureau G, Lafitte J, Recloux P, Brohee D, et al. A phase-ii study testing weekly platinum derivative combination chemotherapy as 2nd-line treatment in patients with advanced small-cell lung-cancer. *Int J Oncol.* (1995) 6:425–9. doi: 10.3892/ijo.6.2.425
22. Nocera M, Baudin E, Pellegriti G, Cailleux AF, Mechelany-Corone C, Schlumberger M. Treatment of advanced medullary thyroid cancer with an alternating combination of doxorubicin-streptozocin and 5 FU-dacarbazine. Groupe d'Etude des Tumeurs a Calcitonine (GETC). *Br J Cancer.* (2000) 83:715–8. doi: 10.1054/bjoc.2000.1314
23. Wu LT, Averbuch SD, Ball DW, de Bustros A, Baylin SB, McGuire WP III. Treatment of advanced medullary thyroid carcinoma with a combination of cyclophosphamide, vincristine, and dacarbazine. *Cancer.* (1994). 73:432–6. doi: 10.1002/1097-0142(19940115)73:2<432::aid-cncr2820730231>3.0.co;2-k
24. Carlomagno F, Vitagliano D, Guida T, Ciardiello F, Tortora G, Vecchio G, et al. ZD6474, an orally available inhibitor of KDR tyrosine kinase activity, efficiently blocks oncogenic RET kinases. *Cancer Res.* (2002) 62:7284–90.
25. Wells SA Jr, Gosnell JE, Gagel RF, Moley J, Pfister D, Skinner M, et al. Vandetanib for the treatment of patients with locally advanced or metastatic hereditary medullary thyroid cancer. *J Clin Oncol.* (2010) 28:767–72. doi: 10.1200/JCO.2009.23.6604
26. Wells SA Jr, Robinson BG, Gagel RF, Dralle H, Fagin JA, Santoro M, et al. Vandetanib in patients with locally advanced or metastatic medullary thyroid cancer: a randomized, double-blind phase III trial. *J Clin Oncol.* (2012) 30:134–41. doi: 10.1200/JCO.2011.35.5040
27. Elisei R, Schlumberger MJ, Muller SP, Schoffski P, Brose MS, Shah MH, et al. Cabozantinib in progressive medullary thyroid cancer. *J Clin Oncol.* (2013) 31:3639–46. doi: 10.1200/JCO.2012.48.4659
28. Viola D, Cappagli V, Elisei R. Cabozantinib (XL184) for the treatment of locally advanced or metastatic progressive medullary thyroid cancer. *Future Oncol.* (2013) 9:1083–92. doi: 10.2217/fon.13.128
29. Drilon AE, Subbiah V, Oxnard GR, Bauer TM, Velcheti V, Lakhani NJ, et al. A phase 1 study of LOXO-292, a potent and highly selective RET inhibitor, in patients with RET-altered cancers. *J Clin Oncol.* (2018) 36(Suppl. 15):102. doi: 10.1200/JCO.2018.36.15_suppl.102
30. Ilanchezhian M, Khan S, Okafor C, Glod J, Del Rivero J. Update on the treatment of medullary thyroid carcinoma in patients with multiple endocrine neoplasia type 2. *Horm Metab Res.* (2020). doi: 10.1055/a-1145-8479. [Epub ahead of print].
31. Hellstrom I, Hellstrom KE, Pierce GE, Yang JP. Cellular and humoral immunity to different types of human neoplasms. *Nature.* (1968) 220:1352–4. doi: 10.1038/2201352a0
32. Rocklin RE, Gagel R, Feldman Z, Tashjian AH Jr. Cellular immune responses in familial medullary thyroid carcinoma. *N Engl J Med.* (1977) 296:835–8. doi: 10.1056/NEJM197704142961502
33. George JM, Williams MA, Almoney R, Sizemore G. Medullary carcinoma of the thyroid. Cellular immune response to tumor antigen in a heritable human cancer. *Cancer.* (1975) 36:1658–61. doi: 10.1002/1097-0142(197511)36:5<1658::AID-CNCR2820360519>3.0.CO;2-0
34. Muller S, Poehnert D, Muller JA, Scheumann GW, Koch M, Luck R. Regulatory T cells in peripheral blood, lymph node, and thyroid tissue in patients with medullary thyroid carcinoma. *World J Surg.* (2010) 34:1481–7. doi: 10.1007/s00268-010-0484-6
35. Cressent M, Pidoux E, Cohen R, Modigliani E, Roth C. Interleukin-2 and interleukin-4 display potent antitumour activity on rat medullary thyroid carcinoma cells. *Eur J Cancer.* (1995) 31A:2379–84. doi: 10.1016/0959-8049(95)00445-9
36. Lausson S, Fournes B, Borrel C, Milhaud G, Treilhou-Lahille F. Immune response against medullary thyroid carcinoma (MTC) induced by parental and/or interleukin-2-secreting MTC cells in a rat model of human familial medullary thyroid carcinoma. *Cancer Immunol Immunother.* (1996) 43:116–23. doi: 10.1007/s002620050311
37. Farsaci B, Higgins JP, Hodge JW. Consequence of dose scheduling of sunitinib on host immune response elements and vaccine combination therapy. *Int J Cancer.* (2012) 130:1948–59. doi: 10.1002/ijc.26219
38. Fu J, Malm IJ, Kadayakkara DK, Levitsky H, Pardoll D, Kim YJ. Preclinical evidence that PD1 blockade cooperates with cancer vaccine TEGVAX to elicit regression of established tumors. *Cancer Res.* (2014) 74:4042–52. doi: 10.1158/0008-5472.CAN-13-2685
39. Antoni R, Caroline RF, Hodi S, Wolchok JD, Joshua AM, Hwu W, et al. Association of response to programmed death receptor 1 (PD-1) blockade with pembrolizumab (MK-3475) with an interferon-inflammatory immune gene signature. *J Clin Oncol.* (2015) 33(Suppl. 15):3001. doi: 10.1200/jco.2015.33.15_suppl.3001
40. Fong L, Carroll P, Weinberg V, Chan S, Lewis J, Corman J, et al. Activated lymphocyte recruitment into the tumor microenvironment following preoperative sipuleucel-T for localized prostate cancer. *J Natl Cancer Inst.* (2014) 106:dju268. doi: 10.1093/jnci/dju268
41. Meijer JA, le Cessie S, van den Hout WB, Kievit J, Schoones JW, Romijn JA, et al. Calcitonin and carcinoembryonic antigen doubling times as prognostic factors in medullary thyroid carcinoma: a structured meta-analysis. *Clin Endocrinol (Oxf).* (2010) 72:534–42. doi: 10.1111/j.1365-2265.2009.03666.x


**Conflict of Interest:** The authors declare that the research was conducted in the absence of any commercial or financial relationships that could be construed as a potential conflict of interest.

frontiers in Endocrinology

ORIGINAL RESEARCH
published: 30 September 2020
doi: 10.3389/fendo.2020.557050

# Prevalence of Parathyroid Carcinoma and Atypical Parathyroid Neoplasms in 153 Patients With Multiple Endocrine Neoplasia Type 1: Case Series and Literature Review

*An Song[1†], Yi Yang[1], Shuzhong Liu[2], Min Nie[1], Yan Jiang[1], Mei Li[1], Weibo Xia[1], Ou Wang[1*†] and Xiaoping Xing[1*†]*

[1] Key Laboratory of Endocrinology, Ministry of Health, Department of Endocrinology, Peking Union Medical College, Peking Union Medical College Hospital, Chinese Academy of Medical Sciences, Beijing, China, [2] Department of Orthopaedic Surgery, Peking Union Medical College Hospital, Peking Union Medical College and Chinese Academy of Medical Sciences, Beijing, China

OPEN ACCESS

**Edited by:**
Antongiulio Faggiano,
Sapienza Università di Roma, Italy

**Reviewed by:**
Amit Tirosh,
Sheba Medical Center, Israel
Subramanian Kannan,
Narayana Health, India

***Correspondence:**
Ou Wang
wang_ou2010@126.com
Xiaoping Xing
xingxp2006@126.com

**†ORCID:**
An Song
orcid.org/0000-0001-6572-1827
Ou Wang
orcid.org/0000-0002-0395-8789
Xiaoping Xing
orcid.org/0000-0002-2759-5177

**Specialty section:**
This article was submitted to Cancer Endocrinology, a section of the journal Frontiers in Endocrinology

**Received:** 10 June 2020
**Accepted:** 20 August 2020
**Published:** 30 September 2020

**Citation:**
Song A, Yang Y, Liu S, Nie M, Jiang Y, Li M, Xia W, Wang O and Xing X (2020) Prevalence of Parathyroid Carcinoma and Atypical Parathyroid Neoplasms in 153 Patients With Multiple Endocrine Neoplasia Type 1: Case Series and Literature Review. Front. Endocrinol. 11:557050. doi: 10.3389/fendo.2020.557050

**Purpose:** The occurrence of parathyroid carcinoma (PC) and atypical parathyroid neoplasm (APN) in multiple endocrine neoplasia type 1 (MEN1) is rare. The present paper reports the cases of 3 MEN1-PC/APN patients at our center and discusses the prevalence in a Chinese MEN1 cohort.

**Methods:** This report is a retrospective analysis of 153 MEN1-associated primary hyperparathyroidism (MEN1-HPT) patients at our center, which included 3 MEN1-associated PC/APN (MEN1-PC/APN) patients. The clinical manifestations, biochemical indices, pathological findings, and therapy have been summarized along with the report of the genetic testing of the 3 patients.

**Results:** Of the 153 MEN1-HPT patients, 1 (0.7%) was histopathologically diagnosed with PC and 2 (1.3%) with APN. Three heterozygous mutations were identified in the 3 MEN1-PC/APN patients (c.917 T > G, c.431T > C, and c.549 G > C). The cumulative findings of 3 cases with 18 previously reported MEN1-PC/APN cases revealed that the mean serum calcium (Ca) level was 3.15 ± 0.44 mmol/L and the median parathyroid hormone (PTH) level was 327 pg/mL (214.1, 673.1), both of which were significantly higher as compared to the respective levels in non-PC/APN MEN1 patients at our center [Ca: 2.78 mmol/L [2.61, 2.88], PTH: 185.5 pg/mL [108.3, 297.0]; $P = 0.0003$, 0.0034, respectively].

**Conclusion:** MEN 1-PC/APN is a rare disease, with a prevalence of only 2.0% among the MEN1-HPT cohort at our center. The affected patients recorded higher serum Ca level and PTH levels than those with MEN1-associated benign tumors. However, the diagnosis of MEN1-PC/APN is based upon pathology most of the times.

**Keywords: multiple endocrine neoplasia type 1, parathyroid carcinoma, atypical parathyroid neoplasms, prevalence, Chinese population**

## INTRODUCTION

Multiple endocrine neoplasia type 1 (MEN1) is an autosomal dominant hereditary syndrome that is characterized by the presence of endocrine tumors affecting the parathyroid, pancreas, and pituitary. In addition, some of these patients also develop adrenal adenoma (AA), carcinoid tumors (CT), angiofibroma, lipomas, collagenoma, and meningiomas (1). MEN1 is diagnosed based on the clinical or genetic criteria, and it has a prevalence of ∼2–20 cases in 100,000 (1). Primary hyperparathyroidism (PHPT) is the most common manifestation of this syndrome, recorded in >95% of cases, with ∼100% penetrance at the age of 50 years (2). The most frequent pathological type of MEN1-associated PHPT (MEN1-HPT) is parathyroid hyperplasia, which often involves multiple glands simultaneously (3, 4).

In contrast, in sync with the tendency of malignant pathology, the occurrence of parathyroid carcinoma (PC) and atypical parathyroid neoplasm (APN) as the causes of PHPT in MEN1 is a rare possibility. Until date, only 17 MEN1-associated PC (MEN1-PC) cases and only 1 MEN1-associated APN (MEN1-APN) case have been reported in the literature, accounting for a prevalence rate of 0.28–1% among MEN1 patients (5, 6). However, these literature are limited to the Caucasian population, and the corresponding data relevant to the Chinese or other Asian population remains lacking.

In this report, we have summarized the clinical manifestations, treatments, and genetic backgrounds of 3 MEN1-PC/APN patients admitted to our center as well as have reported the prevalence of MEN1-PC/APN in a Chinese cohort of MEN1 patients.

## MATERIALS AND METHODS

### Subjects

Between 1999 and 2019, 153 MEN1-HPT patients belonging to 148 families were diagnosed at the Department of Endocrinology, The Peking Union Medical College Hospital (PUMCH), Beijing. Among them, 112 patients underwent surgical treatment for MEN1-HPT, of which 3 were pathologically diagnosed with PC or APN.

### Diagnosis

The diagnosis of MEN1 was established by one of the 3 criteria, namely (2, 4): (i) Clinical criteria: the occurrence of two or more major MEN1-associated endocrine tumors [i.e., parathyroid tumor, pancreatic endocrine tumor (PET), and pituitary adenoma [PIT]]; (ii) Genetic criteria: the identification of a germline MEN1 mutation, who might be asymptomatic with no biochemical or radiological manifestations of MEN1; and (iii) For the first-degree relatives of MEN1-patients: The occurrence of one MEN1-associated tumor.

The diagnostic criteria for PC relied on finding lesions with vascular invasion, perineural invasion, capsular penetration, and/or documented metastases (7). The APN was diagnosed for parathyroid tumors partially sharing some of the atypical features in PC, but not meeting all the histological criteria of PC (6).

### Clinical Investigation

The clinical data were retrospectively collected, including general characteristics, clinical manifestations (e.g., bone involvement, urinary system damage, gastrointestinal symptoms, and hypercalcemia crisis), treatment strategies, pathological features, and follow-up (postoperative recurrence and metastasis). Bone involvement included bone pain, pathological fracture, and the X-ray features of PHPT characterized by bone resorption (such as subperiosteal absorption and osteitis fibrosa cystica). Bone mineral density (BMD) was measured by dual-energy X-ray absorptiometry (DXA; GE-Lunar, USA). Urolithiasis or renal calcification was assessed via ultrasound application.

The hypercalcemia crisis was defined as a serum total calcium (Ca) level of ≥3.5 mmol/L, and it is usually associated with development of acute signs and symptoms of hypercalcemia (8). The definition of recurrence was presentation of hypercalcemia after a disease-free period of at least 6 months after parathyroidectomy (9).

### Laboratory Examinations

Biochemical indices including serum Ca, phosphorus (P), alkaline phosphatase (ALP), and 24-h urine Ca (24-hUCa) were measured with the Beckman Automatic Biochemical Analyzer (AU5800; Beckman Coulter). Ionized-Ca (iCa) levels were measured with a blood-gas analyzer radiometer (ABL800 FLEX; Denmark). The serum parathyroid hormone (PTH) level was measured via chemiluminescence (ADVIA Centaur; Siemens, Germany). Serum 25-dihydroxyvitamin D (25OHD) value was measured using an electrochemiluminescence immunoassay (e601; Roche Cobas, Germany). Normal reference ranges for indices: serum Ca: 2.13–2.70 mmol/L. serum iCa: 1.08–1.28 mmol/L, serum P: 0.81–1.45 mmol/L, ALP: 30–120 U/L, PTH: 13–65 pg/mL, 25OHD: 30–50 ng/mL, 24hUCa: <7.5 mmol.

### DNA Isolation and Gene-Mutation Analysis

Genomic DNA was extracted from the peripheral blood lymphocytes using the QIAamp Blood DNA Kit (Qiagen; Hilden, Germany). All coding exons and exon-intron boundaries of the *MEN1* were amplified via polymerase chain reaction (PCR), followed by Sanger sequencing which was performed as previously prescribed (10).

### Statistical Methods

Statistical analysis was conducted using the Medcalc software (Version 18.2, Ostend, Belgium). All the MEN1-HPT patients at our center, except for the 3 MEN1-PC/APN patients, were placed into the non-PC/APN group. All the 18 reported MEN1-PC/APN cases and 3 from our center were placed in the PC/APN group. All data that were normally distributed were described by mean and standard deviation, and group differences were compared using independent *t*-tests. Data that were non-normally distributed were described in median and 25th and 75th interquartile ranges (Q25, Q75), while group differences were compared using rank-sum tests. The pathological results of the patients were clearly diagnosed by 2 pathologists. For patients with multi-glandular involvement, if the pathological findings were different for different lesions, the diagnosis was based on the

**TABLE 1 |** General characteristics of MEN1-PC/APN cases in our center.

| Case | Sex | Age (years) | Course of disease (years) | MEN1 family history | First involved gland | Other MEN1 diseases |
|---|---|---|---|---|---|---|
| P1 | Female | 51 | 27 | Yes | Parathyroid | Pancreatic non-functional tumor, adrenal non-functional tumor |
| P2 | Female | 52 | 10 | No | Pituitary | Pituitary prolactinoma |
| P3 | Male | 49 | 12 | Suspicious | Parathyroid | Pancreatic neuroendocrine tumor, adrenocortical adenoma, pituitary microadenomas |

findings of the more malignant areas. $P < 0.05$ was considered to be statistically significant.

# RESULTS

## Clinical Data and Genetic Screening of MEN1-PC/APN Patients at Our Center

A total of 153 patients with a clinical and/or genetic diagnosis of MEN1-HPT were identified at our center. Of these, 112 patients (73.2%) underwent surgical treatment, of whom 45 had hyperplasia (40.2%), 64 had adenomas (57.1%), 2 had APN (1.8%), and 1 had PC (0.9%).

The mean disease onset age in the non-PC/APN group ($n = 150$) was 43.0 ± 15.5 years (range: 12–77 years), with a median course of PHPT of 6 years (range: 2 weeks−35 years). This group included 87 women (58%) and 63 men (42%). The involvement of the gastrointestinal tract, urinary tract, and bone were noted in 32, 74, and 70 patients in the non-PC/APN group (21.3, 49.3, and 46.7%), respectively. Bone involvement included 29 cases with bone pain, 14 cases with pathological fracture, 12 cases with subperiosteal absorption, 5 cases with osteitis fibrosa cystica and 43 cases with osteoporosis measured by DXA. The median serum Ca level was 2.78 mmol/L (2.61, 2.88), median PTH was 185.5 pg/mL (108.3, 297.0), and median 24-h UCa was 7.68 mmol (5.09, 10.28) in this group.

**Table 1** summarizes the general characteristics of the 3 MEN1-PC/APN patients. The age at which the disease onset was noted in all 3 cases was >49 years (the mean onset age of the non-PC/APN group was 43.0 ± 15.5 years) with a relatively long course of disease. All the 3 patients had other MEN1 diseases, including PET, PIT, and AA. **Table 2** presents the clinical manifestations and preoperative biochemical markers of the 3 patients. All of them had nephrolithiasis, 2 had bone pain with osteoporosis, and 1 presented with gastrointestinal symptoms such as nausea and vomiting. None of the 3 patients demonstrated hypercalcemia crisis. **Table 3** summarizes the details of the surgical methods, histopathological features, and postoperative follow-up of the 3 patients.

## Case Report

### Case 1

A 51-year-old woman presented with recurrent nephrolithiasis since 1992, along with bone pain-induced restricted movement since 2013. Her laboratory investigations revealed hypercalcemia (3.15 mmol/L, normal range: 2.13–2.70 mmol/L) and elevated serum PTH levels (2,136 pg/mL, normal range: 13–65 pg/mL). Ultrasonography detected bilateral renal calculi. Accordingly, in 2013, the patient underwent left superior parathyroidectomy for the pathology parathyroid adenoma in other hospital. Her postoperative serum Ca level was 1.96 mmol/L and PTH level was 22.8 pg/mL (decreased 98.9%). Until 2019, she experienced recurrent nephrolithiasis, with a serum Ca level of 2.56 mmol/L, iCa level of 1.31 mmol/L, and PTH level of 2189.4 pg/mL. Her BMD, as measured by DXA, was 1.232 in the lumbar spines 1–4 (T score 0.7), 0.887 in the femur neck (T score −0.2), and 0.823 in the total hip (T score −1.1). The parathyroid 99mTc-sestamibi scanning revealed multiple lesions. Meanwhile, 3 abnormal nodules (of size ∼1.3 × 1.1 cm) were detected in the pancreatic tail through Gadolinium-enhanced abdominal MRI. Moreover, nodular masses were detected in both the adrenal glands. No significant abnormalities were recorded in the pituitary MRI. Genetic testing of *MEN1* revealed a heterozygous mutation: c.917T > G (p.L306R, exon 6). The patient had a family history of MEN1 (2 daughters and 1 grandson, 1 elder sister and her son, and 2 younger sisters and one of their sons were clinically diagnosed with PHPT, involving mutation at the same site in *MEN1*). Since the patient was diagnosed as recurrence of MEN-HPT, she underwent the second parathyroidectomy, whereby all of the remaining left inferior, right inferior, and superior parathyroid glands were removed and the left inferior parathyroid tissue (measuring 0.3 × 0.3 × 0.4 cm) were auto-planted into the right sternocleidomastoid muscle. The pathology was found to be atypical parathyroid neoplasm of the right superior and right inferior glands (**Figure 1**), along with the adenoma of the left inferior gland. Her postoperative serum Ca and PTH (decreased 97.1%) levels reverted to the normal since the first day after surgery, without any complications. At 1-year follow-up, the patient showed no signs of recurrence or metastasis, and no new disease associated with MEN1 appeared.

### Case 2

A 52-year-old woman presented with a 10-year history of recurrent nephrolithiasis since 1995. In 2005, her laboratory investigations detected hypercalcemia (3.35 mmol/L), hypercalciuria (22.56 mmol/d), and elevated serum PTH levels (561 pg/mL). Her ultrasound detected bilateral renal calculi. She reported no bone pain or any history of fracture. BMD, as measured by DXA, was 0.998 in lumbar spines 1–4 (T score −0.9), 1.027 in the femur neck (T score 0.9), and 0.993 in the total hip (T score 0.3). At the age of 51 years, the patient

**TABLE 2** | Clinical manifestations and biochemical indices of MEN1-PC/APN cases in our center.

| Case | Skeletal involvement | Urinary involvement | Gastrointestinal symptoms | HypercalcemiaCa (mmol/L) crisis | iCa (mmol/L) | P (mmol/L) | ALP (U/L) | PTH (pg/mL) | 25OHD (ng/mL) | 24hUCa (mmol) | 24hUP (mmol) |
|---|---|---|---|---|---|---|---|---|---|---|---|
| P1* | Yes | Yes | Yes | No | 2.56 | 1.31 | 0.96 | 219 | 2189.4 | 25.4 | 4.13 | 1.89 |
| P2 | No | Yes | No | No | 3.35 | / | 0.87 | 195 | 708.8 | / | 22.56 | / |
| P3 | Yes | Yes | No | No | 2.83 | 1.39 | 0.74 | 113 | 380 | 6.1 | 7.32 | 19.74 |

*Note: 1. * The patient underwent two times operations; the pathology was adenomas for the first time and atypical adenomas for the second time. The results in this table were before the second operation. The results of P2 and P3 were before the first operation.*

*2. Normal reference ranges for indices: Ca (serum calcium): 2.13–2.70 mmol/L. iCa (serum ionized calcium): 1.08–1.28 mmol/L. P (serum phosphorous): 0.81–1.45 mmol/L. ALP (alkaline phosphatase): 30–120 U/L. PTH (serum parathyroid hormone): 13–65 pg/mL. 25OHD (25-hydroxyvitamin D): 30–50 ng/mL. 24hUCa (24h urinary calcium): <7.5 mmol.*

was diagnosed with macroprolactinomas and the chiasmal compression and visual impairment occurred in a short period of time, the patient required pituitary adenoma resection by a single nostril transsphenoidal approach. The patient had no family history of MEN1, nephrolithiasis, or fractures. The genetic testing of *MEN1* revealed a heterozygous mutation: c.431T>C (p.F144S, exon 2). The patient, accordingly, underwent parathyroidectomy for the removal of her left superior and right inferior parathyroid glands—the pathology being atypical parathyroid neoplasm. Her postoperative serum Ca and PTH (decreased 87.5%) levels reverted to the normal since the first day after surgery, without any complications. At her 3-year follow-up, the patient showed no signs of recurrence or metastasis, and no new disease associated with MEN1 appeared. However, the patient has been lost to follow-up since 2008.

## Case 3

A 49-year-old man presented with a 12-year history of recurrent nephrolithiasis since 2004. In 2015, his laboratory investigations revealed hypercalcemia (2.83 mmol/L) and elevated serum PTH levels (380 pg/mL). His ultrasonography detected bilateral renal calculi. His BMD measurement findings by DXA were 1.005 in lumbar spines 1–4 (T score −0.2), 0.83 in the femur neck (T score −0.5), and 0.815 in the total hip (T score −1.2). During the disease course, the patient often suffered from acid reflux and epigastric pain, occasionally accompanied with melena. The contrast-enhanced computed tomography (CT) of his abdomen revealed a highly-vascular lesion in the pancreatic head. The patient was accordingly diagnosed with pancreatic neuroendocrine tumors, for which he underwent $^{125}$I particle implantation and pancreatic biopsy—the pathology being pancreatic neuroendocrine tumors. Meanwhile, a subcutaneous mass of abdominal wall and mediastinum lesion (as per chest CT imaging of a 2.6 × 3.4-cm mass in the right mediastinum) were detected during his regular medical examinations. The patient underwent mediastinal mass resection and abdominal mass resection—the pathology being atypical carcinoid (mediastinum) and lipoma (abdominal wall). The patient had a family history of gastrointestinal diseases: his father died of gastric perforation at the age of 65 years, while his elder brother died of stomach cancer. Genetic testing of *MEN1* revealed a heterozygous mutation: c.549G>C (p.W183C, Exon 3). After clinical and genetic diagnosis as MEN1, the patient underwent left inferior and right superior parathyroidectomy—the pathology being carcinoma. His minimum postoperative serum Ca level was 2.39 mmol/L, while the minimum PTH level was 89 pg/mL (decreased 76.6%). After a year of surgery, his serum Ca level increased to 2.93 mmol/L, while the PTH level was 134 pg/mL. Although the parathyroid 99mTc-sestamibi scanning identified a new lesion in the left superior gland, the patient refused to undergo a second surgery. During the 4-year follow-up, the patient experienced only occasional diarrhea, and his serum Ca level ranged between 2.8 and 3.0 mmol/L, while his PTH level ranged between 120 and 150 pg/mL. No new disease associated with MEN1 appeared during follow-up period.

**TABLE 3 |** Treatment and follow-up of MEN1-PC/APN cases in our center.

| Case | Surgery | Pathology | Histopathologic features | Tumor diameter (cm) | Number of lesions | Postoperative | | Follow-up (year) | Recurrence/ metastasis |
|---|---|---|---|---|---|---|---|---|---|
| | | | | | | Ca (mmol/L) | PTH (pg/ml) | | |
| P1* | Total parathyroidectomy + auto plantation | Atypical adenoma (right superior and right inferior) Hyperplasia (left inferior) | Lobular features, fibrous bands, focal active growth and mitoses | 2.5 | 3 | 2.02 | 120.4 | 1 | No |
| P2 | Left superior and right inferior parathyroidectomy | Atypical adenoma | Active growth, mitoses and thick bands | 2.3 | 2 | 2.24 | 21 | 3 | No |
| P3 | Left inferior and right superior parathyroidectomy | Carcinoma | The cubical or rounded cancer cells are small, stratified in layers as a ridge, focal thick bands, capsular invasion, suspicious vascular invasion, focal oncocytic cells | / | 2 | 2.39 | / | 4 | Recurrence |

*Note: 1. * This patient underwent two times operations. The pathology was adenomas for the first time, and atypical adenomas for the second time. The results in this table are about the second operation.*
*2. Ca (serum calcium): 2.13–2.70 mmol/L. PTH (serum parathyroid hormone): 13–65 pg/mL.*

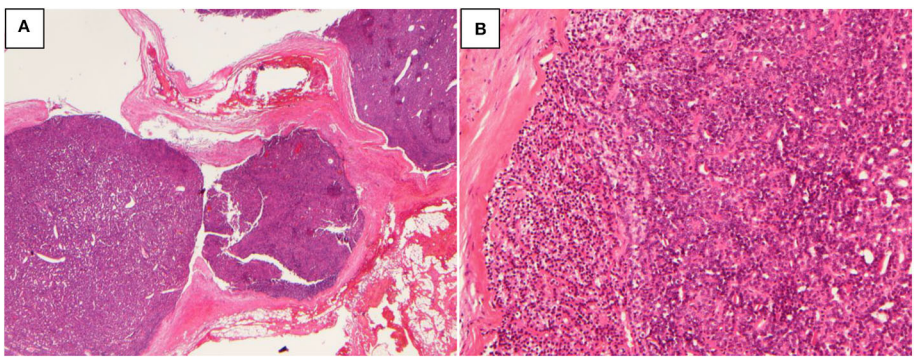


**FIGURE 1 |** Atypical parathyroid neoplasm (patient 1). **(A)** 10× magnification, the tumor grows as multiple nodules with fibrous bands; **(B)** 100× magnification, the tumor cells are arranged in sheets or glands.

## Comparison of the PC/APN Group vs. the Non-PC/APN Group

A total of 18 MEN1-PC cases and 1 MEN1-APN case have been reported previously (3, 5, 6, 11–21). **Table 4** summarizes the general characteristics, biochemical marker, treatments, histopathological features, and *MEN1* genetic testing of the PC/APN group ($n = 21$). Multiple types of gene mutations were detected in the MEN1-PC/APN cases, mainly belonging to missense mutations, followed by nonsense mutations, deletion mutations, insertion mutations, and duplicated mutations. The mean disease onset age of the PC/APN-group patients was 49.7 ± 10.4 years, and the group included 10 women and 11 men. In this group, the mean serum Ca level was 3.15 ± 0.44 mmol/L, and the median PTH level was 327 pg/mL (214.1, 673.1). Both the serum Ca and PTH levels were significantly higher in the PC/APN group than in the non-PC/APN group (Ca: 2.78 mmol/L [2.61, 2.88], PTH: 185.5 pg/mL [108.3, 297.0]; $P = 0.0003$, 0.0034, respectively), while the mean disease onset age was similar between the two groups ($P = 0.065$).

## DISCUSSION

PC is a rare endocrine malignant tumor, with an estimated prevalence rate of 0.005% of all reported cancer cases (22). Until date, <2,000 cases of PC have been reported in the literature (22), which accounts for <1% of all cases of PHPT in the Western countries and among the Caucasian population (23). However, in the Chinese population, carcinoma accounts for 5–7% of PHPT cases (24, 25). The occurrence of parathyroid malignant tendency tumors (PC/APN) in MEN1 is a rare phenomenon, and its prevalence has so far been reported in only 2 centers in the USA. Of the 348 MEN1 patients reported by Mayo Medical

**TABLE 4 |** MEN1-PC/APN reported in the literature and the present study (3, 5, 6, 11–21).

**A**

| Case | Author | Publication year | Sex | Age at diagnosis (years) | Other MEN1 diseases | Ca (mmol/L) | PTH (Normal value) |
|---|---|---|---|---|---|---|---|
| 1 | Wu et al. (11) | 1992 | M | 48 | PIT | 3.15–4.05 | 1.47 nmol/L (0.10–0.46) |
| 2 | Sato et al. (12) | 2000 | F | 51 | N | 2.67 | / |
| 3 | Dionisi et al. (13) | 2002 | M | 35 | PET SL | 3.35 | 75.01 pmol/L (1.1–5.83) |
| 4 | Agha et al. (14) | 2007 | F | 69 | PIT PET | 3.9 | 37.7 pmol/L (0.9–5.4) |
| 5 | Agha et al. (14) | 2007 | M | 32 | PET | 3.7 | 28 pmol/L (0.9–5.4) |
| 6 | Shih et al. (15) | 2009 | F | 53 | PIT PET AA | 3.35 | 143.66 pmol/L (1.59–6.89) |
| 7 | Kalavalapalli et al. (16) | 2010 | F | 40 | PIT PET | 2.65 | 7.2 pmol/L (1.59–6.89) |
| 8 | Del Pozo et al. (17) | 2011 | M | 44 | PET AA | 3.1 | 21.83 pmol/L (0.75–5.67) |
| 9 | Joudele et al. (18) | 2011 | F | 39 | PIT PET AA SL | 3.35 | 34.3 pmol/L (1.18–8.43) |
| 10 | Lee et al. (19) | 2013 | F | 59 | PIT AA | 3.18 | 26.31 pmol/L (1.38–5.73) |
| 11 | Singh Ospina et al. (5) | 2016 | M | 62 | PET AA CT | 3.1 | 14 pmol/L (1–5.2) |
| 12 | Christakis et al. (6) | 2016 | M | 54 | PET CT | 2.63 | 42 pg/mL (9–80) |
| 13 | Christakis et al. (6) | 2016 | M | 55 | PIT PET AA | 3.45 | 673.1 pg/mL (9–80) |
| 14* | Christakis et al. (6) | 2016 | F | 32 | PET CT | 3 | / |
| 15 | Omi et al. (20) | 2018 | M | 40 | PIT PET | 2.7 | 203 pg/mL (16–65) |
| 16 | Cinque et al. (3) | 2017 | M | 61 | PET AA | / | / |
| 17 | Cinque et al. | 2017 | M | 55 | AA | iCa 1.48 (1.12–1.32) | 286 pg/mL (10–65) |
| 18 | Di Meo et al. | 2018 | M | 62 | PET | 2.92 | 391.7 pg/mL |
| 19* | Present study | | F | 51 | PET AA | 2.56 | 2189.4 pg/mL |
| 20* | Present study | | F | 52 | PIT | 3.35 | 708.8 pg/mL |
| 21 | Present study | | M | 51 | PIT PET AA | 2.83 | 380 pg/mL |

**B**

| Case | Surgery | Histopathologic features | Recurrence/metastasis | *MEN1* mutation |
|---|---|---|---|---|
| 1 | Single gland parathyroidectomy | Nests of uniform cells separated by dense collagenous septa and mitotic figures | Neck and sternum metastasis | / |
| 2 | TPTX + autoplantation | Mitoses in parenchymal cells, nuclear polymorphism and capsular invasion | N | c.842delC |
| 3 | First surgery: single gland parathyroidectomy<br>Second surgery: SPTX | Uniform cytology, karyokinesis, fibrous bands, extracapsular, and vascular invasion. | Mediastinal metastasis | / |
| 4 | Resection of 3 parathyroid glands | Dense fibrous capsule, infiltrative cells, mitoses, desmoplasia, fat necrosis, and fibrous banding | Mediastinal metastasis | / |
| 5 | Resection of 2 parathyroid glands | Multiple mitoses with atypical features, fibrous banding, and thick fibrous capsule. | N | / |
| 6 | Surgical resection of 5 benign parathyroid glands plus a combined thyroid/parathyroid mass, followed by radiation therapy | Wide fibrous bands with vascular and perineural invasion and tumor fat necrosis. Focal invasion | N | c.1406_13dup8 |
| 7 | First surgery: single gland parathyroidectomy<br>Second surgery: SPTX | Very cellular parathyroid gland. | Lung metastasis. | / |
| 8 | Resection of 3 parathyroids + Hemithyroidectomy | Dense solid areas are consisting of oncocytic cells, desmoplastic stroma, focal necrosis and atypical cytology. Infiltration of the thyroid gland | Infiltration of the thyroid gland | c.549G>C (p.W183C) |

*(Continued)*

**TABLE 4** | Continued

| B | | | | |
|---|---|---|---|---|
| **Case** | **Surgery** | **Histopathologic features** | **Recurrence/metastasis** | ***MEN1* mutation** |
| 9 | Resection of 2 parathyroids + Hemithyroidectomy + Neck lymphadenectomy | Capsular invasion | Infiltration of the thyroid gland | c.129insA |
| 10 | Single gland parathyroidectomy + Hemithyroidectomy | Abnormal morphology within fibrous connective tissue and capsular invasion | Infiltration of the thyroid gland | / |
| 11 | First surgery: single gland parathyroidectomy Second surgery: single gland parathyroidectomy Third surgery: single gland parathyroidectomy | Histological evidence of local invasion (nerve), fibrous bands and nuclear atypia | Esophageal recurrence | / |
| 12 | First surgery: SPTX Second surgery: TPTX | Lobular features, mitoses, and capsular invasion | Recurrence | c.703G>A (p.E235K) |
| 13 | SPTX | Capsular invasion, fibrosis, nuclear polymorphism | Recurrence | c.1378C>T (p.R460X) |
| 14* | First surgery: resection of 2.5 parathyroids Second surgery: single gland parathyroidectomy | Lobular features and fibrous bands | N | / |
| 15 | First surgery: resection of 3 parathyroids + Hemithyroidectomy + autoplantation Second surgery: Completion thyroidectomy + resection of 1 intrathyroidal mass | Capsular invasion and vascular invasion | Infiltration of the thyroid gland | / |
| 16 | Resection of 2 parathyroids | Capsular invasion | Infiltration of esophageal | c.1252G>A (p.D418N) |
| 17 | Single gland parathyroidectomy | Capsular invasion | Infiltration of surrounding adipose tissue | c.1252G>A (p.D418N) |
| 18 | Resection of 2 parathyroids + Hemithyroidectomy + Neck lymphadenectomy | / | N | / |
| 19* | First surgery: single gland parathyroidectomy, Second surgery: TPTX + autoplantation | Lobular features, fibrous bands, focal active growth, and mitoses | N | c.917T>G (p.L306R) |
| 20* | Resection of 2 parathyroids | Active growth, mitoses, and thick bands | N | c.431T>C (p.F144S) |
| 21 | Resection of 2 parathyroids | The cubical or rounded cancer cells are small, stratified in layers as a ridge, focal thick bands, capsular invasion, suspicious vascular invasion, focal oncocytic cells | Recurrence | c.549G>C (p.W183C) |

*Note: 1. *: MEN1-APN cases.*

*2. PIT, pituitary adenoma; PET, pancreatic endocrine tumor; AA, adrenal adenoma; CT, carcinoid tumor; SL, subcutaneous lipoma; TPTX, total parathyroidectomy; SPTX, subtotal parathyroidectomy; N, no; /, unknown; Ca, serum calcium; PTH, serum parathyroid hormone.*

Center, only 1 (0.28%) had a pathological diagnosis of PC (5). In addition, of the 291 MEN1 patients reported by the MD Anderson Cancer Research Center, only 3 (1%) had parathyroid malignant-tendency tumors (0.7% for PC and 0.3% for APN) (6). In this study, of the 153 MEN1-HPT patients admitted to our center, 2 had APN (1.3%) and 1 had PC (0.7%), with a total prevalence rate of 2.0%. The proportion of both sporadic PC and MEN-PC/APN is relatively high in the Chinese population, probably due to factors such as race and lifestyle (25).

As such, the total number of cases of MEN1-PC/APN patients in the literature and at our center has come to 21. Twelve of these patients have serum Ca level >3.0 mmol/L (**Table 4**) and PTH level about 5-times of the upper limit of the reference range. As compared with that in the non-PC/APN group at our center, the serum Ca and PTH levels of the MEN1 patients were significantly higher in the MEN1-PC/APN group. Singh et al. reported the clinical data of 11 MEN1-PC patients and compared them with those of 510 PC cases unrelated to MEN1 (5). They found no significant differences with respect to the gender, age, and PTH levels between the two groups (5, 26, 27). These results suggest that the clinical features of MEN1-PC/APN are more similar to those of sporadic PC than to those of MEN1-benign

parathyroid tumors. Therefore, MEN1 patients showing a high level of serum Ca and PTH levels should be considered as potential PC/APN cases.

The MEN1-PC/APN patients in the current study presented with a near-normal BMD, which is different from the previous study (20, 21). Because of the small sample size, it could only reflect the individual's condition and might not be consistent with the typical characteristics of MEN1-PC/APN. Eller-Vainicher et al. have reported that MEN1-related PHPT (MHPT) patients showed lower BMD of the lumbar spine and femoral neck than sporadic PHPT (SHPT) patients, even though MHPT patients exhibited milder biochemical presentation than their SHPT counterparts (28). Therefore, increased severity of bone loss in MHPT patients could be partially attributed to the combination of other endocrine dysfunction components, including hypercortisolism, hyperprolactinemia, hypogonadism, and GH deficiency, which also exert negative effects on bone mineralization (29). However, in the previous study of our center, there were no differences between MHPT and SHPT were observed in bone indices as measured using both DXA and high-resolution peripheral computed tomography (HR-pQCT) (4, 30). Therefore, more research is needed in the future to clarify the bone changes in MHPT patients, especially MEN1-PC/APN patients.

Eleven of the 21 MEN1-PC/APN cases carried 9 *MEN1* mutations, 2 of which belonged to the same *MEN1* family (c.1252 G> A, p.D418 N, exon 9). In this study, the mutation of the PC patient was the same as that in a previously reported PC patient (c.549 G> C, p.W183C, exon 3) (19). Two *MEN1* mutations were identified in APN patients (c.917 T> G and c.431T> C). The cases of MEN1-PC/APN were too limited to analyses for the genotype–phenotype relationship, necessitating the analysis of more number of cases for an elaborate study in the future.

The diagnosis of PC and APN depends on the histopathological features, which were relatively complicated and challenging to decipher (21, 31). Presently, the morphological characteristics of PC mainly includes fibrous bands arranged in a trabecular design, mitotic activity, enlarged nucleoli, and capsular and vascular invasion (32). Among all these features, capsular and vascular invasion is considered the most relevant one to indicate tumor recurrence and distant metastasis, and is hence the most reliable evidence for the diagnosis of malignant tumors (33). Moreover, it is believed that immunohistochemical analysis can improve the diagnostic accuracy of PC. The loss of expression of parafibromin combined with those of protein gene product 9.5 (PGP 9. 5) and galectin-3 have also been reported to be common in PC. Moreover, Ki-67 index is usually >5% in malignant tumors. The histopathological characteristics of APN, as a particular pathological type between adenoma and carcinoma, are also not clearly defined. It is generally believed that APN can be diagnosed based on the presentation of some atypical features of carcinoma, except for the lack of the invasion to the neighboring structures (6). Neither of the 2 MEN1-APN patients at our center reported metastases or adhesion with the adjacent tissues, and their pathological findings revealed active growth, mitoses, and thick fibrous bands, but no capsular or vascular invasion. For these 2 patients who were diagnosed with APN, longer term follow-up is required to clarify the biological behavior of their pathology. Interestingly, in case PC is pre-operatively suspected, to prevent the risk of needle tract implantation metastases and the tissue diffusion caused by capsule rupture, fine needle aspiration should be avoided (34, 35).

The surgical removal of abnormally overactive parathyroid glands in MEN1-HPT patients is a definitive treatment (2). As quite a few MEN1-HPT cases involved multiple glands and were susceptible to relapse, the Clinical Practice Guidelines for MEN1 recommend subtotal parathyroidectomy (SPTX, removing at least 3.5 glands) as the first choice of treatment (2). Total parathyroidectomy (TPTX) with auto-plantation can be considered in case of extensive parathyroid lesions. The incidence of hypoparathyroidism after the local resection of parathyroid was reduced in a previous study; however, the recurrence rate was 3.11-times more than that of SPTX or TPTX (36). There is no guideline available for MEN1-PC/APN, considering its relatively rare nature. All the 21 cases of MEN1-PC/APN so far have undergone 1–3 surgeries, and 1 of these even received postoperative radiation therapy for thyroid invasion. Only 1 patient undertook TPTX as the first operation and 2 patients as the second operation, and, in both the situations, no recurrence or metastasis was recorded after TPTX. Seven patients underwent a single gland parathyroidectomy as the first operation, 5 of whom had metastases (of the neck and sternum, mediastinum, lung, thyroid, and esophagus), and 1 of them had a recurrence. All of the metastases/recurrence patients had a second operation, except for 1 who had no report of a subsequent treatment. It is important for the surgeon to be aware of the appearance of PC during surgery. However, PC/APN is often not conclusively identified even during the operation. Based on the accumulated experiences, if MEN1-PC/APN is pre-operatively suspected, it is recommended that a surgical approach be selected in accordance with the nature of PC. Clayman et al. and Shane et al. suggested the following surgery plan: (1) Completely remove the lesion and its adhesion tissues (including the anterior cervical muscle group, esophageal muscle group, and recurrent laryngeal nerve) to avoid tumor rupture and overflowing; (2) also remove the ipsilateral thyroid lobe, paratracheal lymph node, and superior mediastinal lymph node; and (3) if the evidence suggests the involvement of central lymph nodes, the VI level of cervical lymphadenectomy should be performed (37, 38).

More importantly, the management of postoperative patients remains challenging. Both, the recurrence of PC/APN and the proliferative growth of the remaining glands can cause postoperative hypercalcemia. Therefore, if postoperative hypercalcemia is identified, the reason for its occurrence should be clarified immediately. Due to the proliferative growth of the remaining glands, it is suggested that only limited resections be performed via minimally invasive surgery (6). However, if there is sufficient evidence supporting possible PC/APN recurrence in the surrounding tissues, the approach should be open and involving adequate exposure (6).

The authors acknowledge that this study has some limitations. For instance, this being a retrospective study conducted in a single center, there is a possibility of information and confounding biases attributable to the small sample size and overlooked/missed data. However, considering the rarity of MEN1-PC/APN, even a small cohort has the potential to provide valuable data and experience to clinicians.

In summary, MEN1-PC/APN is a relatively rare disease, with an overall prevalence rate of only 2.0% in a Chinese MEN1-HPT cohort. This rate is slightly greater in Chinese population than that reported for Caucasian population. The serum Ca and PTH levels in patients with MEN1-PC/APN are usually greater than in those with MEN1-associated benign parathyroid tumors. However, MEN1-PC/APN is often not conclusively identified pre-operatively and the diagnosis based upon pathology most of the times. If this disease is pre-operatively suspected, surgical treatment is best recommended following PC.

## DATA AVAILABILITY STATEMENT

All datasets presented in this study are included in the article/supplementary material.

## ETHICS STATEMENT

The studies involving human participants were reviewed and approved by the Ethics Committee of PUMCH. Written informed consent was obtained from the individuals for the publication of any potentially identifiable images or data included in this article (No patient was under the age of 16, or otherwise legally or medically unable to provide written informed consent).

## AUTHOR CONTRIBUTIONS

AS, YY, MN, and OW are involved in experimental and analysis. AS, OW, and XX are involved in analysis. SL is involved in conception, analysis, and writing. All authors contributed to the article and approved the submitted version.

## FUNDING

This work was supported by the Chinese Academy of Medical Sciences Innovation Fund for Medical Sciences (CIFMS) 2017-I2M-1-001, National Natural Science Foundation of China (No. 81100559).

## REFERENCES

1. Brandi ML, Gagel RF, Angeli A, Bilezikian JP, Beck-Peccoz P, Bordi C, et al. Guidelines for diagnosis and therapy of MEN type 1 and type 2. *J Clin Endocrinol Metab.* (2001) 86:5658–71. doi: 10.1210/jcem.86.12.8070
2. Thakker RV, Newey PJ, Walls GV, Bilezikian J, Dralle H, Ebeling PR, et al. Clinical practice guidelines for multiple endocrine neoplasia type 1 (MEN1). *J Clin Endocrinol Metab.* (2012) 97:2990–3011. doi: 10.1210/jc.2012-1230
3. Cinque L, Sparaneo A, Cetani F, Coco M, Clemente C, Chetta M, et al. Novel association of MEN1 gene mutations with parathyroid carcinoma. *Oncol Lett.* (2017) 14:23–30. doi: 10.3892/ol.2017.6162
4. Kong J, Wang O, Nie M, Shi J, Hu Y, Jiang Y, et al. Clinical and Genetic Analysis of Multiple Endocrine Neoplasia Type 1-Related Primary Hyperparathyroidism in Chinese. *PLoS ONE.* (2016) 11:e0166634. doi: 10.1371/journal.pone.0166634
5. Singh Ospina N, Sebo TJ, Thompson GB, Clarke BL, Young WFJ. Prevalence of parathyroid carcinoma in 348 patients with multiple endocrine neoplasia type 1 - case report and review of the literature. *Clin Endocrinol.* (2016) 84:244–9. doi: 10.1111/cen.12714
6. Christakis I, Busaidy NL, Cote GJ, Williams MD, Hyde SM, Silva FA, et al. Parathyroid carcinoma and atypical parathyroid neoplasms in MEN1 patients; a clinico-pathologic challenge. The MD Anderson case series and review of the literature. *Int J Surg.* (2016) 31:10–6. doi: 10.1016/j.ijsu.2016.05.035
7. Ritchie LD, Fung EB, Halloran BP, Turnlund JR, Van Loan MD, Cann CE, et al. A longitudinal study of calcium homeostasis during human pregnancy and lactation and after resumption of menses. *Am J Clin Nutr.* (1998) 67:693–701. doi: 10.1093/ajcn/67.4.693
8. Ahmad S, Kuraganti G, Steenkamp D. Hypercalcemic crisis: a clinical review. *Am J Med.* (2015) 128:239–45. doi: 10.1016/j.amjmed.2014.09.030
9. Lou I, Schneider DF, Sippel RS, Chen H, Elfenbein DM. The changing pattern of diagnosing primary hyperparathyroidism in young patients. *Am J Surg.* (2017) 213:146–50. doi: 10.1016/j.amjsurg.2016.03.019
10. Song A, Wang W, Chen S, Wang Y, Liu S, Nie M, et al. Primary hyperparathyroidism during pregnancy: a case series of 8 patients. *Endocr Pract.* (2019) 25:1127–36. doi: 10.4158/EP-2019-0035
11. Wu CW, Huang CI, Tsai ST, Chiang H, Lui WY, P'Eng FK. Parathyroid carcinoma in a patient with non-secretory pituitary tumor: a variant of multiple endocrine neoplasia type-I? *Eur J Surg Oncol.* (1992) 18:517–20.
12. Sato M, Miyauchi A, Namihira H, Bhuiyan MMR, Imachi H, Murao K, et al. A newly recognized germline mutation of MEN1 gene identified in a patient with parathyroid adenoma and carcinoma. *Endocrine.* (2000) 12:223–6. doi: 10.1385/ENDO:12:3:223
13. Dionisi S, Minisola S, Pepe J, De Geronimo S, Paglia F, Memeo L, et al. Concurrent parathyroid adenomas and carcinoma in the setting of multiple endocrine neoplasia type 1: presentation as hypercalcemic crisis. *Mayo Clin Proc.* (2002) 77:866–9. doi: 10.4065/77.8.866
14. Agha A, Carpenter R, Bhattacharya S, Edmonson SJ, Carlsen E, Monson JP. Parathyroid carcinoma in multiple endocrine neoplasia type 1 (MEN1) syndrome: Two case reports of an unrecognised entity. *J Endocrinol Investig.* (2007) 30:145–9. doi: 10.1007/BF03347413
15. Shih RYW, Fackler S, Maturo S, True MW, Brennan J, Wells D. Parathyroid carcinoma in multiple endocrine neoplasia type 1 with a classic germline mutation. *Endocrine Pract.* (2009) 15:567–72. doi: 10.4158/EP09045.CRR1
16. Kalavalapalli S, Talapatra I, O'Connell IPM. A complex case of multiple endocrine neoplasia type 1 with metastatic parathyroid carcinoma. *Central European Journal of Medicine.* (2010) 5:53–58. doi: 10.2478/s11536-009-0116-4
17. Del Pozo C, García-Pascual L, Balsells M, Barahona M, Veloso E, González C, et al. Parathyroid carcinoma in multiple endocrine neoplasia type 1. Case report and review of the literature. *Hormones.* (2011) 10:326–31. doi: 10.14310/horm.2002.1325
18. Juodele L, Serapinas D, Sabaliauskas G, Krasauskiene A, Krasauskas V, Verkauskiene R, et al. Carcinoma of two parathyroid glands caused by a novel MEN1 gene mutation - a rare feature of the MEN 1 syndrome. *Medicina.* (2011) 47:635–9. doi: 10.3390/medicina47110092
19. Lee KM, Kim EJ, Choi WS, Park WS, Kim SW. Intrathyroidal parathyroid carcinoma mimicking a thyroid nodule in a MEN type 1 patient. *J Clin Ultrasound.* (2014) 42:212–4. doi: 10.1002/jcu.22090
20. Omi Y, Horiuchi K, Haniu K, Tokura M, Nagai E, Isozaki O, et al. Parathyroid carcinoma occurred in two glands in multiple endocrine neoplasia 1: a report on a rare case. *Endocr J.* (2018) 65:245–52. doi: 10.1507/endocrj.EJ17-0409
21. Di Meo G, Sgaramella LI, Ferraro V, Prete FP, Gurrado A, Testini M. Parathyroid carcinoma in multiple endocrine neoplasm type 1 syndrome: case report and systematic literature review. *Clin Exp Med.* (2018) 18:585–93. doi: 10.1007/s10238-018-0512-7

22. Ferraro V, Sgaramella LI, Di Meo G, Prete FP, Logoluso F, Minerva F, et al. Current concepts in parathyroid carcinoma: a single Centre experience. *BMC Endocr Disord.* (2019) 19(Suppl. 1):46. doi: 10.1186/s12902-019-0368-1
23. Kearns AE, Thompson GB. Medical and surgical management of hyperparathyroidism. *Mayo Clin Proc.* (2002) 77:87–91. doi: 10.4065/77.1.87
24. DeLellis RA, Mazzaglia P, Mangray S. Primary hyperparathyroidism: a current perspective. *Arch Pathol Lab Med.* (2008) 132:1251–62. doi: 10.1043/1543-2165(2008)132[1251:PHACP]2.0.CO;2
25. Zhao L, Liu JM, He XY, Zhao HY, Sun LH, Tao B, et al. The changing clinical patterns of primary hyperparathyroidism in Chinese patients: data from 2000 to 2010 in a single clinical center. *J Clin Endocrinol Metab.* (2013) 98:721–8. doi: 10.1210/jc.2012-2914
26. Lee PK, Jarosek SL, Virnig BA, Evasovich M, Tuttle TM. Trends in the incidence and treatment of parathyroid cancer in the United States. *Cancer Am Cancer Soc.* (2007) 109:1736–41. doi: 10.1002/cncr.22599
27. Hundahl SA, Fleming ID, Fremgen AM, Menck HR. Two hundred eighty-six cases of parathyroid carcinoma treated in the US. between 1985-1995: a National Cancer Data Base Report. The American College of Surgeons Commission on Cancer and the American Cancer Society. *Cancer Am Cancer Soc.* (1999) 86:538–44. doi: 10.1002/(SICI)1097-0142(19990801)86:3<538::AID-CNCR25>3.0.CO;2-K
28. Eller-Vainicher C, Chiodini I, Battista C, Viti R, Mascia ML, Massironi S, et al. Sporadic and MEN1-related primary hyperparathyroidism: differences in clinical expression and severity. *J Bone Miner Res.* (2009) 24:1404–10. doi: 10.1359/jbmr.090304
29. Kann PH, Bartsch D, Langer P, Waldmann J, Hadji P, Pfutzner A, et al. Peripheral bone mineral density in correlation to disease-related predisposing conditions in patients with multiple endocrine neoplasia type 1. *J Endocrinol Invest.* (2012) 35:573–9. doi: 10.3275/7880
30. Wang W, Nie M, Jiang Y, Li M, Meng X, Xing X, et al. Impaired geometry, volumetric density, and microstructure of cortical and trabecular bone assessed by HR-pQCT in both sporadic and MEN1-related primary hyperparathyroidism. *Osteoporos Int.* (2020) 31:165–73. doi: 10.1007/s00198-019-05186-1
31. Favia G, Lumachi F, Polistina F, D'Amico DF. Parathyroid carcinoma: sixteen new cases and suggestions for correct management. *World J Surg.* (1998) 22:1225–30. doi: 10.1007/s002689900549
32. LiVolsi VA, Montone KT, Baloch ZN. Parathyroid: the pathology of hyperparathyroidism. *Surg Pathol Clin.* (2014) 7:515–31. doi: 10.1016/j.path.2014.08.004
33. Smith JF, Coombs RR. Histological diagnosis of carcinoma of the parathyroid gland. *J Clin Pathol.* (1984) 37:1370–8. doi: 10.1136/jcp.37.12.1370
34. Wei CH, Harari A. Parathyroid carcinoma: update and guidelines for management. *Curr Treat Options Oncol.* (2012) 13:11–23. doi: 10.1007/s11864-011-0171-3
35. Spinelli C, Bonadio AG, Berti P, Materazzi G, Miccoli P. Cutaneous spreading of parathyroid carcinoma after fine needle aspiration cytology. *J Endocrinol Invest.* (2000) 23:255–7. doi: 10.1007/BF03343718
36. Schreinemakers JM, Pieterman CR, Scholten A, Vriens MR, Valk GD, Rinkes IH. The optimal surgical treatment for primary hyperparathyroidism in MEN1 patients: a systematic review. *World J Surg.* (2011) 35:1993–2005. doi: 10.1007/s00268-011-1068-9
37. Clayman GL, Gonzalez HE, El-Naggar A, Vassilopoulou-Sellin R. Parathyroid carcinoma: evaluation and interdisciplinary management. *Cancer Am Cancer Soc.* (2004) 100:900–5. doi: 10.1002/cncr.20089
38. Shane E. Clinical review 122: Parathyroid carcinoma. *J Clin Endocrinol Metab.* (2001) 86:485–93. doi: 10.1210/jcem.86.2.7207


**Conflict of Interest:** The authors declare that the research was conducted in the absence of any commercial or financial relationships that could be construed as a potential conflict of interest.

frontiers in Endocrinology

ORIGINAL RESEARCH
published: 24 February 2021
doi: 10.3389/fendo.2021.624102

# Clinical Prognostic Factors in Patients With Metastatic Adrenocortical Carcinoma Treated With Second Line Gemcitabine Plus Capecitabine Chemotherapy

*Salvatore Grisanti[1], Deborah Cosentini[1], Marta Laganà[1], Alessandra Morandi[1], Barbara Lazzari[1], Laura Ferrari[1], Alberto Dalla Volta[1], Roberta Ambrosini[2], Vittorio Domenico Ferrari[1], Sandra Sigala[3] and Alfredo Berruti[1]**

[1] Medical Oncology Unit, Department of Medical and Surgical Specialties, Radiological Sciences and Public Health, University of Brescia at ASST Spedali Civili, Brescia, Italy, [2] Radiology Unit, Azienda Socio Sanitaria Territoriale (ASST) Spedali Civili, Brescia, Italy, [3] Section of Pharmacology, Department of Molecular and Translational Medicine, University of Brescia, Brescia, Italy

Gemcitabine plus Capecitabine (Gem/Cape) is a frequently adopted second line chemotherapy for metastatic adrenocortical carcinoma (ACC), but only a minority of patients is destined to obtain a clinical benefit. The identification of baseline predictive factors of efficacy is relevant. We retrospectively analyzed clinical data from 50 consecutive patients with metastatic progressing ACC treated between 2011 and 2019. Patients received intravenous Gemcitabine and oral Capecitabine on a metronomic schedule. Previous mitotane therapy was maintained. Clinical benefit (partial response + stable disease) at 4 months was 30%, median progression-free survival (PFS) and disease-specific survival (DSS) from Gem/Cape start were 3 and 8 months, respectively. Among clinical variables evaluated before the start of Gem/Cape, presence of ECOG performance status ≥1 [HR 6.93 95% confidence interval (CI) 0.03–0.54, p.004] and neutrophil-to-lymphocyte ratio (NLR) ≥5 [HR 3.88, 95% (CI) 0.81–0.90, p.003] were independent indicators of poor PFS at multivariate analysis. Conversely, surgery of primary tumor, the presence of lung or lymph-node metastases, blood mitotane level, anemia, and the Advanced Lung cancer Inflammation index (ALI) failed to be independently associated. This study confirms that the Gem/Cape schedule is modestly active in heavily pretreated ACC patients (28% received at least two previous chemotherapy lines). NLR and performance status (PS) are easily available clinical parameters that are helpful to identify patients not likely to derive significant advantage from Gem/Cape chemotherapy.

**Keywords: adrenocortical carcinoma, gemcitabine, capecitabine, prognostic factor, chemotherapy**

OPEN ACCESS

***Edited by:***
*Enzo Lalli, UMR7275 Institut de pharmacologie molèculaire et cellulaire (IPMC), France*

***Reviewed by:***
*Cristina L. Ronchi, University of Birmingham, United Kingdom*
*Alessandra Mosca, Azienda Ospedaliero Universitaria Maggiore della Carità, Italy*

***Correspondence:**
*Alfredo Berruti*
*alfredo.berruti@unibs.it*

***Specialty section:***
*This article was submitted to Cancer Endocrinology, a section of the journal Frontiers in Endocrinology*

***Received:*** *30 October 2020*
***Accepted:*** *11 January 2021*
***Published:*** *24 February 2021*

***Citation:***
*Grisanti S, Cosentini D, Laganà M, Morandi A, Lazzari B, Ferrari L, Volta AD, Ambrosini R, Ferrari VD, Sigala S and Berruti A (2021) Clinical Prognostic Factors in Patients With Metastatic Adrenocortical Carcinoma Treated With Second Line Gemcitabine Plus Capecitabine Chemotherapy. Front. Endocrinol. 12:624102. doi: 10.3389/fendo.2021.624102*

## INTRODUCTION

The clinical management of patients with metastatic adrenocortical carcinoma (ACC) remains a challenging issue for a number of reasons. First, while there are patients with a relatively indolent disease that can be controlled by either mitotane monotherapy or locoregional treatments, the majority of cases displays more aggressive and highly proliferating disease that requires the adoption of systemic chemotherapy (1, 2). Second, according to the results of the FIRM-ACT trial the current first line chemotherapy for locally advanced or metastatic ACC, namely the EDP-M schedule, offers a median progression-free survival (PFS) of 5.1 months (3). Although there is a small proportion of long lasting responder patients, this median PFS indicates that approximately 50% of patients will require additional treatments in the 6 months following EDP failure (4). Third, the EDP regimen administration is associated to manageable but consistent toxicities which causes not all patients can be treated with full dose intensity because of age, performance status (PS), or comorbidity limitations. These patients will require less intensive, alternative schedules following EDP. Fourth, because of its rarity, ACC is an orphan cancer in terms of new drugs selection and thus, very few options exist after failure of standard first-line chemotherapy and the reported overall response rate and duration of response are exceedingly dismal (5–8).

In 2005, based on evidence derived from single case reports, an international consensus conference suggested to incorporate gemcitabine [20,20-difluorodeoxycytidine (Gem)] as a promising agent in the treatment of ACC (9). In a phase 2 clinical trial, 28 patients with advanced ACC were treated with Gem combined with fluoropyrimidines [capecitabine (Cape) or 5-fluorouracil (5FU)] (10). In this pilot study, the overall response rate (CR+PR) was 7%, the disease control rate (CR +PR+SD) was 46.3% and the median progression-free survival was 5.3 months. In a retrospective analysis of a German and Italian series of 145 advanced ACC patients treated outside a clinical trial, Gem/Cape chemotherapy was associated with a disease control rate in approximately 30% of patients and a clinical benefit (disease stabilization or response to therapy for ≥4 months) in approximately 20% of patients (11). These results confirmed that this regimen was moderately active and well tolerated in the real-world practice. To date there is a general consensus in using Gem-Cape chemotherapy as a second line approach in ACC patients after failure of EDP (1).

A central issue in the management of patients with advanced cancers is the preservation of quality of life (QOL) (12). Thus, the prescription of a palliative treatment should be guided by factors enabling the clinician to pre-select the potential responder patient avoiding unnecessary toxicity to the others (13, 14). However, while several studies focused on identification of clinical and pathological indicators (such as the GRAS parameters in the modified ENSAT classification) as adjunct prognostic factors in the setting of advanced ACC (15), less attention has been paid to select patients that have a realistic chance of obtaining benefit from chemotherapy. To address this issue, we analyzed a series of patients with advanced ACC treated with Gem and Cape with the aim of identifying clinical characteristics and laboratory parameters that can easily be found in the daily clinical practice, to be used as predictive factors of efficacy.

## MATERIALS AND METHODS

### Study Design, Patients Selection, and Treatment

This is a retrospective analysis of consecutive patients treated outside a clinical trial at the Medical Oncology Department of the Spedali Civili of Brescia. The study was approved by the Institutional Ethical Review Board (ID: NP 3776/2019) and conducted in accordance with the principles of the Declaration of Helsinki. The decision of starting Gem/Cape chemotherapy was taken within the ACC tumor board discussion for each single case. Patients were included in this retrospective analysis with the following main inclusion criteria: histologically confirmed diagnosis of ACC; clinical, biochemical, and radiological evidence of disease progressing after first–line treatment and not eligible of loco-regional therapies; measurable disease; life expectancy of at least 3 months, age ≥18 years; ECOG performance status (ECOG PS) 0-2; adequate organ function; ability to sign an informed consent.

Main exclusion criteria were: previous treatment with gemcitabine and/or fluoropyrimidines; known hypersensitivity to gemcitabine and/or fluoropyrimidines; history of previous neoplasm within 5 years. The primary objective was to identify clinical and biochemical indicators predictive of response to therapy in terms of progression-free survival (PFS). Secondary endpoints were best objective response, toxicity and disease-specific survival (DSS) analysis from Gem/Cape chemotherapy.

Clinical and biochemical parameters were calculated both at initial diagnosis of ACC and before initiation of Gem/Cape chemotherapy. They included: sex, age, medical history pre- and post-Gemcitabine treatment, ECOG performance status (PS), and the Charlson's Comorbidity Index (CCI) score (16), routine laboratory tests measured at baseline including the mitotane plasma levels, absolute count of white blood cells (WBC), relative counts of neutrophils and lymphocytes, hemoglobin value, platelets absolute count, and the neutrophils-to-lymphocytes ratio (NLR) categorized as <5 or ≥5, derived NLR {dNLR: calculated as [neutrophil count/(leucocyte-neutrophil count)]} (17).

In addition, we assessed the Lung Immune Prognostic Index (LIPI index) which combined the dNLR and LDH levels and categorized patients into three prognostic subsets based on the following cutoffs: dNLR ≤ 3 and LDH ≤UNL; dNLR ≥3 or LDH≥ULN; dNLR≥3 and LDH≥ULN which defined good, intermediate, poor prognostic groups, respectively (17).

The Advanced Lung cancer Inflammation index (ALI index) was calculated as BMI × ALB/NLR. Patients were divided into the low-ALI and high-ALI groups according to the median value (18).

The treatment schedule was based on the regimen previously published by Sperone et al. (10). Briefly, Gem was administered

at 800 mg/sqm over 30 min. intravenous infusion on days 1 and 8 every 21 days, and oral Cape was given at 1500 mg/daily continuously. All patients received concomitant mitotane with the goal of maintaining the 14–20 mg/L target plasma concentration. Chemotherapy was continued until disease progression or unacceptable toxicity. Dose reductions or withdrawal of one drug was permitted according to the clinician's decision.

## Evaluation of Response and Toxicity

Minimum work-up at baseline included physical examination, biochemical and hormonal assessment, and tumor-parameters assessed by imaging techniques not older than 6 weeks. Imaging included total body computed tomography (CT) or FdG-positron emission tomography (CT/PET) or regional nuclear magnetic resonance (MNR). Biochemical and hormonal profiles were assessed at the beginning of each cycle. Radiological assessment was repeated every 12 weeks with the same imaging parameter technique and evaluation of response was classified according to RECISTv1.1 criteria as complete response (CR), partial response (PR), stable disease (SD), or progressive disease (PD). Clinical benefit was defined as stable disease (or better response) lasting at least 4 months. Toxicities were registered during treatment and follow-up and were graded using the Common Terminology Criteria for Adverse Events (CTCAE), version 4.03.

## Statistical Analysis

Descriptive statistics were used to analyze clinical indicators. Continuous variables were categorized by identification of optimal cut-off values. Associations between categorical variables were assessed by two-sided chi-square or Fisher tests as appropriate. PFS and DSS were calculated as the time elapsed from start of Gem/Cape to the first radiological evidence of PD or to the date of death related to ACC, respectively. Survival curves were generated with the Kaplan–Meier method and compared with the log-rank test (Mantel-Cox). Clinical variables with a potential prognostic value at univariate Cox regression (enter level $p \leq .05$) were included in the multivariate Cox model. Results are given as hazard ratio (HR) with 95% confidence intervals (95% CIs). A Bonferroni correction was applied in the multivariate Cox model to correct for multiple comparisons with a small sample size and the new significance level was set at p.006. For all other tests the statistical significance was conventionally set at $p < .05$. All analyses were performed with Statistical Package for Social Science (SPSS Software, Version 23.0, IBM SPSS Statistics, Chicago, IL, USA).

# RESULTS

## Patients Clinicopathological Characteristics, Treatment, and Toxicity

From January 2011 to December 2019, 50 patients with advanced ACC were sequentially treated with Gem/Cape chemotherapy. Patients characteristics are summarized in **Table 1**. At initial diagnosis 50% of the patients had an ENSAT stage IV tumor and 52% had hormonal hypersecretion, respectively. The majority (84%) of patients underwent surgery that was radical (R0) in less than 30% of them. Median Ki67 proliferation index was 25%. All patients received postoperative mitotane therapy. Disease progression/relapse occurred in both visceral and non-visceral anatomical sites in 64% of patients and the most frequent anatomic sites were the lungs, liver, extra-liver abdominal sites and lymphnodes. The most frequent metastatic pattern was represented by lung, liver and abdominal lesions in 26% of patients. The vast majority of patients (70%) had received at least one previous line of chemotherapy for advanced disease and the median time from diagnosis to Gem/Cape chemotherapy was 19 months. Before starting Gem/Cape, more than 60% of the patients had disease-related symptoms (ECOG PS ≥1) and displayed a Charlson's Comorbidity Index score≥5 indicating the presence of at least 3 significant comorbidities. Ten (20%) patients displayed clinical signs of steroid excess. Mitotane levels were available for 45 (90%) patients and 64% of them had a mitotane concentration below the therapeutic range. Laboratory abnormalities showed anemia (Hb <12 g/dl) in 61% of patients while total leukocytes and platelets were within normal range in 27 (66%) and 23 (64%) of cases, respectively. NLR above 5 was observed in 21 (42%) cases. Eight patients (16%) without baseline LDH or dNLR were excluded from the LIPI index calculation. Among the 42 (84%) evaluable patients, 16 (38%) had good LIPI, and 25 (59%) had intermediate-poor LIPI. We additionally calculated the ALI index in the 50 patients in which NLR, BMI, and ALB were available: 25 patients (50%) had an ALI index below-equal the median value (40), the remaining 25 had greater values. No other biochemical parameters are reported because of missing values in >50% of cases.

All patients received combination chemotherapy with both Gem and Cape. A median number of 3 cycles (range 1–17) was administered and the median dose intensity (median mg/sqm administered/mg/sqm calculated per cycle) of Gem and Cape was 93 and 100%, respectively. Treatment was overall well tolerated with all grades asthenia in 33% of patients and grade 3–4 adverse events being reported in less than 10% of patients. In this subgroup of patients, CTCAE grade 3–4 anemia and neutropenia were the most frequent adverse events.

## Response to Therapy and Survival Analysis

All patients were eligible for response and survival. After a median follow-up of 8 months (last update December 2019), all patients but one had progressed with a median PFS of 3 months (range 0.5–23.5) and 45/50 (90%) were dead with a median DSS of 8 months (range 0.5–72) (**Figure 1**). No complete responses were observed. Analysis of best response included 7 (14%) partial responses and 12 (24%) stable diseases. In a landmark analysis at 4 months from Gem/Cape start, 30% of patients obtained a clinical benefit (PR+SD) (**Table 2**). Clinical benefit was however transient and 18% and 4% of patients were progression-free at 6 and 12 months, respectively. After progression, 17 (34%) and 7 (14%) patients further received 1 and ≥2 lines of chemotherapy, respectively.

**TABLE 1** | Patients clinical and pathological characteristics at initial diagnosis and at start of Gem/Cape chemotherapy.

| Characteristic | N. ACC patients (%) |
|---|---|
| Median age (range), years | 49 (16–68) |
| <50 | 26/50 (52) |
| ≥50 | 24/50 (48) |
| Sex | |
| Male | 22/50 (44) |
| Female | 28/50 (56) |
| Initial ENSAT tumor stage: | |
| I-II | 16/50 (32) |
| III | 9/50 (18) |
| IV | 25/50 (50) |
| Hormone secretion: | |
| No secretion | 24/50 (48) |
| Hormone hypersecretion | 26/50 (52) |
| Glucocorticoids | 22/26 (85) |
| Androgens | 3/26 (11) |
| Aldosterone | 1/26 (4) |
| Pathology | |
| Median Ki67 (range), % | 25 (5–85) |
| Median Weiss score (range) | 6 (3–9) |
| Surgery and resection status: | |
| No surgery | 8/50 (16) |
| R0 | 12/42 (28) |
| RX | 4/42 (10) |
| R1/R2 | 26/42 (62) |
| Number of previous chemotherapy lines | 36/50 (72) |
| 1 | |
| ≥2 | 14/50 (28) |
| Time from ACC diagnosis to Gem/Cape start | |
| <19 | 24/47 (51) |
| ≥19 | 23/47 (49) |
| Types of previous chemotherapy lines | |
| Cisplatin-based | 31/50 (62) |
| Anthracyclines-based | 30/50 (60) |
| Streptozotocin/Temozolomide | 4/50 (8) |
| Mitotane concentration during Gem/Cape chemotherapy | |
| <14 mg/L | 29/45 (64) |
| 14–20 mg/L | 16/45 (36) |
| Unknown | 5/50 (18) |
| ECOG performance status at Gem/Cape start | |
| 0 | 19/50 (38) |
| ≥1 | 31/50 (62) |
| Charlson's Comorbidity Index (CCI) at Gem/Cape start | |
| Score 0–2 | 14/45 (31) |
| Score 3–5 | 6/45 (13) |
| Score ≥ 6 | 25/45 (56) |
| Unknown | 5/50 (10) |
| Metastatic sites at Gem/Cape start | |
| Lung | 38/50 (76) |
| Abdomen/peritoneum | 35/50 (70) |
| Liver | 30/50 (60) |
| Lymphnodes | 17/50 (34) |
| Bone | 2/50 (4) |
| White blood cells (WBC) at Gem/Cape start | |
| $<4 \times 10^3/\mu l$ | 9/41 (22) |
| $4–10.8 \times 10^3/\mu l$ | 27/41 (66) |
| $>10.8 \times 10^3/\mu l$ | 5/41 (12) |
| Unknown | 9/50 (18) |
| Lactate dehydrogenase (LDH) at Gem/Cape start | |
| Median LDH (range) | 220 (123-1867) |
| ≤225 U/L | 21/42 (50) |
| >225 U/L | 21/42 (50) |
| Unknown | 8/50 (16) |
| Albumin (ALB) at Gem/Cape start | |
| Median ALB (range) | 3.5 (2–4.6) |
| ≤3.5 g/dl | 28/50 (56) |
| >3.5 g/dl | 22/50 (44) |
| Body mass index (BMI) | |
| Median ALB (range) | 23.5 (17.8–34.4) |
| ≤23.5 | 26/50 (52) |
| >23.5 | 24/50 (48) |
| Hemoglobin (Hb) at Gem/Cape start | |
| ≤12 g/dl | 25/41 (61) |
| >12 g/dl | 16/41 (39) |
| Unknown | 9/50 (18) |
| Platelet (PLT) at Gem/Cape start | |
| $<130 \times 10^3/\mu l$ | 1/36 (3) |
| $130 – 400 \times 10^3/\mu l$ | 23/36 (64) |
| $>400 \times 10^3/\mu l$ | 12/36 (33) |
| Unknown | 14/50 (28) |

## Analysis of Predictive and Prognostic Factors

Two sets of variables were evaluated: traditional prognostic clinico-pathological variables (including ENSAT stage, Ki67, resection status, hormonal hypersecretion) at initial diagnosis and patients clinical characteristics before the start of Gem/Cape chemotherapy (including ECOG PS, comorbidities, pattern of metastases distribution) and laboratory abnormalities. All sets of variables were tested for their predictive and prognostic value in terms of PFS and DSS. Included variables are summarized in **Tables 3** and **4**. Among the variables at initial diagnosis only no-frontline surgery of the primary tumor resulted predictive of shorter PFS during Gem/Cape therapy at univariate analysis (p.014). Clinical variables evaluated before the start of Gem/Cape associated with a higher risk of progression at univariate analysis included: ECOG PS ≥1 (p <.0005), lung metastases (p.040), lymph-node metastases (p.015), neutrophils >70% (p.015), lymphocytes <20% (p.009), neutrophils/lymphocytes ratio (NLR) ≥5 (p.015), Hb <12 g/dl (p.017), ALI index lower than 40 (median value) (p.038), and low mitotane concentrations during Gem/Cape chemotherapy (p.036). At multivariate analysis, no-frontline surgery (HR 2.67, 95% CI 1.00–7.10, p.049), presence of symptoms and pain (ECOG PS ≥1) (HR 6.93, 95% CI 1.86–25.79, p.004) and NLR >5 (HR 3.88, 95% CI 1.57–9.54, p.003) remained significant as independent predictors of poorer PFS. Finally, after Bonferroni correction only ECOG PS ≥1 and NLR >5 maintained a statistical significance (p <.006). Mitotane plasma concentrations and the metastatic sites pattern did not show a prognostic value either for PFS or for DSS. When looking at variables with potential impact on DSS, ENSAT stage IV at initial diagnosis (p.049), time-to Gem/Cape start <19 months (p.008), ECOG PS ≥1 (p.012), and low mitotane concentrations during Gem/Cape chemotherapy (p.037) were significant at univariate analysis. However, none of these covariates maintained a statistical significance at multivariate analysis.

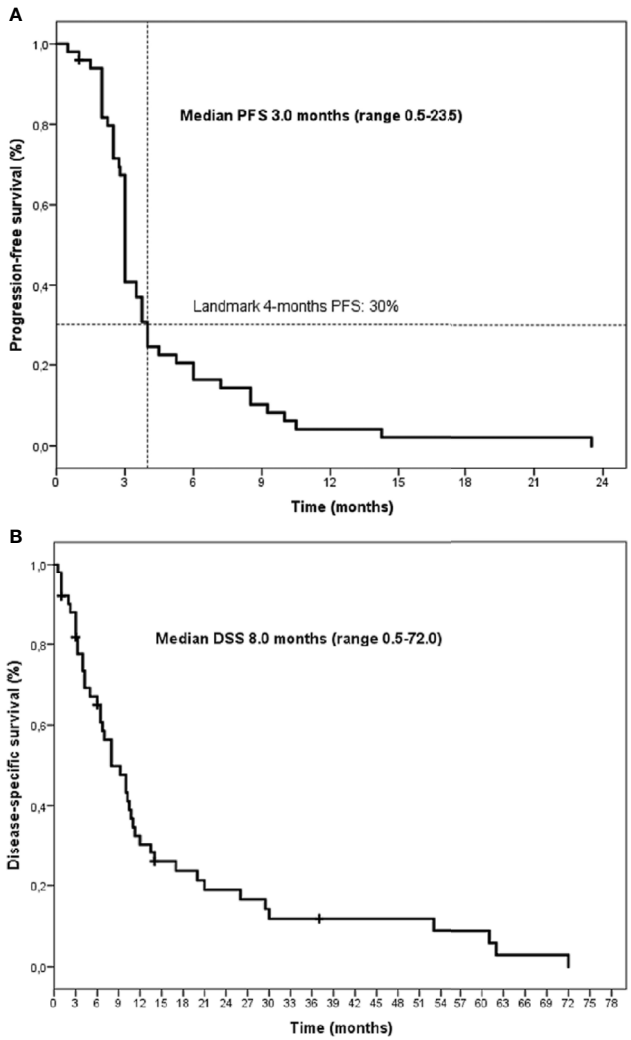


**FIGURE 1** | Kaplan-Meier curves of progression-free survival (PFS) **(A)** and disease-specific survival (DSS) **(B)** for the whole series.

## DISCUSSION

In this paper we performed a retrospective analysis of ACC patients treated with Gem/Cape chemotherapy outside a clinical trial. This series is representative of patients treated with second-line chemotherapy for metastatic ACC who are encountered in the daily clinical practice. Our analysis confirms results from two previous published series (10, 11). Gem/Cape resulted a moderately active regimen with a clinical benefit rate (CBR) at 4 months of 30%, median PFS of 3 months, and median DSS of 8 months. CBR, PFS, and DSS observed in the present series were inferior to those obtained in the Sperone et al. trial (CBR 46%, median PFS 5.3 months, median DSS 9.8 months), while the Henning et al. series reported a lower CBR (20.8%) a similar PFS (median 3 months) and longer DSS (median 10 months) than the present study. Patient selection could account for the differences observed. Patterns and severity of toxicities were also comparable and overall indicate a good tolerability of this schedule. It is well known that PFS is influenced by treatment efficacy while survival mainly depends on disease aggressiveness and efficacy of subsequent treatment lines. We assumed here PFS as surrogate of Gem Cape efficacy. We found that, with the exception of

**TABLE 2** | Analysis of activity of Gem/Cape chemotherapy.

| Endpoints of survival and response to therapy | Outcome |
|---|---|
| Median PFS (range), months | 3.0 (0.5–23.5) |
| Median DSS (range), months | 8 (0.5–72) |
| Best objective response to therapy: | |
| Progressive disease (PD)—n (%) | 31/50 (62) |
| Stable disease (SD)—n (%) | 12/50 (24) |
| Partial response (PR)—n (%) | 7/50 (14) |
| Clinical benefit at 4 months (PR+SD)—n (%) | 15/50 (30) |
| Clinical benefit at 6 months (PR+SD)—n (%) | 9/50 (18) |
| Clinical benefit at 12 months (PR+SD)—n (%) | 2/50 (4) |

**TABLE 3 |** Uni- and multivariate analysis of clinico-pathological factors predictive of progression-free survival (PFS).

| Variable | | Univariate analysis | | | | Multivariate analysis | | |
|---|---|---|---|---|---|---|---|---|
| | | Median PFS (mo) | HR | 95% CIs | p | HR | 95% CIs | p |
| Age at diagnosis | <50 | 3.00 | 1.00 | .65–2.07 | .597 | – | – | – |
| | ≥50 | 3.00 | 1.16 | | | | | |
| Sex | Female | 3.00 | 1.00 | .57–1.82 | .942 | – | – | – |
| | Male | 3.00 | 1.02 | | | | | |
| ENSAT stage at diagnosis | I–III | 3.00 | 1.00 | .83–2.64 | .177 | – | – | – |
| | IV | 3.00 | 1.48 | | | | | |
| Hormone hypersecretion | No | 3.00 | 1.00 | .57–1.78 | .971 | – | – | – |
| | Yes | 3.00 | 1.01 | | | | | |
| Proliferation index (Ki67) | ≤20% | 4.00 | 1.00 | .72–2.54 | .336 | – | – | – |
| | >20% | 3.00 | 1.36 | | | | | |
| Surgery of primary tumor | No | 3.00 | 1.00 | 1.22–6.05 | .014 | 2.67 | 1.00–7.09 | .049 |
| | Yes | 2.50 | 2.72 | | | | | |
| Previous lines of CT | 1 | 3.00 | 1.00 | .74–2.37 | .331 | – | – | – |
| | ≥2 | 3.00 | 1.33 | | | | | |
| Time from ACC diagnosis to Gem/Cape start | <19 | 3.00 | .479 | .257–0.89 | .121 | – | – | – |
| | ≥19 | 3.00 | | | | | | |
| ECOG performance status at Gem/Cape start | 0 | 6.00 | 1.00 | 2.19–10.66 | <.0005 | .145 | .03–0.54 | .004 |
| | ≥1 | 3.00 | 4.83 | | | | | |
| Charlson's Comorbidity Index at Gem/Cape start | Score 0–5 | 3.00 | 1.00 | .56–1.88 | .928 | – | – | – |
| | Score ≥6 | 3.50 | 1.02 | | | | | |
| Metastases lung | No | 6.00 | 1.00 | 1.03–4.37 | .040 | .837 | .24–2.82 | .77 |
| | Yes | 3.00 | 2.12 | | | | | |
| Metastases liver | No | 3.50 | 1.00 | .96–3.32 | .066 | – | – | – |
| | Yes | 3.00 | 1.78 | | | | | |
| Metastases lymphnodes | No | 3.00 | 1.00 | 1.16–4.22 | .015 | .551 | .23–1.3 | .17 |
| | Yes | 2.80 | 2.21 | | | | | |
| Metastases abdomen/peritoneum | No | 3.00 | 1.00 | .55–1.94 | .902 | – | – | – |
| | Yes | 3.00 | 1.04 | | | | | |
| Mitotane concentration during Gem/Cape chemotherapy | 14–20 mg/L | 3.50 | 1.00 | 1.04–3.81 | .036 | 1.25 | .48–3.28 | .64 |
| | <14 mg/L | 3.00 | 1.99 | | | | | |
| Leukocytes (WBC) absolute count at Gem/Cape start | $<4 \times 10^3/\mu l$ | 3.00 | .795 | .26–2.42 | .686 | – | – | – |
| | $4–10 \times 10^3/\mu l$ | 3.00 | 1.00 | .30–1.47 | .318 | | | |
| | $>10 \times 10^3/\mu l$ | 2.00 | 1.25 | .41–3.81 | .686 | | | |
| Neutrophils relative count at Gem/Cape start | <40–70% | 3.00 | 1.00 | 1.21–5.81 | .015 | – | – | – |
| | >70% | 2.50 | 2.65 | | | | | |
| Lymphocyte relative count at Gem/Cape start | <20% | 2.50 | 1.00 | 1.29–6.12 | .009 | – | – | – |
| | 20–>45% | 3.00 | 2.81 | | | | | |
| Albumine (ALB) at Gem/Cape start | >3.5 g/dl | 3.00 | 1.00 | .92–3.17 | .089 | | | |
| | ≤3.5 g/dl | 3.00 | 1.71 | | | | | |
| Lactate dehydrogenase (LDH) at Gem/Cape start | ≤225 U/L | 3.00 | 1.00 | .88–3.11 | .116 | | | |
| | >225 U/L | 3.00 | 1.65 | | | | | |
| Body Mass Index BMI | ≤23.5 | 3.00 | 1.00 | .67–2.24 | .492 | | | |
| | >23.5 | 3.00 | 1.23 | | | | | |
| Neutrophil-to-Lymphocyte Ratio (NLR) at Gem/Cape start | <5 | 3.00 | 1.00 | 1.21–5.81 | .027 | .270 | 0.81–0.90 | .003 |
| | ≥5 | 2.50 | 2.65 | | | | | |
| Hemoglobin (Hb) at Gem/Cape start | ≤12 g/dl | 3.00 | 2.44 | 1.17–5.09 | .017 | .804 | .31–2.03 | .646 |
| | >12 g/dl | 3.00 | 1.00 | | | | | |
| Platelet (PLT) absolute count at Gem/Cape start | $<130\times10^3/\mu l$ | 2.25 | 3.78 | .44–31.87 | .221 | – | – | – |
| | $130–400\times10^3/\mu l$ | 3.00 | .95 | .46–1.97 | .903 | | | |
| | $>400\times10^3/\mu l$ | 3.00 | .26 | .03–2.22 | .221 | | | |
| LIPI index | Good prognosis | 3.50 | 1.00 | .68–2.52 | .413 | – | – | – |
| | Intermediate-poor prognosis | 3.00 | 1.31 | | | | | |
| ALI index | >40 | 3.00 | 1.00 | 1.03–3.50 | .038 | .932 | .29–2.98 | .906 |
| | ≤40 | 3.00 | 1.90 | | | | | |

surgery of the primary tumor (no-surgery HR 2.67, p.049), none of the most important ACC prognostic factors (including ENSAT stage, Ki67 value, hormonal hypersecretion) evaluated at initial diagnosis had any impact in predicting PFS of patients submitted to Gem/Cape chemotherapy and were not associated with DSS. Despite the number of previous chemotherapy lines failed to be associated with outcome, patients who received Gem/Cape after more than 19 months from diagnosis had a better DSS. It should be noted that patients addressed to a second-line therapy are a selected subset who have not died early or have not

**TABLE 4 |** Uni- and multivariate analysis of clinico-pathological factors prognostic of disease-specific survival (DSS).

| Variable | | Univariate analysis | | | | Multivariate analysis | | |
|---|---|---|---|---|---|---|---|---|
| | | Median DSS (mo) | HR | 95% CIs | p | HR | 95% CIs | p |
| Age at diagnosis | <50 | 10.00 | 1.00 | .70–2.25 | .413 | – | – | – |
| | ≥50 | 8.00 | 1.28 | | | | | |
| Sex | Female | 8.00 | 1.00 | .75–2.54 | .292 | – | – | – |
| | Male | 10.25 | 1.38 | | | | | |
| ENSAT stage at diagnosis | I–III | 10.25 | 1.00 | 1.00–3.47 | .049 | 1.19 | .56–2.84 | .680 |
| | IV | 6.50 | 1.86 | | | | | |
| Hormone hypersecretion | No | 10.25 | 1.00 | .69–2.30 | .434 | – | – | – |
| | Yes | 8.00 | 1.26 | | | | | |
| Proliferation index (Ki67) | ≤20% | 10.75 | 1.00 | .68–2.53 | .402 | – | – | – |
| | >20% | 8.00 | 1.32 | | | | | |
| Surgery of primary tumor | No | 10.00 | 1.00 | .79–4.14 | .158 | – | – | – |
| | Yes | 4.25 | 1.81 | | | | | |
| Previous lines of CT | 1 | 9.25 | 1.00 | .55–1.88 | .942 | – | – | – |
| | ≥2 | 8.00 | 1.02 | | | | | |
| Time from ACC diagnosis to Gem/Cape start | ≥19 | 13.5 | 1 | .20–0.78 | .008 | .55 | .22–1.40 | .214 |
| | <19 | 6.5 | 0.40 | | | | | |
| ECOG Performance Status at Gem/Cape start | 0 | 13.50 | 1.00 | 1.20–4.77 | .012 | 1.93 | .75–4.95 | .167 |
| | ≥1 | 6.00 | 2.40 | | | | | |
| Charlson's Comorbidity Index at Gem/Cape start | Score 0–5 | 9.25 | 1.00 | .91–3.61 | .086 | – | – | – |
| | Score ≥6 | 8.00 | 1.82 | | | | | |
| Metastases lung | No | 13.50 | 1.00 | .96–4.12 | .064 | – | – | – |
| | Yes | 7.00 | 1.99 | | | | | |
| Metastases liver | No | 11.00 | 1.00 | .89–3.34 | .103 | – | – | – |
| | Yes | 7.00 | 1.73 | | | | | |
| Metastases lymphnodes | No | 10.25 | 1.00 | .85–3.03 | .143 | – | – | – |
| | Yes | 5.00 | 1.60 | | | | | |
| Metastases abdomen/peritoneum | No | 8.00 | 1.00 | .46–1.71 | .733 | – | – | – |
| | Yes | 9.25 | .89 | | | | | |
| Mitotane concentration during Gem/Cape chemotherapy | 14–20 mg/L | 12.00 | 1.00 | 1.04–4.29 | .037 | 1.10 | .44–2.74 | .837 |
| | <14 mg/L | 7.00 | 2.12 | | | | | |
| Leukocytes (WBC) absolute count at Gem/Cape start | $<4 \times 10^3/\mu l$ | 4.25 | 2.45 | .66–9.13 | .180 | – | – | – |
| | $4–10 \times 10^3/\mu l$ | 8.00 | 1.20 | .35–4.08 | .761 | | | |
| | $>10 \times 10^3/\mu l$ | 8.00 | .40 | .11–1.51 | .180 | | | |
| Neutrophils relative count at Gem/Cape start | <40–70% | 8.00 | 1.00 | .63–3.27 | .377 | – | – | – |
| | >70% | 6.50 | 1.44 | | | | | |
| Lymphocyte relative count at Gem/Cape start | <20% | 6.50 | 1.00 | .68–3.36 | .301 | – | – | – |
| | 20–>45% | 9.25 | 1.52 | | | | | |
| Albumine (ALB) at Gem/Cape start | >3.5 g/dl | 10.25 | 1.00 | .78–2.68 | .242 | | | |
| | ≤3.5 g/dl | 8.00 | 1.44 | | | | | |
| Lactate dehydrogenase (LDH) at Gem/Cape start | ≤225 U/L | 10.00 | 1.00 | .71–2.73 | .324 | | | |
| | >225 U/L | 6.50 | 1.40 | | | | | |
| Body mass index BMI | >23.5 | 9.20 | 1.00 | .61–2.18 | .651 | | | |
| | ≤23.5 | 6.70 | 1.15 | | | | | |
| Neutrophil/lymphocyte ratio (NLR) at Gem/Cape start | <5 | 8.00 | 1.00 | .63–3.27 | .377 | – | – | – |
| | ≥5 | 6.50 | 1.44 | | | | | |
| Hemoglobin (Hb) at Gem/Cape start | ≤12 g/dl | 6.75 | 1.92 | .92–4.00 | .078 | – | – | – |
| | >12 g/dl | 10.75 | 1.00 | | | | | |
| Platelet (PLT) absolute count at Gem/Cape start | $<130\times10^3/\mu l$ | 7.00 | 1.07 | .13–8.57 | .945 | – | – | – |
| | $130–400\times10^3/\mu l$ | 10.00 | .49 | .21–1.12 | .093 | | | |
| | $>400\times10^3/\mu l$ | 6.75 | .92 | .11–7.40 | .945 | | | |
| LIPI index | Good prognosis | 9.25 | 1.00 | .52–2.00 | .943 | – | – | – |
| | Intermadiate-poor prognosis | 6.75 | 1.02 | | | | | |
| ALI index | >40 | 10.00 | 1.00 | .78–2.57 | .252 | – | – | – |
| | ≤40 | 6.50 | 1.41 | | | | | |

had a significant deterioration in performance status after the previous treatment lines and therefore represent a subset with better response rates and overall prognosis.

In this series, mitotane plasma concentration was not predictive of response and survival. Whether mitotane in association with chemotherapy should be continued or not beyond the first line is a matter of controversy (1). The absence of any predictive or prognostic role of plasma mitotane levels in our patient series, confirming a previous observation (11), supports the notion that the drug is not effective in this context and could be withdrawn. When considering patients clinical characteristics at Gem/Cape start,

a more precise definition of those destined to have a poor outcome emerged. The pattern of metastatic sites showed a poor predictive value of PFS for lung, liver, and lymph nodal metastases at univariate analysis but not after adjusting for multiple comparisons. None of them showed to be prognostic for DSS. Surprisingly, the Charlson's Comorbidity Index score ≥6 which defines patient's vulnerabilities at baseline had no impact on PFS and DSS. Our result is in part in contrast with a much larger observation in all ACC patients from the US National Cancer Database in which a Charlson-Deyo comorbidity score >2 was associated with a poorer prognosis (19). On the other hand, the presence of tumor-associated symptoms (ECOG PS ≥1) was highly correlated with a poor PFS (HR 6.93, p.004). While the term "symptoms" is very generic, in our series the symptomatic patient often had pain, discomfort from organ compression or insufficiency, signs of anemia and of systemic inflammation (such as fever). The predictive role for PFS of PS might seem obvious and has wide consensus in clinical oncology. However, its meaning is to practically help the clinician to select patients that have a chance to obtain a benefit from chemotherapy sparing the others in which deterioration of QOL would be the inevitable result. Identification of laboratory parameters of sensitivity to one specific drug has traditionally failed in ACC patients regardless of the nature of the drug, chemotherapy, immunotherapy or molecular target-agent, as a consequence of a low frequency of highly responder patients and the rarity of the disease (20–22). Henning et al., investigated in ACC patients receiving Gem-based chemotherapy the prognostic and predictive role of the tissue expression of the human equilibrative nucleoside transporter type 1 (hENT1) and the subunit M1 of ribonucleotide reductase (RRM1), two enzymatic activities involved in response or resistance to Gemcitabine. Their results showed that both biomarkers were not useful as predictive markers of activity in patients receiving Gem-based chemotherapy (11). The current study additionally investigated the prognostic and predictive value of laboratory characteristics that can be easily found or calculated from clinical records. We found that presence of anemia, high neutrophils and low lymphocytes relative counts and the NLR ≥5 before the start of Gem/Cape chemotherapy were poor predictive factors for PFS at univariate analysis. Among them, only NLR maintained an independent predictive significance at multivariate analysis (HR 3.88, p.003). This observation is based on a very limited number of patients and has, therefore, a weak inferential power. NLR, however, has already shown to be a significant prognostic factor both in ACC (23, 24) and in other neoplasms (25, 26). Further interest of NLR in ACC derives from the fact that it may be increased from endogenous cortisol and/or from exogenous steroid replacement therapy that is a frequent condition in ACC patients (27). In our series NLR correlated with PFS but not with DSS thus appearing to be a predictive factor of Gem/Cape efficacy and not a prognostic factor. ALI and LIPI biomarkers have been described in patients with lung cancer (17, 18) and their role is still unknown in ACC patients. With regard to ALI biomarker, we found a predictive role in terms of PFS at univariate but not at multivariate analysis. Conversely, the LIPI index failed to be significantly associated with PSF and DSS.

In conclusion, the present analysis has some limitations linked to its retrospective nature and the limited number of patients. Nevertheless, it confirms the modest efficacy of Gem/Cape chemotherapy as second or further line of treatment for metastatic ACC patients. Gem/Cape should not be prescribed in patients with poor PS, rapidly progressing ACC and/or with high NLR as they are unlikely to obtain a benefit from this regimen. In line with this, it is unlikely that patients with newly diagnosed, full-blown ACC might derive significant benefit in first line. As Gemcitabine has potential as a demethylating agent and hypermethylation is a distinctive feature of aggressive ACC, in the future tumor methylation status could be evaluated as predictive factor of sensitivity to Gemcitabine. Further investigation is required to best integrate clinical and molecular data to address the correct ACC patient to the correct treatment.

## DATA AVAILABILITY STATEMENT

The raw data supporting the conclusions of this article will be made available by the authors, without undue reservation.

## ETHICS STATEMENT

The studies involving human participants were reviewed and approved. The study was approved by the Institutional Ethical Review Board (ID: NP 3776/2019) and conducted in accordance with the principles of the Declaration of Helsinki. The patients/participants provided their written informed consent to participate in this study.

## AUTHOR CONTRIBUTIONS

Conceptualization, AB. Methodology, SG. Software, AM, DC, and ML. Validation, SG, AB, and VF. Formal analysis, SG and AM. Investigation, SG, DC, ML, VF, BL, SS, and AB. Data curation, SG, AM, DC, ML, AV, and LF. Writing—original draft preparation, SG, AB. Writing—review and editing, SG and AB. Visualization, SG and ML. Supervision, AB and SS. Radiological assessment, RA. Project administration, AB. All authors contributed to the article and approved the submitted version.

## FUNDING

This work was granted by: AIRC project IG14411 (PI: AB), Fondazione Camillo Golgi, Brescia and Fondazione Internazionale di Ricerca in Medicina (F.I.R.M.) ONLUS, Cremona (Italy).

## ACKNOWLEDGMENTS

We are grateful to our patients and their families.

## REFERENCES


1. Fassnacht M, Dekkers OM, Else T, Baudin E, Berruti A, de Krijger R, et al. European Society of Endocrinology Clinical Practice Guidelines on the management of adrenocortical carcinoma in adults, in collaboration with the European Network for the Study of Adrenal Tumors. *Eur J Endocrinol* (2018) 179:G1–G46. doi: 10.1530/EJE-18-0608
2. Terzolo M, Daffara F, Ardito A, Zaggia B, Basile V, Ferrari L, et al. Management of adrenal cancer: a 2013 update. *J Endocrinol Invest* (2014) 37:207–17. doi: 10.1007/s40618-013-0049-2
3. Fassnacht M, Terzolo M, Allolio B, Baudin E, Haak H, Berruti A, et al. Combination chemotherapy in advanced adrenocortical carcinoma. *N Engl J Med* (2012) 366:2189–97. doi: 10.1056/NEJMoa1200966
4. Megerle F, Kroiss M, Hahner S, Fassnacht M. Advanced Adrenocortical Carcinoma - What to do when First-Line Therapy Fails? *Exp Clin Endocrinol Diabetes* (2019) 127:109–16. doi: 10.1055/a-0715-1946
5. Baudin E, Docao C, Gicquel C, Vassal G, Bachelot A, Penfornis A, et al. Use of a topoisomerase I inhibitor (irinotecan, CPT-11) in metastatic adrenocortical carcinoma. *Ann Oncol* (2002) 13:1806–9. doi: 10.1093/annonc/mdf291
6. Khan TS, Imam H, Juhlin C, Skogseid B, Gröndal S, Tibblin S, et al. Streptozocin and o,p'DDD in the treatment of adrenocortical cancer patients: long-term survival in its adjuvant use. *Ann Oncol* (2000) 11:1281–7. doi: 10.1023/a:1008377915129
7. Quinkler M, Hahner S, Wortmann S, Johanssen S, Adam P, Ritter C, et al. Treatment of advanced adrenocortical carcinoma with erlotinib plus gemcitabine. *J Clin Endocrinol Metab* (2008) 93:2057–62. doi: 10.1210/jc.2007-2564
8. Wortmann S, Quinkler M, Ritter C, Kroiss M, Johanssen S, Hahner S, et al. Bevacizumab plus capecitabine as a salvage therapy in advanced adrenocortical carcinoma. *Eur J Endocrinol* (2010) 162:349–56. doi: 10.1530/EJE-09-0804
9. Schteingart DE, Doherty GM, Gauger PG, Giordano TJ, Hammer GD, Korobkin M, et al. Management of patients with adrenal cancer: recommendations of an international consensus conference. *Endocr Relat Cancer* (2005) 12:667–80. doi: 10.1677/erc.1.01029
10. Sperone P, Ferrero A, Daffara F, Priola A, Zaggia B, Volante M, et al. Gemcitabine plus metronomic 5-fluorouracil or capecitabine as a second-/third-line chemotherapy in advanced adrenocortical carcinoma: a multicenter phase II study. *Endocr Relat Cancer* (2010) 17:445–53. doi: 10.1677/ERC-09-0281
11. Henning JEK, Deutschbein T, Altieri B, Steinhauer S, Kircher S, Sbiera S, et al. Gemcitabine-Based Chemotherapy in Adrenocortical Carcinoma: A Multicenter Study of Efficacy and Predictive Factors. *J Clin Endocrinol Metab* (2017) 102:4323–32. doi: 10.1210/jc.2017-01624
12. Steenaard RV, Michon LA, Haak HR. Health-Related Quality of Life in Adrenocortical Carcinoma. *Cancers (Basel)* (2019) 11(10):1500. doi: 10.3390/cancers11101500
13. Payne SA. A study of quality of life in cancer patients receiving palliative chemotherapy. *Soc Sci Med* (1992) 35:1505–9. doi: 10.1016/0277-9536(92)90053-s
14. Hurria A, Togawa K, Mohile SG, Owusu C, Klepin HD, Gross CP, et al. Predicting chemotherapy toxicity in older adults with cancer: a prospective multicenter study. *J Clin Oncol* (2011) 29:3457–65. doi: 10.1200/JCO.2011.34.7625
15. Libé R, Borget I, Ronchi CL, Zaggia B, Kroiss M, Kerkhofs T, et al. Prognostic factors in stage III-IV adrenocortical carcinomas (ACC): an European Network for the Study of Adrenal Tumor (ENSAT) study. *Ann Oncol* (2015) 26:2119–25. doi: 10.1093/annonc/mdv329
16. Charlson ME, Pompei P, Ales KL, MacKenzie CR. A new method of classifying prognostic comorbidity in longitudinal studies: development and validation. *J Chronic Dis* (1987) 40:373–83. doi: 10.1016/0021-9681(87)90171-8
17. Mezquita L, Auclin E, Ferrara R, Charrier M, Remon J, Planchard D, et al. Association of the Lung Immune Prognostic Index With Immune Checkpoint Inhibitor Outcomes in Patients With Advanced Non-Small Cell Lung Cancer. *JAMA Oncol* (2018) 4(3):351–7. doi: 10.1001/jamaoncol.2017.4771
18. Jafri SH, Shi R, Mills G. Advance lung cancer inflammation index (ALI) at diagnosis is a prognostic marker in patients with metastatic non-small cell lung cancer (NSCLC): a retrospective review. *BMC Cancer* (2013) 13(1):158. doi: 10.1186/1471-2407-13-158
19. Tella SH, Kommalapati A, Yaturu S, Kebebew E. Predictors of Survival in Adrenocortical Carcinoma: An Analysis From the National Cancer Database. *J Clin Endocrinol Metab* (2018) 103:3566–73. doi: 10.1210/jc.2018-00918
20. Grisanti S, Cosentini D, Laganà M, Abate A, Rossini E, Sigala S, et al. Are we failing in treatment of adrenocortical carcinoma? Lights and shadows of molecular signatures. *Curr Opin Endocrine Metab Res* (2019) 8:80–7. doi: 10.1016/j.coemr.2019.07.07
21. Cosentini D, Badalamenti G, Grisanti S, Basile V, Rapa I, Cerri S, et al. Activity and safety of temozolomide in advanced adrenocortical carcinoma patients. *Eur J Endocrinol* (2019) 181:681–9. doi: 10.1530/eje-19-0570
22. Berruti A, Sperone P, Ferrero A, Germano A, Ardito A, Priola AM, et al. Phase II study of weekly paclitaxel and sorafenib as second/third-line therapy in patients with adrenocortical carcinoma. *Eur J Endocrinol* (2012) 166:451–8. doi: 10.1530/eje-11-0918
23. Bagante F, Tran TB, Postlewait LM, Maithel SK, Wang TS, Evans DB, et al. Neutrophil-lymphocyte and platelet-lymphocyte ratio as predictors of disease specific survival after resection of adrenocortical carcinoma. *J Surg Oncol* (2015) 112:164–72. doi: 10.1002/jso.23982
24. Mochizuki T, Kawahara T, Takamoto D, Makiyama K, Hattori Y, Teranishi JI, et al. The neutrophil-to-lymphocyte ratio (NLR) predicts adrenocortical carcinoma and is correlated with the prognosis. *BMC Urol* (2017) 17:49. doi: 10.1186/s12894-017-0240-4
25. Suzuki Y, Kan M, Kimura G, Umemoto K, Watanabe K, Sasaki M, et al. Predictive factors of the treatment outcome in patients with advanced biliary tract cancer receiving gemcitabine plus cisplatin as first-line chemotherapy. *J Gastroenterol* (2019) 54:281–90. doi: 10.1007/s00535-018-1518-3
26. Walsh SR, Cook EJ, Goulder F, Justin TA, Keeling NJ. Neutrophil-lymphocyte ratio as a prognostic factor in colorectal cancer. *J Surg Oncol* (2005) 91:181–4. doi: 10.1002/jso.20329
27. Onsrud M, Thorsby E. Influence of in vivo hydrocortisone on some human blood lymphocyte subpopulations. I. Effect on natural killer cell activity. *Scand J Immunol* (1981) 13:573–9. doi: 10.1111/j.1365-3083.1981.tb00171.x


**Conflict of Interest:** The authors declare that the research was conducted in the absence of any commercial or financial relationships that could be construed as a potential conflict of interest.

frontiers in Endocrinology

CASE REPORT
published: 17 March 2021
doi: 10.3389/fendo.2021.652045

# Case Report: Irreversible Watery Diarrhea, Severe Metabolic Acidosis, Hypokalemia and Achloridria Syndrome Related to Vasoactive Intestinal Peptide Secreting Malignant Pheochromocytoma

*Aurelio Negro[1†], Ignazio Verzicco[2†], Stefano Tedeschi[2], Nicoletta Campanini[3], Magda Zanelli[4], Emanuele Negri[5], Enrico Farnetti[6], Davide Nicoli[6], Barbara Palladini[2], Rosaria Santi[1,5], Davide Cunzi[1,2], Anna Calvi[2], Pietro Coghi[2], Luigi Gerra[2], Riccardo Volpi[2], Gallia Graiani[7] and Aderville Cabassi[2*]*

[1] Internal Medicine and Secondary Hypertension Center, Ospedale Sant'Anna di Castelnovo Ne' Monti, Azienda Unità sanitaria Locale – IRCCS di Reggio Emilia, Reggio Emilia, Italy, [2] Centro Ipertensione Arteriosa e Studio Malattie Cardiorenali, S.S. Fisiopatologia Medica, Clinica Medica Generale e Terapia Medica, Parma, Italy, [3] Pathology Unit, Department of Medicine and Surgery, University Hospital of Parma, Parma, Italy, [4] Pathology Unit, Ospedale Sant'Anna di Castelnovo Ne' Monti, Azienda Unità sanitaria Locale – IRCCS di Reggio Emilia, Reggio Emilia, Italy, [5] High Care Internal Medicine Unit, Ospedale Sant'Anna di Castelnovo Ne' Monti, Azienda Unità sanitaria Locale – IRCCS di Reggio Emilia, Reggio Emilia, Italy, [6] Molecular Biology Laboratory, Ospedale Sant'Anna di Castelnovo Ne' Monti, Azienda Unità sanitaria Locale – IRCCS di Reggio Emilia, Reggio Emilia, Italy, [7] Histology and Histopathology Unit, Dental School, University of Parma, Parma, Italy

OPEN ACCESS

**Edited by:**
*Antongiulio Faggiano, Sapienza University of Rome, Italy*

**Reviewed by:**
*Ronald De Krijger, Princess Maxima Center for Pediatric Oncology, Netherlands*
*Fady Hannah-Shmouni, National Institutes of Health (NIH), United States*

***Correspondence:**
*Aderville Cabassi*
*aderville.cabassi@unipr.it*

*[†]These authors have contributed equally to this work*

**Specialty section:**
*This article was submitted to Cancer Endocrinology, a section of the journal Frontiers in Endocrinology*

**Received:** *11 January 2021*
**Accepted:** *01 March 2021*
**Published:** *17 March 2021*

**Citation:**
*Negro A, Verzicco I, Tedeschi S, Campanini N, Zanelli M, Negri E, Farnetti E, Nicoli D, Palladini B, Santi R, Cunzi D, Calvi A, Coghi P, Gerra L, Volpi R, Graiani G and Cabassi A (2021) Case Report: Irreversible Watery Diarrhea, Severe Metabolic Acidosis, Hypokalemia and Achloridria Syndrome Related to Vasoactive Intestinal Peptide Secreting Malignant Pheochromocytoma. Front. Endocrinol. 12:652045. doi: 10.3389/fendo.2021.652045*

**Background:** Pheochromocytoma (PHEO) clinical manifestations generally mirror excessive catecholamines secretion; rarely the clinical picture may reflect secretion of other hormones. Watery diarrhea, hypokalemia and achlorhydria (WDHA) is a rare syndrome related to excessive secretion of vasoactive intestinal peptide (VIP).

**Clinical Case:** A 73-year-old hypotensive man affected by adrenal PHEO presented with weight loss and watery diarrhea associated with hypokalemia, hyperchloremic metabolic acidosis (anion gap 15 mmol/l) and a negative urinary anion gap. Abdominal computed tomography scan showed a right adrenal PHEO, 8.1 cm in maximum diameter, with tracer uptake on $^{68}$GaDOTA-octreotate positron emission tomography. Metastasis in lumbar region and lung were present. Both chromogranin A and VIP levels were high (more than10 times the normal value) with slightly elevated urine normetanephrine and metanephrine excretion. Right adrenalectomy was performed and a somatostatin analogue therapy with lanreotide started. Immunostaining showed chromogranin A and VIP co-expression, with weak somatostatin-receptor-2A positivity. In two months, patient clinical conditions deteriorated with severe WDHA and multiple liver and lung metastasis. Metabolic acidosis and hypokalemia worsened, leading to hemodynamic shock and exitus.

**Conclusions:** A rare case of WDHA syndrome caused by malignant VIP-secreting PHEO was diagnosed. High levels of circulating VIP were responsible of the rapidly evolving clinical picture with massive dehydration and weight loss along with severe hyperchloremic metabolic acidosis and hypokalemia due to the profuse untreatable diarrhea. The rescue treatment with lanreotide was unsuccessful because of the paucity of somatostatin-receptor-2A on VIP-secreting PHEO chromaffin cells.

**Keywords: pheochromocytoma, watery diarrhea hypokalemia achlorhydria syndrome, arterial hypotension, vasointestinal peptide (VIP), metabolic acidosis**

## INTRODUCTION

Pheochromocytomas (PHEO) and sympathetic paragangliomas are rare neuroendocrine tumors arising from chromaffin cells in the medulla of the adrenal glands or from neural crest-derived ganglia. PHEO are usually functional and secrete catecholamines (1). They may manifest with an array of clinical symptoms including headaches, sweating, palpitations, paroxysmal or persistent hypertension, and various signs or symptoms related to catecholamines secretion or, in rare cases, to isolated or combined release of other hormones such as somatostatin, renin, adrenocorticotropic hormone, parathyroid hormone, erythropoietin, enkephalins, calcitonin, neuropeptide Y (2–4). Watery diarrhea associated with hypokalemia and achlorhydria (WDHA) characterizes a rare syndrome first described by Verner and Morrison in 1958 (5) linked to hypersecretion of vasoactive intestinal peptide (VIP). Such a clinical situation was also termed pancreatic cholera because of severe diarrhea resembling those related to Vibrio cholera infection. VIP is a 28-amino acids peptide, member of the secretin/glucagon/pituitary adenylyl cyclase-activating peptide hormone superfamily. VIP is able to regulate gastric acid secretion, intestinal contractility and anion secretion, exocrine pancreas release, vasodilation by acting on two G-protein-coupled receptors VPAC1 and VPAC2 (6). Enteric anion secretion depends from VPAC1 receptor-mediated adenylyl cyclase and protein kinase A activation leading to cystic fibrosis transmembrane conductance regulator stimulation, responsible for the secretion of both $Cl^-$ and $HCO_3^-$ in the ileum and colon (7–9). WDHA associates with severe metabolic acidosis due bicarbonate wasting but also with abnormal glucose tolerance due to VIP-mediated glycogenolytic effect on the liver, with hypercalcemia and tetany-related hypomagnesemia due to diarrhea. The patients also experience facial flushing because of VIP vasodilating effect. VIP-secreting tumors usually originate in the pancreas or much more rarely along the sympathetic chain or in the gut and the skin (10, 11). Here, we report an emblematic case of intractable and refractory WDHA syndrome in a patient with a VIP-secreting malignant adrenal PHEO.

## CASE REPORT

A 73-year-old Caucasian man was referred to our hospital for evaluation of a right PHEO, diagnosed two months before at another hospital, after the identification of a large retroperitoneal mass on abdominal computed tomography (CT). At that time, the patient experienced abdominal discomfort, unintentional weight loss of approximately 5 Kg within the previous 3 months, associated to sporadic episodes of watery diarrhea. At admission to our hospital, the patient was moderately dehydrated and tachypnoic. He denied any history of headache, palpitations, sweating, or hypertension. He reported episodes of watery diarrhea, up to 5-6 times a day and 2-3 times a week, without blood or mucus. He also had no relevant familial history of endocrine nor cancer diseases but only a paternal history of arterial hypertension. Physical examination showed blood pressure (BP) of 100/67 mmHg and heart rate of 88 beats/min; no significant orthostatic pressure gradient was measured. BP values, evaluated on several occasions, were 94/58 and 91/62 mm Hg. Laboratory tests showed a hypokalemia (3.3 mmol/L) with metabolic acidosis (pH 7.29, $HCO3^-$ 19 mmol/L), a serum magnesium level of 1.5 mg/dl and fasting blood glucose of 149 mg/dl. A 24-h urinary sample showed only a slight increase in normetanephrine excretion, 638 µg (normal values: 162-528/day), while metanephrine and methoxytyramine resulted within normal range. Serum chromogranin A was elevated (1028 ng/ml, normal values 20-100), as well as neuron-specific enolase level (NSE 35.7 nl/ml, normal values 1.0-13.5). Plasma cortisol, adrenocorticotropic hormone, thyroid-stimulating hormone, thyroxine, parathyroid hormone, and calcitonin were within the normal ranges. Contrast enhanced abdominal CT scan confirmed the presence of inhomogeneous right adrenal mass measuring 8.1 x 7.7 x 7.9 cm (**Figure 1A**). A $^{18}$F-fluorodeoxyglucose (18F-FDG) positron emission tomography (PET) coupled with CT showed an area of high uptake (maximum standardized uptake value, SUV max 8.6) in the right adrenal gland, with a prevailing peripheral signal and central hypoactivity, and another area of high uptake (SUV max 9.6) in the lumbar region suspicious of lymph node localization (**Figures 1B, C**). In addition, $^{68}$GaDOTA-octreotate (DOTATATE) PET confirmed the peripheral high uptake (SUV max 6) in the right adrenal gland and the high uptake area (SUV max 3.7) in the lumbar region; a high uptake (SUV max 4.5) was also detected at the base of the left lung (**Figure 1D**). Based on these results, patient diagnosis was metastatic adrenal PHEO. Intravenous fluid infusion, sodium bicarbonate, potassium aspartate, magnesium sulphate supplementations were started allowing an improvement of clinical condition and blood pressure levels. Then, after 10-days pre-operative treatment with low dose alpha1-adrenergic antagonist doxazosin (given just before bed), he underwent surgical resection of the tumor. The patient had an uneventful

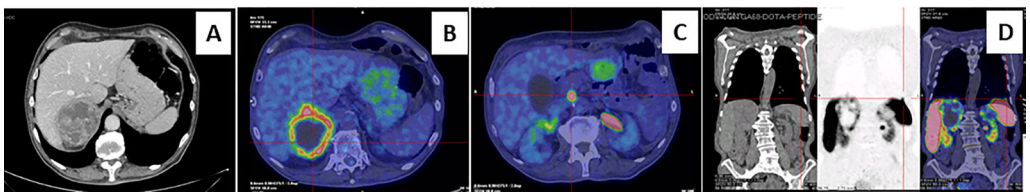


**FIGURE 1** | Abdominal computed tomography scan and Positron emission tomography imaging. Contrast-enhanced abdominal CT scan showed inhomogeneous right adrenal mass measuring 8.1 x 7.7 x 7.9 cm **(A)**. A 18F-fluorodeoxyglucose PET-CT showed an area of high uptake in the right adrenal gland, with a prevailing peripheral signal and central hypoactivity, and in the lumbar region suspected of adenopathic localization **(B, C)**. A 68GaDOTA-octreotate (DOTATATE) PET confirmed previous localizations and also detected a high uptake are at the base of the left lung **(D)**.

postoperative course, except for sporadic watery diarrhea. Gross examination revealed a 10x8x6 cm brownish-yellow, friable adrenal mass. Histology showed a highly cellular tumor made up of monotonous medium-sized cells with discrete nuclear pleomorphism and mild hyperchromasia. Mitotic figures were above 3/10 high power fields, with some atypical mitoses. The cells were arranged in nests with areas of diffuse growth in more than 10% of the tumor. Confluent areas of necrosis were present. Foci of capsular and vascular invasion were noted as well as extension into periadrenal adipose tissue. The histological features were consistent with a malignant PHEO, with a PASS score (Pheochromocytoma of the Adrenal Gland Scaled Score) of 20 (**Figures 2A–D**), indicating a high risk of aggressive cellular behavior (PASS≥4). DNA genetic analysis of the patient with a next generation sequencing (NGS) approach using Trusight One Sequencing Panel by Illumina, revealed a synonymous single nucleotide variant of gene SDHA [rs6555055, NM_004168.2: c.619A>C, (p.Arg207=)] indicated by ClinVar database as associated to "probably benign" catecholamine-secreting PHEO (12). The patient was discharged in satisfactory clinical condition. Therapy with lanreotide, a somatostatin analogue, at a dose of 60 mg once a month was initiated. At 2 months, multiple metastatic pulmonary and hepatic nodules were identified on CT scan (**Figures 3A–D**). The patient once again experienced abdominal discomfort, 4 kg weight loss, yet only sporadic watery diarrhea. Peptide receptor radionuclide therapy and sunitinib, a multi-targeted receptor tyrosine kinase inhibitor, were scheduled. In the meantime, lanreotide therapy was increased to 120 mg once a month. However, after about one month, the patient was re-admitted with a 10-day history of severe watery diarrhea, up to 20 times in 24 hrs, accompanied by nausea, vomiting and occasionally quick flushing. At presentation, he was suffering and markedly dehydrated. Physical examination showed BP of 90/67 mmHg, heart rate of 120 beats/min, the pulse was fast and weak, the breath was fast and short, the skin cold and clammy, and the urination was decreased. Laboratory tests were as follows: blood urea nitrogen 96 mg/dl; serum creatinine 3.5 mg/dl; $Na^+$ 136 mmol/l; $K^+$ 2.5 mmol/l; $Cl^-$ 115 mmol/l; pH 7.08; $HCO_3^-$ 5.5 mmol/l; Pa CO2 30 mm Hg; Pa O2 67 mm Hg; lactate 5 mmol/l (normal values 0.5-2.2); serum anion gap 15 mmol (corrected for serum albumin levels 16 mmol); urine anion gap was negative. Serum prealbumin was 29 mg/dl (normal values 15-35) and albumin 3.9 g/dl (normal values 3.5-5.0). At that time, serum chromogranin A was 2896 ng/ml and neuron-specific enolase 49.6 ng/ml. Twenty-four hours urinary normetanephrine excretion was 920.4 µg, while metanephrine resulted at 432.6 µg (normal

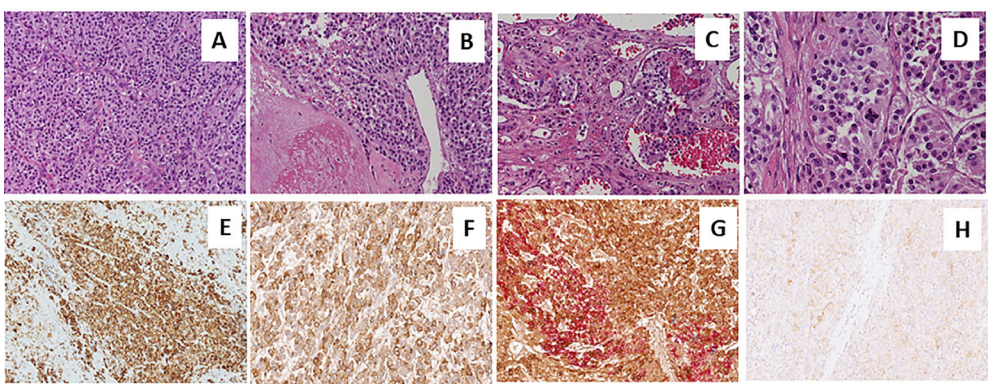


**FIGURE 2** | Sections from right adrenal gland Morphologic analysis with hematoxylin-eosin staining in **(A–D)** at different magnification. Panels show a pheochromocytoma, with a typical zellballen pattern of growth (**A**, 20X), with perivascular cell cuffing around a blood vessel called pseudo-rosette pattern (**B**, 20X), with neoplastic cells inside vascular spaces (**C**, 20X), and at greater magnification (**D**, 40X), an atypical mitotic figure. Positive immunohistochemical staining of Chromogranin A in Panel **(E)**, VIP **(F)** and anti-Somatostatin Receptor 2A (SSTR2A, **H**). Double immunostaining showing the co-expression of Chromogranin A (brown) and VIP (red) **(G)**.

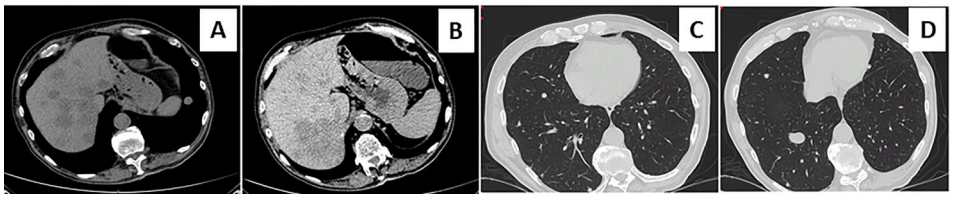


**FIGURE 3** | Metastatic diffusion at chest and hepatic computed tomography scan. Contrast-enhanced abdominal and chest computed tomography scan showed the appearance of multiple metastatic pulmonary and hepatic nodules **(A–D)**.

values 64-302 μg/day). VIP plasma levels were measured, and circulating values were more than 10 times the upper normal limit (1285 pg/ml, normal values 18-100). Cardiac ultrasound showed a reduced left ventricular ejection fraction (35%). Due to the emerging clinical picture, histological sections were re-evaluated with additional immunostainings. Sections were stained with the following primary antibodies: anti-Chromogranin A (clone LK2H10 ready to use; Ventana-Roche), Anti-Vasoactive intestinal polypeptide -VIP (rabbit 1:500; Biogenex) and anti-Somatostatin Receptor 2A -SSTR2A (rabbit 1:100; Bio-Trend). The sections were immunostained with HRP Polymer (Optiview DAB IHC Detection kit; Roche) in accordance with the manufacturer's specifications. Negative controls consisted of substituting normal mouse serum for the primary antibodies. A set of sections adjacent to these used for single labelling with VIP, was used for double labelling with Chromogranin A. The second antibody was immunostained with AP Polymer (Ultraview Universal Alcaline Phosphatase Red Detection Kit; Roche). Permanent red chromogen was used for staining development. Immunostaining revealed strong positivity for neuroendocrine marker chromogranin A and VIP (**Figures 2E, F**); a large number of cells co-expressed chromogranin A and VIP (**Figure 2G**). Weak was the positivity for SSTR2A (**Figure 2H**). A diagnosis of VIP-secreting PHEO was rendered. The patient was then transferred to the intensive care unit. He was managed with intensive intravenous fluid hydration, potassium salts and bicarbonates, as well as with octreotide (0.1 mg/8 h s.c.), sunitinib 50 mg/day and loperamide. However, his diarrhea worsened with further exacerbation of metabolic acidosis (pH 6.99, $HCO_3^-$ 4.3 mmol/l), leading to hemodynamic instability and shock. He died five days later.

## DISCUSSION

Our patient represents a new case of WDHA syndrome caused by a malignant VIP-secreting PHEO with massive dehydration, severe hyperchloremic metabolic acidosis and hypokalemia due to the profuse diarrhea. VIP-secreting PHEO is an extremely rare tumor and from the first description given in 1975 by Lowry et al, only about twenty five cases of PHEO associated with WDHA syndrome have been reported, so far (13–20).

As a general rule, the clinical manifestations of PHEO are very challenging to interpret, reflecting the prevailing hormonal secretion by chromaffin cells, generally represented by catecholamines. In the present case, the modest increase in normetanephrine and metanephrine levels did cause the classic picture of PHEO with arterial paroxysmal or persistent hypertension, headaches, palpitations, anxiety, and diaphoresis. As the main secreted hormone was VIP, diarrhea and arterial hypotension were the main clinical manifestations. VIP elicits a potent vasodilation not only of the splanchnic circulation (gastric, small intestine and colon), but even systemically through a direct effect on VPAC2 receptor of vascular smooth muscle and through VPAC1 receptor-mediated nitric oxide release from endothelial cells (21). VIP systemic vasodilating effect, largely exceeding the vasoconstrictor effect of catecholamines, associated to diarrhea-related volume depletion contributes to the hypotension observed in our patient (14, 16). Episodic facial flushing reported by our patient could be the result of VIP direct arterial skin vasodilatory effect.

Watery diarrhea, hypokalemia, metabolic acidosis due of enteric bicarbonate loss and hypo- or rarely achlorhydria are clinical features of VIP-secreting tumors and generally begin several years before diagnosis. Our patient reported sporadic diarrhea and body weight loss just 3 months before, followed by a rapid clinical worsening. The accelerated time course of WDHA syndrome is a feature of VIP-secreting PHEO compared to pancreatic islet cell tumor, bronchogenic carcinomas, and medullary thyroid carcinomas secreting VIP (14, 16, 17). The clinical condition is clearly dependent from VIP effect on intestinal secretion and motility and inhibition of gastric acid secretion through gastrin release reduction. In a physiologic situation, VIP, derived from the subsequent cleavage and metabolic steps of 170-amino-acid precursor prepro-VIP, is released from several population of enteric nerve terminals, both cholinergic and non-cholinergic, from myenteric and submucosal nerve plexi of gastrointestinal tract, from cholinergic nerves in the pancreatic islet, and from enteric lymphoid tissues (6, 22). Following enterocyte VIP-mediated VPAC1 receptor activation, $HCO3^-$, $Cl^-$ and water secretion is stimulated in the ileum and colon but mainly in the duodenum by the apical $Cl^-/HCO_3^-$ exchanger and the cystic fibrosis transmembrane conductance regulator (9). Pancreatic secretion of $HCO3^-$ is also increased by VIP (23). In our case the autonomous and non-regulated release of massive amount of VIP by the malignant and metastatic PHEO led to refractory and fulminant diarrhea with severe fluid, potassium and bicarbonate

depletion (7–9, 24). A severe hyperchloremic metabolic acidosis with a serum anion gap of 16 mmol and a negative urine anion gap [$(Na^+ + K^+)$-$Cl^-$] was observed in our case. To avoid a wrong interpretation of the acid-base disorder it is important to remember that clinicians still refer to a normal range of the serum gap anion [$Na^+$- ($Cl^-$+ $HCO3^-$)] between 9 and 16 mmol/l but this is no longer true because of the change of measuring electrolyte techniques that brought normal values to lower ranges (4-11 mmol/l) (25). A 16 mmol/l of serum anion gap is just slightly above the normal range and this is an important issue because such a disturbance along with the negative urine anion gap would indicate that kidney is still able to excrete ammonium, and the cause of metabolic acidosis is mainly ascribed to the severe loss of bicarbonates related to VIP-mediated secretory diarrhea. However, while this is the most plausible explanation, we must consider some other factors that can interfere with the acid-base disorder in our case. The patient had an acute reduction in renal function from excessive volume depletion and arterial hypotension. Two conditions have to be taken into account; first, the acute renal functional reduction, that can interfere and reduce the significance of the urinary gap as an indicator of ammonium ion secretion. Second, the arterial hypotension can increase the serum anion gap by the generation of serum lactate, despite being modest the rise observed in our patient (26). Furthermore, a high generation of serum lactate could also be linked to excessive cell proliferation by the VIP-secreting malignant PHEO (27). Therefore, a mixed acidosis both with normal and high serum anion gap can better describe the acid-base disturbance of our patient as also evidenced by the excessive reduction of plasma bicarbonates compared to the slight increase in the serum anion gap. Severe metabolic acidosis determines hemodynamic and inflammatory consequences impairing cardiac contractile function and inducing arterial hyporeactivity through nitrogen and oxygen reactive species generation, altered catecholamine and intracellular calcium signaling (28–32). The altered glucose tolerance of our patient is also related to the effect of VIP high circulating levels, stimulating glucagon release and activating liver glycogenolysis, and to acidosis-mediated insulin resistance development, although a contribution of the modest catecholamines excess cannot be excluded (33, 34).

Based on the concept that neuroendocrine tumors widely express somatostatin receptors and as recommended by Food and Drug Administration and reported in literature (35, 36), we treated our patient with lanreotide acetate, a synthetic cyclical octapeptide analog of somatostatin to inhibit VIP release and improve the WDHA syndrome. Octreotide has been reported to inhibit VIP release from pancreatic tumors reducing diarrhea in 75% of cases (37) and in a case of WDHA syndrome caused by a VIP-producing PHEO to be able to reverse a shock condition (14). The inefficacy of lanreotide treatment in our case was probably due to the paucity of SSTR2A on VIP-secreting PHEO cells observed at immunohistochemistry (**Figure 2H**), as previously reported (19). The combined treatment with sunitinib, a multi-targeted receptor tyrosine kinase inhibitor, reported to be efficacious by Lebowitz-Amit et al. in terms of rapid and complete clinical response, did not show any favorable effects (17). Tumor progression and metastatic expansion in the liver and lung with massive release of VIP, unresponsive to therapies, precipitated the WDHA syndrome and patient clinical condition until his death.

In conclusion, our case showed a rare case of WDHA syndrome due to metastatic VIP-secreting PHEO, with an aggressive clinical behavior and high PASS score. Surgery did not completely eradicate the cancer and the scarcity of SSTR2A expression on tumor cells made the treatment with lanreotide unsuccessful. In order to promptly face clinical symptoms and tumor progression, careful attention should be paid to correctly interpret any non-classic symptoms of PHEO, producing and releasing in rare cases classes of hormones other than catecholamines.

## DATA AVAILABILITY STATEMENT

The raw data supporting the conclusions of this article will be made available by the authors, without undue reservation.

## ETHICS STATEMENT

The studies involving human participants were reviewed and approved by Comitato Etico Unico per la Provincia di Parma. The patients/participants provided their written informed consent to participate in this study.

## AUTHOR CONTRIBUTIONS

Attended the patient and performed diagnostic and laboratory analysis (AN, IV, NC, MZ, EN, EF, BP, RS, DC, GG, ACb). Collected the data and contributed to the analysis of literature data (IV, ST, BP, ACa, PC, LG, ACb). Discussion of the results (AN, IV, ST, PC, RV, ACb). Wrote the paper (AN, IV, ST, ACb). All authors contributed to the article and approved the submitted version.

## REFERENCES

1. Manger WM. The Protean Manifestations of Pheochromocytoma. *Horm Metab Res* (2009) 41:658–63. doi: 10.1055/s-0028-1128139
2. Davison AS, Jones DM, Ruthven S, Helliwell T, Shore SL. Clinical evaluation and treatment of phaeochromocytoma. *Ann Clin Biochem* (2018) 55:34–48. doi: 10.1177/0004563217739931
3. Negro A, Manicardi E, Grasselli C, Babini M, Santi R, Pugni V, et al. Severe ectopic Cushing's syndrome due to ACTH-secreting pheochromocytoma. *Int J Clin Med* (2013) 4(04):228–31. doi: 10.4236/ijcm.2013.44040
4. Negro A, Graiani G, Nicoli D, Farnetti E, Casali B, Verzicco I, et al. Concurrent heterozygous Von-Hippel-Lindau and transmembrane-protein-127 gene mutation causing an erythropoietin-secreting pheochromocytoma

in a normotensive patient with severe erythrocytosis. *J Hypertens* (2020) 38 (2):340–6. doi: 10.1097/HJH.0000000000002253
5. Verner JV, Morrison AB. Islet cell tumor and a syndrome of refractory watery diarrhea and hypokalemia. *Am J Med* (1958) 25:374–80. doi: 10.1016/0002-9343(58)90075-5
6. Harmar AJ, Fahrenkrug J, Gozes I, Laburthe M, May V, Pisegna JR, et al. Pharmacology and functions of receptors for vasoactive intestinal peptide and pituitary adenylate cyclase-activating polypeptide: IUPHAR Review 1. *Br J Pharmacol* (2012) 166:4–17. doi: 10.1111/j.1476-5381.2012.01871.x
7. Clarke LL, Harline MC. Dual role of CFTR in cAMP-stimulated HCO3- secretion across murine duodenum. *Am J Physiol* (1998) 274:G718–26. doi: 10.1152/ajpgi.1998.274.4.G718
8. Hogan DL, Crombie DL, Isenberg JI, Svendsen P, Schaffalitzky de Muckadell OB, Ainsworth MA. CFTR mediates cAMP- and Ca2+-activated duodenal epithelial HCO3- secretion. *Am J Physiol* (1997) 272:G872–8. doi: 10.1152/ajpgi.1997.272.4.G872
9. Seidler U, Blumenstein I, Kretz A, Viellard-Baron D, Rossmann H, Colledge WH, et al. A functional CFTR protein is required for mouse intestinal cAMP-, cGMP- and Ca (2+)-dependent HCO3- secretion. *J Physiol* (1997) 505:411–23. doi: 10.1111/j.1469-7793.1997.411bb.x
10. Bloom SR, Polak JM, Pearse AG. Vasoactive intestinal peptide and watery-diarrhoea syndrome. *Lancet* (1973) 2:14–5. doi: 10.1016/S0140-6736(73)91947-8
11. Said SI. Evidence for secretion of vasoactive intestinal peptide by tumours of pancreas, adrenal medulla, thyroid and lung: support for the unifying APUD concept. *Clin Endocrinol* (1976) 5:201S–4S. doi: 10.1111/j.1365-2265.1976.tb03828.x
12. ClinVar - NCBI – NIH. https://www.ncbi.nlm.nih.gov/clinvar/RCV000263653/#evidence.
13. Loehry CA, Kingham JG, Whorwell PJ. Watery diarrhoea and hypokalemia associated with a phaechromocytoma. *Postgrad Med J* (1975) 51:416–9. doi: 10.1136/pgmj.51.596.416
14. Hu X, Cao W, Zhao M. Octreotide reverses shoch due to vasoactive intestinal peptide-secreting adrenal pheochromocytoma: a case report and review of literature. *World J Clin Cases* (2018) 6(14):862–8. doi: 10.12998/wjcc.v6.i14.862
15. Ikuta S, Yasui C, Kawanaka M, Aihara T, Yoshie H, Yanagi H, et al. Watery diarrhea, hypokalemia and achlorhydria syndrome due to an adrenal pheochromocytoma. *World J Gastroenterol* (2007) 13:4649–52. doi: 10.3748/wjg.v13.i34.4649
16. Smith SL, Slappy AL, Fox TP, Scolapio JS. Pheochromocytoma producing vasoactive intestinal peptide. *Mayo Clin Proc* (2002) 77:97–100. doi: 10.4065/77.1.97
17. Amit RL, Mete O, Asa SL, Ezzat S, Joshua AM. Malignant pheochromocytoma secreting vasoactive intestinal peptide and response to sunitinib: a case report and literature review. *Endocr Pract* (2014) 20:145–50. doi: 10.4158/EP14093.CR
18. Sackel SG, Manson JE, Harawi SJ, Burakoff R. Watery diarrhea syndrome due to an adrenal pheochromocytoma secreting vasoactive intestinal polypeptide. *Dig Dis Sci* (1985) 30:1201–7. doi: 10.1007/BF01314057
19. Jiang J, Zhang L, Wu Z, Ai Z, Hou Y, Lu Z, et al. A rare case of watery diarrhea, hypokalemia and achlorhydria syndrome caused by pheochromocytoma. *BMC Cancer* (2014) 14:553. doi: 10.1186/1471-2407-14-553
20. Quarles Van Ufford Mannesse P, Castro Cabezas M, Vroom TM, Van Gils A, Lips CJ, Niermeijer P. A patient with neurofibromatosis type 1 and watery diarrhoea syndrome due to a VIP-producing adrenal phaechromocytoma. *J Intern Med* (1999) 246(2):231–4. doi: 10.1046/j.1365-2796.1999.00533.x
21. Grant S, Lutz EM, McPhaden AR, Wadsworth RM. Location and function of VPAC1, VPAC2 and NPR-C receptors in VIP-induced vasodilation of porcine basilar arteries. *J Cereb Blood Flow Metab* (2006) 26(1):58–67. doi: 10.1038/sj.jcbfm.9600163
22. Quatrini L, Vivier E, Ugolini S. Neuroendocrine regulation of innate lymphoid cells. *Immunol Rev* (2018) 286(1):120–36. doi: 10.1111/imr.12707
23. Fahrenkrug J, Schaffalitzky de Muckadell OB, Holst JJ, Jensen SL. Vasoactive intestinal polypeptide in vagally mediated pancreatic secretion of fluid and HCO3. *Am J Physiol* (1979) 237:E535–40. doi: 10.1152/ajpendo.1979.237.6.E535
24. Glad H, Ainsworth MA, Svendsen P, Fahrenkrug J. Schaffalitzky de Muckadell OB. Effect of vasoactive intestinal peptide and pituitary adenylate cyclase-activating polypeptide on pancreatic, hepatic and duodenal mucosal bicarbonate secretion in the pig. *Digestion* (2003) 67:56–66. doi: 10.1159/000069707
25. Wesson D, Batlle D, Saleem K, Nithin R. The use of bedside urinary parameters in the evaluation of Metabolic Acidosis. In: D Wesson, editor. *Metabolic Acidosis*. New York: Springer Science (2016). p. 39–51.
26. Regolisti G, Maggiore U, Rossi GM, Cabassi A, Fiaccadori E. Hyperchloremia and acute kidney injury: a spurious association or a worrisome reality? *Internal Emergency Med* (2020) 15:187–9. doi: 10.1007/s11739-019-02213-1
27. Verzicco I, Regolisti G, Quaini F, Bocchi P, Brusasco I, Ferrari M, et al. Electrolyte Disorders Induced by Antineoplastic Drugs. *Front Oncol* (2020) 10:779. doi: 10.3389/fonc.2020.00779
28. Levy B, Collin S, Sennoun N, Ducrocq N, Kimmoun A, Asfar P, et al. Vascular hyporesponsiveness to vasopressors in septic shock: from bench to bedside. *Intensive Care Med* (2010) 16:2019–29. doi: 10.1007/s00134-010-2045-8
29. Cabassi A, Binno SM, Tedeschi S, Ruzicka V, Dancelli S, Rocco R, et al. Low serum ferroxidase I activity is associated with mortality in heart failure and related to both peroxynitrite-induced cysteine oxidation and tyrosine nitration of ceruloplasmin. *Circ Res* (2014) 114:1723–32. doi: 10.1161/CIRCRESAHA.114.302849
30. Cabassi A, Binno SM, Tedeschi S, Graiani G, Galizia C, Bianconcini M, et al. Myeloperoxidase-Related Chlorination Activity Is Positively Associated with Circulating Ceruloplasmin in Chronic Heart Failure Patients: Relationship with Neurohormonal, Inflammatory, and Nutritional Parameters. *BioMed Res Int* (2015) 2015:691693. doi: 10.1155/2015/691693
31. Cabassi A, Vinci S, Quartieri F, Moschini L, Borghetti A. Norepinephrine reuptake is impaired in skeletal muscle of hypertensive rats in vivo. *Hypertension* (2001) 37:698–702. doi: 10.1161/01.HYP.37.2.698
32. Miragoli M, Cabassi A. Mitochondrial Mechanosensor Microdomains in Cardiovascular Disorders. *Adv Exp Med Biol* (2017) 982:247–64. doi: 10.1007/978-3-319-55330-6_13
33. Hauner H, Glatting G, Kaminska D, Pfeiffer EF. Effect of vasoactive intestinal polypeptide (VIP) on glucose and lipid metabolism of isolated rat adipocytes. *Res Exp Med* (1988) 188:189–95. doi: 10.1007/BF01852320
34. Szecówka J, Lins PE, Tatemoto K, Efendić S. Effects of porcine intestinal heptacosapeptide and vasoactive intestinal polypeptide on insulin and glucagon secretion in rats. *Endocrinology* (1983) 112:1469–73. doi: 10.1210/endo-112-4-1469
35. Plouin PF, Bertherat J, Chatellier G, Billaud E, Azizi M, Grouzmann E, et al. Short-term effects of octreotide on blood pressure and plasma catecholamines and neuropeptide Y levels in patients with phaeochromocytoma: a placebo-controlled trial. *Clin Endocrinol (Oxf)* (1995) 42:289–94. doi: 10.1111/j.1365-2265.1995.tb01877.x
36. Lamarre-Cliche M, Gimenez-Roqueplo AP, Billaud E, Baudin E, Luton JP, Plouin PF. Effects of slow-release octreotide on urinary metanephrine excretion and plasma chromogranin A and catecholamine levels in patients with malignant or recurrent phaeochromocytoma. *Clin Endocrinol (Oxf)* (2002) 57:629–34. doi: 10.1046/j.1365-2265.2002.01658.x
37. Gomes-Porras M, Cárdenas-Salas J, Álvarez-Escolá C. Somatostatin Analogs in Clinical Practice: a Review. *Int J Mol Sci* (2020) 21:1682. doi: 10.3390/ijms21051682

**Conflict of Interest:** The authors declare that the research was conducted in the absence of any commercial or financial relationships that could be construed as a potential conflict of interest.

frontiers in Endocrinology

CASE REPORT
published: 19 March 2021
doi: 10.3389/fendo.2021.662377

# Case Report: Ectopic Adrenocortical Carcinoma in the Ovary

*Wen-Hsuan Tsai*[1], *Tze-Chien Chen*[2], *Shuen-Han Dai*[3] *and Yi-Hong Zeng*[1,4]*

[1] Division of Endocrinology and Metabolism, Department of Internal Medicine, Mackay Memorial Hospital, Taipei, Taiwan, [2] Department of Obstetrics and Gynecology, Mackay Memorial Hospital, Taipei, Taiwan, [3] Department of Pathology, Mackay Memorial Hospital, Taipei, Taiwan, [4] Department of Medicine, MacKay Medical College, New Taipei City, Taiwan

Adrenocortical carcinoma (ACC) is a rare malignancy with an incidence of 0.7–2.0 cases/million habitants/year. ACCs are rare and usually endocrinologically functional. We present the case of a 59-year-old woman who experienced abdominal fullness for 6 months and increased abdominal circumference. A large pelvic tumor was observed. She underwent cytoreductive surgery and the pathological test results revealed local tumor necrosis and prominent lympho-vascular invasion. Neuroendocrine carcinoma was the first impression, but positivity for synaptophysin, alpha-inhibin, transcription factor enhancer 3 (TFE-3), calretinin (focal), and CD56 (focal) and high Ki-67-labeling proliferating index (>80%) confirmed the diagnosis of ectopic ACC. Ectopic primary aldosteronism could not be excluded. However, we did not perform saline infusion test or captopril test due to poor performance status. When pathological test reports reveal neuroendocrine features not typically found in the organ being examined, IHC staining should be performed to rule out ectopic ACC. Whether the ectopic ACC is functional or not requires complete survey.

**Keywords: ectopic, adrenocortical carcinoma, ovary, immunohistochemistry, metastasis**

OPEN ACCESS

***Edited by:***
*Barbara Altieri,*
*University Hospital of Wuerzburg, Germany*

***Reviewed by:***
*Letizia Canu,*
*University of Florence, Italy*
*Canan Ersoy,*
*Uludağ University, Turkey*

***Correspondence:**
*Yi-Hong Zeng*
*starrydouchain@gmail.com*

***Specialty section:***
*This article was submitted to Cancer Endocrinology, a section of the journal Frontiers in Endocrinology*

***Received:*** *01 February 2021*
***Accepted:*** *05 March 2021*
***Published:*** *19 March 2021*

***Citation:***
*Tsai W-H, Chen T-C, Dai S-H and Zeng Y-H (2021) Case Report: Ectopic Adrenocortical Carcinoma in the Ovary. Front. Endocrinol. 12:662377. doi: 10.3389/fendo.2021.662377*

## INTRODUCTION

Adrenocortical carcinoma (ACC) is a rare malignancy with an incidence of 0.7–2.0 cases/million habitants/year. It occurs at any age, with two peaks in the first decade of life and between 40 and 50 years. Women are frequently affected (55–60%) (1). The adrenal glands are of dual embryological origin. The adrenal cortex is derived from the coelomic mesoderm of the urogenital ridge, and the adrenal medulla arises from the neural crest tissue (2). Ectopic adrenal rests exist along the migration path of adrenal cortex development, and these anatomic sites include the celiac plexus, kidney, ovary, broad ligament, testis, and spermatic cord (3, 4). The brain, lungs, and stomach have been reported to be rare sites of ectopic rests (3, 4). Ectopic adrenal tissue is found in 50% neonates, and most of the ectopic rests undergo atrophy (5). The occurrence of adrenal rest tissue in adults is 1% (6).

Tumors arising from adrenal rests are uncommon and most of them are functional, resulting in endocrinopathy diagnosed pre-operatively (7). Non-functional tumors are also uncommon and are usually discovered incidentally or during autopsy (7). Malignancies arising from adrenal rests are extremely rare with very few cases reported (8), showing a mean patient age of 36.4 years (0.4–65 years) and equal sex distribution (female:male ratio, 7:6). Studies have reported tumors located in the retroperitoneum (n = 5), testis/scrotum (n = 3), liver (n = 2), kidney (n = 1), spinal cord (n = 1), and pelvis (n = 1); 62% of the tumors were functional, with Cushing's syndrome as the most

common presentation (8). Herein, we present the case of a 59-year-old woman with ectopic ACC in the ovary. Consent has not been obtained because the patient is deceased.

## CASE REPORT

Our patient was a 59-year-old woman who had no past medical history. She delivered three children and entered menopause at the age of 49 years. She complained of lower abdominal fullness for 6 months and increased abdominal circumference. She also experienced stress urinary incontinence, without dysuria, urinary frequency, or urinary urgency. She lost up to 3 kg of body weight in 1 month and had oedema in both feet. There was no fever, bowel habit change, nausea, vomiting, abdominal pain, or tarry/bloody stool. She visited a hospital where a giant pelvic mass was found. She was transferred to our hospital in April 2019. The initial laboratory work report is shown in **Table 1**. Profound elevated Lactate dehydrogenase (4123 IU/L, 98 – 192 IU/L), elevated Carbohydrate antigen 19-9 (39.34 U/mL, <37 U/mL) and Cancer antigen 125 (146.32 U/mL, <35 U/mL) was noted. Gynaecologic sonography showed a huge pelvic mass of approximately 22.5 × 13.3 × 16.1 cm in size. Computed tomography (CT) scans revealed a 23 × 17 × 21 cm heterogeneous mass occupying the lower abdomen and pelvic cavity with indistinct margin from the uterus and bilateral adnexa, suggestive of gynaecologic malignancy. There were multiple small peritoneal nodules, multiple enlarged para-aortic and bilateral iliac lymph nodes, and multiple small pulmonary metastases and lymph nodes over the left lower neck and left supra-clavicular regions (**Figure 1**). The visible liver and adrenal glands were unremarkable. She underwent optimal cytoreductive surgery for symptom relief. Left neck mass excision was performed. The initial pathological test report suggested suspected neuroendocrine carcinoma over bilateral ovaries, bilateral fallopian tubes, and the uterus, with omentum and lymph node metastasis. Right ovarian neuroendocrine carcinoma, stage IVB pT3cN1bM1, was the initially postulated diagnosis.

She underwent postoperative chemotherapy with triweekly Etoposide (100mg/m$^2$) and Cisplatin (100mg/m$^2$). After consultation and discussion with another pathologist, the final pathological test report 2 months later showed ACC, probably arising from the adrenal cortical rest (**Figures 2** and **3**). Weiss score was 8 after discussion with pathologist. Hypertension

**TABLE 1** | Laboratory test for ovary tumor.

| | | |
|---|---|---|
| White blood cell count | 8,500 | (4,000–10,000)/μL |
| Hemoglobin | 13.5 | (11–16) g/dL |
| Platelet count | 291,000 | (140,000–450,000)/μL |
| Creatinine | 0.8 | (0.4–1.2) mg/dL |
| Alanine aminotransferase | 31 | (14–40) IU/L |
| Sodium | 142 | (136–144) mEq/L |
| Potassium | 3.8 | (3.5–5.1) mEq/L |
| Lactate dehydrogenase | 4,123 | (98–192) IU/L |
| Carcinoembryonic antigen | 0.93 | (<5.00) ng/mL |
| Alpha-Fetoprotein | 2.66 | (<10.00) ng/mL |
| Carbohydrate antigen 19-9 | 39.34 | (<37.00) U/mL |
| Cancer antigen 125 | 146.32 | (<35.00) U/mL |

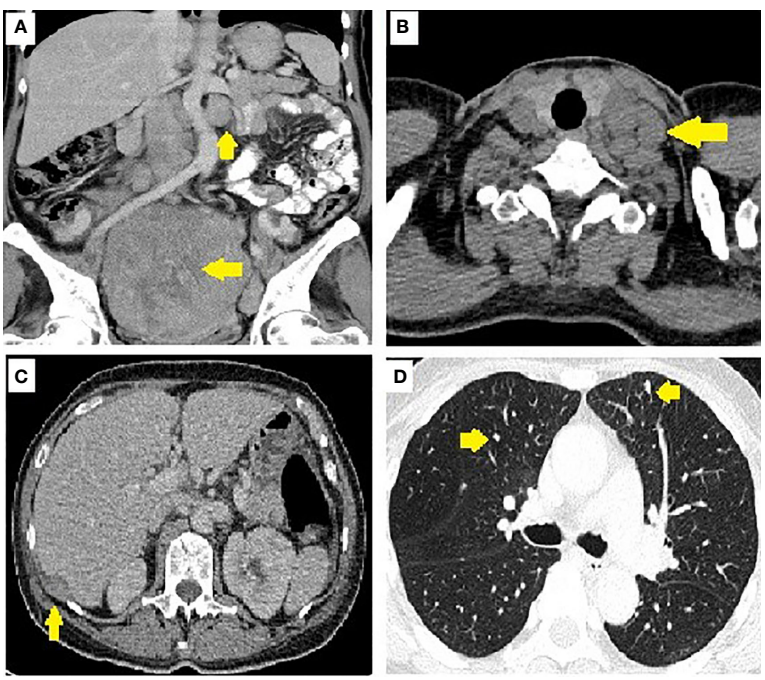


**FIGURE 1** | Image of pelvic tumor and metastasis. **(A)** Para-aortic lymph nodes and pelvic tumor. **(B)** Supraclavicular lymph nodes. **(C)** Sub-diaphragmatic seeding. **(D)** Lung metastasis.

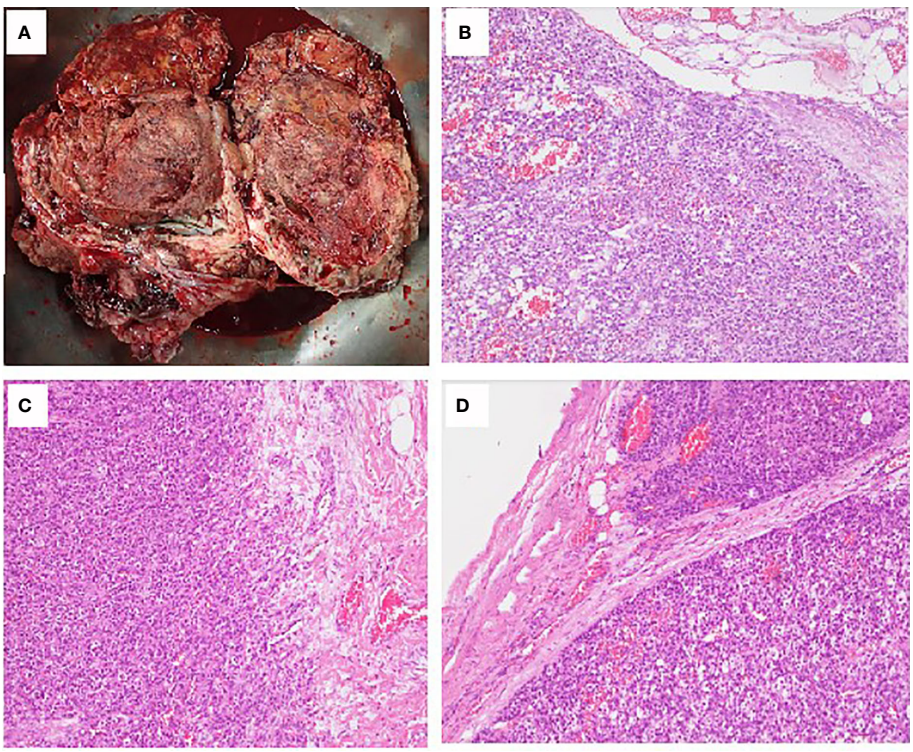


**FIGURE 2** | Pathological findings of ovarian adrenocortical carcinoma. **(A)** A piece of tissue measuring 23 × 17 × 10 cm in size. **(B)** Sections of the huge ovary and uterine body tumor showing solid sheets and nests of tumor cells with monotonous morphology with large, centrally located nuclei and abundant cytoplasm. Focal tumor necrosis is present. Lymphovascular invasion is prominent. **(C)** Biopsy sample of the peritoneum cavity. **(D)** Lymph node metastasis: Lesion cells are arranged in thick trabeculae and in organoid pattern. They contain eosinophilic cytoplasm and small dark nuclei. High prevalence of mitotic figures is seen.

withnormal potassium level was noted during admission. She took amlodipine 5mg per day. The endocrine profile is listed in **Table 2**, which revealed normal aldosterone (12.8 ng/dL, 4.83–27 ng/dL) and decreased plasma renin activity (0.14 ng/mL/hr, 0.6–4.18 ng/mL/hr) level. ARR ratio was 91.4. Hence, ectopic primary aldosteronism could not be excluded. However, we did not perform saline infusion test or captopril test at that time because she was receiving chemotherapy and suffered from abdomen fullness, nausea and vomiting. She received dexamethasone as support therapy during chemotherapy. Leukopenia (900/μL) was noted. Cortisol and ACTH level was checked on the same day. Hence, the normal cortisol (10.54 μg/dL, 9.52–26.21 μg/dL) with elevated ACTH (70.26 pg/mL, 10–70 pg/mL) may be interpreted as acute illness. Follow up cortisol and ACTH level was 17.08 μg/dL and 20.15 pg/mL, respectively.

She received six courses of etoposide and cisplatin regimen and six courses of bevacizumab (900mg). However, LDH level elevated after completion of chemotherapy. Follow-up CT 6 months after the operation showed disease progression, with enlarged left supraclavicular and retrocaval lymph nodes, increased size of lung metastasis, and increased size and number of liver metastases and peritoneal seedings. She received mitotane 500mg per day 6 months after operation and mitotane was titrated to 1000mg per day. She used mitotane intermittently due to nausea, vomiting, poor appetite and dizziness. She was admitted to our hospital several times for poor appetite, vaginal bleeding, anaemia, and renal failure. She expired 9 months after cytoreductive surgery.

## DISCUSSION

We presented the case of a 59-year-old woman who was diagnosed with ectopic ACC in the ovary. Initial pathological studies revealed the presence of local tumor necrosis and prominent lympho-vascular invasion. The Ki-67 proliferation labelling index was very high (>80%). Immunohistochemically, tumor cells were focally positive for CD56 and synaptophysin but also focally positive for calretinin. Two months later, the pathologist confirmed the diagnosis of ectopic ACC based on positivity for synaptophysin, alpha-inhibin, TFE-3, calretinin (focal), and CD56 (focal) and a high Ki-67-labeling proliferating index (>80%), which was much higher than usual ACC. Melan-A and steroidogenic factor-1 (SF1) were not available in our hospital. Adrenal gland was unlikely to be the origin because there was no adrenal lesion identified in the serial image studies. Ectopic primary aldosteronism could not be excluded. However, we did not perform saline infusion test or captopril test at that time because she was receiving chemotherapy and suffered from abdomen fullness, nausea and

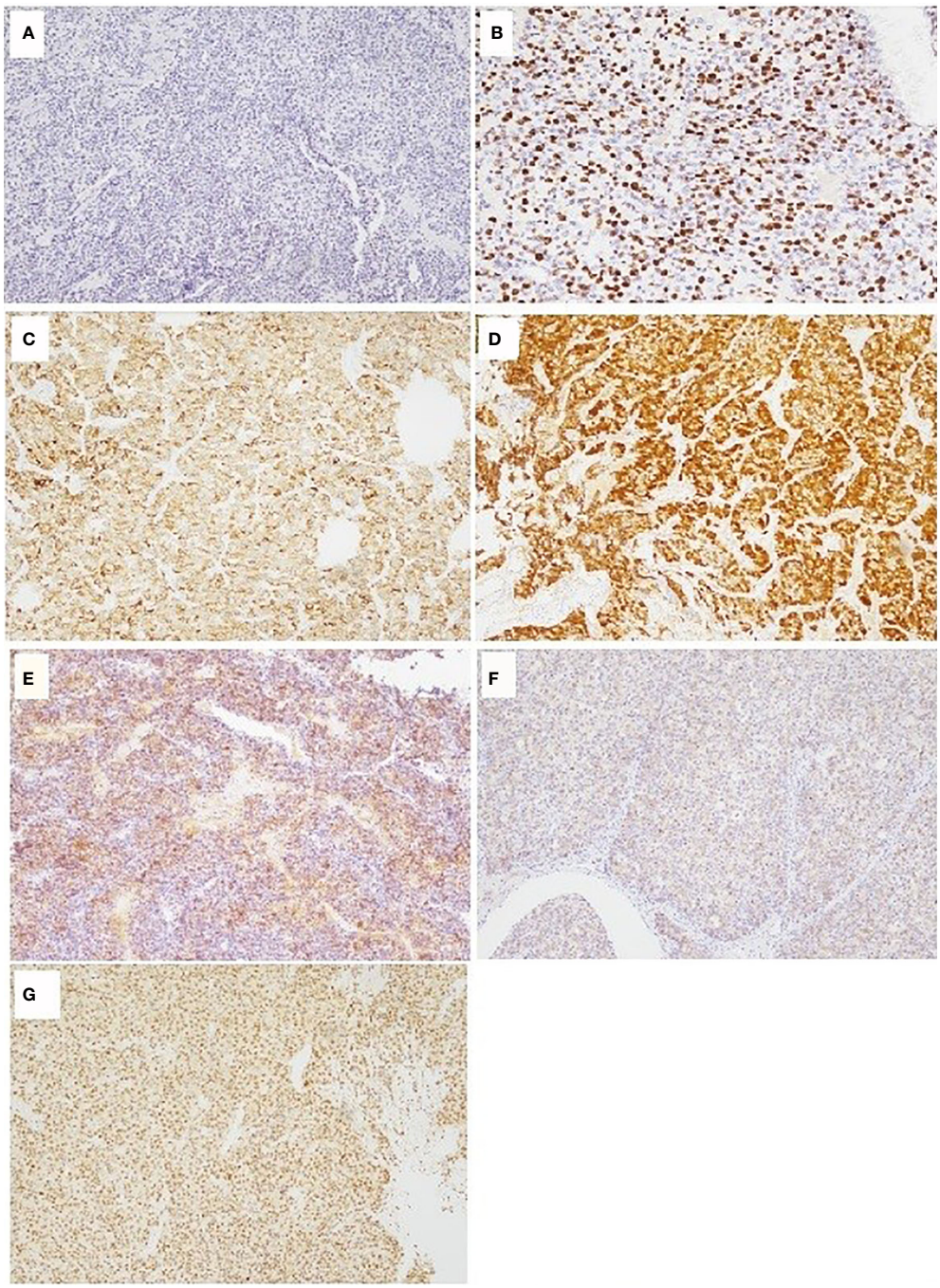


**FIGURE 3** | Immunohistochemistry of ovarian adrenocortical carcinoma. **(A)** Chromogranin A 100×: negative; **(B)** Ki-67 200×: high Ki-67-labeling proliferating index (>80%); **(C)** Alpha-inhibin 100×: positive; **(D)** Calretinin 100×: focally positive; **(E)** CD56 100×: focally positive; **(F)** Synaptophysin 100×: focally positive; **(G)** TFE-3 100×: positive.

vomiting. Hence, we would not define whether this ectopic ACC was functional or non-functional, which was our limitation. Mitotane was immediately considered when ectopic ACC was diagnosed. However, project application was required in Taiwan before we started mitotane. Despite that adjuvant radiotherapy (RT) is important for local tumor control (9), RT was not considered due to multiple distant metastasis in our patient.

To our knowledge, there were only two reported cases of ectopic adrenocortical carcinoma in the ovary. Chentli presented the case of a 34-year-old female referred for Cushing's syndrome in the postpartum period. The adrenal origin of the ectopic tissue was

**TABLE 2** | Hormone profile for ovarian adrenocortical carcinoma.

| | | |
|---|---|---|
| Cortisol | 10.54 | (9.52–26.21) μg/dL |
| Adrenocorticotropic hormone | 70.26 | (10–70) pg/mL |
| Plasma renin activity | 0.14 | (0.6–4.18) ng/mL/hr |
| Aldosterone | 12.8 | (4.83–27) ng/dL |
| Oestrogen | <10 | (menopause <10–28) pg/mL |
| Testosterone | <0.1 | (<0.95) ng/mL |
| Dehydroepiandrosterone sulphate | 12.9 | (3.70–242.4) μg/dL |

confirmed by immunostaining positivity to inhibin-α, melan-A, steroidogenic factor-1 (SF1), and synaptophysin (10). In another study, a 4-year-old girl initially presented with signs of rapid (within 1 month) early puberty (breast development plus pubic and armpit hair) (11). A right ovary mass was noted when she was 15 years old. Pathological examination revealed a 20-cm ovarian steroid tumor. At 21 years of age, pulmonary metastasis was detected. Complete remission of lung metastasis was achieved 5 years after mitotane initiation. The medical history was suggestive of a slowly progressive tumor. The patient was alive for 10 years after the initial operation (11).

Adrenal tumors in the ovary may originate from transformation of the adrenocortical embryonic remnants that break off during adrenal migration or descent of gonadal cells (12). Ectopic adrenal adenomas/carcinomas may result from the mutation of ovarian tissue and its steroid enzymes and/or acquisition of aberrant receptors (13). This pathological situation induces the ovary to synthesize adrenal hormones (14). Steroidogenic factor 1 (SF-1) is the most valid marker of ACC (15). Ki-67 can help define the diagnosis and prognosis of ACC. The general agreement is that ACCs have a Ki-67 labelling index of ≥5% (16). Ki-67 is a powerful prognostic marker in both localized and metastatic ACC (17–19). Positivity for steroid receptor coactivator-1 (SRC-1), inhibin, calretinin, synaptophysin, and melan A and negativity for Pax8, chromogranin, and high-molecular weight cytokeratin (HMWCK) on immunohistochemistry (IHC) studies may help distinguish ACC from other tumors (20).

The 5-year survival of patients with ACC is, respectively, 60–80%, 35–50%, and 0–28% in cases of tumors confined to the adrenal space, locally advanced disease, and metastatic disease (21). There is limited knowledge on the incidence and prognosis of ectopic ACC. In previous studies, the 5- and 10-year survival of patients who underwent resection of ectopic ACC was 26–38% and 7%, respectively (22–24). Surgical resection is the mainstay of treatment (22, 25). Patients with early mortality were found to have high rates of cortisol-secreting tumors and positive resection margins and high disease stages with nodal or synchronous distant metastasis (22–24). The importance of surgery was further confirmed by long-term survival attained with repeat resection of local or distant tumor recurrence (22). According to the presented cases, diagnosis of ectopic ACC is challenging; 50–60% of patients with ACC show clinical hormone excess (21). Hypercortisolism or mixed Cushing's and virilizing symptoms are observed in the majority of these patients (21).

## CONCLUSION

We presented a rare case of ectopic ACC in the ovary. ACC is a rare disease, and ectopic ACC is even rarer. There is limited knowledge of its incidence and prognosis. When encountering hypercortisolism or mixed Cushing's and virilizing symptoms without detectable adrenal nor pituitary tumors, ectopic tumor should be suspected. On the other hand, when pathological tests reveal atypical neuroendocrine feature of the organ, further IHC staining should be performed to rule out ectopic ACC. Whether the ectopic ACC is functional or not requires complete survey.

## DATA AVAILABILITY STATEMENT

The original contributions presented in the study are included in the article/supplementary material. Further inquiries can be directed to the corresponding author.

## ETHICS STATEMENT

The studies involving human participants were reviewed and approved by Mackay Memorial Hospital. Written informed consent for participation was not required for this study in accordance with the national legislation and the institutional requirements. Written informed consent was not obtained from the individual(s) for the publication of any potentially identifiable images or data included in this article.

## AUTHOR CONTRIBUTIONS

W-HT: writing and literature search. T-CC: medical and surgical practices. S-HD: analysis and interpretation. Y-HZ: concept, design, and medical practice. All authors contributed to the article and approved the submitted version.

## ACKNOWLEDGMENTS

The authors hereby thank Editage Taiwan for language assistance during the preparation of the manuscript.

## REFERENCES

1. Kebebew E, Reiff E, Duh QY, Clark OH, McMillan A. Extent of disease at presentation and outcome for adrenocortical carcinoma: have we made progress? *World J Surg* (2006) 30(5):872–8. doi: 10.1007/s00268-005-0329-x
2. Barwick TD, Malhotra A, Webb JA, Savage MO, Reznek RH. Embryology of the adrenal glands and its relevance to diagnostic imaging. *Clin Radiol* (2005) 60(9):953–9. doi: 10.1016/j.crad.2005.04.006
3. Ren PT, Fu H, He XW. Ectopic adrenal cortical adenoma in the gastric wall: case report. *World J Gastroenterol* (2013) 19(5):778–80. doi: 10.3748/wjg.v19.i5.778
4. Makino K, Kojima R, Nakamura H, Morioka M, Iyama K, Shigematsu K, et al. Ectopic adrenal cortical adenoma in the spinal region: case report and review

of the literature. *Brain Tumor Pathol* (2010) 27(2):121–5. doi: 10.1007/s10014-010-0270-z
5. Anderson JR, Ross AH. Ectopic adrenal tissue in adults. *Postgrad Med J* (1980) 56(661):806–8. doi: 10.1136/pgmj.56.661.806
6. Souverijns G, Peene P, Keuleers H, Vanbockrijck M. Ectopic localisation of adrenal cortex. *Eur Radiol* (2000) 10(7):1165–8. doi: 10.1007/s003309900263
7. Goren E, Engelberg IS, Eidelman A. Adrenal rest carcinoma in hilum of kidney. *Urology* (1991) 38(2):187–90. doi: 10.1016/S0090-4295(05)80085-8
8. Cornejo KM, Afari HA, Sadow PM. Adrenocortical Carcinoma Arising in an Adrenal Rest: a Case Report and Review of the Literature. *Endocr Pathol* (2017) 28(2):165–70. doi: 10.1007/s12022-017-9472-9
9. Gharzai LA, Green MD, Griffith KA, Else T, Mayo CS, Hesseltine E, et al. Adjuvant Radiation Improves Recurrence-Free Survival and Overall Survival in Adrenocortical Carcinoma. *J Clin Endocrinol Metab* (2019) 104(9):3743–50. doi: 10.1210/jc.2019-00029
10. Chentli F, Terki N, Azzoug S. Ectopic adrenocortical carcinoma located in the ovary. *Eur J Endocrinol* (2016) 175(4):K17–23. doi: 10.1530/EJE-16-0224
11. Salle L, Mas R, Teissier-Clément MP. Ectopic adrenocortical carcinoma of the ovary: An unexpected outcome. *Ann Endocrinol (Paris)* (2020) 81(5):516–8. doi: 10.1016/j.ando.2020.07.1112
12. Vassiliadi D, Tsagarakis S. Unusual causes of Cushing's syndrome. *Arq Bras Endocrinol Metabol* (2007) 51(8):1245–52. doi: 10.1590/S0004-27302007000800010
13. Lacroix A, Ndiaye N, Tremblay J, Hamet P. Ectopic and abnormal hormone receptors in adrenal Cushing's syndrome. *Endocr Rev* (2001) 22(1):75–110. doi: 10.1210/edrv.22.1.0420
14. Ayala AR, Basaria S, Udelsman R, Westra WH, Wand GS. Corticotropin-independent Cushing's syndrome caused by an ectopic adrenal adenoma. *J Clin Endocrinol Metab* (2000) 85(8):2903–6. doi: 10.1210/jcem.85.8.6749
15. Duregon E, Volante M, Giorcelli J, Terzolo M, Lalli E, Papotti M. Diagnostic and prognostic role of steroidogenic factor 1 in adrenocortical carcinoma: a validation study focusing on clinical and pathologic correlates. *Hum Pathol* (2013) 44(5):822–8. doi: 10.1016/j.humpath.2012.07.025
16. Creemers SG, Hofland LJ, Korpershoek E, Franssen GJ, van Kemenade FJ, de Herder WW, et al. Future directions in the diagnosis and medical treatment of adrenocortical carcinoma. *Endocr Relat Cancer* (2016) 23(1):R43–69. doi: 10.1530/ERC-15-0452
17. Berruti A, Fassnacht M, Baudin E, Hammer G, Haak H, Leboulleux S, et al. Adjuvant therapy in patients with adrenocortical carcinoma: a position of an international panel. *J Clin Oncol* (2010) 28(23):e401–2; author reply e3. doi: 10.1200/JCO.2009.27.5958
18. Beuschlein F, Weigel J, Saeger W, Kroiss M, Wild V, Daffara F, et al. Major prognostic role of Ki67 in localized adrenocortical carcinoma after complete resection. *J Clin Endocrinol Metab* (2015) 100(3):841–9. doi: 10.1210/jc.2014-3182
19. Libé R, Borget I, Ronchi CL, Zaggia B, Kroiss M, Kerkhofs T, et al. Prognostic factors in stage III-IV adrenocortical carcinomas (ACC): an European Network for the Study of Adrenal Tumor (ENSAT) study. *Ann Oncol* (2015) 26(10):2119–25. doi: 10.1093/annonc/mdv329
20. Weissferdt A, Phan A, Suster S, Moran CA. Adrenocortical carcinoma: a comprehensive immunohistochemical study of 40 cases. *Appl Immunohistochem Mol Morphol* (2014) 22(1):24–30. doi: 10.1097/PAI.0b013e31828a96cf
21. Fassnacht M, Dekkers OM, Else T, Baudin E, Berruti A, de Krijger R, et al. European Society of Endocrinology Clinical Practice Guidelines on the management of adrenocortical carcinoma in adults, in collaboration with the European Network for the Study of Adrenal Tumors. *Eur J Endocrinol* (2018) 179(4):G1–g46. doi: 10.1530/EJE-18-0608
22. Tran TB, Postlewait LM, Maithel SK, Prescott JD, Wang TS, Glenn J, et al. Actual 10-year survivors following resection of adrenocortical carcinoma. *J Surg Oncol* (2016) 114(8):971–6. doi: 10.1002/jso.24439
23. Tritos NA, Cushing GW, Heatley G, Libertino JA. Clinical features and prognostic factors associated with adrenocortical carcinoma: Lahey Clinic Medical Center experience. *Am Surg* (2000) 66(1):73–9.
24. Icard P, Goudet P, Charpenay C, Andreassian B, Carnaille B, Chapuis Y, et al. Adrenocortical carcinomas: surgical trends and results of a 253-patient series from the French Association of Endocrine Surgeons study group. *World J Surg* (2001) 25(7):891–7. doi: 10.1007/s00268-001-0047-y
25. Bani-Hani KE. Primary non-functional extra-adrenal adrenocortical carcinoma. *Saudi Med J* (2003) 24(3):301–4.

**Conflict of Interest:** The authors declare that the research was conducted in the absence of any commercial or financial relationships that could be construed as a potential conflict of interest.

frontiers in Endocrinology

CASE REPORT
published: 23 March 2021
doi: 10.3389/fendo.2021.643328

# Case Report: Abdominal Lymph Node Metastases of Parathyroid Carcinoma: Diagnostic Workup, Molecular Diagnosis, and Clinical Management

*Christina Lenschow[1]*, Carmina Teresa Fuss[2], Stefan Kircher[3], Andreas Buck[4], Ralph Kickuth[5], Joachim Reibetanz[1], Armin Wiegering[1], Albrecht Stenzinger[6,7], Daniel Hübschmann[8], Christoph Thomas Germer[1], Martin Fassnacht[2,9], Stefan Fröhling[10], Nicolas Schlegel[1] and Matthias Kroiss[2,9,11]*

*[1] Department of General, Visceral, Transplant, Vascular and Pediatric Surgery, University Hospital Würzburg, University of Würzburg, Würzburg, Germany, [2] Department of Internal Medicine I, Division of Endocrinology and Diabetes, University Hospital, University of Würzburg, Würzburg, Germany, [3] Institute of Pathology, University of Würzburg, Würzburg, Germany, [4] Department of Nuclear Medicine, University Hospital Würzburg, University of Würzburg, Würzburg, Germany, [5] Department of Diagnostic and Interventional Radiology, University Hospital Würzburg, University of Würzburg, Würzburg, Germany, [6] Institute of Pathology, University Hospital Heidelberg, Heidelberg, Germany, [7] Germany and German Cancer Consortium (DKTK), Heidelberg Partner Site, Heidelberg, Germany, [8] Computational Oncology, Molecular Diagnostics Program, NCT Heidelberg and Heidelberg University Hospital, Heidelberg, Germany, [9] Comprehensive Cancer Center Mainfranken, University of Würzburg, Würzburg, Germany, [10] National Center for Tumor Diseases (NCT Heidelberg), Division of Translational Medical Oncology German Cancer Research Center (DKFZ), University Hospital Heidelberg, Heidelberg, Germany, [11] Department of Medicine IV, University Hospital Munich, Ludwig-Maximilians-Universität München, Munich, Germany*

OPEN ACCESS

**Edited by:**
*Enzo Lalli, UMR7275 Institut de pharmacologie moléculaire et cellulaire (IPMC), France*

**Reviewed by:**
*Alfredo Campenni', University of Messina, Italy*
*Christian Albert Koch, Fox Chase Cancer Center, United States*

***Correspondence:**
*Christina Lenschow*
*Lenschow_C@ukw.de*

**Specialty section:**
*This article was submitted to Cancer Endocrinology, a section of the journal Frontiers in Endocrinology*

**Received:** *17 December 2020*
**Accepted:** *04 February 2021*
**Published:** *23 March 2021*

**Citation:**
*Lenschow C, Fuss CT, Kircher S, Buck A, Kickuth R, Reibetanz J, Wiegering A, Stenzinger A, Hübschmann D, Germer CT, Fassnacht M, Fröhling S, Schlegel N and Kroiss M (2021) Case Report: Abdominal Lymph Node Metastases of Parathyroid Carcinoma: Diagnostic Workup, Molecular Diagnosis, and Clinical Management. Front. Endocrinol. 12:643328. doi: 10.3389/fendo.2021.643328*

Parathyroid carcinoma (PC) is an orphan malignancy accounting for only ~1% of all cases with primary hyperparathyroidism. The localization of recurrent PC is of critical importance and can be exceedingly difficult to diagnose and sometimes futile when common sites of recurrence in the neck and chest cannot be confirmed. Here, we present the diagnostic workup, molecular analysis and multimodal therapy of a 46-year old woman with the extraordinary manifestation of abdominal lymph node metastases 12 years after primary diagnosis of PC. The patient was referred to our endocrine tumor center in 2016 with the aim to localize the tumor causative of symptomatic biochemical recurrence. In view of the extensive previous workup we decided to perform [18F]FDG-PET-CT. A pathological lymph node in the liver hilus showed slightly increased FDG-uptake and hence was suspected as site of recurrence. Selective venous sampling confirmed increased parathyroid hormone concentration in liver veins. Abdominal lymph node metastasis was resected and histopathological examination confirmed PC. Within four months, the patient experienced biochemical recurrence and based on high tumor mutational burden detected in the surgical specimen by whole exome sequencing the patient received immunotherapy with pembrolizumab that led to a biochemical response. Subsequent to disease progression repeated abdominal lymph node resection was performed in 10/2018, 01/2019 and in 01/2020. Up to now (12/2020) the patient is biochemically free of

disease. In conclusion, a multimodal diagnostic approach and therapy in an interdisciplinary setting is needed for patients with rare endocrine tumors. Molecular analyses may inform additional treatment options including checkpoint inhibitors such as pembrolizumab.

**Keywords: parathyroid carcinoma, abdominal lymph node metastases, molecular diagnostics, repeated surgery, [18F]FDG-PET-CT, immune check inhibitor, pembrolizumab**

## INTRODUCTION

Parathyroid carcinoma PC is an orphan malignancy occurring in approximately 1%–5% (United States, Europe, Japan) of all patients with primary hyperparathyroidism (pHPT) (1–5). The main pre-operative challenge of PC is to raise the suspicion of malignant disease at diagnosis since clinical outcome and prognosis are largely dependent on the extent of primary surgery. Despite the combination of multiple diagnostic modalities, this rare tumor is often difficult to diagnose preoperatively (6–9). Moreover, diagnosis of malignancy is made in only 15% of the fast-frozen sections. So, in the vast majority of cases, only the final histology or a relapse provides the diagnosis (10).

The high rate of relapse is another considerable problem in PC patients. We have recently published a comprehensive clinical characterization of 83 PC cases and have demonstrated that within a median interval of 48 months 38.6% of cases relapsed (7). However, in case of biochemical recurrence, the precise localization of cancerous tissue is mandatory to enable surgical treatment. The calcimimetic drug cinacalcet is approved to control serum calcium and may be used in case of unsuccessful localization and/or advanced, non-resectable disease. Systemic antitumoral therapy has remained anecdotal (11).

To date, only very few cases of PC with abdominal tumor localization (peripancreatic lymph nodes: n=1, liver n= 6) have been described (12–14).

Here, we present the complex diagnostic workup and multimodal therapy in a 46-year old woman with the uncommon manifestation of abdominal metastases of PC.

## CASE DESCRIPTION

A 46-year old woman was referred to our endocrine tumor center in 2016 with the aim to localize the tumor causative of biochemical recurrence.

Primary surgery due to pHPT had been performed in 2004. Intraoperatively, PC was suspected and en-bloc-resection (hemithyroidectomy, parathyroidectomy and central lymph node dissection of the left side) was performed. PC was confirmed histopathologically and resection margins were free of tumor (R0). The patient experienced a permanent recurrent laryngeal nerve palsy at the left side as complication of the surgical procedure. She underwent postoperative adjuvant external beam radiation of the thyroid region at a total dose of 50.4 Gy. The patient was subsequently free of disease for 12 years.

In 2016, the patient experienced symptoms similar to those at initial diagnosis with thirst, fatigue and visual flashes. Serum calcium was elevated up to 3.4 mmol/L [reference range: 2.0–2.7mmol/L] and parathyroid hormone (PTH) was increased to 203 pg/mL [10–65pg/ml]. Medication with cinacalcet was initiated. Within the three subsequent months, the patient underwent cervical ultrasonography, CT and MRI of the neck and chest, [$^{99m}$Tc] Sestamibi-SPECT/CT, as well as [11C] methionine-PET-CT. None of these imaging modalities localized tumor recurrence. Additionally, the patient underwent re-exploration of the right neck and lymph node dissection of the right cervical lymph nodes. Histopathology was negative for PC and hypercalcemia persisted postoperatively.

Subsequently the patient presented herself at our institution. In view of the extensive previous workup we decided to perform [18F] FDG-PET-CT. Surprisingly, a pathological lymph node (17x24 mm) within the liver hilus showed slightly increased FDG-uptake (**Figures 1A, B**). Due to the unusual localization we questioned relationship with the recurrence of PC and performed selective PTH venous sampling that included the entire neck region, but also sampling from the liver veins in addition to V. cava inferior sampling (**Figure 1C**). Highest PTH was measured in the right V. hepatica with 758 pg/ml and a ratio of 1.3 compared to V. cava inferior. After laparotomy and preparation of the liver hilus, the lymph node was resected with intact capsule without any signs of infiltration (R0) in January 2017. Inspection revealed no further lymph node manifestations (**Figures 1D, E**). Intraoperative PTH dropped from 841 ng/L to 387ng/L The peri-and postoperative course was without any complications. The histological assessment of the resected tissue confirmed lymph node metastasis with blood vessel infiltration (V1) of PC (**Figure 1F**). Histological and immunohistochemical analyses were both consistent with parathyroid carcinoma (positivity for PTH, loss of parafibromin). Furthermore, we stained the lymph node sample for PD-L1 (antibody 28-8). In the tumor cell there was no specific membrane-bound positivity (TC Score 0; Cologne -Score for NSCLS) (15). No tumor associated PD-L1 positivity in the background inflammatory infiltrate was observed. Moreover, we analyzed the DNA-Mismatch-Repair-Protein MLH1, MSH2, MSHG, and PMS2. The results showed no evidence of microsatellite instability. In summary, this was a lymph node metastases of a PD-L1-negative, microsatellite stable parathyroid carcinoma.

After resection, Calcium decreased steadily from 3.4 mmol/L to 2.3 mmol/L. Cinacalcet was discontinued.

## SYSTEMIC TREATMENT

Unfortunately, few days after discharge, PTH level and Calcium level increased slowly again requiring the use of cinacalcet.

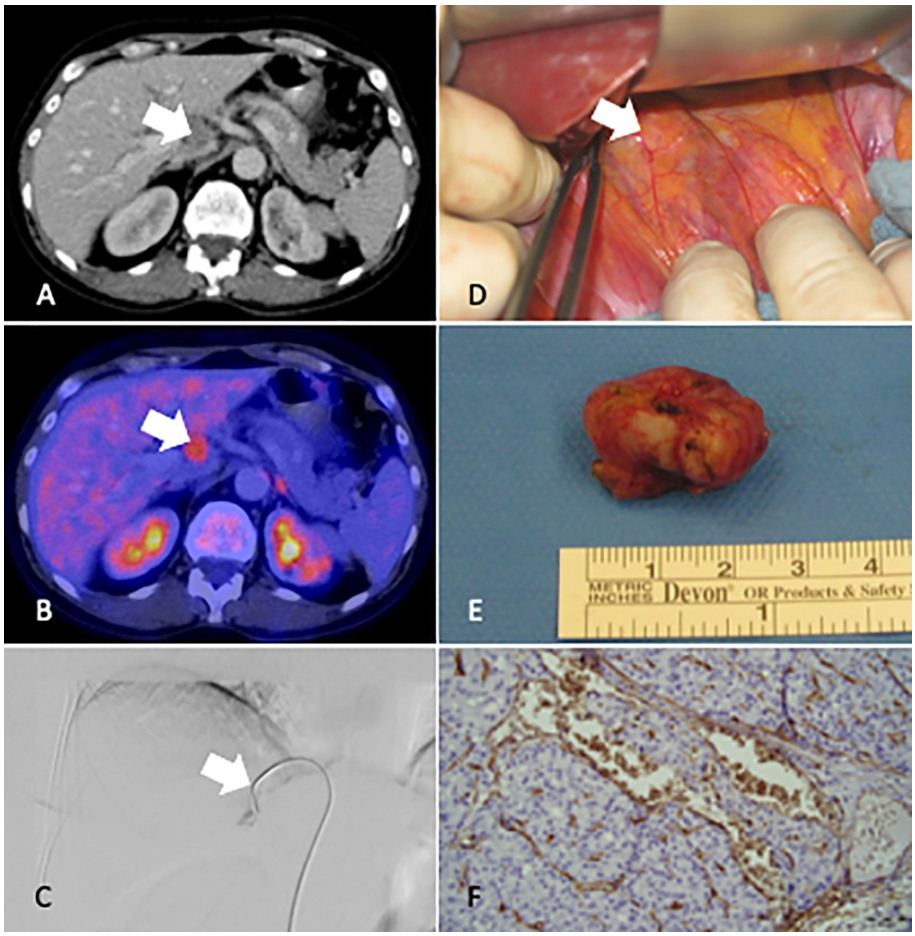


**FIGURE 1** | CT Imaging **(A)**, [18F]FDG-PET-CT **(B)**, Venous sampling V. hepatica **(C)**, intraoperative localization **(D)**, Resected lymph node **(E)**, histological result at time of diagnosis recurrence **(F)**, White arrow marks the lymph node metastases in the hilus of the liver.

The medication was increased to a daily cumulative dose of 150 mg in the following weeks. Four months after resection, PTH rose to 912 ng/L and additionally, denosumab was required to adequately control serum calcium levels (2.6 mmol/l).

Abdominal ultrasonography indicated recurrent lymph node metastases in the hepatic hilus (**Figure 2A**) which was confirmed by [18F]FDG-PET-CT.

The patient was included in NCT/DKTK MASTER (Molecularly Aided Stratification for Tumor Eradication Research), a multicenter, prospective observational study that is based on a common workflow for diagnostics, therapeutic decision making, and structured follow-up in patients with rare tumors failing standard treatment. The formalin-fixed paraffin embedded lymph node tissue obtained at surgery was utilized for whole exome sequencing and 412 single nucleotide variants (SNV) and 2 insertions/deletions (indels) were identified.

Because of the rapid recurrence in the same location, the fact that PTH levels had not returned to normal levels after resection of the previous metastases and in view of controlled serum calcium (2.6 mmol/L) only with 150 mg cinacalcet, we decided to initiate therapy with pembrolizumab on a compassionate use basis at 200 mg every three weeks. Pembrolizumab treatment was started in 09/2017 at a PTH serum concentration of 1,906 ng/L (**Figure 3F**). After four cycles of therapy, PTH dropped significantly (11/2017) to 613 ng/L and [18F]FDG-PET-CT showed stable disease four months later. Pembrolizumab was continued for six infusions every three weeks until [18F]FDG-PET-CT detected a lymph node bulk adjacent to the gallbladder (**Figure 2B**) in 07/2018. After evaluation of resectability, re-laparotomy was performed (10/2018) and the lymph node conglomerate of 3.4x2.0x3.2cm in lymph node station 12 was resected. There were no clinical signs of extra nodal tumor infiltration (**Figures 2C, D**). Intraoperative PTH dropped from 2864 ng/L to 64.3ng/L. Histology confirmed a conglomerate of lymph node metastases of the PC up to 3.8 cm in size exhibiting the same features as the initial specimen. The postoperative course of the patient was unremarkable. In the following months, the patient's serum calcium and PTH levels increased slowly. The patient was normocalcaemic on intermittent medication with denosumab and had stable PTH levels between 197 und 332 pg/L until 06/2019. At this time a progress of

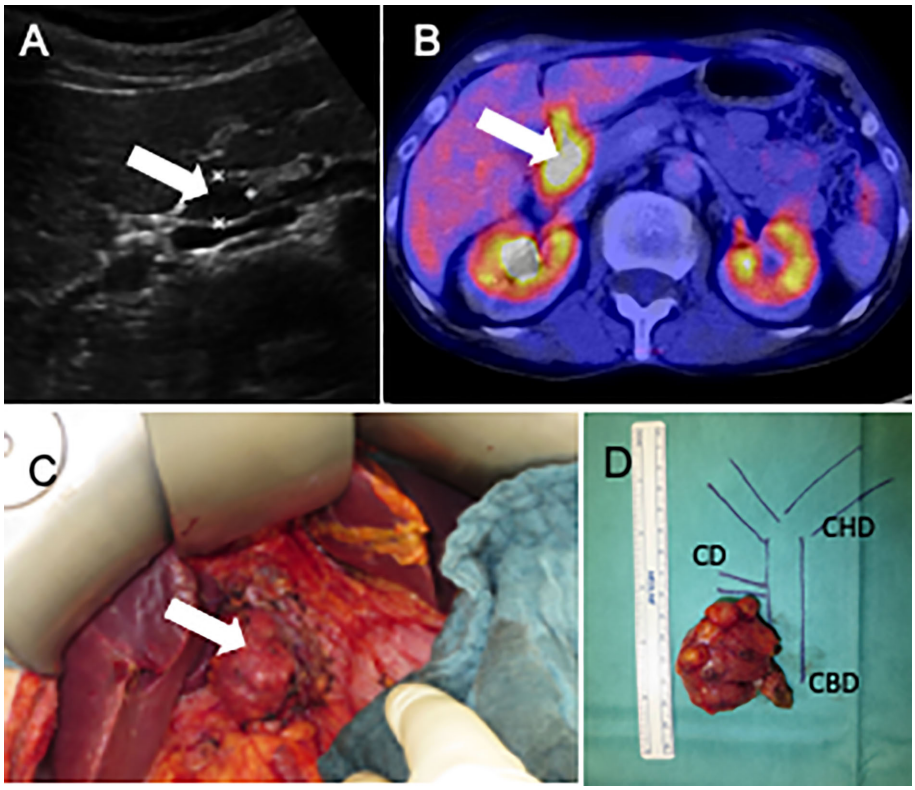


**FIGURE 2** | Abdominal ultrasonography **(A)** [18F]FDG-PET-CT **(B)**, photography surgery 10/2018, Lymph node metastases *in situ* **(C)** (white arrows mark the tumor), and the tumor localization in an anatomical drawing **(D)**. CD, cystic duct; CBD, common bile duct; CHD, common hepatic duct.

increased serum calcium levels (2.8 mmol/L) and PTH (418 ng/L) was detected. A [18F]FDG-PET-CT was performed and showed a new lymph node recurrence near the diaphragm (**Figures 3A–D**). This lymph node was resected as well as a lymph node dorsal of the V. cava inferior in 01/2020 (**Figure 3E**). PTH dropped intraoperatively to 15.8 ng/L (preoperative: 1,831 ng/L). Due to postoperative hypocalcemia, the patient received decostriol (1,25-dihydroxycholecalciferol) at a dose of 0.5 µg twice a day and up to 3 g calcium P.O. per day which could be discontinued during the following 8 weeks. Until 10/2020 the patient was biochemically free of recurrence (serum calcium 2.4 mmol/L, PTH 42.7 pg/ml) without any medication. The whole course of PTH is shown in **Figure 3F**. Interdisciplinary discussion recommended watchful waiting and restaging in case of biochemical progression.

## DISCUSSION

The diagnostic workup and site directed therapy in case of recurrent PC remains challenging. Distant metastases and especially abdominal localization of PC, as presented in this case report, are highly uncommon (7). The review of the literature revealed case reports of distant metastases, specifically abdominal and brain metastases (12–14) (**Table 1**). Interdisciplinary management is crucial to enable focused surgical treatment and adequate medical treatment (16). In this case report, we presented an example for an interdisciplinary workflow in a patient with abdominal recurrent PC 12 years after primary diagnosis.

## [18F]FDG-PET-CT AND SELECTIVE VENOUS SAMPLING IMPROVES LOCALIZATION DIAGNOSTICS

After biochemical recurrence in our patient, tumor localization was not possible by various imaging techniques. However, [18F]FDG-PET-CT was able to visualize the unusual localization of abdominal recurrence. In several a case series, [18F]FDG-PET-CT has been shown to effectively localize PC manifestation sites at initial diagnosis, follow-up or recurrence (17). In the current literature, [18F]choline-PET-CT was compared in small series with [18F]FDG-PET-CT. In 2 cases [18F]FDG-PET-CT detected tumor manifestations in the liver and bone lesions in the pelvis, which was missed by [18F]FDG-PET-CT. The authors of that study discussed that the differences in choline and FDG uptake could be the differences in tumor proliferation and differentiation (18). Another case report demonstrated that [18F]FDG-PET-CT and [18F]choline-PET-CT are feasible, in (recurrent) PC (19). In summary, as long as there is no standardized diagnostic work-up especially in recurrent PC, whole body functional imaging should be considered for

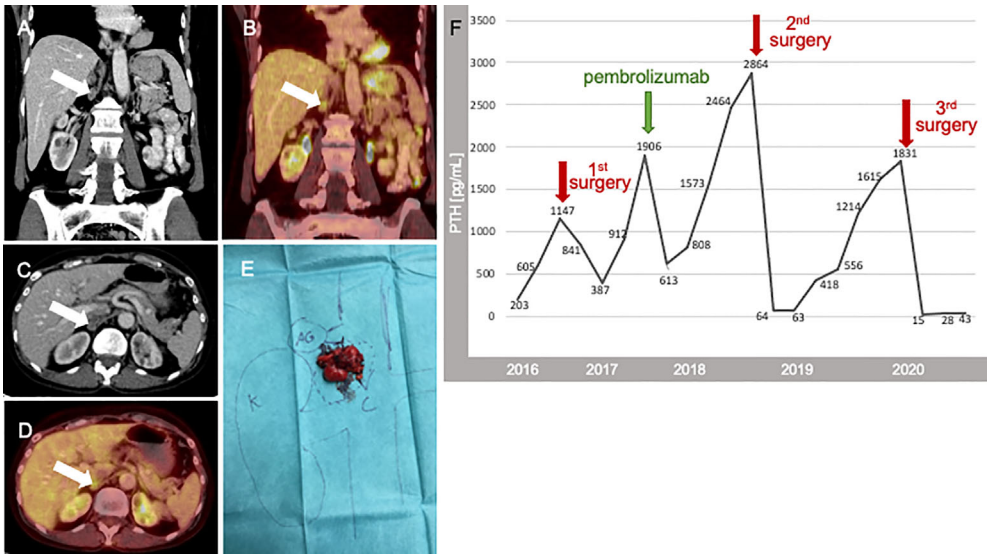


**FIGURE 3** | CT Imaging **(A, C)**, 12/2019), [18F]FDG-PET-CT **(B, D)**, (white arrows mark the tumor), photography surgery 01/2020 **E**; K, Kidney; VC, Vena cava; AG, adrenal gland; PTH course is shown as time scale from the beginning of treatment in our hospital 2016 up to 2020. In this period, we performed three abdominal surgeries (red arrow) and the beginning of therapy within Pembrolizumab (green arrow) **(F)**.

**TABLE 1** | Unusual localizations of distant PC recurrence in the literature.

| First Authors | Publication Year | Patients (n=) | Sites of Distant Metastases (DM) | Finding Modality of DM | Treatment of DM | Outcome | Follow up (years) |
|---|---|---|---|---|---|---|---|
| Manente et al. | 1987 | 1 | Lymph node Pancreas region | Not Reported | Resection | Death | 1 |
| Qiu Zhong-ling et al. | 2013 | 5 | Liver | CT n=5<br>Biopsy n= 3<br>$^{99m}$TC-MIBI n=1 | RFA /EB n=1<br>PR n=3<br>Unknown=1 | Alive n=3<br>Death n=2 | 0.5-9 |
| | | 3 | Brain | MRI n=2<br>CT n=1 | PR | Alive n= 2<br>Unknown n=1 | 5.5-9<br>2.5 |
| Tsoli et al. | 2017 | 1 | Brain | MRI | Resection, RTx | Death | 2 |
| Asare et al. | 2019 | 2 | Liver | Unkown | CTx | Alive n=1<br>Death n=1 | Unkown n=6 |

*Distant metastases were only considered, if they were localized extracervical, extrathoracic and were not localized in bones. RFA, radiofrequency ablation; EB, embolization; PR, palliative resection; CTx, chemotherapy; RTx, Radiotherapy.*

detecting uncommon tumor localization and to avoid repeated cervical surgery.

Furthermore, in our case the selective venous sampling was additionally performed to confirm this uncommon localization. Therefore, selective venous sampling was able to support the localization diagnostics and consecutively, the focused surgical approach we then performed.

## MOLECULAR INFORMED SYSTEMIC TREATMENT

Overall, only few reports have characterized the molecular landscape of PC. Using exome sequencing, Yu et al. (20) in a series of seven cases found an average of 51 somatic variants. This is in stark contrast to the findings in our patient who had high tumor mutational burden (TMBh). TMBh is increasingly recognized as a marker of response to immunotherapy (21) and related to the accumulation of tumoral neoantigens which increase the likelihood of response to inhibition of immune checkpoint molecules.

Molecular guided systemic treatment with pembrolizumab led to stable disease as best response on imaging and a marked clinical and biochemical benefit with a stabilization of serum calcium and drop of PTH for 9 months. Our case demonstrates that in rare tumors, molecular analysis may be useful to detect druggable targets. So far, no case of successful treatment of PC with immune checkpoint inhibitors has been described.

## TARGETED SURGICAL RESECTION PERMITTED LONG-TERM DISEASE CONTROL

After the first two resections of parathyroid metastases, calcium normalization has been achieved. The patient was subsequently clinically and biochemically disease free for 9 months (at last observation 10/2020). Repeated surgery was able to control serum calcium supporting that every effort should be made to localize the disease and evaluate resectability (16, 17). It must be noted that our previous case series suggests that more extended primary surgery (parathyroidectomy and hemithyroidectomy) may be beneficial in lowering the rate of recurrence in general although it is unclear whether this is also true for the very rare distant metastases (7).

## PATIENTS PERSPECTIVE

Our patient has been alive with a "chronic" disease over a long duration which required medical treatment for long periods of time. Uncertainty about prognosis, eventual diagnostic success and risk of surgery have contributed to the disease burden. The present outcome with biochemical remission has significantly improved the well-being of the patient.

## CONCLUSION

Because manifestation of recurrent PC outside of the neck and chest is possible, whole body imaging for tumor localization is useful to allow for focused repeat surgery. The course of the disease in our patient with a recurrence after 12 years after primary surgery suggests that the tumor evaded immune recognition at a certain time point during disease progression which may also explain the unusual systemic spread of the disease. It is tempting to speculate that pembrolizumab treatment inhibited further progression of disease rendering surgical removal effective in a neo-adjuvant manner. A multimodal diagnostic approach and therapy in an interdisciplinary setting is needed for patients with rare endocrine tumors.

## DATA AVAILABILITY STATEMENT

The original contributions presented in the study are included in the article/**Supplementary Material**. Further inquiries can be directed to the corresponding author.

## ETHICS STATEMENT

Written informed consent was obtained from the individual(s) for the publication of any potentially identifiable images or data included in this article.

## AUTHOR CONTRIBUTIONS

CL, NS, and MK designed the study. AB and RK performed diagnostic imaging and procedures. JR and AW performed surgical procedures. CG supervised all surgical procedures. SK examined all histopathological samples. AS, DH, and SF performed whole exome sequencing. CL, CF, and MK provided data. CL and MK analyzed the data. CL, MF, NS, CG, AS, DH, SF, and MK interpreted the data. CL and MK wrote a manuscript draft. All authors contributed to the article and approved the submitted version.

## FUNDING

This publication was supported by the Open Access Publication Fund of the University of Wuerzburg.

## SUPPLEMENTARY MATERIAL

The Supplementary Material for this article can be found online at: https://www.frontiersin.org/articles/10.3389/fendo.2021.643328/full#supplementary-material

## REFERENCES

1. Ryhanen EM, Leijon H, Metso S, Eloranta E, Korsoff P, Ahtiainen P, et al. A nationwide study on parathyroid carcinoma. *Acta Oncol* (2017) 56(7):991–1003. doi: 10.1080/0284186X.2017.1306103
2. Obara T, Fujimoto Y. Diagnosis and treatment of patients with parathyroid carcinoma: an update and review. *World J Surg* (1991) 15(6):738–44. doi: 10.1007/BF01665308
3. Lee PK, Jarosek SL, Virnig BA, Evasovich M, Tuttle TM. Trends in the incidence and treatment of parathyroid cancer in the United States. *Cancer* (2007) 109(9):1736–41. doi: 10.1002/cncr.22599
4. Cetani F, Pardi E, Marcocci C. Parathyroid Carcinoma. *Front Horm Res* (2019) 51:63–76. doi: 10.1159/000491039
5. Harari A, Waring A, Fernandez-Ranvier G, Hwang J, Suh I, Mitmaker E, et al. Parathyroid carcinoma: a 43-year outcome and survival analysis. *J Clin Endocrinol Metab* (2011) 96(12):3679–86. doi: 10.1210/jc.2011-1571
6. Witteveen JE, Haak HR, Kievit J, Morreau H, Romijn JA, Hamdy MA, et al. Challenges and pitfalls in the management of parathyroid carcinoma: 17-year follow-up of a case and review of the literature. *Horm Cancer* (2010) 1(4):205–14. doi: 10.1007/s12672-010-0042-6
7. Lenschow C, Schragle S, Kircher S, Lorenz K, Machens A, Dralle H, et al. Clinical Presentation, Treatment, and Outcome of Parathyroid Carcinoma: Results of the NEKAR Retrospective International Multicenter Study. *Ann Surg* (2020). doi: 10.2139/ssrn.3541131
8. Cetani F, Pardi E, Marcocci C. Update on parathyroid carcinoma. *J Endocrinol Invest* (2016) 39(6):595–606. doi: 10.1007/s40618-016-0447-3
9. Campenni A, Ruggeri RM, Sindoni A, Giovinazzo S, Calbo E, Ieni A, et al. Parathyroid carcinoma presenting as normocalcemic hyperparathyroidism. *J Bone Miner Metab* (2012) 30(3):367–72. doi: 10.1007/s00774-011-0344-y
10. Wang P, Xue S, Wang S, Lv Z, Meng X, Wang G, et al. Clinical characteristics and treatment outcomes of parathyroid carcinoma: A retrospective review of 234 cases. *Oncol Lett* (2017) 14(6):7276–82. doi: 10.3892/ol.2017.7076

11. Machado NN, Wilhelm SM. Parathyroid Cancer: A Review. *Cancers (Basel)* (2019) 11(11):1676. doi: 10.3390/cancers11111676
12. Manente P, Cecchettin M, Infantolino D, Foscolo G, Conte N. Apparently nonfunctioning metastases of parathyroid carcinoma. *Tumori* (1987) 73 (2):191–3. doi: 10.1177/030089168707300218
13. Qiu ZL, Wu CG, Zhu RS, Xue YL, Luo QY. Unusual case of solitary functioning bone metastasis from a "parathyroid adenoma": imagiologic diagnosis and treatment with percutaneous vertebroplasty–case report and literature review. *J Clin Endocrinol Metab* (2013) 98(9):3555–61. doi: 10.1210/jc.2013-2014
14. WEEKLY clinicopathological exercises; parathyroid carcinoma with hyperparathyroidism and with metastases to liver. *N Engl J Med* (1953) 248 (10):426–32. doi: 10.1056/NEJM195303052481007
15. Lloyd RV, Osamura RY, Klöppel G, Rosai J. WHO classification of tumours of endocrine organs by International Agency for Research. In: RV Lloyd, editor. *Cancer*, *4th ed*, vol. 10 th. World Health Organization (WHO, Genf, Switzerland (2017).
16. Storvall S, Ryhanen E, Bensch FV, Heiskanen I, Kytola S, Ebeling T, et al. Recurrent Metastasized Parathyroid Carcinoma-Long-Term Remission After Combined Treatments With Surgery, Radiotherapy, Cinacalcet, Zoledronic Acid, and Temozolomide. *JBMR Plus* (2019) 3(4):e10114. doi: 10.1002/jbm4.10114
17. Evangelista L, Sorgato N, Torresan F, Boschin IM, Pennelli G, Saladini G, et al. FDG-PET/CT and parathyroid carcinoma: Review of literature and illustrative case series. *World J Clin Oncol* (2011) 2(10):348–54. doi: 10.5306/wjco.v2.i10.348
18. Deandreis D, Terroir M, Al Ghuzlan A, Berdelou A, Lacroix L, Bidault F, et al. (1)(8)Fluorocholine PET/CT in parathyroid carcinoma: a new tool for disease staging? *Eur J Nucl Med Mol Imaging* (2015) 42(12):1941–2. doi: 10.1007/s00259-015-3130-6
19. Hatzl M, Roper-Kelmayr JC, Fellner FA, Gabriel M. 18F-Fluorocholine, 18F-FDG, and 18F-Fluoroethyl Tyrosine PET/CT in Parathyroid Cancer. *Clin Nucl Med* (2017) 42(6):448–50. doi: 10.1097/RLU.0000000000001652
20. Yu W, McPherson JR, Stevenson M, van Eijk R, Heng HL, Newey P, et al. Whole-exome sequencing studies of parathyroid carcinomas reveal novel PRUNE2 mutations, distinctive mutational spectra related to APOBEC-catalyzed DNA mutagenesis and mutational enrichment in kinases associated with cell migration and invasion. *J Clin Endocrinol Metab* (2015) 100(2):E360–4. doi: 10.1210/jc.2014-3238
21. Passaro A, Stenzinger A, Peters S. Tumor Mutational Burden as a Pan-cancer Biomarker for Immunotherapy: The Limits and Potential for Convergence. *Cancer Cell* (2020) 38(5):624–5. doi: 10.1016/j.ccell.2020.10.019

**Conflict of Interest:** The authors declare that the research was conducted in the absence of any commercial or financial relationships that could be construed as a potential conflict of interest.

frontiers in Endocrinology

GENERAL COMMENTARY
published: 18 June 2021
doi: 10.3389/fendo.2021.700806

# Commentary: Case Report: Abdominal Lymph Node Metastases of Parathyroid Carcinoma: Diagnostic Workup, Molecular Diagnosis, and Clinical Management

*Giuseppe Fanciulli[1*†], Sergio Di Molfetta[2†], Andrea Dotto[3,4], Tullio Florio[4,5], Tiziana Feola[6,7], Annamaria Colao[8], Antongiulio Faggiano[9] and NIKE Group[‡]*

[1] NET Unit, Department of Medical, Surgical and Experimental Sciences, University of Sassari—Endocrinology Unit, Sassari, Italy, [2] Section of Internal Medicine, Endocrinology, Andrology and Metabolic Diseases, Department of Emergency and Organ Transplantation, University of Bari Aldo Moro, Bari, Italy, [3] Endocrinology Unit, IRCCS Ospedale Policlinico San Martino, Genova, Italy, [4] Department of Internal Medicine, University of Genova, Genova, Italy, [5] IRCCS Ospedale Policlinico San Martino, Genova, Italy, [6] Department of Experimental Medicine, "Sapienza" University of Rome, Rome, Italy, [7] Neuroendocrinology, Neuromed Institute, IRCCS, Pozzilli, Italy, [8] Endocrinology Unit, Department of Clinical Medicine and Surgery, University Federico II, Naples, Italy, [9] Endocrinology Unit, Department of Clinical and Molecular Medicine, Sant'Andrea Hospital, Sapienza University of Rome, Rome, Italy

OPEN ACCESS

**Edited by:**
*Piero Ferolla, Umbria Regional Cancer Network (Rete Oncologica Regionale Umbria, Perugia), Italy*

**Reviewed by:**
*Marco Gallo, Azienda Ospedaliera Nazionale SS. Antonio e Biagio e Cesare Arrigo, Italy*
*Jessica Costa-Guda, University of Connecticut, United States*

***Correspondence:**
*Giuseppe Fanciulli*
*gfanciu@uniss.it*

*[†]These authors share first authorship*

*[‡]Membership of NIKE Group is provided in the Acknowledgments*

**Specialty section:**
*This article was submitted to Cancer Endocrinology, a section of the journal Frontiers in Endocrinology*

**Received:** *26 April 2021*
**Accepted:** *17 May 2021*
**Published:** *18 June 2021*

**Citation:**
*Fanciulli G, Di Molfetta S, Dotto A, Florio T, Feola T, Colao A, Faggiano A and NIKE Group (2021) Commentary: Case Report: Abdominal Lymph Node Metastases of Parathyroid Carcinoma: Diagnostic Workup, Molecular Diagnosis, and Clinical Management. Front. Endocrinol. 12:700806. doi: 10.3389/fendo.2021.700806*

**Keywords: parathyroid carcinoma, immune checkpoint inhibitors, ipilimumab, nivolumab, pembrolizumab**

**A Commentary on**

**Case Report: Abdominal Lymph Node Metastases of Parathyroid Carcinoma: Diagnostic Workup, Molecular Diagnosis, and Clinical Management**
*By Lenschow C, Fuss CT, Kircher S, Buck A, Kickuth R, Reibetanz J, Wiegering A, Stenzinger A, Hübschmann D, Germer CT, Fassnacht M, Fröhling S, Schlegel N and Kroiss M (2021). Front. Endocrinol. 12:643328. doi: 10.3389/fendo.2021.643328*

## INTRODUCTION

In the issue of March 2021, Lenschow et al. reported the case of a 46-year-old woman with recurrent, programmed death-ligand-1 (PD-L1) negative, tumor mutational burden (TMB)-high parathyroid carcinoma (PC), who showed stable disease as her best response on imaging, and a three-fold drop in PTH after treatment with intravenous pembrolizumab (1).

Parathyroid carcinoma is a rare neuroendocrine tumour, accounting for <1% of all cases of primary hyperparathyroidism (2). While surgery represents the mainstay of treatment for both the primary tumour and metastasis, patients no longer amenable to surgical resection often receive unsatisfactory systemic therapies including cinacalcet, adjuvant radiotherapy, and alkylating agents (3).

In recent years, modulation of immune checkpoint proteins expression has been accounted as a prominent mechanism for tumour immune evasion and survival, thus paving the way for new therapeutic approaches (4). Of note, monoclonal antibodies targeting the programmed cell death-1 (PD-1)/PD-L1 and/or the cytotoxic T lymphocyte antigen-4 (CTLA-4)-B7 pathway, hereinafter collectively referred as immune checkpoints inhibitors (ICIs), have shown both clinical effectiveness and a favorable safety profile in patients with advanced solid tumours, and have been included in the treatment repertoire of several malignancies (5).

Given the remarkable results obtained by Lenschow et al. with the anti-PD-1 agent pembrolizumab in the above-mentioned case, we performed an extensive search for possible further relevant data

sources, including a) full published articles in international online databases (PubMed, Web of Science, Scopus, and Embase); b) preliminary reports in selected international meeting abstract repositories (American Society of Clinical Oncology, ASCO; European Neuroendocrine Tumor Society, ENET; European Society for Medical Oncology, ESMO); c) registered clinical trials in the U.S. National Institutes of Health registry of clinical trials (http://clinicaltrials.gov) and in any primary register of the WHO International Clinical Trials Registry Platform (ICTRP).

## FINDINGS

a. The search for full-published articles revealed 263 papers, two of which were pertinent to our aim (one of these being the article by Lenschow et al.). In 2020, Park et al. (6) reported the case of a 65-year-old man with recurrent hyperparathyroidism and histologically confirmed metastatic PC, who showed objective response as defined by the Response Evaluation Criteria in Solid Tumors version 1.1 (RECIST v1.1) (7) after pembrolizumab administration. The tumour was assessed as PD-L1 negative by immunohistochemistry. Mutations in the MSH2 and MSH6 DNA mismatch repair genes, possibly resulting in high replication error at microsatellite loci, were found in tumour samples through comprehensive gene profiling analysis. Therefore, the patient was deemed eligible for treatment with pembrolizumab. Immune blockade of PD-1 resulted in sustained reduction of pulmonary metastatic tumour burden, with concurrent normalization of both calcium and parathyroid hormone levels.
b. We found no preliminary reports in the above-mentioned international meeting abstract repositories.
c. The search in clinical trial registers revealed two active trials, one of which fully matched our aim. NCT02834013 (DART: Dual Anti-CTLA-4 and Anti-PD-1 Blockade in Rare Tumors) is a Phase 2 study evaluating the effects of nivolumab plus ipilimumab (arm I) versus nivolumab alone (arm II) in patients with rare solid tumours (94 listed histotypes, including PC). The primary outcome is the RECIST v1.1 objective response-rate. Major secondary outcomes include incidence of adverse events, best response, clinical benefit rate, overall survival, and progression free survival. The present study status is "Recruiting." However, according to a very recent update of the protocol, accrual of parathyroid gland tumours has been closed.

## DISCUSSION

To date, very limited evidence is available about the efficacy of ICIs in patients with PC. With this regard, some points should be taken into account.

PD-L1 expression in pre-treatment tumour samples has been proposed as a marker for clinical response to anti-PD-1/PD-L1 immunotherapy in patients with advanced malignancies, including melanoma, non-small cell lung cancer, kidney cancer, colorectal cancer, and castration-resistant prostate cancer (8, 9). Notably, immunohistochemistry-assessed PD-L1 expression was found in 4/18 patients (22.2%) with histologically confirmed PC (10), thus suggesting that immune checkpoint blockade may have a rationale in the treatment of this type of tumours. While PD-L1–overexpressing tumours tend to have more intense responses, experience with melanoma suggests that PD-1/PD-L1 blockade may be beneficial also in patients with low PD-L1 expression (11–13), therefore a negative PD-L1 status assessment should not definitively preclude the use of ICIs.

There is growing evidence that the TMB can also predict response to ICIs, with the high TMB-patients exhibiting a higher response rate to anti-PD-1/PD-L1 agents possibly due to increased neo-antigen load and T cell infiltration in the tumour microenvironment (14, 15). In a cohort of 16 patients with PC, Kang et al. have recently found three cases with high (>20 m/Mb) TMB through comprehensive genomic profiling (16). Given the higher response rate observed in the high TMB-patients, assessment of mismatch repair status and/or exome sequencing in tumour samples may help identify those patients possibly benefiting the most from administration of anti-PD-1/PD-L1 agents, in this way enabling a more personalized approach to treatment. The above-mentioned cases of PD-L1 negative, TMB-high tumours benefiting from pembrolizumab therapy further support this approach.

Moreover, PD-1 and CTLA-4 are acknowledged to exert non-redundant immunosuppressive effects (17). As there is robust evidence supporting a greater efficacy of the combined PD-1/CTLA-4 blockade over the two monotherapies in advanced solid cancer (18), the possible inclusion of patients with PC in the NCT02834013 trial is giving rise to great expectations. Of note, ICI two-drug combination therapy is under evaluation also in patients with other aggressive endocrine tumours (19–22).

As a further reason of interest, hypocalcemia due to immune-related hypoparathyroidism has been reported as a rare complication following anti-PD-1 therapy initiation in patients with non-parathyroid tumours (23, 24). As a result, mitigation of hypercalcemia could be hypothesized as a beneficial adjunctive effect of anti-PD-1 agents in patients with PC, irrespective of their imaging response assessment.

In summary, currently available treatments for patients with recurrent PC are insufficient. ICIs, which are considered a milestone in oncology, may provide hope for the future therapy of this rare cancer.

## AUTHOR CONTRIBUTIONS

GF, SDM, AD, TFl, and TFe were responsible for the design, the methodology, the draft preparation, the reviewing, and editing. AC and AF were responsible for the supervision. All authors contributed to the article and approved the submitted version.

## FUNDING

This work was supported by the Italian Ministry of Education, University and Research (MIUR): PRIN 2017Z3N3YC, and by University of Sassari, Italy: Research Funding 2019-2020 to GF.

## ACKNOWLEDGMENTS

This paper is part of the 'Neuroendocrine Tumors Innovation Knowledge and Education' project led by Annamaria Colao and Antongiulio Faggiano, which aims at increasing the knowledge on NET. We would like to acknowledge all the Collaborators of the "NIKE" project: Manuela Albertelli—Genova; Barbara Altieri—Wurzburg; Luigi Barrea—Napoli; Filomena Bottiglieri—Napoli; Severo Campione—Napoli; Federica de Cicco—Napoli; Alessandra Dicitore—Milano; Diego Ferone—Genova; Francesco Ferraù—Messina; Erika Grossrubatscher—Milano; Marco Gallo—Torino; Elisa Giannetta—Roma; Federica Grillo—Genova; Elia Guadagno—Napoli; Valentina Guarnotta—Palermo; Andrea M. Isidori—Roma; Andrea Lania—Milano; Andrea Lenzi—Roma; Fabio Lo Calzo—Avellino; Pasquale Malandrino—Catania; Erika Messina—Messina; Roberta Modica—Napoli; Giovanna Muscogiuri—Napoli; Genoveffa Pizza—Avellino; Riccardo Pofi—Roma; Giulia Puliani—Roma; Carmen Rainone—Napoli; Paola Razzore—Torino; Laura Rizza—Roma; Manila Rubino —Milano; Rosa Maria Ruggieri—Messina; Emilia Sbardella—Roma; Franz Sesti—Roma; Mary Anna Venneri—Roma; Giovanni Vitale—Milano; Maria Chiara Zatelli—Ferrara.

## REFERENCES

1. Lenschow C, Fuss CT, Kircher S, Buck A, Kickuth R, Reibetanz J, et al. Case Report: Abdominal Lymph Node Metastases of Parathyroid Carcinoma: Diagnostic Workup, Molecular Diagnosis, and Clinical Management. *Front Endocrinol (Lausanne)* (2021) 12:643328. doi: 10.3389/fendo.2021.643328
2. Cetani F, Pardi E, Marcocci C. Parathyroid Carcinoma. *Front Horm Res* (2019) 51:63–76. doi: 10.1159/000491039
3. Bollerslev J, Schalin-Jäntti C, Rejnmark L, Siggelkow H, Morreau H, Thakker R, et al. Unmet Therapeutic, Educational and Scientific Needs in Parathyroid Disorders: Consensus Statement From the First European Society of Endocrinology Workshop (PARAT). *Eur J Endocrinol* (2019) 181(3):P1–P19. doi: 10.1530/EJE-19-0316
4. Franzin R, Netti GS, Spadaccino F, Porta C, Gesualdo L, Stallone G, et al. The Use of Immune Checkpoint Inhibitors in Oncology and the Occurrence of AKI: Where do We Stand? *Front Immunol* (2020) 11:574271. doi: 10.3389/fimmu.2020.574271
5. Robert C. A Decade of Immune-Checkpoint Inhibitors in Cancer Therapy. *Nat Commun* (2020) 11. doi: 10.1038/s41467-020-17670-y
6. Park D, Airi R, Sherman M. Microsatellite Instability Driven Metastatic Parathyroid Carcinoma Managed With the Anti-PD1 Immunotherapy, Pembrolizumab. *BMJ Case Rep* (2020) 13(9). doi: 10.1136/bcr-2020-235293
7. Eisenhauer EA, Therasse P, Bogaerts J, Schwartz LH, Sargent D, Ford R, et al. New Response Evaluation Criteria in Solid Tumours: Revised RECIST Guideline (Version 1.1). *Eur J Cancer* (2009) 45(2):228–47. doi: 10.1016/j.ejca.2008.10.026
8. Topalian SL, Hodi FS, Brahmer JR, Gettinger SN, Smith DC, McDermott DF, et al. Safety, Activity, and Immune Correlates of Anti-PD-1 Antibody in Cancer. *N Engl J Med* (2012) 366(26):2443–54. doi: 10.1056/NEJMoa1200690
9. Reck M, Rodríguez-Abreu D, Robinson AG, Hui R, Csőszi T, Fülöp A, et al. KEYNOTE-024 Investigators. Pembrolizumab Versus Chemotherapy for PD-L1-Positive Non-Small-Cell Lung Cancer. *N Engl J Med* (2016) 375(19):1823–33. doi: 10.1056/NEJMoa1606774
10. Du X, Wang L, Shen B, He H, Chang H, Wei B. Clinical Significance of Pd-L1 Expression in Parathyroid Cancer. *Acta Endocrinol (Buchar)* (2016) 12(4):383–6. doi: 10.4183/aeb.2016.383
11. Larkin J, Chiarion-Sileni V, Gonzalez R, Grob JJ, Cowey CL, Lao CD, et al. Combined Nivolumab and Ipilimumab or Monotherapy in Untreated Melanoma. *N Engl J Med* (2015) 373(1):23–34. doi: 10.1056/NEJMoa1504030
12. Wolchok JD, Chiarion-Sileni V, Gonzalez R, Rutkowski P, Grob J-J, Cowey CL, et al. Overall Survival With Combined Nivolumab and Ipilimumab in Advanced Melanoma. *N Engl J Med* (2017) 377(14):1345–56. doi: 10.1056/NEJMoa1709684
13. Bongiovanni M, Rebecchini C, Saglietti C, Bulliard J-L, Marino L, de Leval L, et al. Very Low Expression of PD-L1 in Medullary Thyroid Carcinoma. *Endocr Relat Cancer* (2017) 24(6):L35–8. doi: 10.1530/ERC-17-0104
14. Samstein RM, Lee C-H, Shoushtari AN, Hellmann MD, Shen R, Janjigian YY, et al. Tumor Mutational Load Predicts Survival After Immunotherapy Across Multiple Cancer Types. *Nat Genet* (2019) 51(2):202–6. doi: 10.1038/s41588-018-0312-8
15. Yang RK, Qing Y, Jelloul FZ, Routbort MJ, Wang P, Shaw K, et al. Identification of Biomarkers of Immune Checkpoint Blockade Efficacy in Recurrent or Refractory Solid Tumor Malignancies. *Oncotarget* (2020) 11(6):600–18. doi: 10.18632/oncotarget.27466
16. Kang H, Pettinga D, Schubert AD, Ladenson PW, Ball DW, Chung JH, et al. Genomic Profiling of Parathyroid Carcinoma Reveals Genomic Alterations Suggesting Benefit From Therapy. *Oncologist* (2019) 24(6):791–7. doi: 10.1634/theoncologist.2018-0334
17. Schmidt C. The Benefits of Immunotherapy Combinations. *Nature* (2017) 552(7685):S67–9. doi: 10.1038/d41586-017-08702-7
18. Ma X, Zhang Y, Wang S, Wei H, Yu J. Immune Checkpoint Inhibitor (ICI) Combination Therapy Compared to Monotherapy in Advanced Solid Cancer: A Systematic Review. *J Cancer* (2021) 12(5):1318–33. doi: 10.7150/jca.49174
19. Dai C, Liang S, Sun B, Kang J. The Progress of Immunotherapy in Refractory Pituitary Adenomas and Pituitary Carcinomas. *Front Endocrinol* (2020) 11. doi: 10.3389/fendo.2020.608422
20. Fanciulli G, Di Molfetta S, Dotto A, Florio T, Feola T, Rubino M, et al. Emerging Therapies in Pheochromocytoma and Paraganglioma: Immune Checkpoint Inhibitors in the Starting Blocks. *J Clin Med* (2020) 10(1). doi: 10.3390/jcm10010088. null.
21. Karwacka I, Obołończyk Ł, Kaniuka-Jakubowska S, Sworczak K. The Role of Immunotherapy in the Treatment of Adrenocortical Carcinoma. *Biomedicines* (2021) 9(2). doi: 10.3390/biomedicines9020098
22. Di Molfetta S, Dotto A, Fanciulli G, Florio T, Feola T, Colao A, et al. Immune Checkpoint Inhibitors: New Weapons Against Medullary Thyroid Cancer? *Front Endocrinol* (2021) 12:667784. doi: 10.3389/fendo.2021.667784
23. Manohar S, Kompotiatis P, Thongprayoon C, Cheungpasitporn W, Herrmann J, Herrmann SM. Programmed Cell Death Protein 1 Inhibitor Treatment is Associated With Acute Kidney Injury and Hypocalcemia: Meta-Analysis. *Nephrol Dial Transplant* (2019) 34(1):108–17. doi: 10.1093/ndt/gfy105
24. Nalluru SS, Piranavan P, Ning Y, Ackula H, Siddiqui AD, Trivedi N. Hypocalcemia With Immune Checkpoint Inhibitors: The Disparity Among Various Reports. *Int J Endocrinol* (2020) 2020:7459268. doi: 10.1155/2020/7459268

**Conflict of Interest:** The authors declare that the research was conducted in the absence of any commercial or financial relationships that could be construed as a potential conflict of interest.

The reviewer MG declared a past co-authorship with several of the authors TFe, AC, and AF to the handling editor.

frontiers in Endocrinology

CASE REPORT
published: 31 March 2021
doi: 10.3389/fendo.2021.623756

# Case Report: Metastatic Bronchopulmonary Carcinoid Tumor to the Pineal Region

*Joshua A. Cuoco*[1,2,3†], *Michael W. Kortz*[4,5†], *Edwin McCray*[6], *Evin L. Guilliams*[1,2,3], *Christopher M. Busch*[1,2,3], *Cara M. Rogers*[1,2,3], *Robert W. Jarrett*[2,7] *and Sandeep Mittal*[1,2,3,8*]

[1] Department of Neurosurgery, Carilion Clinic Neurosurgery, Roanoke, VA, United States, [2] Virginia Tech Carilion School of Medicine, Roanoke, VA, United States, [3] School of Neuroscience, Virginia Tech, Blacksburg, VA, United States, [4] Department of Neurosurgery, University of Colorado, Aurora, CO, United States, [5] College of Osteopathic Medicine, Kansas City University, Kansas City, MO, United States, [6] Department of Neurosurgery, Duke University, Durham, NC, United States, [7] Carilion Clinic Pathology and Dominion Pathology Associates, Roanoke, VA, United States, [8] Fralin Biomedical Research Institute, Roanoke, VA, United States

OPEN ACCESS

**Edited by:**
*Enzo Lalli, UMR7275 Institut de Pharmacologie Moléculaire et Cellulaire (IPMC), France*

**Reviewed by:**
*Jean-Yves Scoazec, Institut Gustave Roussy, France*
*Barbara Bardoni, UMR7275 Institut de Pharmacologie Moléculaire et Cellulaire (IPMC), France*

***Correspondence:**
*Sandeep Mittal*
*sandeepmittal@vt.edu*

[†]*These authors share first authorship*

**Specialty section:**
*This article was submitted to Cancer Endocrinology, a section of the journal Frontiers in Endocrinology*

**Received:** *30 October 2020*
**Accepted:** *08 February 2021*
**Published:** *31 March 2021*

**Citation:**
*Cuoco JA, Kortz MW, McCray E, Guilliams EL, Busch CM, Rogers CM, Jarrett RW and Mittal S (2021) Case Report: Metastatic Bronchopulmonary Carcinoid Tumor to the Pineal Region. Front. Endocrinol. 12:623756. doi: 10.3389/fendo.2021.623756*

Intracranial spread of a systemic malignancy is common in advanced staged cancers; however, metastasis specifically to the pineal gland is a relatively rare occurrence. A number of primary lesions have been reported to metastasize to the pineal gland, the most common of which is lung. However, metastasis of a bronchial neuroendocrine tumor to the pineal gland is a seldom-reported entity. Here, we present a 53-year-old female who presented with worsening headaches and drowsiness. MRI brain revealed a heterogeneously enhancing partially cystic mass in the pineal region. The patient had an extensive oncologic history consisting of remote stage IIA invasive breast ductal carcinoma as well as a more recently diagnosed atypical bronchopulmonary neuroendocrine tumor with lymph node metastases. She underwent microsurgical volumetric resection of the large pineal mass and a gross total removal of the tumor was achieved. Histopathology confirmed a metastatic tumor of neuroendocrine origin and the immunohistochemical profile was identical to the primary bronchopulmonary carcinoid tumor. Eight weeks after surgery, she underwent stereotactic radiosurgical treatment to the resection cavity. At 1-year follow-up, the patient remains clinically stable without any new focal neurological deficits and without any evidence of residual or recurrent disease on postoperative MRI. Metastatic neuroendocrine tumors should be considered in the differential diagnosis of pineal region tumors and aggressive surgical resection should be considered in selected patients. Gross total tumor resection may afford excellent local disease control. We discuss the relevant literature on neuroendocrine tumors and current treatment strategies for intracranial metastases of neuroendocrine origin.

**Keywords: metastatic disease, neuroendocrine tumor, lung carcinoid, pineal gland, brain metastasis, CNS tumor**

## BACKGROUND

The brain parenchyma is a common site for the dissemination of metastatic disease; however, metastasis to the pineal region is very rare with a reported incidence of 0.4–3.8% of all intracranial metastases (1, 2). Since Forster's original description of the first case in 1858 (3), various primary malignant tumors have been reported to spread to the pineal region including esophageal, stomach, liver, colon, pancreas, kidney, bladder, prostate, thyroid, breast, melanoma, myeloma, and leukemia (4–6). However, there is only one case reported in the literature of a bronchial neuroendocrine tumor with metastasis to the pineal gland (7).

Neuroendocrine tumors constitute a heterogeneous group of malignancies that originate from neuroendocrine cells throughout the body, most commonly arising from the gastrointestinal tract, tracheobronchial tree, and bladder (8, 9). Complete surgical resection of the primary tumor as well as any metastatic deposits with a curative intent is often recommended in patients with limited extent of metastatic disease (8). However, there is a lack of consensus with respect to standard-of-care for unresectable advanced primary tumors or diffuse metastatic disease given a lack of prospective trials (8).

Here, we present a patient with a pineal region metastasis from a known primary lung carcinoid tumor. We discuss the relevant literature on the neuroendocrine tumors and current treatment strategies for intracranial metastases of neuroendocrine origin. To our knowledge, this is the second reported case in the literature.

## CASE PRESENTATION

### History and Physical Examination

A 53-year-old female presented to our emergency department with 3 weeks of progressively worsening headaches and drowsiness. No focal neurological deficits were present on examination. Relevant history included stage IIA invasive breast ductal carcinoma treated with left mastectomy and chemotherapy two decades prior. Moreover, 2 years prior to presentation, she was diagnosed with atypical bronchopulmonary carcinoid tumor with metastasis to level 5 lymph node and level 6A lymph node with extracapsular extension (T2aN2M0). She initially underwent treatment with octreotide and lobectomy followed by four cycles of adjuvant cisplatin and etoposide 2 years prior to presentation. Given her progressive neurologic symptomatology and history of malignancy, imaging was obtained to rule-out intracranial pathology.

### Neuroimaging Findings

Computed tomography of the head demonstrated a hyperdense, partially cystic pineal region lesion with areas of calcification with supratentorial ventricular dilatation (**Figure 1**). Magnetic resonance imaging of the brain revealed a heterogeneously enhancing 3.9 × 2.6 × 3.1 cm mixed cystic and solid pineal mass extending into the posterior third ventricle and associated obstructive hydrocephalus (**Figure 2**). Metastatic work-up revealed a stable systemic disease burden.

### Neurosurgical Management and Postoperative Imaging

The patient was started on dexamethasone and medically optimized. Given her relatively young age, symptomatic obstructive hydrocephalus, and need for tissue diagnosis as well as local disease control, neurosurgical resection of the pineal region mass was recommended.

A stereotactic right parietal craniotomy with posterior interhemispheric transcallosal approach was utilized for volumetric resection of the large pineal mass. The patient tolerated the procedure well and without complication. Post-operatively, she exhibited a protracted course with transient neurologic symptomatology (i.e., mildly impaired short-term memory, wide-based gait), which subsequently resolved slowly over 3 months.

The patient underwent Cyberknife radiosurgical treatment to the resection cavity 8 weeks after surgery. A total of 27 Gy were delivered in three fractions using a total of 126 beams. Repeat MRI brain at 6-months and 1-year revealed no evidence of residual or recurrent disease (**Figure 3**).

### Histopathological Findings

Histopathology was consistent with metastatic atypical carcinoid tumor of pulmonary origin (**Figure 4**). Routine hematoxylin and eosin (H&E) stained sections demonstrated nests and sheets of cells with speckled chromatin and indistinct to small nucleoli. Thick fibrous bands separated the tumor cell nests. The morphologic appearance was identical to that of the primary lung tumor. Mitoses were present less than 10 per 2 square millimeters. Homer Wright rosettes were not seen. The tumor cells were strongly and diffusely reactive with synaptophysin and neuron specific enolase (NSE) immunohistochemical stains. Cytokeratin AE1/AE3 immunostain was strongly and diffusely reactive helping to exclude a primary pineal tumor. Moreover, glial fibrillary acidic protein (GFAP) and S100 immunostains were completely negative, further helping to exclude a primary pineal tumor which can have similar morphology. The Ki-67 proliferative index was 15%, slightly higher than the 7% labeling index noted in the original bronchopulmonary lesion. Comparatively, tumor morphology of the intracranial metastasis was identical to that of the known atypical bronchopulmonary carcinoid lesion diagnosed 2 years prior (**Figure 5**). The primary atypical bronchopulmonary carcinoid lesion stained positive for synaptophysin, CAM5.2, and cytokeratin AE1/AE3. Additional stains of the primary lesion including CK 5/6, CK7, CK20, p40, TTF-1, Napsin-A, and BRST-2 were negative. Necrosis was noted on histopathology and a mitoses count of no more than one per 2 square millimeters.

## DISCUSSION

The pineal gland is a rare location for the spread of systemic metastasis. In fact, metastasis to this neuroendocrine secretory circumventricular organ has a reported incidence of 0.4–3.8% of

**Abbreviations:** WBRT, whole-brain radiotherapy.

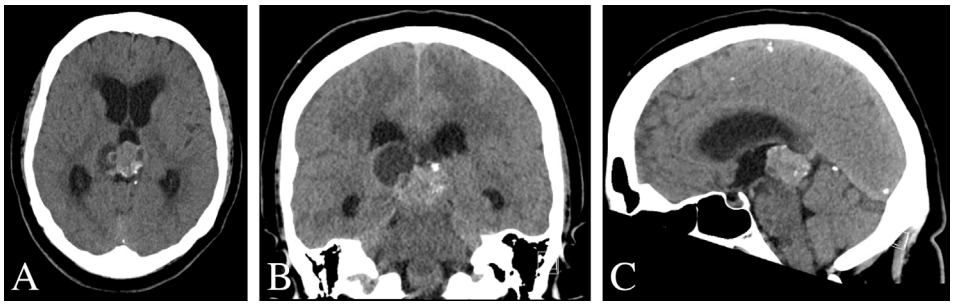


**FIGURE 1** | Pre-operative CT scan of the brain. **(A–C)** Non-contrast CT imaging demonstrating a heterogeneous mass with cystic features and calcification in pineal region causing obstructive hydrocephalus.

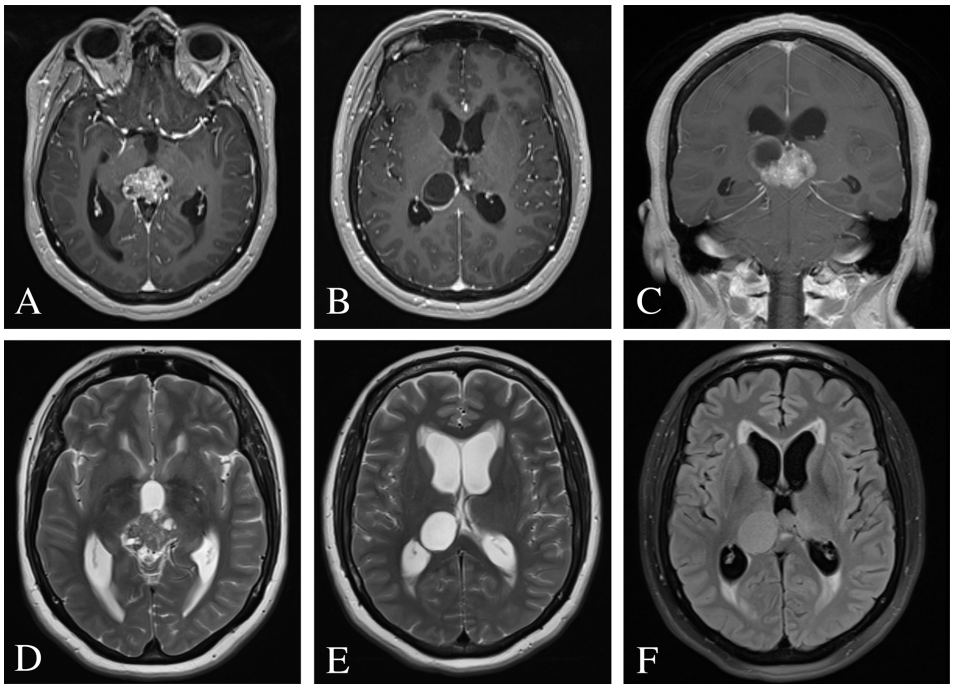


**FIGURE 2** | Pre-operative MRI of the brain. **(A–C)** Post-contrast T1-weighted images demonstrating a heterogeneously enhancing 3.9 × 2.6 × 3.1 cm mixed cystic and solid pineal mass and consequential obstructive hydrocephalus. **(D, E)** T2-weighted images revealed a hyperintense cystic lesion and hypointense solid lesion with mass effect and compression of the cerebral aqueduct resulting in supratentorial ventricular dilatation and periventricular white matter signal abnormality. **(F)** FLAIR image demonstrated periventricular transependymal flow of cerebrospinal fluid indicative of acute hydrocephalus.

all intracranial metastases (1, 2). Although lung cancer is the most common source of disease dissemination to the pineal gland, or epiphysis cerebri, various malignant tumors have been reported to spread to this site including esophageal, stomach, liver, colon, pancreas, kidney, bladder, prostate, thyroid, breast, melanoma, myeloma, and leukemia (4–6, 10). There is only one other report in the literature describing pineal gland metastasis from a bronchopulmonary neuroendocrine tumor (7).

Carcinoid tumors are a rare, diverse group of neoplasms that arise from endodermal precursor cells (11). These lesions primarily originate from the gastrointestinal tract and bronchopulmonary system in 54.5 and 30.1% of cases, respectively; nevertheless, they may also arise from a multitude of other organs such as the thymus, pancreas, liver, uterus, ovary, testes, bladder, and rectum (11, 12). Bronchopulmonary neuroendocrine tumors, arising from pulmonary neuroendocrine cells reside as individual cells or as clusters of cells, account for approximately 25% of all primary lung neoplasms (8). These lesions are classified into four distinct subtypes including: (i) well-differentiated, low-grade typical carcinoids; (ii) well-differentiated, intermediate-grade atypical carcinoids; (iii) poorly differentiated, high-grade large cell neuroendocrine carcinoma; and (iv) poorly differentiated, high-

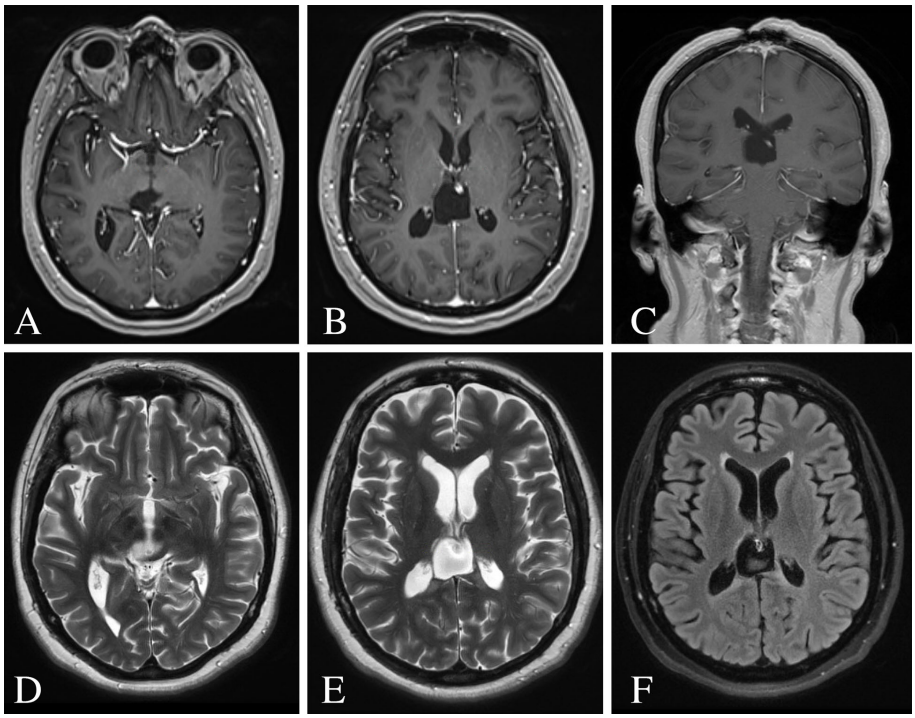


**FIGURE 3** | Post-operative MRI of the brain 12 months following surgery. **(A–C)** Post-contrast T1-weighted images demonstrating no evidence of residual or recurrent disease. **(D, E)** T2-weighted images showing resolution of the ventricular dilatation and flow voids from the internal cerebral veins. **(F)** FLAIR image showing minimal hyperintense signal surrounding the surgical resection cavity.

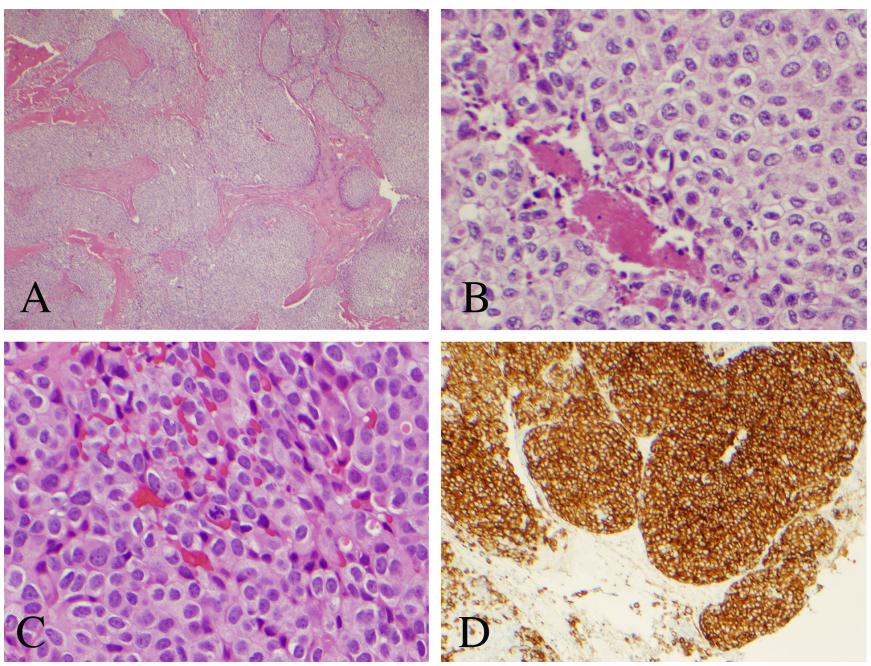


**FIGURE 4** | Histopathological analysis of the resected pineal lesion. **(A)** Hematoxylin and eosin (H&E) stain with nested architecture and sheets of cells (original magnification, 40×). **(B)** H&E stain with sheets of cells with speckled chromatin and indistinct to small nucleoli with multifocal necrosis (original magnification, 200×). **(C)** H&E stain with mitotic figure (original magnification, 400×). **(D)** Strong immunostaining of tumor cells with synaptophysin (original magnification, 100×).

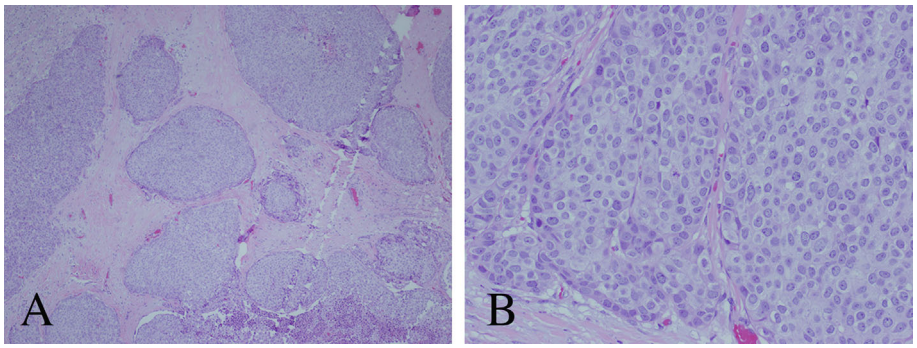


**FIGURE 5** | Histopathological analysis of the primary atypical bronchopulmonary carcinoid tumor. **(A)** Hematoxylin and eosin (H&E) stain with nested architecture and sheets of cells (original magnification, 40×). **(B)** H&E stain with sheets of cells with speckled chromatin and indistinct to small nucleoli (original magnification, 200×).

grade small cell lung cancer (8, 9). Although typical and atypical carcinoids are categorized as low- and intermediate-grade tumors, respectively, these tumors are capable of regional lymph node metastasis as well as spread to distant sites (8, 13–15). Indeed, 5–20% of typical carcinoids and 30–40% of atypical carcinoids are known metastasize. The most common sites of disease dissemination include regional lymph nodes, lung, liver, and bones (8). Brain metastases are an exceptionally rare finding in patients with neuroendocrine tumors with <5% of patients exhibiting intracranial involvement (16, 17). Furthermore, only 1.4% of metastatic brain tumors are of neuroendocrine origin, the majority of which derive from the lung (16, 17). Nevertheless, brain metastases portend a poor prognosis with a median overall survival of 8 months following initial diagnosis of intracranial dissemination (18). However, the most common cause of mortality in patients with intracranial involvement is attributable to the progression of systemic disease rather than sequelae associated with central nervous system dysfunction (11, 16–18).

Given the rarity of intracranial involvement of neuroendocrine tumors, there are no randomized or prospective data to base definitive treatment recommendations. Variable clinical outcomes have been reported in patients treated with neurosurgical resection, stereotactic radiosurgery, whole-brain radiotherapy (WBRT), or a combined treatment approach of intracranial carcinoid metastases (11, 16, 19, 20). Schupak and Wallner assessed treatment response of external-beam radiation therapy in 44 patients with metastatic or unresectable carcinoid tumors including eight patients with brain metastases (19). The authors found that none of the patients with brain metastases exhibited progression of their intracranial disease after radiation therapy with a median dose of 3,300 cGy. Rather, all eight patients ultimately died due to progression of systemic disease (19). Hlatky et al. analyzed treatment modalities and correlates of survival in 24 patients with brain metastases of carcinoid origin (16). The metastases were treated with WBRT alone in seven patients, surgical resection in 12 patients of which seven received adjuvant WBRT (16). The longest median survival (3.2 years) was observed in the cohort that underwent surgical resection plus adjuvant WBRT (16). Mallory and coworkers evaluated 15 patients with primary carcinoid tumors and intracranial metastases who were treated with either surgical resection (n = 12), stereotactic radiosurgery (n = 2), or WBRT (n = 1) (11). The cohort that underwent surgical resection as the primary treatment modality demonstrated longer progression-free intervals, yet this failed to reach statistical significance (p = 0.095) (9). Krug et al. retrospectively analyzed the clinicopathologic factors and outcome data in a cohort of 51 patients with neuroendocrine tumors with associated brain metastases (20). The authors found no significant difference in median overall survival in patients with brain metastases regardless of intervention. Median overall survival times for WBRT alone, surgical resection plus radiation, or observation were 8 months, 7 months, and 18 months, respectively (p = 0.72) (20). These data have begun to lay the groundwork for optimal treatment modalities for intracranial metastases of carcinoid origin; however, further prospective and randomized trials are necessary to define treatment guidelines.

Although carcinoid tumors have been reported to metastasize to various supratentorial and infratentorial locations, dissemination to the pineal gland is an exceedingly rare phenomenon with only one other report to date in the current literature (7). Grozinsky-Glasberg et al. described a 71-year-old male with brochopulmonary neuroendocrine tumor (unspecified subtype) metastasis to the pineal gland 10 years after initial diagnosis of the primary tumor (7). Endoscopic biopsy of the pineal lesion confirmed a diagnosis of bronchopulmonary neuroendocrine tumor. Of note, the intracranial metastasis exhibited a lower Ki-67 proliferation rate than that of the primary lesion (8 *vs* 20%) confirming heterogeneity of proliferation rates between primary and metastatic cells (7). The authors deemed the lesion inaccessible to surgical resection and instead referred for radiosurgery (unspecified type or dose) (7). The tumor regressed on follow-up imaging although no details were provided regarding follow-up neuroimaging findings or clinical status post-radiation.

In the present case, our patient was diagnosed with atypical bronchopulmonary carcinoid with regional lymph nodes metastasis 2 years prior to presentation. We pursued aggressive neurosurgical resection of the lesion with the intent of gross total

resection followed by adjuvant stereotactic radiosurgery to maximize local disease control. One year from the initial operation, she remains clinically stable and follow-up MRI demonstrated no evidence of disease residual intracranially.

Pineal gland lesions are arguably one of the most challenging locations within the intracranial compartment to achieve gross total resection. However, as described herein, aggressive neurosurgical intervention upfront afforded local disease control intracranially at the cost of transient neurologic symptomatology that resolved in the following months. To our knowledge, the present case is first to describe successful neurosurgical resection of a pineal gland lesion of bronchopulmonary neuroendocrine origin. This case highlights a proof-of-concept that aggressive surgical resection of pineal region neuroendocrine metastasis in experienced hands should be considered in the appropriate patient population as gross total resection may afford excellent long-term local disease control.

## CONCLUSIONS

We describe a unique case of bronchopulmonary neuroendocrine tumor metastasis to the pineal gland and our treatment approach. The present case demonstrates that neuroendocrine tumor metastasis should be considered in the differential diagnosis of pineal gland lesions. Although there are no standardized treatment guidelines for brain metastases of neuroendocrine origin, with each reported case we obtain a better understanding of the natural history and optimal treatment approach for these rare lesions. An aggressive management approach, including microsurgical resection of pineal region neuroendocrine metastasis, should be considered in carefully selected patients and can provide excellent long-term outcomes.

## DATA AVAILABILITY STATEMENT

The original contributions presented in the study are included in the article/supplementary material. Further inquiries can be directed to the corresponding author.

## ETHICS STATEMENT

Ethical review and approval was not required for the study on human participants in accordance with the local legislation and institutional requirements. The patients/participants provided their written informed consent to participate in this study. Written informed consent was obtained from the individual(s) for the publication of any potentially identifiable images or data included in this article.

## AUTHOR CONTRIBUTIONS

JC and MK are the primary authors of the manuscript. JC, MK, EM, EG, CB, CR, RJ, and SM provided substantial contributions to the conception and design of the manuscript. JC, MK, EM, EG, CB, CR, RJ, and SM agreed to be accountable for all aspects of the work ensuring that questions related to the accuracy or integrity of any part of the work are investigated and resolved. All authors contributed to the article and approved the submitted version.

## FUNDING

Funding was provided by Carilion Clinic Neurosurgery and the Fralin Biomedical Research Institute at Virginia Tech Carilion School of Medicine.

## REFERENCES

1. Taydas O, Yesilyurt M, Ogul Y, Ogul H. Isolated pineal gland metastasis of acute lymphocytic leukemia: case report. *Cancer Biol Ther* (2020) 21(6):503–5. doi: 10.1080/15384047.2020.1735605
2. Li J, Wang P, Wang B. Unique case report of pineal gland metastasis from bladder carcinoma. *Med (Baltimore)* (2016) 95(18):e3622. doi: 10.1097/MD.0000000000003622
3. örster G. Ein Fall von Markschwamm mit ungewöhnlich vielfacher metastatischer Verbreitung. *Archiv f Pathol Anat* (1858) 13:271–4. doi: 10.1007/BF02822510
4. Ji J, Gu C, Zhang M, Zhang H, Wang H, Qu Y, et al. Pineal region metastasis with intraventricular seeding: A case report and literature review. *Med (Baltimore)* (2019) 98(34):e16652. doi: 10.1097/MD.0000000000016652
5. Lassman AB, Bruce JN, Fetell MR. Metastases to the pineal gland. *Neurology* (2006) 67(7):1303–4. doi: 10.1212/01.wnl.0000238516.29603.33
6. Vaquero J, Ramiro J, Martínez R, Bravo G. Neurosurgical experience with tumours of the pineal region at Clinica Puerta de Hierro. *Acta Neurochir (Wien)* (1992) 116(1):23–32. doi: 10.1007/BF01541249
7. Grozinsky-Glasberg S, Fichman S, Shimon I. Metastatic bronchial neuroendocrine tumor to the pineal gland: a unique manifestation of a rare disease. *Hormones (Athens)* (2010) 9(1):87–91. doi: 10.14310/horm.2002.1258
8. Hendifar AE, Marchevsky AM, Tuli R. Neuroendocrine tumors of the lung: current challenges and advances in the diagnosis and management of well-differentiated disease. *J Thorac Oncol* (2017) 12(3):425–36. doi: 10.1016/j.jtho.2016.11.2222
9. Rekhtman N. Neuroendocrine tumors of the lung: an update. *Arch Pathol Lab Med* (2010) 134(11):1628–38. doi: 10.1043/2009-0583-RAR.1
10. Cao F, Sada DM, Lai S, Sada YH. Stereotactic radiosurgery for carcinoid brain metastasis: a case report. *Cureus* (2019) 11(8):e5509. doi: 10.7759/cureus.5509
11. Mallory GW, Fang S, Giannini C, Van Gompel JJ, Parney IF. Brain carcinoid metastases: outcomes and prognostic factors. *J Neurosurg* (2013) 118(4):889–95. doi: 10.3171/2013.1.JNS121556
12. Modlin IM, Sandor A. An analysis of 8305 cases of carcinoid tumors. *Cancer* (1997) 79(4):813–29. doi: 10.1002/(sici)1097-0142(19970215)79:4<813::aid-cncr19>3.0.co;2-2
13. Soga J, Yakuwa Y. Bronchopulmonary carcinoids: An analysis of 1,875 reported cases with special reference to a comparison between typical carcinoids and atypical varieties. *Ann Thorac Cardiovasc Surg* (1999) 5(4):211–9.
14. Chen X, Pang Z, Wang Y, Bie F, Zeng Y, Wang G, et al. The role of surgery for atypical bronchopulmonary carcinoid tumor: Development and validation of a model based on Surveillance, Epidemiology, and End Results (SEER) database. *Lung Cancer* (2020) 139:94–102. doi: 10.1016/j.lungcan.2019.11.006
15. Yoon JY, Sigel K, Martin J, Jordan R, Beasley MB, Smith C, et al. Evaluation of the prognostic significance of TNM staging guidelines in lung carcinoid tumors. *J Thorac Oncol* (2019) 14(2):184–92. doi: 10.1016/j.jtho.2018.10.166
16. Hlatky R, Suki D, Sawaya R. Carcinoid metastasis to the brain. *Cancer* (2004) 101(11):2605–13. doi: 10.1002/cncr.20659

17. Reed CT, Duma N, Halfdanarson T, Buckner J. Primary neuroendocrine carcinoma of the brain. *BMJ Case Rep* (2019) 12(9):e230582. doi: 10.1136/bcr-2019-230582
18. Akimoto J, Fukuhara H, Suda T, Nagai K, Ichikawa M, Fukami S, et al. Clinicopathological analysis in patients with neuroendocrine tumors that metastasized to the brain. *BMC Cancer* (2016) 16:36. doi: 10.1186/s12885-015-1999-x
19. Schupak KD, Wallner KE. The role of radiation therapy in the treatment of locally unresectable or metastatic carcinoid tumors. *Int J Radiat Oncol Biol Phys* (1991) 20(3):489–95. doi: 10.1016/0360-3016(91)90061-8
20. Krug S, Teupe F, Michl P, Gress TM, Rinke A. Brain metastases in patients with neuroendocrine neoplasms: risk factors and outcome. *BMC Cancer* (2019) 19(1):362. doi: 10.1186/s12885-019-5559-7

**Conflict of Interest:** The authors declare that the research was conducted in the absence of any commercial or financial relationships that could be construed as a potential conflict of interest.

frontiers in Endocrinology

CASE REPORT
published: 07 April 2021
doi: 10.3389/fendo.2021.654638

# Case Report: A New Entity: Multiple Differentiated Variant of Papillary Thyroid Carcinoma With Advanced Clinical Behavior

*Jing Yang*[1], *Rixiang Gong*[1], *Yu Ma*[1], *Jun Gao*[2], *Zhihui Li*[1], *Jingqiang Zhu*[1] *and Yanping Gong*[1]*

[1] Thyroid and Parathyroid Surgery Center, West China Hospital, Sichuan University, Chengdu, China, [2] Department of Toxicological Inspection, Sichuan Center for Disease Control and Prevention, Chengdu, China

OPEN ACCESS

**Edited by:**
*Antongiulio Faggiano, Sapienza University of Rome, Italy*

**Reviewed by:**
*Carmela De Crea, Università Cattolica del Sacro Cuore, Italy*
*Elisa Giannetta, Sapienza University of Rome, Italy*

***Correspondence:**
*Yanping Gong*
*yanpinggong@foxmail.com*

**Specialty section:**
*This article was submitted to Cancer Endocrinology, a section of the journal Frontiers in Endocrinology*

**Received:** *17 January 2021*
**Accepted:** *19 March 2021*
**Published:** *07 April 2021*

**Citation:**
*Yang J, Gong R, Ma Y, Gao J, Li Z, Zhu J and Gong Y (2021) Case Report: A New Entity: Multiple Differentiated Variant of Papillary Thyroid Carcinoma With Advanced Clinical Behavior. Front. Endocrinol. 12:654638. doi: 10.3389/fendo.2021.654638*

There are many histological morphological types of papillary thyroid carcinoma (PTC), but the most frequently seen types are conventional. A single PTC commonly has a conventional and/or a variant morphological pattern. PTC with multiple (more than two) well-differentiated morphological patterns are extremely rare. We herein report the rare case of a 48-year-old male with initial diaphragmatic, pancreatic, and liver tumors from PTC. Then, the PTC was discovered following resection of these tumors, an ultrasound-guided fine-needle aspiration (US-FNA) cytology of a huge mass in the thyroid's left lobe revealed a PTC. After postoperative recovery, physical and ultrasound examinations identified an irregular large nodule in the thyroid's isthmus and left lobe, several swollen lymph nodes in the left neck, a mass in the left gluteus maximus, and several masses in both the bilateral parotid and salivary regions. The US-FNA's pathological examination confirmed metastatic PTCs in the left gluteus maximus and bilaterally in the parotid and salivary glands. An 18-fluorodeoxyglucose positron-emission tomography and computed tomography scan revealed abnormal uptakes in numerous locations (e.g., thyroid's isthmus and left lobe, bilateral parotid gland, and subcutaneous tissues). The patient underwent palliative therapy—including total thyroidectomy, bilateral central neck dissection, left lateral neck dissection, and excision of the bilateral parotid and salivary glands. A whole-body scan post-therapeutic radioactive iodine ablation revealed exclusive thyroid bed uptake. The patient subsequently underwent thyroid stimulating hormone (TSH) repression therapy and chemotherapy with lenvatinib, and thereafter achieved stable clinical conditions. Further histopathological analysis of the PTC revealed multiple differentiated morphological patterns in the single tumor located in the isthmus and left lobe of the thyroid, and in some metastatic lesions. Different metastatic lesions also presented different morphological patterns of PTC. In conclusions, we identified a new entity of PTC as a multiple differentiated variant of PTC (MDV-PTC) with an aggressive clinical nature.

**Keywords: PTC, single tumor, morphological patterns, multiple differentiated variant, entity**

## BACKGROUND

Papillary thyroid carcinoma (PTC) is the most common thyroid carcinoma and has many histological morphological variants, but the conventional type is commonly observed. The variants of PTC as classified by the World Health Organization (WHO) 2017 guidelines are: papillary microcarcinoma, encapsulated, follicular, diffuse sclerosing, tall cell, columnar cell, cribriform-morular, hobnail, fibromatosis/fasciitis-like stroma, solid/trabecular, oncocytic, spindle cell, clear cell, and Warthin-like (1). The follicular variant of PTC is the most common after conventional PTC (2), and other variants, such as diffuse sclerosing, tall cell, columnar cell, and hobnail variant are less often observed. In addition, conventional PTC usually has favorable clinicopathologic features and an excellent prognosis. However, some variants of PTC—such as diffuse sclerosing, tall cell, columnar cell, hobnail variant, and solid variants—behave more aggressively than conventional PTC (3, 4). In a single tumor, PTC commonly presents as conventional and/or a variant morphological pattern. PTC with multiple (more than two) well-differentiated morphological patterns is extremely rare. We herein report a 48-year-old male who presented with a single thyroid tumor composed of conventional PTC morphology with co-existent multiple variant patterns of PTC, as well as cervical lymph node metastases and multiple distant metastases of multiple morphological patterns of PTC.

## CASE PRESENTATION

A 48-year-old male was referred to the Pancreas Surgery Department of West China Hospital, Sichuan University for a mass of the pancreatic body and a nodule of the right liver as identified on abdominal ultrasound examination. The patient had not any significant findings in his past medical history except excision of superficial lipomyoma and pancreatitis. He had a history of smoking, but not drinking or drug abusing. He neither had exposure to radiation. Family history revealed the presence of lung cancer in his father. Subsequently, the patient underwent resection of a firm irregular masse (1.5 × 1.0 × 0.7 cm) located in the diaphragm, a firm irregular masse (measuring 2.5 × 2.0 × 1.5 cm) in pancreatic body, and three firm irregular masses (diameter: 0.5–0.8cm) on the surface of the liver on January 31, 2018. Pathological examination and immunohistochemical analyses of these excised tissues revealed metastatic PTCs. A subsequent cervical ultrasound examination revealed a huge mass (8.1 × 5.1 × 4.1 cm) in the left lobe of the thyroid, and an ultrasound-guided fine-needle aspiration (US-FNA) cytology revealed PTC.

The patient was referred to the Thyroid and Parathyroid Surgery Center of our institution for evaluation for thyroid surgery in June 2018 following a postoperative recovery period of more than four months. A physical examination showed an irregular large nodule in the isthmus and left lobe of the thyroid, a swollen lymph node in the left cervical lateral compartment, and a mass in the right parotid gland. An ultrasound reexamination revealed the following findings: a very large hypoechoic mass (7.3 × 5.9 × 5.1 cm) in the isthmus and entire left lobe of the thyroid, multiple hypoechoic nodules (about 0.2–0.3 cm) in the right lobe of the thyroid, several swollen lymph nodes in the left cervical lateral compartment, several masses in the bilateral parotid region, several nodules in the bilateral salivary region, and a mass in the left gluteus maximus. US-FNA's histological results and immunohistochemical analyses confirmed the presence of metastatic PTCs bilaterally in the parotid gland, and bilaterally in the salivary gland. Both an 18-fluorodeoxyglucose positron-emission tomography and computed tomography scan were ordered for further evaluation and identification of possible occult metastases. The first revealed abnormal uptakes in the following locations: isthmus and left lobe of the thyroid (maximum standardized uptake value [max SUV]:25.22), bilaterally in the parotid gland (left max SUV:16.02, right max SUV:22.51), left salivary gland (max SUV:8.7), left cervical region (max SUV:15.6), bilaterally in the lungs (max SUV:13.41), pancreatic head (max SUV:17.12), right kidney (max SUV:8.71), multiple cones and ribs (max SUV:17.50), and muscles and subcutaneous tissues (max SUV:26.96) (**Figure 1**).

The patient underwent palliative surgical therapy. Specifically, on July 2, 2018, the patient received a total thyroidectomy, bilateral central neck dissection, left lateral neck dissection, and bilateral excision of the parotid and salivary glands. A firm irregular tumor measuring 10.0 × 7.0 × 5.0 cm was observed intraoperatively. The tumor mass replaced the isthmus and left lobe of the thyroid. Additionally, it extended into the tracheoesophageal region and deepened into the superior mediastinum, invading the anterior cervical skeletal muscle. Furthermore, the tumor encapsulated and infiltrated the left recurrent laryngeal nerve and slightly infiltrated the left tracheal surface. Several swollen cervical lymph nodes were identified. The largest one measured 4.0 cm. Bilaterally in the parotid and salivary regions, there were many masses ranging from 0.5–3.5 cm. Of note, some of the masses invaded the facial nerve. Histological examination was performed postoperatively on the paraffin-embedded specimen. The results revealed PTC with multiple regional lymph node metastases, and distant parotid and salivary gland metastases. In addition, $BARF^{V600E}$ and *TERT* promoter mutation (C288T) were identified by next-generation sequencing in the primary thyroid tumor, the pancreatic and cervical lymph node metastases.

Postoperatively, the patient underwent TSH repression therapy (TSH < 0.10 mU/L) with oral administration of sodium levothyroxine (Euthyrox). Oral sodium levothyroxine treatment was suspended in August 2018 in preparation for radioactive iodine ablation therapy. RAI ablation therapy with 200 millicurie of I-131 was administered after two weeks. A whole-body scan following therapeutic RAI ablation showed uptake only in the thyroid bed and no uptake in any of the metastasizing lesions. Subsequently, the patient underwent continuous TSH repression (TSH < 0.10 mU/L) therapy with oral sodium levothyroxine. Additionally, he was treated with lenvatinib chemotherapy from December 2018. Computed tomography revealed that after more than 2 years of treatment, the

**Abbreviations:** PTC, Papillary thyroid carcinoma; WHO, Word Health Organization; US-FNA, Ultrasound-guided fine-needle aspiration; TSH, Thyroid stimulating hormone; HE, Hematoxylin-eosin; PDTC, Poorly-differentiated thyroid cancer; MDV-PTC, Multiple differentiated variant of PTC.

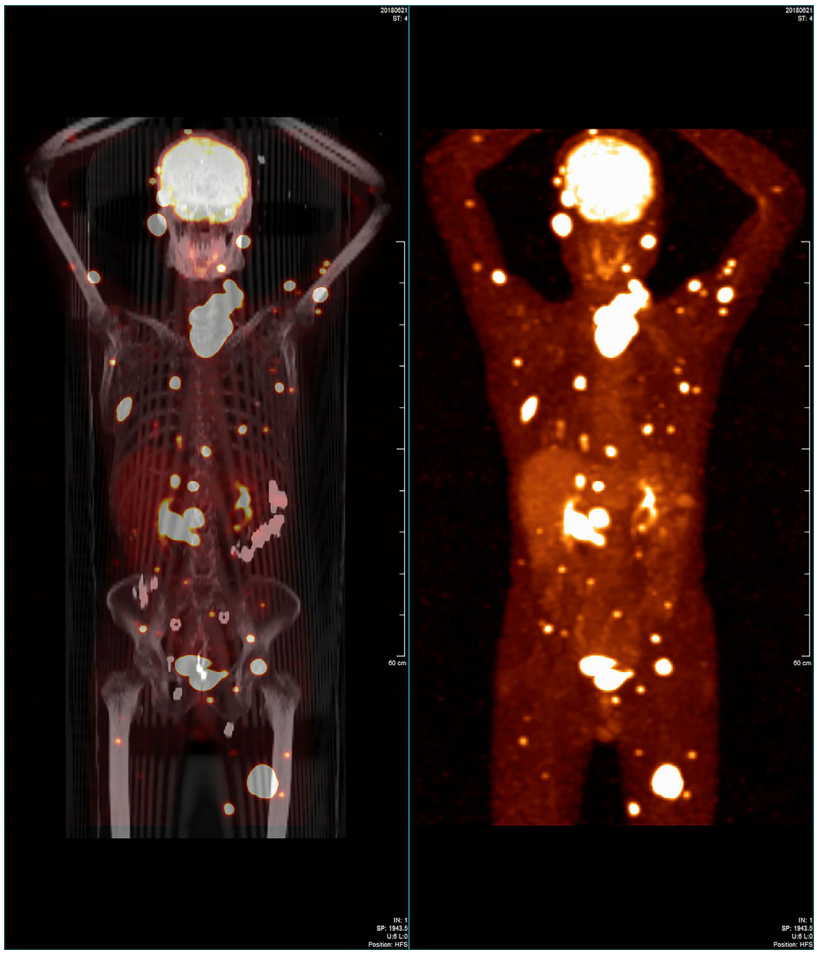

**FIGURE 1** | Whole-body 18-fluorodeoxyglucose positron-emission tomography/computed tomography image showing that many regions in the patient's body had widespread abnormal uptake.

number of metastatic lesions decreased. Additionally, serum thyroglobulin decreased to 15.84~50.60 ug/L (from 313.60 ug/L) as of December 31, 2020. The patient is currently alive with no apparent symptoms. Most of the above medical details have been presented in an other publication regarding the same case by Jing Y et al. (5), which can provide other more detailed medical information.

The postoperative formalin-fixed, paraffin-embedded tissue blocks were selected and hematoxylin–eosin (HE) stained slides were cut for further identification of histopathological subtypes of PTC. The paraffin sections were read after HE staining by Jun Gao's pathology team. These histopathological results showed that there were multiple differentiated morphological patterns in different sections and also in some of the same sections (**Figure 2**). Conventional morphological patterns of PTC were found in all sections. In addition, there was co-existence of columnar cell, tall cell, cribriform-morular, and solid/trabecular morphological patterns of PTC in the single tumor located in the isthmus and left lobe of the thyroid. There was co-existence of columnar, tall cell, and hobnail morphological patterns of PTC in cervical lymph nodes, and co-existence of columnar and tall cell morphological patterns of PTC in masses of the parotid and salivary glands. There was also co-existence of follicular and columnar morphological patterns of PTC in the single pancreatic mass, as well as co-existence of follicular, tall cell, and hobnail morphological patterns of PTC in masses of liver. Additionally, follicular and tall cell morphological patterns of PTC coexisted in a single mass of liver. There were columnar morphological patterns of PTC in a diaphragmatic mass. **Table 1** summarizes these results.

This case report was approved by the Institutional Review Board of West China Hospital of Sichuan University, and the patient has provided written informed consent for publicly publishing the case details and accompanying pictures.

## DISCUSSION

With the exception of a conventional morphological pattern, only a variant morphological pattern of PTC is generally present in a

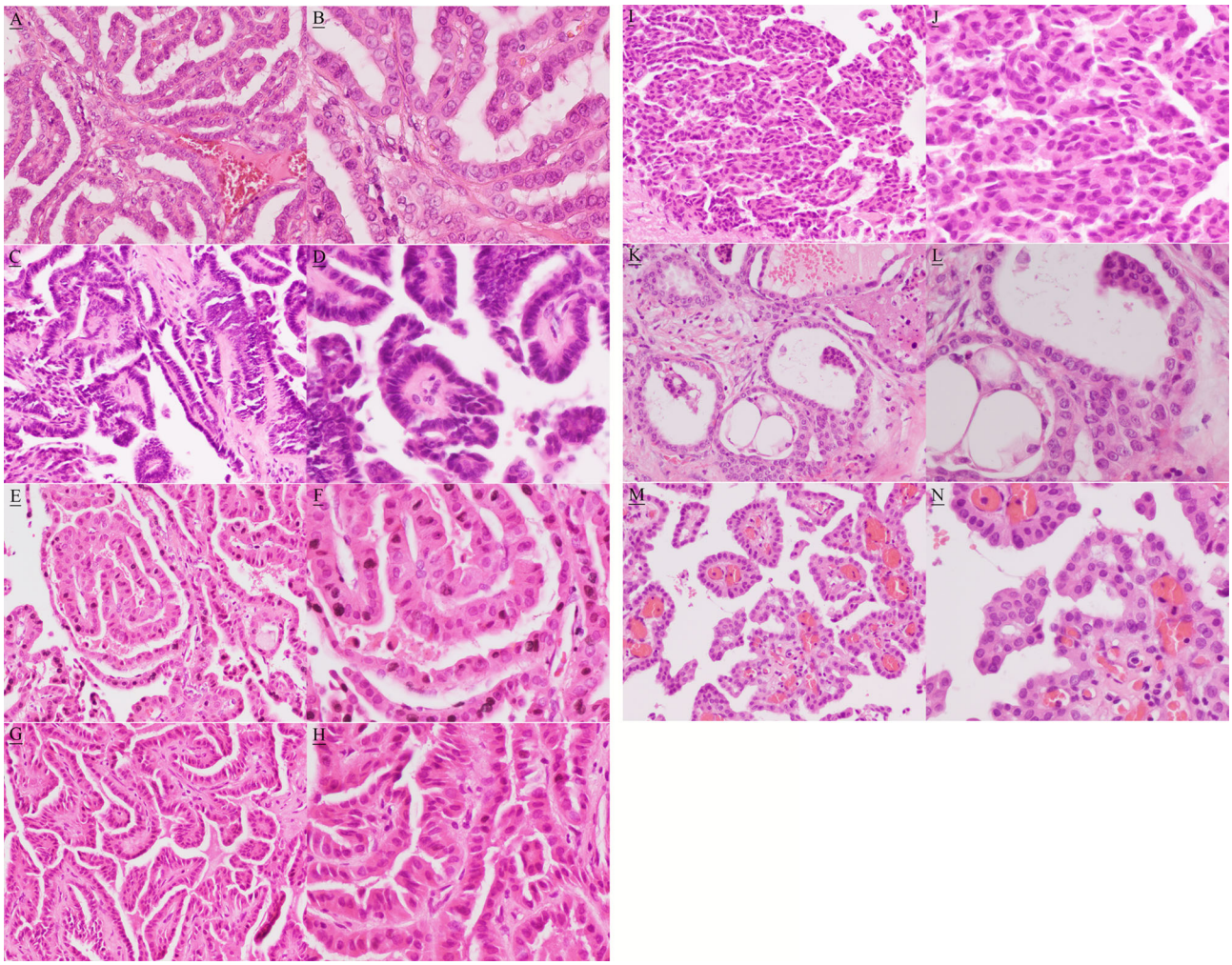


**FIGURE 2** | Hematoxylin and eosin image showing conventional (**A**, magnification, x200; **B**, magnification, x400), columnar (**C**, magnification, x200; **D**, magnification, x400), tall cell (**E**, magnification, x200; **F**, magnification, x400), cribriform-morular (**G**, magnification, x200; **H**, magnification, x400), solid/trabecular (**I**, magnification, x200; **J**, magnification, x400), follicular (**K**, magnification, x200; **L**, magnification, x400), and hobnail (**M**, magnification, x200; **N**, magnification, x400) morphological patterns.

single tumor. A single tumor with co-existing multiple variant morphological patterns of PTC is rare. Schopper HK et al. reported that a single thyroid tumor showed a combination of conventional PTC, follicular variant of PTC, clear cell variant of PTC, columnar cell variant of PTC, and poorly-differentiated thyroid carcinoma (PDTC) (6). In our present case, the single tumor showed multiple well-differentiated morphological patterns, including conventional, tall cell, columnar cell, cribriform-morular, and solid/trabecular morphological patterns. According to the present case and that reported by Schopper HK et al. (6), the entity may have multiple differentiating potential. Of course, it is possible that the multiple morphological patterns of PTC coexisted in initiation as a possibility of a supposed collision tumor. However, we think that the possibility of a collision tumor is less likely for five morphological components in a single primary tumor. In the present case, PDTC was not observed in the primary tumor. Most PDTCs arise from a follicular or PTC (7–10), and some PDTCs are *de novo* (11). Thus, our case may stand a good chance of dedifferentiation into PDTC.

In our present case, besides a single primary tumor presenting multiple well-differentiated variant carcinomas, some single metastatic foci also showed multiple variant carcinomas. The metastatic focus of the pancreas showed co-existence with columnar and follicular variant patterns of PTC, and one metastatic focus of the liver showed co-existence with tall cell and follicular variant patterns of PTC. The case reported by Schopper HK et al. showed that metastatic papillary clear cell carcinoma and columnar cell carcinoma were in juxtaposition in a lymph node deposit (6). However, the follicular variant pattern of PTC was not observed in the primary tumor. Furthermore, the hobnail variant pattern of PTC, which presented in a metastatic lymph node and a liver mass, was also not observed in the primary tumor. This indicates that metastatic lesions may also have multiple differentiating potential by imitating primary

**TABLE 1** | Variant pathological patterns of PTC in different lesions.

| Location of masses | Variant pathological patterns of PTC |
|---|---|
| Primary tumor | Columnar, tall cell, cribriform-morular, and solid/trabecular patterns |
| Cervical lymph nodes | Columnar, tall cell, and hobnail patterns |
| Parotid | Columnar and tall cell patterns |
| Salivary | Columnar and tall cell patterns |
| Pancreas | Follicular and columnar patterns |
| Liver | Follicular, tall cell, and hobnail patterns |
| Diaphragm | Columnar pattern |

tumor behavior, thereby making the possibility of collision tumor less likely. Of course, it is possible that the follicular and hobnail variant patterns of PTC, which may be left out in examining the primary thyroid tumor, directly metastasize to lymph nodes and/or distant locations.

The case by Schopper HK et al. showed vascular invasion and extensive lymph node involvement of the primary tumor (6). Our case presented a more aggressive clinical behavior. The primary tumor has obvious extrathyroidal extension, invading the anterior cervical skeletal muscle, the left recurrent laryngeal nerve, and the left tracheal surface. Additionally, the patient had extensive cervical lymph node metastases and multiple distant metastases (including lung, bone, and other rare distant metastases). The aggressive clinical behavior may be relative to aggressive variants of PTC. Because the primary tumor contains multiple aggressive variant patterns of PTC, such as the columnar variant, tall cell variant and solid/trabecular variant (3, 4), and the histological morphological results of lymph node metastases and distant metastases were mainly columnar and tall cell variant patterns of PTC, co-existing multiple aggressive variant patterns of PTC may contribute to more aggressive behavior, which results in extrathyroidal extension, lymph node metastases, and early multiple distant metastases. The patient may have a poor prognosis based on these aggressive clinicopathological features. Published meta-analyses performed on PTC have shown that co-existent $BRAF^{V600E}$ and *TERT* promoter mutations have a synergistic effect on poor clinical outcomes (12, 13). In this case, *TERT* promoter and $BRAF^{V600E}$ mutations were simultaneously detected in the primary tumor, which also may contribute to a poor prognosis.

From our point of view, this present case is a distinct new entity and extremely rare. We defined the new rare entity as multiple differentiated variant of PTC (MDV-PTC). To the best of our knowledge, we are the first to define MDV-PTC. The diagnosis of MDV-PTC should meet the following criteria: 1) Diagnosis of PTC by conventional criteria, 2) two or more than two different morphological growth patterns existing in a single tumor, except for conventional PTC pattern. Some other variants of PTC, which were defined according to percentage of growth pattern, may present two growth patterns. For instance, the hobnail variant of PTC is defined by > 30% of cell with hobnail features, and 3) absence of poorly-differentiated carcinoma patterns. The fourth edition (2017) of the WHO Classification of Tumors of Endocrine Organs reclassified PDTC as an independent class (1). Also, PDTC is the absence of the conventional nuclear features of PTC according to the histopathological diagnostic criteria for PDTC listed in the Turin consensus proposal (14). Of note, the MDV-PTC should be deemed as an aggressive variant for having aggressive clinicopathological features, including large tumor size, wide extrathyroidal extension, and the presence of lymph node metastases and multiple distant metastases.

## CONCLUDING REMARKS

We report an extremely rare new entity of PTC, and we firstly define the new entity as MDV-PTC. The MDV-PTC has an aggressive clinical behavior. However, additional future studies are needed to help us recognize the new entity.

## DATA AVAILABILITY STATEMENT

The raw data supporting the conclusions of this article will be made available by the authors, without undue reservation.

## ETHICS STATEMENT

The studies involving human participants were reviewed and approved by The Institutional Review Board of West China Hospital of Sichuan University. The patients/participants provided their written informed consent to participate in this study. Written informed consent was obtained from the individual(s) for the publication of any potentially identifiable images or data included in this article.

## AUTHOR CONTRIBUTIONS

JY, RG and YG managed the case. JY and YM collected patient data and image. JG designed method and did histopathological analysis. JY and YG wrote the manuscript. RG, ZL, and JZ conducted the study and revised the manuscript. All authors contributed to the article and approved the submitted version.

## FUNDING

This study was supported by grants from the Department of Sichuan Province, Science and Technology Support Program (grant no. 2018SZ0215).

## ACKNOWLEDGMENTS

We thank JG's pathology team for the support of histopathological analysis. Written informed consent was obtained from the patient to participating in the study and for publication of this manuscript. We thank the patient and his family for participating in this study.

## REFERENCES


1. RV Lloyd, RY Osamura, G Klöppel, J Rosai eds. *WHO Classification of Tumours of Endocrine Organs. 4th*. Lyon: IARC (2017).
2. Tielens ET, Sherman SI, Hruban RH, Ladenson PW. Follicular variant of papillary thyroid carcinoma: a clinicopathologic study. *Cancer* (1994) 73:424–31. doi: 10.1002/1097-0142(19940115)73:2<424::aid-cncr2820730230>3.0.co;2-i
3. Silver CE, Owen RP, Rodrigo JP, Rinaldo A, Devaney KO, Ferlito A. Aggressive variants of papillary thyroid carcinoma. *Head Neck* (2011) 33:1052–59. doi: 10.1002/hed.21494
4. Nath MC, Erickson LA. Aggressive Variants of Papillary Thyroid Carcinoma: Hobnail, Tall Cell, Columnar, and Solid. *Adv Anat Pathol* (2018) 25:172–9. doi: 10.1097/PAP.0000000000000184
5. Yang J, Ma Y, Gong Y, Gong R, Li Z, Zhu J. Multiple Simultaneous Rare Distant Metastases as the Initial Presentation of Papillary Thyroid Carcinoma: A Case Report. *Front Endocrinol (Lausanne)* (2019) 10:759. doi: 10.3389/fendo.2019.00759.
6. Schopper HK, Stence A, Ma D, Pagedar NA, Robinson RA. Single thyroid tumour showing multiple differentiated morphological patterns and intramorphological molecular genetic heterogeneity. *J Clin Pathol* (2017) 70:116–9. doi: 10.1136/jclinpath-2016-203821
7. Kumagai A, Namba H, Mitsutake N, Saenko VA, Ohtsuru A, Ito M, et al. Childhood thyroid carcinoma with BRAFT1799A mutation shows unique pathological features of poor differentiation. *Oncol Rep* (2006) 16:123–6. doi: 10.3892/or.16.1.123
8. Nakazawa T, Celestino R, Machado JC, Cameselle-Teijeiro JM, Vinagre J, Eloy C, et al. Cribriform-morular variant of papillary thyroid carcinoma displaying poorly differentiated features. *Int J Surg Pathol* (2013) 21:379–89. doi: 10.1177/1066896912473355
9. Lee DY, Won JK, Choi HS, Park do J, Jung KC, Sung MW, et al. Recurrence and Survival After Gross Total Removal of Resectable Undifferentiated or Poorly Differentiated Thyroid Carcinoma. *Thyroid* (2016) 26:1259–68. doi: 10.1089/thy.2016.0147
10. Nikitski AV, Rominski SL, Condello V, Kaya C, Wankhede M, Panebianco F, et al. Mouse Model of Thyroid Cancer Progression and Dedifferentiation Driven by STRN-ALK Expression and Loss of p53: Evidence for the Existence of Two Types of Poorly Differentiated Carcinoma. *Thyroid* (2019) 29:1425–37. doi: 10.1089/thy.2019.0284
11. Carcangiu ML, Zampi G, Rosai J. Poorly differentiated ("insular") thyroid carcinoma. A reinterpretation of Langhans' "wuchernde Struma". *Am J Surg Pathol* (1984) 8:655–68. doi: 10.1097/00000478-198409000-00005
12. Moon S, Song YS, Kim YA, Lim JA, Cho SW, Moon JH, et al. Effects of Coexistent BRAFV600E and TERT Promoter Mutations on Poor Clinical Outcomes in Papillary Thyroid Cancer: A Meta-Analysis. *Thyroid* (2017) 27:651–60. doi: 10.1089/thy.2016.0350
13. Chen B, Shi Y, Xu Y, Zhang J. The predictive value of coexisting BRAFV600E and TERT promoter mutations on poor outcomes and high tumour aggressiveness in papillary thyroid carcinoma: A systematic review and meta-analysis. *Clin Endocrinol (Oxf)* (2020). doi: 10.1111/cen.14316
14. Volante M, Collini P, Nikiforov YE, Sakamoto A, Kakudo K, Katoh R, et al. Poorly differentiated thyroid carcinoma: the Turin proposal for the use of uniform diagnostic criteria and an algorithmic diagnostic approach. *Am J Surg Pathol* (2007) 31:1256–64. doi: 10.1097/PAS.0b013e3180309e6a


**Conflict of Interest :** The authors declare that the research was conducted in the absence of any commercial or financial relationships that could be construed as a potential conflict of interest.

frontiers in Endocrinology

CASE REPORT
published: 22 April 2021
doi: 10.3389/fendo.2021.674039

# Case Report: Exceptional Response to Second Line Temozolomide Therapy in a Patient With Metastatic Adrenocortical Carcinoma

*Deborah Cosentini[1†], Antonella Turla[1†], Ornella Carminati[2], Salvatore Grisanti[1], Vittorio Domenico Ferrari[1], Marta Laganà[1], Giovanni Rosti[3], Sandra Sigala[4] and Alfredo Berruti[1*]*

[1] Medical Oncology Unit, Azienda Socio Sanitaria Territoriale (ASST) Spedali Civili, Department of Medical and Surgical Specialties, Radiological Sciences, and Public Health, University of Brescia, Brescia, Italy, [2] Medical Oncology, Department of Oncology and Hematology, Azienda Unità Sanitaria Locale (AUSL), Romagna, Ravenna, Italy, [3] Medical Oncology, Fondazione IRCCS Policlinico San Matteo, Pavia, Italy, [4] Section of Pharmacology, Department of Molecular and Translational Medicine, University of Brescia, Brescia, Italy

OPEN ACCESS

**Edited by:**
Barbara Altieri,
University Hospital of Wuerzburg, Germany

**Reviewed by:**
Peter Igaz,
Semmelweis University, Hungary
Jaydira Del Rivero,
National Cancer Institute (NIH), United States

***Correspondence:**
Alfredo Berruti
alfredo.berruti@gmail.com

[†]These authors have contributed equally to this work and share first authorship

**Specialty section:**
This article was submitted to Cancer Endocrinology, a section of the journal Frontiers in Endocrinology

**Received:** 28 February 2021
**Accepted:** 31 March 2021
**Published:** 22 April 2021

**Citation:**
Cosentini D, Turla A, Carminati O, Grisanti S, Ferrari VD, Laganà M, Rosti G, Sigala S and Berruti A (2021) Case Report: Exceptional Response to Second Line Temozolomide Therapy in a Patient With Metastatic Adrenocortical Carcinoma. Front. Endocrinol. 12:674039. doi: 10.3389/fendo.2021.674039

**Background:** In a recently published retrospective case series, Temozolomide was found active as second line approach in advanced ACC patients. The disease control rate obtained, however, was short-lived. We report here an ACC patient with extensive metastatic disease who obtained a remarkable long lasting response with this alkylating agent.

**Case Presentation:** a 22-year-old female patient with ACC presented at our Medical Oncology Department in poor general condition due the presence of extensive metastatic pulmonary involvement. The disease had progressed to etoposide, doxorubicin and cisplatin plus mitotane therapy. Second line temozolomide therapy was prescribed leading to a progressive improvement of patient general conditions. The disease restaging after 12 cycles revealed a complete response of lung lesions and the patient was free from progression for 14+ months.

**Conclusion:** Temozolomide therapy could be exceptionally efficacious in the management of ACC patients. The molecular mechanisms of sensitivity and resistance to this drug should be carefully studied, in order to select the patients destined to obtain a significant clinical benefit to the drug.

**Keywords: adrenal tumor, alkylating drug, progesterone, treatment, ACC**

## BACKGROUND

Adrenocortical carcinoma (ACC) is a rare and aggressive tumor with an incidence of 0.7-2 new cases per million populations per year (1). Surgery is the mainstay of therapy for localized diseases and patients with moderate to high risk of disease relapse and death are addressed to adjuvant mitotane therapy (2). The standard systemic treatment for advanced/metastatic tumors, not

amenable to surgical resection, is the combination of etoposide, doxorubicin and cisplatin plus mitotane (EDP-M) (3). The results of a large multicenter randomized clinical trial have demonstrated that the efficacy of this regimen is limited with a disease response of about 25% and a median overall survival of 14 months (4). However, a single Institution case series, in which surgery of residual disease after EDP-M was systematically performed when feasible, revealed that few patients (7%) can obtain a pathological complete response and a long term disease control (5). These data suggest that EDP-M scheme can be sometimes very efficacious. Few options are available for patients with disease progression to EDP-M. Gemcitabine plus metronomic capecitabine is a second line approach recommended by international guidelines (1), but the efficacy of this regimen is modest (6). Several target therapies substantially failed to demonstrate activity in ACC (7, 8) and the role of immunotherapy is currently under investigation (9).

In a recently conducted retrospective study, single agent temozolomide was found active as second line approach in advanced ACC patients with a response rate observed in 20% of patients. The disease control rate obtained, however, was short-lived (10).

Here, we presented the case of a 22-year-old female patient with advanced ACC reporting a dramatic disease response to temozolomide therapy.

## CASE PRESENTATION

A 22-year-old woman from Sicily presented in August 2019 at the Medical Oncology Unit of Santa Maria delle Croci hospital in Ravenna, Italy, with severe hypertension, hirsutism, oligomenorrhea, and epigastric pain. A CT scan showed a huge left adrenal mass (100x110mm) and multiple lung metastasis. Hormonal assessment revealed elevated plasma and urinary cortisol levels and elevated androgen levels. The patient's general conditions were compromised due to a severe Cushing's syndrome. A tumor biopsy was performed confirming the ACC diagnosis. The patient was immediately addressed to first line chemotherapy with the EDP-M regimen, administered in association with metyrapone, to rapidly obtain a control of hormone hypersecretion (11). A minimal disease response of lung metastases and no change of the primary tumor lesion was obtained after 2 chemotherapy cycles. The patient general conditions, however, consistently improved. Antineoplastic therapy was continued and, from the 3$^{rd}$ cycles onwards, mitotane serum levels had attained the therapeutic interval, ranging between 14.5 and 20.1 ng/ml. Unfortunately, a huge disease progression was observed at TC restaging after 5 cycles.

The patient was then referred to the Medical Oncology Unit in Brescia in January 2020. On admission her general conditions were poor (ECOG performance status 3). She suffered from uncontrolled pain, nausea, asthenia and dyspnea. Oxygen saturation was low (SpO2 88%), so continuous oxygen therapy was instituted.

The CT scan confirmed the voluminous left adrenal mass (160x110 mm in size) infiltrating the left kidney and revealed a dramatic disease progression in lung with multiple lesions affecting both hemithoraxes (**Figure 1**).

Due her serious conditions we deemed the patient not eligible to further intravenous chemotherapy. She was then discharged and entrusted to home palliative care in Sicily with the prescription of oral temozolomide at the dose of 200 mg/m2/die given for 5 consecutive days every 28 days and daily. Megestrol acetate 160 mg every day was also concomitantly prescribed to support appetite and patient kenesthesis. Mitotane was continued.

Progressively, the patient general conditions improved with a normalization of oxygen saturation and pain control. Temozolomide therapy was well tolerated without any relevant toxicity. After 2 months her quality of life returned to normal and megestrol acetate was interrupted while continuing both temozolomide and mitotane therapies. The CT restaging performed in March 2020 showed a partial response of lung metastases with a minimal response of the adrenal mass. The extent of lung disease further decreased at a subsequent CT in June 2020. In September the patient returned to Brescia for a follow-up visit. A CT scan revealed a complete disease response of lung metastases and a partial response of the abdominal lesion

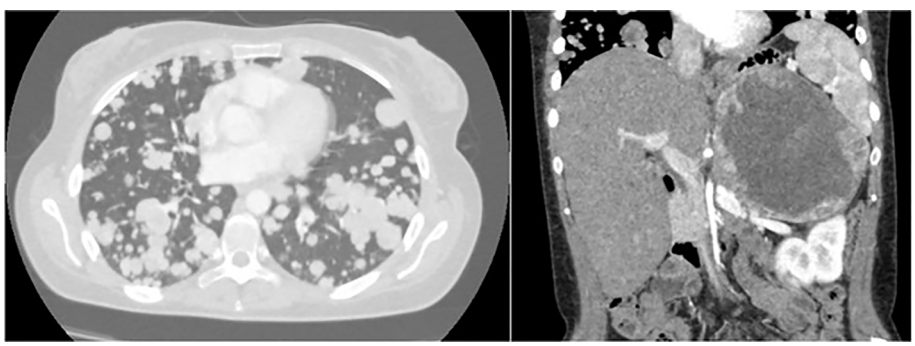

**FIGURE 1** | Multiple pulmonary metastases and adrenal mass detected by CT Scan (January 2020).

with dimension reduction (60 mm) and necrosis increase (**Figure 2**). The FDG PET scan confirmed the complete response of the lung lesions and, as regard the abdominal mass, a small peripheral uptake was described with an extensive central area with no FDG (fluorodesoxyglucose) uptake (necrosis) (**Figure 2**).

The last CT scan (December 2020) revealed a stable disease with respect to the previous control in September. At the last follow-up examination, on February 25$^{th}$, the patient general conditions were excellent (ECOG performance status 0). She was still on Temozolomide treatment (12 total cycles) along with mitotane and was free from progression for 14 months.

A Next Generation Sequencing (NGS) analysis, with a wide panel of genes (genic variant in hotspot regions of 35 genes -AKT1, ALK, AR, BRAF, CDK4, CTNNB1, DDR2, EGFR, ERBB2, ERBB3, ERBB4, ESR1, FGFR2, FGFR3, GNA11, GNAQ, HRAS, IDH1, IDH2, JAK1, JAK2, JAK3, KIT, KRAS, MAP2K1, MAP2K2, MET, MTOR, NRAS, PDGFRA, PIK3CA, RAF1, RET, ROS1, SMO; amplification of 19 genes- ALK, AR, BRAF, CCND1, CDK4, CDK6, EGFR, ERBB2, FGFR1, FGFR2, FGFR3, FGFR4, KIT, KRAS, MET, MYC, MYCN, PDGFRA, PIK3CA; rearrangements of 23 genes- ABL1, AKT3, ALK, AXL, BRAF, ERG, ETV1, ETV4, ETV5, EGFR, ERBB2, FGFR1, FGFR2, FGFR3, MET, NTRK1, NTRK2, NTRK3, FDGFRA, PPARG, RAF1, RET, ROS1) was performed on biopsy tumor samples at diagnosis. A genic variant in CTNN1B exon 3 (p.Met14Leu) was found (**Table 1**). This variant has never been published as pathogenetic in literature and it is not present in ClinVar, whereas it is categorized as VUS (variance of uncertain significance) in the VARSOME database. O6-methylguanine-DNA methyl-transferase (MGMT) and progesterone receptor (PgR) expression could not be assessed, due to insufficient tumor materials.

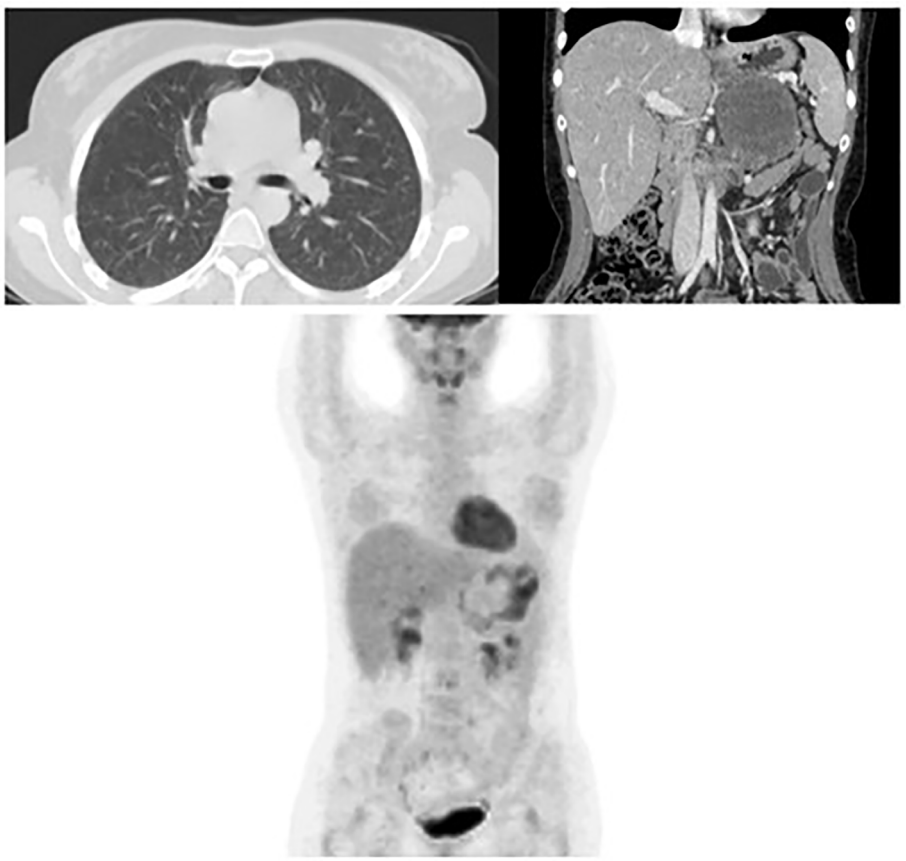

**FIGURE 2** | Complete response of the bilateral lung metastases and reduction of the primary adrenal lesion at the CT Scan after 8 cycles of temozolomide. FDG PET confirming the complete response of lung lesions and a small peripheral area of FDG uptake at the residual adrenal mass. (September 2020).

**TABLE 1** | Genic variant detected by NGS.

| Chromosome | Gene | Genic region | Proteic variant (cDNA) | Variant type | Coverage | Allelic frequency | Reference sequence |
|---|---|---|---|---|---|---|---|
| 3 | CTNN1B | Exon 3 | p.Met14Leu (c.40A>C) | Nucleotide sustitution | 1759 | 39.9% | NM_001098210.1 (GenBank) |

## DISCUSSION

Chemotherapy + mitotane (EDP-M) is modestly active as first first-line approach in the management of patients with advanced/metastatic ACC. At disease progression to EDP-M, the further administration of cytotoxic drugs gave disappointing results. At the best of our knowledge, this is the first ACC case that has obtained a dramatic response with a second-line chemotherapy. This result is even more relevant if we consider that the patient in question had an extensive disease burden and her performance status was very low. The latter condition is known to be an independent factor of poor efficacy of systemic antineoplastic treatments in general and ACC in particular (1).

It is certainly not clear why second-line temozolomide was particularly effective in this case. The drug was found to be able to induce a significant cytotoxic effect in ACC cells *in vitro* (12). However, in a recent Italian case series of pre-treated ACC patients, it proved to be moderately active with a disease response rate observed in 20% of treated cases, but poorly effective, as disease control was short lived (3.5 months on average) (10).

The addition of megestrol acetate for palliation may have contributed in the first weeks to support the patient's performance status and favored the cytotoxic effect of temozolomide. A recent paper by our group has in fact demonstrated an antineoplastic effect of progesterone in ACC cell lines and primary ACC cultures (13). Unfortunately, due to insufficient tissue material, it was not possible to test the expression of the PgR and MGMT in the primary tumor, which are known predictors of efficacy of megestrol acetate and temozolomide, respectively. The NGS performed failed to provide a potentially valuable predictive parameter.

In conclusion, the exceptional and long lasting disease response obtained with temozolomide in this ACC patient, suggests that this drug can be very efficacious in this setting. Temozolomide deserve to be further tested in ACC patients with the aim of identifying predictive factors of efficacy in order to select the patients destined to obtain a significant clinical benefit to the drug.

## DATA AVAILABILITY STATEMENT

The raw data supporting the conclusions of this article will be made available by the authors, without undue reservation.

## ETHICS STATEMENT

The studies involving human participants were reviewed and approved by Brescia ethics committee. The patients/participants provided their written informed consent to participate in this study. Written informed consent was obtained from the individual(s) for the publication of any potentially identifiable images or data included in this article.

## AUTHOR CONTRIBUTIONS

AB conceived the idea of this manuscript. OC, VF, GR, and AB clinically followed the patient. DC, AT, and ML collected and interpreted the patient clinical data and wrote the manuscript. All authors contributed to the article and approved the submitted version.

## FUNDING

This study was supported in part by FIRM onlus, Cremona, Italy and by Associazione Italiana per la Ricerca contro il Cancro (AIRC), IG: 14411.

## REFERENCES

1. Fassnacht M, Assie G, Baudin E, Eisenhofer G, de la Fouchardiere C, Haak HR, et al. Adrenocortical Carcinomas and Malignant Phaeochromocytomas: ESMO-EURACAN Clinical Practice Guidelines for Diagnosis, Treatment and Follow-Up. *Ann Oncol* (2020) 31(11):1476–90. doi: 10.1016/j.annonc.2020.08.2099
2. Berruti A, Grisanti S, Pulzer A, Claps M, Daffara F, Loli P, et al. Long-Term Outcomes of Adjuvant Mitotane Therapy in Patients With Radically Resected Adrenocortical Carcinoma. *J Clin Endocrinol Metab* (2017) 102(4):1358–65. doi: 10.1210/jc.2016-2894
3. Berruti A, Terzolo M, Sperone P, Pia A, Della Casa S, Gross DJ, et al. Etoposide, Doxorubicin and Cisplatin Plus Mitotane in the Treatment of Advanced Adrenocortical Carcinoma: A Large Prospective Phase II Trial. *Endocr Relat Cancer* (2005) 12(3):657–66. doi: 10.1677/erc.1.01025
4. Fassnacht M, Terzolo M, Allolio B, Baudin E, Haak H, Berruti A, et al. Combination Chemotherapy in Advanced Adrenocortical Carcinoma. *N Engl J Med* (2012) 366(23):2189–97. doi: 10.1056/NEJMoa1200966
5. Laganà M, Grisanti S, Cosentini D, Ferrari VD, Lazzari B, Ambrosini R, et al. Efficacy of the EDP-M Scheme Plus Adjunctive Surgery in the Management of Patients With Advanced Adrenocortical Carcinoma: The Brescia Experience. *Cancers (Basel)* (2020) 12(4):941. doi: 10.3390/cancers12040941
6. Sperone P, Ferrero A, Daffara F, Priola A, Zaggia B, Volante M, et al. Gemcitabine Plus Metronomic 5-Fluorouracil or Capecitabine as a Second-/Third-Line Chemotherapy in Advanced Adrenocortical Carcinoma: A Multicenter Phase II Study. *Endocr Relat Cancer* (2010) 17(2):445–53. doi: 10.1677/ERC-09-0281
7. Terzolo M, Daffara F, Ardito A, Zaggia B, Basile V, Ferrari L, et al. Management of Adrenal Cancer: A 2013 Update. *J Endocrinol Invest* (2014) 37(3):207–17. doi: 10.1007/s40618-013-0049-2
8. Grisanti S, Cosentini D, Laganà M, Abate A, Rossini E, Sigala S, et al. Are We Failing in Treatment of Adrenocortical Carcinoma? Lights and Shadows of Molecular Signatures. *Curr Opin Endocr Metab Res* (2019) 8:80–7. doi: 10.1016/j.coemr.2019.07.007
9. Grisanti S, Cosentini D, Laganà M, Volta AD, Palumbo C, Massimo Tiberio GA, et al. The Long and Winding Road to Effective Immunotherapy in Patients With Adrenocortical Carcinoma. *Future Oncol* (2020) 16(36):3017–20. doi: 10.2217/fon-2020-0686
10. Cosentini D, Badalamenti G, Grisanti S, Basile V, Rapa I, Cerri S, et al. Activity and Safety of Temozolomide in Advanced Adrenocortical Carcinoma Patients. *Eur J Endocrinol* (2019) 181(6):681–9. doi: 10.1530/EJE-19-0570
11. Claps M, Cerri S, Grisanti S, Lazzari B, Ferrari V, Roca E, et al. Adding Metyrapone to Chemotherapy Plus Mitotane for Cushing's Syndrome Due to

Advanced Adrenocortical Carcinoma. *Endocrine* (2018) 61(1):169–72. doi: 10.1007/s12020-017-1428-9

12. Creemers SG, van Koetsveld PM, van den Dungen ES, Korpershoek E, van Kemenade FJ, Franssen GJ, et al. Inhibition of Human Adrenocortical Cancer Cell Growth by Temozolomide in Vitro and the Role of the MGMT Gene. *J Clin Endocrinol Metab* (2016) 101(12):4574–84. doi: 10.1210/jc.2016-2768
13. Fragni M, Fiorentini C, Rossini E, Fisogni S, Vezzoli S, Bonini SA, et al. In Vitro Antitumor Activity of Progesterone in Human Adrenocortical Carcinoma. *Endocrine* (2019) 63(3):592–601. doi: 10.1007/s12020-018-1795-x

**Conflict of Interest:** The authors declare that the research was conducted in the absence of any commercial or financial relationships that could be construed as a potential conflict of interest.

frontiers in Endocrinology

REVIEW
published: 03 May 2021
doi: 10.3389/fendo.2021.680609

# Carney Triad, Carney-Stratakis Syndrome, 3PAS and Other Tumors Due to SDH Deficiency

*Georgia Pitsava*[1,2], *Nikolaos Settas*[2], *Fabio R. Faucz*[2*] *and Constantine A. Stratakis*[2]

[1] Division of Intramural Population Health Research, Eunice Kennedy Shriver National Institutes of Child Health and Human Development, National Institutes of Health, Bethesda, MD, United States, [2] Section on Endocrinology and Genetics, Eunice Kennedy Shriver National Institute of Child Health and Human Development, National Institutes of Health, Bethesda, MD, United States

Succinate dehydrogenase (SDH) is a key respiratory enzyme that links Krebs cycle and electron transport chain and is comprised of four subunits SDHA, SDHB, SDHC and SDHD. All *SDH*-deficient tumors are caused by or secondary to loss of SDH activity. As many as half of the familial cases of paragangliomas (PGLs) and pheochromocytomas (PHEOs) are due to mutations of the *SDHx* subunits. Gastrointestinal stromal tumors (GISTs) associated with *SDH* deficiency are negative for *KIT/PDGFRA* mutations and present with distinctive clinical features such as early onset (usually childhood or adolescence) and almost exclusively gastric location. *SDH*-deficient GISTs may be part of distinct clinical syndromes, Carney-Stratakis syndrome (CSS) or dyad and Carney triad (CT). CSS is also known as the dyad of GIST and PGL; it affects both genders equally and is inherited in an autosomal dominant manner with incomplete penetrance. CT is a very rare disease; PGL, GIST and pulmonary chondromas constitute CT which shows female predilection and may be a mosaic disorder. Even though there is some overlap between CT and CSS, as both are due to *SDH* deficiency, CSS is caused by inactivating germline mutations in genes encoding for the SDH subunits, while CT is mostly caused by a specific pattern of methylation of the *SDHC* gene and may be due to germline mosaicism of the responsible genetic defect.

**Keywords: Succinate dehydrogenase (SDH), GIST, paraganglioma, Carney triad, Carney-Stratakis syndrome, SDHB**

OPEN ACCESS

***Edited by:***
*Enzo Lalli,*
*UMR7275 Institut de pharmacologie moléculaire et cellulaire (IPMC), France*

***Reviewed by:***
*Attila Patocs,*
*Semmelweis University, Hungary*
*Andre Lacroix,*
*Université de Montréal, Canada*

***Correspondence:**
*Fabio R. Faucz*
*fabio.faucz@nih.gov*

***Specialty section:***
*This article was submitted to Cancer Endocrinology, a section of the journal Frontiers in Endocrinology*

***Received:*** *15 March 2021*
***Accepted:*** *12 April 2021*
***Published:*** *03 May 2021*

***Citation:***
*Pitsava G, Settas N, Faucz FR and Stratakis CA (2021) Carney Triad, Carney-Stratakis Syndrome, 3PAS and Other Tumors Due to SDH Deficiency. Front. Endocrinol. 12:680609. doi: 10.3389/fendo.2021.680609*

## INTRODUCTION

Succinate dehydrogenase (SDH - also known as mitochondrial complex II or succinate-ubiquinone oxydoreductase) is the only enzyme that is concurrently both a functional member of both the Krebs cycle (or citric acid or tricarboxylic acid cycle) and the electron transport chain (ETC), where it provides electrons for oxidative phosphorylation (1). It is comprised of four mitochondrial subunit proteins: SDHA, SDHB, SDHC, SDHD encoded by nuclear genes, mapped to 5p15.22, 1p36.13, 1q23.3 and 11q23.1, respectively (**Figure 1**). SDHA is a flavoprotein and SDHB is an iron-sulfur protein; together they make up the main catalytic component of the complex. The other two

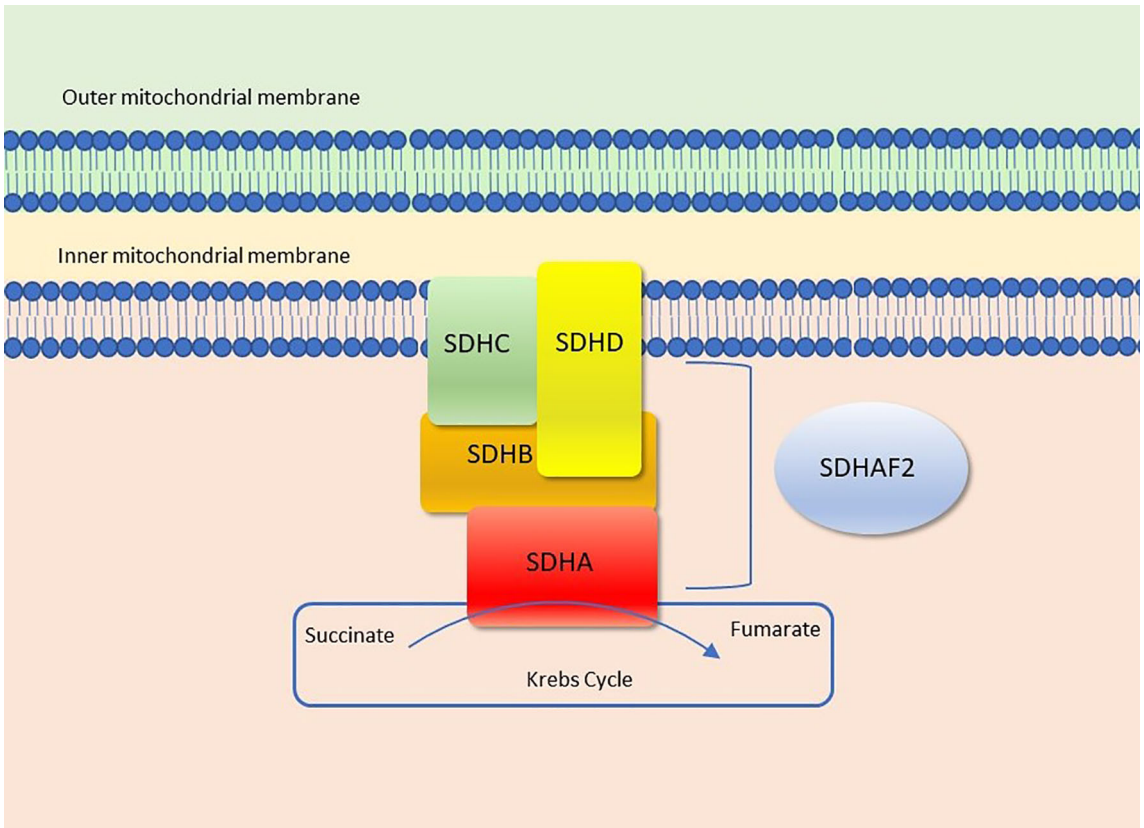


**FIGURE 1** | Succinate dehydrogenase (Complex II). Figure modified from Settas et al. (2).

subunits, SDHC and SDHD are two integral membrane proteins that anchor the complex to the inner mitochondrial membrane (3, 4). Additionally, the succinate dehydrogenase assembly factor 2 (SDHAF2) is required for the flavination and thus normal function of SDHA (4).

Genetic alterations in any of the four *SDHx* genes (*SDHA*, *SDHB*, *SDHC*, *SDHD*) or *SDHAF2* lead to SDH complex dysfunction and loss of SDHB expression (5). This loss of SDHB can be detected rapidly by immunohistochemistry (IHC) and thus, loss of immunohistochemical staining for SDHB is used as the hallmark of *SDH*-deficient tumors (6–9).

## HOW DO *SDHX* MUTATIONS LEAD TO TUMORIGENESIS?

It is not completely clear how the dysfunction of SDH leads to neoplasia; several mechanisms have been proposed. One of them is the activation of pseudohypoxia pathway (10). This mechanism implies that due to *SDH* deficiency, succinate is accumulated; this inhibits propyl hydroxylases (PHDs) resulting in induction of the hypoxic response despite normoxic conditions (pseudohypoxia) (11, 12). At the cellular level, the three α subunits of the hypoxia inducible factor-1 (HIF-1α, HIF2α, HIF3α), are hydroxylated by PHDs 1, 2 and 3 (also known as *Egln2*, *Egln1* and *Egln3*), which are oxygen-dependent enzymes. The hydroxylated HIFαs are then targeted by von Hippel-Lindau (VHL) protein for degradation in the proteasome. In order for the HIFs to be recognized by the VHL, hydroxylation of two proline residues on HIFα is required by PHDs. In the case that the *SHDx* genes are mutated, propyl hydroxylases are inhibited by the accumulated succinate, hydroxylation of HIF-1αs is decreased and therefore they escape degradation. As a result, they translocate to the nucleus, they dimerize with HIFβ and create a complex that activates genes that induce angiogenesis, cell proliferation and glycolysis (12, 13). This mechanism was further supported by additional studies (12, 14–17). Additionally, besides succinate, the accumulation of reactive oxygen species (ROS) in mitochondria, leading to loss of function of the SDH enzyme, has also been implicated in tumor pathogenesis. ROS are mainly produced in complex I (NADH-ubiquinone oxidoreductase) and complex III (ubiquinone-cytochrome c oxidoreductase) in ETC (18). Recently, Xiao et al. demonstrate that *SDHx* knockdown increases intracellular levels of succinate; subsequently, this acts as an alpha-ketoglutarate competitor, inhibiting a-KG-dependent dioxygenases, JIp1, which is involved in sulfur

metabolism and Jhd1 which belongs to the JmjC-domain-containing histone demethylase (JHDM) enzymes. That could lead to tumor formation by causing epigenetic changes (11, 19). The corresponding human JHDM, JMJD2D, was shown to be inhibited by accumulation of succinate as well (20).

Mutations in the *SDHx* subunits have been implicated in familial paragangliomas (PGLs) and pheochromocytomas (PHEOs), gastric stromal tumors (GISTs), Carney-Stratakis syndrome (CSS), and rarely in Carney triad (CT) and a few other tumors (21–30). This review focuses on *SDH*-deficient tumors, the two relevant genetic conditions, CSS and CT, and an association (3PAS), and their clinical, pathological and molecular characteristics.

## SDH-DEFICIENT PARAGANGLIOMAS AND PHEOCHROMOCYTOMAS

Pheochromocytomas and paragangliomas are rare neuroendocrine neoplasms derived from chromaffin cells (31). Tumors arising from the adrenal medulla, which is the largest paraganglion in the body, are termed PHEOs, while those derived from the sympathetic and parasympathetic paraganglia are known as PGLs (31). Extraadrenal locations most commonly include the head and neck, mainly the carotid body, jugular foramen, middle ear, but can also occur in the thorax, abdomen and pelvis (32). PGLs/PHEOs can be either sporadic or hereditary. As many as 35% of them are due to genetic predisposition (33). To date, more than 20 susceptibility genes have been identified (34). Germline mutations of *SDHB*, *SDHC*, and *SDHD* genes are responsible for approximately 50% of hereditary paragangliomas (4, 24, 25, 35–38) and pheochromocytomas (24, 36, 39). Recently, mutations in *SDHA* (21) and *SDHAF2* were also identified in hereditary PHEOs and PGLs (40). In addition, multiple reports have shown that these tumors have high incidence in patients with cyanotic congenital heart disease (41–43).

Depending on the *SDHx* subunit that is mutated, PGL syndromes have different characteristics (**Table 1**): *SDHD* (PGL1) (OMIM#168000)-mutated PGLs are more common in the head and neck and appear to have very high lifetime penetrance as 75% of carriers will have manifestations by 40 years old (44). Mutations in *SDHB* gene as the susceptibility gene for PGL4 (OMIM#115310) are more likely to be in the abdomen and show very high metastatic risk, but lower penetrance compared to PGL1 (~40% of carriers manifest the disease by age 40) (45). On the other hand, in *SDHC* (PGL3) (OMIM#605373) gene mutations, much rarer than the previous two, tumors are more commonly located in the carotid body (35, 46, 47) and have a low malignant potential (45). Mutations in *SDHA* and *SDHAF2* are associated with PGL5 (OMIM#614165) and PGL2 (OMIM#601650) respectively and are very rare. A patient with any type of PGL will present in any of the following contexts: a) because of signs and/or symptoms of excess catecholamine secretion (e.g. hypertension, headache, palpitations, hyperhidrosis, tremor); b) because of an incidental finding on an imaging study; c) because of signs and/or symptoms due to a local mass (various signs and/or symptoms depending on the location); and d) after a genetic testing was performed in the case of familial disease. Histologically, SDH-deficient PHEOs/PGLs have a nested architecture with round cells and prominent vasculature (4).

PHEOs can occur as part of PGL1 and PGL4 and about 3% of them are attributed to *SDH* deficiency (6). The rest of them are either sporadic or they are associated with other familial syndromes such as VHL, MEN2 and NF. What could differentiate SDH-deficient PHEOs is the negative SDHB IHC and the secretion solely of noradrenaline (and/or dopamine) in contrast to the others that secret both adrenaline and noradrenaline (47). In addition, PHEOs caused by *SDHB* mutations show higher malignancy risk (47).

Family history is not always helpful in predicting hereditary PHEOs/PGLs because of phenotypic heterogeneity, incomplete penetrance and in the case of PGL1 and PGL2, maternal imprinting (5, 25, 48). It is interesting that in PHEOs/PGLs that appear to be sporadic based on family history, germline mutations were found in up to 25% of cases (49–51). Therefore, all patients with PHEOs/PGLs (sporadic and hereditary cases) should undergo genetic testing and counseling after IHC is performed (5, 6).

## SDH-DEFICIENT GISTS

GISTs are the most common neoplasms of the gastrointestinal tract of mesenchymal origin and more than 5000 cases are diagnosed each year in the US alone (52). They originate from the interstitial cells of Cajal (53), the pacemaker cells that

**TABLE 1** | Characteristics of SDH-deficient pheochromocytoma and paraganglioma.

| Syndrome | Mutated gene | Mode of inheritance | Frequency | Maternal Imprinting | Affected gender | Associated tumors |
|---|---|---|---|---|---|---|
| **PGL1** | *SDHD* (11q23) | AD | Common | Yes | Both equally | Head and neck, intra-abdominal, adrenals, GIST |
| **PGL2** | *SDHAF2* (11q13) | AD | Very rare | Yes | Both equally | Head and neck |
| **PGL3** | *SDHC* (1q23) | AD | Rare | No | Both equally | Head and neck (carotid body), RCC |
| **PGL4** | *SDHB* (1p36) | AD | Common | No | Both equally | Intra-abdominal, head and neck, RCC |
| **PGL5** | *SDHA* (5p15) | AD | Rare | No | Both equally | GIST |
| **Carney triad** | Hypermethylation of *SDHC* promoter | Unknown | Very rare | No | Mainly females | GIST, abdomen, PCH |

*AD, autosomal dominant; GIST, gastrointestinal stromal tumor; PCH, pulmonary chondroma; PGL, paraganglioma; RCC, renal cell carcinoma.*

regulate peristalsis in the digestive tract (54). Most GISTs occurring in adults are driven by activating mutations in KIT proto-oncogene receptor tyrosine kinase (*KIT*) (75-80% of cases) or platelet-derived growth factor receptor A (*PDGFRA*) (5-15%) genes (55–58). The rest (10-15%), that lack *KIT* and *PDGFRA* gene mutations, are described as 'wild type GISTs' (WT GISTs) and comprise most of pediatric GISTs (59, 60). SDH-deficient GISTs are the majority of WT GISTs (50% of these tumors are associated with hypermethylation of the *SDHC* promoter locus (CT), 30% with germline *SDHA* mutations (4), while 20% is associated with mutations in *SDHB*, *SDHC*, *SDHD* (**Table 2**) (61). The rest harbor mutations in *NF-1, BRAF, ARID1A, ARID1B, CBL, NRAS, HRAS, KRAS, EGFR1, MAX, MEN1, PIK3CA* and *ETV6-NTRK3* fusion genes; these patients are usually older (same as KIT/PDGFRA + tumors) and they have more aggressive disease (62–72) (**Figure 2**). It is important to identify these mutations as it can be useful in the treatment plan.

SDH- deficient GISTs exhibit unique features which are summarized in **Table 2**. Briefly, they manifest predominantly in females, at a young age. They arise almost exclusively in the stomach (61, 73–79) and they frequently have early lymphovascular invasion and consequent involvement of the lymph nodes (76), and less frequently of the liver (61), and do not frequently respond to imatinib (80). However, even in the setting of metastatic disease, they have an indolent clinical course. Histologically, these tumors exhibit multinodular growth pattern with epithelioid cells and they are multifocal. In addition, it was found that SDH-deficient GISTs overexpress insulin-like growth factor receptor (IGF1R) (81), and that this upregulation is highly specific of SDH-deficient GISTs (61, 78, 82, 83). The underlying molecular mechanism is unknown, but it could possibly be due to genetic amplification (61). Stratakis and his group also showed that immunohistochemistry that is negative for SDHB can be used to identify SDH-deficient GISTs caused by *SDHB*, *SDHC* or *SDHD* mutations (75). SDH-deficient GISTs can be sporadic or may present as part of two syndromes, CT (84) and CSS (26, 85).

## Carney Triad (CT)

Going back, in 1977 Dr. J. Aidan Carney described the association of three uncommon tumors- GISTs, PGLs and pulmonary chondroma (PCH) (86). Among other characteristics, the young age (median 18 years old), the female predilection, the multifocality and the concurrence of rare tumors suggested a genetic etiology (87). This association was later referred to as CT (OMIM #604287). Afterwards, adrenocortical adenoma and esophageal leiomyoma were added as components of the triad (88). The etiology of CT is not yet clear but recent data have implicated *SDHC*. In a cohort of 37 patients, comparative genomic hybridization demonstrated no mutations of any of the *SDHx* subunits. Instead, it revealed the most frequent and largest genomic change to be the deletion of 1q12-q21, a region where *SDHC* gene resides (84). Later, Haller et al. demonstrated that aberrant DNA hypermethylation is present at specific sequences of the *SDHC* gene (in the promoter and first exon) in patients with CT; this methylation leads to reduced *SDHC* mRNA expression (89). A genome-wide DNA study confirmed the *SDHC* gene promoter hypermethylation in both CT and WT-GISTs (90). Today, SDHC-specific methylation is considered the molecular signature of CT and is used as simple diagnostic test to identify lesions that may be part of CT in patients that are suspected to be affected by the condition.

## Carney-Stratakis Syndrome (CSS)

In 2002, Dr Carney and Dr Stratakis, described a new condition, that is today known as Carney-Stratakis syndrome (CSS) (OMIM #606864) (also reported as the "paraganglioma and gastric stromal sarcoma syndrome" or Carney-Stratakis dyad) (91). This newly described genetic disorder included only two types of tumors, PGLs/PHEOs and GISTs and is inherited in an autosomal dominant manner with incomplete penetrance. It affects both males and females during childhood and adolescence. Later, in 2007, Dr. Stratakis and his group identified inactivating mutations in the *SDHB*, *SDHC* and *SDHD* subunits as responsible for CSS (26, 92), with subunits B and D being mutated in higher frequency. Pasini et al. studied patients

**TABLE 2** | Comparison of SDH-deficient GISTs and SDH-competent GISTs.

| | SDH-deficient GIST | Non-SHD deficient GIST |
|---|---|---|
| **Gender** | Female > male | Equal |
| **Age** | Children>young adult>older adult | Older adult |
| **Location** | Stomach | Anywhere in GIT |
| ***KIT*/*PDGFRA* mutation** | No | Common (>90%) |
| ***SDHB* IHC** | Positive | Negative |
| **Multifocality** | Rare | Common |
| **Predominant cell** | Spindled | Epithelioid |
| **Metastases to lymph node** | Common | Rare |
| **Response to imatinib** | No | Yes |
| **Associated syndromes/ mutations** | 50% *SDHC* epimutation (Carney triad)<br>30% germline *SDHA* mutation<br>20% *SDHB*, *SDHC*, *SDHD* mutation | Germline *KIT/PDGFRA* mutation,<br>Neurofibromatosis 1<br>*BRAF, KRAS, NRAS, HRAS, ARID1A, ARID1B, CBL, FGFR1, MAX, MEN1, PIK3CA, ETV6-NTRK3* |

*GIST, gastrointestinal stromal tumor; GIT, gastrointestinal tract; IHC, immunohistochemistry; SDH, succinate dehydrogenase.*

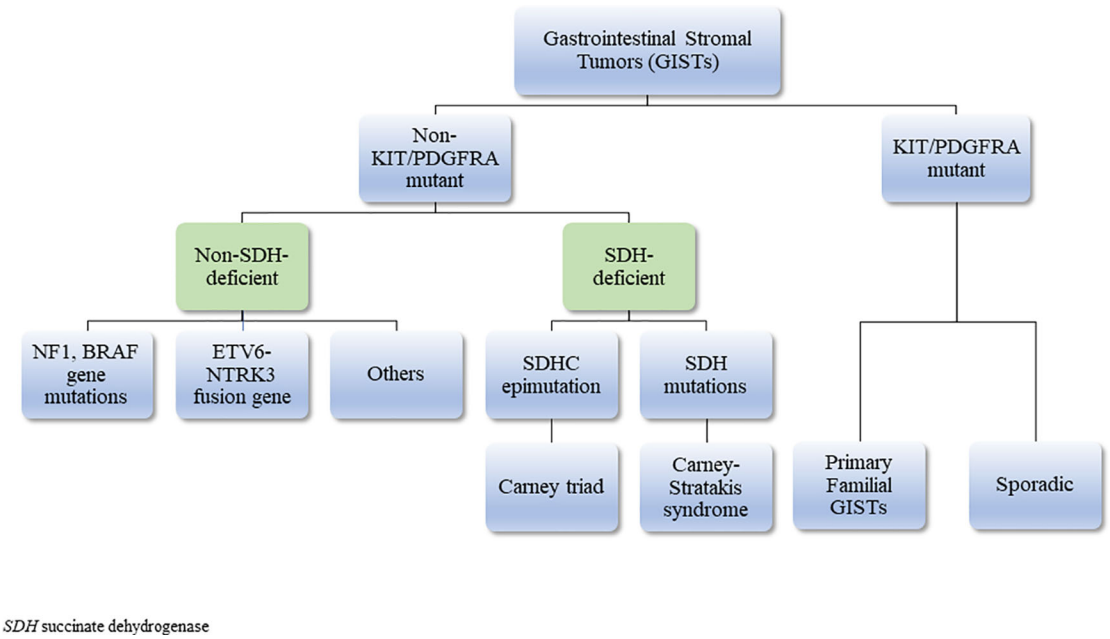


**FIGURE 2** | Classification of gastrointestinal stromal tumors (GISTs).

with CSS who developed GIST and they identified germline mutations in *SDHB*, *SDHC* and *SDHD* (26). Hemizygosity/homozygosity for the mutant allele was found in the GISTs of the affected individuals which is consistent with the tumor suppressor activity of *SDHx* genes (26). *SDHA* loss-of-function mutations have also been identified in patients with CSS (74). Surprisingly, patients harboring *SDHA* mutations demonstrated impressively long survival (93).

## 3PAS

Over the years, the co-existence of PHEOs/PGLs and pituitary adenomas (PAs) was thought to be a coincidence due to the rarity of those endocrine tumors (23). However, in some cases, they may have a common pathogenic mechanism. The first case of a patient with PHEO and acromegaly was described in 1952 (94). Since then, more than 80 such cases have been published (95). In 2012, Xekouki et al. described an individual within a family history with multiple PGLs and PHEOs caused by a germline *SDHD* mutation; in addition, the individual had an aggressive growth hormone (GH)-secreting PA, and loss of heterozygosity at the *SDHD* locus in the pituitary tumor along with increased levels of HIF-1α (96). Since then, the co-existence of those tumors, not recognized as a distinct entity before, has been known as 3PAs. More cases of PAs in patients with *SDH* mutations have been described, supporting the evidence that SDH deficiency plays a role in pituitary tumors (97–99).

SDH-deficient PAs that are part of 3PAs are more commonly macroadenomas and they frequently exhibit different phenotypes within the same family, such as prolactinomas, somatotropinomas and non-functional adenomas (95). Most of the time they respond poorly to somatostatin analogues and they require multiple treatments (95). In addition, PHEOs/PGLs in patients with 3PAs are often bilateral and/or multiple and tend to recur (95). In a cohort study of 19 patients with PHEO/PGL and PA, 9 of them had *SDHx* mutations. In PAs caused by mutations in any of the *SDHx* subunits intracytoplasmic vacuoles were present, a histological characteristic specific to those kinds of tumors (100). One could speculate that those vacuoles could possibly be autophagic bodies, as it is known that activation of autophagy is related to hypoxia-related pathways (101, 102); moreover, autophagy has been found to contribute to chemo- and radio-therapy resistance (103, 104).

## SDH-DEFICIENT RENAL CELL CARCINOMA

SDH-deficient renal carcinoma was first recognized in 2004 (22) and later was accepted as a distinct type of renal cell carcinoma (RCC) (4, 105). It is rare, as it is estimated to account for 0.05-0.2% of all renal carcinomas (106). The mean age is 38 to 40 years (107) and there is a slight male predisposition (106, 108). In most of them, *SDHB* (83%) germline mutation is present (80), but few cases with *SDHC* and *SDHD* mutations have been reported as well (106–109). *SDHA* mutation in RCC was reported for the first time recently by Yakirevich et al. (110), followed by other reports (111, 112). In a cohort study, 36 SDH-deficient RCCs from 27 patients were studied; all of them were negative for SDHB and positive for SDHA by IHC. In addition, genetic testing was performed in 17 of these patients and they all

harbored a germline *SDHx* mutation (16 SDHB, 1 SDHC) (106). In another study, 37 tumors exhibiting morphologic features of SDH-deficient RCC were evaluated; of them 11 showed immunohistochemical loss of SDHB and 1 out of 11 cases loss of SDHA (in this case no *SDHB* gene mutation was detected by sequencing and *SDHA* gene was not evaluated) (108).

Morphologically, SHD-deficient RCCs exhibit distinctive features, being made of cuboidal cells with variable cysts and 'bubbly' eosinophilic cytoplasm with flocculent inclusions. They also exhibit a solid, nested or tubular growth pattern (80, 106–108, 110, 113, 114). The hallmark of these tumors is loss of SDH immunohistochemical expression. Therefore, in renal tumors with morphology suggestive of SDH-deficient RCC or syndromic disease (younger age, family history of RCC, personal or family history of other SDH-deficient tumors) IHC for SDHB should be performed (106, 112). It is possible that SDHA-deficient RCCs may exhibit slightly different morphologic features such as papillary, cribiform-like architecture, higher nuclear grade and areas of solid growth pattern (110–112). However, very few cases have been reported so far and it is difficult to make any definitive associations.

In addition, this distinct type of RCCs is negative for c-kit, cytokeratin 7 (CK7), carbonic anhydrase IX (CAIX), CD117 and vimentin, while it is immunoreactive for PAX8 and kidney-specific cadherin. These markers can be useful in the case that IHC is unavailable (106–108).

Although most SHD-deficient RCCs have a good prognosis, and the risk of metastasis is estimated to be 11%, some of them-those with high-grade nuclear atypia, tumor necrosis or sarcomatoid differentiation- may behave aggressively reaching metastatic rates as high as 70% (106, 108, 115).

## OTHER SDH-DEFICIENT TUMORS

Apart from PGLs/PHEOs, GISTs, PAs and renal cell carcinomas discussed above, there is not much evidence that *SDHx* deficiency contributes significantly to other neoplasms. Thyroid carcinoma associated with either *SDHB* or *SDHD* has been reported in a few individuals (46, 51). Patients with PTEN-negative Cowden and Cowden-like syndromes, have also been reported in association with either *SDHB* or *SDHD* variants (27). Neuroblastoma (28) and bilateral adrenal medullary hyperplasia (29) have been linked to *SDHB* mutations. Moreover, a case of testicular seminoma has been reported in association with *SDHD* mutation (30). While a variety of tumors has been reported in association with SDH mutations we cannot say for sure if there is a causal relationship between them due to the very limited number of cases.

### Loss of SDHB Immunohistochemistry as an Important Tool of Validating SDH Mutations

*SDHx* genes act as tumor suppressor genes (116). *SDHx* germline heterozygous inactivating mutations affect the protein function and predispose to hereditary neoplasms; subsequently, loss of heterozygosity (LOH) in the tumor level results in complete loss of SDH activity (14). Loss of immunohistochemical staining for SDHB has been proved to be a robust and reliable marker for syndromic disease resulting from germline mutation of *SDHA*, *SDHB*, *SDHC* or *SDHD* (6–9). In addition, in the case of double-hit inactivation of *SDHA*, IHC for SDHA becomes negative as well (9, 21). Thus, tumors associated with bi-allelic inactivation of SDHA stain negative for SDHB and SDHA, while tumors caused by inactivating mutations in *SDHB*, *SDHC* or *SDHD* show negative staining only for *SDHB*. In every case, caution should be taken when interpreting the results and further clinical and genetic assessment should ensue.

## SDH-DEFICIENT TUMORS: CLINICAL CONSIDERATIONS AND GENETIC COUNSELING

Clinical features of the tumors discussed above should be taken into careful consideration. It is very important, in the case of PGLs/PHEOs, to be aware of any catecholamine excess symptoms (such as hypertension, hyperhidrosis, palpitations, headache) as well as signs and/or symptoms of a local mass. Depending on the tumor location they may vary. Tumors located in the carotid body may present with voice hoarseness, neck fullness, cough, dysphagia or clinically palpable mass in the lateral upper neck. When located in the middle ear (glomus tympanicum) patients may present with palsies of the cranial nerves VII, IX, X, XI and/or XII (117). It is recommended that these patients undergo imaging in order to detect metastatic disease or new tumors (118–120). In the case of *SDHA*, *SDHC* and *SDHD* mutations, because of the slow-growing tumors, MRI screening is suggested every three to five years (120). In individuals with *SDHB* mutations, due to the rapidly growing nature of these tumors, it should be performed every two years (120). A recent study demonstrated that the most optimal diagnostic imaging included MRI/CT and $^{111}$In-octreotide scintigraphy (121). Other studies showed higher sensitivity and more detailed imaging (regardless of genetic mutation and familial or sporadic cases) using $^{68}$Ga-DOTA-peptides PET/CT, which targets the abundantly expressed somatostatin receptors in those tumors, compared to conventional CT or MRI (122–128); in addition, more lesions were identified in the case of head and neck paragangliomas (HNPGLs) using that compared to all other imaging techniques (126) (including [$^{18}$F]-fluorohydroyphenylalanine ([$^{18}$F]-FDOPA) PET/CT, currently the gold standard for head and neck paragangliomas) (119, 129, 130). Patients with PA should be carefully examined for any symptoms of prolactin (PRL) or GH hypersecretion or visual disturbances, as most PAs that occur in the context of 3PAs are PRL- or GH- secreting macroadenomas or non-functional PAs. Complete pituitary hormone evaluation should also be performed to rule out other pituitary tumors. Hormonal testing should also be performed in the case of concurrent PGLs/PHEOs either in the index case or any family member. If there are no abnormal findings, based on the most recent recommendations, biochemical tests, including testing for PGLs/PHEOs, should be performed annually (118, 119).

Pituitary MRI is indicated in the case of abnormal biochemistry or clinical findings. SDH-deficient PAs are treated the same as sporadic (131–134). In the case of renal cancer, patients may complain about flank pain and/or hematuria, whereas in GISTs abdominal pain or fullness may be the main issue.

## Genetic Counseling and Genetic Testing

It could be suggested that in the presence of SDH deficiency a careful and detailed medical and family history should be obtained even in patients with apparently 'sporadic' PGLs/PHEOs, GISTs or PAs due to the variable expression and decreased penetrance of those conditions. Patients and family members should be referred for genetic counseling. Genetic testing for *SDHx* mutations in any of the above patients, particularly if there are other family members with any of those tumors (do not only include first-degree relatives) should be performed. Doctors should be aware of CT or CSS especially in the case of a *KIT* or *PDFGRA* negative GIST. In the case that genetic testing is unavailable or cannot be performed, SDHB IHC could be performed.

# SUMMARY

*SDH*-deficient tumors are often an indicator of a genetic, tumor-predisposition syndrome, associated with germline mutations in any of the *SDHx* subunits: *SDHA*, *SDHB*, *SDHC*, *SDHD* or rarely *SDHAF2*. In the case of CT, epimutation of *SDHC* promoter locus is the cause. Identifying the genetic basis of *SDH*-deficient tumors has helped in identifying individuals in high risk and introduce screening to them and their families. Thus, better clinical care can be provided as early detection and treatment have become more feasible.

# AUTHOR CONTRIBUTIONS

GP contributed to writing the draft of the paper, to writing the final version of the paper, and critically revised it. FF and NS contributed to writing the final version of the paper and critically revised it. CS conceived the study and contributed to writing the final version of the paper and critically revised it. All authors contributed to the article and approved the submitted version.

# FUNDING

This study was supported by the Intramural Research Program, *Eunice Kennedy Shriver* National Institute of Child Health & Human Development (NICHD), Bethesda, Md 20892, USA.

# REFERENCES

1. Sun F, Huo X, Zhai Y, Wang A, Xu J, Su D, et al. Crystal Structure of Mitochondrial Respiratory Membrane Protein Complex Ii. *Cell* (2005) 121 (7):1043–57. doi: 10.1016/j.cell.2005.05.025
2. Settas N, Faucz FR, Stratakis CA. Succinate dehydrogenase (SDH) deficiency, Carney triad and the epigenome. *Mol Cell Endocrinol* (2017) 469:107–11. doi: 10.1016/j.mce.2017.07.018
3. Huang S, Millar AH. Succinate Dehydrogenase: The Complex Roles of a Simple Enzyme. *Curr Opin Plant Biol* (2013) 16(3):344–9. doi: 10.1016/j.pbi.2013.02.007
4. Gill AJ. Succinate Dehydrogenase (Sdh)-Deficient Neoplasia. *Histopathology* (2018) 72(1):106–16. doi: 10.1111/his.13277
5. Gill AJ. Succinate Dehydrogenase (SDH) and Mitochondrial Driven Neoplasia. *Pathology* (2012) 44(4):285–92. doi: 10.1097/PAT.0b013e3283539932
6. Gill AJ, Benn DE, Chou A, Clarkson A, Muljono A, Meyer-Rochow GY, et al. Immunohistochemistry for SDHB Triages Genetic Testing of SDHB, SDHC, and SDHD in Paraganglioma-Pheochromocytoma Syndromes. *Hum Pathol* (2010) 41(6):805–14. doi: 10.1016/j.humpath.2009.12.005
7. van Nederveen FH, Gaal J, Favier J, Korpershoek E, Oldenburg RA, de Bruyn EM, et al. An Immunohistochemical Procedure to Detect Patients With Paraganglioma and Phaeochromocytoma With Germline Sdhb, SDHC, or SDHD Gene Mutations: A Retrospective and Prospective Analysis. *Lancet Oncol* (2009) 10(8):764–71. doi: 10.1016/S1470-2045(09)70164-0
8. Papathomas TG, Oudijk L, Persu A, Gill AJ, van Nederveen F, Tischler AS, et al. Sdhb/Sdha Immunohistochemistry in Pheochromocytomas and Paragangliomas: A Multicenter Interobserver Variation Analysis Using Virtual Microscopy: A Multinational Study of the European Network for the Study of Adrenal Tumors (EnsT). *Mod Pathol* (2015) 28(6):807–21. doi: 10.1038/modpathol.2015.41
9. Korpershoek E, Favier J, Gaal J, Burnichon N, van Gessel B, Oudijk L, et al. Sdha Immunohistochemistry Detects Germline Sdha Gene Mutations in Apparently Sporadic Paragangliomas and Pheochromocytomas. *J Clin Endocrinol Metab* (2011) 96(9):E1472–6. doi: 10.1210/jc.2011-1043
10. Gottlieb E, Tomlinson IP. Mitochondrial Tumour Suppressors: A Genetic and Biochemical Update. *Nat Rev Cancer* (2005) 5(11):857–66. doi: 10.1038/nrc1737
11. Bardella C, Pollard PJ, Tomlinson I. Sdh Mutations in Cancer. *Biochim Biophys Acta* (2011) 1807(11):1432–43. doi: 10.1016/j.bbabio.2011.07.003
12. Selak MA, Armour SM, MacKenzie ED, Boulahbel H, Watson DG, Mansfield KD, et al. Succinate Links Tca Cycle Dysfunction to Oncogenesis by Inhibiting HIF-Alpha Prolyl Hydroxylase. *Cancer Cell* (2005) 7(1):77–85. doi: 10.1016/j.ccr.2004.11.022
13. Raimundo N, Baysal BE, Shadel GS. Revisiting the TCA Cycle: Signaling to Tumor Formation. *Trends Mol Med* (2011) 17(11):641–9. doi: 10.1016/j.molmed.2011.06.001
14. Gimenez-Roqueplo AP, Favier J, Rustin P, Mourad JJ, Plouin PF, Corvol P, et al. The R22X Mutation of the SDHD Gene in Hereditary Paraganglioma Abolishes the Enzymatic Activity of Complex II in the Mitochondrial Respiratory Chain and Activates the Hypoxia Pathway. *Am J Hum Genet* (2001) 69(6):1186–97. doi: 10.1086/324413
15. Gimenez-Roqueplo AP, Favier J, Rustin P, Rieubland C, Kerlan V, Plouin PF, et al. Functional Consequences of a SDHB Gene Mutation in an Apparently Sporadic Pheochromocytoma. *J Clin Endocrinol Metab* (2002) 87(10):4771–4. doi: 10.1210/jc.2002-020525
16. Pollard PJ, Briere JJ, Alam NA, Barwell J, Barclay E, Wortham NC, et al. Accumulation of Krebs Cycle Intermediates and Over-Expression of HIF1alpha in Tumours Which Result From Germline FH and SDH Mutations. *Hum Mol Genet* (2005) 14(15):2231–9. doi: 10.1093/hmg/ddi227
17. Lopez-Jimenez E, Gomez-Lopez G, Leandro-Garcia LJ, Munoz I, Schiavi F, Montero-Conde C, et al. Research Resource: Transcriptional Profiling Reveals Different Pseudohypoxic Signatures in SDHB and VHL-related Pheochromocytomas. *Mol Endocrinol* (2010) 24(12):2382–91. doi: 10.1210/me.2010-0256
18. Raha S, McEachern GE, Myint AT, Robinson BH. Superoxides From Mitochondrial Complex Iii: The Role of Manganese Superoxide Dismutase. *Free Radic Biol Med* (2000) 29(2):170–80. doi: 10.1016/S0891-5849(00)00338-5

19. Xiao M, Yang H, Xu W, Ma S, Lin H, Zhu H, et al. Inhibition of Alpha-KG-Dependent Histone and DNA Demethylases by Fumarate and Succinate That are Accumulated in Mutations of FH and SDH Tumor Suppressors. *Genes Dev* (2012) 26(12):1326–38. doi: 10.1101/gad.191056.112
20. Smith EH, Janknecht R, Maher LJ,3. Succinate Inhibition of Alpha-Ketoglutarate-Dependent Enzymes in a Yeast Model of Paraganglioma. *Hum Mol Genet* (2007) 16(24):3136–48. doi: 10.1093/hmg/ddm275
21. Burnichon N, Briere JJ, Libe R, Vescovo L, Riviere J, Tissier F, et al. SDHA is a Tumor Suppressor Gene Causing Paraganglioma. *Hum Mol Genet* (2010) 19(15):3011–20. doi: 10.1093/hmg/ddq206
22. Vanharanta S, Buchta M, McWhinney SR, Virta SK, Peczkowska M, Morrison CD, et al. Early-Onset Renal Cell Carcinoma as a Novel Extraparaganglial Component of SDHB-associated Heritable Paraganglioma. *Am J Hum Genet* (2004) 74(1):153–9. doi: 10.1086/381054
23. Xekouki P, Stratakis CA. Succinate Dehydrogenase (Sdhx) Mutations in Pituitary Tumors: Could This be a New Role for Mitochondrial Complex II and/or Krebs Cycle Defects? *Endocr Relat Cancer* (2012) 19(6):C33–40. doi: 10.1530/ERC-12-0118
24. Astuti D, Latif F, Dallol A, Dahia PL, Douglas F, George E, et al. Gene Mutations in the Succinate Dehydrogenase Subunit Sdhb Cause Susceptibility to Familial Pheochromocytoma and to Familial Paraganglioma. *Am J Hum Genet* (2001) 69(1):49–54. doi: 10.1086/321282
25. Baysal BE, Ferrell RE, Willett-Brozick JE, Lawrence EC, Myssiorek D, Bosch A, et al. Mutations in SDHD, a Mitochondrial Complex II Gene, in Hereditary Paraganglioma. *Science* (2000) 287(5454):848–51. doi: 10.1126/science.287.5454.848
26. Pasini B, McWhinney SR, Bei T, Matyakhina L, Stergiopoulos S, Muchow M, et al. Clinical and Molecular Genetics of Patients With the Carney-Stratakis Syndrome and Germline Mutations of the Genes Coding for the Succinate Dehydrogenase Subunits Sdhb, SDHC, and SDHD. *Eur J Hum Genet* (2008) 16(1):79–88. doi: 10.1038/sj.ejhg.5201904
27. Ni Y, Zbuk KM, Sadler T, Patocs A, Lobo G, Edelman E, et al. Germline Mutations and Variants in the Succinate Dehydrogenase Genes in Cowden and Cowden-like Syndromes. *Am J Hum Genet* (2008) 83(2):261–8. doi: 10.1016/j.ajhg.2008.07.011
28. Schimke RN, Collins DL, Stolle CA. Paraganglioma, Neuroblastoma, and a SDHB Mutation: Resolution of a 30-Year-Old Mystery. *Am J Med Genet A* (2010) 152A(6):1531–5. doi: 10.1002/ajmg.a.33384
29. Grogan RH, Pacak K, Pasche L, Huynh TT, Greco RS. Bilateral Adrenal Medullary Hyperplasia Associated With an SDHB Mutation. *J Clin Oncol* (2011) 29(8):e200–2. doi: 10.1200/JCO.2010.32.2156
30. Galera-Ruiz H, Gonzalez-Campora R, Rey-Barrera M, Rollon-Mayordomo A, Garcia-Escudero A, Fernandez-Santos JM, et al. W43x SDHD Mutation in Sporadic Head and Neck Paraganglioma. *Anal Quant Cytol Histol* (2008) 30(2):119–23.
31. Rindi G, Klimstra DS, Abedi-Ardekani B, Asa SL, Bosman FT, Brambilla E, et al. A Common Classification Framework for Neuroendocrine Neoplasms: An International Agency for Research on Cancer (IARC) and World Health Organization (Who) Expert Consensus Proposal. *Mod Pathol* (2018) 31 (12):1770–86. doi: 10.1038/s41379-018-0110-y
32. Lee KY, Oh YW, Noh HJ, Lee YJ, Yong HS, Kang EY, et al. Extraadrenal Paragangliomas of the Body: Imaging Features. *AJR Am J Roentgenol* (2006) 187(2):492–504. doi: 10.2214/AJR.05.0370
33. Raygada M, Pasini B, Stratakis CA. Hereditary Paragangliomas. *Adv Otorhinolaryngol* (2011) 70:99–106. doi: 10.1159/000322484
34. Vicha A, Musil Z, Pacak K. Genetics of Pheochromocytoma and Paraganglioma Syndromes: New Advances and Future Treatment Options. *Curr Opin Endocrinol Diabetes Obes* (2013) 20(3):186–91. doi: 10.1097/MED.0b013e32835fcc45
35. Niemann S, Muller U. Mutations in SDHC Cause Autosomal Dominant Paraganglioma, Type 3. *Nat Genet* (2000) 26(3):268–70. doi: 10.1038/81551
36. Astuti D, Douglas F, Lennard TW, Aligianis IA, Woodward ER, Evans DG, et al. Germline SDHD Mutation in Familial Phaeochromocytoma. *Lancet* (2001) 357(9263):1181–2. doi: 10.1016/S0140-6736(00)04378-6
37. Gimm O, Armanios M, Dziema H, Neumann HP, Eng C. Somatic and Occult Germ-Line Mutations in SDHD, a Mitochondrial Complex II Gene, in Nonfamilial Pheochromocytoma. *Cancer Res* (2000) 60(24):6822–5.
38. Baysal BE, Willett-Brozick JE, Lawrence EC, Drovdlic CM, Savul SA, McLeod DR, et al. Prevalence of SDHB, SDHC, and SDHD Germline Mutations in Clinic Patients With Head and Neck Paragangliomas. *J Med Genet* (2002) 39(3):178–83. doi: 10.1136/jmg.39.3.178
39. van Nederveen FH, Korpershoek E, Lenders JW, de Krijger RR, Dinjens WN. Somatic SDHB Mutation in an Extraadrenal Pheochromocytoma. *N Engl J Med* (2007) 357(3):306–8. doi: 10.1056/NEJMc070010
40. Hao HX, Khalimonchuk O, Schraders M, Dephoure N, Bayley JP, Kunst H, et al. SDH5, a Gene Required for Flavination of Succinate Dehydrogenase, is Mutated in Paraganglioma. *Science* (2009) 325(5944):1139–42. doi: 10.1126/science.1175689
41. Opotowsky AR, Moko LE, Ginns J, Rosenbaum M, Greutmann M, Aboulhosn J, et al. Pheochromocytoma and Paraganglioma in Cyanotic Congenital Heart Disease. *J Clin Endocrinol Metab* (2015) 100(4):1325–34. doi: 10.1210/jc.2014-3863
42. Song MK, Kim GB, Bae EJ, Lee YA, Kim HY, Min SK, et al. Pheochromocytoma and Paraganglioma in Fontan Patients: Common More Than Expected. *Congenit Heart Dis* (2018) 13(4):608–16. doi: 10.1111/chd.12625
43. Agarwal S, Jindal I, Balazs A, Paul D. Catecholamine-Secreting Tumors in Pediatric Patients With Cyanotic Congenital Heart Disease. *J Endocr Soc* (2019) 3(11):2135–50. doi: 10.1210/js.2019-00226
44. Benn DE, Gimenez-Roqueplo AP, Reilly JR, Bertherat J, Burgess J, Byth K, et al. Clinical Presentation and Penetrance of Pheochromocytoma/Paraganglioma Syndromes. *J Clin Endocrinol Metab* (2006) 91(3):827–36. doi: 10.1210/jc.2005-1862
45. Schiavi F, Boedeker CC, Bausch B, Peczkowska M, Gomez CF, Strassburg T, et al. Predictors and Prevalence of Paraganglioma Syndrome Associated With Mutations of the SDHC Gene. *JAMA* (2005) 294(16):2057–63. doi: 10.1001/jama.294.16.2057
46. Ricketts CJ, Forman JR, Rattenberry E, Bradshaw N, Lalloo F, Izatt L, et al. Tumor Risks and Genotype-Phenotype-Proteotype Analysis in 358 Patients With Germline Mutations in SDHB and SDHD. *Hum Mutat* (2010) 31: (1):41–51. doi: 10.1002/humu.21136
47. Benn DE, Robinson BG, Clifton-Bligh RJ. 15 YEARS of PARAGANGLIOMA: Clinical Manifestations of Paraganglioma Syndromes Types 1-5. *Endocr Relat Cancer* (2015) 22(4):T91–103. doi: 10.1530/ERC-15-0268
48. van der Mey AG, Maaswinkel-Mooy PD, Cornelisse CJ, Schmidt PH, van de Kamp JJ. Genomic Imprinting in Hereditary Glomus Tumours: Evidence for New Genetic Theory. *Lancet* (1989) 2(8675):1291–4. doi: 10.1016/S0140-6736(89)91908-9
49. Korpershoek E, Van Nederveen FH, Dannenberg H, Petri BJ, Komminoth P, Perren A, et al. Genetic Analyses of Apparently Sporadic Pheochromocytomas: The Rotterdam Experience. *Ann N Y Acad Sci* (2006) 1073:138–48. doi: 10.1196/annals.1353.014
50. Neumann HP, Bausch B, McWhinney SR, Bender BU, Gimm O, Franke G, et al. Germ-Line Mutations in Nonsyndromic Pheochromocytoma. *N Engl J Med* (2002) 346(19):1459–66. doi: 10.1056/NEJMoa020152
51. Neumann HP, Pawlu C, Peczkowska M, Bausch B, McWhinney SR, Muresan M, et al. Distinct Clinical Features of Paraganglioma Syndromes Associated With SDHB and SDHD Gene Mutations. *JAMA* (2004) 292 (8):943–51. doi: 10.1001/jama.292.8.943
52. Barnett CM, Corless CL, Heinrich MC. Gastrointestinal Stromal Tumors: Molecular Markers and Genetic Subtypes. *Hematol Oncol Clin North Am* (2013) 27(5):871–88. doi: 10.1016/j.hoc.2013.07.003
53. Perez-Atayde AR, Shamberger RC, Kozakewich HW. Neuroectodermal Differentiation of the Gastrointestinal Tumors in the Carney Triad. An Ultrastructural and Immunohistochemical Study. *Am J Surg Pathol* (1993) 17(7):706–14. doi: 10.1097/00000478-199307000-00008
54. Kindblom LG, Remotti HE, Aldenborg F, Meis-Kindblom JM. Gastrointestinal Pacemaker Cell Tumor (Gipact): Gastrointestinal Stromal Tumors Show Phenotypic Characteristics of the Interstitial Cells of Cajal. *Am J Pathol* (1998) 152(5):1259–69.
55. Schaefer IM, Marino-Enriquez A, Fletcher JA. What is New in Gastrointestinal Stromal Tumor? *Adv Anat Pathol* (2017) 24(5):259–67. doi: 10.1097/PAP.0000000000000158
56. Huss S, Kunstlinger H, Wardelmann E, Kleine MA, Binot E, Merkelbach-Bruse S, et al. A Subset of Gastrointestinal Stromal Tumors Previously

Regarded as Wild-Type Tumors Carries Somatic Activating Mutations in KIT Exon 8 (P.D419del). *Mod Pathol* (2013) 26(7):1004–12. doi: 10.1038/modpathol.2013.47
57. Rossi S, Gasparotto D, Miceli R, Toffolatti L, Gallina G, Scaramel E, et al. Kit, PDGFRA, and BRAF Mutational Spectrum Impacts on the Natural History of Imatinib-Naive Localized Gist: A Population-Based Study. *Am J Surg Pathol* (2015) 39(7):922–30. doi: 10.1097/PAS.0000000000000418
58. Hirota S, Isozaki K, Moriyama Y, Hashimoto K, Nishida T, Ishiguro S, et al. Gain-of-Function Mutations of C-Kit in Human Gastrointestinal Stromal Tumors. *Science* (1998) 279(5350):577–80. doi: 10.1126/science.279.5350.577
59. Mei L, Smith SC, Faber AC, Trent J, Grossman SR, Stratakis CA, et al. Gastrointestinal Stromal Tumors: The GIST of Precision Medicine. *Trends Cancer* (2018) 4(1):74–91. doi: 10.1016/j.trecan.2017.11.006
60. Boikos SA, Pappo AS, Killian JK, LaQuaglia MP, Weldon CB, George S, et al. Molecular Subtypes of KIT/PDGFRA Wild-Type Gastrointestinal Stromal Tumors: A Report From the National Institutes of Health Gastrointestinal Stromal Tumor Clinic. *JAMA Oncol* (2016) 2(7):922–8. doi: 10.1001/jamaoncol.2016.0256
61. Miettinen M, Lasota J. Succinate Dehydrogenase Deficient Gastrointestinal Stromal Tumors (Gists) - a Review. *Int J Biochem Cell Biol* (2014) 53:514–9. doi: 10.1016/j.biocel.2014.05.033
62. Agaram NP, Wong GC, Guo T, Maki RG, Singer S, Dematteo RP, et al. Novel V600E Braf Mutations in Imatinib-Naive and Imatinib-Resistant Gastrointestinal Stromal Tumors. *Genes Chromosomes Cancer* (2008) 47(10):853–9. doi: 10.1002/gcc.20589
63. Brenca M, Rossi S, Polano M, Gasparotto D, Zanatta L, Racanelli D, et al. Transcriptome Sequencing Identifies ETV6-NTRK3 as a Gene Fusion Involved in GIST. *J Pathol* (2016) 238(4):543–9. doi: 10.1002/path.4677
64. Hostein I, Faur N, Primois C, Boury F, Denard J, Emile JF, et al. Braf Mutation Status in Gastrointestinal Stromal Tumors. *Am J Clin Pathol* (2010) 133(1):141–8. doi: 10.1309/AJCPPCKGA2QGBJ1R
65. Lasota J, Felisiak-Golabek A, Wasag B, Kowalik A, Zieba S, Chlopek M, et al. Frequency and Clinicopathologic Profile of PIK3CA Mutant GISTs: Molecular Genetic Study of 529 Cases. *Mod Pathol* (2016) 29(3):275–82. doi: 10.1038/modpathol.2015.160
66. Miettinen M, Fetsch JF, Sobin LH, Lasota J. Gastrointestinal Stromal Tumors in Patients With Neurofibromatosis 1: A Clinicopathologic and Molecular Genetic Study of 45 Cases. *Am J Surg Pathol* (2006) 30(1):90–6. doi: 10.1097/01.pas.0000176433.81079.bd
67. Miranda C, Nucifora M, Molinari F, Conca E, Anania MC, Bordoni A, et al. KRAS and BRAF Mutations Predict Primary Resistance to Imatinib in Gastrointestinal Stromal Tumors. *Clin Cancer Res* (2012) 18(6):1769–76. doi: 10.1158/1078-0432.CCR-11-2230
68. Patil DT, Rubin BP. Genetics of Gastrointestinal Stromal Tumors: A Heterogeneous Family of Tumors? *Surg Pathol Clin* (2015) 8(3):515–24. doi: 10.1016/j.path.2015.05.006
69. Weldon CB, Madenci AL, Boikos SA, Janeway KA, George S, von Mehren M, et al. Surgical Management of Wild-Type Gastrointestinal Stromal Tumors: A Report From the National Institutes of Health Pediatric and Wildtype Gist Clinic. *J Clin Oncol* (2017) 35(5):523–8. doi: 10.1200/JCO.2016.68.6733
70. Shi E, Chmielecki J, Tang CM, Wang K, Heinrich MC, Kang G, et al. FGFR1 and NTRK3 Actionable Alterations in "Wild-Type" Gastrointestinal Stromal Tumors. *J Transl Med* (2016) 14(1):339. doi: 10.1186/s12967-016-1075-6
71. Pantaleo MA, Urbini M, Indio V, Ravegnini G, Nannini M, De Luca M, et al. Genome-Wide Analysis Identifies MEN1 and MAX Mutations and a Neuroendocrine-Like Molecular Heterogeneity in Quadruple Wt Gist. *Mol Cancer Res* (2017) 15(5):553–62. doi: 10.1158/1541-7786.MCR-16-0376
72. Nannini M, Urbini M, Astolfi A, Biasco G, Pantaleo MA. The Progressive Fragmentation of the KIT/PDGFRA Wild-Type (Wt) Gastrointestinal Stromal Tumors (Gist). *J Transl Med* (2017) 15(1):113. doi: 10.1186/s12967-017-1212-x
73. Elston MS, Sehgal S, Dray M, Phillips E, Conaglen JV, Clifton-Bligh RJ, et al. A Duodenal Sdh-Deficient Gastrointestinal Stromal Tumor in a Patient With a Germline Sdhb Mutation. *J Clin Endocrinol Metab* (2017) 102(5):1447–50. doi: 10.1210/jc.2017-00165
74. Dwight T, Benn DE, Clarkson A, Vilain R, Lipton L, Robinson BG, et al. Loss of SDHA Expression Identifies Sdha Mutations in Succinate Dehydrogenase-Deficient Gastrointestinal Stromal Tumors. *Am J Surg Pathol* (2013) 37(2):226–33. doi: 10.1097/PAS.0b013e3182671155
75. Gaal J, Stratakis CA, Carney JA, Ball ER, Korpershoek E, Lodish MB, et al. Sdhb Immunohistochemistry: A Useful Tool in the Diagnosis of Carney-Stratakis and Carney Triad Gastrointestinal Stromal Tumors. *Mod Pathol* (2011) 24(1):147–51. doi: 10.1038/modpathol.2010.185
76. Miettinen M, Wang ZF, Sarlomo-Rikala M, Osuch C, Rutkowski P, Lasota J. Succinate Dehydrogenase-Deficient Gists: A Clinicopathologic, Immunohistochemical, and Molecular Genetic Study of 66 Gastric Gists With Predilection to Young Age. *Am J Surg Pathol* (2011) 35(11):1712–21. doi: 10.1097/PAS.0b013e3182260752
77. Janeway KA, Kim SY, Lodish M, Nose V, Rustin P, Gaal J, et al. Defects in Succinate Dehydrogenase in Gastrointestinal Stromal Tumors Lacking KIT and PDGFRA Mutations. *Proc Natl Acad Sci USA* (2011) 108(1):314–8. doi: 10.1073/pnas.1009199108
78. Chou A, Chen J, Clarkson A, Samra JS, Clifton-Bligh RJ, Hugh TJ, et al. Succinate Dehydrogenase-Deficient Gists are Characterized by IGF1R Overexpression. *Mod Pathol* (2012) 25(9):1307–13. doi: 10.1038/modpathol.2012.77
79. Wagner AJ, Remillard SP, Zhang YX, Doyle LA, George S, Hornick JL. Loss of Expression of SDHA Predicts SDHA Mutations in Gastrointestinal Stromal Tumors. *Mod Pathol* (2013) 26(2):289–94. doi: 10.1038/modpathol.2012.153
80. Evenepoel L, Papathomas TG, Krol N, Korpershoek E, de Krijger RR, Persu A, et al. Toward an Improved Definition of the Genetic and Tumor Spectrum Associated With SDH Germ-Line Mutations. *Genet Med* (2015) 17(8):610–20. doi: 10.1038/gim.2014.162
81. Janeway KA, Zhu MJ, Barretina J, Perez-Atayde A, Demetri GD, Fletcher JA. Strong Expression of IGF1R in Pediatric Gastrointestinal Stromal Tumors Without Igf1r Genomic Amplification. *Int J Cancer* (2010) 127(11):2718–22. doi: 10.1002/ijc.25247
82. Lasota J, Wang Z, Kim SY, Helman L, Miettinen M. Expression of the Receptor for Type I Insulin-Like Growth Factor (IGF1R) in Gastrointestinal Stromal Tumors: An Immunohistochemical Study of 1078 Cases With Diagnostic and Therapeutic Implications. *Am J Surg Pathol* (2013) 37(1):114–9. doi: 10.1097/PAS.0b013e3182613c86
83. Wang YM, Gu ML, Ji F. Succinate Dehydrogenase-Deficient Gastrointestinal Stromal Tumors. *World J Gastroenterol* (2015) 21(8):2303–14. doi: 10.3748/wjg.v21.i8.2303
84. Matyakhina L, Bei TA, McWhinney SR, Pasini B, Cameron S, Gunawan B, et al. Genetics of Carney Triad: Recurrent Losses At Chromosome 1 But Lack of Germline Mutations in Genes Associated With Paragangliomas and Gastrointestinal Stromal Tumors. *J Clin Endocrinol Metab* (2007) 92(8):2938–43. doi: 10.1210/jc.2007-0797
85. Stratakis CA, Carney JA. The Triad of Paragangliomas, Gastric Stromal Tumours and Pulmonary Chondromas (Carney Triad), and the Dyad of Paragangliomas and Gastric Stromal Sarcomas (Carney-Stratakis Syndrome): Molecular Genetics and Clinical Implications. *J Intern Med* (2009) 266(1):43–52. doi: 10.1111/j.1365-2796.2009.02110.x
86. Carney JA, Sheps SG, Go VL, Gordon H. The Triad of Gastric Leiomyosarcoma, Functioning Extra-Adrenal Paraganglioma and Pulmonary Chondroma. *N Engl J Med* (1977) 296(26):1517–8. doi: 10.1056/NEJM197706302962609
87. Zhang L, Smyrk TC, Young WF Jr, Stratakis CA, Carney JA. Gastric Stromal Tumors in Carney Triad are Different Clinically, Pathologically, and Behaviorally From Sporadic Gastric Gastrointestinal Stromal Tumors: Findings in 104 Cases. *Am J Surg Pathol* (2010) 34(1):53–64. doi: 10.1097/PAS.0b013e3181c20f4f
88. Carney JA. Gastric Stromal Sarcoma, Pulmonary Chondroma, and Extra-Adrenal Paraganglioma (Carney Triad): Natural History, Adrenocortical Component, and Possible Familial Occurrence. *Mayo Clin Proc* (1999) 74(6):543–52. doi: 10.4065/74.6.543
89. Haller F, Moskalev EA, Faucz FR, Barthelmess S, Wiemann S, Bieg M, et al. Aberrant DNA Hypermethylation of SDHC: A Novel Mechanism of Tumor Development in Carney Triad. *Endocr Relat Cancer* (2014) 21(4):567–77. doi: 10.1530/ERC-14-0254

90. Killian JK, Miettinen M, Walker RL, Wang Y, Zhu YJ, Waterfall JJ, et al. Recurrent Epimutation of SDHC in Gastrointestinal Stromal Tumors. *Sci Transl Med* (2014) 6(268):268ra177. doi: 10.1126/scitranslmed.3009961
91. Carney JA, Stratakis CA. Familial Paraganglioma and Gastric Stromal Sarcoma: A New Syndrome Distinct From the Carney Triad. *Am J Med Genet* (2002) 108(2):132–9. doi: 10.1002/ajmg.10235
92. McWhinney SR, Pasini B, Stratakis CA, International Carney T. Carney-Stratakis Syndrome C. Familial Gastrointestinal Stromal Tumors and Germ-Line Mutations. *N Engl J Med* (2007) 357(10):1054–6. doi: 10.1056/NEJMc071191
93. Pantaleo MA, Lolli C, Nannini M, Astolfi A, Indio V, Saponara M, et al. Good Survival Outcome of Metastatic SDH-Deficient Gastrointestinal Stromal Tumors Harboring SDHA Mutations. *Genet Med* (2015) 17 (5):391–5. doi: 10.1038/gim.2014.115
94. Iversen K. Acromegaly Associated With Phaeochromocytoma. *Acta Med Scand* (1952) 142(1):1–5. doi: 10.1111/j.0954-6820.1952.tb13837.x
95. Xekouki P, Brennand A, Whitelaw B, Pacak K, Stratakis CA. The 3pas: An Update on the Association of Pheochromocytomas, Paragangliomas, and Pituitary Tumors. *Horm Metab Res* (2019) 51(7):419–36. doi: 10.1055/a-0661-0341
96. Xekouki P, Pacak K, Almeida M, Wassif CA, Rustin P, Nesterova M, et al. Succinate Dehydrogenase (Sdh) D Subunit (Sdhd) Inactivation in a Growth-Hormone-Producing Pituitary Tumor: A New Association for SDH? *J Clin Endocrinol Metab* (2012) 97(3):E357–66. doi: 10.1210/jc.2011-1179
97. Dwight T, Mann K, Benn DE, Robinson BG, McKelvie P, Gill AJ, et al. Familial SDHA Mutation Associated With Pituitary Adenoma and Pheochromocytoma/Paraganglioma. *J Clin Endocrinol Metab* (2013) 98(6): E1103–8. doi: 10.1210/jc.2013-1400
98. Papathomas TG, Gaal J, Corssmit EP, Oudijk L, Korpershoek E, Heimdal K, et al. Non-Pheochromocytoma (Pcc)/Paraganglioma (Pgl) Tumors in Patients With Succinate Dehydrogenase-Related PCC-PGL Syndromes: A Clinicopathological and Molecular Analysis. *Eur J Endocrinol* (2014) 170 (1):1–12. doi: 10.1530/EJE-13-0623
99. Gill AJ, Toon CW, Clarkson A, Sioson L, Chou A, Winship I, et al. Succinate Dehydrogenase Deficiency is Rare in Pituitary Adenomas. *Am J Surg Pathol* (2014) 38(4):560–6. doi: 10.1097/PAS.0000000000000149
100. Denes J, Swords F, Rattenberry E, Stals K, Owens M, Cranston T, et al. Heterogeneous Genetic Background of the Association of Pheochromocytoma/Paraganglioma and Pituitary Adenoma: Results From a Large Patient Cohort. *J Clin Endocrinol Metab* (2015) 100(3):E531–41. doi: 10.1210/jc.2014-3399
101. Zhang H, Bosch-Marce M, Shimoda LA, Tan YS, Baek JH, Wesley JB, et al. Mitochondrial Autophagy is an HIF-1-dependent Adaptive Metabolic Response to Hypoxia. *J Biol Chem* (2008) 283(16):10892–903. doi: 10.1074/jbc.M800102200
102. Zakeri Z, Lockshin RA. Cell Death: History and Future. *Adv Exp Med Biol* (2008) 615:1–11. doi: 10.1007/978-1-4020-6554-5_1
103. Lee JG, Shin JH, Shim HS, Lee CY, Kim DJ, Kim YS, et al. Autophagy Contributes to the Chemo-Resistance of non-Small Cell Lung Cancer in Hypoxic Conditions. *Respir Res* (2015) 16:138. doi: 10.1186/s12931-015-0285-4
104. Chaachouay H, Fehrenbacher B, Toulany M, Schaller M, Multhoff G, Rodemann HP. Ampk-Independent Autophagy Promotes Radioresistance of Human Tumor Cells Under Clinical Relevant Hypoxia In Vitro. *Radiother Oncol* (2015) 116(3):409–16. doi: 10.1016/j.radonc.2015.08.012
105. Srigley JR, Delahunt B, Eble JN, Egevad L, Epstein JI, Grignon D, et al. The International Society of Urological Pathology (Isup) Vancouver Classification of Renal Neoplasia. *Am J Surg Pathol* (2013) 37(10):1469–89. doi: 10.1097/PAS.0b013e318299f2d1
106. Gill AJ, Hes O, Papathomas T, Sedivcova M, Tan PH, Agaimy A, et al. Succinate Dehydrogenase (Sdh)-Deficient Renal Carcinoma: A Morphologically Distinct Entity: A Clinicopathologic Series of 36 Tumors From 27 Patients. *Am J Surg Pathol* (2014) 38(12):1588–602. doi: 10.1097/PAS.0000000000000292
107. Wang G, Rao P. Succinate Dehydrogenase-Deficient Renal Cell Carcinoma: A Short Review. *Arch Pathol Lab Med* (2018) 142(10):1284–8. doi: 10.5858/arpa.2017-0199-RS
108. Williamson SR, Eble JN, Amin MB, Gupta NS, Smith SC, Sholl LM, et al. Succinate Dehydrogenase-Deficient Renal Cell Carcinoma: Detailed Characterization of 11 Tumors Defining a Unique Subtype of Renal Cell Carcinoma. *Mod Pathol* (2015) 28(1):80–94. doi: 10.1038/modpathol.2014.86
109. Gill AJ, Lipton L, Taylor J, Benn DE, Richardson AL, Frydenberg M, et al. Germline SDHC Mutation Presenting as Recurrent Sdh Deficient GIST and Renal Carcinoma. *Pathology* (2013) 45(7):689–91. doi: 10.1097/PAT.0000000000000018
110. Yakirevich E, Ali SM, Mega A, McMahon C, Brodsky AS, Ross JS, et al. A Novel Sdha-Deficient Renal Cell Carcinoma Revealed by Comprehensive Genomic Profiling. *Am J Surg Pathol* (2015) 39(6):858–63. doi: 10.1097/PAS.0000000000000403
111. Jiang Q, Zhang Y, Zhou YH, Hou YY, Wang JY, Li JL, et al. A Novel Germline Mutation in SDHA Identified in a Rare Case of Gastrointestinal Stromal Tumor Complicated With Renal Cell Carcinoma. *Int J Clin Exp Pathol* (2015) 8(10):12188–97.
112. Ozluk Y, Taheri D, Matoso A, Sanli O, Berker NK, Yakirevich E, et al. Renal Carcinoma Associated With a Novel Succinate Dehydrogenase A Mutation: A Case Report and Review of Literature of a Rare Subtype of Renal Carcinoma. *Hum Pathol* (2015) 46(12):1951–5. doi: 10.1016/j.humpath.2015.07.027
113. Miettinen M, Sarlomo-Rikala M, McCue P, Czapiewski P, Langfort R, Waloszczyk P, et al. Mapping of Succinate Dehydrogenase Losses in 2258 Epithelial Neoplasms. *Appl Immunohistochem Mol Morphol* (2014) 22 (1):31–6. doi: 10.1097/PAI.0b013e31828bfdd3
114. Gill AJ, Pachter NS, Chou A, Young B, Clarkson A, Tucker KM, et al. Renal Tumors Associated With Germline SDHB Mutation Show Distinctive Morphology. *Am J Surg Pathol* (2011) 35(10):1578–85. doi: 10.1097/PAS.0b013e318227e7f4
115. Ricketts CJ, Shuch B, Vocke CD, Metwalli AR, Bratslavsky G, Middelton L, et al. Succinate Dehydrogenase Kidney Cancer: An Aggressive Example of the Warburg Effect in Cancer. *J Urol* (2012) 188(6):2063–71. doi: 10.1016/j.juro.2012.08.030
116. Hensen EF, Bayley JP. Recent Advances in the Genetics of SDH-related Paraganglioma and Pheochromocytoma. *Fam Cancer* (2011) 10(2):355–63. doi: 10.1007/s10689-010-9402-1
117. Suarez C, Rodrigo JP, Bodeker CC, Llorente JL, Silver CE, Jansen JC, et al. Jugular and Vagal Paragangliomas: Systematic Study of Management With Surgery and Radiotherapy. *Head Neck* (2013) 35(8):1195–204. doi: 10.1002/hed.22976
118. Plouin PF, Amar L, Dekkers OM, Fassnacht M, Gimenez-Roqueplo AP, Lenders JW, et al. European Society of Endocrinology Clinical Practice Guideline for Long-Term Follow-Up of Patients Operated on for a Phaeochromocytoma or a Paraganglioma. *Eur J Endocrinol* (2016) 174(5): G1–G10. doi: 10.1530/EJE-16-0033
119. Lenders JW, Duh QY, Eisenhofer G, Gimenez-Roqueplo AP, Grebe SK, Murad MH, et al. Pheochromocytoma and Paraganglioma: An Endocrine Society Clinical Practice Guideline. *J Clin Endocrinol Metab* (2014) 99 (6):1915–42. doi: 10.1210/jc.2014-1498
120. CI NSW. *Risk Management for SDH-related Paraganglioma-Phaeochromocytoma Predisposition Syndromes*. Available at: https://www.eviq.org.au/cancer-genetics/risk-management/3558-risk-management-for-sdh-related-paraganglioma#cancer-and-tumour-risk-management-guidelines.
121. Gimenez-Roqueplo AP, Caumont-Prim A, Houzard C, Hignette C, Hernigou A, Halimi P, et al. Imaging Work-Up for Screening of Paraganglioma and Pheochromocytoma in SDHx Mutation Carriers: A Multicenter Prospective Study From the PGL.EVA Investigators. *J Clin Endocrinol Metab* (2013) 98(1):E162–73. doi: 10.1210/jc.2012-2975
122. Han S, Suh CH, Woo S, Kim YJ, Lee JJ. Performance of (68)Ga-DOTA-Conjugated Somatostatin Receptor-Targeting Peptide PET in Detection of Pheochromocytoma and Paraganglioma: A Systematic Review and Metaanalysis. *J Nucl Med* (2019) 60(3):369–76. doi: 10.2967/jnumed.118.211706
123. Janssen I, Chen CC, Millo CM, Ling A, Taieb D, Lin FI, et al. Pet/Ct Comparing (68)Ga-DOTATATE and Other Radiopharmaceuticals and in Comparison With CT/MRI for the Localization of Sporadic Metastatic

Pheochromocytoma and Paraganglioma. *Eur J Nucl Med Mol Imaging* (2016) 43(10):1784–91. doi: 10.1007/s00259-016-3357-x

124. Chang CA, Pattison DA, Tothill RW, Kong G, Akhurst TJ, Hicks RJ, et al. (68)Ga-DOTATATE and (18)F-FDG PET/CT in Paraganglioma and Pheochromocytoma: Utility, Patterns and Heterogeneity. *Cancer Imaging* (2016) 16(1):22. doi: 10.1186/s40644-016-0084-2
125. Castinetti F, Kroiss A, Kumar R, Pacak K, Taieb D. 15 YEARS of PARAGANGLIOMA: Imaging and Imaging-Based Treatment of Pheochromocytoma and Paraganglioma. *Endocr Relat Cancer* (2015) 22 (4):T135–45. doi: 10.1530/ERC-15-0175
126. Janssen I, Chen CC, Taieb D, Patronas NJ, Millo CM, Adams KT, et al. 68Ga-DOTATATE PET/CT in the Localization of Head and Neck Paragangliomas Compared With Other Functional Imaging Modalities and CT/MRI. *J Nucl Med* (2016) 57(2):186–91. doi: 10.2967/jnumed.115.161018
127. Janssen I, Blanchet EM, Adams K, Chen CC, Millo CM, Herscovitch P, et al. Superiority of [68Ga]-DOTATATE PET/CT to Other Functional Imaging Modalities in the Localization of SDHB-Associated Metastatic Pheochromocytoma and Paraganglioma. *Clin Cancer Res* (2015) 21 (17):3888–95. doi: 10.1158/1078-0432.CCR-14-2751
128. Archier A, Varoquaux A, Garrigue P, Montava M, Guerin C, Gabriel S, et al. Prospective Comparison of (68)Ga-DOTATATE and (18)F-FDOPA PET/CT in Patients With Various Pheochromocytomas and Paragangliomas With Emphasis on Sporadic Cases. *Eur J Nucl Med Mol Imaging* (2016) 43 (7):1248–57. doi: 10.1007/s00259-015-3268-2
129. Taieb D, Timmers HJ, Hindie E, Guillet BA, Neumann HP, Walz MK, et al. Eanm 2012 Guidelines for Radionuclide Imaging of Phaeochromocytoma and Paraganglioma. *Eur J Nucl Med Mol Imaging* (2012) 39(12):1977–95. doi: 10.1007/s00259-012-2215-8
130. King KS, Chen CC, Alexopoulos DK, Whatley MA, Reynolds JC, Patronas N, et al. Functional Imaging of SDHx-related Head and Neck Paragangliomas: Comparison of 18F-Fluorodihydroxyphenylalanine, 18f-Fluorodopamine, 18f-Fluoro-2-Deoxy-D-Glucose PET, 123i-Metaiodobenzylguanidine Scintigraphy, and 111In-Pentetreotide Scintigraphy. *J Clin Endocrinol Metab* (2011) 96(9):2779–85. doi: 10.1210/jc.2011-0333
131. Aghi MK, Chen CC, Fleseriu M, Newman SA, Lucas JW, Kuo JS, et al. Congress of Neurological Surgeons Systematic Review and Evidence-Based Guidelines on the Management of Patients With Nonfunctioning Pituitary Adenomas: Executive Summary. *Neurosurgery* (2016) 79(4):521–3. doi: 10.1227/NEU.0000000000001386
132. Katznelson L, Laws ER Jr, Melmed S, Molitch ME, Murad MH, Utz A, et al. Acromegaly: An Endocrine Society Clinical Practice Guideline. *J Clin Endocrinol Metab* (2014) 99(11):3933–51. doi: 10.1210/jc.2014-2700
133. Melmed S, Casanueva FF, Hoffman AR, Kleinberg DL, Montori VM, Schlechte JA, et al. Diagnosis and Treatment of Hyperprolactinemia: An Endocrine Society Clinical Practice Guideline. *J Clin Endocrinol Metab* (2011) 96(2):273–88. doi: 10.1210/jc.2010-1692
134. Freda PU, Beckers AM, Katznelson L, Molitch ME, Montori VM, Post KD, et al. Pituitary Incidentaloma: An Endocrine Society Clinical Practice Guideline. *J Clin Endocrinol Metab* (2011) 96(4):894–904. doi: 10.1210/jc.2010-1048

**Conflict of Interest:** CAS holds patent on the *PRKAR1A*, *PDE11A*, and *GPR101* genes and/or their function and his laboratory has received research funding from Pfizer Inc. FRF holds patent on the *GPR101* gene and/or its function. CAS is receiving compensation by ELPEN, Inc. Neither Pfizer, Inc nor ELPEN, Inc had any role in the study design, data collection and analysis, decision to publish, or preparation of the manuscript.

The remaining authors declare that the research was conducted in the absence of any commercial or financial relationships that could be construed as a potential conflict of interest.

frontiers in Endocrinology

CASE REPORT
published: 01 July 2021
doi: 10.3389/fendo.2021.687809

# Case Report: Three Rare Cases of Ectopic ACTH Syndrome Caused by Adrenal Medullary Hyperplasia

*Yu Cheng*[1†], *Jie Li*[2†], *Jingtao Dou*[1], *Jianming Ba*[1], *Jin Du*[1], *Saichun Zhang*[1], *Yiming Mu*[1*], *Zhaohui Lv*[1*] *and Weijun Gu*[1*]

[1] *Department of Endocrinology, Chinese PLA General Hospital, Beijing, China,* [2] *Department of Pathology, Chinese PLA General Hospital, Beijing, China*

OPEN ACCESS

**Edited by:**
*Barbara Altieri, University Hospital of Wuerzburg, Germany*

**Reviewed by:**
*Marcio Machado, University of São Paulo, Brazil*
*Carl Christofer Juhlin, Karolinska Institutet (KI), Sweden*

***Correspondence:**
*Yiming Mu*
*muyiming@301hospital.com.cn*
*Zhaohui Lv*
*metabolism301@126.com*
*Weijun Gu*
*guweijun301@163.com*

[†]*These authors have contributed equally to this work*

**Specialty section:**
*This article was submitted to Cancer Endocrinology, a section of the journal Frontiers in Endocrinology*

**Received:** *30 March 2021*
**Accepted:** *07 June 2021*
**Published:** *01 July 2021*

**Citation:**
*Cheng Y, Li J, Dou J, Ba J, Du J, Zhang S, Mu Y, Lv Z and Gu W (2021) Case Report: Three Rare Cases of Ectopic ACTH Syndrome Caused by Adrenal Medullary Hyperplasia. Front. Endocrinol. 12:687809. doi: 10.3389/fendo.2021.687809*

Ectopic ACTH syndrome (EAS) accounts for 10–20% of endogenous Cushing's syndrome (CS). Hardly any cases of adrenal medullary hyperplasia have been reported to ectopically secrete adrenocorticotropic hormone (ACTH). Here we describe a series of three patients with hypercortisolism secondary to ectopic production of ACTH from adrenal medulla. Cushingoid features were absent in case 1 but evident in the other two cases. Marked hypokalemia was found in all three patients, but hyperglycemia and osteoporosis were present only in case 2. All three patients showed significantly elevated serum cortisol and 24-h urinary cortisol levels. The ACTH levels ranged from 19.8 to 103.0pmol/L, favoring ACTH-dependent Cushing's syndrome. Results of bilateral inferior petrosal sinus sampling (BIPSS) for case 1 and case 3 confirmed ectopic origin of ACTH. The extremely high level of ACTH and failure to suppress cortisol with high dose dexamethasone suppression test (HDDST) suggested EAS for patient 2. However, image studies failed to identify the source of ACTH secretion. Bilateral adrenalectomy was performed for rapid control of hypercortisolism. After surgery, cushingoid features gradually disappeared for case 2 and case 3. Blood pressure, blood glucose and potassium levels returned to normal ranges without medication for case 2. The level of serum potassium also normalized without any supplementation for case 1 and case 3. The ACTH levels of all three patients significantly decreased 3-6 months after surgery. Histopathology revealed bilateral adrenal medullary hyperplasia and immunostaining showed positive ACTH staining located in adrenal medulla cells. In summary, our case series reveals the adrenal medulla to be a site of ectopic ACTH secretion. Adrenal medulla-originated EAS makes the differential diagnosis of ACTH-dependent Cushing's syndrome much more difficult. Control of the hypercortisolism is mandatory for such patients.

**Keywords: ACTH-dependent Cushing's syndrome, ectopic ACTH syndrome, adrenal medullary hyperplasia, immunohistochemical staining, bilateral adrenalectomy**

## INTRODUCTION

Adrenocorticotropic hormone (ACTH)-dependent Cushing's syndrome can be classified as either Cushing's disease or ectopic ACTH syndrome (EAS). It is estimated that EAS is responsible for 10–20% of all cases of Cushing's syndrome. The frequencies of tumors associated with EAS vary among series (1). In the 1970s, EAS were mainly represented by small-cell lung carcinomas (SCLCs). But the most prevalent tumor of EAS has recently shifted from SCLCs to neuroendocrine tumors (NETs), and particularly bronchial carcinoids in the recent literature (2–4). Other origins of tumors responsible for EAS are the thymus (5), pancreas, and thyroid. Pheochromocytoma also has been reported to have ectopic ACTH secretion and accounts for approximately 5% of EAS cases (6). Adrenal medullary hyperplasia, characterized by an increased medullary cell mass, is even more rare for excess catecholamine production (7, 8). Hardly any case of adrenal medullary hyperplasia was previously reported to ectopically secrete ACTH according to our systematic search of publications. Here, we reported three cases of EAS associated with adrenal medullary hyperplasia in our center.

## CASE DESCRIPTION

Case series results are summarized in **Tables 1** and **2** and are individually described here.

### Case 1

A 23-year-old woman was admitted to our department presented with a one-month history of general fatigue, acne and hirsutism. Blood pressure was 130/80 mmHg. Her weight was 55 kg, and height was 162.5 cm (Body mass index 20.8Kg/m$^2$). She had no typical symptoms of Cushing's syndrome such as moon face, central obesity, supraclavicular fat accumulation, or buffalo hump. Stria was also invisible. Hypokalemia was evident, which could not be normalized with oral and intravenous potassium supplementation until spironolactone (60mg tid) was added. The level of HbA1c was 5.4%, and blood glucose levels were within normal range after a 75-g oral glucose tolerance test (OGTT). Dual-energy X-ray absorptiometry (DXA) bone densitometry suggested osteopenia with a Z-score of -1.3 at L1-L4 spine. Biochemical workup (**Table 1**) revealed loss of circadian rhythm, elevated 24-h urinary cortisol levels and failure to suppress cortisol with classical low dose dexamethasone

**TABLE 1** | Summary of Characteristics and Laboratory Findings at Presentation.

| | Case 1 | Case 2 | Case 3 | Normal Range |
|---|---|---|---|---|
| Age at diagnosis | 23y | 28y | 31y | |
| Sex | Female | Male | Male | |
| BMI | 20.8 | 28.0 | 31.6 | <28kg/m$^2$ |
| HbA1c | 5.7 | 5.6 | 5.4 | <6.5% |
| Glucose after 75g OGTT | | | | |
| 0min | 3.9 | 8.65 | 4.8 | 3.4-6.1mmol/L |
| 60min | 6.95 | 16.48 | 8.34 | <11.1mmol/L |
| 120min | 7.06 | 17.12 | 7.26 | ≥7.8mmol/L |
| Blood pressure | 130/80 | 150/100 | 130/90 | <140/90mmHg |
| Z score | -1.3 | -4.0 | 0.2 | >-1 |
| L1-L4 spine | | | | |
| Serum potassium | 2.56 | 1.29 | 2.66 | 3.5-4.5mmol/L |
| Serum cortisol | | | | |
| 0AM | 1007.19 | 3048.0 | 785.28 | 0-165.7nmol/L |
| 8AM | 1229.25 | 3577.9 | 1080.58 | 198.7-797.5nmol/L |
| 4PM | 1152.32 | 3394.7 | 164.21 | 85.3-459.6nmol/L |
| Urine free cortisol | 6674.8 | 47862 | 6358.8 | 98.0-500.1nmol/24h |
| Serum ACTH | | | | |
| 0AM | 13.3 | 88.8 | 38.4 | |
| 8AM | 19.8 | 103.0 | 42.0 | <10.12pmol/L |
| 4PM | 23.5 | 62.6 | 66.4 | |
| **LDDST** | | | | |
| Serum cortisol | 1997.19 | | 850.21 | <50nmol/L |
| Serum ACTH | 24.4 | _ | 28.4 | |
| Urine free cortisol | 7499.5 | | 6419.9 | <98.0nmol/24h |
| **HDDST** | | | | |
| Serum cortisol | 1673.45 (136%) | 3789.9 (106%) | 1793.09 (166%) | <50% |
| Serum ACTH | 22.6 | 100.0 | 15.7 | |
| Urine free cortisol | 4243.3 (63%) | 50800 (106%) | 5697.0 (90%) | <50% |
| **DDAVP** | | | | |
| ACTH max/ACTH basal | 7.11 | _ | 5.77 | |
| **BIPSS** | | | | |
| Central/peripheral ACTH at basal | 0.93 | _ | 1.02 | |
| Central/peripheral ACTH after DDAVP stimulation | 1.5 | _ | 0.67 | |

**TABLE 2** | Assessment Before and After Bilateral Adrenalectomy.

| | Case 1 | Case 2 | Case 3 |
|---|---|---|---|
| Serum ACTH (pmol/L) | Before 3m 12m | Before 3m 12m | Before 3m 12m |
| 0AM | 13.3 1.77 - | 88.8 1.1 1.1 | 38.4 3.53 7.3 |
| 8AM | 19.8 11.9 - | 103.0 4.06 54.2 | 42.0 7.33 86.1 |
| 4PM | 23.5 10.1 - | 62.6 4.00 12.6 | 66.4 6.64 49.3 |
| Serum Cortisol (nmol/L) | Before 3m 12m | Before 3m 12m | Before 3m 12m |
| 0AM | 1007.19 197.34 - | 3048.0 134.65 40.50 | 785.28 121.81 <25.7 |
| 8AM | 1229.25 304.11 - | 3577.9 <25.7 31.37 | 1080.58 342.89 231.36 |
| 4PM | 1152.32 123.76 - | 3394.7 130.54 85.81 | 164.21 <25.7 <25.7 |

suppression test (LDDST). Plasma ACTH level was elevated to 19.8 pmol/L, favoring ACTH-dependent Cushing's syndrome. Desmopressin stimulation resulted in ACTH increase by about 700%. But cortisol was not suppressed after high dose dexamethasone intake. Magnetic resonance imaging (MRI) showed normal pituitary gland (**Supplementary Figure 1A**). So next, bilateral inferior petrosal sinus sampling (BIPSS) was performed and showed a central-to-peripheral ACTH gradient < 2 at baseline and < 3 after desmopressin stimulation. Finally, diagnosis of EAS was considered. The lesion was not localized by CT scans. Further evaluation with $^{68}$Ga-DOTATATE PET/CT and 18F-PET/CT still failed to identify the source of ACTH secretion. Only bilateral adrenal hyperplasia was observed *via* image studies (**Figure 1A**). As steroidogenesis inhibitors are unavailable in China, mifepristone can aggravate hypokalemia, and the cortisol level remained unchangeable after short-acting octreotide injection, bilateral adrenalectomy was performed for rapid control of hypercortisolism. Transperitoneal approach was used with the patient positioned in left and right lateral positions for right and left glands, respectively. A meticulous surgical technique was used to best expose the adrenal veins to clip them before division followed by excising the glands. The patient had minimal blood pressure variations during surgery. After surgery, a 20mg dose of hydrocortisone per day was given. The level of serum potassium normalized without any supplementation. The level of serum sodium was around 140mmol/L. Blood pressure maintained between 100-110/60-70mmHg. ACTH level significantly decreased at the latest follow-up (3 months after surgery, **Table 2**), indicating adrenal glands to be the origin of excess ACTH. Consistently, the low power view of histopathological image showed a thickened adrenal medulla, more than a third of the total adrenal thickness in both glands, which met the criteria of adrenal medulla hyperplasia in WHO 2017 classification of endocrine tumors (**Figure 2A**). The high power view showed diffuse hyperplasia of the medullary cells, and the medullary cells showed size and shape variability in areas of diffuse hyperplasia (**Figure 2B**). The medullary cells stained positive for chromogranin A (**Figure 2C**). Histopathology revealed bilateral diffuse cortex hyperplasia (**Figure 2D**). Immunostaining showed sporadic positive ACTH staining (**Figure 3A**) located in adrenal medulla cells. To rule out the possibility of non-specific staining, ACTH staining was simultaneously performed in adrenal tissues from a patient undergoing adrenalectomy due to renal cell carcinoma, and no positive cells were spotted neither in adrenal cortex nor adrenal medulla (**Figures 3D, E**).

## Case 2

A 28-year-old man complained with a six-month history of acne and three-month history of moon face, general fatigue and hypertension. Physical examination revealed a blood pressure of 150/90 mmHg, weight of 78 kg, and height of 167 cm (BMI 27.9 Kg/m$^2$). He displayed overt cushingoid features with central obesity, dorsocervical and supraclavicular fat pads, abdominal striae, skin

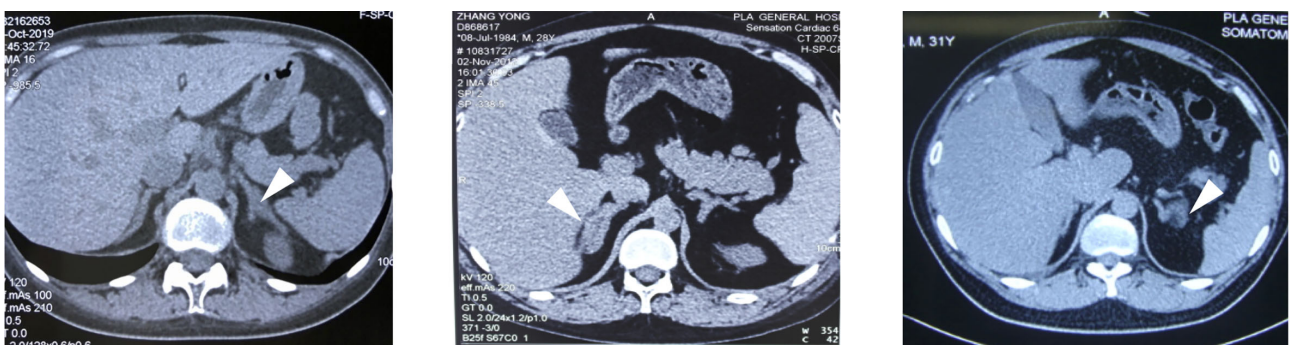


**FIGURE 1** | The CT images of the adrenal glands for case1 **(A)**, case 2 **(B)** and case 3 **(C)**. Adrenal contrast-enhanced CT showed adrenal hyperplasia (arrows).

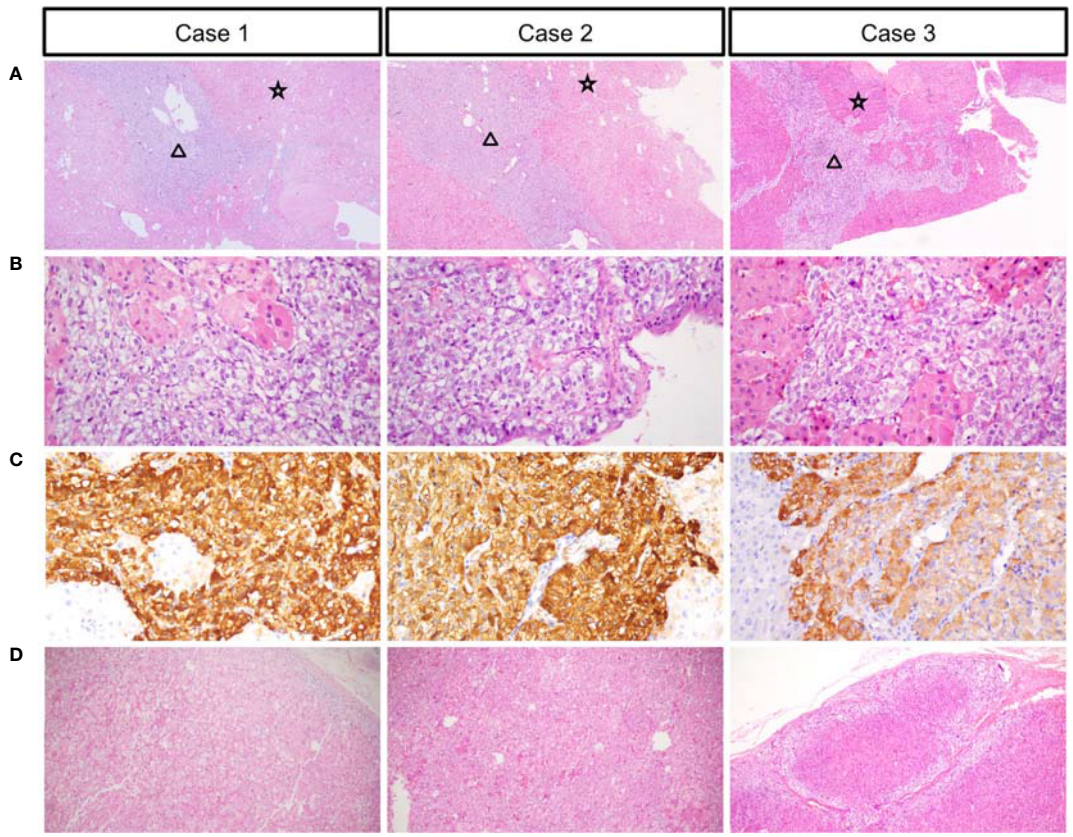


**FIGURE 2** | Low power views showing the thickened medulla (black triangle) and hyperplastic adrenal cortex (black star) **(A)**. High-power views of the medulla **(B)**. Chromogranin expression in the medullary cells **(C)**. High-power views of the cortex **(D)**.

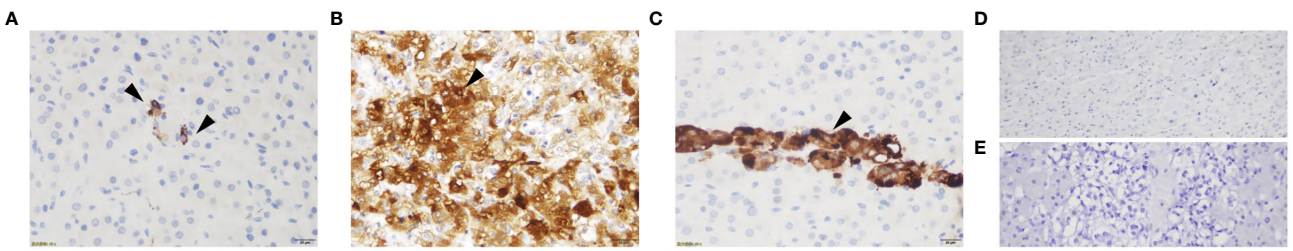


**FIGURE 3** | ACTH immunostaining of the adrenal glands for case1 **(A)**, case 2 **(B)**, case 3 **(C)**, adrenal cortex of normal control **(D)** and adrenal medulla of normal control **(E)**. ACTH staining showed sporadic positive ACTH staining for case 1, numerous adrenal medulla cells positive for ACTH for case 2, focal positive ACTH staining for case 3 and negative ACTH staining for normal control.

bruises, acne, and facial plethora. Laboratory examination showed severe hypokalemia (1.2mmol/L). A 75-g OGTT confirmed diabetes mellitus with a fasting blood glucose level of 8.65 mmol/l and a 2-h glucose level of 17.12 mmol/L, although HbA1c level was only 5.6%. DXA showed severe osteoporosis with a Z-score of -4.0 at the L1-L4 spine. Endocrinological investigation (**Table 1**) identified severe hypercortisolism with loss of circadian rhythm and elevated 24-h urinary cortisol levels. Plasma ACTH level was significantly elevated to 103 pmol/L, confirming ACTH-dependent Cushing's syndrome. The serum cortisol level was not suppressed after a high dose dexamethasone suppression test (HDDST). MRI revealed no pituitary adenoma (**Supplementary Figure 1B**). We offered BIPSS for ACTH assays to identify the origin of ACTH, but the patient refused. Nonetheless, EAS was considered given the ACTH level, results of HDDST and pituitary MRI. No lesion was detected in thoracic

CT scan. Abdominal CT showed hyperplasia of the right adrenal gland (**Figure 1B**). Pituitary MRI showed a mass in the left nasal cavity and left ethmoidal sinus (**Supplementary Figure 2**), and PET-CT confirmed intense metabolic activity of the mass. The mass was thereafter biopsied. Pathology showed that the mass was composed of small round blue cells with a high nuclear-to-cytoplasmic ratio, rare nucleoli and a nuclear chromatin pattern typical of neuroendocrine-like tumors. The diagnosis of olfactory neuroblastoma was supported by immunohistochemical staining for multiple neuro-endocrine markers, such as CD56, synaptophysin, chromogranin A and S-100. Previously, more than 20 cases of olfactory neuroblastoma presenting with EAS have been reported (9, 10). However, biopsy did not show positive ACTH staining. Surgical removal of the tumor was delayed due to poor general condition of the patient. Upon admission, ketoconazole was still available. At a dose of 800mg/d, the serum cortisol level dropped from 3577.9 to 1159.3nmol/L, but liver damage was already induced with ALT level reaching 300U/L. Therefore, ketoconazole was discontinued and bilateral adrenalectomy was next performed. Similarly, no sudden rise of blood pressure was observed during surgery. After surgery, cushingoid features gradually disappeared. Blood pressure, blood glucose and potassium levels returned to normal ranges without medication. He needed a 7.5-mg dose of prednisone acetate per day. At 3 month after surgery, the ACTH level decreased to 4.06 pmol/L. As the general condition significantly improved, the patient next underwent transnasal endoscopic resection of the tumour mass. ACTH and CRH staining were both negative for the tumor, whereas histopathology showed an increased adrenal medullary cell mass and diffuse hyperplasia of the medullary cells in both adrenal glands (**Figures 2A, B**). The medullary cells stained positive for chromogranin A (**Figure 2C**). Histopathology also revealed bilateral diffuse cortex hyperplasia (**Figure 2D**). Immunohistochemical staining showed numerous adrenal medulla cells positive for ACTH (**Figure 3B**). A year after bilateral adrenalectomy, the patient was admitted for regular follow-up. The 8AM ACTH markedly elevated to 54.2pmol/L but was suppressed below 1.11pmol/L after 1mg dexamethasone administration, suggesting that the up-regulated ACTH level was a result of adrenocortical insufficiency. The patient is currently under regular follow-up and remains well for 7 years.

## Case 3

A 31-year-old man presented with a two-month history of general fatigue, acne, moon face and hyperpigmentation. Physical examination revealed a blood pressure of 130/90 mmHg, weight of 99 kg, and height of 177 cm (BMI 31.6 Kg/$m^2$). He showed cushingoid features including moon face, supraclavicular fat accumulation, buffalo hump, facial and truncal acne, ecchymoses and striae. Laboratory examination showed hypokalemia. The level of HbA1c was 5.4%. A 75-g OGTT showed normal glucose homeostasis. Z score at L1-L4 spine was 0.2. The serum levels of ACTH, cortisol, and 24-h urine free cortisol were markedly elevated (**Table 1**). Results of LDDST showed a cortisol value of 840.21 nmol/L after the dexamethasone administration. There was no suppression after HDDST. MRI of the pituitary gland did not showed signs of pituitary adenoma (**Supplementary Figure 1C**). Just like case 1, ACTH max/ACTH basal was as high as 5.77 after desmopressin stimulation. BIPSS showed that there was no evidence of a central-to-peripheral gradient of ACTH at baseline or after desmopressin stimulation. According to these findings, the patient was diagnosed with EAS. Thoracic CT scan was normal. Abdominal CT only showed nodular hyperplasia of the left adrenal gland (**Figure 1C**). The 18F-PET/CT showed increased uptake in both adrenal glands. Octreotide scanning also revealed negative results. As steroidogenesis inhibitors were unavailable, bilateral adrenalectomy was then performed *via* the same approach as case 1 without arterial variations. After surgery, a 20mg dose of hydrocortisone per day was added. Cushingoid features gradually disappeared. The levels of serum potassium remained normal without potassium supplement. Similarly, immunohistochemical staining showed focal positive ACTH staining in hyperplastic adrenal medulla cells (**Figures 2A–C**, **3C**) and nodular hyperplasia of adrenal cortex in both adrenal glands (**Figure 2D**). ACTH level significantly decreased 3 months after surgery (**Table 2**). At the latest follow-up, a year after surgery, the patient complained about hyperpigmentation. Laboratory tests showed that 8AM ACTH level relapsed to 86.1 pmol/L. After LDDST, ACTH level significantly decreased to 18.4 pmol/L. $^{68}$Ga-DOTATATE PET/CT and pituitary MRI still showed no signs for lesions. All the data indicated that increase of ACTH was the result of cortisol hypofunction. In order to suppress ACTH secretion, we added dexamethasone 0.1875mg at 10PM.

# DISCUSSION

Our case series suggest that severe Cushing's syndrome can be induced by ectopic production of ACTH caused by adrenal medulla hyperplasia, supported by a drastic decrease of ACTH level after bilateral adrenalectomy, positive ACTH staining in adrenal medulla cells, and the number of ACTH positive cells in proportion to serum ACTH level.

Back in 1980s, researchers showed the presence of immunoreactive ACTH and corticotropin-releasing hormone (CRH) in adrenals (combined cortex and medulla) by radioimmunity assay, immunoaffinity chromatography, and gel filtration chromatography (11). Interestingly, in patients with proven deficiency of pituitary ACTH, administration of 100ug human CRH induced an increase in plasma ACTH level, indicating extra-pituitary source of ACTH (12). Animal experiments revealed the role of the adrenal medulla as the production site of ACTH after CRH stimulation (13). Subsequently, it was demonstrated that human adrenal medulla expressed CRH receptors (14). Strong evidence supports a local, intra-adrenal CRH/ACTH system (15). Adrenal medullary cells possess the potential to secret ACTH into plasma. So it would be reasonable to infer that in our series, the adrenal medulla was the source of ectopic ACTH secretion.

Compared to pheochromocytomas, adrenal medullary hyperplasia is less common. Only case reports or small case series about adrenal medullary hyperplasia have been reported (16, 17), in

which patients often represented with a medical history of symptoms and signs of excessive catecholamine excretion, slightly elevated level of catecholamine, and increased adrenal medullary tissue relative to the cortex. However, in our case series, blood pressure only slightly elevated for case 2, most probably related with hypercortisolism. Given the prominent Cushing's syndrome in our series, the levels of catecholamine was not detected in any of the three cases. But absence of paroxysmal symptoms and blood pressure variations during the adrenal surgery made the possibility of catecholamine excess relatively low. We hypothesized that the potential of ACTH secretion might be limited to a certain subtype of adrenal medulla cells, and hyperplasia of such cells mainly resulted in hypercortisolism rather than excess catecholamine production. The underlying mechanism needs further exploration.

Occult EAS is not rare. A lack of tumor identification has been documented from 12 to 36.5% in different series (1). In some cases, a non-metastatic well-differentiated and indolent neuroendocrine tumor can be discovered after several months or years of follow-up (4). However, some cases remain truly occult. Our findings provide reasonable explanations for, if not all, parts of these truly occult cases. The adrenal medulla has rarely been identified to be the ectopic source of ACTH before, and its incidence might have been underestimated. There might be two reasons. First, in cases with occult EAS, pharmacological treatments of hypercortisolism are fist-line choices in many countries (18), which would not affect the ACTH level. Without removal of adrenal glands, there would be no evidence to suggest adrenal medulla hyperplasia. Secondly, in cases with bilateral adrenalectomy to control hypercortisolism, the ACTH would rapidly relapse to a high level due to adrenocortical hypofunction. If in the short time-window when ACTH level dropped, the patients did not have the ACTH level checked, the clue would also have been missed.

Differential diagnosis between Cushing's disease and occult EAS can be challenging. Typically, in EAS, the degree of ACTH hypersecretion is much higher compared to Cushing's disease. CRH or desmopressin stimulation usually results in increase in ACTH and cortisol levels in Cushing's disease, but not in EAS. The cortisol level is not suppressed with HDDST. However, these tests may not be completely reliable (19). A review concluded that the sensitivity of desmopressin stimulation in the differential diagnosis of ACTH-dependent Cushing's syndrome was 83% and the specificity was only 62% (20). In certain researches, EAS patients even responded to desmopressin test in about 30-40% of cases (21). So if ACTH-dependent Cushing's syndrome were biochemically supported and a pituitary adenoma was detected on MRI, the diagnosis of Cushing's disease would have been arbitrarily made. However, given that pituitary adenoma can be detected in 5~20% normal people (22), we might have preformed pituitary resection to a patient with occult EAS and concomitant non-functional pituitary adenoma. So it must be born in mind that occult EAS is not rare (23). Under such circumstances, BIPSS is very important. BIPSS combined with CRH and/or desmopressin administration is considered the gold standard for distinguishing EAS from Cushing's disease (24). Absence of a central to peripheral ACTH gradient confirms an ectopic source of ACTH secretion. EAS associated with adrenal medulla hyperplasia might raise another diagnostic problem as in case 2, when a tumor, which has been reported to be associated with EAS, is indeed identified. It is very likely that surgical excision of the tumor is the first-line choice as surgery offers a good chance for cure while maintains adrenal function. With no doubt, hypercortisolism would persist afterwards.

Desmopressin is a long-acting vasopressin analog with selective V2 agonist activity (25). Pituitary ACTH-producing adenoma expresses V2 receptors (V2R). As a result, desmopressin administration produces a significant rise of ACTH secretion in the majority of patients with Cushing's disease whereas patients with EAS were unresponsive (26). Since CRH is unavailable in China, desmopressin stimulation test instead is applied to distinguishing EAS from Cushing's disease. Taken the ACTH max/ACTH basal ratio of 1. 5 as a cut point, a significant overlap of the ACTH response to the desmopressin test was found between patients with Cushing's disease and EAS. But the ratio rarely exceeds 3 in EAS (20). However, we notice that after desmopressin stimulation, ACTH increment was up to 711% for case 1 and 577% for case 3. It has been reported that the adrenal medulla, from many species, exhibits V1 vasopressin receptors, and *via* V1 receptors, arginine-vasopressin stimulates intramedullary the CRH-ACTH system (27). So we hypothesize that the adrenal medulla also exhibit V2R and desmopressin stimulates the intramedullary ACTH production, making distinguishing adrenal medulla-originated EAS from Cushing's disease more difficult.

In our study, age of three patients at diagnosis was relatively younger than that in previously published series regarding EAS (2–4, 23, 28, 29). The medical history was short, and most common signs were general fatigue and acne. Cushingoid features were absent in case 1 but evident in the other two cases. With respect to cortisol-induced comorbidities, marked hypokalemia was found in all three patients, but hyperglycemia and osteoporosis were present only in case 2. The clinical heterogeneity is probably due to the large span of ACTH levels from 19.8 to 103.0pmol/L. Bilateral adrenalectomy rapidly and effectively halted hypercortisolism in our case series. The surgery has been traditionally considered a safe option to achieve a radical and fast treatment of hypercortisolism. In a meta-analysis of 23 studies, 30-day morbidity and mortality were acceptable (18% and 3%, respectively) (30). Clinical remission of Cushing's syndrome was greater than 95%. But the downside of bilateral adrenalectomy is also very obvious, including the need for lifelong glucocorticoid and mineralocorticoid replacement therapy, and the risk of adrenal crisis (4.1 to 9.1 per 100 patient-years). In recent guidelines and reviews regarding EAS, bilateral adrenalectomy has been reconsidered and restricted to very severe cases, when steroidogenesis inhibitors are unavailable, ineffective or poorly tolerated (18). The therapeutic effect of steroidogenesis inhibitors on adrenal medulla-originated EAS needs further exploration. When medical treatment fails, bilateral adrenalectomy should be performed as soon as possible. Survival of patients with EAS is dependent on tumor histology and by the severity of hypercortisolemia. Patients with SCLCs and thymic carcinoids seem to have the worst prognosis, while patients with tumors with endocrine differentiation have a better outcome. Adrenal medulla-originated EAS is relatively benign. Just as our case series, when hypercortisolemia is well controlled, the patients will survive with improved health-related quality of life.

In summary, our case series reveals the adrenal medulla to be a site of ectopic ACTH secretion, which is previously ignored. Adrenal medulla-originated EAS makes the differential diagnosis of ACTH-dependent Cushing's syndrome much more difficult. Control of the hypercortisolism is mandatory for such patients. When steroidogenesis inhibitors are unavailable, response to somatostatin analogues is limited, or the adverse effects are intolerable, bilateral adrenalectomy is the last choice. If hypercortisolemia is promptly and effectively controlled, the prognosis is often favorable.

## DATA AVAILABILITY STATEMENT

The original contributions presented in the study are included in the article/**Supplementary Material**. Further inquiries can be directed to the corresponding authors.

## ETHICS STATEMENT

Written informed consent was obtained from the individual(s) for the publication of any potentially identifiable images or data included in this article.

## AUTHOR CONTRIBUTIONS

YC analyzed the data. She was a major contributor in writing the manuscript. WG made substantial contributions in interpretation of data, and have been involved in revising the manuscript critically for important intellectual content. JL supervised histological examination. JD, JB, JTD, and SZ made substantial contributions to acquisition of data, or analysis. YM and ZL were the superior advisors. They agreed to be accountable for all aspects of the work in ensuring that questions related to the accuracy or integrity of any part of the work are appropriately investigated and resolved. All authors contributed to the article and approved the submitted version.

## ACKNOWLEDGMENTS

We thank Dr Nan Jin, Hong liao, Chunjing Zhu, Huali Ming and Zewei Li for kindly providing **Figures 1–3**.

## SUPPLEMENTARY MATERIAL

The Supplementary Material for this article can be found online at: https://www.frontiersin.org/articles/10.3389/fendo.2021.687809/full#supplementary-material

**Supplementary Figure 1 |** Pituitary MRI images for case1 **(A)**, case 2 **(B)** and case 3 **(C)**. Pituitary contrast-enhanced MRI did not showed signs of pituitary adenoma.

**Supplementary Figure 2 |** Pituitary MRI image for case 2, revealing the presence of a mass in the left nasal cavity and left ethmoidal sinus (arrow).

## REFERENCES

1. Alexandraki KI, Grossman AB. The Ectopic ACTH Syndrome. *Rev Endocrine Metab Disord* (2010) 11(2):117–26. doi: 10.1007/s11154-010-9139-z
2. Isidori AM, Kaltsas GA, Pozza C, Frajese V, Newell–Price J, Reznek RH, et al. The Ectopic Adrenocorticotropin Syndrome: Clinical Features, Diagnosis, Management, and Long-Term Follow-Up. *J Clin Endocrinol Metab* (2006) 91 (2):371–7. doi: 10.1210/jc.2005-1542
3. Hernández I, Espinosa-de-los-Monteros AL, Mendoza V, Cheng S, Molina M, Sosa E, et al. Ectopic ACTH-Secreting Syndrome: A Single Center Experience Report With a High Prevalence of Occult Tumor. *Arch Med Res* (2006) 37 (8):976–80. doi: 10.1016/j.arcmed.2006.05.015
4. Espinosa-de-los-Monteros AL, Ramírez-Rentería C, Mercado M. Clinical Heterogeneity of the Ectopic Acth Syndrome: A Long-Term Follow Up Study. *Endocrine Pract* (2020) 26(12):1435–41. doi: 10.1016/j.eprac.2020.06.001
5. Chen Y-y, Li S-q, Liu H-s, Qin Y-z, Li L, Huang C, et al. Ectopic Adrenocorticotropic Hormone Syndrome Caused by Neuroendocrine Tumors of the Thymus: 30-Year Experience With 16 Patients at a Single Institute in the People’s Republic of China. *OncoTargets Ther* (2016) 2193. doi: 10.2147/OTT.S100585
6. Ballav C, Naziat A, Mihai R, Karavitaki N, Ansorge O, Grossman AB. Mini-Review: Pheochromocytomas Causing the Ectopic ACTH Syndrome. *Endocrine* (2012) 42(1):69–73. doi: 10.1007/s12020-012-9646-7
7. Falhammar H, Stenman A, Calissendorff J, Juhlin CC. Presentation, Treatment, Histology, and Outcomes in Adrenal Medullary Hyperplasia Compared With Pheochromocytoma. *J Endocrine Soc* (2019) 3(8):1518–30. doi: 10.1210/js.2019-00200
8. Rudy FR, Bates RD, Cimorelli AJ, Hill GS, Engelman K. Unilateral Adrenal Medullary Hyperplasia: Another Form of Curable Hypertension? *Int J Clin Pract* (1999) 53(2):149–51. doi: 10.1016/s0046-8177(80)80076-1
9. Decaestecker K, Wijtvliet V, Coremans P, Van Doninck N. Olfactory Neuroblastoma (Esthesioneuroblastoma) Presenting as Ectopic ACTH Syndrome: Always Follow Your Nose. *Endocrinol Diabetes Metab Case Rep* (2019) 2019. doi: 10.1530/EDM-19-0093
10. Koo BK, An JH, Jeon KH, Choi SH, Cho YM, Jang HC, et al. Two Cases of Ectopic Adrenocorticotropic Hormone Syndrome With Olfactory Neuroblastoma and Literature Review. *Endocr J* (2008) 55(3):469–75. doi: 10.1507/endocrj.K07E-005
11. Suda T, Tomori N, Tozawa F, Mouri T, Demura H, Shizume K. Distribution and Characterization of Immunoreactive Corticotropin-Releasing Factor in Human Tissues. *J Clin Endocrinol Metab* (1984) 59(5):861–6. doi: 10.1210/jcem-59-5-861
12. Fehm HL, Holl R, Späth–Schwalbe E, Born J, Voigt KH. Ability of Corticotropin Releasing Hormone to Stimulate Cortisol Secretion Independent From Pituitary Adrenocorticotropin. *Life Sci* (1988) 42 (6):679–86. doi: 10.1016/0024-3205(88)90459-6
13. Andreis PG, Neri G, Mazzocchi G, Musajo F, Nussdorfer GG. Direct Secretagogue Effect of Corticotropin-Releasing Factor on the Rat Adrenal Cortex: The Involvement of the Zona Medullaris. *Endocrinology* (1992) 131 (1):69–72. doi: 10.1210/endo.131.1.1319330
14. Willenberg HS, Bornstein SR, Hiroi N, Päth G, Goretzki PE, Scherbaum WA, et al. Effects of a Novel Corticotropin-Releasing-Hormone Receptor Type I Antagonist on Human Adrenal Function. *Mol Psychiatry* (2000) 5(2):137–41. doi: 10.1038/sj.mp.4000720
15. Vrezas I, Willenberg HS, Mansmann G, Hiroi N, Fritzen R, Bornstein SR. Ectopic Adrenocorticotropin (ACTH) and Corticotropin-Releasing Hormone (CRH) Production in the Adrenal Gland: Basic and Clinical Aspects. *Microscopy Res Technique* (2003) 61(3):308–14. doi: 10.1002/jemt.10340
16. Montebello A, Ceci MA, Vella S. Adrenal Medullary Hyperplasia Mimicking Pheochromocytoma. *BMJ Case Rep* (2020) 13(9):e236209. doi: 10.1136/bcr-2020-236209

17. Rivas Mejia AM, Cameselle-Teijeiro JM, Thavaraputta S, Lado–Abeal J. Adrenal Medullary Hyperplasia, An Under the Radar Cause of Endocrine Hypertension. *Am J Med Sci* (2020). doi: 10.1016/j.amjms.2020.06.031
18. Young J, Haissaguerre M, Viera-Pinto O, Chabre O, Baudin E, Tabarin A. Management OF Endocrine DISEASE: Cushing's Syndrome Due to Ectopic ACTH Secretion: An Expert Operational Opinion. *Eur J Endocrinol* (2020) 182(4):R29–58. doi: 10.1530/EJE-19-0877
19. Suda T, Kageyama K, Nigawara T, Sakihara S. Evaluation of Diagnostic Tests for ACTH-dependent Cushing's Syndrome. *Endocr J* (2009) 56(3):469–76. doi: 10.1507/endocrj.K08E-353
20. Vassiliadi DA, Tsagarakis S. Diagnosis OF Endocrine DISEASE: The Role of the Desmopressin Test in the Diagnosis and Follow-Up of Cushing's Syndrome. *Eur J Endocrinol* (2018) 178(5):R201–14. doi: 10.1530/EJE-18-0007
21. Terzolo M, Reimondo G, Ali A, Borretta G, Cesario F, Pia A, et al. The Limited Value of the Desmopressin Test in the Diagnostic Approach to Cushing's Syndrome. *Clin Endocrinol (Oxf)* (2001) 54(5):609–16. doi: 10.1046/j.1365-2265.2001.01260.x
22. Tabarin A, Laurent F, Catargi B, Olivier–Puel F, Lescene R, Berge J, et al. Comparative Evaluation of Conventional and Dynamic Magnetic Resonance Imaging of the Pituitary Gland for the Diagnosis of Cushing's Disease. *Clin Endocrinol (Oxf)* (1998) 49(3):293–300. doi: 10.1046/j.1365-2265.1998.00541.x
23. Ilias I, Torpy DJ, Pacak K, Mullen N, Wesley RA, Nieman LK. Cushing's Syndrome Due to Ectopic Corticotropin Secretion: Twenty Years' Experience at the National Institutes of Health. *J Clin Endocrinol Metab* (2005) 90 (8):4955–62. doi: 10.1210/jc.2004-2527
24. Oldfield EH, Doppman JL, Nieman LK, Chrousos GP, Miller DL, Nieman DA, et al. Petrosal Sinus Sampling With and Without Corticotropin-Releasing Hormone for the Differential Diagnosis of Cushing's Syndrome. *N Engl J Med* (1991) 325(13):897–905. doi: 10.1056/NEJM199109263251301
25. Sawyer WH, Acosta M, Balaspiri L, Judd J, Manning M. Structural Changes in the Arginine Vasopressin Molecule That Enhance Antidiuretic Activity and Specificity. *Endocrinology* (1974) 94(4):1106–15. doi: 10.1210/endo-94-4-1106
26. Tsagarakis S, Tsigos C, Vasiliou V, Tsiotra P, Kaskarelis J, Sotiropoulou C, et al. The Desmopressin and Combined CRH-desmopressin Tests in the Differential Diagnosis of ACTH-dependent Cushing's Syndrome: Constraints Imposed by the Expression of V2 Vasopressin Receptors in Tumors With Ectopic ACTH Secretion. *J Clin Endocrinol Metab* (2002) 87(4):1646–53. doi: 10.1210/jcem.87.4.8358
27. Mazzocchi G, Malendowicz LK, Rebuffat P, Tortorella C, Nussdorfer GG. Arginine-Vasopressin Stimulates CRH and ACTH Release by Rat Adrenal Medulla, Acting Via the V1 Receptor Subtype and a Protein Kinase C-dependent Pathway. *Peptides* (1997) 18(2):191–5. doi: 10.1016/S0196-9781(96)00294-X
28. Ejaz S, Vassilopoulou-Sellin R, Busaidy NL, Hu MI, Waguespack SG, Jimenez C, et al. Cushing Syndrome Secondary to Ectopic Adrenocorticotropic Hormone Secretion. *Cancer* (2011) 117(19):4381–9. doi: 10.1002/cncr.26029
29. Kakade H, Kasaliwal R, Jagtap V, Bukan A, Budyal S, Khare S, et al. Ectopic ACTH-Secreting Syndrome: A Single-Center Experience. *Endocrine Pract* (2013) 19(6):1007–14. doi: 10.4158/EP13171.OR
30. Guerin C, Taieb D, Treglia G, Brue T, Lacroix A, Sebag F, et al. Bilateral Adrenalectomy in the 21st Century: When to Use it for Hypercortisolism? *Endocrine-Related Cancer* (2016) 23(2):R131–42. doi: 10.1530/ERC-15-0541

**Conflict of Interest:** The authors declare that the research was conducted in the absence of any commercial or financial relationships that could be construed as a potential conflict of interest.

frontiers in Endocrinology

CASE REPORT
published: 22 July 2021
doi: 10.3389/fendo.2021.705271

# Highly Symptomatic Progressing Cardiac Paraganglioma With Intracardiac Extension Treated With $^{177}$Lu-DOTATATE: A Case Report

*Alexis Huot Daneault[1], Mélanie Desaulniers[1], Jean-Mathieu Beauregard[2], Alexis Beaulieu[2], Frédéric Arsenault[2], Geneviève April[2], Éric Turcotte[1] and François-Alexandre Buteau[2]**

[1] Département de médecine nucléaire et radiobiologie, Université de Sherbrooke, Sherbrooke, QC, Canada, [2] Département d'imagerie médicale, Division médecine nucléaire, CHU de Québec, Québec, QC, Canada

OPEN ACCESS

**Edited by:**
*Antongiulio Faggiano, Sapienza University of Rome, Italy*

**Reviewed by:**
*Annibale Versari, Local Health Authority of Reggio Emilia, Italy*
*Paraskevi Xekouki, University of Crete, Greece*
*Mauro Cives, University of Bari Aldo Moro, Italy*

***Correspondence:**
*François-Alexandre Buteau*
*francois.buteau.med@ssss.gouv.qc.ca*

**Specialty section:**
*This article was submitted to Cancer Endocrinology, a section of the journal Frontiers in Endocrinology*

**Received:** *05 May 2021*
**Accepted:** *08 July 2021*
**Published:** *22 July 2021*

**Citation:**
*Huot Daneault A, Desaulniers M, Beauregard J-M, Beaulieu A, Arsenault F, April G, Turcotte É and Buteau F-A (2021) Highly Symptomatic Progressing Cardiac Paraganglioma With Intracardiac Extension Treated With $^{177}$Lu-DOTATATE: A Case Report. Front. Endocrinol. 12:705271. doi: 10.3389/fendo.2021.705271*

**Introduction:** Primary cardiac paragangliomas are rare tumors. Metastatic disease is even rarer. Surgical management is technically challenging, and sometimes even impossible. Available therapeutic modalities for metastatic disease include external beam radiation therapy as well as systemic treatments, namely $^{131}$I-MIBG and more recently, peptide receptor radionuclide therapy (PRRT) with $^{177}$Lu-DOTATATE. To our knowledge, this is the first case of progressive unresectable cardiac paraganglioma with intracardiac extension treated with dosimetry based personalized PRRT to be reported. This case is of particular interest since it documents for the first time the efficacy, and especially the safety of the $^{177}$Lu-DOTATATE PRRT in this precarious context for which therapeutic options are limited.

**Case Presentation:** A 47-year-old man with no medical history consulted for rapidly decreasing exercise tolerance. The investigation demonstrated an unresectable progressing metastatic cardiac paraganglioma with intracardiac extension. The patient was treated with personalized $^{177}$Lu-DOTATATE PRRT and showed complete symptomatic and partial anatomical responses, with a progression-free survival of 13 months.

**Conclusions:** PRRT with $^{177}$Lu-DOTATATE should be considered for inoperable cardiac paraganglioma. No major hemodynamic complications were experienced. Therapy resulted in safety and substantially improved quality of life.

**Keywords: PRRT, 177Lu-DOTATATE, metastatic cardiac paraganglioma, personalized activity, dosimetry**

**Abbreviations:** FDG, Fluorodeoxyglucose; DOPA, Dihydroxyphenylalanine; MIBG, Metaiodobenzylguanidine; PC, Pheochromocytoma; PGL, Paraganglioma; PRRT, Peptide receptor radionuclide therapy; SDH, Succinate dehydrogenase; SSTR, Somatostatin receptor.

## INTRODUCTION

Paragangliomas (PGLs) are rare neuroendocrine tumors arising from the chromaffin cells of the neural crest (1). Their incidence is estimated to be less than 1 per 100,000 people per year (2). PGLs can be distributed along sympathetic or parasympathetic chains from the base of the skull to the prostate, but the majority are located in the abdomen (3). Cardiac PGLs are extremely rare tumors and account for only 2% of all PGLs (4, 5) and less than 1% of cardiac primary malignancy. Clinical presentation is driven by mass effect related symptoms or hormonal related symptoms from excessive production of catecholamines. Cardiac PGLs can be found in any part of the heart; however, case series data have shown propensity for the left atrium. PGLs of the right atrium are much rarer (6). Approximately 10% of PGLs show malignancy, usually characterized by the presence of metastases (7).

The treatment of metastatic cardiac PGLs is multimodal, including a combination of surgery and/or external beam radiation therapy for the primary tumor and/or systemic treatment. Up to 90% of those tumors express somatostatin receptor (SSTR), making peptide receptor radionuclide therapy (PRRT) with lutetium-177 or yttrium-90-labeled somatostatin receptor ligands a very promising therapeutic avenue. Preliminary data suggest higher response rates and a more favorable toxicity profile for PRRT as compared with $^{131}$I-MIBG (8).

To our knowledge, this is the only case of metastatic PGL with substantial intracardiac extension treated with personalized $^{177}$Lu-DOTATATE reported in the literature. Although other cases of cardiac PGLs treated with PRRT have been reported, these included patients with little intracardiac extension or $^{90}$Y-DOTATATE based PRRT, and did not provide a detailed history, treatment details like injected activity nor follow-up (9).

## CASE PRESENTATION

A 47-year-old male, marathon runner, with no medical history developed progressive fatigue following a 65 km run. Over the following months, the patient experienced a few episodes of paroxysmal tachyarrhythmia and his exercise tolerance decreased substantially. After 6 months, he developed a grade 3 dyspnea and persistent tachycardia.

The transthoracic echocardiogram showed a right atrial mass obstructing the tricuspid valve and extending in the atrioventricular groove. Given the degree of valvular obstruction and rapidly progressive symptoms, the patient was referred for urgent open-heart surgery. Only two thirds of the tumor could be safely removed. Post-operative imaging demonstrated a 7.3-cm residual lesion attached to the posterior aspect of the right atrium occupying majority of the cavity and extending in the ventricle, causing mild obstruction of the tricuspid valve. The right systolic function was preserved. Histopathological analysis showed a PGL with a Ki-67 of 30-40%. Genetic testing identified the presence of SDHB gene mutation. Serum and urinary metanephrines and norepinephrines were elevated. Alpha and beta-blocking medication was initiated.

The $^{123}$I-MIBG scintigraphy was negative. A $^{18}$F-FDG PET/CT showed marked hypermetabolism ($SUV_{max}$ 36) and central necrosis of the right intra-auricular mass. $^{111}$In-pentetreotide SPECT/CT demonstrated a high avidity of the cardiac lesion (**Figure 1**). There was no distant metastasis. Two months later, a $^{68}$Ga-DOTATATE PET/CT showed intense uptake ($SUV_{max}$ 14) of the cardiac lesion and three new lytic bone lesions consistent with metastases. As these were also new on the accompanying low dose CT scan, their detection was not due to the $^{68}$Ga-DOTATATE PET-CT superior sensitivity.

Because of the metastatic status, heart transplantation was initially dismissed. Without treatment, the patient symptomatology quickly worsened. The patient was referred for $^{177}$Lu-DOTATATE treatment as part of our clinical trial of personalized PRRT (NCT02754297). At the time of the first treatment, the primary lesion had progressed to 8,5 x 7,2 x 8,8 cm. The mass was now transgressing the right atrial wall and encasing the right coronary artery over 11 cm. Thus, administration of the highest activity was considered critical in order to maximize the RECIST response (Response Evaluation Criteria in Solid Tumours version 1.1). As a precautionary measure

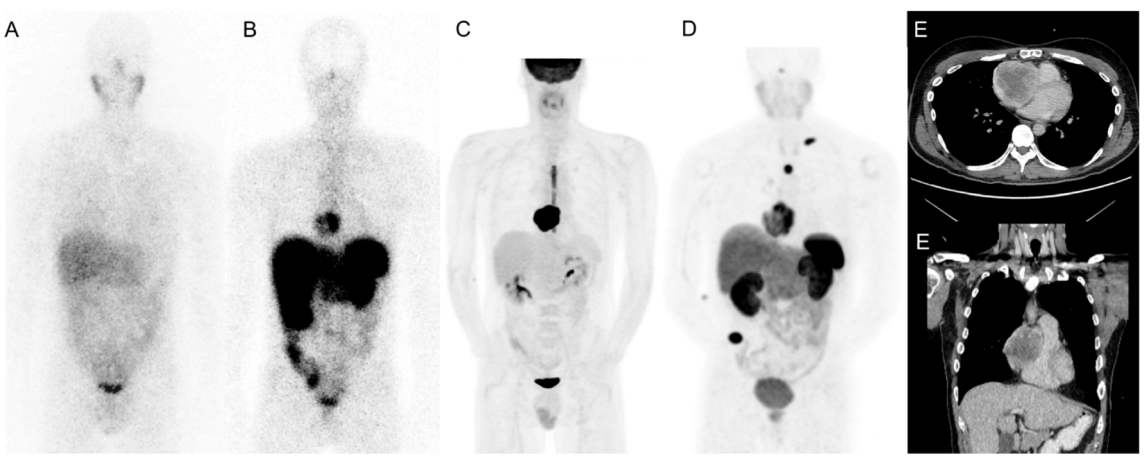


**FIGURE 1** | Staging imaging; $^{123}$I-MIBG scintigraphy **(A)**, $^{111}$In-Pentetreotide scintigraphy **(B)**, $^{18}$F-FDG PET/CT **(C)**, $^{68}$Ga-DOTATATE SPECT-CT PET/CT **(D)**, Contrast-enhanced CT **(E)**.

for the theoretical risk of hormonal release, hemodynamic compromise and bleeding, the patient was hospitalized for the first treatment. The protocol included 4 induction cycles every 8-10 weeks administered over 25 minutes in combination with an amino acid infusion. The patient was on alpha and beta blockers. He was also premedicated with dexamethasone and ondansetron for each cycle. Total administered activity was based on a cumulative kidney absorbed dose of 23 Gy and dose was distributed over 4 cycles. The first cycle administered activity was estimated with body surface area and renal function (10). Subsequent ones were estimated with SPECT/CT-based dosimetry with two time points (11). The patient received four cycles of $^{177}$Lu-DOTATATE and a cumulative activity of 40.7 GBq (1100 mCi), including 12.6 GBq (340 mCi) in the first cycle, well above the empiric activity of 7.4 GBq (200 mCi) per cycle used for GEP-NETs (29.6 GBq total). We estimated that, at 69 Gy, the maximum tumor dose was 37% higher than what would have been delivered during empiric PRRT.

Given the high risk of bleeding, pre-PRRT angioembolization of the main tumor feeder vessels had been initially planned. However, considering the tumor growth rate and the progression of dyspnea, chest pain and tachycardia, the procedure was abandoned and PRRT prioritized. The patient underwent the 4 induction cycles without substantial acute or subacute side effects. He had no hemodynamic toxicity or bleeding. Over the course of his treatments, he had episodes of grade 2 thrombocytopenia and neutropenia, all of which were self-limited (**Table 1**). At the end of the 4 cycles, fatigue, chest pain and dyspnea resolved, and episodes of tachyarrhythmia disappeared. The dosage of metoprolol and prazocin was considerably reduced, decreasing respectively from 125 mg to 50 mg and 2 mg to 1 mg TID. The chromogranin A decreased from 585 to 205 ng/mL and the serum norepinephrine decreased from 104 to 37 nmol/L after 4 cycles.

SPECT/CTs (**Figure 2**) performed following each treatment showed incremental anatomical response. $^{68}$Ga-DOTATATE PET/CT obtained at three months after the last treatment confirmed the partial response with the main cardiac lesion measuring 5.5 x 4.7 x 6.0 cm compared to 8.5 x 7.2 x 8.8 cm initially (32% reduction in largest dimension). The metabolic tumor volume, as defined by SSTR positive viable tumor identified on $^{68}$Ga-DOTATATE PET/CT decreased by 62%, from 257 to 99 cc. Unfortunately, the follow-up $^{68}$Ga-DOTATATE PET/CT (**Figure 3**) at seven months after the last induction cycle showed a significant increase of the primary tumor size (6.8 x 5.6 x 6.8 cm) equivalent to 117 cc, the development of mediastinal adenopathy and diffuse bone metastatic infiltration.

**TABLE 1** | Transient hematotoxicity from $^{177}$Lu-DOTATATE therapy.

| Treatment cycle | Platelets (x $10^9$/L) | Neutrophils (x $10^9$/L) | Hemoglobin (g/L) |
|---|---|---|---|
| **1** | 211 | 5.60 | 120 |
| **2** | 170 | 3.10 | 134 |
| **3** | 157 | 1.70 | 131 |
| **4** | 74 | 1.60 | 122 |
| **3 months after PRRT** | 92 | 1.92 | 120 |
| **6 months after PRRT** | 127 | 3.00 | 123 |

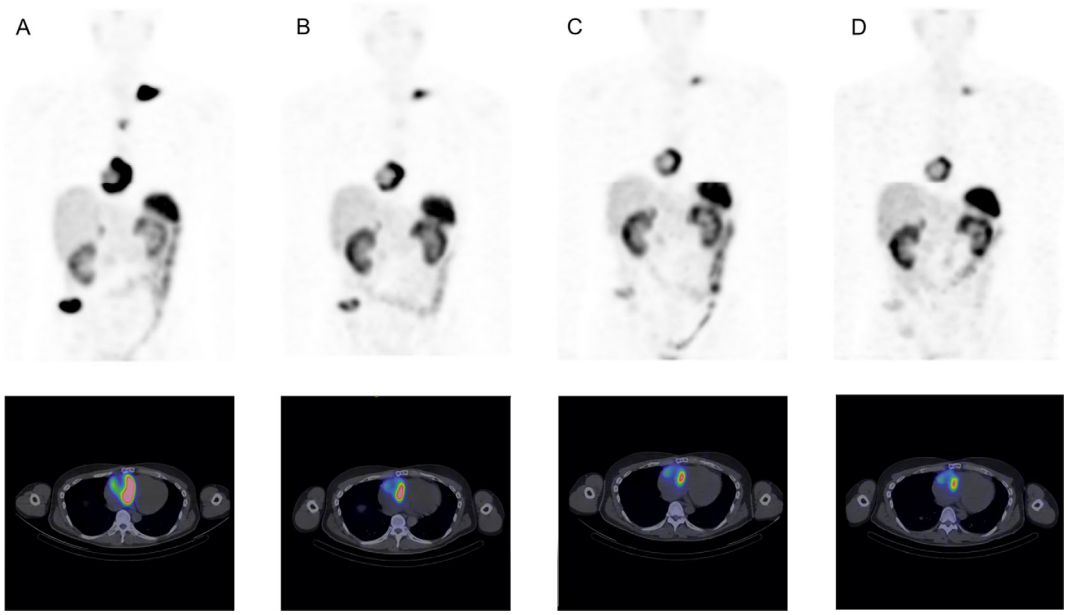


**FIGURE 2** | Post-treatment $^{117}$Lu-DOTATATE maximum intensity projection (MIP) and axial fusion images. Post-treatment images 1 **(A)**, 2 **(B)**, # 3 **(C)** and 4 **(D)**.

The progression-free survival was thus 13 months. Given the rapidity and the extent of recurrence, and subacute bone marrow toxicity, salvage PRRT treatments were not considered.

The patient was evaluated for Sunitinib. The treatment was poorly tolerated and was discontinued after 6 months despite numerous breaks and doses adjustments. Then, he received temozolomide for 6 months until disease progression. Cabozatinib was tried but was discontinued after only one cycle due to persistent thrombocytopenia and poor tolerability. As of May 2021, the patient is receiving best supporting care including external radiation therapy targeted on painful bone metastases.

## DISCUSSION

The main treatment of cardiac PGLs is surgical resection. Complete resection is complex because of their large size, relationship to vital structures, lack of capsule and clear delineation (12). In addition, they have substantial vascularization often originating from the coronary network (6) increasing risk for hemorrhage. A few cases of preoperative embolization have shown a decrease in the risk of bleeding (13). Adrenergic blockade with alpha- and beta-adrenergic antagonists is also recommended to avoid the effect of catecholamine release secondary to surgical manipulation. Partial resection is sometimes considered to reduce symptoms, prevent complications, or promote response to systemic therapy. In our case, a second surgical resection was dismissed because the tumor had become too large and invaded the right atrial wall with important right coronary encasement, making the procedure too risky.

Cytotoxic chemotherapy efficacy for metastatic paraganglioma is not well defined in the literature. A meta-analysis of 50 patients with metastatic paraganglioma treated with chemotherapy regimen comprising cyclophosphamide, vincristine and dacarbazine showed an objective response rate of 41% but only a disease control rate of 55% (combination of complete response, partial response and stable disease according to RECIST 1.1 criteria) (14).

Treatments of metastatic diseases also include β- particles emitting radiopharmaceuticals. Up to 60% of PGL and pheochromocytoma (PC) demonstrate high enough uptake to consider $^{131}$I-MIBG therapy (15). The benefits of $^{131}$I-MIBG are poorly defined in the literature due to the lack of prospective studies. The available studies are mostly retrospective and are performed on very heterogeneous populations with variable dose administration protocols. A recent meta-analysis of 243 patients receiving various regimes of $^{131}$I-MIBG showed a partial response in 27% and disease stability in 52% (16).

$^{177}$Lu-DOTATATE, another medium-energy beta-emitting radiopharmaceutical, is also part of the available therapeutic arsenal. A recent metanalysis including 201 cases of PGL or (PC) treated with $^{177}$Lu-DOTATATE or $^{90}$Y-DOTATOC showed an objective response rate of 25% and a disease control rate of 84%. Clinical and biochemical responses were observed in 61 and 64% of patients (17). The median progression-free survival was 37.1 months. Myelotoxicity (grade > 2) as neutropenia occurred in 3%, thrombocytopenia in 9%, and lymphopenia in 11% of cases. Nephrotoxicity (grade > 2), defined as a gradual and usually permanent loss of kidney function resulting in a decreased glomerular filtration rate of 59-30 mL/min, was reported in 4% of cases (17). It should be noted, however, that the patients included in this study were heterogeneous. Neither tumors grade nor the proportion of SDH mutations were provided.

More recently, a retrospective study including 22 patients with PGLs or PCs treated with 3 to 11 cycles of $^{177}$Lu-DOTATATE, with a median total administered activity of 29.6 GBq (800 mCi) showed

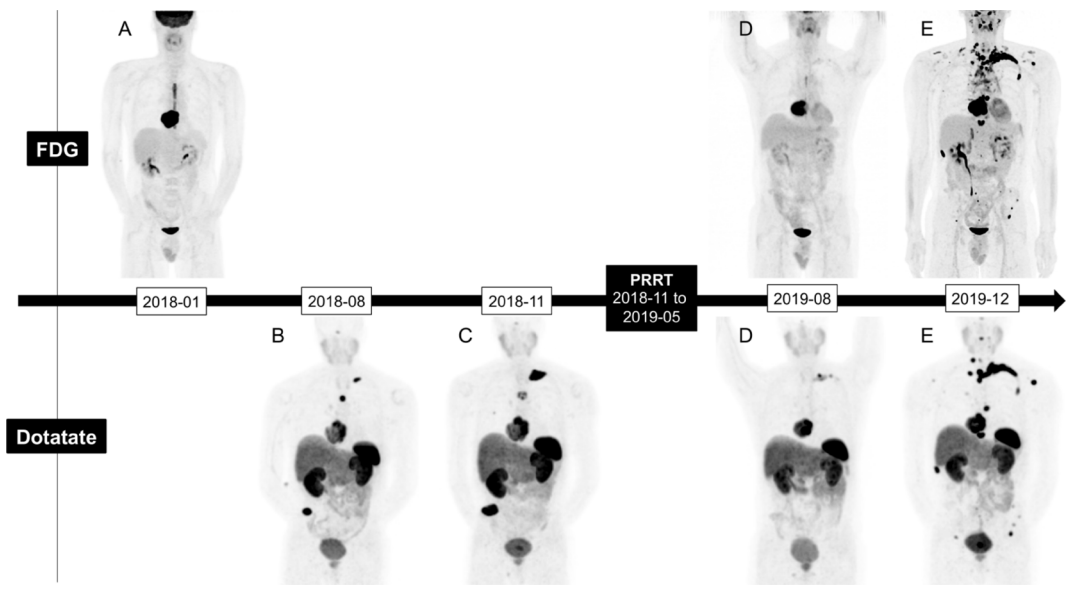


**FIGURE 3** | $^{18}$F-FDG and $^{68}$Ga-DOTATATE PET/CT maximum intensity projection (MIP) imaging evolution; Staging **(A, B)** Pre-treatment **(C)**, 3 months post-treatment **(D)**, 7 months post-Treatment **(E)**.

a progression-free survival of 21.6 months (18). A subgroup analysis showed a significant increase in progression-free survival for tumors with Ki-67 < 15% and patients treated as first-line therapy. No significant toxicity was noted.

Given the lack of controlled studies or comparative studies between $^{131}$I-MIBG and $^{177}$Lu-DOTATATE, it is not possible to determine the superiority of either agent nor can definitive conclusion be drawn from this current case report. The best approach for now is based on tumor characterisation from SSTR and MIBG imaging, opting for the treatment with the highest uptake, considering the toxicity profiles, the characteristics and comorbidities of the patient, and local availability (19). In the case of our patient, $^{177}$Lu-DOTATATE was the only remaining radiopharmaceutical therapeutic agent in view of the lack of $^{131}$I-MIBG uptake. A few cases in the literature have shown a benefit in this particular situation (20).

The administration of dexamethasone with PRRT as premedication is controversial for the treatment of PGLs and PCs. Dexamethasone has antiemetic properties, reduces the radiation-induced tumor edema and in this case, reduces the risk of vascular compromise. However, it is thought to increase the risk of a catecholaminergic crisis by increasing the production and release of catecholamines into the circulation, and by its synergistic pharmacodynamic effects, particularly at the level of the vascular endothelium (21). In view of the few cases of catecholaminergic crises reported following treatment of PRRT in patients who have received premedication with dexamethasone, some authors discourage its use (22). For our patient, it was judged that there were more benefits than risks to administer dexamethasone premedication given the location of the PGL and the risk of vascular compromise. Other than a hot flush during the first cycle relieved by temporarily stopping the $^{177}$Lu-DOTATATE infusion, there were no other reactions related to the release of catecholamines.

A recent phase II registry study from Sistani G and al (23). suggests a potential benefit of increasing the treatment intervals and the number of cycles, each with a lower activity in comparison to phase III NETTER-1 trial (24). Considering the high ki-67 of 30-40% and the rapid recurrence of our patient tumor, it is possible to believe that he could have benefited more from this longer-term, continuous PRRT approach, albeit keeping the cycle intervals short.

## CONCLUSION

Cardiac PGL is an exceedingly rare tumor and may lead to hemodynamic compromise. Surgical resection, if indicated, is technically challenging and frequently not feasible. This case demonstrates that personalized $^{177}$Lu-DOTATATE PRRT can be considered as a safe and effective palliative treatment for unresectable MIBG negative tumor which can substantially improve quality of life.

## PATIENT PERSPECTIVE

Our patient was very grateful for his treatments. Each treatment, he gained more energy and enjoyed a better quality of life with his family, including his soon to be graduated daughter. He was also grateful to his community for helping him make the trip to treatments.

## DATA AVAILABILITY STATEMENT

The original contributions presented in the study are included in the article/supplementary material. Further inquiries can be directed to the corresponding author.

## ETHICS STATEMENT

The studies involving human participants were reviewed and approved by CHU de Québec - Université Laval research committee. The patients/participants provided their written informed consent to participate in this study. Written informed consent was obtained from the individual(s) for the publication of any potentially identifiable images or data included in this article.

## AUTHOR CONTRIBUTIONS

AHD and MD are the main contributor of the manuscript. JMB, AB, FA, GA, ET, and FAB acted as a reviewer. FAB is the senior author. All authors contributed to the article and approved the submitted version.

## ACKNOWLEDGMENTS

Thank you to our patient for allowing us to share our experience with the entire scientific community.

## REFERENCES

1. Kiernan CM, Solorzano CC. Pheochromocytoma and Paraganglioma: Diagnosis, Genetics, and Treatment. *Surg Oncol Clin N Am* (2016) 25 (1):119–38. doi: 10.1016/j.soc.2015.08.006
2. DeLellis RA LR, Heitz PU, Eng C. *Pathology and Genetics of Tumours of Endocrine Organs. 3rd Ed.* Lyon: IARC Publications (2004).
3. Bravo EL. Evolving Concepts in the Pathophysiology, Diagnosis, and Treatment of Pheochromocytoma. *Endocr Rev* (1994) 15(3):356–68. doi: 10.1210/edrv-15-3-356
4. Tam DY, Cusimano RJ. Cardiac Paraganglioma. *CMAJ* (2017) 189(30):E996. doi: 10.1503/cmaj.170067
5. Polito MV, Ravera A, Silverio A, Prota C, Lambiase C, Dellegrottaglie S, et al. A Peculiar Etiology of Acute Heart Failure: Adrenergic Myocarditis. *Am J Emergency Med* (2015) 33(10):1545. doi: 10.1016/j.ajem.2015.07.025
6. Khan MF, Datta S, Chisti MM, Movahed MR. Cardiac Paraganglioma: Clinical Presentation, Diagnostic Approach and Factors Affecting Short and Long-Term Outcomes. *Int J Cardiol* (2013) 166(2):315–20. doi: 10.1016/j.ijcard.2012.04.158

7. Richard E, Goldstein JAON, Holcomb GW, Morgan WM, Neblett WW, Oates JA, et al. Clinical Experience Over 48 Years With Pheochromocytoma. *Ann Surg* (1999) 229(6):755–66. doi: 10.1097/00000658-199906000-00001
8. Mak IYF, Hayes AR, Khoo B, Grossman A. Peptide Receptor Radionuclide Therapy as a Novel Treatment for Metastatic and Invasive Phaeochromocytoma and Paraganglioma. *Neuroendocrinology* (2019) 109 (4):287–98. doi: 10.1159/000499497
9. Ultan Healy MT, Grossman A, Weaver A, Jafar-Mohammadi B. Utility of PRRT Therapy in Invasive Intra-Cardiac Paraganglioma. *Endocrine Abstracts* (2018) 60:21. doi: 10.1530/endoabs.60.P21
10. Del Prete M, Buteau FA, Beauregard JM. Personalized (177)Lu-Octreotate Peptide Receptor Radionuclide Therapy of Neuroendocrine Tumours: A Simulation Study. *Eur J Nucl Med Mol Imaging* (2017) 44(9):1490–500. doi: 10.1007/s00259-017-3688-2
11. Del Prete M, Arsenault F, Saighi N, Zhao W, Buteau FA, Celler A, et al. Accuracy and Reproducibility of Simplified QSPECT Dosimetry for Personalized (177)Lu-Octreotate PRRT. *EJNMMI Phys* (2018) 5(1):25. doi: 10.1186/s40658-018-0224-9
12. Ramlawi B, David EA, Kim MP, Garcia-Morales LJ, Blackmon SH, Rice DC, et al. Contemporary Surgical Management of Cardiac Paragangliomas. *Ann Thorac Surg* (2012) 93(6):1972–6. doi: 10.1016/j.athoracsur.2012.02.040
13. Jun Matsumoto JN, Takeuchi E, Fukami T, Nawata K, Takamoto S-i. Successful Perioperative Management of a Middle Mediastinal Paraganglioma. *J Thorac Cardiovasc Surg* (2006) 132(3):705–6. doi: 10.1016/j.jtcvs.2006.02.061
14. Niemeijer ND, Alblas G, van Hulsteijn LT, Dekkers OM, Corssmit EP. Chemotherapy With Cyclophosphamide, Vincristine and Dacarbazine for Malignant Paraganglioma and Pheochromocytoma: Systematic Review and Meta-Analysis. *Clin Endocrinol (Oxf)* (2014) 81(5):642–51. doi: 10.1111/cen.12542
15. Pryma DA, Chin BB, Noto RB, Dillon JS, Perkins S, Solnes L, et al. Efficacy and Safety of High-Specific-Activity (131)I-MIBG Therapy in Patients With Advanced Pheochromocytoma or Paraganglioma. *J Nucl Med* (2019) 60 (5):623–30. doi: 10.2967/jnumed.118.217463
16. van Hulsteijn LT, Niemeijer ND, Dekkers OM, Corssmit EP. (131)I-MIBG Therapy for Malignant Paraganglioma and Phaeochromocytoma: Systematic Review and Meta-Analysis. *Clin Endocrinol (Oxf)* (2014) 80(4):487–501. doi: 10.1111/cen.12341
17. Swayamjeet Satapathy BRM. Anil Bhansali Peptide Receptor Radionuclide Therapy in the Management of Advanced Pheochromocytoma and Paraganglioma: A Systematic Review and Meta-Analysis. *Clin Endocrinol (Oxf)* (2019) 91(6):718–27. doi: 10.1111/cen.14106
18. Vyakaranam AR, Crona J, Norlen O, Granberg D, Garske-Roman U, Sandstrom M, et al. Favorable Outcome in Patients With Pheochromocytoma and Paraganglioma Treated With (177)Lu-DOTATATE. *Cancers (Basel)* (2019) 11(7):909. doi: 10.3390/cancers11070909
19. Jha A, Taieb D, Carrasquillo JA, Pryma DA, Patel M, Millo C, et al. High-Specific-Activity-(131)I-MIBG Versus (177)Lu-DOTATATE Targeted Radionuclide Therapy for Metastatic Pheochromocytoma and Paraganglioma. *Clin Cancer Res* (2021) 27(11):2989–95. doi: 10.1158/1078-0432.CCR-20-3703
20. Parghane RV. TSBS. 131i-MIBG Negative Progressive Symptomatic Metastatic Paraganglioma: Response and Outcome Witj 177Lu-DOTATATE Peptide Receptor Radionuclide Therapy. *Ann Nucl Med* (2021) 35:92–101. doi: 10.1007/s12149-020-01541-z
21. Rosas AL, Kasperlik-Zaluska AA, Papierska L, Bass BL, Pacak K, Eisenhofer G. Pheochromocytoma Crisis Induced by Glucocorticoids: A Report of Four Cases and Review of the Literature. *Eur J Endocrinol* (2008) 158(3):423–9. doi: 10.1530/EJE-07-0778
22. Del Olmo-Garcia MI, Muros MA, Lopez-de-la-Torre M, Agudelo M, Bello P, Soriano JM, et al. Prevention and Management of Hormonal Crisis During Theragnosis With LU-DOTA-TATE in Neuroendocrine Tumors. A Systematic Review and Approach Proposal. *J Clin Med* (2020) 9(7):2203. doi: 10.3390/jcm9072203
23. Sistani G, Sutherland DEK, Mujoomdar A, Wiseman DP, Khatami A, Tsvetkova E, et al. Efficacy of 177Lu-Dotatate Induction and Maintenance Therapy of Various Types of Neuroendocrine Tumors: A Phase II Registry Study. *Curr Oncol* (2020) 28(1):115–27. doi: 10.3390/curroncol28010015
24. Strosberg J, El-Haddad G, Wolin E, Hendifar A, Yao J, Chasen B, et al. Phase 3 Trial of (177)Lu-Dotatate for Midgut Neuroendocrine Tumors. *N Engl J Med* (2017) 376(2):125–35. doi: 10.1056/NEJMoa1607427


**Conflict of Interest:** The authors declare that the research was conducted in the absence of any commercial or financial relationships that could be construed as a potential conflict of interest.

frontiers in Endocrinology

CASE REPORT
published: 04 August 2021
doi: 10.3389/fendo.2021.724766

# Parathyroid Adenoma With Respiratory-Like Epithelium: Case Report of a Potential Mimic With Unknown Etiology

*C. Christofer Juhlin*[1,2*] *and Jan Zedenius*[3,4]

[1] Department of Oncology-Pathology, Karolinska Institutet, Stockholm, Sweden, [2] Department of Pathology and Cytology, Karolinska University Hospital, Stockholm, Sweden, [3] Department of Molecular Medicine and Surgery, Karolinska Institutet, Stockholm, Sweden, [4] Department of Breast, Endocrine Tumors and Sarcoma, Karolinska University Hospital, Stockholm, Sweden

Parathyroid adenoma is a tumor composed of increased parenchymal tissue, often built-up by chief cells, transitional cells or oncocytic cells arranged in acinar or solid formations. Occasionally, rare histological patterns are reported, including cystic or trabecular arrangements. We present a 47 year-old male patient with primary hyperparathyroidism who underwent focused parathyroidectomy for a right inferior adenoma. Surgery was uneventful, but histologically, normal parathyroid tissue adjacent to a tumorous structure displaying a cystic growth pattern was detected. The cells lining the cyst walls appeared cylindrical and pseudo-stratified, vaguely reminiscent of a respiratory type of epithelium usually associated to branchial cleft cysts or thyroglossal cyst remnants, albeit with a tumorous appearance. The respiratory-like epithelium stained positive for parathyroid markers PTH and GATA3, thereby confirming them as parathyroid-derived. The patient was cured from surgery as he displayed normal calcium and PTH levels postoperatively, and is currently alive and well without signs of relapse 4 years after surgery. This is to our knowledge the first report of a parathyroid tumor displaying a respiratory-like epithelium. Experimentally, canine parathyroid glands can develop ciliated respiratory epithelium in response to inhalation of ozone. Our patient is a construction worker with a hypothetically increased risk of continuous ozone exposure. Although this association remains purely speculative, future investigations of this tumor phenotype could perhaps yield novel insights regarding the frequency of this histological variant, potential clinical associations, and clues regarding influencing factors.

**Keywords: respiratory, epithelium, case report, parathyroid, adenoma**

OPEN ACCESS

***Edited by:***
*Barbara Altieri, University Hospital of Wuerzburg, Germany*

***Reviewed by:***
*Liborio Torregrossa, University of Pisa, Italy*
*Alessandro Galani, Bolognini Hospital, Italy*

****Correspondence:***
*C. Christofer Juhlin*
*christofer.juhlin@ki.se*

***Specialty section:***
*This article was submitted to Cancer Endocrinology, a section of the journal Frontiers in Endocrinology*

***Received:*** *14 June 2021*
***Accepted:*** *22 July 2021*
***Published:*** *04 August 2021*

***Citation:***
*Juhlin CC and Zedenius J (2021) Parathyroid Adenoma With Respiratory-Like Epithelium: Case Report of a Potential Mimic With Unknown Etiology. Front. Endocrinol. 12:724766. doi: 10.3389/fendo.2021.724766*

## INTRODUCTION

Parathyroid adenomas are benign, parenchymal tumors that often secrete parathyroid hormone (PTH), causing hypercalcemia (1). The most common presentation is uniglandular disease in a patient with primary hyperparathyroidism. The acinar component is usually composed of chief cells, transitional cells or oncocytic cells, although rare histological variants such as cystic adenomas, water-clear cell adenomas

and lipoadenomas have been described (2–6). In some instances, parathyroid tissue may present in ectopic locations as a consequence of aberrant embryological migration during the fetal stage, and in some instances also present as a component of a branchial cleft anomaly (7).

The parathyroid chief cells, the main cell type of most parathyroid adenomas, are usually polygonal with a neutral to slight eosinophilic cytoplasm, and the nuclei are often round with little atypia (2). In normal parathyroid tissue, the cells are usually arranged in delicate palisading cords, whereas the growth pattern in adenomas usually tend to be acinar or diffuse. Even though the chief cell nuclei often are enlarged in adenomas compared to normal parathyroid tissue, the cells retain their polygonal shape and do not exhibit metaplastic features (2). In this case report, we describe a parathyroid adenoma with a cystic growth, lined by a cell component highly reminiscent of respiratory type epithelium, and describe the histological, expressional and clinical features of this exceedingly unusual manifestation.

## CASE DESCRIPTION

The patient was a 47 year-old male of Swedish ethnicity without previous medical history. He had no family history suggestive of parathyroid disorders. He worked as a construction worker, did not smoke and only reported moderate use of alcohol. In 2017, he developed fatigue and was subsequently diagnosed with hypercalcemia with an ionized calcium of 1.52 mmol/L (reference 1.15-1.33). His plasma PTH levels were also elevated at 18 pmol/L (reference: 1.6-6.0). The patient was referred to our department for a surgical consult. Clinical examination showed no palpable neck mass. Neck ultrasound identified a 10 mm enlarged right inferior parathyroid gland. No further localization study was performed. The patient was planned for a focused parathyroidectomy, which was performed a month later. The excised gland weighed 700 mg and measured 19 mm. Upon macroscopic examination, the tumor exhibited a cystic appearance. Histologically, the lesion demonstrated a multilobar, cord-like cystic growth pattern, with a single-lined, pseudostratified epithelium built-up by cylindrical cells with basal-positioned nuclei and vacuolated cytoplasm (**Figure 1**). Focally, structures reminiscent of cilia were noted. Tumor nuclei displayed a compact chromatin, and atypia was generally absent. Small foci of infiltrating lymphocytes were also detected, as was an adjacent rim of normal parathyroid tissue. There was no thymic or thyroid tissue present.

Immunohistochemistry was performed, and the cylindrical cells displayed diffuse positivity for the AE1/AE1 pan-keratin cocktail, PTH, GATA binding protein 3 (GATA3) and polyclonal Paired box 8 (PAX8), thereby verifying them as parathyroid-derived (**Figure 1**). Stains for Thyroid transcription factor 1 (TTF1) and Napsin A were negative. To rule out malignant potential, parafibromin and Adenomatous polyposis coli (APC) stains were ordered, and both showed widespread positivity. The Ki-67 proliferation index was determined to 2% by manual counting of 500 cells using an ocular grid. A periodic acid-Shiff (PAS) staining displayed magenta-colored intracytoplasmatic droplets that were absent on a subsequent PAS diastase stain, indicating that these droplets were glycogen-derived. The final diagnosis was a parathyroid adenoma.

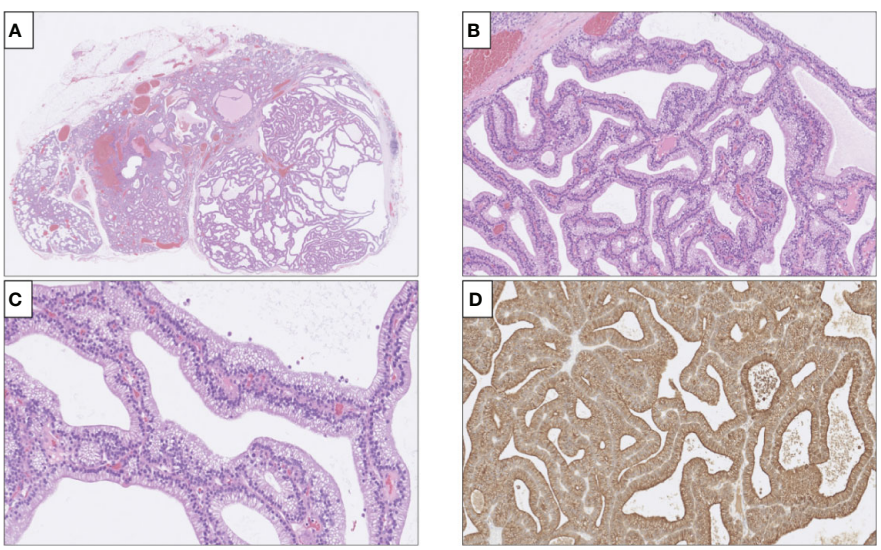


**FIGURE 1** | Histological and immunohistochemical attributes of the parathyroid adenoma with respiratory-like epithelium. **(A)** Hematoxylin-eosin (H&E) stain of the excised lesion depicting a cystic appearance (right), with normal rim of parathyroid tissue to the left. Magnification x20. **(B, C)** Cells were pseudo-stratified and cylindrical with palisading nuclei and, appearing focally, processes reminiscent of apical cilia, magnification x200 and x400 respectively. **(D)** Diffuse and strong PTH immunoreactivity was noted.

Immediately postoperatively, the patient's PTH levels decreased, indicating cure (1.3 pmol/L), and he was discharged the same day. Subsequent ionized calcium measurements 3 weeks later showed normalized levels at 1.25 mmol/L, and values remains normal at follow-up, although PTH levels one year postoperatively was just above normal range, probably secondary to a synchronous vitamin D deficiency at the time. The patient is well and without any related symptoms as of May 2021.

## DISCUSSION

We report a parathyroid adenoma with a highly unusual growth pattern, characterized by cysts lined by a respiratory-like epithelium. The parathyroid origin was proven by immunohistochemistry, and the functionality of the lesion was also established as surgical removal cured the patient from hypercalcemia. The finding is of potential value for practicing endocrine pathologists as a novel differential diagnosis when investigating cystic lesions lined by a ciliated, cylindric epithelium in the neck.

Usually, the finding of cystic structures lined with cylindrical epithelium in the neck could lead the pathologist to suspect a thyroglossal duct cyst (8). However, the index lesion was tumorous in nature, was not located along the midline, lacked association to the hyoid bone and there was no thyroid tissue within the excised specimen. Moreover, rare cases of third branchial cleft cyst anomalies can present with parathyroid tissue, but the lesion presented herein did not contain thymic tissue, and the respiratory epithelium lining branchial cleft cysts are not immunoreactive to PTH or GATA3 (9). Therefore, the lesion was indeed a parathyroid adenoma displaying a morphology reminiscent of airway epithelium. As no fresh-frozen tissue was kept from the tumor, we could not perform electron microscopy to investigate the suspected cilia component more closely, but previous ultrastructural studies in parathyroid tumors may support the notion that subsets of cases may exhibit ciliated structures (10).

When searching online repositories for similar findings, no credible descriptions of this phenomenon was identified, and the incidence of this type of parathyroid tumor is therefore assumed to be exceedingly low. On an experimental basis, ozone exposure in dogs has been found to prompt the development of ciliated cystic structures within the parathyroid glands (10, 11). Even though the index patient is a construction worker (a profession associated to ozone exposure), we can neither rule out nor confirm that exposure to this substance in any way influenced the development of a parathyroid tumor with respiratory-like epithelium (12). Therefore, it is currently not known if our observations indeed indicate a metaplastic transformation involving parathyroid cells. From a prognostic perspective, the patient did not display persistent or recurrent hypercalcemia, neither were there any signs of atypia in the excised tumor. Retained parafibromin and APC expression in any parathyroid tumor also argues against malignant potential.

To conclude, we describe a parathyroid adenoma with a previously unreported histological growth pattern. Future retrospective analyses of large tumor series can possibly uncover similar cases in which the cellular features were initially overlooked.

## DATA AVAILABILITY STATEMENT

The original contributions presented in the study are included in the article/supplementary material. Further inquiries can be directed to the corresponding author.

## ETHICS STATEMENT

Ethics approval no. 01-133 was obtained by KI Forskningsetikkommitté Nord. The patients/participants provided their written informed consent to participate in this study. Written informed consent was obtained from the individual(s) for the publication of any potentially identifiable images or data included in this article.

## AUTHOR CONTRIBUTIONS

CCJ conceived the idea, reviewed the histology and drafted the manuscript. JZ reviewed the clinical history and edited the manuscript. All authors contributed to the article and approved the submitted version.

## FUNDING

CCJ is a Junior Clinical Investigator sponsored by the Swedish Cancer Society.

## REFERENCES

1. Juhlin CC, Erickson LA. Genomics and Epigenomics in Parathyroid Neoplasia: From Bench to Surgical Pathology Practice. *Endocr Pathol* (2021) 32:17–34. doi: 10.1007/s12022-020-09656-9
2. Weltgesundheitsorganisation. International Agency for Research on Cancer. In: RV Lloyd, RY Osamura, G Klöppel, J Rosai, editors. *WHO Classification of Tumours of Endocrine Organs, 4th*. Lyon: International Agency for Research on Cancer (2017).
3. Juhlin CC, Nilsson I-L, Falhammar H, Zedenius J. Institutional Characterisation of Water Clear Cell Parathyroid Adenoma: A Rare Entity Often Unrecognised by TC-99m-Sestamibi Scintigraphy. *Pathology* (2021) S0031-3025(21)00107-0. doi: 10.1016/j.pathol.2021.02.011 Online ahead of print.
4. Hyrcza MD, Sargın P, Mete O. Parathyroid Lipoadenoma: A Clinicopathological Diagnosis and Possible Trap for the Unaware Pathologist. *Endocr Pathol* (2016) 27:34–41. doi: 10.1007/s12022-015-9404-5
5. Juhlin CC, Falhammar H, Zedenius J, Nilsson I-L, Höög A. Lipoadenoma of the Parathyroid Gland: Characterization of an Institutional Series Spanning 28 Years. *Endocr Pathol* (2020) 31:156–65. doi: 10.1007/s12022-020-09616-3
6. Juhlin C, Larsson C, Yakoleva T, Leibiger I, Leibiger B, Alimov A, et al. Loss of Parafibromin Expression in a Subset of Parathyroid Adenomas. *Endocr Relat Cancer* (2006) 13:509–23. doi: 10.1677/erc.1.01058
7. Noussios G, Anagnostis P, Natsis K. Ectopic Parathyroid Glands and Their Anatomical, Clinical and Surgical Implications. *Exp Clin Endocrinol Diabetes* (2012) 120:604–10. doi: 10.1055/s-0032-1327628

8. Thompson LDR, Herrera HB. Lau SK. A Clinicopathologic Series of 685 Thyroglossal Duct Remnant Cysts. *Head Neck Pathol* (2016) 10:465–74. doi: 10.1007/s12105-016-0724-7
9. Salido S, Gómez-Ramírez J, Bravo JM, Martín-Pérez E, Fernández-Díaz G, Múñoz de Nova JL, et al. Parathyroid Adenoma in Third Pharyngeal Pouch Cyst as a Rare Case of Primary Hyperparathyroidism. *Ann R Coll Surg Engl* (2014) 96:e8–10. doi: 10.1308/003588414X13946184900804
10. Pemsingh RS, Atwal OS, MacPherson RB. Atypical Cilia in Ciliated Cysts of the Parathyroid Glands of Dogs Exposed to Ozone. *Exp Pathol* (1985) 28:105–10. doi: 10.1016/s0232-1513(85)80021-9
11. Pemsingh RS, Atwal OS. Occurrence of APUD-Type Cells in the Ciliated Cyst of the Parathyroid Gland of Ozone-Exposed Dogs. *Acta Anat (Basel)* (1983) 116:97–105. doi: 10.1159/000145731
12. Hall RM, Page E. Ozone Exposure at a Construction Site. *Appl Occup Environ Hyg* (1999) 14:203–7. doi: 10.1080/104732299302945

**Conflict of Interest:** The authors declare that the research was conducted in the absence of any commercial or financial relationships that could be construed as a potential conflict of interest.

frontiers in Endocrinology

CASE REPORT
published: 20 August 2021
doi: 10.3389/fendo.2021.731579

# Case Report: Consecutive Adrenal Cushing's Syndrome and Cushing's Disease in a Patient With Somatic *CTNNB1*, *USP8*, and *NR3C1* Mutations

*Mario Detomas[1]*, Barbara Altieri[1], Wiebke Schlötelburg[2,3], Silke Appenzeller[4], Sven Schlaffer[5], Roland Coras[6], Andreas Schirbel[3], Vanessa Wild[7], Matthias Kroiss[1,8], Silviu Sbiera[1], Martin Fassnacht[1] and Timo Deutschbein[1,9]*

*[1] Department of Internal Medicine I, Division of Endocrinology and Diabetes, University Hospital Würzburg, University of Würzburg, Würzburg, Germany, [2] Department of Diagnostic and Interventional Radiology, University Hospital Würzburg, University of Würzburg, Würzburg, Germany, [3] Department of Nuclear Medicine, University Hospital Würzburg, University of Würzburg, Würzburg, Germany, [4] Core Unit Bioinformatics, Comprehensive Cancer Center Mainfranken, University Hospital of Würzburg, University of Würzburg, Würzburg, Germany, [5] Department of Neurosurgery, University Hospital Erlangen, Erlangen, Germany, [6] Department of Neuropathology, University Hospital Erlangen, Erlangen, Germany, [7] Institute of Pathology, University of Würzburg, Würzburg, Germany, [8] Department of Internal Medicine IV, University Hospital Munich, Ludwig-Maximilians-Universität München, Munich, Germany, [9] Medicover Oldenburg MVZ, Oldenburg, Germany*

OPEN ACCESS

**Edited by:**
*Dragana Nikitovic, University of Crete, Greece*

**Reviewed by:**
*Marcio Machado, University of São Paulo, Brazil*
*Anna Aulinas, Hospital de la Santa Creu i Sant Pau, Spain*

***Correspondence:**
*Mario Detomas*
*detomas_m@ukw.de*

**Specialty section:**
*This article was submitted to Cancer Endocrinology, a section of the journal Frontiers in Endocrinology*

**Received:** *27 June 2021*
**Accepted:** *29 July 2021*
**Published:** *20 August 2021*

**Citation:**
*Detomas M, Altieri B, Schlötelburg W, Appenzeller S, Schlaffer S, Coras R, Schirbel A, Wild V, Kroiss M, Sbiera S, Fassnacht M and Deutschbein T (2021) Case Report: Consecutive Adrenal Cushing's Syndrome and Cushing's Disease in a Patient With Somatic CTNNB1, USP8, and NR3C1 Mutations. Front. Endocrinol. 12:731579. doi: 10.3389/fendo.2021.731579*

The occurrence of different subtypes of endogenous Cushing's syndrome (CS) in single individuals is extremely rare. We here present the case of a female patient who was successfully cured from adrenal CS 4 years before being diagnosed with Cushing's disease (CD). The patient was diagnosed at the age of 50 with ACTH-independent CS and a left-sided adrenal adenoma, in January 2015. After adrenalectomy and histopathological confirmation of a cortisol-producing adrenocortical adenoma, biochemical hypercortisolism and clinical symptoms significantly improved. However, starting from 2018, the patient again developed signs and symptoms of recurrent CS. Subsequent biochemical and radiological workup suggested the presence of ACTH-dependent CS along with a pituitary microadenoma. The patient underwent successful transsphenoidal adenomectomy, and both postoperative adrenal insufficiency and histopathological workup confirmed the diagnosis of CD. Exome sequencing excluded a causative germline mutation but showed somatic mutations of the β-catenin protein gene (*CTNNB1*) in the adrenal adenoma, and of both the ubiquitin specific peptidase 8 (*USP8*) and the glucocorticoid receptor (*NR3C1*) genes in the pituitary adenoma. In conclusion, our case illustrates that both ACTH-independent and ACTH-dependent CS may develop in a single individual even without evidence for a common genetic background.

**Keywords: Cushing's syndrome, Cushing's disease, hypercortisolism, glucocorticoid excess, USP8, CTNNB1, NR3C1**

## INTRODUCTION

Endogenous Cushing´s syndrome (CS) is a rare disorder with an incidence of 0.2–5.0 per million people per year (1, 2). The predominant subtype (accounting for about 80%) is adrenocorticotropic hormone (ACTH)-dependent CS. The vast majority of this subtype is due to an ACTH-secreting pituitary adenoma [so called Cushing´s disease (CD)], whereas ectopic ACTH-secretion (e.g. through pulmonary carcinoids) is much less common. In contrast, ACTH-independent CS can mainly be attributed to cortisol-producing adrenal adenomas. Adrenocortical carcinomas, uni-/bilateral adrenal hyperplasia, and primary pigmented nodular adrenocortical disease (PPNAD) may account for some of these cases as well (3, 4).

Coexistence of different subtypes of endogenous CS in single individuals is even rarer but has been described in few reports. These cases were usually observed in the context of prolonged ACTH stimulation on the adrenal glands, resulting in micronodular or macronodular hyperplasia (5–9). A sequence of CD and PPNAD was also described in presence of Carney complex, a genetic syndrome characterized by the loss of function of the gene encoding for the regulatory subunit type 1α of protein kinase A (*PRKAR1A*) (10). Moreover, another group reported the case of a patient with Cushing's disease followed by ectopic Cushing's syndrome more than 30 years later (8). To our knowledge, however, we here describe the first case report on a single patient with a cortisol-producing adrenocortical adenoma and subsequent CD.

## CASE DESCRIPTION

In March 2014, a 49-year old female underwent an abdominal magnetic resonance imaging (MRI) because of recurrent abdominal pain and irregular hypermenorrhea. This revealed the presence of a left-sided adrenal lesion of 4.5 x 4.2 cm (**Figure 1A**). Due to the

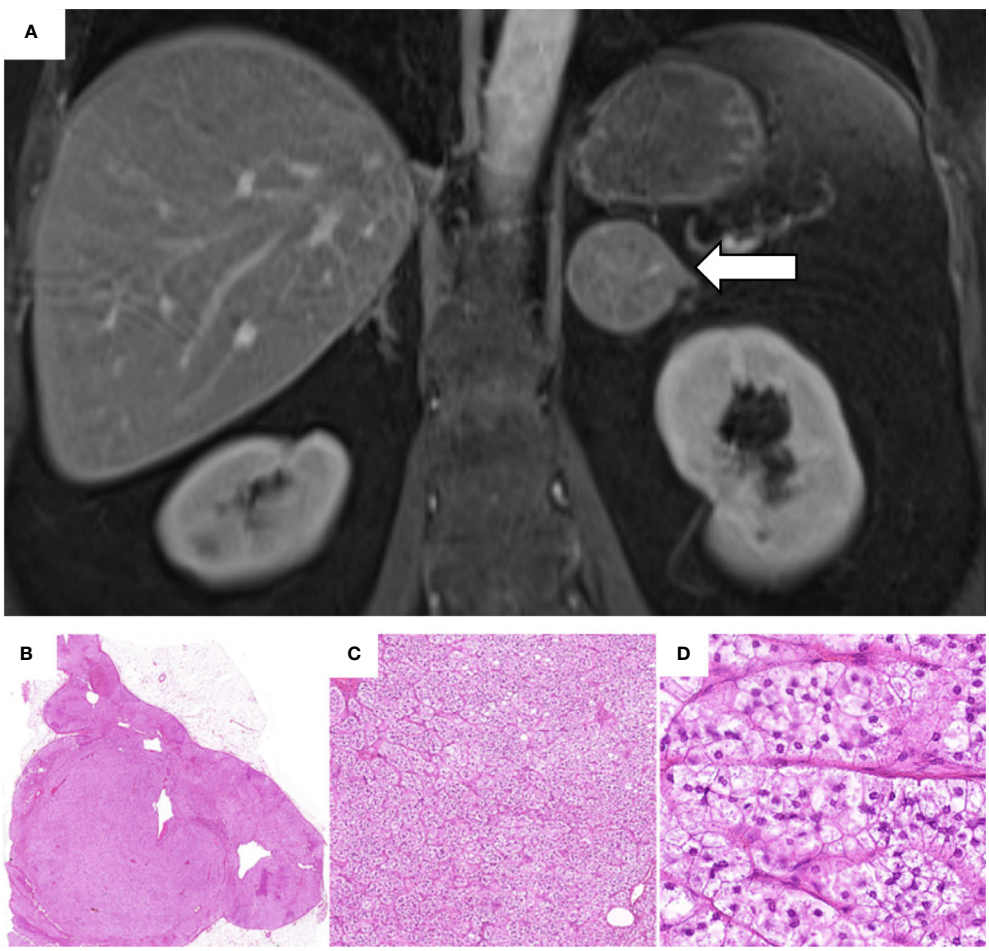


**FIGURE 1** | Abdominal magnetic resonance imaging performed in March 2014 and histological analysis of the adrenal adenoma. **(A)** Contrast-enhanced coronal T1-weighted MRI showing a 4.5 x 4.2 cm adenoma of the left adrenal gland (white arrow). **(B–D)** Histological investigation of the adrenal adenoma with hematoxylin and eosin staining: **(B)** Solitary, well circumscribed intra-adrenal mass confined to the gland; **(C)** Nested/fasciculated growth pattern of uniform tumor cells; **(D)** Tumor cells showing lipid-rich foamy cytoplasm with small uniform nuclei. Absent mitosis or necrosis. (H.E. 6.5x, 10.0x, 40.0x).

persistence of menstrual cycle irregularities and the development of hirsutism, the general practitioner finally suspected a cortisol-producing adrenal tumor and the patient was, therefore, referred to our outpatient clinic.

At the time of her first examination at our outpatient clinic (January 2015), the patient reported muscle-weakness, asthenia, and hirsutism. She suffered from arterial hypertension and was treated with a triple anti-hypertensive therapy. Other comorbidities and medical therapies were not reported. Both parents had arterial hypertension, and the familial history was positive for breast cancer (mother). The physical examination revealed classical signs of CS such as centripetal obesity (body mass index: 45.2 kg/m$^2$), striae rubrae, hirsuitism, facial plethora, skin atrophy, and multiple hematomas. Her glycated hemoglobin was slightly elevated (HbA1c 6.4%). The routine laboratory (including electrolytes) was unremarkable. The endocrine workup was conducted according to published guidelines (12), involved commercially available analytical procedures (i.e., the Immulite 2000 Xpi from Siemens for the analysis of ACTH and serum cortisol, a manual luminescence immunoassay from IBL for the analysis of salivary cortisol, and a manual radioimmunoassay from Immuntech for the analysis of urinary free cortisol) and indicated presence of ACTH-independent CS (as shown in **Table 1**). Of note, basal ACTH was repeatedly <10 ng/l (reference range 0-46 ng/l). Furthermore, there was no evidence for primary hyperaldosteronism or a catecholamine excess.

**TABLE 1** | Endocrine evaluation in our outpatient clinic (January 2015) and at our endocrine ward (April 2019).

| Initial evaluation (January 2015) - diagnosis of ACTH-independent Cushing's syndrome | Result | Reference range |
|---|---|---|
| ACTH (ng/l) | 6.3 | 0 - 46 |
| Basal serum cortisol (µg/dl) | **27.6** | 5-25 |
| Serum cortisol after 1 mg dexamethasone (µg/dl) | **16.3** | 0 - 1.8 |
| Late-night salivary cortisol (µg/dl) | **0.34** | 0 - 0.15 |
| 24-hour urinary free cortisol (µg/24h) | **182** | 8 - 70 |
| Aldosterone (ng/l) | 36 | 38 - 313 |
| Plasma renin concentration (ng/l) | 14 | 3 - 57 |
| Plasma metanephrine (ng/l) | 57.7 | 0 - 90 |
| Plasma normetanephrine (ng/l) | 59.3 | 0 - 200 |
| Total testosterone (µg/l) | 0.2 | 0 - 0.73 |
| DHEA-S (µg/dl) | 55 | 26 - 200 |
| Androstendione (µg/l) | 3.03 | 0.47 -2.68 |
| 17α-hydroxyprogesterone (µg/l) | 1.5 | 0.3 - 3.6 |
| **Follow-up evaluation (April 2019) – diagnosis of ACTH-dependent Cushing's syndrome** | **Result** | **Reference range** |
| ACTH (ng/l) | **69.3** | 0 - 46 |
| Basal serum cortisol (µg/dl) | 23.5 | 5-25 |
| Serum cortisol after 1 mg dexamethasone (µg/dl) | **28.0** | 0 - 1.8 |
| Late-night salivary cortisol (µg/dl) | **0.21** | 0 - 0.15 |
| 24-hour urinary free cortisol (µg/24h) | **206.7** | 8 - 70 |

*The biochemical results of January 2015 (with pathological results reported in bold letters) were suggestive for ACTH-independent Cushing's syndrome and excluded several potential differential diagnoses (e.g. primary hyperaldosteronism, and catecholamine excess).*
*The pathological biochemical results of April 2019 were instead suggestive for ACTH-dependent Cushing's syndrome.*
*ACTH, adrenocorticotropic hormone; DHEA-S, dehydroepiandrosterone-sulfate.*

In February 2015, the patient underwent successful laparoscopic left-sided adrenalectomy. Postoperatively, morning serum cortisol was < 5 µg/dl and glucocorticoid replacement therapy was initiated. The histopathological analysis revealed a well-circumscribed tumor, with foamy lipid-rich cytoplasm, a Ki-67 <1%, and no signs of malignancy (Weiss score: 1) (13). The analysis was compatible with a cortisol-producing adrenocortical adenoma. Slides from the histological investigations are exemplarily shown in **Figures 1B–D**.

Between February and May 2015, anti-hypertensive therapy could already be reduced to only one drug, and subsequent blood pressure levels were normal. Hydrocortisone was stopped in May 2015, taking into account a normalized adrenal function measured by an ACTH stimulation test and no clinical evidence for an ongoing glucocorticoid withdrawal syndrome.

In August 2015, the patient reported a weight loss of 5 kg and an improvement of her general condition. The 1 mg dexamethasone suppression test (DST) and the late-night salivary cortisol (LNSC) results were remarkably lower than preoperatively, but not normalized (**Figure 2**). In contrast, 24-hour urinary free cortisol (UFC) was within the reference range and the ACTH was no longer suppressed. The patient was subsequently followed up for three years on an annual basis. The course of the four most relevant endocrine parameters (i.e., ACTH, 1 mg DST, LNSC, and 24-hour UFC) during our observation is provided in **Figure 2**. Two years after adrenalectomy, the antihypertensive therapy was discontinued and the patient did not take any medication at all. Additionally, the HbA1c was clearly improved (the lowest level was 5.5% in April 2017) compared to preoperative levels.

In April 2018, however, the patient reported symptoms suggestive for recurrent CS (i.e., proximal myopathy, moderate fatigue, and weight gain of 5 kg in 6 months) for the first time. Her general practitioner had already restarted anti-hypertensive medication because of uncontrolled blood pressure. Biochemical workup revealed recurrent glucocorticoid excess, surprisingly without suppressed ACTH (**Figure 2**). Due to the patient's medical history, an abdominal contrast enhanced computer tomography (CT) scan was performed. This showed an inhomogeneous, hypodense, non-enhancing soft tissue mass of 2.3 x 1.6 cm in position of the removed left adrenal gland. For further investigations, we performed a [$^{123}$I](R)-1-[1-(4-iodophenyl)ethyl]-1H-imidazole-5-carboxylic acid azetidinylamide imaging (($^{123}$I)-MAZA) whole body scintigraphy and single-photon emission computed tomography (SPECT)/CT. ($^{123}$I)-MAZA is a tracer that binds specifically to the two adrenocortical enzymes 11ß-hydroxylase (CYP11B1) and aldosterone synthase (CYP11B2). However, these imaging methods did not show the supposed adrenal remnant at the level of the former left-sided cortisol-producing adrenal adenoma (**Supplementary Figure 1**). Furthermore, basal ACTH was above 50 ng/l. Further clinical and biochemical workup was delayed because the patient had the impression that her general condition was not severely affected.

In January 2019, she described that fatigue and myopathy were now more intense and that arterial hypertension was very difficult to control. At that time, the biochemical tests were once again clearly pathological (**Figure 2**). Accordingly, we suggested

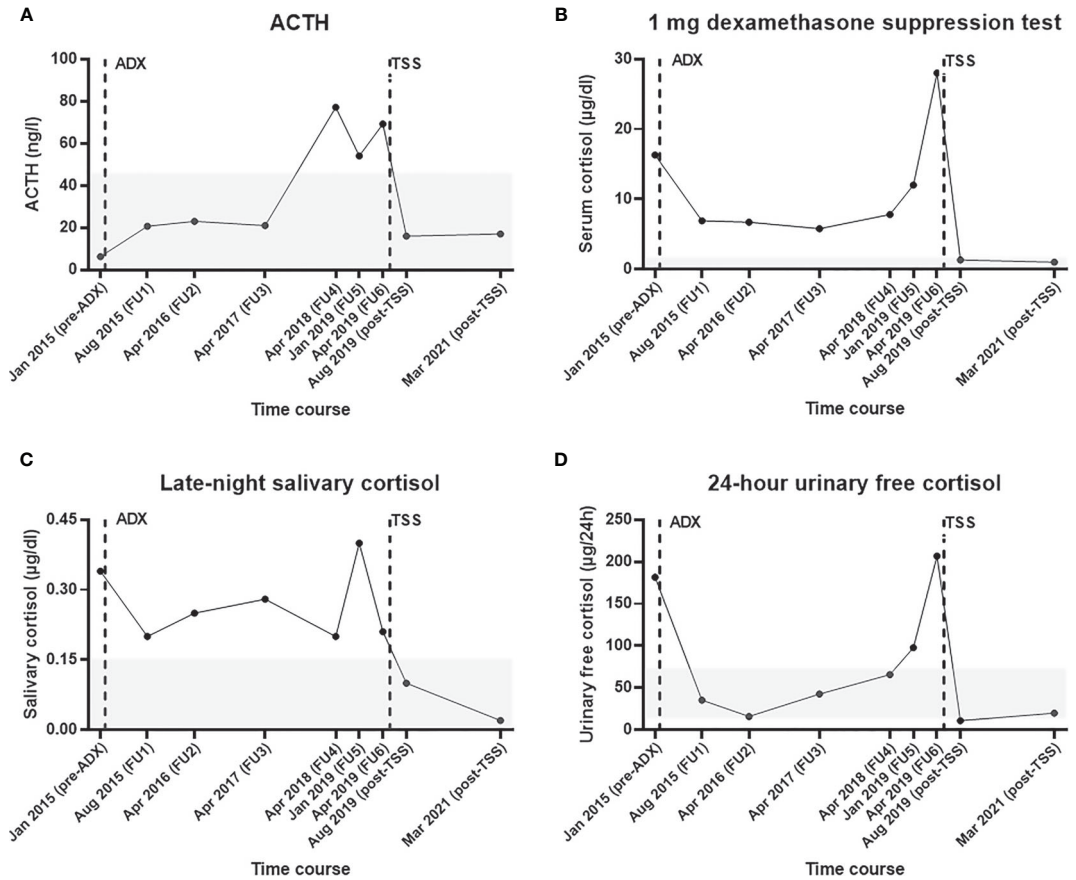


**FIGURE 2** | Selected endocrine parameters from initial diagnosis of adrenal Cushing's syndrome until recovery after transsphenoidal surgery for Cushing's disease. Course of **(A)** plasma ACTH, **(B)** serum cortisol during the 1 mg dexamethasone suppression test, **(C)** late-night salivary cortisol, and **(D)** 24-hour urinary free cortisol. The time of adrenalectomy (in February 2015) and transsphenoidal adenomectomy (in June 2019) are illustrated with vertical broken bars. The reference range of each test is shown as a grey area. ACTH, adrenocorticotropin hormone; ADX, adrenalectomy; FU, follow up; TSS, transsphenoidal surgery.

additional diagnostic and therapeutic measures, but she refused them and gave priority to a gynecological surgery.

After successful removal of uterine leiomyomas in March 2019, we performed a comprehensive endocrine re-evaluation in April 2019. In a first step, ACTH-dependent CS was confirmed (**Table 1**). In a second step, dynamic diagnostic procedures were performed to establish the subtype of CS (i.e., pituitary vs. ectopic ACTH source). As recommended in such cases (1), both a corticotropin-releasing hormone (CRH) test and a desmopressin test were carried out, showing an ACTH-increase of more than 40% each (**Supplementary Table 1**). Furthermore, a pituitary MRI revealed a hypointense focal lesion of 0.5 x 0.4 x 0.4 cm in the dorsal part of the adenohypophysis compatible with a pituitary microadenoma (**Figures 3A, B**). In order to rule out the presence of a non-functioning pituitary adenoma and to confirm pituitary origin of the ACTH excess, a bilateral inferior petrosal sinus sampling was performed. This procedure revealed ACTH central to peripheral (IPS:P) ratios of 8.6 at baseline and 65.2 after CRH stimulation, indicating CD. According to these results, a central ACTH source was assumed.

The patient was, therefore, referred to pituitary surgery. In June 2019, she underwent successful transsphenoidal adenomectomy. The histopathological analysis described a 0.5 x 0.5 x 0.2 cm pituitary adenoma. The histological analysis (exemplarily shown in **Figures 3C, D**) and the immunohistochemistry revealed ACTH-expression in >50% of the cells, whereas staining for prolactin, thyroid-stimulating hormone (TSH), follicle-stimulating hormone (FSH), and luteinizing (LH) was negative. As an indirect hint for hypercortisolism, some Crooke cells were also identified in the normal adenohypophysis tissue (14).

Postoperatively, basal ACTH was <5 ng/l and cortisol levels were suppressed. Accordingly, glucocorticoid replacement was initiated. In the first postoperative follow-up 10 weeks after surgery (August 2019), an ACTH stimulation test revealed a persistent partial adrenal insufficiency (serum cortisol after 1 hour: 17.5 µg/dl), while the basal ACTH level was 16 ng/l. As reported in **Figure 2**, the biochemical workup (including 1 mg DST, UFC, and LNSC) indicated remission from CS.

Because we suspected the presence of a germline mutation and in order to discover potential driver mutations, whole exome

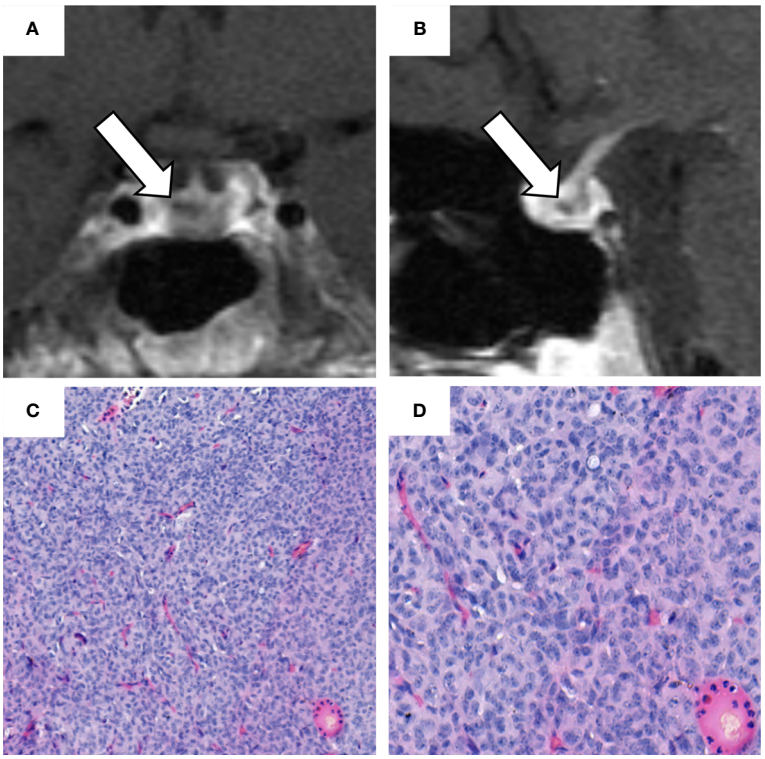


**FIGURE 3** | Sellar magnetic resonance imaging (MRI) performed in April 2019 and histological analysis of the pituitary adenoma. **(A)** coronal and **(B)** sagittal contrast-enhanced T1-weighted sellar magnetic resonance imaging. The white arrows indicate a hypointense focal lesion of 0.5 x 0.4 x 0.4 cm in the dorsal part of the adenohypophysis, reaching to the right side of the gland. This lesion was radiologically regarded as compatible with a microadenoma. **(C, D)** hematoxylin and eosin staining of the ACTH-secreting pituitary adenoma with: fragmented parts of a good differentiated epithelial tumor; cells present with medium size and oval nuclei (with an interspersed chromatin structure); occasional detection of nucleoli; no evidence of high mitotic activity; cytoplasm predominantly chromophobe. (H.E. 10x, 20x).

sequencing analysis was performed (using tumor material from both the adrenal and the pituitary adenomas, with germline DNA from whole blood as a reference). The methodic of the analysis is described in the "Materials and Methods" section. Nineteen somatic mutations were identified in the adrenal adenoma, facing 16 somatic mutations in the pituitary adenoma (**Supplementary Table 2**). None of these mutations were shared, rendering independent development of both tumor entities. Among the observed somatic mutations, we identified a pathogenic somatic *CTNNB1* alteration (NM_001098209.2:exon3:c.133T>G: p.Ser45Ala; variant allele frequency (VAF) 33.6%) in the adrenal adenoma; in the pituitary adenoma, a pathogenic *USP8* mutation (NM_001128610.3:exon14:c.2152T>C:p.Ser718Pro; VAF 40.2%) as well as a pathogenic alteration in the glucocorticoid receptor gene *NR3C1* (NM_000176.3:exon5:c.1729_1735del: p.Trp577Argfs*15; VAF 31.7%) were observed.

The patient provided written informed consent to two disease-specific clinical registries and agreed in the current case presentation. The approval numbers from the local ethics committee of the University Hospital of Würzburg are 88/11 (for the European Network for the Study of Adrenal Tumors registry) and 85/12 (for the Network of Excellence for Neuroendocrine Tumors registry). In the last follow up (conducted in March 2021), the patient was in complete clinical and biochemical remission (**Figure 2**) and reported no signs and symptoms suggestive for Cushing's syndrome.

## MATERIALS AND METHODS

### DNA Extraction

DNA was isolated from snap-frozen adrenocortical adenoma sample with the Maxwell® 16 Tissue DNA Purification Kit (#AS1030, Promega, Madison, WI, USA) and from formalin-fixed paraffin-embedded (FFPE) pituitary adenoma with the QIAamp DNA FFPE Tissue Kit (#56404, Qiagen, Hilden, Germany) according to the manufacturer's instructions. Leukocyte DNA was extracted from whole blood using NucleoSpin® Blood L (#740954.20, Macherey-Nagel, Düren, Germany), as previously described (15). The quality of DNA was analyzed by the Qubit® dsDNA BR (Broad-Range) Assay Kits (#Q32850, Thermo Fisher Scientific, Waltham, MA USA).

Tumor and leukocyte DNA was enriched with the Twist Human Core Exome Plus Kit (Twist Bioscience, San Francisco, CA, USA). Paired end sequencing with a length of 100 bps was performed on a NovaSeq 6000, 2 x 100 bp (CeGaT, Thüringen, Germany), according to the manufacturer's protocol (yielding a coverage of 281x in the blood samples, of 525x in the adrenocortical adenoma, and of 284 x in the pituitary adenoma).

## Genetic Analysis

After an initial quality assessment using FastQC, v0.11.5 (Available online at: http://www.bioinformatics.babraham.ac.uk/projects/fastqc), adapters and low-quality reads were trimmed with TrimGalore, v0.4.0 (Available online at: http://www.bioinformatics.babraham.ac.uk/projects/trim_galore/) powered by Cutadapt, v1.8. The trimmed reads were mapped to the UCSC human genome (hg19) with BWA mem, v0.7.17 (16) before being sorted and indexed using Picard, v1.125 (available online at: http://broadinstitute.github.io/picard/) and SAMtools, v1.3 (17), respectively. Duplicates were marked with Picard. For coverage calculations and base quality score recalibration, GATK3, v3.5 and GATK4, v4.0.11.0 were used (18).

GATK3 and GATK4 were used for germline variant calling. Additionally, small germline indels were called using Scalpel v 0.5.312 (19). MuTect1, v1.1.410 (20) and MuTect2 (that is integrated in the GATK4 package),samtools (mpileup) with VarScan2, v2.4.111 (21) and Scalpel were used for somatic variant calling. All variants were annotated with ANNOVAR, v2019-10-24 (22) and considered if they were below a frequency of 2% in the databases 1000g2015aug_all, ExAC_nontcga_ALL, gnomAD_exome_ALL and gnomAD_genome_ALL (if the position is covered by at least 20 reads, and the alternative allele is covered by at least 8 reads and comprised at least 5% of the total reads). Each variant was visually verified using IGV, v2.7.2 (23).

# DISCUSSION

To our knowledge, this is the first published case reported describing a histologically confirmed ACTH-dependent CS in a patient who had suffered from an ACTH-independent adrenal CS few years earlier. In our opinion, this case is remarkably not only from a clinical, but also from a pathophysiological perspective.

The major clinical challenge was to accept the unexpected, i.e. to agree to the diagnosis of CD after former adrenal CS. Of course, our first hypothesis was a relapse of adrenal CS, particularly as the abdominal CT scan report described an uncertain mass at the level of the formerly resected adrenal gland. At that time, the relatively high plasma ACTH was interpreted as part of the recovery process from adrenal CS. However, doubts arose when an adrenocortical remnant could not be confirmed by the ($^{123}$I)-MAZA whole body scintigraphy and SPECT/CT. Therefore, the unclear mass was finally regarded as scar soft tissue. Recently, some authors reported assay-specific spurious ACTH levels leading to diagnostic and therapeutic obstacles (24). However, our analytical methodology did not change throughout the diagnostic process, making falsely elevated ACTH levels very unlikely.

It is certainly tempting to speculate on the starting point of ACTH oversecretion in our case. Postoperative improvement of both the patient´s clinical and biochemical condition seem to prove the development of CD many months after surgery for adrenal CS. As outlined in **Figure 3**, there was an increase in the ACTH and cortisol levels throughout the years despite initial normalization of UFC following adrenalectomy. The fact that 1 mg DST and LNSC only improved (but not normalized) may be explained by a physiologic/non-neoplastic hypercortisolism related to the obesity of the patient (25), but does not exclude an initial coexistence of a more pronounced adrenal CS and a - at that time - less relevant CD.

In the literature, the coexistence of the two subtypes of endogenous CS has already been described in few patients. Hernandez-Ramirez et al. (10) reported a case of ACTH-dependent and ACTH-independent CS coexisting in a patient with Carney complex. In this case, PPNAD developed 5 years after CD. In our patient, Carney complex was clinically unlikely due to the lack of typical signs and symptoms (such as pigmented lesions of the skin and mucosa, cardiac, cutaneous and other myxomas). Moreover, exome sequencing excluded a causative germline mutation of *PRKAR1A* but also of *MEN1*. With respect to the latter, Dal Verme et al. (11) reported the case of a patient who suffered from ectopic Cushing's syndrome due to a thymic carcinoid 32 years after being treated for Cushing's disease, possibly pointing to a *MEN1* germline mutation.

Schteingart et al. (26) presented a patient with suspected coexistence of CD and a cortisol-producing adrenal adenoma. However, histopathological analysis finally revealed an adrenocortical hyperplasia (as origin of hypercortisolism) along with a solitary non-functioning adrenocortical adenoma. Recently, Di Dalmazi et al. (7) described two cases with transition from ACTH-dependent to ACTH-independent hypercortisolism associated to micronodular adrenal hyperplasia and a catalytic α subunit of protein kinase A (*PRKACA*) somatic-mutation.

Two other case reports described persistent hypercortisolemia after transspehoidal removal of an ACTH-secreting pituitary microadenoma (8, 9). However, at least in one of these cases, the causative adrenal macronodule was already present at the time of the initial diagnosis of Cushing's syndrome (8); in the other case, the adrenal mass was detected 10 months after pituitary surgery (making an ACTH-driven nodular autonomy instead of the consecutive occurrence of two independent Cushing subtypes very likely) (9).

Our own case, however, differs significantly from the already published cases. Firstly, in the two patients reported by Di Dalmazi et al. (7) and in the patient reported by Timmers et al. (9), CD was present before the adrenal CS and the initial stimulation of ACTH/Pro-opiomelanocortin (POMC) might therefore be pathophysiologically involved in the development of the adrenal hyperplasia. Secondly, in our case the histopathological analysis of the adrenal tumor clearly described an adrenocortical adenoma and no micronodular or macronodular hyperplasia. Thirdly, we performed whole exome

sequencing of both adenomas and could clearly demonstrate that they are genetically distinct, whereas none of the previous reports could (dis)prove a similar situation.

*CNTNNB1* is a gene encoding for the β-catenin protein, which has a principal role in the Wnt signaling pathway. The role of β-catenin in the embryonic development of adrenal cortical cells and in the renewal of the adult adrenal cortex is well known (27). Additionally, the mutation of this protein and the constitutive Wnt pathway activation is reported in the context of the development of benign and malignant adrenal tumors (28–32). Although studies suggested that mutations in *CTNNB1* are more common in inactive adrenal adenomas (28, 29, 33), they have also often been reported in cortisol-producing adrenal adenomas (28, 29, 33, 34). The genetic analysis of the present adrenal tumor revealed a somatic mutation p.Ser45Ala of the *CTNNB1*-gene. This mutation has already been reported in the context of autonomous cortisol secretion (33, 34); of note, our current case was not part of these studies. Differently from previous reports, our case was associated with signs and symptoms of CS, which clearly improved after adrenalectomy. Moreover, as previously reported (28, 33, 34), a *CTNNB1*-mutation is associated with larger tumors, explaining the size greater than 40 mm of the adrenal adenoma in our case. Nevertheless, malignancy was excluded by a Weiss score of 1 and a Ki 67 index of <1%.

The exome analysis on the ACTH-secreting pituitary adenoma revealed a p.Ser718Pro-*USP8* somatic mutation. *USP8* is a gene which encodes for a protein named Ubiquitin specific peptidase 8 (35–38). This deubiquitinase enzyme removes the ubiquitin residues that physiologically target proteins for recycling or destruction. According to current knowledge, somatic USP8 mutations are present in about 24-40% of all CD cases (35–38). The most common mutation site of *USP8* in the context of CD has been found at the level of the exon 14 (NM_001128610.3), between the amino acids 713 and 720, in the 14-3-3 binding motif (36–38). In our case, exome analysis revealed a somatic mutation exactly in this region of exon 14 (p.Ser718Pro2-*USP8*). This mutation impairs the binding of 14-3-3 proteins (which have a regulatory role on *USP8*), thus increasing the deubiquitination of the Epidermal Growth Factor Receptor (EGFR), favoring its overexpression (36–38).

It is worth mentioning that the genetic analysis of the pituitary adenoma also revealed a frameshift deletion of the nuclear receptor subfamily 3 group C member 1 (*NR3C1*) gene that encodes for the glucocorticoid receptor. Somatic mutations of this gene have already been reported in 4 out of 64 (6.2%) ACTH-secreting pituitary adenomas analyzed by exome sequencing (38). While the mutation that we found now (NM_000176.3:exon5:c.1729_1735del:p.W577Rfs*15) has not yet been reported previously, the somatic mutations reported were all either inactivating point mutations or deletions. The recurring mutation-induced inactivation of the glucocorticoid receptor suggests that this process may be partly responsible for the manifestation of CD. This assumption is supported by analyses of the frequent inactivating germline polymorphisms showing that such disturbances in hypothalamic-pituitary-adrenal signaling homeostasis have important functional effects (39–41). Possibly, the distinct difference in cortisol levels before and after adrenalectomy could have influenced the glucocorticoid receptor turnover in the pituitary, resulting in increased glucocorticoid resistance and cell proliferation, and finally leading to the formation of an autonomous adenoma.

In conclusion, no association between somatic mutations of *CTNNB1* (in cortisol-producing adrenal adenomas), *USP8* and *NR3C1* (in ACTH-secreting pituitary adenomas) has been reported so far. To our knowledge, this is the first published case reporting two independent ACTH-independent and ACTH-dependent subtypes of CS developing in a single patient. Accordingly, the extremely rare event of recurrent hypercortisolism due to different subtypes of CS must be taken into account if corresponding (but unexpected) findings are observed during follow-up.

## ETHICS STATEMENT

The studies involving human participants were reviewed and approved by the local ethics committee of the University Hospital of Würzburg Approval numbers: 88/11 and 85/12. The patients/participants provided their written informed consent to participate in this study. Written informed consent was obtained from the individual(s) for the publication of any potentially identifiable images or data included in this article.

## AUTHOR CONTRIBUTIONS

Clinical data were obtained by MD, MK, MF, and TD. Imaging data were provided by WS and AS. Tumor material was provided by SSc, RC, and VW. Genetic analyses were performed by BA and SA, and results were interpreted by SSb. MD and TD wrote the first draft of the manuscript which was then revised by all co-authors. All authors contributed to the article and approved the submitted version.

## FUNDING

This study was funded by the German Research Foundation (Deutsche Forschungsgemeinschaft (DFG); project numbers: 314061271 – CRC/TRR 205.

## ACKNOWLEDGMENTS

We would like to thank Laura Landwehr and Joachim Bernhardt for facilitating the preparation of our case report.

## SUPPLEMENTARY MATERIAL

The Supplementary Material for this article can be found online at: https://www.frontiersin.org/articles/10.3389/fendo.2021.731579/full#supplementary-material

**Supplementary Figure 1 |** (123I)-MAZA whole body scintigraphy and single-photon emission computed tomography performed in July 2018. **(A)** Whole body scintigraphy in LDR projection showing a physiological tracer uptake of the right adrenal gland (black arrow), **(B)** transversal, and **(C)** coronal (123I)-MAZA SPECT/CT fusion of the upper abdomen showing no tracer uptake of the inhomogeneous, hypodense soft tissue mass detected in the position of the formerly resected left adrenal gland (white arrows), but expected physiological tracer uptake of the right adrenal gland. $^{123}$I-MAZA, [$^{123}$I](R)-1-[1-(4-iodophenyl)ethyl]-1H-imidazole-5-carboxylic acid azetidinylamide; CT, computed tomography; LDR, left side, dorsal view, right side; SPECT, single-photon emission computed tomography.

**Supplementary Table 1 |** Dynamic tests for the differentiation of ACTH dependent Cushing´s syndrome performed at our endocrine ward in April 2019. Both the CRH and the desmopressin test indicated a pituitary ACTH source, whereas the 8 mg dexamethasone favored an ectopic ACTH source. Pathological parameters are presented in bold letters. ACTH, adrenocorticotropic hormone; CRH, corticotropin-releasing hormone.

**Supplementary Table 2 |** Table of somatic mutations identified in the adrenal and in the pituitary adenoma. Detailed description of the somatic mutations identified in both adrenal and pituitary adenoma.

# REFERENCES


1. Lacroix A, Feelders RA, Stratakis CA, Nieman LK. Cushing's Syndrome. *Lancet* (2015) 386(9996):913–27. doi: 10.1016/S0140-6736(14)61375-1
2. Sharma ST, Nieman LK, Feelders RA. Cushing's Syndrome: Epidemiology and Developments in Disease Management. *Clin Epidemiol* (2015) 7:281–93. doi: 10.2147/CLEP.S44336
3. Else T, Kim AC, Sabolch A, Raymond VM, Kandathil A, Caoili EM, et al. Adrenocortical Carcinoma. *Endocr Rev* (2014) 35(2):282–326. doi: 10.1210/er.2013-1029
4. Vassiliadi DA, Tsagarakis S. Diagnosis and Management of Primary Bilateral Macronodular Adrenal Hyperplasia. *Endocr Relat Cancer* (2019) 26(10):R567–81. doi: 10.1530/ERC-19-0240
5. Smals AG, Pieters GF, van Haelst UJ, Kloppenborg PW. Macronodular Adrenocortical Hyperplasia in Long-Standing Cushing's Disease. *J Clin Endocrinol Metab* (1984) 58(1):25–31. doi: 10.1210/jcem-58-1-25
6. Hermus AR, Pieters GF, Smals AG, Pesman GJ, Lamberts SW, Benraad TJ, et al. Transition From Pituitary-Dependent to Adrenal-Dependent Cushing's Syndrome. *N Engl J Med* (1988) 318(15):966–70. doi: 10.1056/NEJM198804143181506
7. Di Dalmazi G, Timmers H, Arnaldi G, Kusters B, Scarpelli M, Bathon K, et al. Somatic PRKACA Mutations: Association With Transition From Pituitary-Dependent to Adrenal-Dependent Cushing Syndrome. *J Clin Endocrinol Metab* (2019) 104(11):5651–7. doi: 10.1210/jc.2018-02209
8. Santos J, Paiva I, Gomes L, Batista C, Geraldes E, Rito M, et al. [Recurrent Hypercortisolism After Removal of an ACTH Secretor Pituitary Adenoma Associated With an Adrenal Macronodule]. *Acta Med Port* (2010) 23(1):107–12.
9. Timmers HJ, van Ginneken EM, Wesseling P, Sweep CG, Hermus AR. A Patient With Recurrent Hypercortisolism After Removal of an ACTH-Secreting Pituitary Adenoma Due to an Adrenal Macronodule. *J Endocrinol Invest* (2006) 29(10):934–9. doi: 10.1007/BF03349200
10. Hernandez-Ramirez LC, Tatsi C, Lodish MB, Faucz FR, Pankratz N, Chittiboina P, et al. Corticotropinoma as a Component of Carney Complex. *J Endocr Soc* (2017) 1(7):918–25. doi: 10.1210/js.2017-00231
11. Dal Verme A, Cejas C, Margan M, Siguelboim D, Canosa V, Peralta C. [Acth's Ectopic Secretion in a Patient With Precedents of Cushing's Disease]. *Med (B Aires)* (2015) 75(4):218–20.
12. Nieman LK, Biller BM, Findling JW, Newell-Price J, Savage MO, Stewart PM, et al. The Diagnosis of Cushing's Syndrome: An Endocrine Society Clinical Practice Guideline. *J Clin Endocrinol Metab* (2008) 93(5):1526–40. doi: 10.1530/EJE-09-0695
13. Giordano TJ, Berney D, de Krijger RR, Erickson L, Fassnacht M, Mete O, et al. Data Set for Reporting of Carcinoma of the Adrenal Cortex: Explanations and Recommendations of the Guidelines From the International Collaboration on Cancer Reporting. *Hum Pathol* (2020) 110(2021):50–61. doi: 10.1016/j.humpath.2020.10.001
14. Oldfield EH, Vance ML, Louis RG, Pledger CL, Jane JA Jr, Lopes MB. Crooke's Changes In Cushing's Syndrome Depends on Degree of Hypercortisolism and Individual Susceptibility. *J Clin Endocrinol Metab* (2015) 100(8):3165–71. doi: 10.1210/JC.2015-2493
15. Altieri B, Sbiera S, Herterich S, De Francia S, Della Casa S, Calabrese A, et al. Effects of Germline CYP2W1*6 and CYP2B6*6 Single Nucleotide Polymorphisms on Mitotane Treatment in Adrenocortical Carcinoma: A Multicenter ENSAT Study. *Cancers (Basel)* (2020) 12(2):359. doi: 10.3390/cancers12020359
16. Li H, Durbin R. Fast and Accurate Short Read Alignment With Burrows-Wheeler Transform. *Bioinformatics* (2009) 25(14):1754–60. doi: 10.1093/bioinformatics/btp324
17. Li H, Handsaker B, Wysoker A, Fennell T, Ruan J, Homer N, et al. The Sequence Alignment/Map Format and SAMtools. *Bioinformatics* (2009) 25(16):2078–9. doi: 10.1093/bioinformatics/btp352
18. McKenna A, Hanna M, Banks E, Sivachenko A, Cibulskis K, Kernytsky A, et al. The Genome Analysis Toolkit: A MapReduce Framework for Analyzing Next-Generation DNA Sequencing Data. *Genome Res* (2010) 20(9):1297–303. doi: 10.1101/gr.107524.110
19. Fang H, Bergmann EA, Arora K, Vacic V, Zody MC, Iossifov I, et al. Indel Variant Analysis of Short-Read Sequencing Data With Scalpel. *Nat Protoc* (2016) 11(12):2529–48. doi: 10.1038/nprot.2016.150
20. Cibulskis K, Lawrence MS, Carter SL, Sivachenko A, Jaffe D, Sougnez C, et al. Sensitive Detection of Somatic Point Mutations in Impure and Heterogeneous Cancer Samples. *Nat Biotechnol* (2013) 31(3):213–9. doi: 10.1038/nbt.2514
21. Koboldt DC, Chen K, Wylie T, Larson DE, McLellan MD, Mardis ER, et al. VarScan: Variant Detection in Massively Parallel Sequencing of Individual and Pooled Samples. *Bioinformatics* (2009) 25(17):2283–5. doi: 10.1093/bioinformatics/btp373
22. Wang K, Li M, Hakonarson H. ANNOVAR: Functional Annotation of Genetic Variants From High-Throughput Sequencing Data. *Nucleic Acids Res* (2010) 38(16):e164. doi: 10.1093/nar/gkq603
23. Robinson JT, Thorvaldsdottir H, Winckler W, Guttman M, Lander ES, Getz G, et al. Integrative Genomics Viewer. *Nat Biotechnol* (2011) 29(1):24–6. doi: 10.1038/nbt.1754
24. Greene LW, Geer EB, Page-Wilson G, Findling JW, Raff H. Assay-Specific Spurious ACTH Results Lead to Misdiagnosis, Unnecessary Testing, and Surgical Misadventure-A Case Series. *J Endocr Soc* (2019) 3(4):763–72. doi: 10.1210/js.2019-00027
25. Findling JW, Raff H. DIAGNOSIS OF ENDOCRINE DISEASE: Differentiation of Pathologic/Neoplastic Hypercortisolism (Cushing's Syndrome) From Physiologic/non-Neoplastic Hypercortisolism (Formerly Known as Pseudo-Cushing's Syndrome). *Eur J Endocrinol* (2017) 176(5):R205–R16. doi: 10.1530/EJE-16-0946
26. Schteingart DE, Tsao HS. Coexistence of Pituitary Adrenocorticotropin-Dependent Cushing's Syndrome With a Solitary Adrenal Adenoma. *J Clin Endocrinol Metab* (1980) 50(5):961–6. doi: 10.1210/jcem-50-5-961
27. Kim AC, Reuter AL, Zubair M, Else T, Serecky K, Bingham NC, et al. Targeted Disruption of Beta-Catenin in Sf1-Expressing Cells Impairs Development and Maintenance of the Adrenal Cortex. *Development* (2008) 135(15):2593–602. doi: 10.1242/dev.021493
28. Bonnet S, Gaujoux S, Launay P, Baudry C, Chokri I, Ragazzon B, et al. Wnt/beta-Catenin Pathway Activation in Adrenocortical Adenomas is Frequently Due to Somatic CTNNB1-Activating Mutations, Which are Associated With Larger and Nonsecreting Tumors: A Study in Cortisol-Secreting and -Nonsecreting Tumors. *J Clin Endocrinol Metab* (2011) 96(2):E419–26. doi: 10.1210/jc.2010-1885
29. Bonnet-Serrano F, Bertherat J. Genetics of Tumors of the Adrenal Cortex. *Endocr Relat Cancer* (2018) 25(3):R131–R52. doi: 10.1530/ERC-17-0361
30. Faillot S, Foulonneau T, Neou M, Espiard S, Garinet S, Vaczlavik A, et al. Genomic Classification of Benign Adrenocortical Lesions. *Endocr Relat Cancer* (2021) 28(1):79–95. doi: 10.1530/ERC-20-0128
31. Zheng S, Cherniack AD, Dewal N, Moffitt RA, Danilova L, Murray BA, et al. Comprehensive Pan-Genomic Characterization of Adrenocortical Carcinoma. *Cancer Cell* (2016) 29(5):723–36. doi: 10.1016/j.ccell.2016.04.002
32. Altieri B, Ronchi CL, Kroiss M, Fassnacht M. Next-Generation Therapies for Adrenocortical Carcinoma. *Best Pract Res Clin Endocrinol Metab* (2020) 34(3):101434. doi: 10.1016/j.beem.2020.101434
33. Ronchi CL, Di Dalmazi G, Faillot S, Sbiera S, Assie G, Weigand I, et al. Genetic Landscape of Sporadic Unilateral Adrenocortical Adenomas Without

PRKACA P.Leu206Arg Mutation. *J Clin Endocrinol Metab* (2016) 101 (9):3526–38. doi: 10.1530/endoabs.41.OC1.1
34. Di Dalmazi G, Altieri B, Scholz C, Sbiera S, Luconi M, Waldman J, et al. RNA Sequencing and Somatic Mutation Status of Adrenocortical Tumors: Novel Pathogenetic Insights. *J Clin Endocrinol Metab* (2020) 105(12):e4459–73. doi: 10.1210/clinem/dgaa616
35. Losa M, Mortini P, Pagnano A, Detomas M, Cassarino MF, Pecori Giraldi F. Clinical Characteristics and Surgical Outcome in USP8-Mutated Human Adrenocorticotropic Hormone-Secreting Pituitary Adenomas. *Endocrine* (2019) 63(2):240–6. doi: 10.1007/s12020-018-1776-0
36. Reincke M, Sbiera S, Hayakawa A, Theodoropoulou M, Osswald A, Beuschlein F, et al. Mutations in the Deubiquitinase Gene USP8 Cause Cushing's Disease. *Nat Genet* (2015) 47(1):31–8. doi: 10.1038/ng.3166
37. Sbiera S, Deutschbein T, Weigand I, Reincke M, Fassnacht M, Allolio B. The New Molecular Landscape of Cushing's Disease. *Trends Endocrinol Metab* (2015) 26(10):573–83. doi: 10.1016/j.tem.2015.08.003
38. Sbiera S, Kunz M, Weigand I, Deutschbein T, Dandekar T, Fassnacht M. The New Genetic Landscape of Cushing's Disease: Deubiquitinases in the Spotlight. *Cancers (Basel)* (2019) 11(11):1761. doi: 10.3390/cancers11111761
39. Briassoulis G, Damjanovic S, Xekouki P, Lefebvre H, Stratakis CA. The Glucocorticoid Receptor and its Expression in the Anterior Pituitary and the Adrenal Cortex: A Source of Variation in Hypothalamic-Pituitary-Adrenal Axis Function; Implications for Pituitary and Adrenal Tumors. *Endocr Pract* (2011) 17(6):941–8. doi: 10.4158/EP11061.RA
40. Lamberts SW. Glucocorticoid Receptors and Cushing's Disease. *Mol Cell Endocrinol* (2002) 197(1-2):69–72. doi: 10.1016/S0303-7207(02)00280-0
41. Antonini SR, Latronico AC, Elias LL, Cukiert A, Machado HR, Liberman B, et al. Glucocorticoid Receptor Gene Polymorphisms in ACTH-Secreting Pituitary Tumours. *Clin Endocrinol (Oxf)* (2002) 57(5):657–62. doi: 10.1046/j.1365-2265.2002.01639.x

**Conflict of Interest:** The authors declare that the research was conducted in the absence of any commercial or financial relationships that could be construed as a potential conflict of interest.

**Publisher's Note:** All claims expressed in this article are solely those of the authors and do not necessarily represent those of their affiliated organizations, or those of the publisher, the editors and the reviewers. Any product that may be evaluated in this article, or claim that may be made by its manufacturer, is not guaranteed or endorsed by the publisher.

frontiers in Endocrinology

ORIGINAL RESEARCH
published: 01 September 2021
doi: 10.3389/fendo.2021.727327

# Comparison of 68Ga-DOTANOC and 18F-FDG PET-CT Scans in the Evaluation of Primary Tumors and Lymph Node Metastasis in Patients With Rectal Neuroendocrine Tumors

*Zhihao Zhou[1†], Zhixiong Wang[1†], Bing Zhang[2], Yanzhang Wu[1], Guanghua Li[1*] and Zhao Wang[1*]*

[1] Department of Gastrointestinal Surgery, First Affiliated Hospital of Sun Yat-sen University, Guangzhou, Guangdong, China,
[2] Department of Nuclear Medicine, First Affiliated Hospital of Sun Yat-sen University, Guangzhou, Guangdong, China

**Background:** Lymph node metastasis of rectal neuroendocrine tumors (RNETs) predicts poor prognosis. However, the assessment of lymph node metastasis remains a challenge. It has been reported that 68Ga-DOTANOC and 18F-FDG PET-CT scans could be employed in the work-up of rectal neuroendocrine tumors (RNETs). This study aimed to assess both tracers' ability to identify primary tumors and lymph node (LN) metastasis in RNETs.

**Methods:** A total of 537 patients with RNETs were enrolled from January 2014 to January 2021. Both 68Ga-DOTANOC and 18F-FDG PET-CT scans were used to evaluate primary tumors and LN group metastasis. PET images were evaluated through visual and semiquantitative assessment. Receiver Operating Characteristics (ROC) curve analysis was used to investigate the performance of SUVmax of 68Ga-DOTANOC and 18F-FDG PET in predicting LN group metastasis.

**Results:** Fifty-two patients with preoperative 68Ga-DOTANOC with 18F-FDG PET-CT scans underwent endoscopic biopsy or dissection of the primary tumor, while 11 patients underwent rectal surgery together with regional LN dissection. For primary tumors, 68Ga-DOTANOC had a sensitivity of 89.58% and a positive predictive value (PPV) of 95.56% through visual assessment, while 18F-FDG PET-CT showed 77.08% sensitivity and 97.37% PPV. For the prediction of LN group metastasis, 68Ga-DOTANOC PET-CT had 77.78% sensitivity and 91.67% specificity, while 18F-FDG PET-CT had 38.89% sensitivity and 100% specificity according to visual assessment. The area under the ROC curves (AUC) for 68Ga-DOTANOC PET/CT was 0.852 (95%CI:0.723-0.981) with an optimal SUVmax cut-off value of 2.25, while the AUC for 18F-FDG PET were 0.664 (95% CI:0.415-0.799) with an optimal SUVmax cut-off value of 1.05.

OPEN ACCESS

**Edited by:**
*Barbara Altieri, University Hospital of Wuerzburg, Germany*

**Reviewed by:**
*Mick Welling, Leiden University Medical Center, Netherlands*
*Pasqualino Malandrino, University of Catania, Italy*

***Correspondence:**
*Zhao Wang*
*wangzhao@mail.sysu.edu.cn*
*Guanghua Li*
*ligh26@mail.sysu.edu.cn*

*†These authors have contributed equally to this work and share first authorship*

**Specialty section:**
*This article was submitted to Cancer Endocrinology, a section of the journal Frontiers in Endocrinology*

**Received:** *18 June 2021*
**Accepted:** *16 August 2021*
**Published:** *01 September 2021*

**Citation:**
*Zhou Z, Wang Z, Zhang B, Wu Y, Li G and Wang Z (2021) Comparison of 68Ga-DOTANOC and 18F-FDG PET-CT Scans in the Evaluation of Primary Tumors and Lymph Node Metastasis in Patients With Rectal Neuroendocrine Tumors. Front. Endocrinol. 12:727327. doi: 10.3389/fendo.2021.727327*

**Conclusions:** This study showed that 68Ga-DOTANOC PET-CT was a promising tool for detecting LN metastasis in RNETs with high sensitivity and specificity in visual assessment and semiquantitative assessment, which was better than 18F-FDG PET-CT.

**Keywords: rectal neuroendocrine tumors, lymph node metastasis, 68Ga-DOTANOC PET, 18F-FDG PET, PET-CT**

## INTRODUCTION

Neuroendocrine tumors (NETs) are considered rare tumors and constitute only 0.5% of all malignant conditions (1). NETs can arise in different organs, including the gastrointestinal tract, pancreas, lungs, gallbladder, thymus, thyroid gland, testes, ovary, and skin (2). Rectal NETs (RNETs) only account for 1% to 2% of rectal tumors (3). In 2010, the World Health Organization proposed that rectal neuroendocrine tumors (NETs) are classified as malignant tumors (4), and the 5-year survival rates for RNETs were 64.1% and 88% in Europe and North America, respectively (5–7).

RNETs were mostly limited to local (8) and endoscopic dissection for most cases, which was sufficient (9). However, lymph node (LN) metastases were found in nearly 10% of cases (10). Surgery with lymphadenectomy represents the gold standard for the curative treatment of localized disease with LN metastasis (11). Although tumor size, endoscopic aspect, CT appearance, etc. could predict LN metastasis (12), how to diagnose LN metastases accurately remains uncertain.

NETs typically express somatostatin receptors (SSTRs) on their cell membranes (13). Due to the high expression of SST in most NETs, SST imaging has become the current standard for staging and preoperative assessment of NET patients (14, 15). Of all methods available, PET-CT with 68Ga-labeled somatostatin analogs (SSAs) (68Ga-DOTATATE, 68Ga-DOTANOC, and 68Ga-DOTATOC) showed the best mix of diagnostic accuracy (16). However, the predictive value of LN metastasis for SST imaging remains to be explored.

FDG is a glucose analog that is actively transported into the cell and subsequently remains in the cell. Tumor cells, due to their higher metabolic activity, usually have a higher FDG uptake than normal tissues (17). 18F-FDG PET/CT was considered the preferred radiotracer for G3 tumors, as well as for some high-grade G2 tumors (18). 18F-FDG PET-CT had a high diagnostic accuracy to identify progression in enteropancreatic NETs (19) and was a useful tool to predict the therapeutic effect in patients who underwent peptide receptor radionuclide therapy (20). However, 18F-FDG PET-CT shows high false negative findings, which could be related to the indolent tumor behavior of most NETs, such as G1 and low G2 tumors (21). The diagnostic role of 18F-FDG PET-CT is still controversial due to these conflicting results (22).

**Abbreviations:** NETs, neuroendocrine tumors; NENs, neuroendocrine neoplasms; RNETs, Rectal NETs; LN, lymph node; SSAs, somatostatin analogs; TNM, tumor node metastasis; SUVmax, maximum standard uptake value; IQRs, interquartile ranges; ROC, Receiver Operating Characteristics; CI, confidence interval; ESD, endoscopic submucosal dissection; PPV, positive predictive value; NPV, negative predictive value; AUC, The area under the ROC curves.

68Ga-DOTANOC PET-CT seems to be superior to 18F-FDG PET-CT in the diagnostic performance of primary and LN metastases of pancreatic NETs (23, 24). However, whether 68Ga-DOTANOC PET-CT can identify primary tumors and LN metastasis better than 18F-FDG PET-CT in patients with RNETs remains unclear.

In our study, we explored the diagnostic ability of 68Ga-DOTANOC PET-CT and 18F-FDG PET-CT for RNET primary tumors and regional LN group metastasis.

## MATERIALS AND METHODS

### Patients

Patients who were diagnosed with RNETs from January 2014 to January 2021 were enrolled. The study was approved by the Ethics Committee of the First Affiliated Hospital of Sun Yat-sen University in China. All research was undertaken following the provisions of the Declaration of Helsinki. Patients with the following criteria were included: (1) confirmed RNETs according to 2019 World Health Organization (WHO) digestive system tumor classification criteria; (2) underwent 68Ga-DOTANOC PET-CT and 18F-FDG PET-CT within a 1-month period; and (3) absence of therapeutic intervention or change in disease status between the two PET studies. The exclusion criteria were as follows: (1) other colorectal malignancies; (2) uncertain diagnosis lacking pathology; and (3) long-acting radiolabeled somatostatin analog treatment in the 4 weeks prior to the study (25). All patients provided written informed consent and complied with the ethical guidelines in the Declaration of Helsinki.

### Pathological Diagnosis

The histological type of rectal NETs was defined according to the 2019 WHO classification (26), and tumor node metastasis (TNM) staging was characterized in our study according to the 2017 AJCC 8th edition (27). All NETs were graded according to the current guidelines of the 2019 WHO classification system based on mitotic counts and the Ki-67 labeling index. G1, G2, and G3 were classified according to the Ki-67 index. In brief, G1 was assigned to tumors with a mitotic rate <2/10 HPFs and/or a Ki-67 labeling index <3%, G2 to tumors with a mitotic rate 2 to 20/HPFs and/or a Ki-67 labeling index of 3% to 20%, and G3 to tumors with a mitotic rate >20/HPFs and/or a Ki-67 labeling index >20%.

### LN Group Classification

According to the Japanese Classification of Colorectal, Appendiceal, and Anal Carcinoma (28), regional LNs were mainly classified into pericolic, intermediate, main LN group,

and lateral LN groups. For some cases, the surgeon selected the enlarged LN individually during surgery according to preoperative imaging.

## Reference Standard

Histopathology was taken as the reference standard.

## 68Ga-DOTANOC and 18F-FDG PET-CT Imaging

As Qiao He reported (29), no specific preparation of the patients was required before 68Ga-DOTANOC PET-CT and 18F-FDG examination. PET-CT imaging was performed with a Gemini GXL 16 PET scanner (Philips Healthcare). One hundred eleven to 185 MBq (3–5 mCi) 68Ga-DOTANOC or a dose of 5.18 MBq (0.14 mCi)/kg FDG was injected intravenously, and serial scanning was performed. Serial scanning from head to mid-thigh was performed approximately 45–60 min after the injection. Following low radiation dose CT acquisition with a slice thickness of 5 mm, PET acquisition was performed for 1.5 min per bed position for 7–8 beds using a slice thickness of 4 mm. CT-based attenuation correction of the emission data was employed. PET images were reconstructed by the Line of Response RAMLA algorithm.

18F-FDG and 68Ga-DOTANOC PET-CT studies were performed at least 24 h apart.

## Image Analysis

68Ga-DOTANOC and 18F-FDG PET-CT images were evaluated both visually and semi-quantitatively by two experienced nuclear medicine physicians in consensus. For the PET-CT studies, areas with focal activity greater than the background that could not be identified as physiological activity were considered to indicate tumor tissue (defined as visual assessment). The location and radioactivity uptake (maximum standard uptake value, SUVmax) of the lesions were observed or measured (defined as semiquantitative analysis).

## Statistical Analysis

Normally distributed variables were expressed as the means and standard deviations (SD), with variables not following a normal distribution presented as medians and interquartile ranges (IQRs) and categorical variables as frequencies and proportions. The Shapiro-Wilk test was used to test deviations from a normal distribution. The nonparametric analyses were performed using the Mann–Whitney U test. A receiver operating characteristic (ROC) curve was then constructed to determine the optimal SUVmax cutoff for predicting LN metastasis. A p value of $<0.05$ was considered statistically significant. The data analysis was performed using GraphPad Prism 8 software (GraphPad Software, Inc., La Jolla, CA, USA) and MedCalc statistical software.

# RESULTS

## Patients Characteristics

A total of 52 patients who underwent both 68Ga-DOTANOC and 18F-FDG PET-CT scans were included in the study. Of the 11 patients who underwent regional LN dissection, 1 patient underwent salvage surgery after endoscopic submucosal dissection (ESD), 5 patients with distant metastases underwent surgery when intestinal obstruction occurred, and the other 5 patients underwent radical surgery. Another 41 patients underwent endoscopic biopsy or dissection only. More details are shown in **Figure 1** and **Table 1**.

## Comparison of the Performance of 68Ga-DOTANOC and 18F-FDG PET-CT in Primary Tumors

### Visual Assessment

Of the 52 patients included, 48 patients were pathologically diagnosed with NETs for the primary tumor, while the remaining 4 patients were determined to be negative by pathology for the primary tumor due to preoperative endoscopic dissection.

68Ga-DOTANOC PET-CT successfully identified 43/48 primary tumors with a sensitivity of 89.58% and 95.56% PPV, while 18F-FDG PET-CT identified 37/48 primary tumors with a

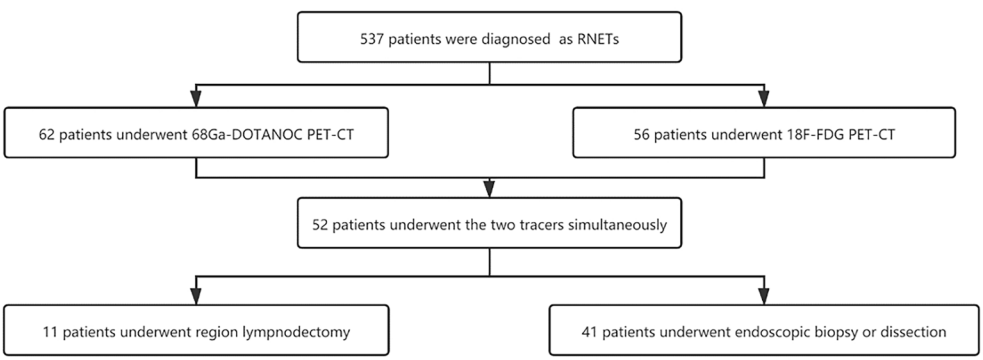


**FIGURE 1** | The flowchart of study patients.

**TABLE 1** | Basic clinicopathological characteristics in patients who underwent 68Ga-DOTANOC and 18F-FDG PET-CT.

| Characteristics | value |
|---|---|
| Sex | |
| Male | 32 |
| Female | 20 |
| Age (years) | 28-75 |
| TNM stage | |
| I-III | 11 |
| IV | 41 |
| Grade | |
| G1 | 15 |
| G2 | 31 |
| G3 | 6 |

*TNM, tumor node metastasis.*

sensitivity of 77.08% and 97.37% PPV. The sensitivity of 68Ga-DOTANOC PET-CT was not statistically different from that of FDG 18F-FDG PET-CT (p = 0.109). The combination of 68Ga-DOTANOC and 18F-FDG PET-CT could increase the sensitivity to 93.75%.

For 6 cases with G3 primary tumors, 68Ga-DOTANOC PET-CT identified 4 of these 6 patients and showed false negatives in 2 cases, while 18F-FDG PET-CT diagnosed 5 of these 6 patients and reported false negatives in one case (**Figure 2**). At the same time, among 42 patients with G1-2 primary tumors, 68Ga-DOTANOC PET-CT identified 39 patients (39/42), while 18F-FDG PET-CT identified only 32 patients (32/42) (p =0.039).

## The Value of 68Ga-DOTANOC and 18F-FDG PET-CT in Predicting LN Group Metastasis

Among the 11 patients who underwent regional lymphadenectomy, 10 patients were pathologically diagnosed with LN group metastasis. Forty-two groups of regional LNs were harvested after surgery, of which 18 groups were diagnosed with metastases. More details are shown in **Table 2**.

### Visual Assessment

68Ga-DOTANOC PET-CT was true positive in 14 LN groups and true negative in 22 LN groups; thus, the sensitivity of 68Ga-DOTANOC PET-CT for detecting RNETs was 77.78%, and the specificity was 91.67%. Meanwhile, 18F-FDG PET-CT was true positive in 7 LN groups and true negative in 24 LN groups, with 38.89% sensitivity and 100% specificity. The overall sensitivity, specificity, and accuracy of 68Ga-DOTANOC and 18F-FDG PET-CT in predicting LN group metastasis are presented in **Table 3**.

Among the 18 positive LN groups, both 68Ga-DOTANOC PET-CT and 18F-FDG PET-CT were true positive in 7 LN groups. Among the 24 negative LN groups, 18F-FDG PET-CT defined all true negatives (24/24), while 68Ga-DOTANOCPET-CT assessed 2 of 24 LN groups as false positives (2/24). Both 68Ga-DOTANOC and 18F-FDG PET-CT were positive in 7 LN groups and negative in 22 LN groups. However, discordance was noted in 13 groups between the two tracers (**Figure 3**).

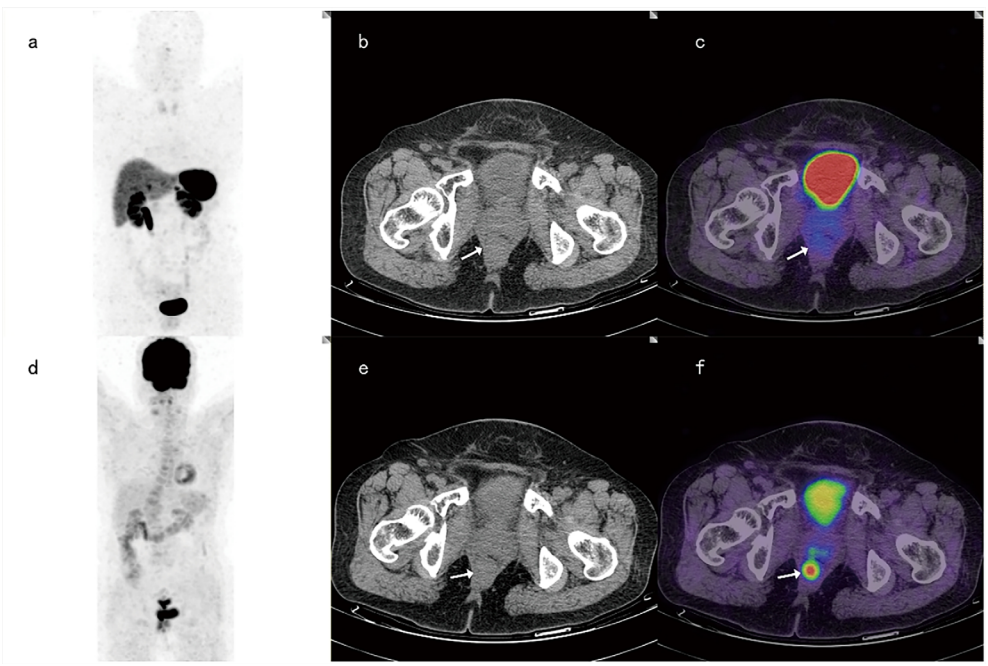


**FIGURE 2** | A 65-year-old female patient with rectal neuroendocrine carcinoma (Ki-67 was 90%). 68Ga-DOTANOC PET-CT images and corresponding MIP images **(A–C)** showed no focal uptake of 68Ga-DOTANOC, while 18F-FDG PET-CT imaging **(D–F)** showed focal uptake of 18F-FDG.

**TABLE 2** | General characteristics of patients who underwent region LN dissection.

| Variables | Value |
|---|---|
| Sex | |
| Male | 6 |
| Female | 5 |
| Age (years) | 38-70 |
| TNM stage | |
| I-III | 6 |
| IV | 5 |
| Grade | |
| G1 | 2 |
| G2 | 8 |
| G3 | 1 |
| LN group metastases | |
| Positive | 18 |
| Negative | 24 |

*TNM, tumor node metastasis; LN, Lymph node.*

### Semiquantitative Assessment

ROC analysis showed that the optimal SUVmax cut-off value with the highest accuracy for predicting malignant nodes through 68Ga-DOTANOC PET was 2.25 with 77.78% sensitivity, 91.67% specificity, 87.50% PPV, 84.62% NPV and 85.71% accuracy. The AUC was 0.824 (95%CI:0.723-0.981) (**Figure 4A** and **Table 4**).

Meanwhile, the optimal SUVmax cut-off value with the highest accuracy for predicting malignant nodes through 18F-FDG PET was 1.05 with 61.11% sensitivity, 75.00% specificity, 64.71% PPV,72.00% NPV and 69.05% accuracy. The AUC was 0.664 (95%CI: 0.485-0.844) (**Figure 4B** and **Table 4**).

## DISCUSSION

This was the first study to evaluate the impact of 68Ga-DOTANOC and 18F-FDG PET-CT in predicting LN metastasis in patients with RNETs. Our study showed that 68Ga-DOTANOC PET-CT showed prospective ability to predict LN metastasis through visual assessment and semiquantitative assessment, which was better than 18F-FDG PET-CT. Meanwhile, the sensitivity of 68Ga-DOTANOC in primary tumors were better than those of 18F-FDG PET-CT.

In our study, the overall sensitivity of 68Ga-DOTANOC PET-CT was 89.58%, and the PPV was 95.56% in primary tumors. Even for G3 tumors, 4/6 of primary tumors could be detected by 68Ga-DOTANOC PET-CT. Several previous studies have shown that the sensitivity of 68GA-DOTANOC PET-CT for detecting gastrointestinal pancreatic primary lesions was 71.4%-94.4% (30–32), suggesting that 68Ga-DOTANOC had good diagnostic sensitivity. Meanwhile, 18F-FDG PET-CT identified 37/48 primary tumors with 77.08% sensitivity in our research, which was similar to the results of Zhang, P et al. (33). Other studies have shown that 18F-FDG PET-CT was not sensitive for diagnosing NETs (sensitivity 33%-66.7%) (19, 34, 35). In our study, the sensitivity of 68Ga-DOTANOC PET-CT was higher than that of 18F-FDG PET-CT for patients with G1-G2 tumors (p=0.039), indicating that 68Ga-DOTANOC was more reliable for the diagnosis of G1-G2 RNETs.

We also found that the combination of 68Ga-DOTANOC and 18F-FDG PET-CT slightly increased the sensitivity to 93.75% in detecting primary tumors. Similarly, a study by Partelli, S. et al. (22) also showed that 68Ga-DOTANOC PET-CT combined with 18F-FDG PET-CT could only slightly increase the sensitivity in pancreatic neuroendocrine tumors, suggesting that 18F-FDG PET-CT is unnecessary for detecting RNETs.

The current literature evaluating 68Ga-DOTANOC PET-CT for diagnosing LN metastasis is limited. Our research showed that 68Ga-DOTANOC PET-CT had 77.78% sensitivity and 91.67% specificity in both visual assessment and semiquantitative assessment for diagnosing LN group metastasis in RNETs, showing that the two evaluation methods were highly consistent. As reported by Ansquer, C (36). 68Ga-DOTANOC PET-CT had a sensitivity of 86.4% in midgut neuroendocrine tumors, and Niraj Naswa reported that 68Ga-DOTANOC had a sensitivity of 92.8% and specificity of 100% in diagnosing LN metastasis for gastroenteropancreatic neuroendocrine tumors (23), indicating that 68Ga-DOTANOC was a good tool for screening LN metastasis.

A study by Majala S. showed that only 33% of LN metastases could be diagnosed through 18F-FDG PET-CT in nonfunctional pancreatic neuroendocrine tumors (24). Meanwhile, another study showed that 68Ga-DOTANOC PET-CT had 94.2% sensitivity, 87.5% specificity, and 92.1% accuracy while 18F-FDG PET-CT had 25.7% sensitivity, 100% specificity, and 49% accuracy in gastroenteropancreatic neuroendocrine tumors (23). In concordance with the above research, our research showed that the sensitivity of 18F-FDG PET-CT for detecting LN group metastasis was only 38.89% in visual assessment and 61.11% in semiquantitative assessment with an AUC of 0.664, which was lower than the sensitivity and AUC of 68Ga-DOTANOC PET-CT (sensitivity was 77.78% and the AUC was 0.854). Therefore, we concluded that 68Ga-DOTANOC

**TABLE 3** | Sensitivity, specificity, positive and negative predictive value and accuracy for the prediction of LN group metastasis by 68Ga-DOTANOC and 18F-FDG PET through visual assessment.

| | 68Ga-DOTANOC PET | 18F-FDG PET | p value |
|---|---|---|---|
| Sensitivity (%) (95% CI) | 77.78 (52.36-93.59) | 38.89 (17.30-64.25) | 0.018 |
| Specificity (%) (95% CI) | 91.67 (73.00-98.97) | 100 | 0.489 |
| PPV (%) (95% CI) | 87.5 (64.48-96.43) | 100 | 1.000 |
| NPV (%) (95% CI) | 84.62 (69.68-92.94) | 69.57 (55.20-80.92) | 0.150 |
| Accuracy (%) (95% CI) | 85.71 (71.46-94.57) | 68.57 (60.15-75.93) | 0.175 |

*PPV, positive predictive value; NPV, negative predictive value.*

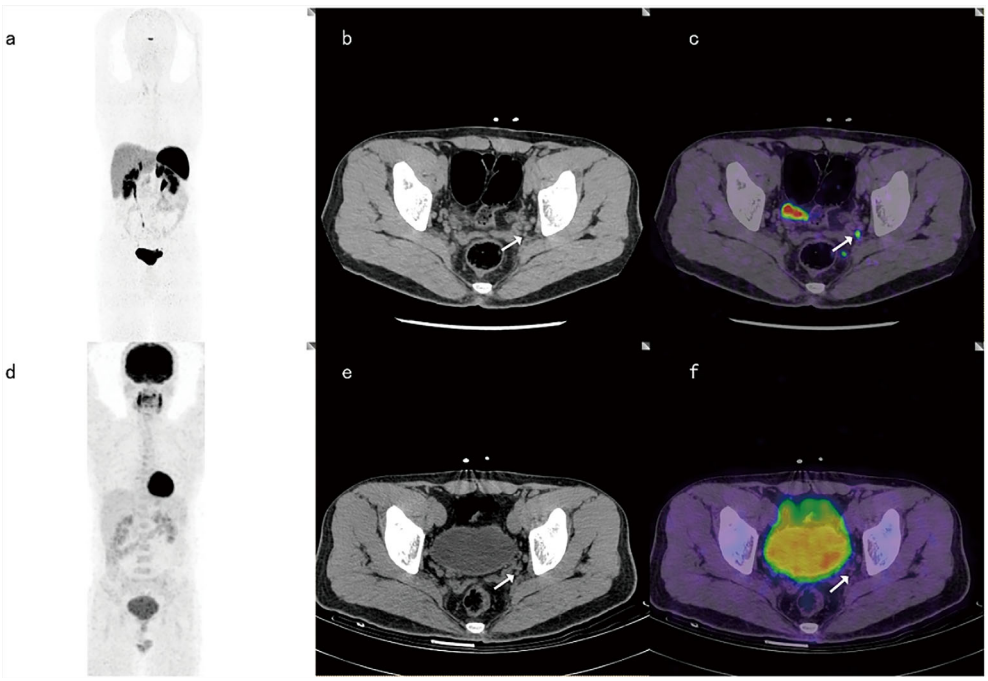


**FIGURE 3** | A 37-year-old male with LN metastasis adjacent to the left iliac blood vessel. The focal uptake of 68Ga-DOTANOC in LNs (as shown by the arrow) was obviously increased **(A–C)**, while the focal uptake of 18F-FDG was similar to that in the background **(D–F)**.

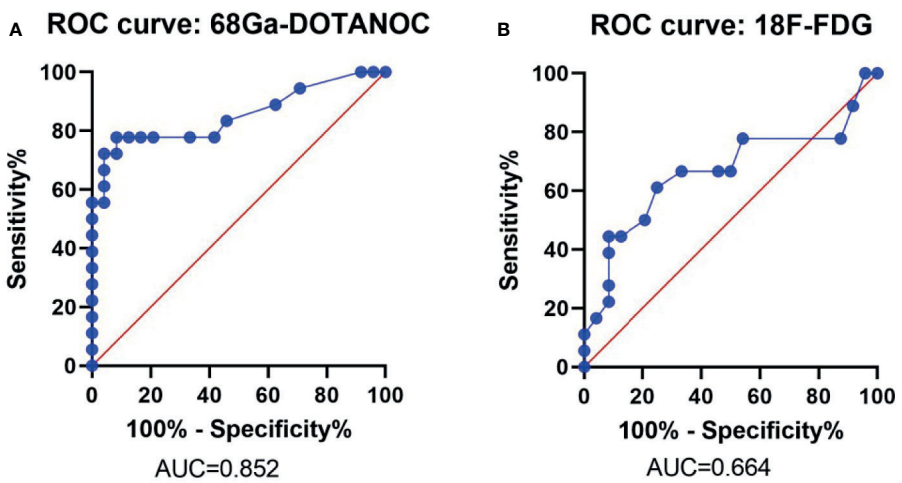


**FIGURE 4** | ROC Curve of the SUVmax of 68Ga-DOTANOC and 18F-FDG PET in predicting LN group metastasis. ROC Curve of 68Ga-DOTANOC PET, The AUC was 0.852 **(A)**; ROC Curve of 18F-FDG PET. The AUC was 0.664 **(B)**. ROC, Receiver Operating Characteristics; AUC, The area under the ROC curves.

PET-CT was more suitable for screening LN group metastasis than 18F-FDG PET-CT.

68Ga-DOTANOC and 18F-FDG PET-CT had similar diagnostic capabilities in evaluating primary tumors but had different diagnostic capabilities in LN metastases. The result may be due to the active lymph node inflammation in the rectal network (37), which affects FDG uptake (38) and cause FDG PET is not reliable for detecting LN metastases of RNETs or maybe 68Ga-DOTANOC is actually better than FDG as N. Naswa reported (23).

**TABLE 4 |** Sensitivity, specificity, positive and negative predictive value, accuracy and AUC for the prediction of LN group metastasis by 68Ga-DOTANOC and 18F-FDG PET through semiquantitative assessment.

| | 68Ga-DOTANOC PET | 18F-FDG PET | p value |
|---|---|---|---|
| Sensitivity (%) (95% CI) | 77.78 (52.36-93.59) | 61.11 (35.75-82.70) | 0.278 |
| Specificity (%) (95% CI) | 91.67 (73.00-98.97) | 75.00 (53.29-90.23) | 0.121 |
| PPV (%) (95% CI) | 87.50 (64.48-96.43) | 64.71 (45.54-80.08) | 0.127 |
| NPV (%) (95% CI) | 84.62 (69.68-92.94) | 72.00 (57.96-82.75) | 0.274 |
| Accuracy (%) (95% CI) | 85.71 (71.46-94.57) | 69.05 (52.91-82.38) | 0.015 |
| AUC (95% CI) | 0.852 (0.723-0.981) | 0.664 (0.485-0.844) | 0.0583 |

*PPV, positive predictive value; NPV, negative predictive value; AUC, Area under ROC curve.*

Usually, in parallel with an increasing tumor proliferation rate (Ki-67 index), 68 Ga-DOTA- somatostatin receptor expression in NETs decreases (39). For NETs with Ki-67 greater than 15%, metabolic imaging with 18 FDG PET-CT is usually preferred rather than 68 Ga-DOTA-somatostatin analog PET-CT because of the low or absent somatostatin receptor expression in NET lesions (40). In our study, most patients had Ki-67 less than 15%, which may explain why the performance of 68Ga-DOTANOC PET-CT was better than 18F-FDG PET-CT. Therefore, 68Ga-DOTANOC PET-CT seems to be more suitable for RNET assessment than 18F-FDG PET-CT, especially in G1-G2 RNETs.

With the emergence of molecular imaging, surgeons are using molecular imaging to image-guided surgery (41). Hybrid detection modalities for image-guided surgery has been applied such as the application of indocyanine green (ICG)-99mTc-nanolloid for cancers (42). Similarly, Håkan Orlefors reported that 11C-5-Hydroxytryptophane PET can localize the NETs (43). However, the hybrid detection modalities for image-guided surgery in NETs are rare. SSTRs such as 68Ga-DOTANOC have high specificity, but whether it is suitable for guided surgery needs further study; meanwhile, combination of image-guided surgery and robot-assisted with laparoscopic surgery may reduce surgical complications in the future (44).

The strengths of the present study are that we evaluated simultaneously the primary tumors and regional LN group histologically of RNETs. However, there are some limitations. Firstly, the major limitation of the present study was the number of patients, as RNETs are rare; therefore, the conclusion should be treated carefully, and more cases need to be studied in the future. Secondly, as the study was retrospective, RCT research is needed.

## DATA AVAILABILITY STATEMENT

The original contributions presented in the study are included in the article/supplementary material. Further inquiries can be directed to the corresponding author.

## ETHICS STATEMENT

The studies involving human participants were reviewed and approved by Ethics Committee of the First Affiliated Hospital of Sun Yat-sen University. The patients/participants provided their written informed consent to participate in this study.

## AUTHOR CONTRIBUTIONS

ZW and GL designed this study. ZZ interpreted the patient data and drafted the manuscript. BZ and YW contributed to data collection. GL and ZXW revised the manuscript. All authors contributed to the article and approved the submitted version.

## FUNDING

This study was funded by the Natural Science Foundation of Guangdong Province, China (Grant Nos. 2016A030310155, 2017A030313577, and 2018A030313978) and the National Natural Science Foundation of China (Grant Nos. 81602049 and 81802342).

## REFERENCES

1. Moertel CG. Karnofsky Memorial Lecture. An Odyssey in the Land of Small Tumors. *J Clin Oncol* (1987) 5:1502–22. doi: 10.1200/JCO.1987.5.10.1502
2. Ahmed M. Gastrointestinal Neuroendocrine Tumors in 2020. *World J Gastrointest Oncol* (2020) 12:791–807. doi: 10.4251/wjgo.v12.i8.791
3. Maggard MA, O'Connell JB, Ko CY. Updated Population-Based Review of Carcinoid Tumors. *Ann Surg* (2004) 240:117–22. doi: 10.1097/01.sla.0000129342.67174.67
4. Kim JY, Hong S-M, Ro JY. Recent Updates on Grading and Classification of Neuroendocrine Tumors. *Ann Diagn Pathol* (2017) 29:11–6. doi: 10.1016/j.anndiagpath.2017.04.005
5. Hauso O, Gustafsson BI, Kidd M, Waldum HL, Drozdov I, Chan AKC, et al. Neuroendocrine Tumor Epidemiology: Contrasting Norway and North America. *Cancer* (2008) 113:2655–64. doi: 10.1002/cncr.23883
6. Garcia-Carbonero R, Capdevila J, Crespo-Herrero G, Díaz-Pérez JA, Martínez Del Prado MP, Alonso Orduña V, et al. Incidence, Patterns of Care and Prognostic Factors for Outcome of Gastroenteropancreatic Neuroendocrine Tumors (GEP-NETs): Results From the National Cancer Registry of Spain (RGETNE). *Ann Oncol* (2010) 21:1794–803. doi: 10.1093/annonc/mdq022
7. Yao JC, Hassan M, Phan A, Dagohoy C, Leary C, Mares JE, et al. One Hundred Years After "Carcinoid": Epidemiology of and Prognostic Factors for Neuroendocrine Tumors in 35,825 Cases in the United States. *J Clin Oncol* (2008) 26:3063–72. doi: 10.1200/JCO.2007.15.4377
8. Masui T, Ito T, Komoto I, Uemoto S. Recent Epidemiology of Patients With Gastro-Entero-Pancreatic Neuroendocrine Neoplasms (GEP-NEN) in Japan: A Population-Based Study. *BMC Cancer* (2020) 20:1104. doi: 10.1186/s12885-020-07581-y
9. Bertani E, Ravizza D, Milione M, Massironi S, Grana CM, Zerini D, et al. Neuroendocrine Neoplasms of Rectum: A Management Update. *Cancer Treat Rev* (2018) 66:45–55. doi: 10.1016/j.ctrv.2018.04.003
10. Goretzki PE, Mogl MT, Akca A, Pratschke J. Curative and Palliative Surgery in Patients With Neuroendocrine Tumors of the Gastro-Entero-Pancreatic (GEP) Tract. *Rev Endocr Metab Disord* (2018) 19:169–78. doi: 10.1007/s11154-018-9469-9

11. Andreasi V, Partelli S, Muffatti F, Manzoni MF, Capurso G, Falconi M. Update on Gastroenteropancreatic Neuroendocrine Tumors. *Dig Liver Dis* (2021) 53:171–82. doi: 10.1016/j.dld.2020.08.031
12. de Mestier L, Lorenzo D, Fine C, Cros J, Hentic O, Walter T, et al. Endoscopic, Transanal, Laparoscopic, and Transabdominal Management of Rectal Neuroendocrine Tumors. *Best Pract Res Clin Endocrinol Metab* (2019) 33:101293. doi: 10.1016/j.beem.2019.101293
13. Refardt J, Hofland J, Kwadwo A, Nicolas GP, Rottenburger C, Fani M, et al. Theranostics in Neuroendocrine Tumors: An Overview of Current Approaches and Future Challenges. *Rev Endocr Metab Disord* (2020) 22:581–4. doi: 10.1007/s11154-020-09552-x
14. Sundin A, Arnold R, Baudin E, Cwikla JB, Eriksson B, Fanti S, et al. ENETS Consensus Guidelines for the Standards of Care in Neuroendocrine Tumors: Radiological, Nuclear Medicine & Hybrid Imaging. *Neuroendocrinology* (2017) 105:212–44. doi: 10.1159/000471879
15. Sanli Y, Garg I, Kandathil A, Kendi T, Zanetti MJB, Kuyumcu S, et al. Neuroendocrine Tumor Diagnosis and Management: Ga-DOTATATE PET/Ct. *AJR Am J Roentgenol* (2018) 211:267–77. doi: 10.2214/AJR.18.19881
16. Tirosh A, Kebebew E. The Utility of Ga-DOTATATE Positron-Emission Tomography/Computed Tomography in the Diagnosis, Management, Follow-Up and Prognosis of Neuroendocrine Tumors. *Future Oncol* (2018) 14:111–22. doi: 10.2217/fon-2017-0393
17. Carideo L, Prosperi D, Panzuto F, Magi L, Pratesi MS, Rinzivillo M, et al. Role of Combined [Ga]Ga-DOTA-SST Analogues and [F]FDG PET/CT in the Management of GEP-NENs: A Systematic Review. *J Clin Med* (2019) 8:1032. doi: 10.3390/jcm8071032
18. Deroose CM, Hindié E, Kebebew E, Goichot B, Pacak K, Taïeb D, et al. Molecular Imaging of Gastroenteropancreatic Neuroendocrine Tumors: Current Status and Future Directions. *J Nucl Med* (2016) 57:1949–56. doi: 10.2967/jnumed.116.179234
19. Rinzivillo M, Partelli S, Prosperi D, Capurso G, Pizzichini P, Iannicelli E, et al. Clinical Usefulness of (18) F-Fluorodeoxyglucose Positron Emission Tomography in the Diagnostic Algorithm of Advanced Entero-Pancreatic Neuroendocrine Neoplasms. *Oncologist* (2018) 23:186–92. doi: 10.1634/theoncologist.2017-0278
20. Alevroudis E, Spei M-E, Chatziioannou SN, Tsoli M, Wallin G, Kaltsas G, et al. Clinical Utility of F-FDG PET in Neuroendocrine Tumors Prior to Peptide Receptor Radionuclide Therapy: A Systematic Review and Meta-Analysis. *Cancers (Basel)* (2021) 13:1813. doi: 10.3390/cancers13081813
21. Imperiale A, Meuter L, Pacak K, Taïeb D. Variants and Pitfalls of PET/CT in Neuroendocrine Tumors. *Semin Nucl Med* (2021) 51:519–28. doi: 10.1053/j.semnuclmed.2021.03.001
22. Partelli S, Rinzivillo M, Maurizi A, Panzuto F, Salgarello M, Polenta V, et al. The Role of Combined Ga-DOTANOC and (18)FDG PET/CT in the Management of Patients With Pancreatic Neuroendocrine Tumors. *Neuroendocrinology* (2014) 100:293–9. doi: 10.1159/000368609
23. Naswa N, Sharma P, Gupta SK, Karunanithi S, Reddy RM, Patnecha M, et al. Dual Tracer Functional Imaging of Gastroenteropancreatic Neuroendocrine Tumors Using 68Ga-DOTA-NOC PET-CT and 18F-FDG PET-CT: Competitive or Complimentary? *Clin Nucl Med* (2014) 39:e27–34. doi: 10.1097/RLU.0b013e31827a216b
24. Majala S, Seppänen H, Kemppainen J, Sundström J, Schalin-Jäntti C, Gullichsen R, et al. Prediction of the Aggressiveness of Non-Functional Pancreatic Neuroendocrine Tumors Based on the Dual-Tracer PET/Ct. *EJNMMI Res* (2019) 9:116. doi: 10.1186/s13550-019-0585-7
25. Ayati N, Lee ST, Zakavi R, Pathmaraj K, Al-Qatawna L, Poon A, et al. Long-Acting Somatostatin Analog Therapy Differentially Alters Ga-DOTATATE Uptake in Normal Tissues Compared With Primary Tumors and Metastatic Lesions. *J Nucl Med* (2018) 59:223–7. doi: 10.2967/jnumed.117.192203
26. Nagtegaal ID, Odze RD, Klimstra D, Paradis V, Rugge M, Schirmacher P, et al. The 2019 WHO Classification of Tumours of the Digestive System. *Histopathology* (2020) 76:182–8. doi: 10.1111/his.13975
27. Yang M, Zeng L, Yao WQ, Ke NW, Tan CL, Tian BL, et al. A Comprehensive Validation of the Novel 8th Edition of American Joint Committee on Cancer Staging Manual for the Long-Term Survivals of Patients With non-Functional Pancreatic Neuroendocrine Neoplasms. *Med (Baltimore)* (2020) 99:e22291. doi: 10.1097/md.0000000000022291
28. Japanese Society for Cancer of the Colon and Rectum. Japanese Classification of Colorectal, Appendiceal, and Anal Carcinoma: The 3D English Edition [Secondary Publication]. *J Anus Rectum Colon* (2019) 3:175–95. doi: 10.23922/jarc.2019-018
29. He Q, Zhang B, Zhang L, Chen Z, Shi X, Yi C, et al. Diagnostic Efficiency of Ga-DOTANOC PET/CT in Patients With Suspected Tumour-Induced Osteomalacia. *Eur Radiol* (2021) 31:2414–21. doi: 10.1007/s00330-020-07342-2
30. Wild D, Bomanji JB, Benkert P, Maecke H, Ell PJ, Reubi JC, et al. Comparison of 68Ga-DOTANOC and 68Ga-DOTATATE PET/CT Within Patients With Gastroenteropancreatic Neuroendocrine Tumors. *J Nucl Med* (2013) 54:364–72. doi: 10.2967/jnumed.112.111724
31. Sharma A, Das CJ, Makharia GK, Arora G, Kumar R. Comparison of Contrast-Enhanced CT + CT Enterography and 68Ga-DOTANOC PET/CT in Gastroenteropancreatic Neuroendocrine Tumors. *Clin Nucl Med* (2020) 45:848–53. doi: 10.1097/RLU.0000000000003188
32. Naswa N, Sharma P, Kumar A, Nazar AH, Kumar R, Chumber S, et al. Gallium-68-DOTA-NOC PET/CT of Patients With Gastroenteropancreatic Neuroendocrine Tumors: A Prospective Single-Center Study. *AJR Am J Roentgenol* (2011) 197:1221–8. doi: 10.2214/AJR.11.7298
33. Zhang P, Yu J, Li J, Shen L, Li N, Zhu H, et al. Clinical and Prognostic Value of PET/CT Imaging With Combination of (68)Ga-DOTATATE and (18)F-FDG in Gastroenteropancreatic Neuroendocrine Neoplasms. *Contrast Media Mol Imaging* (2018) 2018:2340389. doi: 10.1155/2018/2340389
34. Has Simsek D, Kuyumcu S, Turkmen C, Sanlı Y, Aykan F, Unal S, et al. Can Complementary 68Ga-DOTATATE and 18F-FDG PET/CT Establish the Missing Link Between Histopathology and Therapeutic Approach in Gastroenteropancreatic Neuroendocrine Tumors? *J Nucl Med* (2014) 55:1811–7. doi: 10.2967/jnumed.114.142224
35. Kayani I, Bomanji JB, Groves A, Conway G, Gacinovic S, Win T, et al. Functional Imaging of Neuroendocrine Tumors With Combined PET/CT Using 68Ga-DOTATATE (DOTA-DPhe1,Tyr3-Octreotate) and 18F-FDG. *Cancer* (2008) 112:2447–55. doi: 10.1002/cncr.23469
36. Ansquer C, Touchefeu Y, Faivre-Chauvet A, Leux C, Le Bras M, Régenet N, et al. Head-To-Head Comparison of 18F-DOPA PET/CT and 68Ga-DOTANOC PET/CT in Patients With Midgut Neuroendocrine Tumors. *Clin Nucl Med* (2021) 46:181–6. doi: 10.1097/RLU.0000000000003450
37. Pijl JP, Nienhuis PH, Kwee TC, Glaudemans AWJM, Slart RHJA, Gormsen LC. Limitations and Pitfalls of FDG-PET/CT in Infection and Inflammation. *Semin Nucl Med* (2021) S0001-2998(21)00040-4. doi: 10.1053/j.semnuclmed.2021.06.008
38. Kubota K. From Tumor Biology to Clinical Pet: A Review of Positron Emission Tomography (PET) in Oncology. *Ann Nucl Med* (2001) 15:471–86. doi: 10.1007/BF02988499
39. Sundin A. Novel Functional Imaging of Neuroendocrine Tumors. *Endocrinol Metab Clin North Am* (2018) 47:505–23. doi: 10.1016/j.ecl.2018.04.003
40. Binderup T, Knigge U, Loft A, Mortensen J, Pfeifer A, Federspiel B, et al. Functional Imaging of Neuroendocrine Tumors: A Head-to-Head Comparison of Somatostatin Receptor Scintigraphy, 123I-MIBG Scintigraphy, and 18F-FDG PET. *J Nucl Med* (2010) 51:704–12. doi: 10.2967/jnumed.109.069765
41. Mondal SB, O'Brien CM, Bishop K, Fields RC, Margenthaler JA, Achilefu S. Repurposing Molecular Imaging and Sensing for Cancer Image-Guided Surgery. *J Nucl Med* (2020) 61:1113–22. doi: 10.2967/jnumed.118.220426
42. Van Oosterom MN, Rietbergen DDD, Welling MM, van der Poel HG, Maurer T, Van Leeuwen FWB. Recent Advances in Nuclear and Hybrid Detection Modalities for Image-Guided Surgery. *Expert Rev Med Devices* (2019) 16:711–34. doi: 10.1080/17434440.2019.1642104
43. Orlefors H, Sundin A, Eriksson B, Skogseid B, Oberg K, Akerström G, et al. PET-Guided Surgery - High Correlation Between Positron Emission Tomography With 11C-5-Hydroxytryptophane (5-HTP) and Surgical Findings in Abdominal Neuroendocrine Tumours. *Cancers (Basel)* (2012) 4:100–12. doi: 10.3390/cancers4010100
44. Meershoek P, van Oosterom MN, Simon H, Mengus L, Maurer T, van Leeuwen PJ, et al. Robot-Assisted Laparoscopic Surgery Using DROP-IN

Radioguidance: First-in-Human Translation. *Eur J Nucl Med Mol Imaging* (2019) 46:49–53. doi: 10.1007/s00259-018-4095-z

**Conflict of Interest:** The authors declare that the research was conducted in the absence of any commercial or financial relationships that could be construed as a potential conflict of interest.

**Publisher's Note:** All claims expressed in this article are solely those of the authors and do not necessarily represent those of their affiliated organizations, or those of the publisher, the editors and the reviewers. Any product that may be evaluated in this article, or claim that may be made by its manufacturer, is not guaranteed or endorsed by the publisher.

frontiers in Endocrinology

CASE REPORT
published: 08 September 2021
doi: 10.3389/fendo.2021.693004

# Catecholaminergic Crisis After a Bleeding Complication of COVID-19 Infection: A Case Report

*Angel Rebollo-Román[1,2†], Maria R. Alhambra-Expósito[1,2†], Yiraldine Herrera-Martínez[3], F. Leiva-Cepas[2,4], Carlos Alzas[1], Concepcion Muñoz-Jiménez[1,2], R. Ortega-Salas[2,4], María J. Molina-Puertas[1,2], Maria A. Gálvez-Moreno[1,2*] and Aura D. Herrera-Martínez[1,2*]*

[1] Endocrinology and Nutrition Service, Reina Sofia University Hospital, Córdoba, Spain, [2] Maimonides Institute for Biomedical Research of Córdoba, Córdoba, Spain, [3] Nuclear Medicine Service, Virgen del Rocio University Hospital, Seville, Spain, [4] Pathology Service, Reina Sofia University Hospital, Córdoba, Spain

The severe acute respiratory syndrome coronavirus 2 (SARS-CoV-2) presents in some cases with hemostatic and thrombotic complications. Pheochromocytomas are unusual, though potentially lethal tumors. Herein we describe the first case of hemorrhage in a pheochromocytoma related to SARS-CoV-2 infection. A 62-year-old man consulted for syncope, fever, and palpitations. He was diagnosed with SARS-CoV-2 pneumonia and presented with a hemorrhage in a previously unknown adrenal mass, which resulted in a catecholaminergic crisis. Medical treatment and surgery were required for symptom control and stabilization. We hereby alert clinicians to watch for additional/unreported clinical manifestations in COVID-19 infection.

**Keywords: bleeding, pheochromocytoma, COVID19, catecholamines, complication**

OPEN ACCESS

***Edited by:***
*Antongiulio Faggiano, Sapienza University of Rome, Italy*

***Reviewed by:***
*Ana Laura Márquez-Aguirre, CONACYT Centro de Investigación y Asistencia en Tecnología y Diseño del Estado de Jalisco (CIATEJ), Mexico*
*Jose Alberto Choreño Parra, Instituto Politécnico Nacional de México (IPN), Mexico*

***Correspondence:**
*Aura D. Herrera-Martínez*
*aurita.dhm@gmail.com*
*Maria A. Gálvez-Moreno*
*mariaa.galvez.sspa@juntadeandalucia.es*

*†These authors have contributed equally to this work*

***Specialty section:***
*This article was submitted to Cancer Endocrinology, a section of the journal Frontiers in Endocrinology*

***Received:*** *09 April 2021*
***Accepted:*** *04 June 2021*
***Published:*** *08 September 2021*

***Citation:***
*Rebollo-Román A, Alhambra-Expósito MR, Herrera-Martínez Y, Leiva-Cepas F, Alzas C, Muñoz-Jiménez C, Ortega-Salas R, Molina-Puertas MJ, Gálvez-Moreno MA and Herrera-Martínez AD (2021) Catecholaminergic Crisis After a Bleeding Complication of COVID-19 Infection: A Case Report. Front. Endocrinol. 12:693004. doi: 10.3389/fendo.2021.693004*

## INTRODUCTION

Pheochromocytomas are rare tumors derived from the adrenal medulla. Usually germline or somatic gene mutations are implicated, resulting in sporadic tumors, or associated with hereditary syndromes. These tumors might be diagnosed incidentally or due to clinical symptoms due to catecholamine overproduction or to a mass effect, but are rarely diagnosed because of intratumoral hemorrhage. Diagnosis is confirmed by elevated plasma/urine metanephrines or normetanephrines; additionally, imaging is necessary for tumor location and the evaluation of local invasion or metastases (1).

**Abbreviations:** SARS-CoV-2, severe acute respiratory syndrome coronavirus 2; COVID-19, Coronavirus disease 2019; HBP, high blood pressure; CT, computed tomography; PCR, polymerase chain reaction; [$^{18}$ F] DOPA-PET, 6-fluoro-($^{18}$F)-L-3,4-dihydroxyphenylalanine positron emission tomography; MRI, magnetic resonance imaging.

Coronavirus disease 2019 (COVID-19), caused by severe acute respiratory syndrome coronavirus 2 (SARS-CoV-2), has resulted in an emerging respiratory infection with pandemical diffusion since January 2020 (2). SARS-Cov-2 infection has been associated with several complications, including thrombosis and bleeding in comparable rates in patients with similar degrees of critical illness (3).

Although intratumoral hemorrhage in pheocromocytomas is a very rare manifestation of this tumor, some cases have been previously described, especially related with trauma or systemic

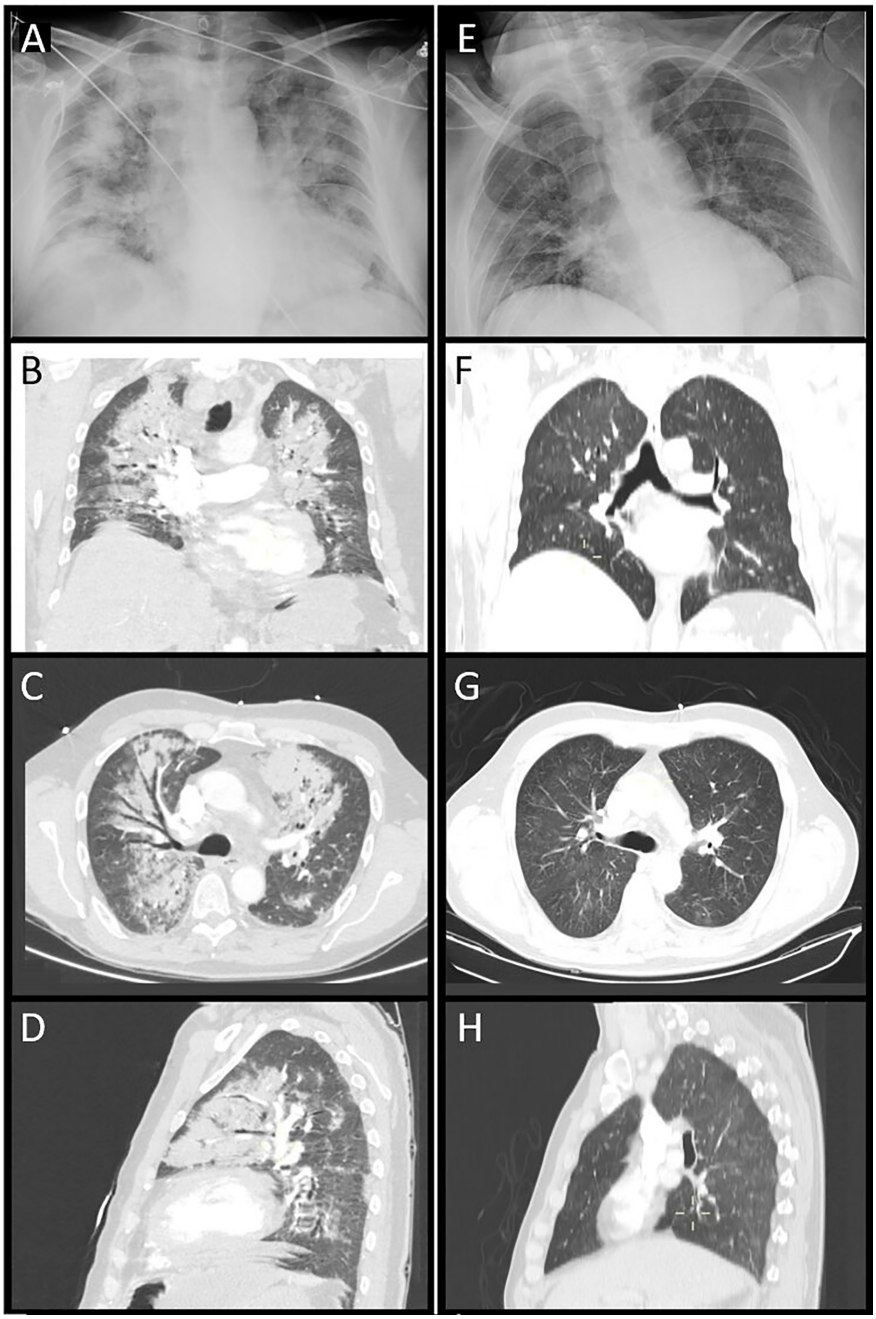


**FIGURE 1** | Thorax radiography **(A)** and CT images [coronal view, **(B)**; axial view, **(C)**; sagittal view, **(D)**]. Diffuse bilateral patched consolidations with open bronchi inside and ground-glass opacities due to COVID-19 infection. Thorax radiography **(E)** and CT control images. Two weeks after treatment [coronal view, **(F)**; axial view, **(G)**; sagittal view, **(H)**], significant improvement of the pneumonia is observed.

anticoagulation (4–6); in most cases, any underlying cause was identified (7). In these patients, less than 30% had a previous history that suggested a pheochromocytoma (8, 9). Mortality rate in these cases reaches 28–31%, but lower rates should be currently expected due to early diagnosis and appropriate alpha blockage (7, 10).

It is suggested that paroxysms of hypertension or necrosis increase intratumoral intravascular pressure and may produce hemorrhage (11, 12). Trauma, thrombolysis, anticoagulants, or alpha-blockers could act as initiating factors (4–7, 10). Viral infections have not been previously described as precipitator of intratumor hemorrhage in pheocromocytomas.

Herein, we report, to the best of our knowledge, the first case of intratumoral hemorrhage of a pheochromocytoma in the context of a SARS-CoV-2 infection.

## CASE REPORT

A 62-year-old patient presented to the emergency department with recurrent fainting episodes accompanied by asthenia and dry cough. Clinical symptoms appeared one week before consultation. The patient had a personal history of high blood pressure (HBP) treated with four drugs (losartan, hydrochlorothiazide, amlodipine, and furosemide). No previous history of bleeding or any other disease was described.

Upon his arrival, blood pressure was 97/52 mmHg with a heart rate of 100 bpm. The chest X-ray showed converging diffuse condensations in both pulmonary fields, predominantly central, suggestive of evolutioned SARS-CoV-2 infection (**Figure 1A**). Arterial blood gas analysis showed hypoxemia and hypocapnia; additionally, high white blood cell count with neutrophilia and elevated D-dimer were observed (**Table 1**). Given the low BP, the global respiratory insufficiency and a high suspicion of SARS-Cov-2 infection, a CT pulmonary angiogram was performed in order to rule out a pulmonary embolism. Bilateral patched consolidations with open bronchi inside and ground-glass opacities and no filling defects were observed in the pulmonary arteries (**Figures 1B–D**). The lower images of the scan revealed an adrenal left mass (8 × 7.4 cm) with a cystic component and a big calcification, suggestive of a hematoma or pseudocyst (**Figures 2A, B**). These results were confirmed in a MRI (**Figures 2C, D**).

**TABLE 1** | Laboratory parameters.

| Parameter | Admission | Discharge |
|---|---|---|
| Hemoglobin | 14.5 g/dl | 8.5 g/dl |
| White blood cell count | 19,350 WBC/mcL | 13,390 WBC/mcL |
| C-reactive protein | 166 mg/L | 166 mg/L |
| pO2 (mmHg) | 53 | 94 |
| pCO2 (mmHg) | 26 | 40 |
| Plasma free metanephrines (N < 90 pg/ml) | 350 | <15 |
| Plasma free normetanephrines (N < 180 pg/ml) | 231 | 18 |
| 24-h urine fractionated metanephrines (N < 341 mcg/24 h) | 4,032.6 | – |
| 24-h urine fractionated normetanephrines (N < 444 mcg/24 h) | 1,990.34 | – |

*N, normal.*

Given the hemodynamic instability and the global respiratory insufficiency secondary to SARS-Cov-2 infection, the patient was admitted to the intensive care unit. Previous SARS-CoV-2 infection was confirmed using serological tests, nasopharyngeal swab, and bronchoalveolar lavage PCR. Two days after admission, respiratory symptoms improved but the patient remained hemodynamically unstable, alternating hypotension and hypertensive crises. Initially, intravenous treatment with noradrenaline 0.2 mcg/kg/min was administered but after 48 h, it was stopped.

Elevated plasma and 24-h urinary metanephrine and normetanephrine were detected (**Table 1**). Simultaneously, hemoglobin levels dropped 2 g/dl. An 18-F-DOPA PET/CT was performed and revealed high aminoacidic metabolism in the peripheral area of the adrenal mass, with a central hypodense area with calcifications without metabolism, suggesting a pheochromocytoma with internal necrotic/cystic/hemorrhagic component (**Figures 2E, F**). An open adrenalectomy with splenectomy was performed after adequate alpha- and beta-blockade using low-doses of doxazosin (2 mg/12 h) and bisoprolol (5 mg/d). The histological analysis reported a pseudoencapsulated pheochromocytoma of 7 × 5 × 4 cm and 340 g, with focal calcification, intratumor hemorrhage and 60% of necrosis without vascular or peritumoral invasion (**Figure 3**). Clinical and radiological improvements of the pneumonia were also observed (**Figures 1E–H**). A summary of biochemical parameters at admission and at discharged are depicted in **Table 1**. Eleven months after surgery the patient remains asymptomatic, without evidence of relapsed disease and requires any antihypertensive drugs.

## DISCUSSION

SARS-Cov-2 infection has several clinical presentations, ranging from asymptomatic patients to mild symptoms and acute severe respiratory stress (2). Global mortality reaches 5.44% of cases, mostly related to respiratory insufficiency with hypoxia or multiple organ dysfunction (13), additionally some patients suffer severe systemic hyperinflammatory reaction (cytokine storm), which reminds that hemophagocytic lymphohistiocytosis is also triggered by other viral infections (5).

SARS-CoV-2 infection can be associated with coagulopathy alterations, probably due to infection-induced inflammatory changes, similar to those observed in patients with disseminated intravascular coagulation. Initially, coagulopathy presents with prominent elevation of D-dimer and fibrin/fibrinogen degradation products; in contrast, abnormalities in prothrombin time, partial thromboplastin time or platelet count are uncommon at a first stage of disease (3).

In this context, some cases of post-COVID19 spontaneous hemorrhage, including intracranial, pulmonary, abdominal, pelvic, and muscular hemorrhage, have been described (14). In some patients, this spontaneous hemorrhage has been reported as the presenting symptom of SARS-Cov-2 infection (15, 16). A multicenter, retrospective study performed in 400 hospital-admitted SARS-Cov-2 infected patients reported thrombocytopenia and decreased fibrinogen as clinical factors associated with significant

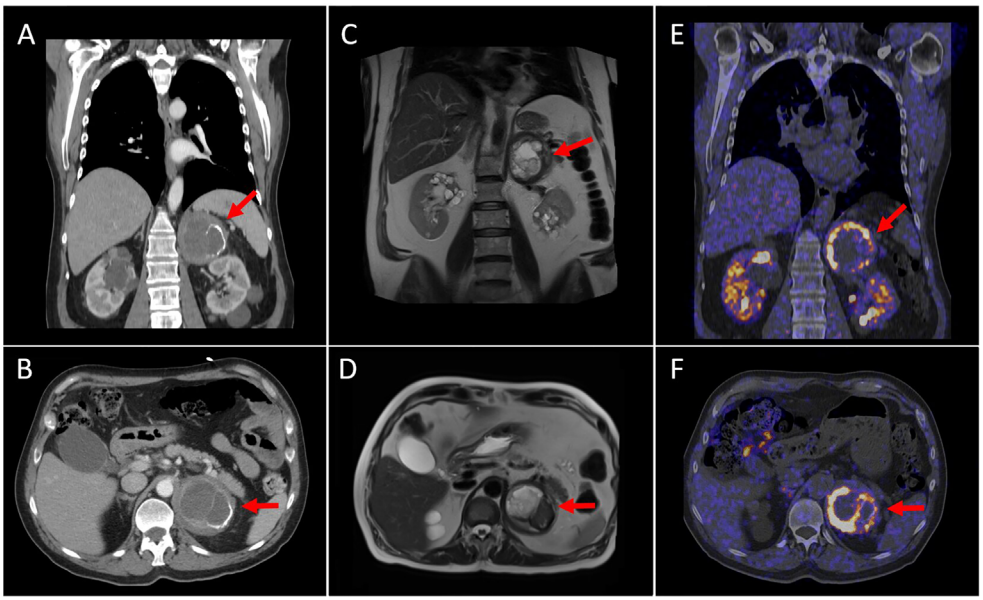


**FIGURE 2** | Coronal and axial CT views **(A, B)** show an 8 cm left adrenal tumor with a cystic component inside and partially calcified wall. Coronal and axial MRI views **(C, D)** reveal a left adrenal mass with a heterogeneous content (necrotic-cystic areas). Coronal and axial [$^{18}$ F] DOPA PET/CT images **(E, F)** demonstrate intense and heterogeneous DOPA-uptake in the periphery of the mass (SUVmax of 20.9). These findings were compatible with the existence of pheochromocytoma with a cystic–necrotic–hemorrhagic component.

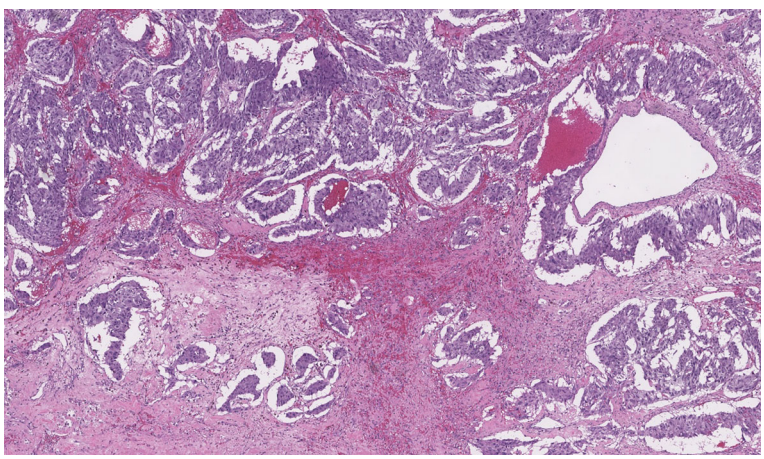

**FIGURE 3** | Histological characteristics of the resected tumor. Hematoxylin eosin images that show intratumor hemorrhage and 60% of necrosis without vascular or peritumoral invasion.

bleeding manifestations (17); in this study, the overall bleeding rate was 4.8% (95% CI, 2.9–7.3%), specifically 3.1% (95% CI, 1.4–6.1%) in non-critically ill patients and 7.6% (95% CI, 3.9–13.3%) in critically ill patients. Remarkably, the major bleeding rate (WHO grade 3–4) was 2.3% (95% CI, 1.0–4.2%) (17), compared with the 5.6% rate observed in critically ill patients without SARS-Cov-2 infection and heparin thromboprophylaxis (18).

Furthermore, increased mortality rate has been described in patients with spontaneous intraabdominal hemorrhage; for example, a spontaneous hematoma in the ileo-psoas increases mortality rate by 28% in an intensive care unit (14). In this context, several institutions recommend personalizing the use of low molecular weight heparin or unfractionated heparin infusions in patients with SARS-Cov-2 infection (with elevated

D-dimer levels and without known thrombotic complications), since the risk of hemorrhage is also present in these patients (19).

Herein we report a case with probable coagulation disturbances after a SARS-Cov-2 infection, which provoked adrenal mass bleeding and consequently catecholamine liberation; as a result, a catecholaminergic crisis was observed in this patient with incidental pheochromocytoma. Importantly, acute hemorrhage represents a differential diagnosis in this patient, but acute hemorrhagic rupture as the initial manifestation of pheochromocytoma is rare (10), and might be related with increased intratumoral intravascular pressure that may be precipitated by paroxysms of hypertension or necrosis (11, 20).

In our patient, D-dimer was elevated at the moment of his arrival. During the early phase of SARS-CoV-2 infection, coagulation test abnormalities are seen, but they do not result in clinical bleeding. Whether the initial coagulation changes seen in infected patients progress linearly to sepsis-induced coagulopathy and then to disseminated intravascular coagulopathy as a result of SARS-CoV-2 infection is still to be determined (3). Currently, it is not known whether the underlying cause of the elevated D-dimer levels, bleeding, and thrombotic manifestations in the SARS-Cov-2 infection are related to a pathophysiological-distinct viral coagulopathy or a coagulation system activation due to severe inflammation (17).

In summary, to the best of our knowledge, this is the first case report of adrenal hemorrhage in a pheochromocytoma related to SARS-CoV-2. Based on the current short experience and the chronological association, SARS-CoV-2 may be considered accountable for the hemorrhage in this patient.

## DATA AVAILABILITY STATEMENT

The raw data supporting the conclusions of this article will be made available by the authors, without undue reservation.

## ETHICS STATEMENT

Written informed consent was obtained from the individual(s) for the publication of any potentially identifiable images or data included in this article.

## AUTHOR CONTRIBUTIONS

All authors have equally contributed to clinical follow-up of the patient and the preparation of this manuscript. All authors contributed to the article and approved the submitted version.

## FUNDING

This work was funded by Instituto de Salud Carlos III, co-funded by European Union (ISCIII-AES-2019/002525). Abbott Nutrition kindly contributed with the publication fee of this article. The funder was not involved in the study design, collection, analysis, interpretation of data, the writing of the manuscript or the decision to submit it for publication.

## REFERENCES

1. Farrugia FA, Charalampopoulos A. Pheochromocytoma. *Endocr Regul* (2019) 53:191–212. doi: 10.2478/enr-2019-0020
2. Zhu N, Zhang D, Wang W, Li X, Yang B, Song J, et al. A Novel Coronavirus From Patients With Pneumonia in China, 2019. *N Engl J Med* (2020) 382:727–33. doi: 10.1056/NEJMoa2001017
3. Connors JM, Levy JH. Covid-19 and Its Implications for Thrombosis and Anticoagulation. *Blood* (2020) 135:2033–40. doi: 10.1182/blood.2020006000
4. Shaw TR, Rafferty P and Tait GW. Transient Shock and Myocardial Impairment Caused by Phaeochromocytoma Crisis. *Br Heart J* (1987) 57:194–8. doi: 10.1136/hrt.57.2.194
5. Primhak RA, Spicer RD and Variend S. Sudden Death After Minor Abdominal Trauma: An Unusual Presentation of Phaeochromocytoma. *Br Med J (Clin Res Ed)* (1986) 292:95–6. doi: 10.1136/bmj.292.6513.95
6. May EE, Beal AL and Beilman GJ. Traumatic Hemorrhage of Occult Pheochromocytoma: A Case Report and Review of the Literature. *Am Surg* (2000) 66:720–4.
7. Brown H, Goldberg PA, Selter JG, Cabin HS, Marieb NJ, Udelsman R and Setaro JF. Hemorrhagic Pheochromocytoma Associated With Systemic Corticosteroid Therapy and Presenting as Myocardial Infarction With Severe Hypertension. *J Clin Endocrinol Metab* (2005) 90:563–9. doi: 10.1210/jc.2004-1077
8. Kobayashi T, Iwai A, Takahashi R, Ide Y, Nishizawa K, Mitsumori K. Spontaneous Rupture of Adrenal Pheochromocytoma: Review and Analysis of Prognostic Factors. *J Surg Oncol* (2005) 90:31–5. doi: 10.1002/jso.20234
9. Habib M, Tarazi I and Batta M. Arterial Embolization for Ruptured Adrenal Pheochromocytoma. *Curr Oncol* (2010) 17:65–70. doi: 10.3747/co.v17i6.597
10. Souiki T, Tekni Z, Laachach H, Bennani A, Zrihni Y, Tadmori A, et al. Catastrophic Hemorrhage of Adrenal Pheochromocytoma Following Thrombolysis for Acute Myocardial Infarction: Case Report and Literature Review. *World J Emerg Surg* (2014) 9:50. doi: 10.1186/1749-7922-9-50
11. Kumar S, Nanjappa B, Kumar S, Prasad S, Pushkarna A and Singh SK. Adrenal Artery Pseudoaneurysm in Pheochromocytoma Presenting With Catastrophic Retroperitoneal Haemorrhage. *Can Urol Assoc J* (2013) 7:E254–6. doi: 10.5489/cuaj.541
12. Park JH, Kang KP, Lee SJ, Kim CH, Park TS, Baek HS. A Case of a Ruptured Pheochromocytoma With an Intratumoral Aneurysm Managed by Coil Embolization. *Endocr J* (2003) 50:653–6. doi: 10.1507/endocrj.50.653
13. Wu Z, McGoogan JM. Characteristics of and Important Lessons From the Coronavirus Disease 2019 (Covid-19) Outbreak in China: Summary of a Report of 72314 Cases From the Chinese Center for Disease Control and Prevention. *JAMA* (2020) 23(13):1239–42. doi: 10.1001/jama.2020.2648
14. Artzner T, Clere-Jehl R, Schenck M, Greget M, Merdji H, De Marini P, et al. Spontaneous Ilio-Psoas Hematomas Complicating Intensive Care Unit Hospitalizations. *PloS One* (2019) 14:e0211680. doi: 10.1371/journal.pone.0211680
15. Craen A, Logan G and Ganti L. Novel Coronavirus Disease 2019 and Subarachnoid Hemorrhage: A Case Report. *Cureus* (2020) 12:e7846. doi: 10.7759/cureus.7846
16. Ghosh R, Dubey S, Kanti Ray B, Chatterjee S, Benito-Leon J. Covid-19 Presenting With Thalamic Hemorrhage Unmasking Moyamoya Angiopathy. *Can J Neurol Sci* (2020) 1–3. doi: 10.1017/cjn.2020.117
17. Al-Samkari H, Karp Leaf RS, Dzik WH, Carlson JC, Fogerty AE, Waheed A, et al. COVID and Coagulation: Bleeding and Thrombotic Manifestations of SARS-CoV2 Infection. *Blood* (2020) 136(4):489–500. doi: 10.1182/blood.2020006520
18. Lauzier F, Arnold DM, Rabbat C, Heels-Ansdell D, Zarychanski R, Dodek P, et al. Risk Factors and Impact of Major Bleeding in Critically Ill Patients Receiving Heparin Thromboprophylaxis. *Intensive Care Med* (2013) 39:2135–43. doi: 10.1007/s00134-013-3044-3
19. Obi AT, Barnes GD, Wakefield TW, Brown S, Eliason JL, Arndt E and Henke PK. Practical Diagnosis and Treatment of Suspected Venous Thromboembolism During COVID-19 Pandemic. *J Vasc Surg Venous Lymphat Disord* (2020) 8:526–34. doi: 10.1016/j.jvsv.2020.04.009

20. Mussig K, Horger M, Haring HU and Wehrmann M. Spontaneous Rupture of Malignant Adrenal Phaeochromocytoma. *Emerg Med J* (2008) 25:242. doi: 10.1136/emj.2007.052076

**Conflict of Interest:** The authors declare that the research was conducted in the absence of any commercial or financial relationships that could be construed as a potential conflict of interest.

**Publisher's Note:** All claims expressed in this article are solely those of the authors and do not necessarily represent those of their affiliated organizations, or those of the publisher, the editors and the reviewers. Any product that may be evaluated in this article, or claim that may be made by its manufacturer, is not guaranteed or endorsed by the publisher.

frontiers in Endocrinology

CASE REPORT
published: 25 October 2021
doi: 10.3389/fendo.2021.766234

# Spontaneous Remission After a Hypercalcemic Crisis Caused by an Intracystic Hemorrhage of Bilateral Parathyroid Adenomas: A Case Report and Literature Review

*Yaoxia Liu[1,2,3†], Jianwei Li[1†], Hui Liu[1], Han Yang[1], Jingtao Qiao[1], Tao Wei[4], Tao Wang[5,6,7*] and Yerong Yu[1*]*

[1] Department of Endocrinology and Metabolism, West China School of Medicine/West China Hospital of Sichuan University, Chengdu, China, [2] Department of Geriatrics, Sichuan Provincial People's Hospital, University of Electronic Science and Technology of China, Chengdu, China, [3] Department of Geriatrics, Chinese Academy of Sciences Sichuan Translational Medicine Research Hospital, Chengdu, China, [4] Department of Thyroid Surgery, West China School of Medicine/West China Hospital of Sichuan University, Chengdu, China, [5] Department of Pediatrics, West China Second University Hospital, Sichuan University, Chengdu, China, [6] The Cardiac Development and Early Intervention Unit, West China Institute of Women and Children's Health, West China Second University Hospital, Sichuan University, Chengdu, China, [7] Key Laboratory of Birth Defects and Related Diseases of Women and Children (Sichuan University), Ministry of Education, Chengdu, China

**Background:** Hyperparathyroidism is a common cause of hypercalcemia; however, spontaneous remission after a hypercalcemic crisis caused by an intracystic hemorrhage of parathyroid adenomas is very rare. The question, then, is "What is the best treatment strategy for this type of case?"

**Method:** A 47-year-old male patient with primary hyperparathyroidism and a hypercalcemic crisis is reported. Hypercalcemia was spontaneously relieved thereafter. Postoperative paraffin pathology results indicated an intracystic hemorrhage of bilateral parathyroid adenomas.

**Results:** After the case report, a literature review is also included to summarize the clinical features of this patient and to provide special reference for clinical diagnosis and treatment of similar cases.

**Conclusions:** The choice of surgical timing for such cases can be made based on the comprehensive consideration of clinical symptoms and changes in parathyroid function.

**Keywords: hypercalcemic crisis, spontaneous remission, hemorrhage, parathyroid adenoma, primary hyperparathyroidism**

OPEN ACCESS

***Edited by:***
*Antongiulio Faggiano, Sapienza University of Rome, Italy*

***Reviewed by:***
*Gallia Graiani, University of Parma, Italy*
*Zhenyu Li, Chongqing University, China*

***Correspondence:**
*Tao Wang*
*44871875@qq.com*
*Yerong Yu*
*yuyerong0919@163.com*

*†These authors have contributed equally to this work and share first authorship*

***Specialty section:***
*This article was submitted to Cancer Endocrinology, a section of the journal Frontiers in Endocrinology*

***Received:*** *28 August 2021*
***Accepted:*** *28 September 2021*
***Published:*** *25 October 2021*

***Citation:***
*Liu Y, Li J, Liu H, Yang H, Qiao J, Wei T, Wang T and Yu Y (2021) Spontaneous Remission After a Hypercalcemic Crisis Caused by an Intracystic Hemorrhage of Bilateral Parathyroid Adenomas: A Case Report and Literature Review. Front. Endocrinol. 12:766234. doi: 10.3389/fendo.2021.766234*

## INTRODUCTION

Hyperparathyroidism is the most common cause of hypercalcemia, but spontaneous remission after a hypercalcemic crisis caused by hemorrhage of parathyroid adenomas is very rare. There have been no reports involving an intracystic hemorrhage of bilateral parathyroid adenomas. It is generally believed that hemorrhage of parathyroid adenomas may be caused by rapid tumor growth with an insufficient blood supply to the tumor (1). The patients may present with a diversity of clinical features due to differing degrees of hemorrhage and necrosis of the parathyroid adenoma cells (2). Indeed, there has not been a literature review on the appropriate clinical decision for spontaneous remission of parathyroid function following an intracystic hemorrhage of parathyroid adenomas.

## CASE DESCRIPTION

A 47-year-old male patient was referred to onset of excessive thirst and polydipsia more than 1 month ago, accompanied by general malaise and anorexia. Two weeks ago he went to a local hospital due to abdominal discomfort and the blood biochemical test revealed both elevated serum creatinine (172.9 umol/L,Ref. 63-109 umol/L) and calcium level(4.66 mmol/l, Ref. 2.1-2.7 mmol/L), a declined phosphorus level(1.76 mmol/l, Ref. 0.81-1.45 mmol/L). The blood sodium, potassium, and glucose levels were all normal. The patient was then referred to our hospital for further evaluation. The patient was previously healthy, without psycho-social disease,trauma history, nor drug use. He also denied the family history of hypercalcemia. Physical examination revealed the following: T, 36.5°C; P, 91/min; R, 20/min; and BP, 139/96 mmHg. No abnormalities were detected on examination of the heart, lungs, and abdomen. There was a grade II goiter (**Figure 1A**), with a 4 x 4 cm mass palpable in front of the neck. The masses had hard texture with poor mobility and no tenderness. The results of blood biochemical testing on the day after admission were as follows: creatinine 195 umol/L; estimated glomerular filtration rate 34.3 ml/min/1.73m$^2$; calcium 3.80 mmol/L; phosphorus 1.24 mmol/L; and PTH, 320.7 pmol/L (Ref. 1.6-6.9 pmol/L).

The patient was given isotonic saline infusion (200 to 300 mL/hour) to correct volume depletion, a loop diuretic [furosemide (20 mg iv qd for 2 days)] to increase calcium excretion, and a single dose of salmon calcitonin (300 IU ivgtt). Third day after admission, the patient's serum calcium level decreased to 2.17 mmol/l and the PTH level was 182.5 pmol/L. Then rehydration and calcium-lowering therapy were stopped, and the serum calcium concentration was monitored every one to two days. During the next one week the serum calcium levels had been within the normal range and phosphorus level fluctuated between 0.36 and 0.50 mmol/L. The serum creatinine levels returned to normal and PTH gradually decreased, but still above normal (**Figure 2**).

A CT scan of the neck (**Figure 1B**) revealed bilateral slightly hypointense cystic mass deep the thyroid, 4.4 x 3.2 cm size on the right, 4.2 x 2.1 cm size on the left, with a uniform density and clear borders. A contrast-enhanced scan revealed intracystic septa within the lesions, with apparent enhancement of the cystic wall and septa. An ultrasound examination of the neck revealed mixed cystic-solid nodules posterior to the two lateral lobes of the thyroid, the size was 5.0 x 2.3 x 3.7 cm(right) and 5.3×3.5×3.1cm(left) respectively. Both nodules had clear borders and a regular morphology without apparent internal blood flow signals. Contrast-enhanced ultrasound of neck mass shows mixed cystic-solid nodules behind the two lateral lobes of the thyroid. SPECT/CT fusion imaging (MIBI; **Figures 1C, D**) revealed an abnormal increase uptake during MIBI in part of the mass posterior to the right lobe of the thyroid, which point the possibility of parathyroid adenoma. A bone density test and X-ray examination of the hands and four limbs did not demonstrate a reduction in bone mass and osteoporosis. At 11th day post-admission, the patient underwent an ultrasound-guided biopsy of the bilateral cystic nodules posterior to the thyroid. Ten milliliters of dark red bloody fluid were collected from the cystic nodules bilaterally. Exfoliative cytology indicated a small number of hyperplastic epithelial and tissue cells, possibly indicating benign cystic lesions. The neck masses shrank in size after fine needle aspiration; however, ultrasonography of the thyroid gland 2 days later revealed cystic space regains its size before aspiration which suggested new hemorrhage after the fine needle aspiration.

According to the guidelines for the diagnosis and treatment of primary hyperparathyroidism (3) and considering the patient's surgical requirements, the neck mass resection was performed at three weeks post-admission, during which the bilateral cystic-solid masses were found, 5 x 3 x 3.5 cm in size on the right (**Figure 1E**) and 5.5 x 4 x 3.5 cm on the left (**Figure 1F**). The mass adhered closely to the thyroid gland and the surrounding tissues, with obscure borders and an irregular morphology. At last, the patient underwent resection of bilateral inferior parathyroid adenomas and a total thyroidectomy. Bilateral superior parathyroids were preserved. Postoperative paraffin pathology results indicated intracystic hemorrhage of bilateral parathyroid adenomas. (**Figures 1G, H**). Thyroid pathology suggested nodular goiter in both bilateral lobes and isthmus of the thyroid gland.

The patient recovered well after surgery. At day 1 post-operatively, the serum PTH level was 1.95 pmol/L, and the blood calcium level was 2.23 mmol/L. According the clinical guideline, The patient was given calcitriol [1,25(OH)2D] 0.5ug twice daily, calcium supplement (10% calcium gluconate 100ml diluted intravenous infusion each day) after surgery. At 2 and 4 days post-operatively, the blood calcium level was 1.87 and 1.65 mmol/L, respectively, and the patient had no tetany. At 9 days post-operatively, the normal blood calcium level was restored and discharged from hospital with oral calcium carbonate 600mg twice daily and osteopontin 0.5ug twice daily. The blood calcium and PTH levels were monitored at 3 weeks, 2 months, 4 months, post-operatively and the results were all normal. The dose of the above drugs was reduced at month 4 and then discontinued at month 5. Calcium and phosphorus were still normal at the 6th month recheck.

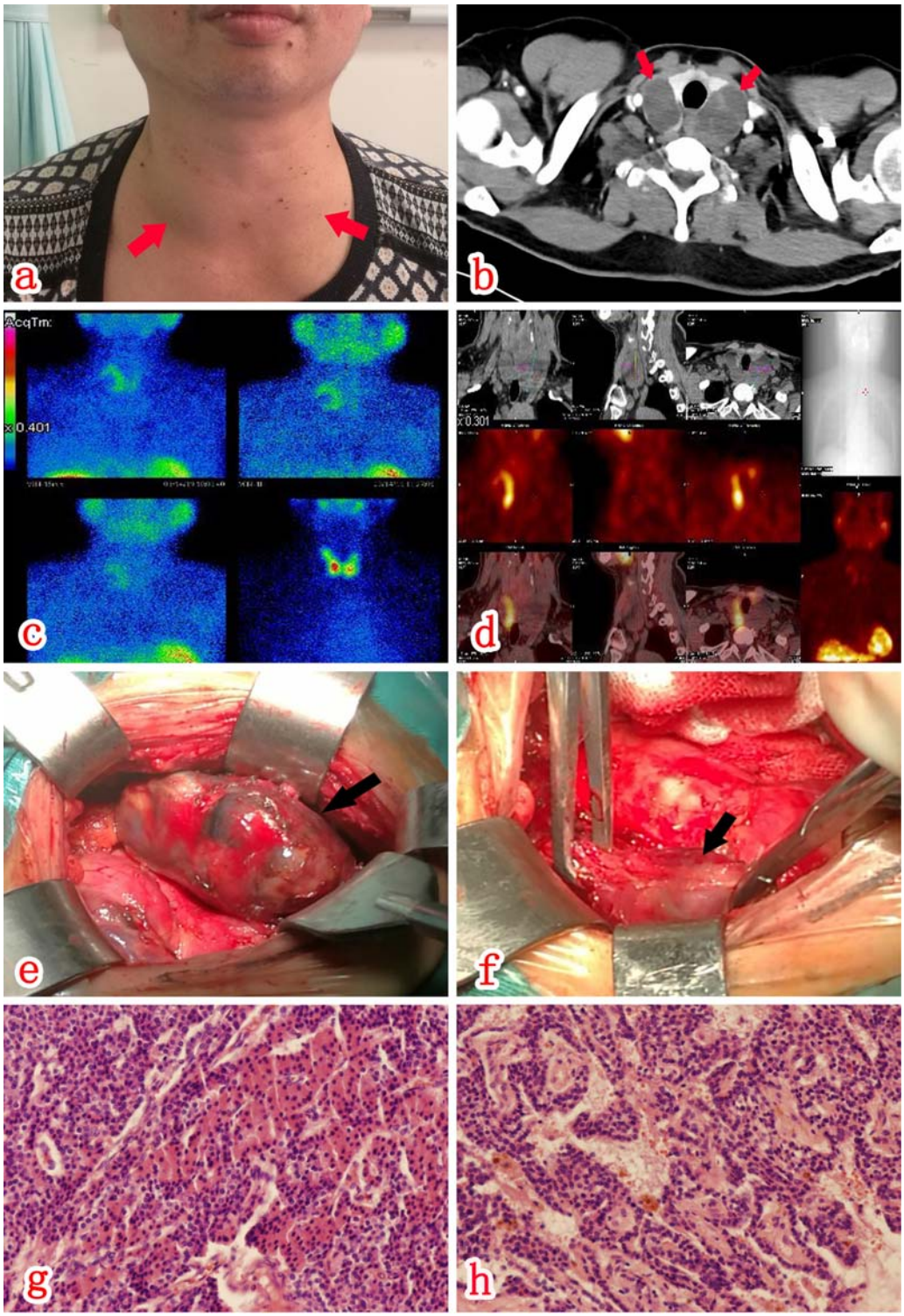


**FIGURE 1** | There was a grade II goiter **(A)**, with a 4 x 4 cm mass palpable near the thyroid bilaterally. CT scan **(A, B)** of the neck revealed bilateral slightly hypointense cystic shadows below the thyroid. SPECT/CT fusion imaging **(C, D)** revealed an abnormal increase in uptake in part of the mass behind the right lobe of the thyroid during MIBI, which was considered relevant to hyperparathyroidism. There were a cystic-solid mass **(E)** on the posterolateral aspect of the right lateral lobe of the thyroid and a cystic-solid mass **(F)** on the left lateral lobe of the thyroid. Postoperative paraffin pathology (HE staining x100) results indicated that both the right **(G)** and left **(H)** space-occupying lesions represented parathyroid adenomas with cystic change.

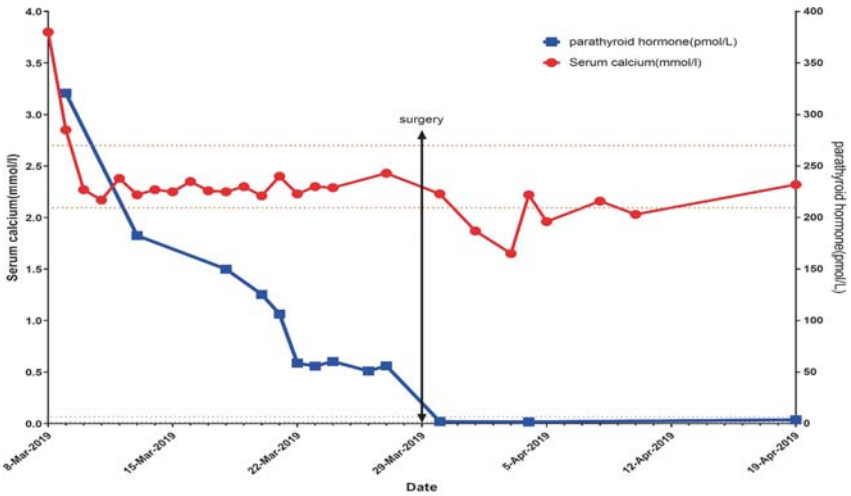


**FIGURE 2** | After admission, the blood calcium level was 3.6 mmol/L. After 2000-4000 ml of NS for 5 days and salmon calcitonin (300 IU ivgtt), the blood calcium level gradually decreased and remained within the normal range. After surgery, the blood calcium level decreased, reaching the lowest level (1.65 mmol/L). After that, the calcium level was gradually restored to normal. There was a progressive decrease in the PTH level; however, the PTH level was stabilized at 50-60 pmol/L at 12 days post-admission, and this situation persisted for 1 week. One day post-operatively the PTH level rapidly decreased to 1.95 pmol/L, followed by a slow, gradual increase.

Through screening tests,the patient was finally ruled out multiple endocrine neoplasia. He and his relatives also underwent testing of genes associated with MEN, none were carriers of the MEN related genes.

## DISCUSSION

### The Mismatch Between Tumor Rapid Growth and Blood Supply Might Result in Infarction of Parathyroid Adenoma and Hemorrhage

Intracystic hemorrhage of parathyroid adenomas is very rare. There are only about 100 cases reported with intracystic hemorrhage of parathyroid adenomas in the literatures. Some studies have shown that the use of anti-coagulation drugs (4) non-steroidal anti-inflammatory drugs (5) and trauma (6) may be risk factors; however, the cause of intracystic hemorrhage of parathyroid adenomas is unknown. It is currently believed that if tumor growth is too rapid and the blood supply to the tumor is insufficient, hemorrhage of parathyroid adenomas may occur (1). In 1953, Howard reported spontaneous remission after hyperparathyroidism due to infarction in parathyroid adenomas (7), which was called Parathyroidectomy. Nylen (8) suggested that infarction and hemorrhage represented two stages of the same phenomenon. Parathyroid adenoma apoplexy is divided into infarction of the adenoma (without hemorrhage), infarction with intracystic hemorrhage, and extracystic hemorrhage (8).

For our patient, he was in good health before and without trauma nor drug use history. Combined with the changes of blood calcium level, it is speculated that the rapid growth of adenoma and the massive release of PTH lead to the hypercalcemic crisis. However, the mismatch between tumor growth and blood supply resulted in infarction of parathyroid adenoma and intracystic hemorrhage, followed by spontaneous remission of hyperparathyroidism and hypercalcium crisis.

### The Clinical Manifestations of Bleeding Parathyroid Adenomas and the Accompanying Changes in Parathyroid Function Are Diverse

Symptoms of hemorrhage of parathyroid adenomas depend on the speed and volume of hemorrhage, as well as the position of the parathyroid gland (*in situ* or ectopic). Simple necrosis of parathyroid adenomas is associated with a smaller hematoma and few local symptoms. This condition may remain undetected until an incidental finding of spontaneous remission of hypercalcemia (9). Some patients are free from local discomfort in intracystic hemorrhage of *in situ* parathyroid adenomas (2), and may present with neck pain, a mass, and hoarseness (2). In *in situ* extracystic hemorrhage, the blood may diffuse to the neck or mediastinum, leading to compression of tracheal and esophagus (2), may cause dyspnea and dysphagia. Compression of the recurrent laryngeal nerve will lead to hoarseness and vocal cord paralysis with local swelling, pain, a mass, and ecchymosis (2) Spread of the hematoma may cause a pleural effusion (10, 11). Life-threatening hemorrhage of parathyroid adenomas usually needs surgical treatment as soon as possible. Hemorrhage of ectopic parathyroid adenomas often leads to a mediastinal hematoma, (6, 11–16) which also requires emergency surgery.

Parathyroid adenoma cells may also be involved and become necrotic after necrosis and hemorrhage of parathyroid adenomas, so parathyroid function will be influenced too. The

changes of parathyroid function vary to what extent the adenoma cells are involved. Some patients with hypercalcemia fail to achieve remission (17–19) or even progress to refractory hypercalcemic crisis (20). Others with hypercalcemia may show a reduction in the PTH level and achieve remission or even have the blood calcium level restored to normal (7, 21). In a few cases, hungry bone syndrome may occur due to the rapid decrease in the PTH level, leading to hypocalcemia (2, 22–24). Patients with hyperparathyroidism and complete necrosis of the parathyroid adenoma usually achieve full remission (21, 24–28), i.e., parathyroid adenomectomy in the real sense; however, some patients with hypercalcemia only achieve temporary remission and relapse later (22, 24, 27, 29). The time of relapse varies from one patient to another and ranges from several weeks to several years. The longest reported time of relapse after remission is 7 years (30).

In our case, only bilateral thyroid mass was present because of bilateral *in situ* parathyroid adenoma intracystic hemorrhage. Bone X-ray and bone density testing did not reveal bone mass changes in our case, indicating a relatively short course of disease of hyperparathyroidism. This patient showed a significant increase in the PTH level upon the onset, indicating rapid growth of the parathyroid adenoma and the secretion of a large amount of hormone before the hemorrhage. The blood calcium level was restored spontaneously to normal after the hypercalcemic crisis; however, there was no further decrease in the PTH level beyond 50-60 pmol/L. Based on an increased uptake in MIBI, it was concluded that there were residual parathyroid adenoma cells. The PTH level of this patient was still above the normal range, while the blood calcium level was low, which was possibly due to the decrease in PTH receptor sensitivity under a high PTH level. Considering the possibility of recurrent hypercalcemia and the surgical requirement of the patient, and according to the guidelines (3) this patient finally received surgical treatment. The post-operative pathologic results confirmed intracystic hemorrhage of bilateral parathyroid adenomas.

## Fine-Needle Aspiration Biopsy of Parathyroid Adenoma Hematoma Is of Limited Diagnostic Value and Carries Some Risk

In our patient, fine needle aspiration was performed to determine the etiology of bilateral parathyroid cystic lesions and collected bloody fluid eventually. Pathologic evaluation results showed a small amount of hyperplastic epithelial and tissue cells. After the fine needle aspiration biopsy, the cystic space-occupying lesions shrank in size, but soon grew to the original size. We further reviewed the relevant literature to explore the value and risks of fine-needle aspiration biopsy in such cases.

There have been previous reports on fine needle aspiration biopsy for hemorrhage of parathyroid adenomas. Givens (31) reported one case with hemorrhage of parathyroid adenoma who underwent a CT-guided biopsy. Pathologic biopsy showed epithelioid cells in well-ordered sheets and rare atypical cells. Other studies (8, 32) described bloody fluid from fine needle biopsy aspiration, which confirmed hemorrhage, but without a pathologic diagnosis. Novodvorsky (24) and Taguchi (33) reported that the finding of an increase in PTH level in the puncture fluid could help establish the diagnosis of parathyroid adenomas. Simcic (34) reported decompression of the hematoma by fine needle aspiration. The patient had immediate relief of his discomfort, and the mass regressed considerably in size, only to recur within 24 h of the puncture. This situation was similar to that observed in our patient. But Shim report that for patients with neck swelling and pain due to hemorrhage of the parathyroid adenoma, conservative management with intermittent sono-guided aspiration was performed without specific events (35).

The finding of bloody fluid by fine needle aspiration biopsy and an increase in PTH level in puncture fluid can help to make the diagnosis of hemorrhage of parathyroid mass and hyperparathyroidism for patients with cystic space-occupying lesions in the parathyroid gland, but it is difficult to obtain valuable pathologic cells in the puncture fluid. Although decompression of hematoma by fine needle aspiration is conducive to the remission of compression, the risk of another hemorrhage and recurrent hematoma exists.

In addition, there are two case reports on hemorrhage of parathyroid adenomas after fine needle aspiration biopsy so far. One of them was followed up for 105 months, and finally achieved full remission of hyperparathyroidism after hemorrhage of the parathyroid adenoma (25), the other case received surgical treatment at 1 month after aspiration-reduced hemorrhage (36).

Therefore, we believe that fine-needle aspiration biopsy of parathyroid adenoma hematoma is of limited diagnostic value and carries some risk. For patients requiring fine needle aspiration for decompression, the decision should be made carefully by weighing the pros and cons, unless the compression symptoms are severe and urgent.

## Through Literature Review, It Is Believed That There Is No Consensus On the Timing of Surgery for Intracapsular Hemorrhage in Primary *In Situ* Parathyroid Adenomas and That a Comprehensive Assessment Should be Made Based on the Clinical Features of the Case and the Patient's Wishes

In our case, it was found that the parathyroid adenoma adhered closely to the surrounding tissues and the hematoma tension was high. Both of the hematomas burst open during the surgery. Considering the hyperparathyroidism may relieve after intracystic hemorrhage of parathyroid adenoma and the difficulty of surgery in the acute phase, as well as the risk of extracapsular hemorrhage due to hematoma rupture, we conducted a literature review to answer the following questions. Do these patients require aggressive surgery? What is the appropriate time for surgery?

There has been no consensus on the choice of surgical timing for intracystic hemorrhage of primary *in situ* parathyroid adenomas.

According to previous literature reports, some cases had severe adhesions following intracystic hemorrhage of the parathyroid adenomas, as noted during surgery (6, 8, 37). One such case underwent surgery 7 months after the onset (38). The evidence is still insufficient to prove that prolonging conservative treatment can reduce adhesions found by subsequent surgery. In another report (37), a parathyroid adenoma (6.9 cm x 5.2 cm x 4.8 cm) ruptured during surgery. A large amount of unclear and bloody fluid flowed out, as was observed in our case; however, there have been no case reports on extracystic hemorrhage of a parathyroid adenoma due to hematoma rupture during the conservative treatment for intracystic hemorrhage of parathyroid adenomas.

Whether the patients underwent surgery after intracystic hemorrhage of parathyroid adenomas, and the specific duration of conservative treatment vary across the literature reports. We reviewed literature reports on 120 cases with hemorrhage or necrosis of parathyroid adenomas (including primary and secondary hyperparathyroidism, *in situ* ectopic parathyroid adenomas, and intracystic and extracystic hemorrhage of the parathyroid adenomas). Among the cases, we performed a detailed analysis of 34 cases with clinical or pathologic diagnosis of intracystic hemorrhage or necrosis of *in situ* primary parathyroid adenomas, parathyroid cysts and hyperplasia, described in Chinese or English (**Tables 1**, **2**). Of these cases, 12 did not undergo surgical treatment and all of them achieved spontaneous remission of hyperparathyroidism(**Table 1**). Five patients achieved full restoration of parathyroid function and complete absorption of the lesions. Four patients were followed up for 6, 9, 16, and 29 months, and none relapsed. Three patients relapsed at 16 days, 1 year, and 2 years afterwards, although the patients had not undergone surgical treatment upon the time of the literature report. Eight patients finally underwent surgical treatment after conservative treatment. Among the 8 patients, 4 achieved spontaneous remission of hyperparathyroidism, but later underwent surgical treatment due to recurrent hyperparathyroidism at 1 month, 6 years, 20 months, 11 months, and 8 years later. One patient underwent surgery at 2 months after conservative treatment due to failure to achieve remission of hyperparathyroidism; 2 patients achieved remission of hyperparathyroidism to a certain degree, but still received surgical treatment after 1 month and 3 months of conservative treatment, respectively. There were some patients who directly received surgical treatment, but the duration of conservative treatment before surgery was not mentioned in the literature. All patients had their parathyroid adenomas resected en bloc and achieved full remission of hyperparathyroidism after surgery. Whether hyper parathyroidism can be relieved, and hyperparathyroidism will recur later are independent of the size of the hematoma.

**TABLE 1** | Case analysis of intracystic hemorrhage or necrosis of *in situ* primary parathyroid adenomas (Unoperated patients, n = 12).

| Author | Age | Sex | Signs/symptoms | Hematoma size (cm) | [Ca++] | PTH | Surgery | Follow-up time | Changes in PHPT | Clinic Diagnosis |
|---|---|---|---|---|---|---|---|---|---|---|
| Wootten (2) | 63 | M | tetanic contractures of the hands | N/A | ↓9.4 mg/dL | ↑69pg/mL | N | 6M | Spontaneous remission | spontaneously resolving primary hyperparathyroidism |
| Nylen (8) | 64 | M | Abrupt neck swelling and pain, neck tenderness | 1.58 | 8.6mg/dl | ↓27pg/ml | N | 16M | Spontaneous remission | parathyroid apoplexy. |
| Baskar (9) | 30 | F | Chronic symptomatic hypercalcemia | N/A | → 2.37mmol/L† | ↑255ng/L | N | 5Y | Spontaneous remission | MEN1 |
| Ferrari (21) | 48 | M | symptoms of sever symptomatic hypercalcemia | 2.8 | ↑18 mg/dL | ↑1315pg/mL | N | 2Y | Spontaneous remission | parathyroid apoplexy |
| Micale Sara J (23) | 71 | F | neck discomfort, sore throat, difficulty swallowing | 2.1 × 2.4 × 3.6 | ↓8.1 mg/dL | →64.3pg/m | N | 16D | Spontaneous remission | infarction of parathyroid adenoma |
| Novodvorsky (24) | 54 | F | symptomatic hypocalcaemia | 4.4 | ↓1.88 mmol/L | ↑17.6 pmol/L | N | 11M | Spontaneous remission | Infarct hemorrhage of parathyroid adenoma |
| Kara (25) | 67 | F | slight neck swelling | N/A | →9.3mg/dl | ↑90.1 | N | 105M | Spontaneous remission | hemorrhage of parathyroid adenoma |
| Schinner (26) | 68 | M | Chronic symptomatic hypercalcemia | 3.7×1.2×1.7 | ↓3.3 mmol / l | ↑9.7 pmol/ l | N | 4Y | Spontaneous remission | infarction of the parathyroid adenoma |
| Onoda (28) | 67 | F | Asymptomatic | 1.4X1.1X1.0 | → | → | N | 2Y | Spontaneous remission | parathyroid infarction or homeorrhagic infarction |
| Lucas (29) | 53 | F | Acute neck pain, dysphagia, neck mass dyspnea | 3 | →8.6mg/dl | →38pg/ml | N | 10M | spontaneous remission, but recurrence in 10 months | infarction of parathyroid adenoma |
| Kovacs (39) | 49 | F | Abrupt neck pain, dyspnea,tenderness, | N/A | → 2.17mmol/L (2.1-2.6)* | ↑6.41 (1.38-5.72) pmol/L | N | 29M | Spontaneous remission | infarction of the parathyroid adenoma |
| Chan (40) | 78 | F | Chronic symptomatic hypercalcemia | 2.5 × 1.5 | ↓ 1.37mmol/L (2.20–2.62 mmol/l)† | ↑32.5 pmol/l | N | 1Y | Spontaneous remission, but recurrence in 1 year | Parathyroid apoplexy |

**total calcium; †Corrected calcium; PTH, parathyroid hormone; ↓Below normal; ↑Above normal; →Within the normal range.*

**TABLE 2 |** Case analysis of intracystic hemorrhage or necrosis of *in situ* primary parathyroid adenomas (Operated patients, n = 22).

| Author | Age | Sex | Signs/symptoms | Hematoma size (cm) | [Ca++] | PTH | Surgery | Time before operation | Changes in PHPT | Pathological diagnosis |
|---|---|---|---|---|---|---|---|---|---|---|
| Howard (7) | 57 | F | neck pain, nausea, vomiting and tachycardia supervened | 3.5×2×2 | ↑20 mg. per 100 ml | N/A | surgery | N/A | Spontaneous remission after Hypercalcemia | infarction of the adenoma |
| DeGroote (17) | 45 | F | symptomatic hypercalcemia, suddenly neck pain, neck tenderness, Severe dehydration | 3x3 | 20 mg/100 ml | N/A | Neck exploration | 4D | N/A | parathyroid adenoma, chief cell type, with a fresh hemorrhagic 1.5-cm cystic area and multiple areas of cystic necrosis within the gland |
| Chodack (18) | 61 | F | symptomatic hypercalcemia, gradual increase in sleepiness and confused, neck nontender mass, Tracheal displacement, fever | 6.5x4 | ↑18.5 mg/100 cc | N/A | emergency exploration | emergency exploration | N/A | chief-cell parathyroid adenoma |
| Mizunashi (20) | 62 | F | progressive symptomatic hypercalcemia., confusion | 2.5x2.0x1.6 | ↑4.25 mmol/L | ↑2300 ng/L | surgery | Emergency operation | Intractable hypercalcemia | Parathyroid adenoma with intratumoral hemorrhage |
| Johnston (22) | 19 | M | tetany, neck | 3.5x2.5 | ↓5.1 mg. per 100 ml. | N/A | surgical exploration | N/A | N/A | The capsule surrounding the adenoma was intact and the central area was necrotic, with a rim of viable "Wasserhelle" cells around the periphery. |
| Novodvorsky (24) | 51 | M | Asymptomatic | 1.7 ×0.5 × 1.0 | →2.43 mmol/L | ↑8.7 pmol/L | uneventful bilateral neck exploration | 20M | spontaneous remission, but recurrence in 17 months | parathyroid autoinfarction |
| Cetani (27) | 39 | F | neck pain, swelling, tenderness | 2.5 | →1.23mmol/L | →40ng/L | parathyroidectomy | 11M | spontaneous remission, but recurrence in 11months | parathyroid adenoma |
| Lucas (29) | 67 | M | Chronic symptomatic hypercalcemia | 1.5x1.0 | →9.9mg/dl | ↑67pg/ml | Neck exploration | N/A | Spontaneous remission | Spontaneous infarction of a parathyroid adenoma |
| Pereira (30) | 24 | F | hand muscle contraction, Chvostek's sign | 7.4 cm3 (Volume) | ↓ 6.8 mg/dl | ↑110 pg/ml | bilateral neck exploration | 8Y | spontaneous remission, but recurrence in 7 years | benign proliferation of parathyroid cells |
| Daniel (31) | 51 | F | intermittent hoarseness, breathy voice, coughing, right vocal fold paresis | 3.4 | 10.8 mg/dL | 118pg/mL | minimally invasive parathyroidectomy | N/A | N/A | hypercellular parathyroid tissue |
| Taguchi (33) | 85 | F | neck mass and symptomatic hypercalcemia | 3.6 | ↑11.7 mg/dl | ↑1348pg/ml | surgery | N | N/A | cystic parathyroid adenoma with intracystic hemorrhage |

*(Continued)*

**TABLE 2** | Continued

| Author | Age | Sex | Signs/symptoms | Hematoma size (cm) | [Ca++] | PTH | Surgery | Time before operation | Changes in PHPT | Pathological diagnosis |
|---|---|---|---|---|---|---|---|---|---|---|
| Maxwell (36) | 63 | F | neck pain and swelling, difficulty swallowing liquids, choking sensation, voice change | 4 | →22pg/mL | ↑10.4 mg/dL | parathyroidectomy and thyroid lobectomy, | 1M | Spontaneous remission. but recurrence in 2 weeks | hypercellular parathyroid adenoma, focus of inflammation, cystic change, fibrosis, and hemosiderin deposition |
| Kataoka (38) | 52 | F | Abrupt neck pain and swelling, dysphagia, fever, mass | 3.1×2.3×1.8 | ↓8.4 mg/dl | →40.8pg/ml‡ | parathyroid surgery | 6Y | Incomplete remission, and recurrence in 4 months | parathyroid adenoma with oxyphilic cells surrounded by normal rims |
| Chen (37) | 82 | M | abrupt thyroid enlargement and neck mass, hoarseness, trachea compression and displacement | 6.9x5.2x4.8 | ↑1.43mmol/L | ↑210.4pg/mL | surgery | N/A | N/A | cystic ectopic intrathyroidal parathyroid adenoma |
| Natsui (41) | 59 | M | symptoms of symptomatic hypercalcemia subsided. mass | 3.4x2.1 | →8.6mg/dl | 86pg/dl‡ | Nodulectomy | 1M | Spontaneous remission | Parathyroid adenoma (erative or necrotic tissues with the hemosiderin deposition) |
| Ozaki (42) | 64 | M | symptomatic hypercalcemia, left thyroid lobe nodule | 4.0x2.5x1.0 | → | N/A | cervical exploration | 3M | Spontaneous remission | cystic degeneration of parathyroid adenoma. |
| Gooding (43) | 58 | M | N/A | 2.7×3 | 12mg/dl | ↑129 pg/mL | surgery | N/A | N/A | hemorrhagic parathyroid cyst. |
| Ben-Shlomo (44) | 59 | M | neck pain, acute hoarseness, Abrupt dysphonia, mass, complete paralysis of the right vocal cord. | 2x3 | → | N/A | surgery | N/A | N/A | hyperplastic parathyroid tissue embedded in blood |
| Ahadizadeh (45) | 55 | F | neck swelling, dysphonia. | 4 | 11.1 mg/dL | 467 pg/mL | parathyroid exploration, Left hemithyroidectomy | N/A | Spontaneous remission | parathyroid adenoma with infarction |
| McLatchie (46) | 51 | M | renal colic.renal pelvic calculus | 2 | → | → | neck exploration | N/A | Spontaneous remission | infarcted chief cell adenoma |
| Efremidou (47) | 59 | M | abrupt neck pain, | 2.2×1.8×2.9 | ↑12.9 mg/dl | ↑146.5 pg/ml | cervical exploration and thyroidectomy | 2M | Incomplete remission | parathyroid adenoma cells surrounding a central region of cystic degeneration |
| Govindaraj (48) | 46 | F | Neck mass, throat pain, chronic symptomatic hypercalcemia | 2 × 1.2 × 2 | → | 533 pg/mL, | left neck exploration | N/A | Spontaneous remission | infarcted parathyroid gland with neovascularizing granulation tissue |

**total calcium; PTH, parathyroid hormone; ‡iPTH, intact parathyroid hormone assay; ↓Below normal; ↑Above normal; →Within the normal range.*

As shown by the literature review, conservative observation may be feasible for those achieving spontaneous remission of hyperparathyroidism after intracystic hemorrhage of a parathyroid adenoma. Given the probability of relapse, the parathyroid function and hematoma changes should be closely monitored. Surgical treatment is recommended if hyperparathyroidism recurs. Those failing to achieve remission of hyperparathyroidism after the hemorrhage can be treated by elective surgery. The choice of surgical timing should be made based on parathyroid function, health economics considerations, and the patient's will.

## CONCLUSION

We present a case of a 47-year-old male patient with primary hyperparathyroidism and a hypercalcemic crisis, and hypercalcemia spontaneously relieved thereafter. Pathology results indicated an intracystic hemorrhage of bilateral parathyroid adenomas. The mismatch between tumor rapid growth and blood supply might result in infarction of parathyroid adenoma and hemorrhage. The clinical manifestations of bleeding parathyroid adenomas and the accompanying changes in parathyroid function are diverse, because of the diversity of speed and volume of hemorrhage, as well as the position of the parathyroid gland. Fine-needle aspiration biopsy of parathyroid adenoma hematoma is of limited diagnostic value and carries some risk. After literature review, it is believed that there is no consensus on the timing of surgery for intracapsular hemorrhage in primary *in situ* parathyroid adenomas and that a comprehensive assessment should be made based on the Clinical manifestations, changes in parathyroid function and the patient's wishes. We will continue to collect such case reports and keep the literature review updated to provide the best evidence for clinical decision making.

## DATA AVAILABILITY STATEMENT

The original contributions presented in the study are included in the article/supplementary material. Further inquiries can be directed to the corresponding authors.

## ETHICS STATEMENT

The studies involving human participants were reviewed and approved by Medical Ethics Committee of West China Hospital, Sichuan University. The patients/participants provided their written informed consent to participate in this study. Written informed consent was obtained from the individual(s) for the publication of any potentially identifiable images or data included in this article.

## AUTHOR CONTRIBUTIONS

YL was involved in study concept, study design, and manuscript preparation. JL carried out the definition of intellectual content and manuscript review. HL handled data analysis and statistical analysis. HY carried out data acquisition. JQ and TWe conducted the clinical studies. TWa was involved in the literature research and manuscript editing. YY performed the role of guarantor for the integrity of the entire study. All authors contributed to the article and approved the submitted version.

## FUNDING

This article was supported by the National Natural Science Foundation of China (No 81701888); Science and Technology Program of Sichuan (2019YFS0239); and Health and Family Planning Commission Foundation of Sichuan Province (No. 17PJ262).

## REFERENCES

1. Kozlow W, Demeure MJ, Welniak LM, Shaker JL. Acute Extracapsular Parathyroid Hemorrhage: Case Report and Review of the Literature. *Endocr Pract* (2001) 7(1):32–6. doi: 10.4158/EP.7.1.32
2. Wootten Christopher T, Orzeck Eric A. Spontaneous Remission of Primary Hyperparathyroidism: A Case Report and Meta-Analysis of the Literature. *Head Neck* (2006) 28(1):81–8. doi: 10.1002/hed.20316
3. Chinese Medical Association, Osteoporosis and Bone Mineral Diseases Branch and Metabolic Bone Diseases Group of Endocrine Branch. Guidelines for the Diagnosis and Treatment of Primary Hyperparathyroidism. *Chin J Osteoporosis Bone Mineral Dis* (2014) 7(3):1–60.
4. van den Broek JJ, Poelman MM, Wiarda BM, Bonjer HJ, Houdijk AP. Extensive Cervicomediastinal Hematoma Due to Spontaneous Hemorrhage of a Parathyroid Adenoma: A Case Report. *J Surg Case Rep* (2015) 2015(5):1–3. doi: 10.1093/jscr/rjv039
5. Khan S, Choe CC, Shabaik A. Parathyroid Adenoma Presenting With Spontaneous Cervical and Anterior Mediastinal Hemorrhage: A Case Report. *Med (Baltimore)* (2019) 98(5):e14347. doi: 10.1097/MD.0000000000014347
6. Zhao C, Wang X, Wei H, Ma G. Parathyroid Adenoma Causing a Spontaneous Cervical and Mediastinal Massive Hematoma. *Int J Clin Exp Med* (2015) 8(11):21826–9.
7. Howard JE, Follis RH Jr, Yendt ER, Connor TB. Hyperparathyroidism; Case Report Illustrating Spontaneous Remission Due to Necrosis of Adenoma, and a Study of the Incidence of Necroses in Parathyroid Adenomas. *J Clin Endocrinol Metab* (1953) 13(8):997–1008. doi: 10.1210/jcem-13-8-997
8. Nylen E, Shah A, Hall J. Spontaneous Remission of Primary Hyperparathyroidism From Parathyroid Apoplexy. *J Clin Endocrinol Metab* (1996) 81(4):1326–8. doi: 10.1210/jcem.81.4.8636326
9. Baskar V, Kamalakannan D, Singh BM, Odum J. Spontaneous Regression of Hypercalcemia in a Patient With Primary Hyperparathyroidism and Prolactinoma. *J Endocrinol Invest* (2004) 27(5):462–4. doi: 10.1007/BF03345292
10. Huang J, Soskos A, Murad SM, Krawisz BR, Yale SH, Urquhart AC. Spontaneous Hemorrhage of a Parathyroid Adenoma Into the Mediastinum. *Endocr Pract* (2012) 18(4):e57–60. doi: 10.4158/EP11329.CR
11. Santelmo N, Hirschi S, Sadoun D, Kambouchner M, Cohen R, Valeyre D, et al. Bilateral Hemothorax Revealing Mediastinal Parathyroid Adenoma. *Respiration* (1999) 66(2):176–8. doi: 10.1159/000029364
12. Bürgesser MV, Debernardi DM, Bustos ME. Spontaneous Mediastinal Hematoma as an Initial Manifestation of Ectopic Parathyroid Cystadenoma. *Arch Bronconeumol* (2012) 48(5):185–6. doi: 10.1016/j.arbr.2011.12.002
13. Devèze A, Sebag F, Pili S, Henry JF. Parathyroid Adenoma Disclosed by a Massive Cervical Hematoma. *Otolaryngol Head Neck Surg* (2006) 134(4):710–2. doi: 10.1016/j.otohns.2005.03.075
14. Akimoto T, Saito O, Muto S, Hasegawa T, Nokubi M, Numata A, et al. A Case of Thoracic Hemorrhage Due to Ectopic Parathyroid Hyperplasia With Chronic Renal Failure. *Am J Kidney Dis* (2005) 45(6):e109–14. doi: 10.1053/j.ajkd.2005.03.004
15. Berry BE, Carpenter PC, Fulton RE, Danielson GK. Mediastinal Hemorrhage From Parathyroid Adenoma Simulating Dissecting Aneurysm. *Arch Surg* (1974) 108(5):740–1. doi: 10.1001/archsurg.1974.01350290102019
16. Nakajima J, Takamoto S, Tanaka M, Takeuchi E, Murakawa T, Kitagawa H, et al. Parathyroid Adenoma Manifested by Mediastinal Hemorrhage: Report of a Case. *Surg Today* (2002) 32(9):809–11. doi: 10.1007/s005950200155
17. DeGroote JW. Acute Intermittent Hyperparathyroidism With Hemorrhage Into a Parathyroid Adenoma. *JAMA* (1969) 208(11):2160–1. doi: 10.1001/jama.1969.03160110132027

18. Chodack P, Attie JN, Groder MG. Hypercalcemic Crisis Coincidental With Hemorrhage In Parathyroid Adenoma. *Arch Intern Med* (1965) 116:416–23. doi: 10.1001/archinte.1965.03870030096016
19. Manouras A, Toutouzas KG, Markogiannakis H, Lagoudianakis E, Papadima A, Antonakis PT, et al. Intracystic Hemorrhage in a Mediastinal Cystic Adenoma Causing Parathyrotoxic Crisis. *Head Neck* (2008) 30(1):127–31. doi: 10.1002/hed.20661
20. Mizunashi K, Takaya K, Sato H, Mori S, Abe K, Furukawa Y. The Time Course of Renal Function and Bone Turnover in Parathyroid Crisis Due to Intratumoral Hemorrhage. *Clin Investig* (1994) 72(6):448–50. doi: 10.1007/BF00180519
21. Ferrari F, Marcocci C, Cetani F. Acute Severe Primary Hyperparathyroidism: Spontaneous Remission After 2 Years Follow-Up. *J Endocrinol Invest* (2019) 42(2):243–4. doi: 10.1007/s40618-018-0971-4
22. Johnston CC, Schnute RB. A Case of Primary Hyperparathyroidism With Spontaneous Remission Following Infarction of the Adenoma With Development of Hypocalcemic Tetany. *J Clin Endocrinol Metab* (1961) 21:196–200. doi: 10.1210/jcem-21-2-196
23. Micale SJ, Kane MP, Busch RS. Spontaneous Resolution of Primary Hyperparathyroidism in Parathyroid Adenoma. *Case Rep Endocrinol* (2012) 2012:793753. doi: 10.1155/2012/793753
24. Novodvorsky P, Hussein Z, Arshad MF, Iqbal A, Fernando M, Munir A, et al. Two Cases of Spontaneous Remission of Primary Hyperparathyroidism Due to Auto-Infarction: Different Management and Their Outcomes. *Endocrinol Diabetes Metab Case Rep* (2019) 2019:18–0136. doi: 10.1530/EDM-18-0136
25. Kara E, Della Valle E, De Vincentis S. Cured Primary Hyperparathyroidism After Fine-Needle Aspiration Biopsy-Induced Parathyroid Disappearance. *Endocrinol Diabetes Metab Case Rep* (2017) 2017:17–0125. doi: 10.1530/EDM-17-0125
26. Schinner S, Fritzen R, Schott M, Willenberg HS, Scherbaum WA. Spontaneous Remission of Primary Hyperparathyroidism. *Exp Clin Endocrinol Diabetes* (2007) 115(9):619–21. doi: 10.1055/s-2007-985358
27. Cetani F, Ambrogini E, Faviana P, Vitti P, Berti P, Pinchera A, et al. Spontaneous Short-Term Remission of Primary Hyperparathyroidism From Infarction of a Parathyroid Adenoma. *J Endocrinol Invest* (2004) 27(7):687–90. doi: 10.1007/BF03347505
28. Onoda N, Miyakawa M, Sato K, Demura H, Uchida E. Spontaneous Remission of Parathyroid Adenoma Followed With Ultrasonographic Examinations. *J Clin Ultrasound* (1994) 22(2):134–6. doi: 10.1002/jcu.1870220213
29. Lucas DG, Lockett MA, Cole DJ. Spontaneous Infarction of a Parathyroid Adenoma: Two Case Reports and Review of the Literature. *Am Surg* (2002) 68 (2):173–6.
30. Pereira FA, Brandão DF, Elias J, Paula FJ. Parathyroid Adenoma Apoplexy as a Temporary Solution of Primary Hyperparathyroidism: A Case Report. *J Med Case Rep* (2007) 1:139. doi: 10.1186/1752-1947-1-139
31. Givens DJ, Hunt JP, Bentz BG. Uncommon Presentations of Parathyroid Adenoma. *Head Neck* (2013) 35(9):E265–268. doi: 10.1002/hed.23124
32. Taniguchi I, Maeda T, Morimoto K, Miyasaka S, Suda T, Yamaga T. Spontaneous Retropharyngeal Hematoma of a Parathyroid Cyst: Report of a Case. *Surg Today* (2003) 33(5):354–7. doi: 10.1007/s005950300080
33. Taguchi T, Sugimoto T, Terada Y. Cystic Parathyroid Adenoma With Intracystic Hemorrhage. *Endocrine* (2016) 52(2):399–400. doi: 10.1007/s12020-015-0743-2
34. Simcic KJ, McDermott MT, Crawford GJ, Marx WH, Ownbey JL, Kidd GS. Massive Extracapsular Hemorrhage From a Parathyroid Cyst. *Arch Surg* (1989) 124(11):1347–50. doi: 10.1001/archsurg.1989.01410110109023
35. Shim WS, Kim IK, Yoo SD, Kim DH. Non-Functional Parathyroid Adenoma Presenting as a Massive Cervical Hematoma: A Case Report. *Clin Exp Otorhinolaryngol* (2008) 1(1):46–8. doi: 10.3342/ceo.2008.1.1.46
36. Maxwell JH, Giroux L, Bunner J, Duvvuri U. Fine-Needle Thyroid Aspiration-Induced Hemorrhage of an Unsuspected Parathyroid Adenoma Misdiagnosed as a Thyroid Nodule: Remission and Relapse of Hyperparathyroidism. *Thyroid* (2011) 21(7):805–8. doi: 10.1089/thy.2010.0200
37. Chen J, Ma Z, Yu J. Diagnostic Pitfalls in a Cystic Ectopic Intrathyroidal Parathyroid Adenoma Mimicking a Nodular Goiter: A Care-Compliant Case Report. *Med (Baltimore)* (2019) 98(5):e14351. doi: 10.1097/MD.0000000000014351
38. Kataoka K, Taguchi M, Takeshita A, Miyakawa M, Takeuchi Y. Recurrence of Primary Hyperparathyroidism Following Spontaneous Remission With Intracapsular Hemorrhage of a Parathyroid Adenoma. *J Bone Miner Metab* (2008) 26(3):295–7. doi: 10.1007/s00774-007-0816-2
39. Kovacs KA, Gay JD. Remission of Primary Hyperparathyroidism Due to Spontaneous Infarction of a Parathyroid Adenoma. Case Report and Review of the Literature. *Med (Baltimore)* (1998) 77(6):398–402. doi: 10.1097/00005792-199811000-00006
40. Chan WB, Chow CC, King AD, et al. Spontaneous Necrosis of Parathyroid Adenoma: Biochemical and Imaging Follow-Up for Two Years. *Postgrad Med J* (2000) 76(892):96–8. doi: 10.1136/pmj.76.892.96
41. Natsui K, Tanaka K, Suda M, et al. Spontaneous Remission of Primary Hyperparathyroidism Due to Hemorrhagic Infarction in the Parathyroid Adenoma. *Intern Med* (1996) 35(8):646–9. doi: 10.2169/internalmedicine.35.646
42. Ozaki O, Sakamoto M, Matsui Y. Spontaneous Remission of Hypercalcemia in a Functioning Parathyroid Cyst. *Jpn J Surg* (1984) 14(4):315–9. doi: 10.1007/BF02469648
43. Gooding GA, Duh QY. Primary Hyperparathyroidism: Functioning Hemorrhagic Parathyroid Cyst. *J Clin Ultrasound* (1997) 25(2):82–4. doi: 10.1002/(SICI)1097-0096(199702)25:2<82::AID-JCU6>3.0.CO;2-F
44. Ben-Shlomo I, Zohar S, Turani H, Cozacov C. Sudden Dysphonia Due to Parathyroid Apoplexy: A Rare Case of Recurrent Laryngeal Nerve Palsy. *Head Neck* (1990) 12(4):355–6. doi: 10.1002/hed.2880120415
45. Ahadizadeh EN, Manzoor NF, Wasman J, Lavertu P. Spontaneous Resolution of Hypercalcemia. *Am J Otolaryngol* (2017) 38(4):496–7. doi: 10.1016/j.amjoto.2017.03.003
46. McLatchie GR, Morris EW, Forrester A, Fogelman I. Autoparathyroidectomy: A Case Report. *Br J Surg* (1979) 66(8):552–3. doi: 10.1002/bjs.1800660810
47. Efremidou EI, Papageorgiou MS, Pavlidou E, et al. Parathyroid Apoplexy, the Explanation of Spontaneous Remission of Primary Hyperparathyroidism: A Case Report. *Cases J* (2009) 2:6399. doi: 10.1186/1757-1626-2-6399
48. Govindaraj S, Wasserman J, Rezaee R, Manolas KJ, Liratzopoulos N. Parathyroid Adenoma Autoinfarction: A Report of a Case. *Head Neck* (2003) 25(8):695–9. doi: 10.1002/hed.10244


**Conflict of Interest:** The authors declare that the research was conducted in the absence of any commercial or financial relationships that could be construed as a potential conflict of interest.

frontiers in Endocrinology

ORIGINAL RESEARCH
published: 05 November 2021
doi: 10.3389/fendo.2021.756523

# Adrenocortical Tumors in Children With Constitutive Chromosome 11p15 Paternal Uniparental Disomy: Implications for Diagnosis and Treatment

*Emilia Modolo Pinto*[1*], *Carlos Rodriguez-Galindo*[2,3], *Catherine G. Lam*[2,3], *Robert E. Ruiz*[1], *Gerard P. Zambetti*[1] *and Raul C. Ribeiro*[2]

[1] Department of Pathology, St. Jude Children's Research Hospital, Memphis, TN, United States, [2] Department of Oncology, St. Jude Children's Research Hospital, Memphis, TN, United States, [3] Department of Global Pediatric Medicine, St. Jude Children's Research Hospital, Memphis, TN, United States

OPEN ACCESS

**Edited by:**
Barbara Altieri,
University Hospital of Wuerzburg, Germany

**Reviewed by:**
Ronald De Krijger,
Princess Maxima Center for Pediatric Oncology, Netherlands
Sandra Sigala,
University of Brescia, Italy

***Correspondence:**
Emilia Modolo Pinto
emilia.pinto@stjude.org

**Specialty section:**
This article was submitted to Cancer Endocrinology, a section of the journal Frontiers in Endocrinology

**Received:** 10 August 2021
**Accepted:** 04 October 2021
**Published:** 05 November 2021

**Citation:**
Pinto EM, Rodriguez-Galindo C, Lam CG, Ruiz RE, Zambetti GP and Ribeiro RC (2021) Adrenocortical Tumors in Children With Constitutive Chromosome 11p15 Paternal Uniparental Disomy: Implications for Diagnosis and Treatment. Front. Endocrinol. 12:756523. doi: 10.3389/fendo.2021.756523

Pediatric adrenocortical tumors (ACTs) are rare and heterogeneous. Approximately 50% of children with ACT carry a germline *TP53* variant; however, the genetic underpinning of remaining cases has not been elucidated. In patients having germline *TP53* variants, loss of maternal chromosome 11 and duplication of the paternal copy [paternal uniparental disomy, (UPD)] occurs early in tumorigenesis and explains the overexpression of *IGF2*, the hallmark of pediatric ACT. Beckwith-Wiedemann syndrome (BWS) is also associated with overexpression of *IGF2* due to disruption of the 11p15 loci, including segmental UPD. Here, we report six children with ACT with wild type *TP53* and germline paternal 11p15 UPD. Median age of five girls and one boy was 3.2 years (range 0.5-11 years). Two patients met the criteria for BWS before diagnosis of ACT. However, ACT was the first and only manifestation of paternal 11p15 UPD in four children. Tumor weight ranged from 21.5 g to 550 g. Despite poor prognostic features at presentation, such as pulmonary metastasis, bilateral adrenal involvement, and large tumors, all patients are alive 8-21 years after cancer diagnosis. Our observations suggest that children with ACT and wild type *TP53*, irrespective of their age, should be screened for germline abnormalities in chromosome 11p15.

**Keywords: Beckwith-Wiedemann syndrome, adrenocortical cancer, hemihypertrophia, chromosome 11p15, TP53, UPD**

## INTRODUCTION

Pediatric adrenocortical tumors (ACTs) are associated with germline *TP53* mutations in 50% of cases (1, 2). For ACT cases without a germline *TP53* alteration, germline abnormalities at chromosome 11p15 loci, typically seen in the Beckwith-Wiedemann syndrome (BWS, OMIM 130650) (3–8), have been reported (1). BWS is a pediatric overgrowth and cancer predisposition syndrome. The clinical presentation is highly variable and viewed as a spectrum of *classical* (macroglossia, anterior abdominal wall defects, and prenatal and post-natal overgrowth), *atypical*

(patients with isolated features of BWS) and *isolated lateralized overgrowth* (3). Affected individuals are usually born macrosomic and develop rapid growth starting either at birth or before the first year of life (3, 4). However, asymmetry may not be apparent at birth, and overall signs of overgrowth may appear subtle. Patients with BWS are also at risk of having early onset tumors such as Wilms tumor, hepatoblastoma, ACT, and neuroblastoma which are considered to originate from dysregulation of cellular processes during early embryogenesis (3–8). The variability in phenotype is due to genetic and epigenetic alterations of chromosome 11p15, with specific gene mutations, chromosomal copy number changes, or methylation status of chromosome 11p15 imprinting centers, leading to dysregulation of specific genes affecting growth, development, and cancer (5–8). Cancer risk depends on the genetic/epigenetic defect. Segmental paternal 11p15 paternal uniparental disomy (UPD) accounts for 20% of cases of BWS (3), and a 25-30% cancer risk including Wilms tumor, hepatoblastoma and ACTs (5–8). Most of the cases clinically defined as BWS who develop ACT have germline UPD (7, 8). However, since 11p15 UPD occurs as a somatic mosaic event, the true incidence of UPD might be higher than that reported in literature.

Chromosome 11p15 contains a cluster of imprinted genes important for the control of fetal and postnatal growth (**Figure 1**). The telomeric domain includes the long non-coding RNA *H19*, which is maternally expressed in the embryo and placenta (9) but silenced in most tissues after birth except in cardiac and skeletal muscles (10). Also contained within this domain is *IGF2*, which encodes, a growth factor paternally expressed in the fetus and placenta, and biallelically expressed in the liver after birth (11). The ICR1 (imprinting control region) located upstream of the *H19*, is a methylation sensitive chromatin insulator that in conjunction with enhancers, modulates the transcription of *IGF2* and *H19* in an allele-specific manner. The ICR1 is usually unmethylated in the maternal allele and therefore allows the binding of CTCF (CCCTC-binding factor), a zinc finger protein with insulating activity, thereby preventing the expression of *IGF2*, and allowing transcription of *H19* by downstream enhancers on the maternal chromosome (**Figure 1**). Conversely, the ICR1 is methylated on the paternal allele which interferes with CTCF binding, thus silencing *H19* and allowing *IGF2* expression *via* access to enhancers (12) (**Figure 1**). The centromeric ICR2 is located at the 5′ end of long non-coding RNA *KCNQ1OT1*(antisense transcript of *KCNQ1*) and mediates the silencing of several genes, including *CDKN1C*, which encodes the G1 cyclin-dependent kinase inhibitor ($p57^{KIP2}$), that negatively regulates cell growth and proliferation. *CDKN1C* is maternally expressed in the embryo and placenta as well as postnatally throughout the body (13) (**Figure 1**). *KCNQ1* is initially maternally expressed during early embryogenesis but is then biallelically expressed during development (14). On the maternal chromosome, ICR2 is methylated, *KCNQ1OT1* is not transcribed, and the flanking imprinted genes (*KCNQ1* and *CDKN1C*) are expressed. On the paternal chromosome, the *KCNQ1OT1* promoter is not methylated, the transcript is expressed in the opposite direction of *KCNQ1*, and silences *in cis* genes of the centromeric domain on the paternal chromosome (15) (**Figure 1**).

In this study, we describe the clinical and molecular findings of six pediatric cases of ACTs with germline paternal 11p15 UPD and discuss the implications of these findings for the management of children with ACT associated with these genetic abnormalities.

## PATIENTS AND METHODS

### Case Selection

Six pediatric patients with ACT, all with wild type *TP53*, were selected from the International Pediatric Adrenocortical Tumor Registry (IPACTR) at St. Jude Children's Research Hospital (St. Jude). Written informed consent was obtained from parents or legal guardians for inclusion in the St Jude Children's Research Hospital (St. Jude) International Pediatric Adrenocortical Tumor Registry (IPACTR; http://clinicaltrials.gov/show/NCT00700414). One patient (#1) was diagnosed with BWS at the time of cancer diagnosis. A second patient (#2) developed lateralized overgrowth and the ACT was found when surveilling for abdominal tumors. No features of BWS were seen during cancer diagnosis for the remaining four cases (#3,4,5,6) but patients were subsequently found to harbor constitutional chromosome 11p15 alterations (**Table 1**).

### Molecular Analysis

Due to the complexity of the chromosome 11p15 imprinting regions and their interactions, the interpretation of copy number variations (16) and epigenetic changes (6, 16) in that region requires a series of molecular assays. In this series of 6 patients, whole genome or whole exome sequencing was examined for three (#1,5,6) patients and single nucleotide polymorphism array was offered to patient #3.

Targeted techniques were combined to determine 11p15 status in germline DNA for all 6 patients. Genotyping of a panel of five microsatellite markers (D11S1363, D11S922, D11S4046, HUMTH01 and D11S988) covering positions 1,061,991 to 4,539,851 at chromosome 11p15 (GRCh37/hg19) was performed by using a fluorescently labeled forward and conventional reverse primers as previously described (1). An informative result allows us to discriminate maternal and paternal alleles for each marker. A pattern of homozygosity is suggestive of paternal uniparental disomy (UPD). In addition, genomic DNA was analyzed by using a methylation-specific multiplex ligation-dependent probe amplification (MS-MLPA; ME030-C3 BWS/RSS, MRC-Holland), commercially designed specifically for the 11p15 region and currently the most rapid and robust technique to assess methylation. DNA was processed in parallel with and without digestion with the methylation sensitive *Hha*I enzyme to detect both chromosome copy number alteration and methylation deregulation. Data analysis was performed using the Coffalyser software (MRC Holland) which provides two outputs, one related to chromosome 11p15

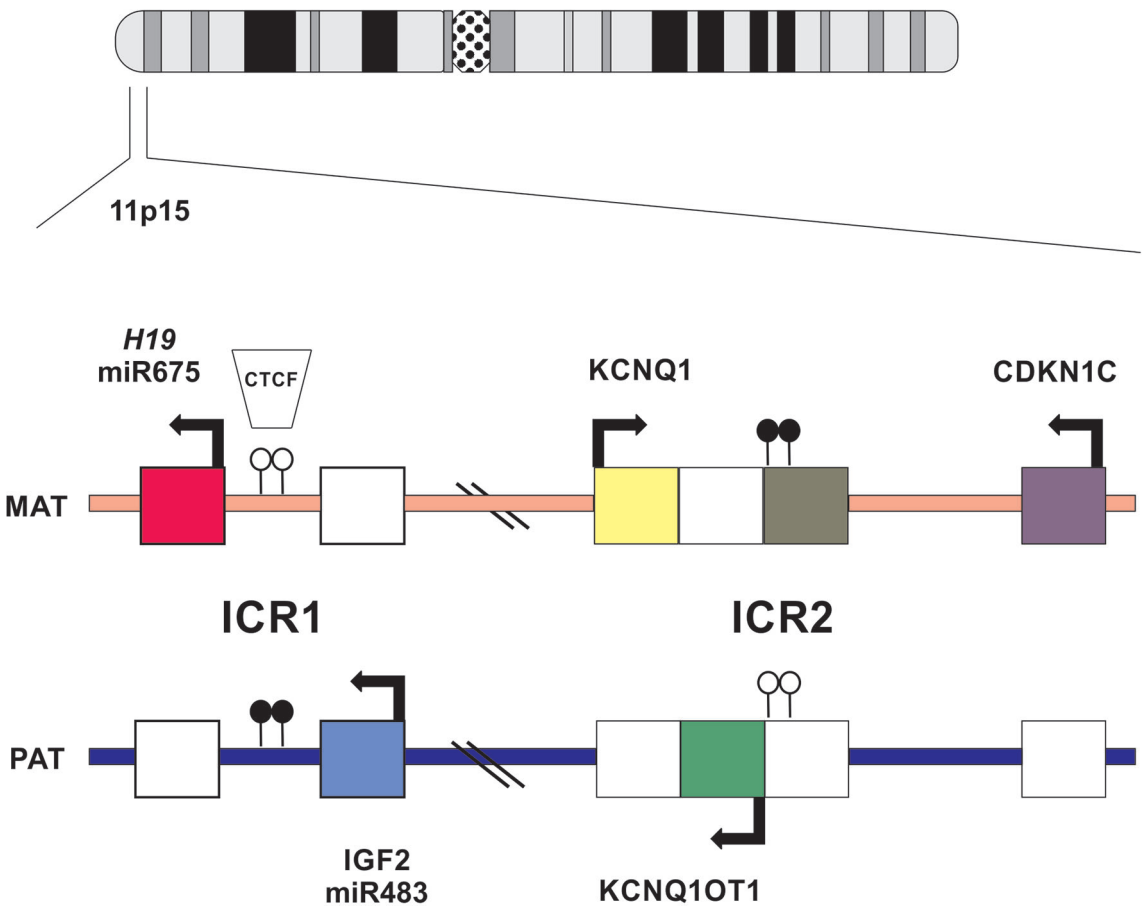


**FIGURE 1** | Schematic representation of imprinted gene cluster on chromosome 11p15. Genes and their directions of transcription are shown. Maternally or paternally expressed genes are indicated by filled squares. Open circles show the location on normally unmethylated ICR and filled circles indicate normally methylated ICR.

**TABLE 1** | Clinical findings of pediatric adrenocortical patients included in this study.

| Case | Gender | Age (yrs) | Clinical Presentation | Additional findings | Tumor weight (g)/ side | Pathologic diagnosis | Ki-67 LI | p53 | *CTNNB1* | Inhibin-α | Treatment | Status (yrs) |
|---|---|---|---|---|---|---|---|---|---|---|---|---|
| 1 | F | 8.5 | BWS | Bilateral adrenal masses/ Bilateral breast masses | 21.5 (left) | ACA | <2% | <2% | WT | Subset positive | Surgery | Alive (18) |
| 2 | M | 2.4 | BWS | Hepatic mass | 56 (left) | ACC | <5% | Negative | ND | Negative | Surgery | Alive (13) |
| 3 | F | 0.5 | Cushing syndrome | | >100* (left) | ACC | 30% | <1% | S45P | Ocassional cells | Surgery | Alive (8) |
| 4 | F | 1.3 | Routine visit | Bilateral pulmonary nodules | 130 (left) | ACC | ND | ND | WT | ND | Surgery + Chemotherapy | Alive (28) |
| 5 | F | 4 | Abdominal pain | Tumor extension into the inferior cava and right atrium | 550 (right) | UMP | low | 20% | positive (IHC) | Negative | Surgery + Chemotherapy | Alive (21) |
| 6 | F | 11 | Hypertension | Tumor rupture during surgery | 388 (left) | UMP | <5% | Occasional area | G34E | Negative | Surgery | Alive (23) |

**Weight estimated from tumor volume (276cm$^3$). BWS, Beckwith-Wiedemann syndrome; ACA, adrenocortical adenoma; ACC, adrenocortical carcinoma; UMP, uncertain malignant potential; ND, not determined.*

*Partial results (patients #1,3,4 and 6) has been previously published (1, 9).*

copy number changes and the other methylation status of imprinting control 1 (ICR1; regulating *H19* and *IGF2*; position 1,976,280 to 1,982,450) and ICR2 (regulating *CDKN1C*, *KCNQ1* and *KCNQ1OT1*; position 2,677,130 to 2,678,030) by the ratio of digested to undigested DNA. DNA from control individuals shows reduction of 50% of the MS-MLPA signal, corresponding to the presence of methylated alleles (ICR1 is unmethylated in maternal allele and ICR2 unmethylated in the paternal allele) and the contribution of both parental chromosomes (**Figure 2A**). Patients with UPD exhibited hypermethylation at ICR1 and hypomethylation at ICR2 consistent with the absence of maternal chromosome and duplication of paternal chromosome (**Figure 2B**). These epigenetic and structural changes at chromosome 11p15 leads to biallelic expression of *IGF2* and inactivation of *H19* and *CDKN1C*.

## Histological and Immunohistochemistry Studies

Enrollment on the IPACTR requires central review for the diagnosis of pediatric adrenocortical tumors in individuals up to 21 years of age at the time of initial diagnosis. The histological diagnosis was based on a combination of morphologic (hematoxylin and eosin) and histochemical criteria including chromogranin, cytokeratin, Cam 5.2, inhibin (**Figure 3**), Melan-A and synaptophysin. In addition, Ki-67 and beta-catenin were analyzed using standard assays (1). The p53 expression by immunohistochemistry was performed on deparaffinized tissue sections using the avidin-biotin complex method. The slides were incubated with monoclonal antibodies directed against p53 protein (1:50, DO-7; Dako Carpinteria, CA) (**Table 1**). There was no attempt to reclassify the tumors using specific histological criteria.

# RESULTS

## Case 1

The patient was an 8.5-year-old female with presumptive diagnosis of BWS who presented to the local physician in 2003 with new onset of herculean habitus, clitoromegaly, pubic hair, acne, and apocrine odor. Abdominal computed tomography imaging revealed synchronous bilateral adrenal masses. There

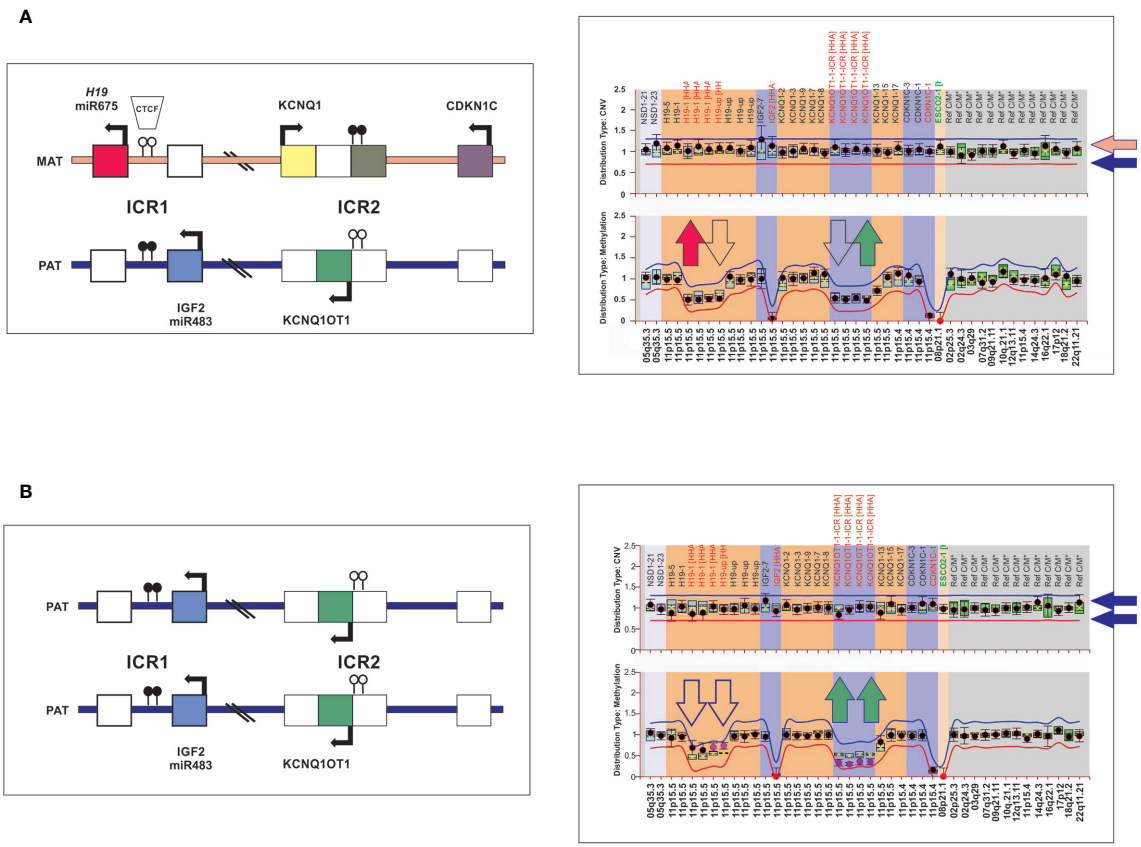


**FIGURE 2** | Schematic representation of the chromosome 11p15 covered by the MS-MLPA assay. **(A)** The left panel shows a diagram of the imprinted gene cluster on chromosome 11p15 with normal chromosomal copy number and methylation status. The right panel, MS-MLPA showing a diploid content of chromosome 11p15 (upper panel) and ICR1 and ICR2 for methylated probes (lower panel) in the normal range, consistent with the presence of maternal and paternal chromosomes 11p15. **(B)** Individuals with paternal 11p15 UPD as visualized by MS-MLPA. ICR1 hypermethylated and ICR2 hypomethylated consistent with loss of maternal chromosome 11p15.

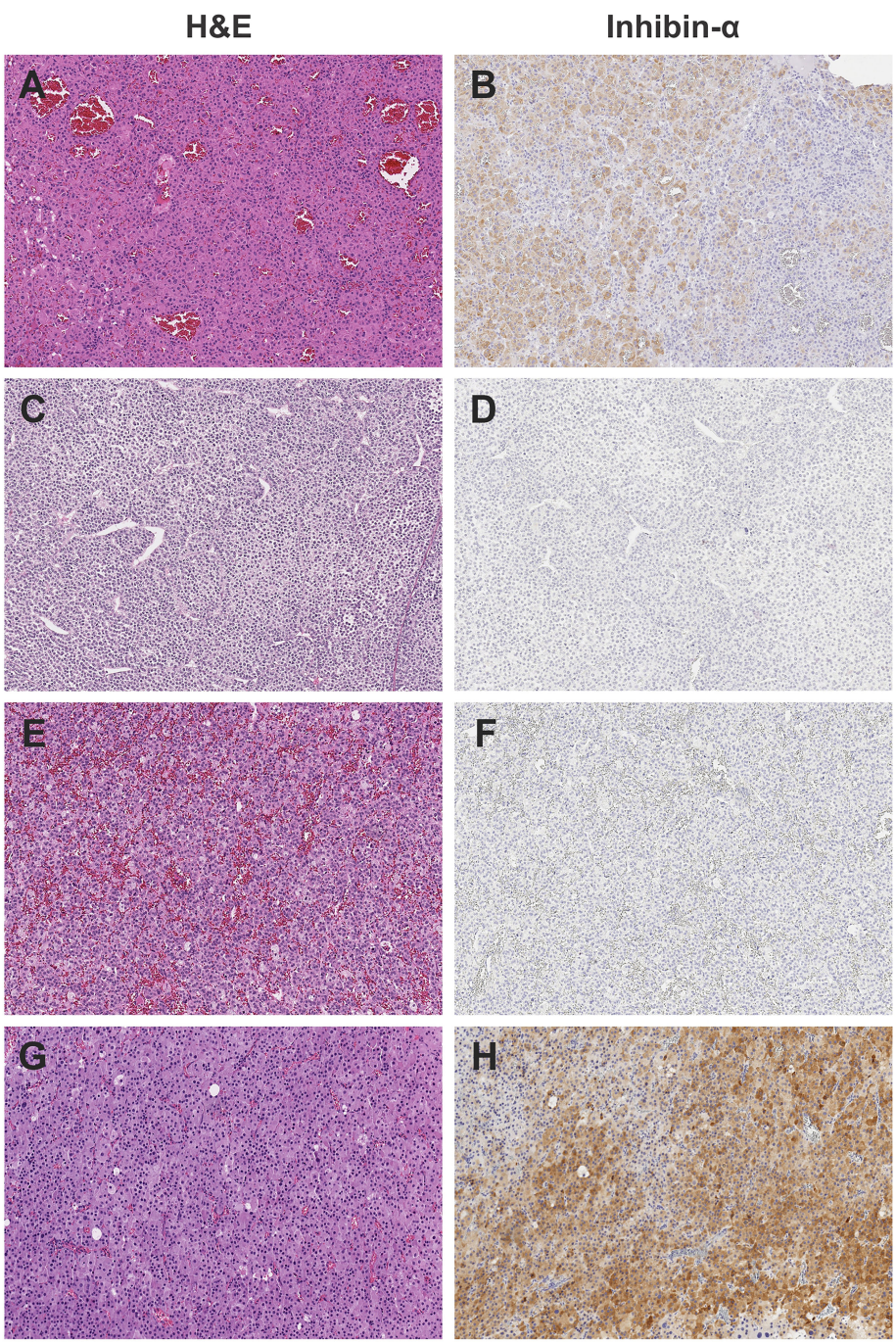


**FIGURE 3** | Representative histology of study cases, showing the heterogeneous appearance of adrenocortical tumors by H&E staining and weak to absent inhibin staining. All images photographed at 10x magnification using Leica Biosystems Aperio ImageScope. **(A)** H&E, **(B)** Inhibin, positive in subset of cells of Case #1; Adrenocortical adenoma. **(C)** H&E, **(D)** Inhibin, negative of case #3; Adrenocortical carcinoma. **(E)** H&E, **(F)** Inhibin, negative of Case #6; Adrenocortical tumor of uncertain malignant potential. **(G)** H&E, **(H)** Inhibin positive, patchy, adrenocortical carcinoma.

was no evidence of disease elsewhere. The patient underwent laparotomy with excision of the left adrenal gland and tumor enucleation of the right gland. The left tumor weighed 21.5 g and measured 5.5 × 1.5 × 0.7 cm, and right tumor measured 1.3 × 1.2 × 1.0 cm. Sections of both tumors showed similar cellular constituents. Tumors were composed of a uniform population of cells with ample acidophilic cytoplasm and moderate anisonucleosis that recapitulated the zona reticularis, consistent

with the diagnosis of adrenocortical adenoma. The p53 staining was negative and Ki-67 labeling index (LI) was less than 2%. Inhibin-α was positive in a subset of cells. No chemotherapy was indicated. The patient remained asymptomatic until 2008, and then developed bilateral small breast nodules. The right breast mass measured 3.5 × 2.5 × 2.0 cm and the left inferior breast mass measured 3.0 × 2.0 × 2.0 cm and both were surgically removed. Histology of the first mass had features of tubular adenoma and that of the left mass of juvenile fibroadenoma. The patient remained clinically stable until the age of 18 years when she was taken off the protocol.

*Molecular findings*: Blood and tumor DNA of this patient was examined by whole exome sequencing (WES) (17). Results showed that the patient had a wild type sequence for *TP53* in both germline and tumor DNA as well as wild type sequence for *CTNNB1* and *ATRX* in the tumor (1, 17). Additional findings included the somatic p.E150K variant in the imprinted *MKRN3* and the p.D155fs in the cytochrome P450 Family 17 Subfamily A Member 1, *CYP17A1*. Of note, the patient harbored a germline p.E257K variant in *EGFR* (17) and the p.M595T variant in the regulator of epigenetic gene silencing *SIRT1*. Both variants were present in the tumor in the heterozygous state (17). The variant in *EGFR* was classified as likely benign in CLINVAR (variant ID 1123013) and the *SIRT1* variant was not reported. Therefore, both variants have been reported in the Genome Aggregation Database (gnomAD) originated from unrelated individual sequences as part of population genetic studies supporting lack of biological significance for both variants in the context of adrenocortical tumors. WES analysis of blood-derived DNA did not detect 11p15 UPD. However, a pattern of homozygosity at chromosome 11p15 was verified by microsatellite markers analyses and confirmed by MS-MLPA consistent with paternal uniparental disomy (UPD) in the germline sample (**Figure 2**).

## Case 2

Patient was a 2.4-year-old male with a past medical history consistent with BWS (hemihypertrophy) who had an abdominal mass in the left adrenal gland during surveillance for abdominal tumors. In addition, a hepatic mass was noted. The patient underwent laparotomy with resection of the left adrenal gland and partial hepatectomy. The adrenal tumor weighed 56 g and measured 5.9 × 5.9 × 3.6 cm. The liver lesion weighed 73 g and measured 6.5 × 4.5 × 4.0 cm. Tumors in adrenal gland and liver were histologically identical. The immune profile of both tumors was positive for pan keratin, vimentin, synaptophysin, melan-A, and was negative for inhibin-α, chromogranin, and alpha-feto protein, anti-endomysial antibody (EMA), and calretinin. Liver and adrenal masses were also negative for p53, and Ki-67 LI was <5% in both tumors. There was vascular invasion in the adrenal tumor. Peri-aortic lymph nodes were negative. Tumor margins were free of tumor. The patient was not treated with chemotherapy and remains free of disease 11 years after the diagnosis of adrenocortical carcinoma (ACC).

*Molecular findings*: Molecular studies were done for the germline sample and the patient was wild type for *TP53*. Microsatellite analysis covering the position 1,061,991 to 4,539,851 at chromosome 11p15 (GRCh37/hg19) revealed a heterozygous pattern for all studied markers but MS-MLPA revealed a pattern consistent with mosaic paternal UPD.

## Case 3

The patient was an 8.4-year-old girl diagnosed with stage II ACC at age 7 months. In 2013, she went to the local pediatric endocrinologist as she had Cushing syndrome. Her medical history revealed that she was a full-term infant with a birth weight of 6lb 12 oz (~3kg). She did not have umbilical hernia, omphalocele, macroglossia, nevus flammeus or lateralized overgrowth. An ultrasound imaging study revealed an abdominal mass in the adrenal gland region. The mass, which measured 8.2 × 7.5 × 4.5 cm was completely resected and the diagnosis of ACC confirmed. Tumor was positive for vimentin and melan-A and inhibin-α was moderate in occasional tumor cells. The Ki-67 LI was 30%. The patient was not treated with chemotherapy and has remained disease-free.

*Molecular findings*: Blood and tumor samples were available for molecular studies. No *TP53* variants were observed in the germline or tumor (1). The tumor harbored the p.S45P missense variant in *CTNNB1* and was wild type for *ATRX*. Whole genome SNP microarray (Reveal; Integrated Genetics) analysis of germline DNA revealed normal chromosome copy number but 50% mosaicism for chromosome 11p covering a 45.6 Mb region. A pattern consistent with mosaic paternal UPD was confirmed by MS-MLPA.

## Case 4

Patient was a 28-year-old healthy female diagnosed with non-functional metastatic ACT at age 15 months. She did not have an antecedent of endocrine manifestations, and the tumor was discovered during the one-year routine visit to the pediatrician. She did not have a history of growth and developmental abnormalities. CT imaging of the abdomen and chest revealed a left supra-renal mass measuring 5 cm in the largest diameter and bilateral pulmonary nodules (Stage IV). She underwent resection of the primary tumor that measured 7.0 × 6.0 × 4.0 cm and weighed 130 g. The histopathological examination confirmed the diagnosis of ACC. She was transferred to St. Jude and treated with cisplatin, etoposide and mitotane. However, after four courses of chemotherapy, several pulmonary lesions remained. She underwent resection of the bilateral pulmonary metastatic nodules, and most of them showed viable metastatic tumor by histology. Chemotherapy was stopped and the patient was monitored for tumor progression. The pulmonary lesions regressed and remained very small for over 10 years. She continues to be free of disease and in good health to date, 26.5 years after the diagnosis.

*Molecular findings*: No *TP53* variants were observed in blood and tumor samples (1). In addition, the primary tumor was negative for *CTNNB1* and *ATRX*. Furthermore, microsatellite analysis of germline DNA revealed a pattern of homozygosity consistent with paternal UPD that was confirmed by MS-MLPA.

## Case 5

The patient was a 21-year-old female with past history of stage 3 ACT diagnosed at 4.9 years. Her development was normal except

for an incidental note per the family of longer and larger right upper and lower extremities throughout her life that had not been specifically investigated as far as the patient and her family were aware, but was associated with chronic left-leaning posture and asymmetric shoe size. She had been in her usual state of good health until the age 4 years when she complained of abdominal pain. She also had weight loss, increased headaches, decreased activity and energy, increased tiredness, and sweating. Given the persistence of symptoms, she was examined by a physician who palpated an abdominal mass and noted hypertension and slight androgen elevations. Magnetic resonance imaging showed a large abdominal mass in the right adrenal gland, with direct extension into the inferior vena cava and nearly completely filling of the right atrium. She underwent a partial sternotomy, and extraction of the caval portion of the adrenal tumor and resection of the right retroperitoneal tumor. The tumor weight was 550 g and measured 13.5 × 10.5 × 6.0 cm. The pathology confirmed ACC (low Ki-67 LI, rare mitotic figures and negative for inhibin-α). There were large areas of necrosis, and vascular invasion with tumor penetration through the capsule. Immunohistochemistry analysis was negative for p53 and positive for beta-catenin. She was treated with the combination of cisplatin, doxorubicin, etoposide, and mitotane. Features of right-sided lateral overgrowth, including right-sided tongue enlargement as well as increased right *vs*. left arm circumferences (51 cm *vs* 50 cm), calf circumferences (39 cm *vs* 37 cm), and a slight leg length discrepancy (88 cm *vs* 85 cm) were first noted during exams performed at St. Jude as part of a multidisciplinary rare endocrine tumor clinic when she was 18 years old, and led to additional testing subsequently confirming chromosome 11p15 UPD. She has been alive and tumor free for 17 years.

*Molecular findings:* Blood DNA of this patient was analyzed by whole exome sequencing (WES). No reportable structural, single nucleotide variants, and indel or copy number changes were identified in *APC*, *CDKN1C*, *MEN1*, *PRKAR1A*, and *TP53*. Chromosome paternal 11p15 UPD was confirmed by MS-MLPA.

## Case 6

The patient was a 23-year-old female who had hypertension during a routine medical visit in 2009 at age 11 years. Examination for causes of hypertension revealed a large, and well-defined mass in the left upper quadrant above the left kidney and deep to the spleen. The mass was approximately 8.7 × 9.7 × 9.7 cm and was relatively round. The kidneys and liver were normal in appearance. There was no regional adenopathy. Laboratory investigation showed remarkably elevated levels of deoxycorticosterone, aldosterone, and dehydroepiandrosterone. The mass was removed one month later, and weighed 388 g and measured 11 × 10 × 6 cm. There was a 3 × 3 cm defect on the surface suggestive of tumor rupture. The tumor was composed of nests of moderate-sized cells with round nuclei, prominent nucleoli, and moderate to abundant foamy to amphophilic non-foamy cytoplasm. There was only one mitosis per ten 400× fields and there was no atypical mitosis. However, the tumor demonstrated prominent venous invasion, necrosis, and extracapsular extension. Calcifications were noted. Immunohistochemical stains were positive for melan-A, vimentin, and cytokeratin (focal). Epithelial membrane antigen, chromogranin, and inhibin-α were negative. Ki-67 LI was <5%. Occasional areas of the tumor showed moderate nuclear staining for p53. The patient was referred to St. Jude for treatment. At that time, her adrenal hormones had returned to normal levels. She underwent comprehensive imaging studies, including FDG-PET scans. There was no evidence of residual disease. The recommendation was observation. She remains disease free 12 years from diagnosis.

*Molecular findings:* Blood and tumor DNA of this patient was analyzed by whole genome sequencing (WGS) (17). The patient had a wild type sequence for *TP53* in both germline and tumor DNA (1, 17). ACT was wild type for *ATRX* and acquired the p.G34E variant in *CTNNB1* and p.R201H in *GNAS* (17). In addition, the patient harbored the germline p.R307* variant in the PDE11A (18). WES analysis of blood-derived DNA was not sufficiently sensitive to detect chromosome 11p15 UPD, but MS-MLPA revealed a mosaic pattern of paternal 11p15 UPD.

# DISCUSSION

This study suggests that ACT can be the first and only clinical manifestation of germline paternal uniparental disomy (UPD) at chromosome 11p15. The association between chromosome 11p15 rearrangements and embryonal tumors, including pediatric ACT, in patients with clinical diagnosis of BWS/lateralized overgrowth is well established (3–8). Wilms tumor is the most common tumor (52% of all tumors) (3), and pediatric ACT accounts for a minority of cases (3%) (3). The risk for embryonal tumors in BWS results primarily from dysregulation at the telomeric domain of 11p15 (gain of methylation at ICR1 and UPD) rather than at the centromeric domain (loss of methylation at ICR2 and pathogenic variants in *CDKN1C*) (19, 20). The loss of methylation at the ICR2 confers a low risk of developing embryonal tumors (19, 20). ACTs have been reported in a BWS patient with concomitant neuroblastoma and hypomethylation at ICR2 (21). However, most studies associate ACT exclusively with 11p15 UPD (19, 22, 23). In addition to paternal 11p15 UPD, germline rearrangements at this region have also been observed in 12% of children with ACT without germline *TP53* mutations (1), making abnormalities in these loci the most common recurrent constitutional driver events in wild type *TP53* pediatric ACT.

Remarkably, four of the patients with germline paternal 11p15 UPD (cases #3,4,5,6), and three previously reported cases of ACT with hypomethylation at ICR2 (24, 25) did not have clinical manifestations of BWS. These findings suggest that chromosome 11p15 abnormalities are associated with diverse phenotypes ranging from cases that fulfil the entire criteria of classic BWS to those with embryonal tumors-only. This concept is supported by a study reporting that among 437 cases of non-syndromic Wilms tumor, 13 (3%) had constitutional 11p15 abnormalities, including 6 with germline paternal segmental 11p15 UPD (26).

Although mechanisms underlying the phenotypic variations are not established, the length of the uniparental disomic region has been implicated in the degree of severity (27). This is consistent with molecular findings observed in three of the patients (cases #1,5,6) included in this study. In these patients, microsatellite and MS-MLPA analysis detected mosaic paternal 11p15 UPD that was not detected by WGS or WES. These findings highlight the technical challenges of detecting genetic mosaicism and underscore the need to incorporate multiple techniques with higher diagnostic yield to determine the (epi)genotype-phenotype associated to cancer risk.

A diversity of adrenal gland lesions is observed in BWS, including adrenal hyperplasia, hemorrhage, cysts, neuroendocrine tumors, neuroblastoma, hemangioendothelioma, ovarian thecal metaplasia, and adrenal cortical tumors (adenoma and carcinoma) (28). Moreover, ectopic adrenal tissue (29) has been found in liver, renal hilum, and spinal cord. A panel of markers (CD56, vimentin, melan-A, inhibin-α, synaptophysin, chromogranin and SF-1) are used to establish the origin of adrenal tumors (30, 31). Notably inhibin-α is expressed in the normal adrenal cortex and frequently in both adrenocortical adenoma and carcinoma, which is useful to differentiate adrenal cortex tumors from other embryonal pediatric tumors. Normal adrenal glands show strong immunoreactivity against the inhibin-α subunit, especially in the zona reticularis (32, 33) and both fetal and definitive zones of the fetal cortex (32, 33). In addition, immunopositivity is seen in most ACTs (33). In our series, inhibin-α was negative in three cases and had weak focal expression (occasional cells) in two cases. Focal immunoreactivity for inhibin-α was also seen in heterotopic ACT in a patient with BWS (29). However, the clinical and pathological significance of immunoreactivity for inhibin α remains unclear.

*IGF2* expression is increased in virtually all cases of pediatric ACT, irrespective of the *TP53* status, and is considered an early driver event in tumorigenesis of the adrenal cortex (17). However, the mechanism of *IGF2* overexpression, and likely its degree, may vary. Most cases of ACT in carriers of germline *TP53* variants, have lost the whole maternal chromosome 11, followed by duplication of the paternal [copy neutral loss of heterozygosity (LOH)] (17). In this context, there is biallelic *IGF2* expression and loss of *IGF2* regulatory elements located in maternal chromosome 11. In contrast, in ACT of children with germline paternal 11p15 UPD, rearrangements appear to be confined to the 11p15 loci and *IGF2* expression could still be regulated by remaining regulators on maternal chromosome 11. Moreover, in ACT driven by *TP53* germline mutations, there is an association between tumor weight and the number of genomic alterations (17). It is not surprising that tumor size is a reliable prognostic indicator in patients with germline *TP53* variants, in which patients with small tumors (<100 g) have excellent outcomes (34–36) whereas those with large tumors can have metastatic disease at diagnosis and a high relapse rate after complete resection. These observations are consistent with the proposed mechanism of pediatric ACT associated with germline *TP53* variants that lose both the wild type *TP53* and maternal chromosome 11 early in tumorigenesis (17). As the tumor grows, these two molecular events are followed by acquisition of multiple genomic abnormalities and poor clinical outcomes in patients (17). Conversely, it appears that tumor weight in cases of ACT with constitutional paternal 11p15 UPD is not associated with high number of genomic aberrations as seen in carriers of *TP53* variants even when the former has larger tumors. In our series, all six patients with ACT associated with paternal 11p15 UPD are alive and free of disease despite bilateral pulmonary metastasis at diagnosis in one patient, bilateral tumors in another patient, and tumor extending and nearly filling the right atrium in a third patient. Of note, independent of the germline *TP53* status, copy neutral LOH with preferential loss of maternal chromosome 11 leading to *IGF2* overexpression from the paternal allele is observed in 90% of pediatric ACTs (17). Although not related to prognosis in children, chromosome 11p15 abnormalities and IGF2 overexpression are malignancy markers in adult patients with ACC (37).

Recommendations for cancer surveillance of children with BWS have been suggested by consensus panels (5, 38). For non-syndromic children with paternal UPD 11p15 who develop ACT, it is unclear whether surveillance is required beyond that for relapsed ACT. In our series, no patients developed other embryonal tumors. However, case #1, who had a clinical diagnosis of BWS preceding the diagnosis of ACT, developed bilateral breast fibroadenomas at age 14 years. This complication is seen in women with BWS (39). Until more data are available, we suggest that patients with ACT associated with paternal UPD 11p15 follow the surveillance recommendations for BWS (5, 38).

Case #1 was also interesting because in addition to paternal 11p15 UPD, it also carried a germline mutation in *EGFR* (p.E257K). A germline mutation in *EGFR* (p.D1080N) has been reported in another patient with bilateral ACT, but without overt clinical signs of BWS. Unfortunately, in the reported case (40), chromosome 11p15 copy number changes and methylation studies were not performed to determine whether the patient did or did not have germline paternal UPD 11p15. Whether germline *EGFR* mutations contributes to pediatric ACT remains to be elucidated.

In conclusion, we demonstrate that germline paternal 11p15 UPD is a relatively common event in pediatric ACT without germline *TP53* variants or somatic manifestation of BWS. Given the therapeutic implications and tumor surveillance, we recommend using chromosome 11p15 molecular assays in routine clinical work-up of patients with pediatric adrenocortical tumors, particularly those with wild type *TP53* sequence, with genetic predisposition evaluation and counseling.

## DATA AVAILABILITY STATEMENT

The raw data supporting the conclusions of this article will be made available by the authors, without undue reservation.

## ETHICS STATEMENT

The studies involving human participants were reviewed and approved by St. Jude Children's Research Hospital. Written informed consent to participate in this study was provided by the participants' legal guardian/next of kin. Written informed consent was obtained from the minor(s)' legal guardian/next of kin for the publication of any potentially identifiable images or data included in this article.

## AUTHOR CONTRIBUTIONS

All authors co-wrote the manuscript and are accountable for all aspects of the work. All authors contributed to the article and approved the submitted version.

## FUNDING

This work was supported by the American Lebanese Syrian Associated Charities (ALSAC), Speer Charitable Trust, and Cancer Center Support Grant CA21765. The content is solely the responsibility of the authors and does not necessarily represent the official views of the National Institutes of Health.

## ACKNOWLEDGMENTS

We thank the patients and their family members for indirect participation in this study. We also thank Vani Shanker, PhD, for editing the manuscript.

## REFERENCES

1. Pinto EM, Rodriguez-Galindo C, Pounds S, Wang L, Clay MC, Neale G, et al. Identification of Clinical and Biologic Correlates Associated With Outcome in Children With Adrenocortical Tumors Without Germline TP53 Mutations: A St. Jude Adrenocortical Tumor Registry and Children's Oncology Group Study. *J Clin Oncol* (2017) 35:3956e63. doi: 0.1200/JCO.2017.74.2460
2. Wasserman JD, Novokmet A, Eichler-Jonsson C, Ribeiro RC, Rodriguez-Galindo C, Zambetti GP, et al. Prevalence and Functional Consequence of TP53 Mutations in Pediatric Adrenocortical Carcinoma: A Children's Oncology Group Study. *J Clin Oncol* (2015) 33:602–9. doi: 10.1200/JCO.2013.52.6863
3. Brioude F, Kalish JM, Mussa A, Foster AC, Bliek J, Ferrero GB, et al. Expert Consensus Document: Clinical and Molecular Diagnosis, Screening and Management of Beckwith-Wiedemann Syndrome: An International Consensus Statement. *Nat Rev Endocrinol* (2018) 14:229–49. doi: 10.1038/nrendo.2017.166
4. Pettenati MJ, Haines JL, Higgins RR, Wappner RS, Palmer CG, Weaver DD, et al. Wiedemann-Beckwith Syndrome: Presentation of Clinical and Cytogenetic Data on 22 New Cases and Review of the Literature. *Hum Genet* (1986) 74:143–54. doi: 10.1007/BF00282078
5. Tan TY, Amor DJ. Tumour Surveillance in Beckwith-Wiedemann Syndrome and Hemihyperplasia: A Critical Review of the Evidence and Suggested Guidelines for Local Practice. *J Paed Child Health* (2006) 42:486–90. doi: 10.1111/j.1440-1754.2006.00908.x
6. Cooper WN, Luharia A, Evans GA, Raza H, Haire AC, Grundy R, et al. Molecular Subtypes and Phenotypic Expression of Beckwith-Wiedemann Syndrome. *Eur J Hum Genet* (2005) 13:1025–32. doi: 10.1038/sj.ejhg.5201463
7. Maas SM, Vansenne F, Kadouch DJM, Ibrahim A, Bliek J, Hopman S, et al. Phenotype, Cancer Risk, and Surveillance in Beckwith–Wiedemann Syndrome Depending on Molecular Genetic Subgroups. *Am J Hum Genet* (2016) 170:2248–60. doi: 10.1002/ajmg.a.37801
8. Rump P, Zeegers MPA, van Essen AJ. Tumor Risk in Beckwith-Wiedemann Syndrome: A Review and Meta-Analysis. *Am J Med Genet A* (2005) 136:95–104. doi: 10.1002/ajmg.a.30729
9. Jinno Y, Ideda Y, Yun K, Maw M, Masuzaki H, Fukuda H, et al. Establishment of Functional Imprinting of the H19 Gene in Human Developing Placentae. *Nat Genet* (1995) 10:318–24. doi: 10.1038/ng0795-318
10. Leibovitch MP, Nguyen VC, Gross MS, The human ASM. (Adult Skeletal Muscle) Gene: Expression and Chromosomal Assignment to 11p15. *Biochem Biophys Res Commun* (1991) 180:1241–50. doi: 10.1016/S0006-291X(05)81329-4
11. Monk D, Sanches R, Arnaud P, Apostolidou S, Hills FA, Abu-Amero S, et al. Imprinting of IGF2 P0 Transcript and Novel Alternatively Spliced INS-IGF2 Isoforms Show Differences Between Mouse and Human. *Hum Moll Genet* (2006) 15:1259–69. doi: 10.1093/hmg/ddl041
12. Schmidt JV, Levorse JM, Tilghman SM. Enhancer Competition Between H19 and Igf2 Does Not Mediate Their Imprinting. *PNAS* (1999) 96:9733–8. doi: 10.1073/pnas.96.17.9733
13. Stampone E, Caldarelli I, Zullo A, Bencivenga D, Mancini FP, Ragione FD, et al. Genetic and Epigenetic Control of CDKN1C Expression: Importance in Cell Commitment and Differentiation, Tissue Homeostasis and Human Diseases. *Int J Mol Sci* (2018) 19:1055. doi: 10.3390/ijms19041055
14. Korostowski L, Raval A, Breuer G, Engel N. Enhancer-Driven Chromatin Interactions During Development Promote Escape From Silencing by a Long Non-Coding RNA. *Epigenet Chromatin* (2011) 4:21. doi: 10.1186/1756-8935-4-21
15. Mancini-Dinardo D, Steele SJS, Levorse JM, Ingram RS, Tilghman SM. Elongation of the Kcnq1ot1 Transcript Is Required for Genomic Imprinting of Neighboring Genes. *Genes Dev* (2006) 20:1268–82. doi: 10.1101/gad.1416906
16. Begemann M, Spengler S, Gogiel M, Grasshoff U, Bonin M, Betz RC, et al. Clinical Significance of Copy Number Variations in the 11p15.5 Imprinting Control Regions: New Cases and Review of the Literature. *J Med Genet* (2012) 49:547–53. doi: 10.1136/jmedgenet-2012-100967
17. Pinto EM, Chen X, Easton J, Finkelstein D, Liu Z, Pounds S, et al. Genomic Landscape of Paediatric Adrenocortical Tumours. *Nat Commun* (2015) 6:6302. doi: 10.1038/ncomms7302
18. Pinto EM, Faucz FR, Paza LZ, Wu G, Fernandes ES, Bertherat J, et al. Germline Variants in Phosphodiesterase Genes and Genetic Predisposition to Pediatric Adrenocortical Tumors. *Cancers* (2020) 12:506. doi: 10.3390/cancers12020506
19. Mussa A, Molinatto C, Baldassarre G, Riberi E, Russo S, Larizza L, et al. Cancer Risk in Beckwith-Wiedemann Syndrome: A Systematic Review and Meta-Analysis Outlining a Novel (Epi)Genotype Specific Histotype Targeted Screening Protocol. *J Pediatr* (2016) 176:142–9. doi: 10.1016/j.jpeds.2016.05.038
20. Bliek J, Gicquel C, Maas S, Gaston V, Bouc YL, Mannens M. Epigenotyping as a Tool for the Prediction of Tumor Risk and Tumor Type in Patients With Beckwith-Wiedemann Syndrome (BWS). *J Pediatr* (2004) 145:796–9. doi: 10.1016/j.jpeds.2004.08.007
21. Alsultan A, Lovell MA, Hayes KL, Allshouse MJ, Garrington TP. Simultaneous Occurrence of Right Adrenocortical Tumor and Left Adrenal Neuroblastoma in an Infant With Beckwith–Wiedemann Syndrome. *Pediatr Blood Cancer* (2008) 51:695–8. doi: 10.1002/pbc.21694
22. Papulino C, Chianese U, Nicoletti MM, Benedetti R, Altucci L. Preclinical and Clinical Epigenetic-Based Reconsideration of Beckwith-Wiedemann Syndrome. *Front Genet* (2020) 11:563718. doi: 10.3389/fgene.2020.563718
23. Brioude F, Lacoste A, Netchine I, Vazquez M-P, Auber F, Audry G, et al. Beckwith-Wiedemann Syndrome: Growth Pattern and Tumor Risk According to Molecular Mechanism, and Guidelines for Tumor Surveillance. *Horm Res Paediatr* (2013) 80:457–65. doi: 10.1159/000355544
24. Wijnen M, Alders M, Zwaan C, Wagner A, van den Heuvel-Eibrink MM. KCNQ1OT1 Hypomethylation: A Novel Disguised Genetic Predisposition in Sporadic Pediatric Adrenocortical Tumors? *Pediatr Blood Cancer* (2012) 59:565–6. doi: 10.1002/pbc.23398

25. Eltan M, Arslan Ates E, Cerit K, Menevse TS, Kaygusuz SB, Eker N, et al. Adrenocortical Carcinoma in Atypical Beckwith-Wiedemann Syndrome Due to Loss of Methylation at Imprinting Control Region 2. *Pediatr Blood Cancer* (2020) 67:e28042. doi: 10.1002/pbc.28042
26. Scott RH, Douglas J, Baskcomb L, Huxter N, Barker K, Hanks S, et al. Constitutional 11p15 Abnormalities, Including Heritable Imprinting Center Mutations, Cause Nonsyndromic Wilms Tumor. *Nat Genet* (2008) 40:1329–34. doi: 10.1038/ng.243
27. Smith AC, Shuman C, Chitayat D, Steele L, Ray PN, Bourgeois J, et al. Severe Presentation of Beckwith-Wiedemann Syndrome Associated With High Levels of Constitutional Paternal Uniparental Disomy for Chromosome 11p15. *Am J Med Genet* (2007) 143A:3010–5. doi: 10.1002/ajmg.a.32030
28. MacFarland SP, Mostoufi-Moab S, Zelley K, Mattei PA, States LJ, Bhatti TR, et al. Managemente of Adrenal Masses in Patients With Beckwith-Wiedemann Syndrome. *Pediatr Blood Cancer* (2017) 64(8):e26432. doi: 10.1002/pbc.26432
29. Kim EN, Song DE, Yoon HM, Lee BH, Kim CJ. Adrenal Cortical Neoplasm With Uncertain Malignant Potential Arising in the Heterotopic Adrenal Cortex in the Liver of a Patient With Beckwith-Wiedemann Syndrome. *J Pathol Transl Med* (2019) 53:129–35. doi: 10.4132/jptm.2018.11.13
30. Sangoi AR, Fujiwara M, West RB, Montgomery KD, Bonventre JV, Higgins JP, et al. Immunohistochemical Distinction of Primary Adrenal Cortical Lesions From Metastatic Clear Cell Renal Cell Carcinoma: A Study of 248 Cases. *Am J Surg Pathol* (2011) 35:678–86. doi: 10.1097/PAS.0b013e3182152629
31. Munro LMA, Kennedy A, McNicol AM. The Expression of Inhibin/Activin Subunits in the Human Adrenal Cortex and Its Tumours. *J Endocrinol* (1999) 161:341–7. doi: 10.1677/joe.0.1610341
32. Hofland J, de Jong FH. Inhibins and Activins: Their Roles in the Adrenal Gland and the Development of Adrenocortical Tumors. *Mol Cell Endocrinol* (2012) 359:92–100. doi: 10.1016/j.mce.2011.06.005
33. Arola J, Liu J, Heikkila P, Ilvesmaki V, Salmenkivi K, Voutilainen R, et al. Expression of Inhibin Alpha in Adrenocortical Tumours Reflects the Hormonal Status of the Neoplasm. *J Endocrinol* (2000) 165:223–9. doi: 10.1677/joe.0.1650223
34. Michalkiewicz E, Sandrini R, Figueiredo B, Miranda ECM, Caran E, Oliveira-Filho AG, et al. Clinical and Outcome Characteristics of Children With Adrenocortical Tumors: A Report From the International Pediatric Adrenocortical Tumor Registry. *J Clin Oncol* (2004) 22:838–45. doi: 10.1200/JCO.2004.08.085
35. Rodriguez-Galindo C, Krailo MD, Pinto EM. Treatment of Pediatric Adrenocortical Carcinoma With Surgery, Retroperitoneal Lymph Node Dissection, and Chemotherapy: The Children's Oncology Group ARAR0332 Protocol. *J Clin Oncol* (2021) 39:2463–73. doi: 10.1200/JCO.20.02871
36. McAteer JP, Huaco JA, Gow KW. Predictors of Survival in Pediatric Adrenocortical Carcinoma: A Surveillance, Epidemiology, and End Results (SEER) Program Study. *J Pediatr Surg* (2013) 48:1025–31. doi: 10.1016/j.jpedsurg.2013.02.017
37. Gicquel C, Bertagna X, Schneid H, Francillard-Leblond M, Luton JP, Girard F, et al. Rearrangements at 11p15 Locus and Overexpression of Insulin-Like Growth Factor-II Gene in Sporadic Adrenocortical Tumors. *J Clin Endocrinol Metab* (1994) 78:1444–53. doi: 10.1016/j.jpedsurg.2013.02.017
38. Wang KH, Kupa J, Duffy KA and Kalish JM. Diagnosis and Management of Beckwith-Wiedemann Syndrome. *Front Pediatr* (2020) 7562. doi: 10.3389/fped.2019.00562
39. Oktay A, Esmart HA, Aslan O. Fibroepithelial Breast Tumors in a Teenager With Beckwith-Wiedemann Syndrome: A Case Report and Review of Literature. *Eur J Breast Health* (2021) 17:288–91. doi: 10.4274/ejbh.galenos.2021.6271
40. Akhavanfard S, Yehia L, Padmanabhan R, Reynolds JP, Ni Y, Eng C. Germline EGFR Variants Are Over-Represented in Adolescents and Young Adults (AYA) With Adrenocortical Carcinoma. *Hum Mol Genet* (2020) 29:3679–90. doi: 10.1093/hmg/ddaa268


**Conflict of Interest:** The authors declare that the research was conducted in the absence of any commercial or financial relationships that could be construed as a potential conflict of interest.

frontiers in Endocrinology

CASE REPORT
published: 11 November 2021
doi: 10.3389/fendo.2021.731631

# Aggressive Pituitary Macroadenoma Treated With Capecitabine and Temozolomide Chemotherapy Combination in a Patient With Nelson's Syndrome: A Case Report

*Oriol Mirallas[1]*, Francesca Filippi-Arriaga[2], Irene Hernandez Hernandez[3], Anton Aubanell[4], Anas Chaachou[5], Alejandro Garcia-Alvarez[1], Jorge Hernando[1], Elena Martínez-Saez[5], Betina Biagetti[3] and Jaume Capdevila[1]*

[1] Medical Oncology Department, Gastrointestinal and Endocrine Tumor Unit, Vall d'Hebron University Hospital and Vall d'Hebron Institute of Oncology (VHIO), Barcelona, Spain, [2] Clinical Pharmacology Department, Vall d'Hebron University Hospital, Barcelona, Spain, [3] Endocrinology & Nutrition Service, Vall d'Hebron University Hospital, Barcelona, Spain, [4] Radiology Department, Vall d'Hebron University Hospital, Barcelona, Spain, [5] Pathology Department, Vall d'Hebron University Hospital, Barcelona, Spain

OPEN ACCESS

**Edited by:**
*Antongiulio Faggiano, Sapienza University of Rome, Italy*

**Reviewed by:**
*Salvatore Cannavo, University of Messina, Italy*
*Franz Sesti, Sapienza University of Rome, Italy*

***Correspondence:**
*Oriol Mirallas*
*omirallas@vhebron.net*

**Specialty section:**
*This article was submitted to Cancer Endocrinology, a section of the journal Frontiers in Endocrinology*

**Received:** *27 June 2021*
**Accepted:** *12 October 2021*
**Published:** *11 November 2021*

**Citation:**
*Mirallas O, Filippi-Arriaga F, Hernandez Hernandez I, Aubanell A, Chaachou A, Garcia-Alvarez A, Hernando J, Martínez-Saez E, Biagetti B and Capdevila J (2021) Aggressive Pituitary Macroadenoma Treated With Capecitabine and Temozolomide Chemotherapy Combination in a Patient With Nelson's Syndrome: A Case Report. Front. Endocrinol. 12:731631. doi: 10.3389/fendo.2021.731631*

Nelson's syndrome is considered a severe side effect that can occur after a total bilateral adrenalectomy in patients with Cushing's disease. It usually presents with clinical manifestations of an enlarging pituitary tumor including visual and cranial nerve alterations, and if not treated, can cause death through local brain compression or invasion. The first therapeutic option is surgery but in extreme cases of inaccessible or resistant aggressive pituitary tumors; the off-label use of chemotherapy with capecitabine and temozolomide can be considered. However, the use of this treatment is controversial due to adverse events, lack of complete response, and inability to predict results. We present the case of a 48-year-old man diagnosed with Nelson's syndrome with prolonged partial response and significant clinical benefit to treatment with capecitabine and temozolomide.

**Keywords: capecitabine, temozolomide, aggressive pituitary tumors, Nelson's syndrome, case report**

## INTRODUCTION

Nelson's syndrome (NS) is characterized by an elevation of adrenocorticotropic hormone (ACTH), hyperpigmentation, and an expanding pituitary mass. NS is considered a severe side effect of total bilateral adrenalectomy (TBA) that occurs as a consequence of missing glucocorticoid feedback to control adenoma cells in patients with Cushing's disease (CD), which results in an invasive macroadenoma of the pituitary gland (1). CD represents around 70% of the forms of chronic endogenous hypercortisolism and is caused by excessive secretion of cortisol from the adrenal glands secondary to stimulation of an ACTH-producing pituitary tumor (2). CD has a prevalence of 40 cases per million with an incidence from 1.2 to 2.4 per million per year (2, 3). Usually, CD presents in the fourth to sixth decade of life and is more common in

women than in men with a ratio of 3:1 (2, 3). Almost 10% of patients with CD eventually undergo TBA and the incidence of NS in patients with TBA shows a high variation, ranging from 0% to 47% with a median of 21% at a median follow-up of 61 months (1). The first-line treatment for CD is transsphenoidal surgery since it is the only curative treatment. When surgery fails, other options include repeating surgery (if feasible), radiotherapy, bilateral adrenalectomy, and/or medical treatment (4, 5). Treatment with TBA is performed in patients in whom all other treatment options have failed; the advantage of this procedure is usually the immediate control of hypercortisolism (1). The criteria for the diagnosis of NS include a plasma ACTH level above 200 ng/L, imaging evidence of pituitary mass enlargement, and hyperpigmentation (4). If a patient develops NS after TBA, the primary treatment is surgery, but in patients with inaccessible or resistant aggressive pituitary tumors, the off-label use of chemotherapy or the experimental use of peptide receptor radionuclide therapy (PRRT) may be considered (6, 7). Treatment with temozolomide (TMZ) alone has demonstrated favorable responses in some case reports against a variety of aggressive pituitary tumors (8). However, the use of this treatment can be controversial due to adverse events and lack of complete response to it. In some cases, the addition of capecitabine (CAP) has been proposed; however, the effect of the combination of these drugs in NS has been less defined and the long-term repercussions are unknown (9). Untreated NS adenomas often become markedly aggressive and may cause death, usually through local brain compression or invasion (5). Herein, we present the case of a Nelson's syndrome patient treated with CAP-TMZ, who achieved a prolonged partial response with great tolerance.

## CASE PRESENTATION

A 48-year-old man was referred to our hospital for the study of cushingoid phenotype. Medical history included allergy to penicillin and dyslipidemia. He presented an ACTH of 152 pg/ml (range, 4.7–48.8 pg/ml) cortisol of 47 μg/dl (range, 5.27–22.45 μg/dl), dynamic endocrine laboratory tests were suggestive of CD, and the magnetic resonance imaging (MRI) revealed a macroadenoma. Therefore, initial treatment with a transsphenoidal resection was performed. The morphological changes were consistent with a pituitary adenoma, with a loss of reticulin network (**Figure 1B**). The cells displayed a pathological appearance with a glassy pale eosinophilic cytoplasm, with intranuclear or perinuclear vacuoles, consistent with Crooke's hyaline change (**Figure 1A**). ACTH cytoplasmic immunoreactivity was found at the periphery of the cell (**Figure 1C**); PAS positivity was found, stronger at the periphery (**Figure 1D**). The proliferation index (Ki-67) reached 2% to 4% of cells. Pituitary surgery was unsuccessful, and the follow-up pituitary MRI showed an 8-mm lesion on the right margin of the sella turcica. With this finding, a second surgical intervention was performed and the histology reported a pituitary adenoma with mild and diffuse expression of ACTH, absence of p53 overexpression, and a Ki-67 of 2%–3%. Despite surgical rescue, the patient remained with active Cushing and an increasing tumor volume in follow-up. Thus, a third surgical intervention was performed with adjuvant stereotaxic radiotherapy at a dose of 54 Gy in 27 fractions to prevent NS but was not expected to be curative. The last histological study showed again a pituitary adenoma with ACTH expression, absence of p53 overexpression, and a Ki-67 of 2%. The patient failed to control hypercortisolism with ketoconazole (200 mg/8 h) and pasireotide (40 mg/month). Therefore, the case was presented to the endocrine tumors

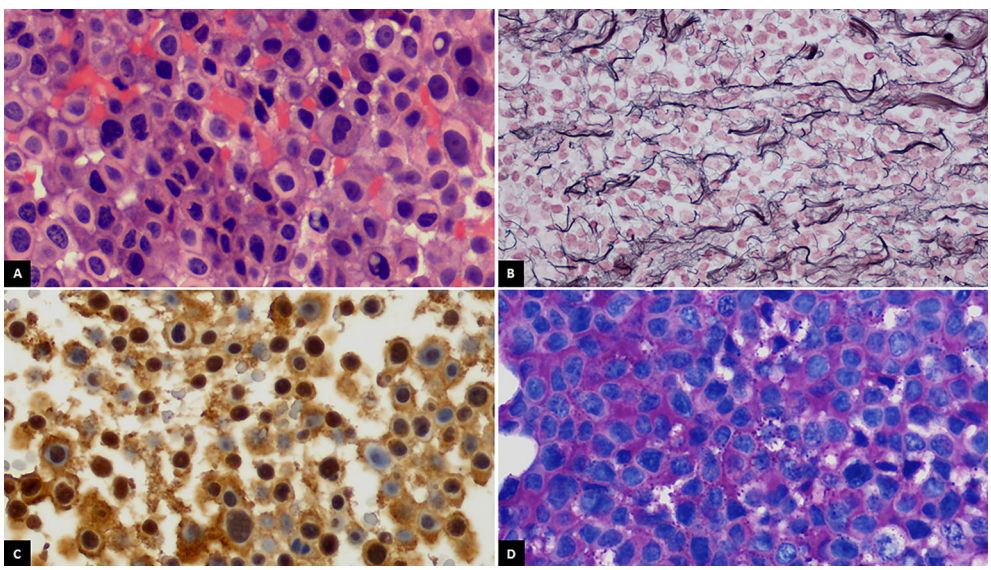


**FIGURE 1** | **(A)** Crooke cells exhibiting wide glassy pale eosinophilic cytoplasm with intranuclear or perinuclear vacuoles (H&E, ×400). **(B)** Breakdown of reticulin network in the lesion (Gordon's reticulin, ×400). **(C)** ACTH cytoplasmic immunoreactivity at the periphery of the cell (ACTH, ×400). **(D)** Periodic acid-Schiff (PAS) positivity staining stronger at the periphery of the cell (×400).

committee, and treatment with TBA was indicated. After TBA, the cortisol levels became undetectable and steroid replacement was initiated with hydrocortisone 300 mg iv during the first 24 h. After the initial treatment, the corticosteroid dose was gradually decreased until an oral dose of hydrocortisone at 30 mg/day was reached. Moreover, oral fludrocortisone at 0.1 mg/day was initiated. The pathological anatomy report of the adrenal glands showed diffuse corticoadrenal hyperplasia with an absence of malignancy. During postsurgical TBA follow-up, the annual pituitary MRIs showed tumor stability for 2 years.

Two years and eleven months after the TBA, the patient presented to the emergency room with an intermittent bilateral diplopia of 3 weeks of evolution. He denied ocular symptoms like exudate, chemosis, or ecchymosis. He also denied fever, bulbar symptoms, nausea, vomiting, headache, or head trauma. On physical examination, he presented generalized skin and mucosa hyperpigmentation, horizontal diplopia to dextroversion, without ptosis or clear restrictions in the oculomotor muscles, and no peripheral sensory or motor neurological alterations were present. The ophthalmic funduscopy and ultrasound biomicroscopy were unremarkable. The presentation of diplopia to dextroversion as the main clinical sign suggested differential diagnoses such as lens ectopias, cataracts, and corneal opiates. The ocular fundus examination without pathological findings helped to dismiss these possible diagnoses. The diplopia was not accompanied by ocular exudate, chemosis, or ecchymosis, which made it unlikely to relate the symptom to an infectious process. The neurological evaluation with an absence of peripheral sensory or motor alterations made diagnoses such as multiple sclerosis or Eaton-lambert syndrome very unlikely. Diplopia was not associated with systemic symptoms such as fever or chills, which could suggest an orbital or brain abscess or cavernous sinus thrombosis. An emergency CT scan was requested and did not show growth of the lesion or signs of compression. However, during follow-up, the patient persisted with intermittent diplopia and subsequently presented ACTH levels at 1,838 pg/ml and chromogranin A of 41.5 ng/ml (range, 0–101.9 ng/ml). A pituitary MRI (**Figures 2A, C**) reported an increase in the size of the pituitary tumor that invaded the clivus, a subacute bleeding component that affected the right margin of the tumor (9 × 14 mm), and an invasion of both cavernous sinuses extending to the lateral carotid line (Knosp grade III). With the three criteria of plasma ACTH level increase, imaging evidence of pituitary mass enlargement, and hyperpigmentation, the patient was diagnosed with NS. No other surgery was performed due to the low probability of success and no clear clinical benefit. Prior to the committee, a thoracic and abdominal CT scan was performed and was negative for extracranial disease. The case was presented to the endocrine tumors committee and the patient started treatment with CAP 2,500 mg daily on days 1 to 14 every 28 days for 14 days and TMZ 140 mg/m$^2$ once daily on days 10 to 14 every 28 days. After two cycles of CAP-TMZ, the diplopia disappeared, hyperpigmentation improved, and ACTH levels decreased to 80% (from 1,838 to 414 pg/ml). The patient reported asthenia and diarrhea grade one during the first two cycles, which disappeared after four cycles. The patient completed four cycles of CAP-TMZ and started maintenance treatment with TMZ 140 mg/m$^2$ once daily on days 10 to 14 every 28 days. After 14 months of initial CAP-TMZ treatment, the last pituitary MRI showed a 65% shrinkage of the tumor (**Figures 2** and **3B, D**) compared with the prior brain MRI (**Figures 3A, C**). At the time of this article's publication, after 18 months of the first dose of CAP-TMZ, the patient continues treatment with hormone replacement therapy and TMZ with excellent tolerance, maintaining a PS ECOG of 0 without new neurological focality in the last follow-up visit (**Table 1**).

## DISCUSSION

The choice of treatment for a complicated case of NS is challenging due to the inability to predict a good outcome. Like in the case of our patient, Nelson's syndrome usually presents with clinical manifestations of an enlarging pituitary tumor, including visual and cranial nerve alterations, due to tumor compressive effects or invasion into surrounding structures (6). To gain a rapid reduction in tumor size and ACTH secretion, pituitary surgery with maximal resection of the adenoma is the first-line treatment for NS, but when this approach is dismissed, there is no specific standardized systemic treatment (10). Regarding the chemotherapy options for the treatment of aggressive pituitary adenomas (APA), the use of TMZ has been described since 2006. TMZ exerts its cytotoxic activity by alkylating DNA at the O6-methylguanine DNA methyltransferase (MGMT) position of guanine resulting in irreversible DNA damage and cell death (11). Principal controversies to determine the adequate use of TMZ in patients with APA are related to the optimal duration of treatment and whether TMZ should be used in combination with other therapies. Based on the results of a European Society of Endocrinology survey in 2016, TMZ was endorsed as first-line chemotherapeutic treatment of APA (8). A previous case of a 64-year-old woman with NS treated with TMZ reported a significant improvement in symptoms, a reduction of plasma ACTH, and regression of tumor on magnetic resonance imaging scan after four cycles of treatment (12). Another review describes at least 11 separate cases of pituitary tumors treated with TMZ with sustained effects (12). In general, clinically functioning tumors and concurrent radiotherapy are associated with a better response to treatment with TMZ (8). A systematic review of 31 cases of APA reported that the objective response rate (complete response plus partial response) was 48.4%, and a stable disease occurred in 29%, and lack of response to TMZ was 22.5%. Among patients who received more than 12 months of treatment with TMZ, the majority stayed free of disease progression for relatively long periods of time (14 to 120 months). Although these data strongly argue for use of long-term TMZ in the treatment of APA, the duration of TMZ therapy remains unknown (13). A literature review that included 31 patients reported that 25 patients (80.6%) had disease control during TMZ treatment, while six patients (19.4%) had disease progression with a median follow-up after beginning TMZ of 43 months. The 2-year progression-free survival was 47.7% (95% CI, 29.5%–65.9%), while the 2-year disease control duration was 59.1% (95% CI, 39.1%–79.1%) (14).

The results of the combination of CAP-TMZ for the treatment of NS remain uncertain due to the lack of current

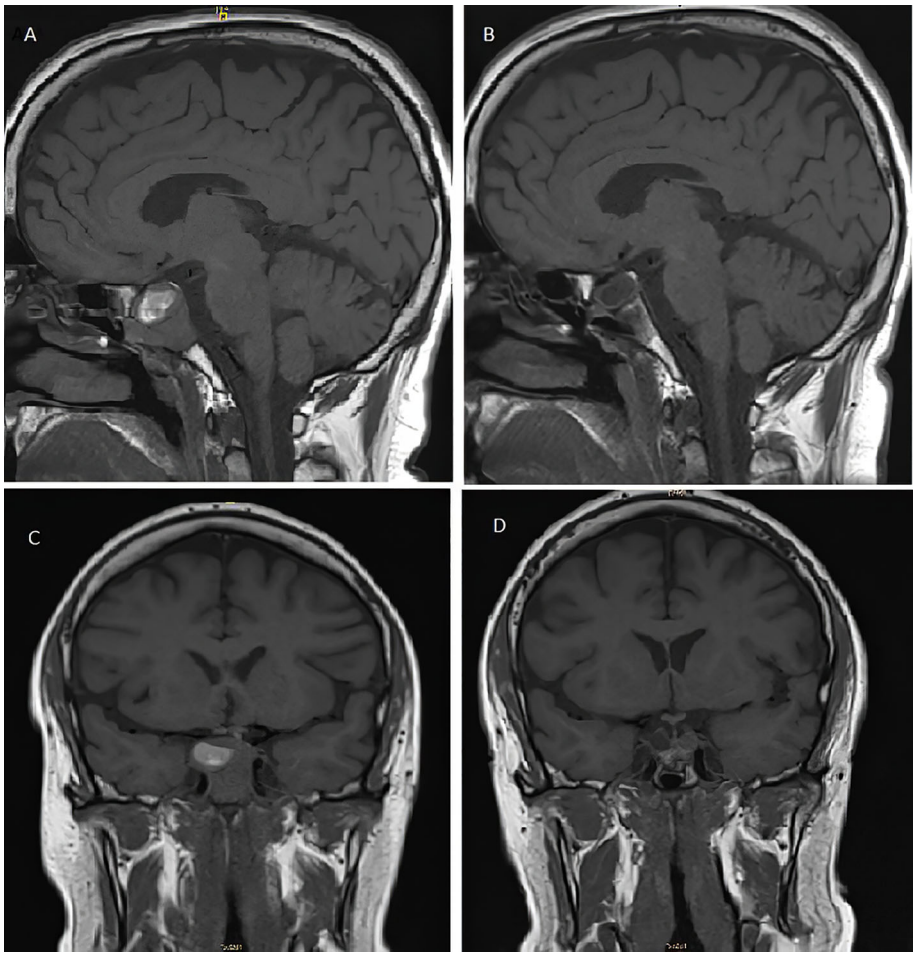


**FIGURE 2** | T1-weighted pituitary magnetic resonance imaging before **(A, C)** and after **(B, D)** treatment with capecitabine and temozolomide. **(A)** Pre-CAPTEM sagittal image shows an increase in the size of the seal tumor (26 mm) with a subacute bleeding component. **(B)** Post-CAPTEM sagittal image shows a decrease of 65% with a total size of 9 mm. **(C)** Pre-CAPTEM pituitary coronal image shows invasion of clivus and protrusion into the sphenoid sinus. **(D)** Post-CAPTEM coronal image shows a decrease in size of the lesion, more prominent at the right level.

evidence. CAP is metabolized to 5-fluorouracil and interferes with DNA synthesis and replication. Its use can lead to adverse reactions like bone marrow suppression, diarrhea, hand-foot syndrome, nausea, or fatigue (11). A synergism between CAP-TMZ has been hypothesized due to a reduction in thymidine levels (12). Previous reports that could support this theory include the case of a 48-year-old man with an aggressive corticotrope tumor who was treated with 12 cycles of CAP-TMZ, leading to tumor shrinkage and no tumor regrowth after 22 months of therapy cessation (15). A case series of four patients with aggressive ACTH producing pituitary tumors were treated with CAP-TMZ; two out of four patients demonstrated complete regression of the disease, one patient had a 75% regression, and one had an ongoing stable disease for 4.5 years at the time of the report (9). In our case, a neurological and radiological partial response was observed after 18 months of starting treatment with CAP-TMZ. These data suggest that CAP-TMZ may be a promising option for the treatment of NS with a low toxicity profile. However, some limitations must be considered. This was a single reported case; we cannot specifically determine whether the initial clinical and radiological effect of the treatment was due to the combination of CAP-TMZ or to one of the agents by themselves. The known cases of APA tend to become malignant after several years, so we cannot yet indicate if this will be the evolution of our patient. The patient received CAP-TMZ as the best possible medical treatment, according to our expertise, but from the patient's perspective, he would prefer a drug that does not cause fatigue and allows him to go back to work. It is important to always keep in mind that the ideal treatment should be the most effective, best tolerated, and least harmful.

APA can exhibit histological features like increased proliferation, a Ki-67 index above 3%, increased mitotic cells, and p53 expression. However, the presence of these features does not predict future aggressive behavior, and the prognostic value of these markers is controversial (8). There is no correlation between the Ki-67 index and response to treatment with TMZ.

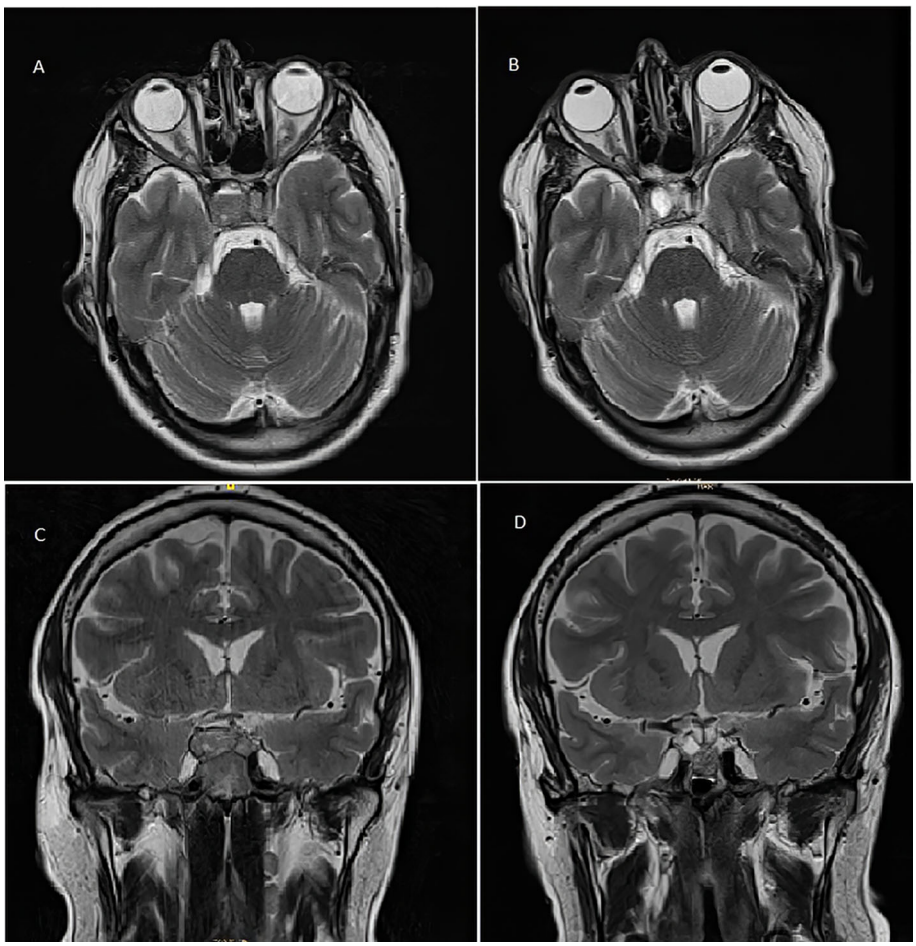


**FIGURE 3** | T2-weighted pituitary magnetic resonance imaging before **(A, C)** and after **(B, D)** treatment with capecitabine and temozolomide. **(A)** Pre-CAPTEM axial image. **(B)** Post-CAPTEM axial image shows a decrease in size of 65% with prominent cystic degeneration. **(C)** Pre-CAPTEM pituitary coronal image. **(D)** Post-CAPTEM coronal image shows a decrease in lesion.

Otherwise, the negative expression of the enzyme MGMT was associated with TMZ response among patients with APA (13). The MGMT repairs DNA and counteracts the effect of TMZ (8). All pathology reports of our patient showed low mitosis indicators, absence of overexpression of p53, and low KI-67 levels. MGMT expression was not available, but it might be negative due to a good response to treatment. Although the response to TMZ has been favorable for our patient, its use may limit other experimental therapies in the future. A recent study reported that peptide receptor radionuclide therapy (PRRT) can induce tumor shrinkage and clinical or biochemical improvement in 33% of patients with APA, but PRRT failure was significantly associated with previous TMZ treatment, noting that PRRT could be effective in 80% of patients not previously treated with TMZ (7).

In our case, the short latency between the tumor progression and the last session of radiotherapy, a single exposure to adjuvant stereotaxic radiotherapy with a total dose of 54 Gy, and the fact that it was a young patient make it unlikely that adjuvant radiotherapy was directly responsible for the tumor progression or a change of aggressiveness (16). Despite local tumor progression, the patient did not show new lesions at other locations of the central nervous system nor extracranial metastasis by CT scan. Thus, we treated a benign tumor with CAP-TMZ because it was rapidly growing and locally compressive. A future problem to consider is that by exposing this kind of tumor to chemotherapeutic pharmacological stress, there is a possibility of creating mechanisms of cellular resistance, mutations, and thus, malignancy. A case of a 42-year-old man with ACTH-secreting pituitary tumor evolved to a carcinoma in which the tumor progressively increased from 2.2 to 31.1 $cm^3$, Ki-67 increased from 2% to 18%, and an intradural metastasis at the foramen magnum was detected. Despite these findings, the tumor presented a 90% reduction after five cycles of TMZ (200 $mg/m^2$/day during the first cycle and 150 $mg/m^2$/day during the following cycles) (17). Another case involved a 46-year-old woman with an APA being treated with CAP-TMZ and showing a complete biochemical and radiological response by

**TABLE 1** | Treatment timeline.

| Months | Case evolution |
|---|---|
| 0 | Diagnosis of pituitary macroadenoma |
| 0 | First transsphenoidal endoscopic resection + biopsy |
| 21 | Recurrence: second transsphenoidal endoscopic resection + biopsy |
| 29 | Recurrence: third transsphenoidal endoscopic resection + biopsy + adjuvant stereotaxic radiotherapy (54 Gy in 27 fractions) |
| 29 | Ketoconazole (200 mg/8 h) |
| | Pasireotide (40 mg/month) |
| 33 | Total bilateral adrenalectomy |
| 68 | Diagnosis of Nelson's syndrome |
| 72 | CAP 2,500 mg daily on days 1 to 14 every 28 days for 14 days and TMZ 140 mg/m$^2$ once daily on days 10 to 14 every 28 days. (Total 4 cycles) |
| 76 | Maintenance treatment with TMZ 140 mg/m$^2$ once daily on days 10 to 14 every 28 days |
| 90 | Follow-up: 18 months with good tolerance since first dose of CAP + TMZ treatment |

*CAP, capecitabine; TMZ, temozolomide.*

MRI after 10 cycles. At first, each cycle was every 28 days, and then they were subsequently extended to every 42 days and every 3 months. After 8 years of treatment, the patient progressed biochemically and developed liver metastases. Due to insufficient tumor from liver biopsy, whole-exome sequencing of recurrent sellar tumor and a matched normal tissue was performed. This tumor was found to be hypermutated in the absence of microsatellite instability or mismatch repair deficiency (11). Another case of a 50-year-old man with a giant invasive corticotrope pituitary tumor treated with CAP-TMZ also presented a decrease in size and ACTH levels, but the tumor recurred after 5 months with increased avidity on PET scan, suggesting a transformation to a more aggressive phenotype (12).

All these data suggest that treatment with CAP-TMZ could be an effective option for patients with APA and NS, but treatment should be properly supervised in order to avoid secondary effects. Additionally, the use of CAP-TMZ could be explored as neoadjuvant treatment of pituitary tumors to achieve shrinkage of the tumor before surgery if complete extirpation is impossible (9). The limited or unknown long-term effect of treatment with CAP-TMZ in NS resistant to standard treatment modalities highlights the need to identify additional effective therapies.

## PATIENT'S PERSPECTIVE

When they told me I had to receive chemotherapy, I did not take it too well, I was not amused at all, I wished there were other treatment options; however, they explained to me that it was very risky to have surgery again. I am the first person in my family that has problems with the pituitary gland, and everything that has happened to me from the beginning caught me off guard. The chemotherapy treatment has been very strong; it made me feel very tired. The first thing I noticed when starting the chemotherapy treatment was burning, pain, and erythema in the palms and soles of my hands and feet, later it made me feel very discouraged. In the aspects of my personal life, I think that the hormonal disorders and symptoms in my body increased after my pituitary gland was "fried" with radiotherapy. Sometimes, I have been discouraged because I do not feel like being intimate with my girlfriend due to my hormonal disorder. At this moment, I am following all the indications and hormonal treatments that my doctors have told me to do, in order to make these symptoms disappear. Regarding the good aspect of the treatment, I noticed that after 2 months of chemotherapy, the double vision that I was experiencing totally disappeared. I also noticed an improvement in the spots and color of my skin. In general, this is not a treatment that I would like to follow all my life, and I hope in the future there may be some other treatment options that do not make me feel tired and that allow me to return to my work and the activities that I used to do.

## PERMISSION TO REUSE AND COPYRIGHT

An abstract of the case participated in the 13th SEOM MIR Clinical Case Contest and its intellectual property rights were assigned to SEOM, who authorizes the present publication. The current updated version of this case includes new content, the patient's perspective, and posttreatment MRI images that have not been published before.

## DATA AVAILABILITY STATEMENT

The original contributions presented in the study are included in the article/**Supplementary Material**. Further inquiries can be directed to the corresponding author.

## ETHICS STATEMENT

Written informed consent was obtained from the minor(s)' legal guardian/next of kin for the publication of any potentially identifiable images or data included in this article.

## AUTHOR CONTRIBUTIONS

OM and FF-A were major contributors in the literature review and writing the manuscript. All authors contribute to the

discussion of the case. AA contributed with image description. EM-S contributed with pathological anatomy description. BB, JH, and JC contributed with their expert review of the manuscript. All authors contributed to the article and approved the submitted version.

## REFERENCES


1. Ritzel K, Beuschlein F, Mickisch A, Osswald A, Schneider HJ, Schopohl J, et al. Outcome of Bilateral Adrenalectomy in Cushing's Syndrome: A Systematic Review. *J Clin Endocrinol Metab* (2013) 98(10):3939–48. doi: 10.1210/jc.2013-1470
2. Pivonello R, De Leo M, Cozzolino A, Colao A. The Treatment of Cushing's Disease. *Endocr Rev* (2015) 36(4):385–486. doi: 10.1210/er.2013-1048
3. Lindholm J, Juul S, Jørgensen JOL, Astrup J, Bjerre P, Feldt-Rasmussen U, et al. Incidence and Late Prognosis of Cushing's Syndrome: A Population-Based Study. *J Clin Endocrinol Metab* (2001) 86(1):117–23. doi: 10.1210/jc.86.1.117
4. Banasiak MJ, Malek AR. Nelson Syndrome: Comprehensive Review of Pathophysiology, Diagnosis, and Management. *Neurosurg Focus* (2007) 23 (3):1–10. doi: 10.3171/foc.2007.23.3.15
5. Nieman LK, Biller BMK, Findling JW, Murad MH, Newell-Price J, Savage MO, et al. Treatment of Cushing's Syndrome: An Endocrine Society Clinical Practice Guideline. *J Clin Endocrinol Metab* (2015) 100(8):2807–31. doi: 10.1210/jc.2015-1818
6. Barber TM, Adams E, Ansorge O, Byrne JV, Karavitaki N, Wass JAH. Nelson's Syndrome. *Eur J Endocrinol* (2010) 163(4):495–507. doi: 10.1530/EJE-10-0466
7. Giuffrida G, Ferraù F, Laudicella R, Cotta OR, Messina E, Granata F, et al. Peptide Receptor Radionuclide Therapy for Aggressive Pituitary Tumors: A Monocentric Experience. *Endocr Connect* (2019) 8(5):528–35. doi: 10.1530/EC-19-0065
8. McCormack A, Dekkers OM, Petersenn S, Popovic V, Trouillas J, Raverot G, et al. Treatment of Aggressive Pituitary Tumours and Carcinomas: Results of a European Society of Endocrinology (ESE) Survey 2016. *Eur J Endocrinol* (2018) 178(3):265–76. doi: 10.1530/EJE-17-0933
9. Zacharia BE, Gulati AP, Bruce JN, Carminucci AS, Wardlaw SL, Siegelin M, et al. High Response Rates and Prolonged Survival in Patients With Corticotroph Pituitary Tumors and Refractory Cushing Disease From Capecitabine and Temozolomide (CAPTEM): A Case Series. *Neurosurgery* (2014) 74(4):447–55. doi: 10.1227/NEU.0000000000000251
10. Azad TD, Veeravagu A, Kumar S, Katznelson L. Nelson Syndrome: Update on Therapeutic Approaches. *World Neurosurg* (2015) 83(6):1135–40. doi: 10.1016/j.wneu.2015.01.038
11. Lin AL, Donoghue MTA, Wardlaw SL, Yang TJ, Bodei L, Tabar V GE. Approach to the Treatment of a Patient With an Aggressive Pituitary Tumor. *J Clin Endocrinol Metab* (2020) 105(12):3807–20. doi: 10.1210/clinem/dgaa649
12. Thearle MS, Freda PU, Bruce JN, Isaacson SR, Lee Y, Fine RL. Temozolomide (Temodar®) and Capecitabine (Xeloda®) Treatment of an Aggressive Corticotroph Pituitary Tumor. *Pituitary* (2011) 14(4):418–24. doi: 10.1007/s11102-009-0211-1
13. Ji Y, Vogel RI, Lou E. Temozolomide Treatment of Pituitary Carcinomas and Atypical Adenomas: Systematic Review of Case Reports. *Neurooncol Pract* (2016) 3(3):188–95. doi: 10.1093/nop/npv059
14. Losa M, Bogazzi F, Cannavo S, Ceccato F, Curtò L, De Marinis L, et al. Temozolomide Therapy in Patients With Aggressive Pituitary Adenomas or Carcinomas. *J Neurooncol* (2016) 126(3):519–25. doi: 10.1007/s11060-015-1991-y
15. Nakano-Tateno T, Satou M, Inoshita N, van Landeghem FKH, Easaw J, Mehta V, et al. Effects of CAPTEM (Capecitabine and Temozolomide) on a Corticotroph Carcinoma and an Aggressive Corticotroph Tumor. *Endocr Pathol* (2020) 32(3):418–26. doi: 10.1007/s12022-020-09647-w
16. Chowdhary A, Spence AM, Sales L, Rostomily RC, Rockhill JK, Silbergeld DL. Radiation Associated Tumors Following Therapeutic Cranial Radiation. *Surg Neurol Int* (2012) 3(48):1–6 doi: 10.4103/2152-7806.96068
17. Curtò L, Torre ML, Ferraù F, Pitini V, Altavilla G, Granata F, et al. Temozolomide-Induced Shrinkage of a Pituitary Carcinoma Causing Cushing's Disease - Report of a Case and Literature Review. *ScientificWorldJournal* (2010) 10:2132–8. doi: 10.1100/tsw.2010.210


## SUPPLEMENTARY MATERIAL

The Supplementary Material for this article can be found online at: https://www.frontiersin.org/articles/10.3389/fendo.2021.731631/full#supplementary-material

**Conflict of Interest:** The authors declare that the research was conducted in the absence of any commercial or financial relationships that could be construed as a potential conflict of interest.

frontiers in Endocrinology

ORIGINAL RESEARCH
published: 09 December 2021
doi: 10.3389/fendo.2021.795116

# Role of FGF Receptors and Their Pathways in Adrenocortical Tumors and Possible Therapeutic Implications

*Iuliu Sbiera[1], Stefan Kircher[2], Barbara Altieri[1], Kerstin Lenz[1], Constanze Hantel[3,4], Martin Fassnacht[1,5,6], Silviu Sbiera[1*†] and Matthias Kroiss[1,6,7*†]*

*[1] Department of Internal Medicine I, Division of Endocrinology and Diabetes, University Hospital, University of Würzburg, Würzburg, Germany, [2] Institute of Pathology, University of Würzburg, Würzburg, Germany, [3] Department of Endocrinology, Diabetology and Clinical Nutrition, University Hospital Zürich (USZ) and University of Zürich (UZH), Zürich, Switzerland, [4] Medizinische Klinik und Poliklinik III, University Hospital Carl Gustav Carus Dresden, Dresden, Germany, [5] Clinical Chemistry and Laboratory Medicine, University Hospital, University of Würzburg, Würzburg, Germany, [6] Comprehensive Cancer Center Mainfranken, University of Würzburg, Würzburg, Germany, [7] Department of Internal Medicine IV, University Hospital, Ludwig-Maximilians-Universität München, Munich, Germany*

Adrenocortical carcinoma (ACC) is a rare endocrine malignancy and treatment of advanced disease is challenging. Clinical trials with multi-tyrosine kinase inhibitors in the past have yielded disappointing results. Here, we investigated fibroblast growth factor (FGF) receptors and their pathways in adrenocortical tumors as potential treatment targets. We performed real-time RT-PCR of 93 FGF pathway related genes in a cohort of 39 fresh frozen benign and malignant adrenocortical, 9 non-adrenal tissues and 4 cell lines. The expression of FGF receptors was validated in 166 formalin-fixed paraffin embedded (FFPE) tissues using RNA *in situ* hybridization (RNAscope) and correlated with clinical data. In malignant compared to benign adrenal tumors, we found significant differences in the expression of 16/94 FGF receptor pathway related genes. Genes involved in tissue differentiation and metastatic spread through epithelial to mesechymal transition were most strongly altered. The therapeutically targetable FGF receptors 1 and 4 were upregulated 4.6- and 6-fold, respectively, in malignant compared to benign adrenocortical tumors, which was confirmed by RNAscope in FFPE samples. High expression of FGFR1 and 4 was significantly associated with worse patient prognosis in univariate analysis. After multivariate adjustment for the known prognostic factors Ki-67 and ENSAT tumor stage, FGFR1 remained significantly associated with recurrence-free survival (HR=6.10, 95%CI: 1.78 – 20.86, p=0.004) and FGFR4 with overall survival (HR=3.23, 95%CI: 1.52 – 6.88, p=0.002). Collectively, our study supports a role of FGF pathways in malignant adrenocortical tumors. Quantification of FGF receptors may enable a stratification of ACC for the use of FGFR inhibitors in future clinical trials.

**Keywords: normal adrenal glands, adrenocortical tumors, FGF-pathway, FGFR, RNA Expression, RNAScope, unsupervised clustering, patient survival**

OPEN ACCESS

***Edited by:***
*Natalia Simona Pellegata, Helmholtz Association of German Research Centres (HZ), Germany*

***Reviewed by:***
*Carl Christofer Juhlin, Karolinska Institutet (KI), Sweden*
*Pierre Val, Centre National de la Recherche Scientifique (CNRS), France*
*Gallia Graiani, University of Parma, Italy*

***Correspondence:**
*Silviu Sbiera*
*Sbiera_S@ukw.de*
*Matthias Kroiss*
*Matthias.Kroiss@med.uni-muenchen.de*

*†These authors have contributed equally to this work*

***Specialty section:***
*This article was submitted to Cancer Endocrinology, a section of the journal Frontiers in Endocrinology*

***Received:*** *14 October 2021*
***Accepted:*** *23 November 2021*
***Published:*** *09 December 2021*

***Citation:***
*Sbiera I, Kircher S, Altieri B, Lenz K, Hantel C, Fassnacht M, Sbiera S and Kroiss M (2021) Role of FGF Receptors and Their Pathways in Adrenocortical Tumors and Possible Therapeutic Implications. Front. Endocrinol. 12:795116. doi: 10.3389/fendo.2021.795116*

## INTRODUCTION

Adrenocortical carcinoma (ACC) is a rare endocrine malignancy, the pathogenesis of which is still poorly understood. Complete surgical resection is the treatment of choice in localized ACC and virtually the only option to achieve cure. As recurrence is frequent, adjuvant therapy is recommended in most patients (1, 2). The use of mitotane for adjuvant ACC treatment is mainly based on a large retrospective multicentre study conducted in Italy and Germany (3, 4). In advanced metastatic disease, the first and largest randomized phase III study in advanced ACC established etoposide, doxorubicin, cisplatin plus mitotane (EDP-M) as the cytotoxic chemotherapy of first choice (5). However, with a median overall survival of only 14.8 months in the group receiving EDP-M, the prognosis is still poor. Accordingly, there has been a growing interest in targeted therapies for the treatment of ACC.

Since insulin-like growth factor (IGF) 2 is the single most overexpressed molecule in the majority of ACC (6), clinical investigation of inhibitors of the IGF pathway yielded high expectations (7). However, this first industry-sponsored randomized phase III clinical trial in ACC with the IGF1R-inhibitor linsitinib (OSI-906) did not significantly prolong progression free survival in the vast majority of patients although some remarkable responses were observed (8). High expression of vascular endothelial growth factor (VEGF) and its receptor VEGF-R2 in many ACC specimens (9) led to several studies targeting the tumor vasculature in ACC with bevacizumab, an anti-VEGF monoclonal antibody, and sorafenib, a multi-tyrosine kinase inhibitor in combination with paclitaxel which however failed to demonstrate clinical efficacy (10). Previous *in vitro* data in ACC cell lines (11) led to the conception of a phase II clinical trial of the receptor tyrosine kinase (RTK) inhibitor sunitinib targeting VEGFR2, and PDGFRβ among others. 29 patients were evaluated in the study (SIRAC), all patients had progressed despite prior cytotoxic chemotherapy and suffered from significant tumor burden, however, sunitinib showed modest antitumor effects (12). Despite these setbacks, tyrosine kinase inhibitors have still potential in the treatment of ACC, as demonstrated by a small study using the multi-tyrosine kinase inhibitor cabozantinib in 16 patients with progressive ACC that showed prolonged disease control in half of the patients (13). However, overall, advanced disease still remains a major therapeutic challenge in patients with ACC (14).

In humans, the family of fibroblast growths factors (FGFs) comprises 22 different genes that encode proteins binding with high affinity to receptor tyrosine kinases (FGFRs) (15). Members of the FGF family function in the earliest stages of embryonic development and during organogenesis to maintain progenitor cells and mediate their growth, differentiation, survival, and patterning (16, 17). Four of the five FGF receptors (FGFR1-4) are highly conserved membrane bound RTK. After ligand binding, dimerization of the receptor causes phosphorylation of intracellular tyrosine residues that subsequently activate several crucial intracellular signaling pathways (18) like Phospholipase-C (PLC), Protein Kinase C (PKC) and Ras/Mitogen-activated protein kinase (MAPK). Activation of FGFR signaling may lead to carcinogenesis in several types of tissues (19, 20). Aberrant expression of some of the FGFs has been implicated in the development and progression of different tumor types (21, 22). Although FGF signaling can drive tumorigenesis, it has also been shown to mediate tumor protective functions (21). Importantly, the association of FGFRs with tumorigenesis led to the development of tyrosine kinase inhibitors (TKI) with FGFR specificity (23, 24), with high response rates in the first clinical studies in other types of cancer (25). Notably, response to FGFR inhibition is correlating with copy number amplification (26, 27) and mRNA expression levels (28).

The knowledge about the FGF/FGFR pathway in the adrenal gland is sparse and fragmented. As early as 1975, Gospodarowicz et al. demonstrated that some fibroblast growth factors increased proliferation in the mouse Y1-adrenocortical tumor cell line (29) and in bovine and human foetal adrenocortical cells (30). Later, FGF1 and 2 were identified as growth-stimulating factors in adrenocortical cells and adrenocortical tumors (31–33) indicating a dual role of the FGF/FGFR system in both organogenesis and tumorigenesis in the adrenal system. FGF signaling through Fgfr2 isoform IIIb was shown to regulate adrenal cortex development in mice (34) while in humans a study in 22 ACC patients has shown a variable expression of FGFR2 that did not correlate with either clinical data or CTNNB1 genotype (35). Regarding possible FGFR gene amplifications, no study is specifically reporting such data for adrenocortical tumors but a quick query in the COSMIC (https://cancer.sanger.ac.uk/cosmic) database revealed gene amplifications in FGFR1, 3 and 4 genes in 1, 4 and 3 samples in the data of Zheng et al. (36) out of 89 samples analyzed, similar to that in other types of cancer (37).

However, until now, no single study has been published that focused on the FGF/FGFR pathway as a central mechanism that can potentially be targeted therapeutically. Our study aims at closing this gap and we expect the results to represent a promising step towards a better understanding at the molecular level and improved treatment in this disease with dismal outcome.

## MATERIAL AND METHODS

### Patient Material

We used patient material from three normal adrenal glands (NAG), 29 adrenocortical adenomas (ACA) and 149 ACC. Of these, three NAG, 15 ACA and 21 ACC were used for the Real-time PCR experiments as frozen samples, and three NAG, 21 ACA and 142 ACC were used for RNAScope as Formalin fixed, paraffin embedded (FFPE) tissue samples (**Table 1**). For an overview of the sample overlap please see the Venn diagram in the **Supplementary Figure 1**. Informed consent was obtained from all subjects involved and the study was conducted according to the guidelines of the Declaration of Helsinki, approved by the Ethics Committee of the University of Würzburg (approval # 88/11). An overview of key clinical

**TABLE 1** | Patient and tumor statistic for the FFPE (A) and frozen tissue (B) samples.

| A | NAG | ACA | ACC |
|---|---|---|---|
| *n* | 3 | 15 | 21 |
| Sex (male/female) | 1/2 | 7/8 | 12/9 |
| Age [yr (sd)] | 49 (11) | 46 (12) | 51 (13) |
| Size of the tumor [cm (sd)] | | 3.2 (1.5) | 10 (4.9) |
| Hormone secretion | | | |
| Cortisol – *n* (%) | | 8 (53%) | 10 (47%) |
| Androgen – *n* (%) | | 0 (0%) | 3 (14%) |
| Aldosterone – *n* (%) | | 3 (20%) | 1 (5%) |
| Inactive – *n* (%) | | 4 (27%) | 0 (0%) |
| Unknown – *n* (%) | | 0 (0%) | 7 (34%) |
| Tumor localization – *n* (%) | | | |
| Primary - ENSAT stage I+II | | | 8 (38%) |
| Primary - ENSAT stage III | | | 8 (38%) |
| Primary - ENSAT stage IV | | | 5 (24%) |
| Local recurrences | | | 0 (0%) |
| Distant metastases | | | 0 (0%) |
| Ki67 index [median (range)] | | | 20 (3-70) |
| Weiss Score [median (range)] | | | 7 (3-9) |
| **B** | **NAG** | **ACA** | **ACC** |
| *n* | 3 | 29 | 142 |
| Sex (male/female) | 1/2 | 11/18 | 52/90 |
| Age [yr (sd)] | 49 (11) | 51 (14) | 49 (14) |
| Size of the tumor [cm (sd)] | | 3.3 (1.2) | 9.8 (4.7) |
| Hormone secretion | | | |
| Cortisol – *n* (%) | | 11 (38%) | 52 (37%) |
| Androgen – *n* (%) | | 0 (0%) | 10 (7%) |
| Aldosterone – *n* (%) | | 7 (24%) | 6 (4%) |
| Inactive – *n* (%) | | 11 (38%) | 16 (11%) |
| Unknown – *n* (%) | | 0 (0%) | 58 (41%) |
| Tumor localization – *n* (%) | | | |
| Primary - ENSAT stage I+II | | | 47 (33%) |
| Primary - ENSAT stage III | | | 36 (25%) |
| Primary - ENSAT stage IV | | | 26 (18%) |
| Local recurrences | | | 22 (16%) |
| Distant metastases | | | 11 (8%) |
| Ki67 index [median (range)] | | | 10 (1-70) |
| Weiss Score [median (range)] | | 0 (0-1) | 5 (2-9) |

*NAG, normal adrenal gland; ACA, adrenocortical adenoma; ACC, adrenocortical carcinoma.*

characteristics of the patients can be found in **Table 1**. The differential diagnosis between ACA and ACC was based on established clinical, biochemical and morphological criteria, and all histological diagnoses, including Weiss score and Ki67 expression, were confirmed by the reference pathologist. The normal adrenal glands used in this study were obtained in an anonymized fashion as a byproduct of kidney cancer surgery when the adrenal gland had to be also removed. RNA from four different ACC cell lines [NCI-H295-R, MUC-1 (38), CU-ACC1 and CU-ACC2 (39)] was included as well. The following samples served for comparison: 1 normal thyroid, 1 normal colon, 2x colon carcinoma, 2x osteosarcoma, 2x liposarcoma, 1x synovial sarcoma together with two cell lines deriving from liver cancer (Hep G2) and embryonic kidney (HEK 293).

## Real-Time PCR

For quantification of mRNA expression, real-time RT-PCR was performed. RNA was extracted from previously cryo-preserved tissues using the RNeasy Lipid Tissue Kit and from cell lines using the RNeasy Mini Kit (both from Qiagen, Germany). This mRNA was then reverse transcribed with the High-Capacity cDNA Reverse Transcription Kit (Thermo Fisher Scientific, USA) and subsequently 10ng/well were used for the real-time RT-PCR amplification using the TaqMan Gene Expression Assay kit (Thermo Fisher Scientific, USA) with the probe primers for each specific gene. The pre-made FGF pathway PCR plate from Thermo Fisher (catalogue number 4418781) was utilized. The probe list and plate layout can be seen in **Supplementary Table 1**. Since the plate did not contain a probe for FGFR4, this gene was amplified separately using a specific TaqMan probe (Hs01106908_m1, Thermo Fisher), and as housekeeping genes for the expression normalization 18S (Hs99999901_s1) and ACTB (Hs99999903_m1) were amplified in parallel. The amplification and the quantification steps were performed using a StepOnePlus Real-Time PCR System (Thermo Fisher Scientific, USA). Raw expression data of the 92 genes of the FGF pathway plate were normalized to the expression of the four house keeping genes (**Supplementary Table 1**, green background) and expression of FGFR4 was normalized to the expression of the two house keeping genes listed above using the ΔCT method (Microsoft Excel). As the ribosomal 18S rRNA was one of the house keeping genes that have been used to normalize the expression data and its expression levels are much higher than the expression levels of any other gene involved in cellular function, the relative expression values resulting are expected to be quite low numerically.

## RNAScope

RNAScope is a custom RNA *in-situ* hybridization solution from Advanced Cell Diagnostics, USA. Version 2.0 of the kit was utilized for our experiments following the manufacturer's instructions as described before (40). In short, the FFPE tissue sections of ~2µm thickness were mounted on SuperFrost glass slides (Langenbrinck, Germany), deparaffinized in xylene then washed with 100% ethanol followed by endogenous enzyme blocking in hydrogen peroxide solution (ref. part number 322335, Advanced Cell Diagnostics) at room temperature for 10 min. Permeabilization was performed by boiling in a pressure cooker for 15 minutes in target retrieval reagent (ref. 322000, ACD). Afterwards, protein digestion was achieved with the help of Protease Plus (ref. 322331, ACD) for 20 min at 40°C. All steps at 40°C were performed in a HybEZ Oven (also from ACD) that ensures quick heating up of the samples. FGFR 1, 2 and 4 probes (Hs-FGFR1 – ref. 310071; Hs-FGFR2 – ref. 311171; Hs-FGFR4-CD5 – ref. 412301, ACD) were then hybridized at 40°C for 2h. As a positive control, a probe detecting the mRNA for Cyclophilin B (PPIB) was used, which is expressed at a sufficiently low level so as to provide a rigorous control for sample quality and technical performance (ref. 313901). To ensure that there is no background staining related to the RNAscope assay a negative control probe targeting the dihydrodipicolinate reductase (DapB, accession nr. EF191515) gene from the *Bacillus subtilis* strain SMY, a soil bacterium (so unspecific for humans), was used (ref. 310043). Unbound probes were subsequently washed away. Starting with this step and until final DAB detection, the slides were washed in wash buffer (ref. 31009, ACD) instead of water. Afterwards, the slides were treated in order with Amplifier

solution 1 to 6. Amplifier 1 (ref. 322311, ACD) and Amplifier 3 (ref. 22313, ACD) at 40°C for 40 min, Amplifier 2 (ref. 322312, ACD) and Amplifier 4 (ref.322314, ACD) at 40°C for 20 min, while Amplifier 5 (ref. 322315, ACD) for 50min and Amplifier 6 (ref. 322316, ACD) for 20 min at RT. Then equal amounts of DAB-A (ref. 320052, ACD) and DAB-B (ref. 320053, ACD) were mixed and applied to the slides for 10 minutes at RT. Counterstaining of nuclei was performed using Meyer's Hematoxylin (Carl Roth, Germany) for 2 minutes, followed by washing in running tap water for 5 minutes. After dehydration, the slides were mounted using Entellan (Merck, Germany) and borosilicate glass coverslips (A. Hartenstein, Germany).

Three pictures of representative areas of each slide were taken with the Leica Aperio Versa brightfield scanning microscope (Leica, Germany) at 40x magnification. Scoring the RNAScope slides was done with the help of Aperio ImageScope software (version 12.x, Leica, Germany) on the entirety of the pictures using the optional image analysis algorithm 'RNA ISH v1' (Leica, Germany). This algorithm automatically detects and counts the number of RNA molecules (each brown stained spot is one molecule of RNA) and the number of cells (by detecting the hematoxylin stained nuclei) in a defined area. Thresholds for the detection were manually adjusted for a high fidelity assessment of the signal. In **Figure 1** there is an example of only a selected area for detection from a high scoring sample. We used the ratio of RNA spots per number of cells for each slide to quantify the target gene expression.

## Bioinformatic and Statistical Analyses

Normalized expression data were Log 2 transformed and loaded into the Gene-E software (v. 3.0.215, Broad Institute ©2013). The unsupervised cluster analysis of all the samples was performed using the column distance/similarity matrix algorithm and the average linkage method with Pearson correlation. Hierarchical clustering of the gene expression between different phenotype clusters was performed using the marker selection algorithm, using a two-sided test with 1000 permutations. The most significantly differential expressed genes were considered those where the false discovery rate (FDR) values were <0.05.

For subsequent analyses at single gene level, non-parametrical comparisons between two groups the two-tailed Mann-Whitney test was used. A two tailed p-value <0.05 was considered statistically significant. Statistical analyses were performed with Graph Pad Prism v 7 for Windows (La Jolla, CA, USA). For ACC patients, the Kaplan-Meier method was used to estimate overall survival (OS, in all patients with primary tumors) and recurrence-free survival (RFS, in patients with complete resection of the primary tumor) while the Cox proportional hazards model was used for univariate and multivariate analyses using IBM SPSS v 26 for Windows (SPSS Inc., Chicago, IL, USA).

# RESULTS

## FGF Pathway mRNA Expression

Similarity matrix clustering of real-time RT-PCR assessment comprising 93 genes from the FGF pathway showed a distinctive phenotype of adrenocortical tissue compared to all the other tissue samples (**Figure 2**). A separate cluster that contained all three NAG and most of the ACA had a distinct expression pattern compared to the majority of ACC. At variance, typical epithelial (from thyroid and colon) and mesenchymal tissues (from sarcomas) and all cell lines showed divergent expression patterns and clustered in several small groups separately from the adrenocortical tissues. Notably, colon tissues, whether normal or malignant clustered together as did most of the sarcomas. The different cell lines, whether of adrenocortical origin or not, did not cluster with their tissue counterparts (**Figure 2**).

Several genes of the FGF pathway were significantly differentially expressed among the different clusters, including 16 genes differentially expressed between ACA and ACC (**Table 2** and **Supplementary Figure 2**). Among the 11 genes expressed at lower levels in ACC compared to ACA, there were the genes encoding for FGFs and their receptors like the *FGF12*, *FGF14*, and *FGFR2*, for phospholipases like Phospholipase D1, Phosphatidylcholine-Specific (*PLD1*) and Glycosyl-phosphatidylinositol Specific Phospholipase D1 (*GPLD1*), Ras-

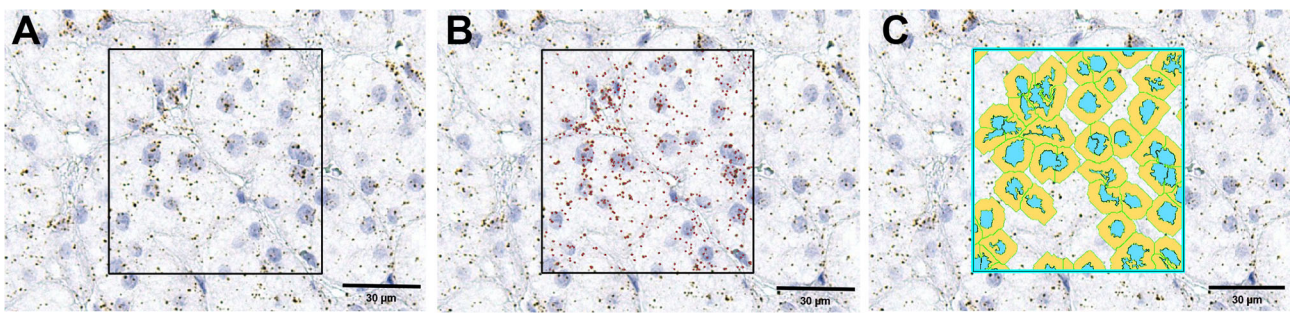


**FIGURE 1** | An example of RNAScope signal detection using the ImageScope software. The first image **(A)** is the original image; in the square is the selected area for detection. **(B)** the same image with the detected mRNA molecules marked in red by the software, while **(C)** is the same image with the detected cells marked in blue (nuclei) and yellow (cytoplasm).

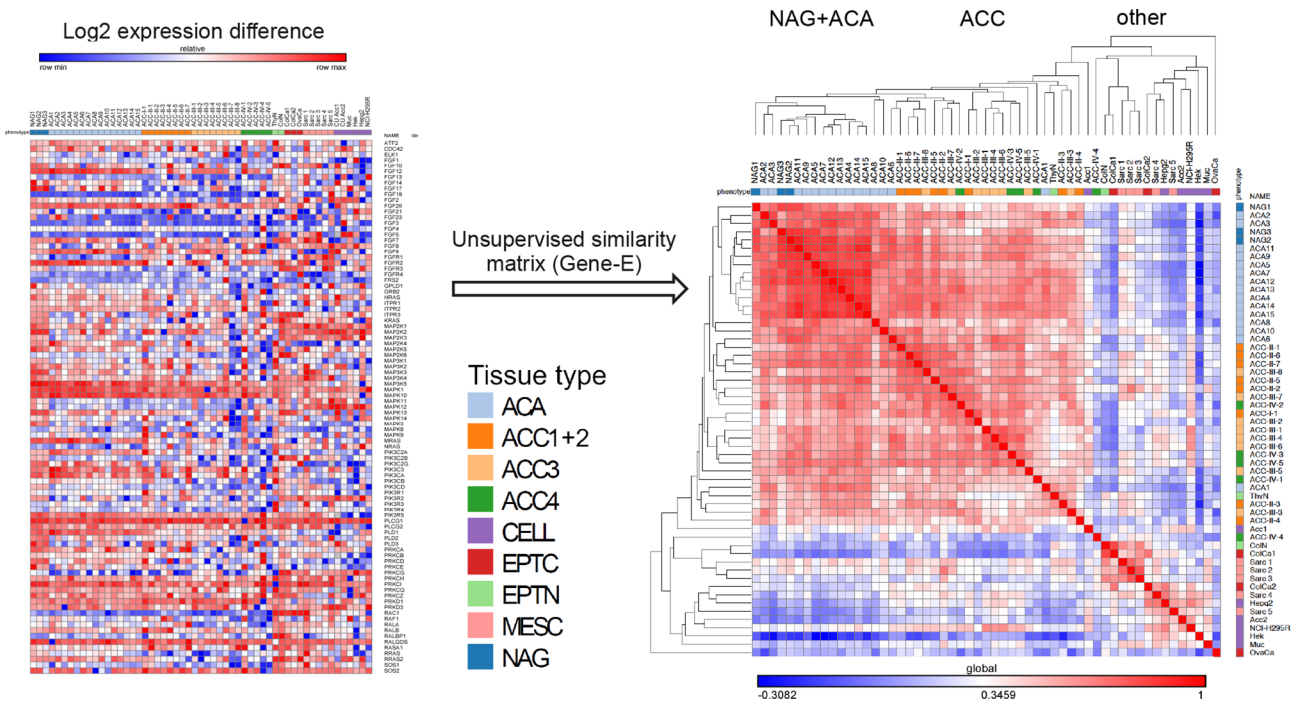


**FIGURE 2** | Unsupervised clustering of RT-PCR data of the FGF pathway genes. Unsupervised hierarchical matrix based on FGF pathway expression. On the left side is a graphical representation of the log 2 transformed normalized expression data arranged vertically by tissue name, and horizontally by gene name in the order that they were arranged on the PCR plate. To the right side is the data rearranged through the unsupervised similarity matrix clustering. The colored bar under the tissue names is encoding the different types of tissues analyzed: NAG=normal adrenal glands, ACA, adrenocortical adenomas; ACC1+2, ACC in ENSAT stages I and II; ACC3, ACC in ENSAT stage III; ACC4, ACC in ENSAT stage IV; EPTN, normal (non-neoplastic) classical epithelial tissues; EPTC, malignant tumors of classical epithelial tissues/carcinomas; MESC, malignant tumors of classical mesenchymal tissues/sarcomas and CELL, cell-lines.

Related Protein R-Ras 1 (*RRAS*), 2 (*RRAS2*) and 3 (*MRAS*) and the Mitogen-Activated Protein Kinases 10 (*MAPK10*) and 5 (*MAP3K5*) as well as Phosphatidylinositol-4-Phosphate 3-Kinase Catalytic Subunit Type 2 Gamma (*PIK3C2G*). The five genes significantly upregulated in ACCs vs ACAs encoded for the *FGFR1*, *FGFR4*, *FGF8*, and *FGF19*, and the Neuroblastoma RAS Viral Oncogene Homolog (*NRAS*).

The differences between ACCs with localized, ENSAT I/II tumors compared to stage III/IV ACCs were less prominent with only 8 genes with statistically significant differential expression between the two groups (**Table 2** and **Supplementary Figure 3**). Most of these genes were expressed at lower in advanced ACC: RAS Like Proto-Oncogene A (*RALA*), Raf-1 Proto-Oncogene (*RAF1*) and the kinases Protein Kinase C Alpha (*PRKCA*), Mitogen-Activated Protein Kinase 9 (*MAPK9*), Mitogen-Activated Protein Kinase Kinase Kinase 1 (*MAP3K1*) and 2 (*MAP3K2*), and Phosphoinositide-3-Kinase Regulatory Subunit 1 (*PIK3R1*). Fibroblast growth factor 21 (*FGF21*) was the only one of the analyzed genes that was expressed at significantly higher levels in advanced ACC.

## RNAScope *In Situ* RNA Hybridization

To assess the tissue distribution of the FGF receptors *FGFR1*, *2* and *4* as potential treatment targets, and to confirm real-time PCR results in a larger sample set (n=166), we applied *RNAScope in situ RNA hybridization.*

We did not differentiate between the different subcellular localizations of the hybridization signal (cytoplasmic, perinuclear and nuclear) as a means to assess the complete gene specific RNA in the cells. The housekeeping gene *PPIB* (Peptidylprolyl Isomerase B) showed a relatively constant average expression in all ACC samples analyzed (between 10 and 15 molecules per cell, **Figure 3A**), and the hybridization with the bacterial DapB was negative in all the samples. The expression of *FGFRs* was variable between the samples but homogenously distributed within most samples (**Figures 3B–D**). *FGFR* expression was nearly exclusively in tumoral cells. Significantly more FGFR1 and FGFR4 mRNAs were detected in ACC compared to ACA (5.1 ± 4.3 mRNA molecules/cell vs 1.7 ± 1.4 mRNA molecules/cell, p=0.03 in the case of *FGFR1* and 5.5 ± 4.9 mRNA molecules/cell vs 2.1 ± 1.4 mRNA molecules/cell, p=0.002 in the case of *FGFR4*) (**Figure 4A**). In contrast, *FGFR2* was significantly higher expressed in ACA (5.2 ± 2.7 mRNA molecules/cell for ACA vs 2.5 ± 2.5 mRNA molecules/cell for ACC, p=0.0001) confirming our real-time RT-PCR results in frozen tissues.

Next, we compared expression between tumors in early and advanced stages and found significantly higher expression only of *FGFR4* in ENSAT stage 3 + 4 (6.2 ± 5.2 mRNA molecules/cell)

**TABLE 2** | Statistically significant differential mRNA expression between different groups of adrenocortical tissues.

| Tissue<br>Gene symbol | ACA (n = 15)<br>relative expression (average ± SD) | ACC (n = 21)<br>relative expression (average ± SD) | ACC vs. ACA<br>fold-change (95% CI) | *p* -value |
|---|---|---|---|---|
| *PLD1* | 0.027 ± 0.0124 | 0.008 ± 0.004 | -3.40 (-2.41 to -4.39) | p<0.0001 |
| *FGF12* | 0.056 ± 0.041 | 0.015 ± 0.024 | -3.74 (-1.50 to -7.71) | p<0.0001 |
| *RRAS2* | 0.002 ± 0.0008 | 0.0009 ± 0.0007 | -2.15 (-1.24 to -3.06) | p=0.0002 |
| *PIK3C2G* | $8.3x10^{-5}$ ± $1x10^{-5}$ | $1.2x10^{-5}$ ± $1.6x10^{-5}$ | -6.77 (-1.70 to -11.83) | p=0.021 |
| *MRAS* | 0.025 ± 0.011 | 0.011 ± 0.008 | -2.21 (-1.30 to -3.13) | p=0.0003 |
| ***FGFR2*** | 0.021 ± 0.013 | 0.013 ± 0.017 | -1.63 (-1.03 to -2.23) | p=0.014 |
| *MAPK10* | 0.043 ± 0.028 | 0.021 ± 0.032 | -2.00 (-1.02 to -2.98) | p=0.001 |
| *RRAS* | 0.005 ± 0.001 | 0.003 ± 0.002 | -1.59 (-1.04 to -2.13) | p=0.006 |
| *MAP3K5* | 0.029 ± 0.018 | 0.011 ± 0.009 | -2.52 (-1.44 to -3.59) | p=0.001 |
| *GPLD1* | $2.1x10^{-4}$ ± $1.3x10^{-4}$ | $1.2x10^{-4}$ ± $7.8x10^{-5}$ | -1.76 (-1.15 to -2.36) | p=0.009 |
| *FGF14* | $1.1x10^{-4}$ ± $1.2x10^{-4}$ | $6.6x10^{-5}$ ± $9.8x10^{-5}$ | -1.70 (-1.05 to -2.35) | p=0.04 |
| ***FGFR1*** | 0.005 ± 0.003 | 0.023 ± 0.015 | 4.11 (2.58 to 5.63) | p<0.0001 |
| ***FGFR4*** | $3.3x10^{-5}$± $2.4x10^{-5}$ | $2.0x10^{-4}$± $1.8x10^{-4}$ | 6.16 (3.17 to 9.14) | p<0.007 |
| *NRAS* | 0.012 ± 0.003 | 0.020 ± 0.009 | 1.45 (1.06 to 1.84) | p=0.049 |
| *FGF8* | $3.4x10^{-6}$± $4.7x10^{-6}$ | $2.8x10^{-5}$± $5.9x10^{-5}$ | 8.32 (1.26 to 15.39) | p=0.010 |
| *FGF19* | $1.7x10^{-7}$± $1.02x10^{-7}$ | $1.71x10^{-6}$± $3.0x10^{-6}$ | 9.81 (1.11 to 18.51) | p=0.047 |
| Tissue | ACC 1 + 2 (n=8) | ACC 3 + 4 (n=13) | ACC 3 + 4 vs. ACC 1 + 2 | |
| Gene symbol | relative expression (average ± SD) | relative expression (average ± SD) | fold-change (average ± SD) | *p* -value |
| *RALA* | 0.016 ± 0.012 | 0.006 ± 0.002 | -2.67 (-2.01 to -3.32) | p=0.001 |
| *PRKCA* | 0.047 ± 0.042 | 0.006 ± 0.006 | -7.85 (-3.32 to -12.39) | p=0.004 |
| *MAPK9* | 0.031 ± 0.017 | 0.013 ± 0.008 | -2.74 (-1.55 to -2.98) | p=0.012 |
| *MAP3K2* | 0.013 ± 0.005 | 0.007 ± 0.005 | -1.66 (-1.04 to -2.28) | p=0.024 |
| *PIK3R1* | 0.081 ± 0.102 | 0.021 ± 0.019 | -3.85 (-1.93 to -5.76) | p=0.024 |
| *RAF1* | 0.007 ± 0.003 | 0.004 ± 0.002 | -1.61 (-1.11 to -2.11) | p=0.036 |
| *MAP3K1* | 0.008 ± 0.003 | 0.005 ± 0.002 | -1.52 (-1.12 to -1.92) | p=0.036 |
| *FGF21* | $5.1x10^{-7}$± $5.0x10^{-7}$ | $8.8x10^{-6}$± $7.6x10^{-6}$ | 17.38 (9.24 to 25.51) | p=0.007 |

*ACA, adrenocortical adenoma; ACC, adrenocortical carcinoma; ACC 1 + 2, adrenocortical carcinoma in ENSAT stages I and II; ACC 3 + 4, adrenocortical carcinoma in ENSAT stages III and IV. The higher values between two subgroups are squared in black. The significantly differentially expressed FGF- receptors are in bold type. A negative fold change is represented by the "-" sign. The p-values refer to the Mann-Whitney statistical comparison between the two groups of samples. A p-value <0.05 was considered statistically significant.*

compared to ENSAT 1 + 2 (4.1 ± 3.7 mRNA molecules/cell, p=0.02) ACC (**Figure 4B**). Similarly, we found significantly higher expression *FGFR4* (**Figure 4C**) in recurrences/metastasis compared to primary tumors (8.8 ± 6.6 mRNA molecules/cell for recurrences vs 4.7 ± 4.1 mRNA molecules/cell for primary tumors).

## Influence on Patient Survival

In a next step we assessed the influence of the *FGFR 1*, *2* and *4* on patient survival in the RNAScope ACC patient cohort. The median expression value for each receptor was chosen as cut-off between low and high expression and was 3.9 spots per cell for *FGFR1*, 1.9 for *FGFR2* and 4.4 for *FGFR4*. High *FGFR1* expression was associated with both a shorter OS of 84.12 ± 16.75 *vs* 147.98 ± 23.20 months (HR=1.8, 95%CI: 1.01-3.25, p=0.047) (**Figure 5A**) and a shorter RFS of 24.84 ± 6.71 *vs* 74.71 ± 15.06 months (HR=2.93, 95%CI: 1.25-6.84, p=0.013) (**Figure 5B**), whereas *FGFR2* was not associated with either OS and RFS (**Figures 5C, D** and **Table 3**). *FGFR4*, while significantly associated with a shorter OS of 50.52 ± 7.59 *vs* 154.60 ± 19.64 months (HR=2.44, 95%CI: 1.41-4.22, p=0.001) (**Figure 5E**), was not associated with RFS (**Figure 5F** and **Table 3**). Interestingly, in a multivariate analysis, including ENSAT tumor stage and proliferation index Ki-67, two well established prognostic factors for ACC (41, 42), the association between *FGFR1* expression and the recurrence-free survival and between *FGFR4* expression and the OS remained significant (HR=6.10, 95%CI: 1.78 – 20.86, p=0.004 and HR=3.23, 95%CI: 1.52 – 6.88, p=0.002, respectively) (**Table 3**).

# DISCUSSION

Almost half of the patients with metastatic ACC disease die of the disease already in the first year after diagnosis, one of the worst survival rates among solid cancers. This urges the need for better therapeutic options but while targeting receptor tyrosine kinases was hailed as game changing in other solid cancers, the trials with e.g. VEGFR and IGFR inhibitors in ACC were disappointing (14). This is the largest study screening the FGF/FGFR pathway in adrenocortical tissues with the declared scope of finding potential treatment targets.

The analysis of pan-FGF/FGFR pathway expression data showed that there are significant differences in the expression pattern of constituents of this pathway between the different subtypes of adrenocortical tissues but also between these and normal and neoplastic tissues of other organs. The normal and benign adrenocortical tissues clustered close together in unsupervised analyses but separately from the malignant adrenocortical carcinomas. This indicates that the different members of the pathway have similar expression patterns between the normal and benign adrenocortical tissues but different from the ACC. Interestingly, the expression in all adrenocortical tissues clustered again separately from the expression in other normal and neoplastic

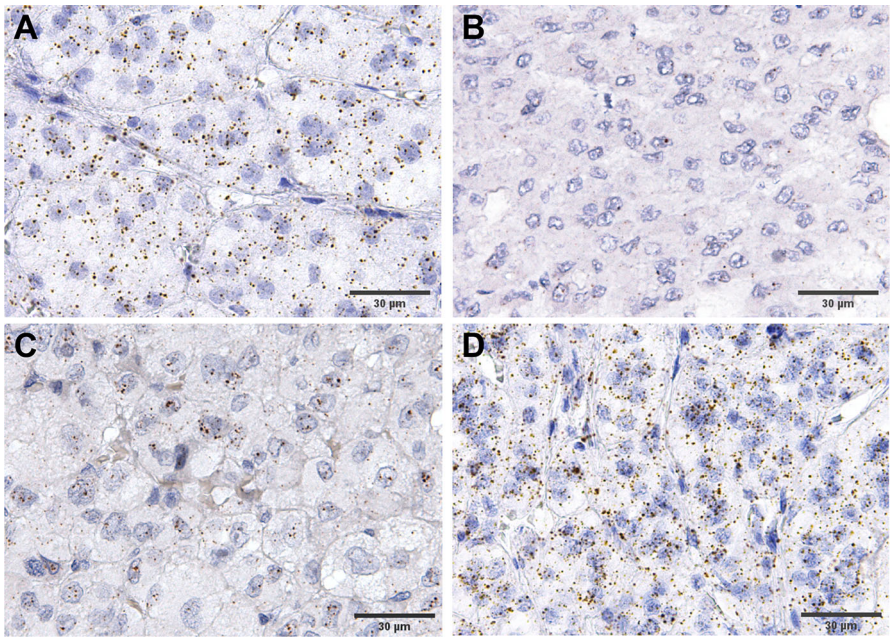


**FIGURE 3** | Examples of expression RNAScope staining in ACC. **(A)** an example of house keeping gene, PPIB, staining, while **(B–D)** show various levels of FGFR4 expression, from low to high.

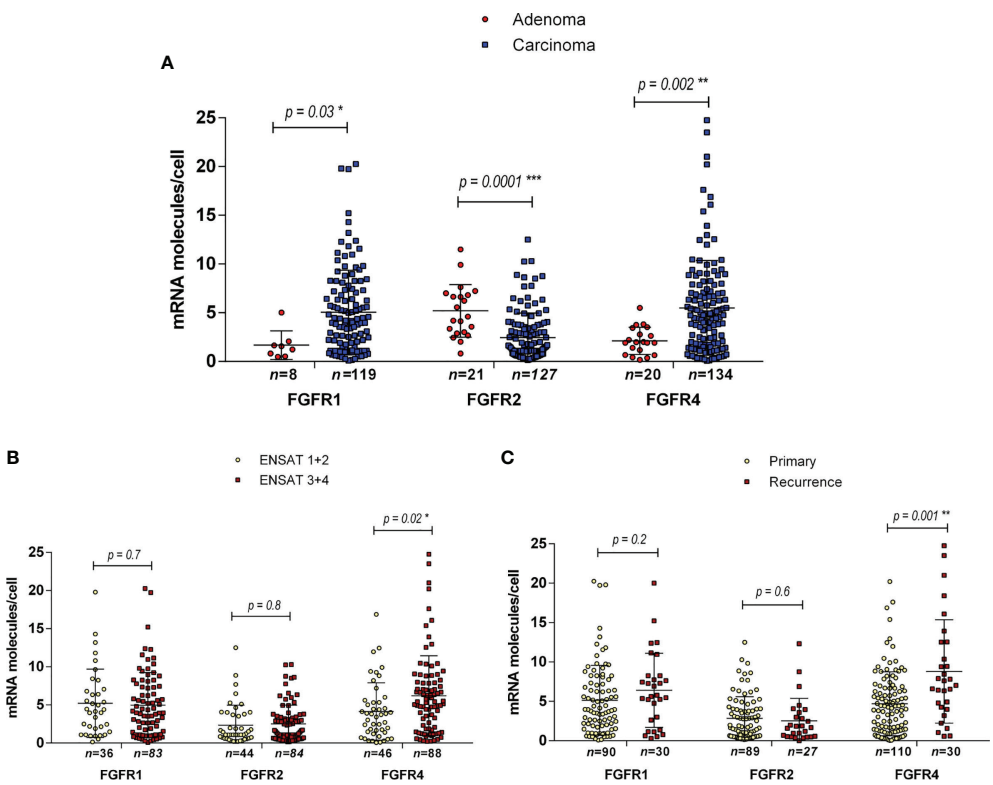


**FIGURE 4** | Expression of FGF receptors 1, 2 and 4 in adrenocortical tissues as assessed by RNAScope. Expression levels in ACA vs ACC **(A)**, in ACC ENSAT stages 1 + 2 vs 3 + 4 **(B)** and in ACC primary tumor samples vs local or distant recurrences **(C)**. Statistical significance: *p<0.05, **p<0.01, ***p<0.001.

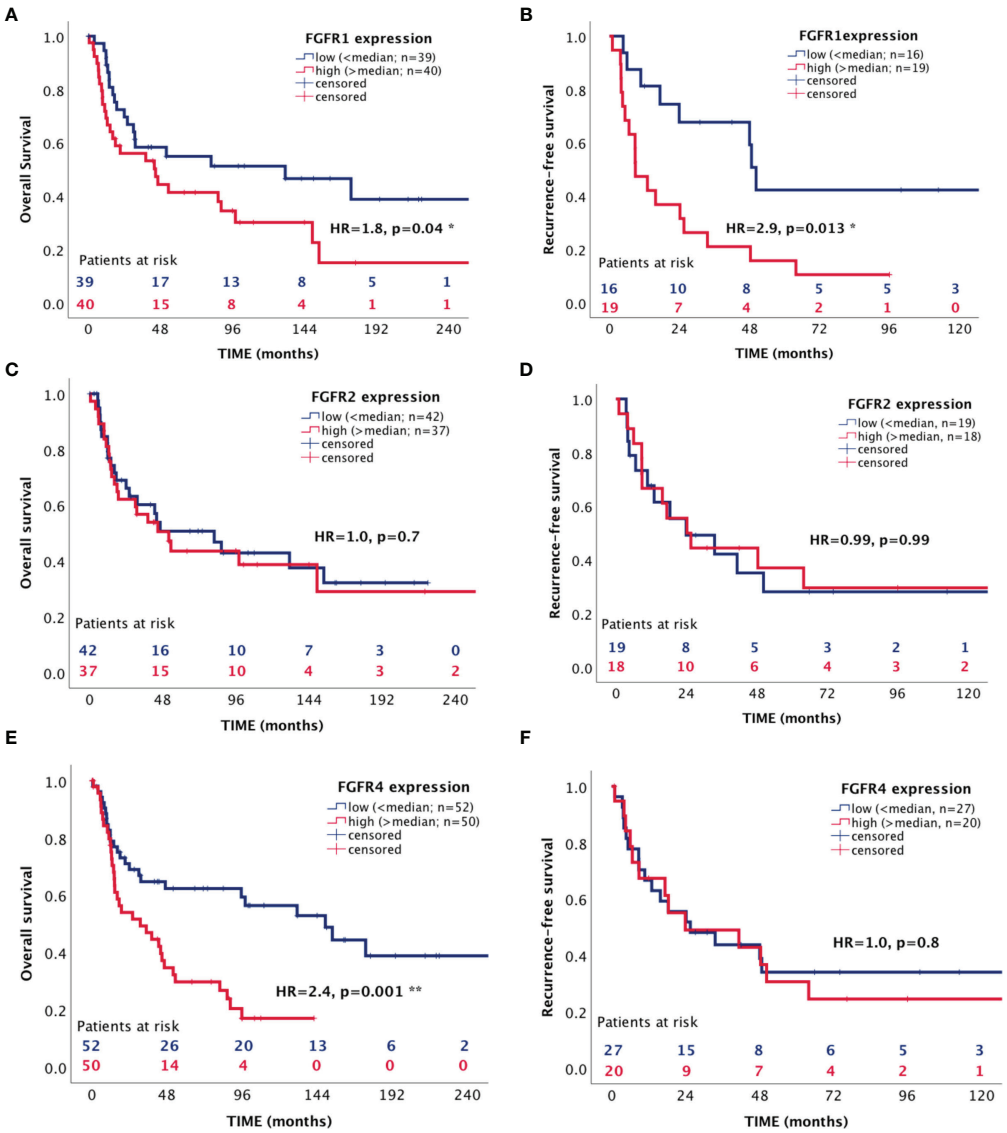


**FIGURE 5** | Association between expression of FGF receptors 1, 2 and 4 with patient survival. **(A, C, E)** overall survival **(B, D, F)** recurrence-free survival. *p < 0.05 and **p < 0.01.

tissues of both epithelial and mesenchymal origin indicating that adrenocortical tissues represent a particular tissue type as we could show before (43). A defining property of FGFs and their receptors is that they bind to heparin and heparan sulfate and are therefore intimately connected with the extracellular matrix of tissues (44) where they play an important role during epithelial morphogenesis (45). As the loss of connectivity with the extracellular matrix is an important process necessary in the establishment of 2D cell-lines (46), it was not surprising that all cell-lines, including those of adrenocortical origin, had completely divergent FGF/FGFR pathway gene expression pattern from the corresponding tissues. Hence these cell-lines may not be regarded as a reliable research model for FGF signaling in adrenocortical tissues and future studies addressing the therapeutic potential of modulating these pathways will need to use more physiological models such as patient-derived tumor xenograft or spontaneous adrenocortical carcinoma mouse models.

A quantitative analysis of the genes significantly differentially expressed between the benign ACA and ACC revealed quite a high number of genes (16/93) with altered expression in ACC. A qualitative analysis of these genes showed that several of the genes that were expressed at lower levels in ACC are associated with patterns of expression indicative of tissues differentiation. Thus, a downregulation of these genes would lead to less differentiated, more disorganized tissues. For example in the adrenal, *PLD1* and *MRAS* are associated with hormonal secretion patterns (47–49), *FGFR2* is known to regulate the differentiation (50) and the spatial organization of the adrenal gland (51) while

**TABLE 3 |** Influence of FGFR - 1, 2 and 4 expression on overall and recurrence-free survival of ACC patients in univariate and multivariate analyses including Ki-67 and ENSAT stage.

| **overall survival** | | | | | | | |
|---|---|---|---|---|---|---|---|
| **Variables** | **univariate analysis** | | | | **multivariate analysis** | | |
| | **time (months)** | **HR** | **95%CI** | ***p*** | **HR** | **95%CI** | ***p*** |
| Tumor stage (ENSAT) | | | | | | | |
| I+II (n=46) | 171.68 ± 22.82 | | | | | | |
| III (n=33) | 90.17 ± 17.74 | 2.11 | 1.13 – 3.94 | 0.018* | 5.23 | 1.95 – 14.01 | 0.001** |
| IV (n=25) | 36.94 ± 11.28 | 4.60 | 2.35 – 8.98 | <0.001*** | 5.64 | 1.43 – 22.18 | 0.013* |
| Ki67 | | | | | | | |
| low (<20) (n=53) | 143.21 ± 17.61 | | | | | | |
| high (≥20) (n=19) | 30.11 ± 6.77 | 4.31 | 2.12 – 8.78 | <0.001*** | 17.44 | 5.83 – 52.20 | <0.001*** |
| FGFR1 | | | | | | | |
| low (<median) (n=39) | 147.9 ± 23.20 | | | | | | |
| high (>median) (n=40) | 84.12 ± 16.75 | 1.80 | 1.01 – 3.25 | 0.047* | 2.11 | 0.91 – 4.89 | 0.07 |
| FGFR2 | | | | | | | |
| low (<median) (n=42) | 103.09 ± 15.94 | | | | | | |
| high (>median) (n=37) | 117.81 ± 23.76 | 1.09 | 0.60 – 1.98 | 0.75 | 1.19 | 0.50 – 2.83 | 0.68 |
| FGFR4 | | | | | | | |
| low (<median) (n=50) | 154.60 ± 19.64 | | | | | | |
| high (>median) (n=52) | 50.52 ± 7.59 | 2.44 | 1.41 – 4.22 | 0.001** | 3.23 | 1.52 – 6.88 | 0.002** |
| recurrence-free survival | | | | | | | |
| | | **univariate analysis** | | | | **multivariate analysis** | |
| **Variables** | **time (months)** | **HR** | **95%CI** | ***p*** | **HR** | **95%CI** | ***p*** |
| Tumor stage (ENSAT) | | | | | | | |
| I+II (n=35) | 63.35 ± 11.58 | | | | | | |
| III (n=14) | 43.65 ± 14.25 | 1.36 | 0.66 – 2.81 | 0.40 | 1.74 | 0.67 – 4.51 | 0.25 |
| Ki67 | | | | | | | |
| low (<20) (n=29) | 71.22 ± 11.85 | | | | | | |
| high (≥20) (n=10) | 13.89 ± 5.57 | 4.34 | 1.87 – 10.09 | 0.001** | 8.66 | 2.64 – 28.44 | <0.001*** |
| FGFR1 | | | | | | | |
| low (<median) (n=16) | 74.71 ± 15.06 | | | | | | |
| high (>median) (n=19) | 24.84 ± 6.71 | 2.9 | 1.25 – 6.84 | 0.009** | 6.10 | 1.78 – 20.86 | 0.004** |
| FGFR2 | | | | | | | |
| low (<median) (n=19) | 59.56 ± 16.40 | | | | | | |
| high (>median) (n=18) | 53.44 ± 12.71 | 0.99 | 0.45 – 2.18 | 0.99 | 0.87 | 0.32 – 2.39 | 0.79 |
| FGFR4 | | | | | | | |
| low (<median) (n=27) | 62.94 ± 13.21 | | | | | | |
| high (>median) (n=20) | 52.62 ± 13.07 | 1.06 | 0.52 – 2.18 | 0.86 | 0.77 | 0.33 – 1.80 | 0.55 |

*Statistical significance:*p<0.05,**p<0.01,***p<0.001.*

*PIK3C2G* has been identified as a novel X-zone marker and is downregulated in the adrenal glands of Gata6 knockout (cKO) mice (52). Importantly, *FGFR1* and *FGFR4* were considerably higher expressed in ACC (53–55). The concordant up-regulation of their ligands *FGF8* and *FGF19* suggests an autocrine/paracrine growth promoting loop (56).

The differences between the localized (ENSAT I and II) and more aggressive (ENSAT III and IV) ACCs were more subtle as can be observed also by the lower number of genes that had significantly different expression levels between the two subgroups. Most of the genes were associated with metastatic processes such as what was classically defined as epithelial to mesenchymal transition suggesting its involvement in the adrenocortical cancer progression. For example *RalA* plays an important role during embryogenesis and regulation of epithelial-mesenchymal interaction in tissues of mesenchymal origin including the fetal adrenal (57). The same is true for *MAPK9/JNK2* the phosphorylation status of which is controlling metastatic processes by promoting the switch of tumor cells from mesenchymal-epithelial transition to epithelial-mesenchymal transition (58) and its inactivation was identified as a carcinogenic factor in other types of cancer (59). *PIK3R1* was also reported to negatively regulate the epithelial-mesenchymal transition and stem-like phenotype of renal cancer (60) so its downregulation would lead to mobilization of cells and support establishment of metastases. Interestingly, *FGF21*, the only gene found significantly upregulated in advanced vs localized ACC is a secreted endocrine factor that functions as a major metabolic regulator stimulating the uptake of glucose and as such has been associated with aggressiveness in several types of cancer (61–63) but also with outcome in other types of diseases (64). All these findings, and especially the upregulation of the secreted factor *FGF21* in advanced ACC are important discoveries for ACC and should be addressed in more detail in further studies.

Importantly, from the therapeutic potential point of view, the three FGFRs that we could show to be differentially expressed between benign and malignant adrenocortical tumors, *FGFR1*, *2* and *4*, were also confirmed in the larger cohort of FFPE tissues. The partial cross reactivity of FGFR antibodies due to the sequence similarity of the FGFR family rendered immunohistochemistry unreliable as a validation method. That is why most studies assessing FGFR expression as a prognostic marker for selective

FGFR inhibitors use an *in situ* RNA detection method instead of immunohistochemistry (28, 65, 66). We opted for the *in-situ* hybridization technique RNAScope that allowed us to both quantify and also determine the tissue distribution of the mRNA of interest, a major advantage when compared to the bulk measurement used in the targeted screening. RNAscope confirmed the previous finding that *FGFR1* and *4* are overexpressed in ACC when compared to ACA while *FGFR2* is higher expressed in the latter. Not surprisingly *FGFR1* and *4* expression was significantly negatively associated with patient survival endpoints while their individual role in recurrence and metastasis remains unclear from these clinical analyses.

The high expression of the *FGFR1* and *4* in ACCs is a promising first indication that FGFR inhibitors like ponatinib (pan-FGFR, PDGFR, SRC, RET, KIT and FLT1 inhibitor) (24), lenvatinib (VEGFR, pan-FGFR, PDGFRα, KIT and RET inhibitor) (23), rogaratinib (selective FGFR 4 inhibitor) (65) or others may have better therapeutic efficacy than the other RTK inhibitors that have been tested until now for the treatment of ACC.

To summarize our data, we could show that FGF/FGFR pathways are expressed in adrenocortical tissues and that their expression pattern is different from other tissues. Expression changes in different member molecules of this pathway are associated with tumor progression (*FGFR1* and *4*) and loss of tissue differentiation, and aggressiveness. These include factors that are generally associated with what is classically known as epithelial to mesechymal transition including cell mobilization and metastatic spread. It must be noted however from our previous work that the adrenal cortex shares less similarity with epithelial compared to mesenchymal tissues based on marker protein expression. Furthermore, *FGFR1* and *4* were also associated with patient prognosis in a relatively large cohort of ACC patients. All this data is raising the hopes that future studies with FGFR inhibitors will show the therapeutic potential of these novel targets in the treatment of refractory ACC.

## DATA AVAILABILITY STATEMENT

The original contributions presented in the study are included in the article and **Supplementary Material**. Further inquiries can be directed to the corresponding authors.

## ETHICS STATEMENT

The studies involving human participants were reviewed and approved by Ethics Committee of the University of Würzburg, Josef-Schneider-Straße 4, 97080, Würzburg, Germany. The patients/participants provided their written informed consent to participate in this study.

## AUTHOR CONTRIBUTIONS

MF, SS, and MK designed the study. IS and KL performed experiments. SK, BA, and CH provided samples and clinical data. IS and SS analysed the data. IS, MF, SS, and MK interpreted the data. IS, MF, SS, and MK wrote a manuscript. All authors contributed to the article and approved the submitted version.

## FUNDING

This study was supported by the Else Kröner-Fresenius Foundation (Else Kröner-Fresenius-Stiftung; project number: 2016_A96 to SS and MK and the German Research Foundation (Deutsche Forschungsgemeinschaft; project numbers 314061271 – CRC/TRR 205 and 237292849 to MF, SS and MK). This work was also supported by the Uniscientia Foundation (Keyword Tumor Model) to CH.

## ACKNOWLEDGMENTS

The authors wish to thank all patients, their families and caregivers for providing clinical data and tumor sections for this study. The APC was partially funded by the Open Access Publication Fund of the University of Würzburg.

## SUPPLEMENTARY MATERIAL

The Supplementary Material for this article can be found online at: https://www.frontiersin.org/articles/10.3389/fendo.2021.795116/full#supplementary-material

## REFERENCES

1. Fassnacht M, Dekkers OM, Else T, Baudin E, Berruti A, de Krijger R, et al. European Society of Endocrinology Clinical Practice Guidelines on the Management of Adrenocortical Carcinoma in Adults, in Collaboration With the European Network for the Study of Adrenal Tumors. *Eur J Endocrinol* (2018) 179(4):G1–G46. doi: 10.1530/EJE-18-0608
2. Fassnacht M, Assie G, Baudin E, Eisenhofer G, de la Fouchardiere C, Haak HR, et al. Adrenocortical Carcinomas and Malignant Phaeochromocytomas: ESMO-EURACAN Clinical Practice Guidelines for Diagnosis, Treatment and Follow-Up. *Ann Oncol* (2020) 31(11):1476–90. doi: 10.1016/j.annonc.2020.08.2099
3. Terzolo M, Angeli A, Fassnacht M, Daffara F, Tauchmanova L, Conton PA, et al. Adjuvant Mitotane Treatment for Adrenocortical Carcinoma. *N Engl J Med* (2007) 356(23):2372–80. doi: 10.1056/NEJMoa063360
4. Berruti A, Fassnacht M, Baudin E, Hammer G, Haak H, Leboulleux S, et al. Adjuvant Therapy in Patients With Adrenocortical Carcinoma: A Position of an International Panel. *J Clin Oncol* (2010) 28(23):e401–2; author reply e3. doi: 10.1200/JCO.2009.27.5958
5. Fassnacht M, Terzolo M, Allolio B, Baudin E, Haak H, Berruti A, et al. Combination Chemotherapy in Advanced Adrenocortical Carcinoma. *N Engl J Med* (2012) 366(23):2189–97. doi: 10.1056/NEJMoa1200966
6. Soon PS, Gill AJ, Benn DE, Clarkson A, Robinson BG, McDonald KL, et al. Microarray Gene Expression and Immunohistochemistry Analyses of Adrenocortical Tumors Identify IGF2 and Ki-67 as Useful in Differentiating Carcinomas From Adenomas. *Endocr Relat Cancer* (2009) 16(2):573–83. doi: 10.1677/ERC-08-0237
7. Altieri B, Colao A, Faggiano A. The Role of Insulin-Like Growth Factor System in the Adrenocortical Tumors. *Minerva Endocrinol* (2019) 44(1):43–57. doi: 10.23736/S0391-1977.18.02882-1

8. Fassnacht M, Berruti A, Baudin E, Demeure MJ, Gilbert J, Haak H, et al. Linsitinib (OSI-906) Versus Placebo for Patients With Locally Advanced or Metastatic Adrenocortical Carcinoma: A Double-Blind, Randomised, Phase 3 Study. *Lancet Oncol* (2015) 16(4):426–35. doi: 10.1016/S1470-2045(15)70081-1
9. Xu YZ, Zhu Y, Shen ZJ, Sheng JY, He HC, Ma G, et al. Significance of Heparanase-1 and Vascular Endothelial Growth Factor in Adrenocortical Carcinoma Angiogenesis: Potential for Therapy. *Endocrine* (2011) 40(3):445–51. doi: 10.1007/s12020-011-9502-1
10. Berruti A, Sperone P, Ferrero A, Germano A, Ardito A, Priola AM, et al. Phase II Study of Weekly Paclitaxel and Sorafenib as Second/Third-Line Therapy in Patients With Adrenocortical Carcinoma. *Eur J Endocrinol* (2012) 166 (3):451–8. doi: 10.1530/EJE-11-0918
11. Kroiss M, Reuss M, Kuhner D, Johanssen S, Beyer M, Zink M, et al. Sunitinib Inhibits Cell Proliferation and Alters Steroidogenesis by Down-Regulation of HSD3B2 in Adrenocortical Carcinoma Cells. *Front Endocrinol (Lausanne)* (2011) 2:27. doi: 10.3389/fendo.2011.00027
12. Kroiss M, Quinkler M, Johanssen S, van Erp NP, Lankheet N, Pollinger A, et al. Sunitinib in Refractory Adrenocortical Carcinoma: A Phase II, Single-Arm, Open-Label Trial. *J Clin Endocrinol Metab* (2012) 97(10):3495–503. doi: 10.1210/jc.2012-1419
13. Kroiss M, Megerle F, Kurlbaum M, Zimmermann S, Wendler J, Jimenez C, et al. Objective Response and Prolonged Disease Control of Advanced Adrenocortical Carcinoma With Cabozantinib. *J Clin Endocrinol Metab* (2020) 105(5):1461–8. doi: 10.1210/clinem/dgz318
14. Altieri B, Ronchi CL, Kroiss M, Fassnacht M. Next-Generation Therapies for Adrenocortical Carcinoma. *Best Pract Res Clin Endocrinol Metab* (2020) 34 (3):101434. doi: 10.1016/j.beem.2020.101434
15. Lieu C, Heymach J, Overman M, Tran H, Kopetz S. Beyond VEGF: Inhibition of the Fibroblast Growth Factor Pathway and Antiangiogenesis. *Clin Cancer Res* (2011) 17(19):6130–9. doi: 10.1158/1078-0432.CCR-11-0659
16. Itoh N, Ornitz DM. Fibroblast Growth Factors: From Molecular Evolution to Roles in Development, Metabolism and Disease. *J Biochem* (2011) 149 (2):121–30. doi: 10.1093/jb/mvq121
17. Ornitz DM, Itoh N. The Fibroblast Growth Factor Signaling Pathway. *Wiley Interdiscip Rev Dev Biol* (2015) 4(3):215–66. doi: 10.1002/wdev.176
18. Itoh N. The Fgf Families in Humans, Mice, and Zebrafish: Their Evolutional Processes and Roles in Development, Metabolism, and Disease. *Biol Pharm Bull* (2007) 30(10):1819–25. doi: 10.1248/bpb.30.1819
19. Thisse B, Thisse C. Functions and Regulations of Fibroblast Growth Factor Signaling During Embryonic Development. *Dev Biol* (2005) 287(2):390–402. doi: 10.1016/j.ydbio.2005.09.011
20. Haugsten EM, Wiedlocha A, Olsnes S, Wesche J. Roles of Fibroblast Growth Factor Receptors in Carcinogenesis. *Mol Cancer Res* (2010) 8(11):1439–52. doi: 10.1158/1541-7786.MCR-10-0168
21. Turner N, Grose R. Fibroblast Growth Factor Signalling: From Development to Cancer. *Nat Rev Cancer* (2010) 10(2):116–29. doi: 10.1038/nrc2780
22. Korc M, Friesel RE. The Role of Fibroblast Growth Factors in Tumor Growth. *Curr Cancer Drug Targets* (2009) 9(5):639–51. doi: 10.2174/156800909789057006
23. Capozzi M, De Divitiis C, Ottaiano A, von Arx C, Scala S, Tatangelo F, et al. Lenvatinib, a Molecule With Versatile Application: From Preclinical Evidence to Future Development in Anti-Cancer Treatment. *Cancer Manag Res* (2019) 11:3847–60. doi: 10.2147/CMAR.S188316
24. Tan FH, Putoczki TL, Stylli SS, Luwor RB. Ponatinib: A Novel Multi-Tyrosine Kinase Inhibitor Against Human Malignancies. *Onco Targets Ther* (2019) 12:635–45. doi: 10.2147/OTT.S189391
25. Bedrose S, Miller KC, Altameemi L, Ali MS, Nassar S, Garg N, et al. Combined Lenvatinib and Pembrolizumab as Salvage Therapy in Advanced Adrenal Cortical Carcinoma. *J Immunother Cancer* (2020) 8(2):e001009. doi: 10.1136/jitc-2020-001009
26. Cha Y, Kim HP, Lim Y, Han SW, Song SH, Kim TY. FGFR2 Amplification Is Predictive of Sensitivity to Regorafenib in Gastric and Colorectal Cancers In Vitro. *Mol Oncol* (2018) 12(7):993–1003. doi: 10.1002/1878-0261.12194
27. Pearson A, Smyth E, Babina IS, Herrera-Abreu MT, Tarazona N, Peckitt C, et al. High-Level Clonal FGFR Amplification and Response to FGFR Inhibition in a Translational Clinical Trial. *Cancer Discov* (2016) 6(8):838–51. doi: 10.1158/2159-8290.CD-15-1246
28. Sanchez-Guixe M, Hierro C, Jimenez J, Viaplana C, Villacampa G, Monelli E, et al. High FGFR1-4 mRNA Expression Levels Correlate With Response to Selective FGFR Inhibitors in Breast Cancer. *Clin Cancer Res* (2021). doi: 10.1158/1078-0432.CCR-21-1810
29. Gospodarowicz D, Handley HH. Stimulation of Division of Y1 Adrenal Cells by a Growth Factor Isolated From Bovine Pituitary Glands. *Endocrinology* (1975) 97(1):102–7. doi: 10.1210/endo-97-1-102
30. Gospodarowicz D, Ill CR, Hornsby PJ, Gill GN. Control of Bovine Adrenal Cortical Cell Proliferation by Fibroblast Growth Factor. Lack of Effect of Epidermal Growth Factor. *Endocrinology* (1977) 100(4):1080–9. doi: 10.1210/endo-100-4-1080
31. Boulle N, Gicquel C, Logie A, Christol R, Feige JJ, Le Bouc Y. Fibroblast Growth Factor-2 Inhibits the Maturation of Pro-Insulin-Like Growth Factor-II (Pro-IGF-II) and the Expression of Insulin-Like Growth Factor Binding Protein-2 (IGFBP-2) in the Human Adrenocortical Tumor Cell Line NCI-H295R. *Endocrinology* (2000) 141(9):3127–36. doi: 10.1210/endo.141.9.7632
32. Haase M, Schott M, Bornstein SR, Malendowicz LK, Scherbaum WA, Willenberg HS. CITED2 is Expressed in Human Adrenocortical Cells and Regulated by Basic Fibroblast Growth Factor. *J Endocrinol* (2007) 192(2):459–65. doi: 10.1677/JOE-06-0083
33. Feige JJ, Baird A. Growth Factor Regulation of Adrenal Cortex Growth and Function. *Prog Growth Factor Res* (1991) 3(2):103–13. doi: 10.1016/s0955-2235(05)80002-x
34. Guasti L, Candy Sze WC, McKay T, Grose R, King PJ. FGF Signalling Through Fgfr2 Isoform IIIb Regulates Adrenal Cortex Development. *Mol Cell Endocrinol* (2013) 371(1-2):182–8. doi: 10.1016/j.mce.2013.01.014
35. Haase M, Thiel A, Scholl UI, Ashmawy H, Schott M, Ehlers M. Subcellular Localization of Fibroblast Growth Factor Receptor Type 2 and Correlation With CTNNB1 Genotype in Adrenocortical Carcinoma. *BMC Res Notes* (2020) 13(1):282. doi: 10.1186/s13104-020-05110-5
36. Zheng S, Cherniack AD, Dewal N, Moffitt RA, Danilova L, Murray BA, et al. Comprehensive Pan-Genomic Characterization of Adrenocortical Carcinoma. *Cancer Cell* (2016) 29(5):723–36. doi: 10.1016/j.ccell.2016.04.002
37. Krook MA, Reeser JW, Ernst G, Barker H, Wilberding M, Li G, et al. Fibroblast Growth Factor Receptors in Cancer: Genetic Alterations, Diagnostics, Therapeutic Targets and Mechanisms of Resistance. *Br J Cancer* (2021) 124(5):880–92. doi: 10.1038/s41416-020-01157-0
38. Hantel C, Shapiro I, Poli G, Chiapponi C, Bidlingmaier M, Reincke M, et al. Targeting Heterogeneity of Adrenocortical Carcinoma: Evaluation and Extension of Preclinical Tumor Models to Improve Clinical Translation. *Oncotarget* (2016) 7(48):79292–304. doi: 10.18632/oncotarget.12685
39. Kiseljak-Vassiliades K, Zhang Y, Bagby SM, Kar A, Pozdeyev N, Xu M, et al. Development of New Preclinical Models to Advance Adrenocortical Carcinoma Research. *Endocr Relat Cancer* (2018) 25(4):437–51. doi: 10.1530/ERC-17-0447
40. Adam P, Kircher S, Sbiera I, Koehler VF, Berg E, Knosel T, et al. FGF-Receptors and PD-L1 in Anaplastic and Poorly Differentiated Thyroid Cancer: Evaluation of the Preclinical Rationale. *Front Endocrinol (Lausanne)* (2021) 12:712107. doi: 10.3389/fendo.2021.712107
41. Fassnacht M, Johanssen S, Quinkler M, Bucsky P, Willenberg HS, Beuschlein F, et al. Limited Prognostic Value of the 2004 International Union Against Cancer Staging Classification for Adrenocortical Carcinoma: Proposal for a Revised TNM Classification. *Cancer* (2009) 115(2):243–50. doi: 10.1002/cncr.24030
42. Beuschlein F, Weigel J, Saeger W, Kroiss M, Wild V, Daffara F, et al. Major Prognostic Role of Ki67 in Localized Adrenocortical Carcinoma After Complete Resection. *J Clin Endocrinol Metab* (2015) 100(3):841–9. doi: 10.1210/jc.2014-3182
43. Sbiera I, Kircher S, Altieri B, Fassnacht M, Kroiss M, Sbiera S. Epithelial and Mesenchymal Markers in Adrenocortical Tissues: How Mesenchymal Are Adrenocortical Tissues? *Cancers* (2021) 13(7):1736. doi: 10.3390/cancers13071736
44. Burgess WH, Maciag T. The Heparin-Binding (Fibroblast) Growth Factor Family of Proteins. *Annu Rev Biochem* (1989) 58:575–606. doi: 10.1146/annurev.bi.58.070189.003043
45. Li X, Chen Y, Scheele S, Arman E, Haffner-Krausz R, Ekblom P, et al. Fibroblast Growth Factor Signaling and Basement Membrane Assembly are Connected During Epithelial Morphogenesis of the Embryoid Body. *J Cell Biol* (2001) 153(4):811–22. doi: 10.1083/jcb.153.4.811
46. Schiller JH, Bittner G. Loss of the Tumorigenic Phenotype With *In Vitro*, But Not *In Vivo*, Passaging of a Novel Series of Human Bronchial Epithelial Cell

Lines: Possible Role of an Alpha 5/Beta 1-Integrin-Fibronectin Interaction. *Cancer Res* (1995) 55(24):6215–21.
47. Tsai YY, Rainey WE, Pan ZQ, Frohman MA, Choudhary V, Bollag WB. Phospholipase D Activity Underlies Very-Low-Density Lipoprotein (VLDL)-Induced Aldosterone Production in Adrenal Glomerulosa Cells. *Endocrinology* (2014) 155(9):3550–60. doi: 10.1210/en.2014-1159
48. Rabano M, Pena A, Brizuela L, Macarulla JM, Gomez-Munoz A, Trueba M. Angiotensin II-Stimulated Cortisol Secretion is Mediated by Phospholipase D. *Mol Cell Endocrinol* (2004) 222(1-2):9–20. doi: 10.1016/j.mce.2004.05.006
49. Romero DG, Plonczynski M, Vergara GR, Gomez-Sanchez EP, Gomez-Sanchez CE. Angiotensin II Early Regulated Genes in H295R Human Adrenocortical Cells. *Physiol Genomics* (2004) 19(1):106–16. doi: 10.1152/physiolgenomics.00097.2004
50. Hafner R, Bohnenpoll T, Rudat C, Schultheiss TM, Kispert A. Fgfr2 Is Required for the Expansion of the Early Adrenocortical Primordium. *Mol Cell Endocrinol* (2015) 413:168–77. doi: 10.1016/j.mce.2015.06.022
51. Leng S, Pignatti E, Khetani RS, Shah MS, Xu S, Miao J, et al. Beta-Catenin and FGFR2 Regulate Postnatal Rosette-Based Adrenocortical Morphogenesis. *Nat Commun* (2020) 11(1):1680. doi: 10.1038/s41467-020-15332-7
52. Pihlajoki M, Gretzinger E, Cochran R, Kyronlahti A, Schrade A, Hiller T, et al. Conditional Mutagenesis of Gata6 in SF1-Positive Cells Causes Gonadal-Like Differentiation in the Adrenal Cortex of Mice. *Endocrinology* (2013) 154 (5):1754–67. doi: 10.1210/en.2012-1892
53. Laurell C, Velazquez-Fernandez D, Lindsten K, Juhlin C, Enberg U, Geli J, et al. Transcriptional Profiling Enables Molecular Classification of Adrenocortical Tumours. *Eur J Endocrinol* (2009) 161(1):141–52. doi: 10.1530/EJE-09-0068
54. De Martino MC, Al Ghuzlan A, Aubert S, Assie G, Scoazec JY, Leboulleux S, et al. Molecular Screening for a Personalized Treatment Approach in Advanced Adrenocortical Cancer. *J Clin Endocrinol Metab* (2013) 98 (10):4080–8. doi: 10.1210/jc.2013-2165
55. Brito LP, Ribeiro TC, Almeida MQ, Jorge AA, Soares IC, Latronico AC, et al. The Role of Fibroblast Growth Factor Receptor 4 Overexpression and Gene Amplification as Prognostic Markers in Pediatric and Adult Adrenocortical Tumors. *Endocr Relat Cancer* (2012) 19(3):L11–3. doi: 10.1530/ERC-11-0231
56. Kuro OM. Klotho and Endocrine Fibroblast Growth Factors: Markers of Chronic Kidney Disease Progression and Cardiovascular Complications? *Nephrol Dial Transplant* (2019) 34(1):15–21. doi: 10.1093/ndt/gfy126
57. Zhao Z, Rivkees SA. Tissue-Specific Expression of GTPas RalA and RalB During Embryogenesis and Regulation by Epithelial-Mesenchymal Interaction. *Mech Dev* (2000) 97(1-2):201–4. doi: 10.1016/s0925-4773(00)00427-5
58. Hu S, Dong X, Gao W, Stupack D, Liu Y, Xiang R, et al. Alternative Promotion and Suppression of Metastasis by JNK2 Governed by its Phosphorylation. *Oncotarget* (2017) 8(34):56569–81. doi: 10.18632/oncotarget.17507
59. Lessel W, Silver A, Jechorek D, Guenther T, Roehl FW, Kalinski T, et al. Inactivation of JNK2 as Carcinogenic Factor in Colitis-Associated and Sporadic Colorectal Carcinogenesis. *Carcinogenesis* (2017) 38(5):559–69. doi: 10.1093/carcin/bgx032
60. Lin Y, Yang Z, Xu A, Dong P, Huang Y, Liu H, et al. PIK3R1 Negatively Regulates the Epithelial-Mesenchymal Transition and Stem-Like Phenotype of Renal Cancer Cells Through the AKT/GSK3beta/CTNNB1 Signaling Pathway. *Sci Rep* (2015) 5:8997. doi: 10.1038/srep08997
61. Kang YE, Kim JT, Lim MA, Oh C, Liu L, Jung SN, et al. Association Between Circulating Fibroblast Growth Factor 21 and Aggressiveness in Thyroid Cancer. *Cancers (Basel)* (2019) 11(8):1154. doi: 10.3390/cancers11081154
62. Kim SH, Kim JW, Hwang IG, Jang JS, Hong S, Kim TY, et al. Serum Biomarkers for Predicting Overall Survival and Early Mortality in Older Patients With Metastatic Solid Tumors. *J Geriatr Oncol* (2019) 10(5):749–56. doi: 10.1016/j.jgo.2019.03.015
63. Osawa T, Muramatsu M, Watanabe M, Shibuya M. Hypoxia and Low-Nutrition Double Stress Induces Aggressiveness in a Murine Model of Melanoma. *Cancer Sci* (2009) 100(5):844–51. doi: 10.1111/j.1349-7006.2009.01105.x
64. Ebrahimi F, Wolffenbuttel C, Blum CA, Baumgartner C, Mueller B, Schuetz P, et al. Fibroblast Growth Factor 21 Predicts Outcome in Community-Acquired Pneumonia: Secondary Analysis of Two Randomised Controlled Trials. *Eur Respir J* (2019) 53(2):1800973. doi: 10.1183/13993003.00973-2018
65. Schuler M, Cho BC, Sayehli CM, Navarro A, Soo RA, Richly H, et al. Rogaratinib in Patients With Advanced Cancers Selected by FGFR mRNA Expression: A Phase 1 Dose-Escalation and Dose-Expansion Study. *Lancet Oncol* (2019) 20(10):1454–66. doi: 10.1016/S1470-2045(19)30412-7
66. Grunewald S, Politz O, Bender S, Heroult M, Lustig K, Thuss U, et al. Rogaratinib: A Potent and Selective Pan-FGFR Inhibitor With Broad Antitumor Activity in FGFR-Overexpressing Preclinical Cancer Models. *Int J Cancer* (2019) 145(5):1346–57. doi: 10.1002/ijc.32224

**Conflict of Interest:** The authors declare that the research was conducted in the absence of any commercial or financial relationships that could be construed as a potential conflict of interest.

**Publisher's Note:** All claims expressed in this article are solely those of the authors and do not necessarily represent those of their affiliated organizations, or those of the publisher, the editors and the reviewers. Any product that may be evaluated in this article, or claim that may be made by its manufacturer, is not guaranteed or endorsed by the publisher.

frontiers in Endocrinology

CASE REPORT
published: 15 December 2021
doi: 10.3389/fendo.2021.793718

# Case Report and Systematic Review: Sarcomatoid Parathyroid Carcinoma —A Rare, Highly Malignant Subtype

*Yongchao Yu, Yue Wang, Qingcheng Wu, Xuzi Zhao, Deshun Liu, Yongfu Zhao, Yuguo Li, Guangzhi Wang, Jingchao Xu, Junzhu Chen, Ning Zhang* and Xiaofeng Tian**

*Department of Thyroid Surgery, The Second Hospital of Dalian Medical University, Dalian, China*

**Background:** Parathyroid carcinoma (PC) is a rare malignancy, the incidence of which is less than 1/1 million per year. Sarcomatoid parathyroid carcinoma (SaPC) is an extremely peculiar subtype; only three cases have been reported internationally. It consists of both malignant epithelial components and sarcomatoid components (mesenchymal origin) simultaneously. This "confusing" cancer exhibits higher invasiveness, and traditional surgery does not appear to achieve the expectation, which differs significantly from that of general PC.

**Objective:** To characterize the clinicopathologic features of SaPC and explore similarities and differences between SaPC and general PC.

**Materials and Methods:** We collected clinical data of SaPC cases from our center and literature. The SaPC case in our center was presented. To better understand the characteristics of SaPC, we also reviewed clinical information in general PC cases from our center and literature within the last 5 years, and a systematic review was performed for further comparison.

**Results:** A 60-year-old woman was admitted for a neck mass and hoarseness. After the surgery, she was confirmed as SaPC and ultimately developed local recurrence at 3 months. Together with the reported cases from literature, four cases of SaPC (three cases from literature) and 203 cases of general PC (200 cases from literature) were reviewed. Both tumors showed obvious abnormalities in parathormone (PTH) level and gland size. Compared to general PC, SaPC has a later age of onset (60.50 ± 7.42 vs. 51.50 ± 8.29), relatively low levels of PTH (110.28 ± 59.32 vs. 1,156.07 ± 858.18), and a larger tumor size (6.00 ± 1.63 vs. 3.14 ± 0.70). For SaPC, all four cases were initially misdiagnosed as thyroid tumors (4/4). Spindle cell areas or transitional zones were common pathological features in SaPC cases (3/4).

**Conclusion:** SaPC is a very rare pathologic subtype of PC and appears to be much more easily misdiagnosed as a thyroid tumor. Spindle cell areas or transitional zones are highly possible to be pathological features in its sarcomatoid components. Despite many similarities, there are some differences between SaPC and general PC—SaPC does not show the obvious endocrine feature but stronger aggressiveness. Surgical treatment of

OPEN ACCESS

***Edited by:***
*Enzo Lalli, UMR7275 Institut de Pharmacologie Moléculaire et Cellulaire (IPMC), France*

***Reviewed by:***
*Jessica Costa-Guda, University of Connecticut, United States*
*Gallia Graiani, University of Parma, Italy*

****Correspondence:***
*Xiaofeng Tian*
*txfdl@dmu.edu.cn*
*Ning Zhang*
*drdorischang@yeah.net*

***Specialty section:***
*This article was submitted to Cancer Endocrinology, a section of the journal Frontiers in Endocrinology*

***Received:*** *12 October 2021*
***Accepted:*** *24 November 2021*
***Published:*** *15 December 2021*

***Citation:***
*Yu Y, Wang Y, Wu Q, Zhao X, Liu D, Zhao Y, Li Y, Wang G, Xu J, Chen J, Zhang N and Tian X (2021) Case Report and Systematic Review: Sarcomatoid Parathyroid Carcinoma —A Rare, Highly Malignant Subtype. Front. Endocrinol. 12:793718. doi: 10.3389/fendo.2021.793718*

SaPC does relieve life-threatening symptoms and improve quality of life even with recurrence in the short term.

**Keywords: sarcomatoid, PTH, parathyroid carcinoma, diagnosis, surgery**

## INTRODUCTION

Parathyroid carcinoma (PC) is a rare malignant neoplasm. The incidence is less than 1 in 1 million per year (1). At present, general PC is believed to be a slowly progressive disease characterized by specific clinical features (2), and radical surgery is believed to be the only effective curative treatment for this disease (3–5). Sarcomatoid carcinoma is an exceedingly rare tumor subtype. It refers to a bipolar malignancy with both carcinoma and sarcomatoid components. In PC, this tumor subtype was initially named parathyroid carcinosarcoma or parathyroid carcinoma with sarcomatoid differentiation (6–8). We utilized the term "sarcomatoid carcinoma" referring to nomenclature of other tumors with similar features. Sarcomatoid parathyroid carcinoma (SaPC) was first reported in 2002 by Nacamuli et al. (6) and characterized by strong invasiveness and life-threatening recurrence shortly after the operation, which is quite different from general PC. For sarcomatoid carcinoma, there are several hypotheses about its formation, and epithelial–mesenchymal transformation (EMT) appears to play a major role (9, 10).

Here, we introduce similarities and differences between SaPC and general PC based on our experience with cases in our center and the literature. In addition, we provide more insights into the diagnosis and surgical strategies of SaPC.

## MATERIALS AND METHODS

### The Collection of Medical Records

From January 2016 to September 2021, four patients with PC were enrolled in this study, including one patient with SaPC (one female) and three patients with general PC (three females). They underwent surgery in our department and were followed up. We obtained clinicopathologic and prognostic information of the patients after approval by the Ethics Committee of the Second Hospital of Dalian Medical University.

### Systematic Review

The systematic review was conducted under the Preferred Reporting Items for Systematic reviews and Meta-Analyses (PRISMA) guidelines (11). Literature that contained general PC cases was searched using terms "parathyroid carcinoma" OR "parathyroid cancer" in PubMed (MeSH) and Cochrane Library (Title Abstract Keyword) from 2016 to present. General PC cases were defined as an age of onset >18 years old, having elevated preoperative parathormone (PTH) level (>65 pg/ml), and finally diagnosed with PC (based on postoperative histopathology). Literature related to SaPC was obtained by manual searches. Only publications in English were considered. The date of the last retrieval was September 18, 2021, and literature was reviewed independently by two authors. For all enrolled cases, we reviewed age, gender, preoperative total serum calcium level, preoperative PTH, and tumor size (the greatest diameter) for further analysis. Prognostic information is also reviewed in SaPC cases. SPSS software 23.0 is used for statistical analyses, and GraphPad Prism 8.0 software is used for data plotting. Data are expressed as mean ± SD. Two-tailed independent samples t-test is used for evaluating statistical differences; $p < 0.05$ is considered significant (*), and $p < 0.01$ is considered extremely significant (**).

## RESULTS

### Case Presentation

A 60-year-old woman was admitted with a continuously enlarged neck mass for 1 year and hoarseness for 1 week. In addition, she presented with dyspnea for 5 months. The patient had no family history of parathyroid diseases or hyperparathyroidism-jaw tumor syndrome. Physical examination showed a firm left neck mass of approximately 6.0 cm * 5.0 cm. Laboratory findings revealed elevated serum PTH (188.1 pg/ml, reference range: 15–65 pg/ml) and hypercalcemia (total serum calcium: 3.29 mmol/L, reference range: 2.1–2.6 mmol/L). Indicators related to thyroid function were within normal limits. Laryngoscopy showed left vocal cord paralysis. Ultrasonography showed that the left thyroid lobe was enlarged significantly, a hypoechoic lesion nearly occupied the whole lobe, and comparable signs were presented on the neck CT (**Figure 1A**). Tc-99m sestamibi scintigraphy demonstrated two-phase nuclide accumulation on the left thyroid (**Figure 1B**). Chest CT showed multiple micro pulmonary nodules (**Figure 1C**).

During the surgical exploration, we found that the tumor invaded the anterior cervical muscle group and left recurrent laryngeal nerve. Only the superior parathyroid was found in the left neck. *En bloc* resection (including part of the invaded recurrent laryngeal nerve and muscle tissue and entire thyroid) and left central lymph node dissection were performed to completely remove the affected tissue. The tumor profile showed that the thyroid was markedly infiltrated, and the normal gland was almost invisible (**Figure 1D**). Postoperative histopathological findings revealed that SaPC widely invaded the ipsilateral thyroid, and 1/6 of the lymph nodes showed metastasis. Immunohistochemical staining was further performed to confirm the diagnosis (**Figure 2**); results were presented below: (1) Carcinomatous components: Some PC cells show negative nuclear staining of parafibromin (**Figure 2A**); Cytokeratin (AE1/AE3) (+); Chromogranin A (+); E-Cadherin

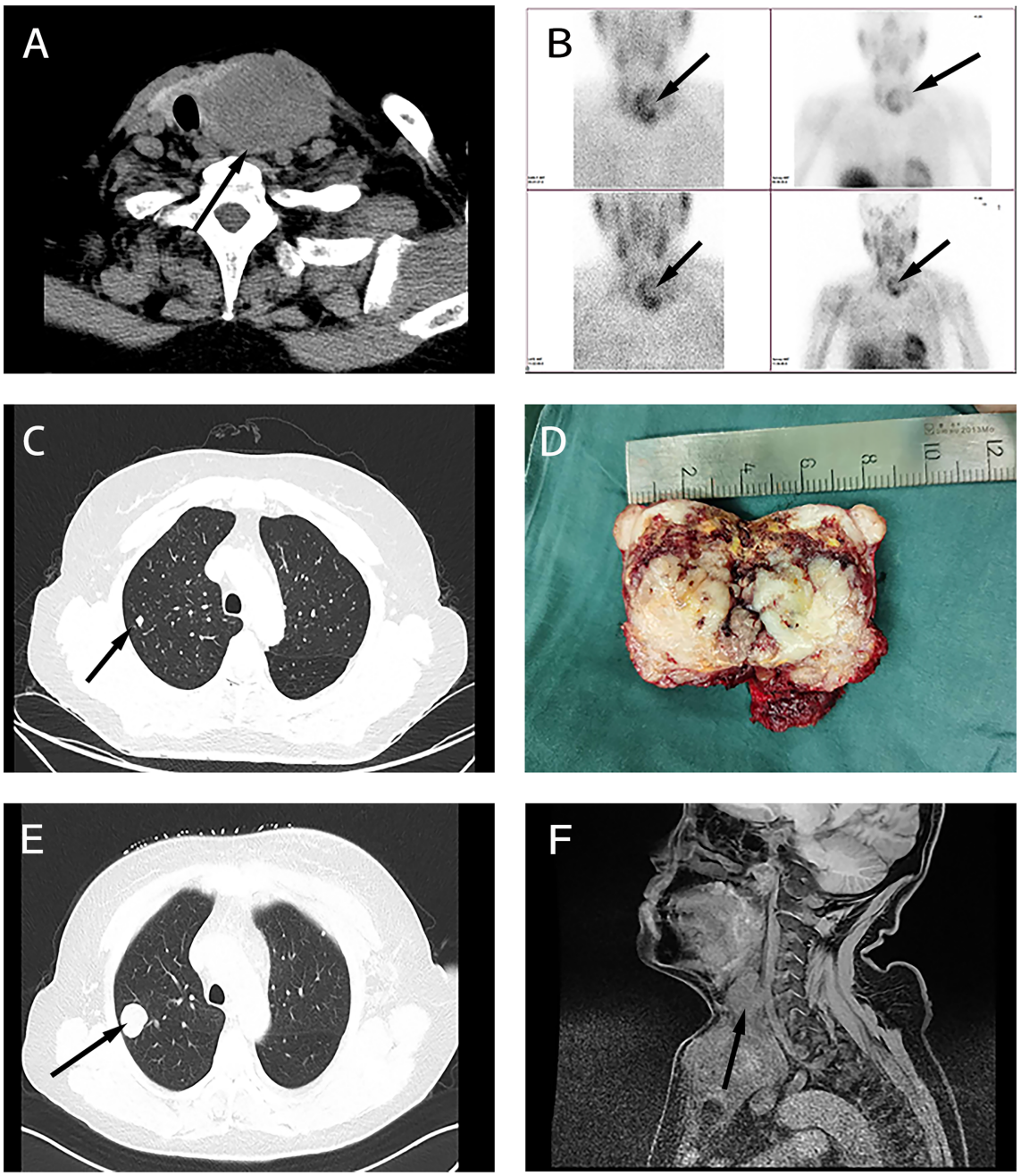


**FIGURE 1** | Clinical characteristics of the sarcomatoid parathyroid carcinoma (SaPC) case. **(A)** Neck CT showed the giant tumor. **(B)** Tc-99m sestamibi scintigraphy suggests abnormal nuclide uptake in the left thyroid. **(C)** Chest CT presented micro pulmonary nodule before surgery. **(D)** The profile of the resected tumor. **(E)** Chest CT shows pulmonary metastasis at the closely located position in preoperative chest CT **(C)**. **(F)** Enhanced MRI showed extensive local organ and tissue invasion.

(+); PTH (+); Calcitonin (–); Thyroglobulin (-); Desmin (-); KI-67 index 10%; (2) Spindle cell components: Desmin (+; **Figure 2B**); Cytokeratin (AE1/AE3) (-); Chromogranin A (-); E-Cadherin (-); Calcitonin (-); KI-67 index 30%. In addition, the existence of transition zones (**Figure 2C**) and positive N-cad staining in both carcinomatous and sarcomatoid components (**Figure 2D**) was found during pathological examination.

The patient recovered soon postoperatively and remained hoarse. She did not experience choking when drinking water, and dyspnea significantly improved. Three months later, the patient complained of progressively aggravating dyspnea and a gradually growing neck mass. Serum calcium and PTH levels were without abnormal elevation during this time (**Figure S1**). Clinical examinations suggested regional relapse and multiple

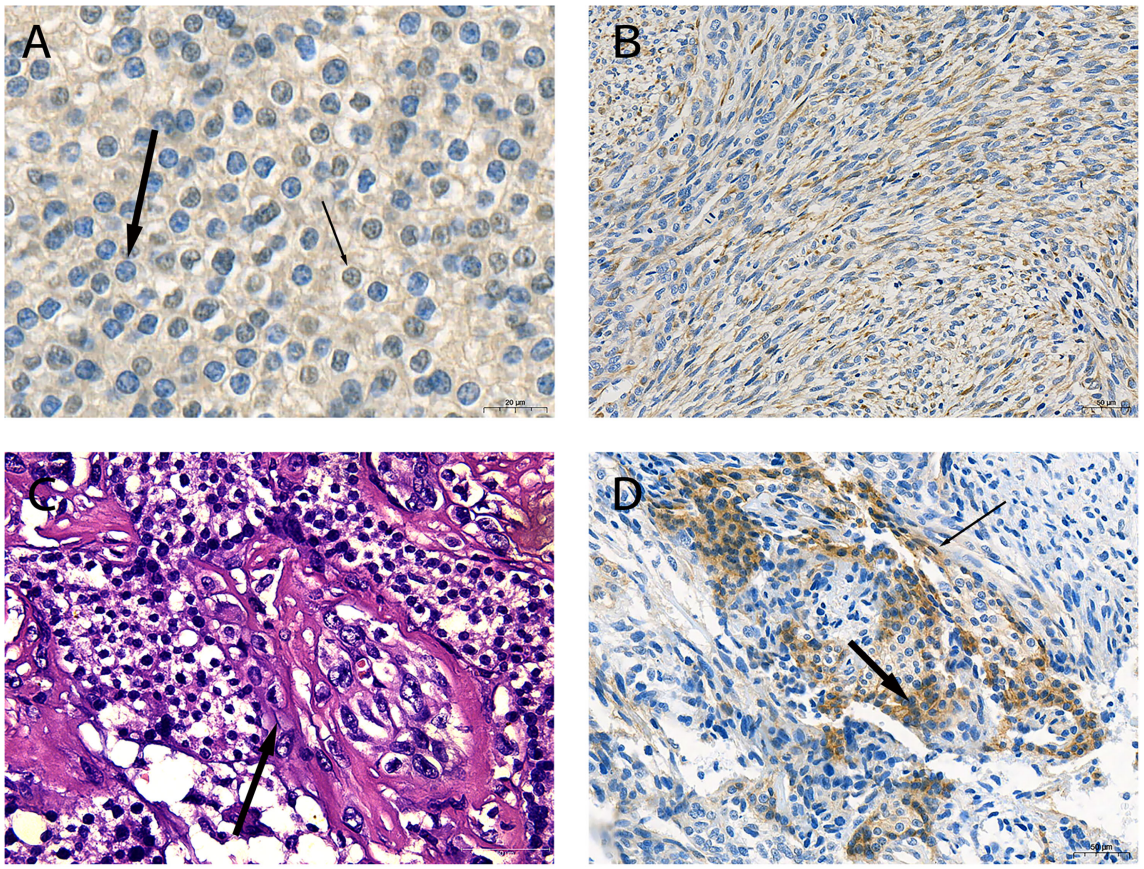


**FIGURE 2** | Pathological characteristics of the sarcomatoid parathyroid carcinoma (SaPC) case. **(A)** Negative staining of parafibromin in the nucleus (thick arrow) and contrast-positive staining (thin arrow) of parathyroid carcinoma (PC) cells (×630). **(B)** Spindle cells shuttled through carcinomatous component regions showed positive desmin staining (×200). **(C)** The morphology of cell changes between two component regions (arrow) (H&E, ×400). **(D)** N-cad was positive in carcinomatous (thick arrow) and spindle cell components (thin arrow) (×200).

pulmonary metastases (**Figure 1E**). In contrast to the chest CT before, it seemed that pulmonary metastasis had occurred before the first surgery. Enhanced MRI showed extensive local organ and tissue invasion by the recurred tumor (**Figure 1F**). At last, the patient gave up the medical treatments.

## Systematic Review

Together with the reported cases, four cases of SaPC (male: female = 1:1, three cases from literature) and 203 cases of general PC (male:female = 0.85:1, 200 cases from literature) were included in this study. The process of the assessment of literature related to general PC was shown in the PRISMA flowchart (**Figure 3**). The details of all four SaPC cases are present in **Table 1**. A total of 197 PTH results, 169 total serum calcium results and 189 tumor size results of general PC cases are reviewed, which are presented in the online supplementary material [**Table S1** (12–47)]. Overall, both SaPC and general PC cases showed abnormal PTH levels and gland size. Compared with general PC, SaPC presented a later age of onset (60.50 ± 7.42 vs. 51.50 ± 8.29, p = 0.032*), lower levels of PTH (110.28 ± 59.32 vs. 1,156.07 ± 858.18, p = 0.016*), and larger tumor size (6.00 ± 1.63 vs. 3.14 ± 0.70, p = 0.039*). Besides, SaPC also shows a lower serum calcium level (2.70 ± 0.42 vs. 3.41 ± 0.91), but it is not significant (p = 0.120) due to small samples. For SaPC cases (**Table 1**), all four cases were initially suspected as thyroid tumors (4/4), three of four patients showed hoarseness (3/4), and two of four patients showed a neck mass (2/4). Spindle cell areas or transitional zones are common pathological features in SaPC cases (3/4).

## DISCUSSION

PC is a rare malignancy in the endocrine system (48). The prevalence of PC in the USA is approximately 30 cases per year (49). For most patients, uncontrolled hypercalcemia is the main cause of death (50). SaPC is a rare and special subtype of PC, and only three cases have been reported internationally. Tumor invasion and metastasis seem to be associated with a patient's death in SaPC.

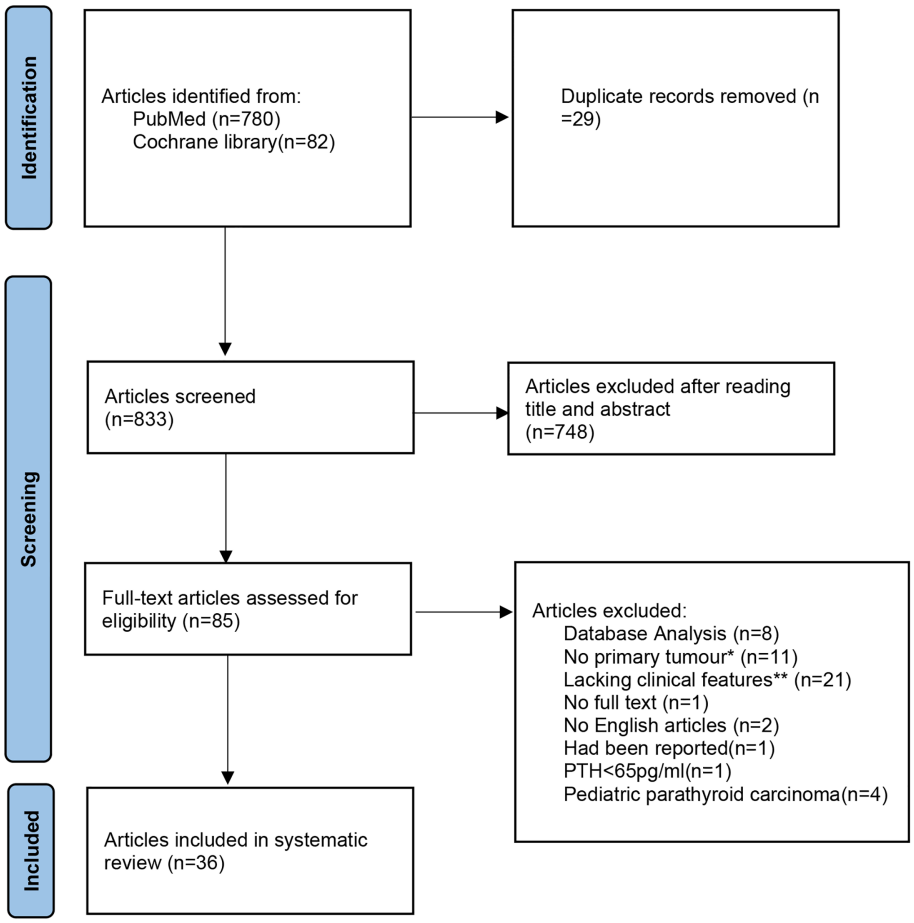


**FIGURE 3** | The detailed literature search process presented in a Preferred Reporting Items for Systematic reviews and Meta-Analyses (PRISMA) flowchart. *No primary tumours: secondary to other parathyroid diseases or not identified as parathyroid cancer in the initial surgery. **Lacking clinical features: Articles which lacking more than two study elements in the systematic review (age, gender, preoperative PTH, preoperative total serum calcium or tumour size.

Collectively, it is difficult to do the differentiation diagnosis of PC before surgery—how to distinguish malignant from benign, or how to distinguish PC from thyroid tumors, especially in non-functional PC (51) and SaPC. In recent years, the medical circle has made a breakthrough in the management of thyroid cancer, especially with the publication of the 2015 American Thyroid Association (ATA) guidelines (52) in the year 2016. According to the 2015 ATA guidelines, all patients suspected of thyroid cancer need assessment of parathyroid function. Thus, more atypical PC can be found, just like our case. Simultaneously, more cases and clinical experience of PC have been accumulated in recent years. Recognition of parathyroid carcinoma has been enlarged and deepened than any before. Well-recognized clinical manifestations of PC include extremely elevated serum calcium levels and serum PTH levels and a prominent neck mass (53). The significantly increased level of serum alkaline phosphatase has a predictive value for PC (54). Owing to the unclear cytologic atypia between benign and malignant parathyroid tumors, fine-needle aspiration (FNA) results do not diagnose the disease preoperatively instead of increasing the risk of needle tract metastasis (40). Therefore, unlike the thyroid cancer (52), FNA is not applicable when parathyroid diseases are suspected. Imaging examination is routinely used to localize the abnormal parathyroid gland. Ultrasonography and CT are common preoperative examinations before surgery. Methoxy Isobutyl Isonitrile (MIBI) scan is effective in differentiating parathyroid and thyroid tumors when high PTH levels are found in patients. It can also distinguish PC from benign parathyroid diseases by differences in the retention level of 99mTc-MIBI (55). In our study, MIBI scan showed that a large range of abnormal uptake occurred on the left thyroid (**Figure 1B**); this might be a useful adjunct to reveal evidence of invasion when PC is suspected. Definitive diagnosis of PC is restricted to histological findings, which contain observable vascular or peripheral nerve invasion, penetration of the capsule, and infiltration of surrounding tissues (56). Currently, it is believed that parafibromin (encoded by CDC73/HRPT2) is a significant immunohistochemical marker, and there is evidence that its negative expression in parathyroid

**TABLE 1** | Basic clinical data of SaPC cases in our center and literature.

| References | | | Basic information | | | | Laboratory findings | | Tumor basic characteristics | | | Surgery | Postoperative therapy | | Prognosis | | |
|---|---|---|---|---|---|---|---|---|---|---|---|---|---|---|---|---|---|
| Number | Author | Publication date | Sex | Age | Clinical features | Primary diagnosis | PTH (pg/ml) | Ca (mmol/L) | Pathological features | Tumor size (cm) | Local invasion | | Radiation therapy | Chemo-therapy | Local recurrence | Metastasis | Survival (after the surgery) |
| No. 1 | Our case | 2021 | Female | 60 | Left neck mass; hoarseness | Thyroid cancer | 188.1 | 3.29 | transitional zone; spindle cell component | 6.00 | Yes | En bloc resection, left central lymph node dissection | No | No | Yes | Yes | Alive at 6 months |
| No. 2 | Nacamuli (6) | 2002 | Male | 54 | Left neck mass | Lymphocytic thyroiditis | 117 | 2.7 | transitional zone | 8.00 | No | En bloc resection | No | Yes | No | Yes | Dead at 7 months |
| No. 3 | Taggart (7) | 2013 | Female | 57 | Left neck mass; hoarseness | Thyroid cancer | 47 | 2.45 | spindle cell component | 4.00 | Yes | En bloc resection; cervical lymph node | Yes | Yes | No | Yes | Unknown |
| No.4 | Hu (8) | 2020 | Male | 71 | hoarseness | Thyroid cancer | 89 | 2.34 | necrosis | 6.00 | Yes | palliative resection | No | No | Yes | Yes | Dead at 6 months |

*PTH, parathormone; SaPC, sarcomatoid parathyroid carcinoma.*

cells indicates PC (57). Similarly, invasion and negative staining of parafibromin (**Figure 2A**) can be seen in SaPC cases. Recent studies showed that germline CDC73 mutation is closely related to HPT-JT syndrome and other variant phenotypes of sporadic PC (58, 59). There might be a connection between germline CDC73 mutation and SaPC. Unfortunately, we did not conserve the blood sample for the gene test. And the patient was lost to follow-up from December 2020. This is the limitation of this work, and more studies are needed to pursue this connection.

Interestingly, there are some differences in manifestations between SaPC and general PC. Firstly, the endocrine feature of SaPC is less distinct—although the PTH level is higher than normal, it is about one-tenth of general PC, which may be related to functional carcinomatous regions replaced by non-functional sarcomatoid regions at different levels. Moreover, all four cases of SaPC were suspected as thyroid tumors before surgery, which might be associated with the anatomical location and tumor invasiveness, but more cases are needed for validation. Notable signs, such as hoarseness and a larger tumor size, are common in this subtype, which might be an embodiment of the fast disease progression. Pathologically, the diagnosis of SaPC also includes the presence of mesenchymal cell areas and corresponding immunohistochemical markers. Specific spindle cell regions or transitional zones can also be observed in reported cases and our case of SaPC (**Table 1; Figures 2B, C**), which might be potential histomorphological characteristics of this subtype. In addition, the positive staining of N-cad in both components (**Figure 2D**) and the appearance of transitional zones seem to support the hypothesis of EMT. Combined with our case (**Figure 2B**), sarcomatoid regions showed a positive expression of different mesenchymal tissue markers (desmin or vimentin), indicating that the direction of sarcomatoid differentiation in PC may be different between individuals.

Presently, surgery is the overriding therapeutic modality for PC patients (12, 20, 60). Margin status in the initial surgery is crucial to the prognosis (61), and early salvage surgery can still achieve reasonably good therapeutic efficacy (19). *En bloc* resection with ipsilateral thyroid lobectomy and ipsilateral central lymph node dissection seems to be an appropriate surgical approach (62). However, a study suggested that resection of the ipsilateral thyroid cannot prolong survival (63). Thus, in-depth studies on the extent of resection are needed.

Nevertheless, the effect and extent of surgery in SaPC require further study. In our case (No. 1, **Table 1**), we performed the radical surgical procedure, and dyspnea improved temporarily, but tumor recurrence occurred 3 months later. Combined with reported cases, SaPC showed early recurrence after radical surgery. Surgical treatments in SaPC indeed achieve improvements in clinical symptoms, but recurrence and death occurred about 6 months later. In general, surgery for SaPC does relieve tumor compression, correct hypercalcemia, and improve quality of life even with recurrence in the short term.

According to the literature, radiotherapy and chemotherapy after surgery for general PC are ineffective (64, 65). The result shows no difference in SaPC with these treatments—the first two

patients received postoperative chemotherapy but relapsed in months. In terms of sarcomatoid carcinoma in other organs such as kidney (66) and lung (67), they show the similar clinicopathological characteristics as SaPC, and targeted therapy has been confirmed to be potentially beneficial. This may be the future direction of treatment for SaPC.

Due to the rarity of the disease, there are currently no well-accepted staging criteria for PC. Patients who receive radical resection often have a favorable outcome, with a 5-year survival of up to 82.3% and 66% in 10 years (68). In our center, all four patients with typical PC received radical surgery, and none experienced recurrence (follow-up period was between 15 and 66 months; data not shown). However, SaPC was highly aggressive, with postoperative recurrence and early systemic metastases in all four patients (**Table 1**), which led to the patient's death in a short time—two of the four patients with SaPC died within 7 months. We noticed that a longer period of the systematic review might benefit the research, which is a limitation of this work. We will continue to concern relative research henceforth.

## CONCLUSION

SaPC is a highly unusual subtype of PC, and patients eventually succumb to direct tumor invasion and metastasis, while general PC has a good prognosis after radical surgery. Patients with SaPC seem to be easily misdiagnosed as thyroid tumors. Spindle cell areas or transitional zones are likely to be pathological features of SaPC. Despite many similarities, there are also some differences between SaPC and general PC—SaPC does not present a significant endocrinological feature but presents more aggressiveness. Surgery in SaPC cases indeed improves severe symptoms and quality of life even in patients experiencing a relapse in the short term, and other effective treatments are needed to explore.

## DATA AVAILABILITY STATEMENT

The original contributions presented in the study are included in the article/**Supplementary Material**. Further inquiries can be directed to the corresponding authors.

## ETHICS STATEMENT

The studies involving human participants were reviewed and approved by the Ethics Committee of the Second Hospital of Dalian Medical University. The patients/participants provided their written informed consent to participate in this study.

## AUTHOR CONTRIBUTIONS

YY designed the study. YY, YW, QW, and XZ reviewed the literature and collected data. DL, GW, JX, and JC analyzed data and assessed the accuracy of results. YY wrote the first paper draft of the article. YL and YZ provided assistance during the writing process. XT and NZ reviewed and edited the article. All authors contributed to the article and approved the submitted version.

## FUNDING

This study was supported by the Scientific Research Fund of Liaoning Provincial Education Department, China (grant no. LZ2019057).

## SUPPLEMENTARY MATERIAL

The Supplementary Material for this article can be found online at: https://www.frontiersin.org/articles/10.3389/fendo.2021.793718/full#supplementary-material

## REFERENCES

1. Lee PK, Jarosek SL, Virnig BA, Evasovich M, Tuttle TM. Trends in the Incidence and Treatment of Parathyroid Cancer in the United States. *Cancer* (2007) 109(9):1736–41. doi: 10.1002/cncr.22599
2. Quaglino F, Manfrino L, Cestino L, Giusti M, Mazza E, Piovesan A, et al. Parathyroid Carcinoma: An Up-To-Date Retrospective Multicentric Analysis. *Int J Endocrinol* (2020) 2020:7048185. doi: 10.1155/2020/7048185
3. Wei CH, Harari A. Parathyroid Carcinoma: Update and Guidelines for Management. *Curr Treat Options Oncol* (2012) 13(1):11–23. doi: 10.1007/s11864-011-0171-3
4. Shane E. Clinical Review 122: Parathyroid Carcinoma. *J Clin Endocrinol Metab* (2001) 86(2):485–93. doi: 10.1210/jcem.86.2.7207
5. Rubello D, Casara D, Dwamena BA, Shapiro B. Parathyroid Carcinoma. A Concise Review. *Minerva Endocrinol* (2001) 26(2):59–64.
6. Nacamuli R, Rumore GJ, Clark G. Parathyroid Carcinosarcoma: A Previously Unreported Entity. *Am Surg* (2002) 68(10):900–3.
7. Taggart JL, Summerlin DJ, Moore MG. Parathyroid Carcinosarcoma: A Rare Form of Parathyroid Carcinoma With Normal Parathyroid Hormone Levels. *Int J Surg Pathol* (2013) 21(4):394–8. doi: 10.1177/1066896913480830
8. Hu L, Xie X. Parathyroid Carcinoma With Sarcomatoid Differentiation: A Case Report and Literature Review. *Diagn Pathol* (2020) 15(1):142. doi: 10.1186/s13000-020-01060-5
9. Pang A, Carbini M, Moreira AL, Maki RG. Carcinosarcomas and Related Cancers: Tumors Caught in the Act of Epithelial-Mesenchymal Transition. *J Clin Oncol* (2018) 36(2):210–6. doi: 10.1200/jco.2017.74.9523
10. McCluggage WG. Malignant Biphasic Uterine Tumours: Carcinosarcomas or Metaplastic Carcinomas? *J Clin Pathol* (2002) 55(5):321–5. doi: 10.1136/jcp.55.5.321
11. Page MJ, McKenzie JE, Bossuyt PM, Boutron I, Hoffmann TC, Mulrow CD, et al. The PRISMA 2020 Statement: An Updated Guideline for Reporting Systematic Reviews. *Bmj* (2021) 372:n71. doi: 10.1136/bmj.n71
12. Ferraro V, Sgaramella LI, Di Meo G, Prete FP, Logoluso F, Minerva F, et al. Current Concepts in Parathyroid Carcinoma: A Single Centre Experience. *BMC Endocr Disord* (2019) 19(Suppl 1):46. doi: 10.1186/s12902-019-0368-1
13. Campennì A, Giovinazzo S, Pignata SA, Di Mauro F, Santoro D, Curtò L, et al. Association of Parathyroid Carcinoma and Thyroid Disorders: A Clinical Review. *Endocrine* (2017) 56(1):19–26. doi: 10.1007/s12020-016-1147-7
14. Takenobu M, Moritani S, Kawamoto K, Yoshioka K, Kitano H. Parathyroid Carcinoma Coexisting With Multiple Parathyroid Adenomas: A Case Report. *Endocr J* (2020) 67(9):963–7. doi: 10.1507/endocrj.EJ20-0139
15. Xin Y, Zhao T, Wei B, Gu H, Jin M, Shen H, et al. Intrapericardial Parathyroid Carcinoma: A Case Report. *Endocrine* (2020) 69(2):456–60. doi: 10.1007/s12020-020-02283-8

16. Vodopivec DM, Thomas DD, Palermo NE, Steenkamp DW, Lee SL. Looking for the Outsider. *N Engl J Med* (2020) 383(23):2275–81. doi: 10.1056/NEJMcps2004935
17. Medas F, Erdas E, Loi G, Podda F, Pisano G, Nicolosi A, et al. Controversies in the Management of Parathyroid Carcinoma: A Case Series and Review of the Literature. *Int J Surg* (2016) 28 Suppl 1:S94–8. doi: 10.1016/j.ijsu.2015.12.040
18. Tkachenko R, Zakhartseva L, Golovko A, Kuryk O, Lazarenko G. Parathyroid Carcinoma: A Case Report. *Exp Oncol* (2019) 41(1):72–5. doi: 10.32471/exp-oncology.2312-8852.vol-41-no-1.12775
19. Xue S, Chen H, Lv C, Shen X, Ding J, Liu J, et al. Preoperative Diagnosis and Prognosis in 40 Parathyroid Carcinoma Patients. *Clin Endocrinol (Oxf)* (2016) 85(1):29–36. doi: 10.1111/cen.13055
20. Ryhänen EM, Leijon H, Metso S, Eloranta E, Korsoff P, Ahtiainen P, et al. A Nationwide Study on Parathyroid Carcinoma. *Acta Oncol* (2017) 56(7):991–1003. doi: 10.1080/0284186x.2017.1306103
21. Libánský P, Adámek S, Broulík P, Fialová M, Kubinyi J, Lischke R, et al. Parathyroid Carcinoma in Patients That Have Undergone Surgery for Primary Hyperparathyroidism. *In Vivo* (2017) 31(5):925–30. doi: 10.21873/invivo.11148
22. Gao Y, Yu C, Xiang F, Xie M, Fang L. Acute Pancreatitis as an Initial Manifestation of Parathyroid Carcinoma: A Case Report and Literature Review. *Med (Baltimore)* (2017) 96(44):e8420. doi: 10.1097/md.0000000000008420
23. Shruti S, Siraj F. Parathyroid Carcinoma: An Unusual Presentation of a Rare Neoplasm. *Ger Med Sci* (2017) 15:Doc21. doi: 10.3205/000262
24. Dikmen K, Bostanci H, Gobut H, Yildiz A, Ertunc O, Celik A, et al. Nonfunctional Double Parathyroid Carcinoma With Incidental Thyroid Micropapillary Carcinoma: A Rare Case. *Pan Afr Med J* (2017) 27:241. doi: 10.11604/pamj.2017.27.241.11503
25. Liu R, Xia Y, Chen C, Ye T, Huang X, Ma L, et al. Ultrasound Combined With Biochemical Parameters Can Predict Parathyroid Carcinoma in Patients With Primary Hyperparathyroidism. *Endocrine* (2019) 66(3):673–81. doi: 10.1007/s12020-019-02069-7
26. Shah R, Gosavi V, Mahajan A, Sonawane S, Hira P, Kurki V, et al. Preoperative Prediction of Parathyroid Carcinoma in an Asian Indian Cohort. *Head Neck* (2021) 43(7):2069–80. doi: 10.1002/hed.26677
27. Triggiani V, Castellana M, Basile P, Renzulli G, Giagulli VA. Parathyroid Carcinoma Causing Mild Hyperparathyroidism in Neurofibromatosis Type 1: A Case Report and Systematic Review. *Endocr Metab Immune Disord Drug Targets* (2019) 19(3):382–8. doi: 10.2174/1871530318666180910123316
28. Sadacharan D, Mahadevan S, Ferdinant J, Rakeshchandru K. Hypercalcaemic Encephalopathy Due to Metastatic Parathyroid Carcinoma. *BMJ Case Rep* (2017) 2017. doi: 10.1136/bcr-2017-219664
29. Rizwan A, Jamal A, Uzzaman M, Fatima S. Case Report: Lady With Bone Pains for 5 Years-Parathyroid Carcinoma. *BMC Res Notes* (2018) 11(1):617. doi: 10.1186/s13104-018-3711-0
30. Takumi K, Fukukura Y, Hakamada H, Nagano H, Kumagae Y, Arima H, et al. CT Features of Parathyroid Carcinomas: Comparison With Benign Parathyroid Lesions. *Jpn J Radiol* (2019) 37(5):380–9. doi: 10.1007/s11604-019-00825-3
31. Baek CO, Kim KH, Song SK. Synchronous Parathyroid Carcinoma and Papillary Thyroid Carcinoma in a Patient With Long-Standing Schizophrenia. *Korean J Intern Med* (2017) 32(6):1104–7. doi: 10.3904/kjim.2015.072
32. Agarwal S, Kumar T, Sharma MC, Damle NA, Gandhi AK. Parathyroid Carcinoma With Contralateral Subcutaneous and Breast Recurrences: A Rare Presentation. *Head Neck* (2016) 38(5):E115–8. doi: 10.1002/hed.24317
33. Kapur A, Singh N, Mete O, Hegele RA, Fantus IG. A Young Male With Parafibromin-Deficient Parathyroid Carcinoma Due to a Rare Germline HRPT2/CDC73 Mutation. *Endocr Pathol* (2018) 29(4):374–9. doi: 10.1007/s12022-018-9552-5
34. Shahid A, Iftikhar F. Pathological Bone Fractures in a Patient With Parathyroid Carcinoma - A Case Report. *J Pak Med Assoc* (2017) 67(12):1956–8.
35. Singh P, Vadi SK, Saikia UN, Sood A, Dahiya D, Arya AK, et al. Minimally Invasive Parathyroid Carcinoma-A Missing Entity Between Parathyroid Adenoma and Carcinoma: Scintigraphic and Histological Features. *Clin Endocrinol (Oxf)* (2019) 91(6):842–50. doi: 10.1111/cen.14088
36. Morand GB, Helmchen BM, Steinert HC, Schmid C, Broglie MA. 18f-Choline-PET in Parathyroid Carcinoma. *Oral Oncol* (2018) 86:314–5. doi: 10.1016/j.oraloncology.2018.09.009
37. Mahajan G, Sacerdote A. Previously Unreported Deletion of CDC73 Involving Exons 1-13 was Detected in a Patient With Recurrent Parathyroid Carcinoma. *BMJ Case Rep* (2018) 11(1):e225784. doi: 10.1136/bcr-2018-225784
38. Chen Z, Fu J, Shao Q, Zhou B, Wang F. 99mtc-MIBI Single Photon Emission Computed Tomography/Computed Tomography for the Incidental Detection of Rare Parathyroid Carcinoma. *Med (Baltimore)* (2018) 97(40):e12578. doi: 10.1097/md.0000000000012578
39. Dagang DJ, Gutierrez JB, Sandoval MA, Lantion-Ang FL. Multiple Brown Tumours From Parathyroid Carcinoma. *BMJ Case Rep* (2016) 2016. doi: 10.1136/bcr-2016-215961
40. Song A, Yang Y, Liu S, Nie M, Jiang Y, Li M, et al. Prevalence of Parathyroid Carcinoma and Atypical Parathyroid Neoplasms in 153 Patients With Multiple Endocrine Neoplasia Type 1: Case Series and Literature Review. *Front Endocrinol (Lausanne)* (2020) 11:557050. doi: 10.3389/fendo.2020.557050
41. Tarbunova M, Trimaldi J, Saremian J. A Case of Parathyroid Carcinoma Accompanied by a Brown Tumor. *Diagn Cytopathol* (2016) 44(8):685–7. doi: 10.1002/dc.23511
42. Balakrishnan M, George SA, Rajab SH, Francis IM, Kapila K. Cytological Challenges in the Diagnosis of Intrathyroidal Parathyroid Carcinoma: A Case Report and Review of Literature. *Diagn Cytopathol* (2018) 46(1):47–52. doi: 10.1002/dc.23847
43. Kawagishi S, Funaki S, Ose N, Kimura K, Mukai K, Otsuki M, et al. Debulking Surgery for Functional Pleural Dissemination of Parathyroid Carcinoma-Case Report. *J Cardiothorac Surg* (2021) 16(1):86. doi: 10.1186/s13019-021-01477-z
44. Russo M, Borzì G, Ilenia M, Frasca F, Malandrino P, Gullo D. Challenges in the Treatment of Parathyroid Carcinoma: A Case Report. *Hormones (Athens)* (2019) 18(3):325–8. doi: 10.1007/s42000-019-00104-w
45. do Vale RH, Queiroz MA, Coutinho AM, Buchpiguel CA, de Menezes MR. 18f-FDG PET/CT Osteometabolic Activity in Metastatic Parathyroid Carcinoma. *Clin Nucl Med* (2016) 41(9):724–5. doi: 10.1097/rlu.0000000000001278
46. Omi Y, Horiuchi K, Haniu K, Tokura M, Nagai E, Isozaki O, et al. Parathyroid Carcinoma Occurred in Two Glands in Multiple Endocrine Neoplasia 1: A Report on a Rare Case. *Endocr J* (2018) 65(2):245–52. doi: 10.1507/endocrj.EJ17-0409
47. Çalapkulu M, Sencar ME, Unsal IO, Sakiz D, Duger H, Özbek M, et al. Tumor Volume Can Be Used as a Parameter Indicating the Severity of Disease in Parathyroid Cancer. *Endocr Pract* (2021) 27(7):706–9. doi: 10.1016/j.eprac.2021.01.006
48. Cetani F, Pardi E, Marcocci C. Parathyroid Carcinoma. *Front Horm Res* (2019) 51:63–76. doi: 10.1159/000491039
49. Dudney WC, Bodenner D, Stack BCJr. Parathyroid Carcinoma. *Otolaryngol Clin North Am* (2010) 43(2):441–53, xi. doi: 10.1016/j.otc.2010.01.011
50. Salcuni AS, Cetani F, Guarnieri V, Nicastro V, Romagnoli E, de Martino D, et al. Parathyroid Carcinoma. *Best Pract Res Clin Endocrinol Metab* (2018) 32(6):877–89. doi: 10.1016/j.beem.2018.11.002
51. Wang L, Han D, Chen W, Zhang S, Wang Z, Li K, et al. Non-Functional Parathyroid Carcinoma: A Case Report and Review of the Literature. *Cancer Biol Ther* (2015) 16(11):1569–76. doi: 10.1080/15384047.2015.1070989
52. Haugen BR, Alexander EK, Bible KC, Doherty GM, Mandel SJ, Nikiforov YE, et al. American Thyroid Association Management Guidelines for Adult Patients With Thyroid Nodules and Differentiated Thyroid Cancer: The American Thyroid Association Guidelines Task Force on Thyroid Nodules and Differentiated Thyroid Cancer. *Thyroid* (2016) 26(1):1–133. doi: 10.1089/thy.2015.0020
53. Givi B, Shah JP. Parathyroid Carcinoma. *Clin Oncol (R Coll Radiol)* (2010) 22(6):498–507. doi: 10.1016/j.clon.2010.04.007
54. Bae JH, Choi HJ, Lee Y, Moon MK, Park YJ, Shin CS, et al. Preoperative Predictive Factors for Parathyroid Carcinoma in Patients With Primary Hyperparathyroidism. *J Korean Med Sci* (2012) 27(8):890–5. doi: 10.3346/jkms.2012.27.8.890
55. Zhang M, Sun L, Rui W, Guo R, He H, Miao Y, et al. Semi-Quantitative Analysis of (99m)Tc-Sestamibi Retention Level for Preoperative Differential

Diagnosis of Parathyroid Carcinoma. *Quant Imaging Med Surg* (2019) 9 (8):1394–401. doi: 10.21037/qims.2019.07.02
56. Schulte KM, Talat N. Diagnosis and Management of Parathyroid Cancer. *Nat Rev Endocrinol* (2012) 8(10):612–22. doi: 10.1038/nrendo.2012.102
57. Erickson LA, Mete O. Immunohistochemistry in Diagnostic Parathyroid Pathology. *Endocr Pathol* (2018) 29(2):113–29. doi: 10.1007/s12022-018-9527-6
58. Shattuck TM, Välimäki S, Obara T, Gaz RD, Clark OH, Shoback D, et al. Somatic and Germ-Line Mutations of the HRPT2 Gene in Sporadic Parathyroid Carcinoma. *N Engl J Med* (2003) 349(18):1722–9. doi: 10.1056/NEJMoa031237
59. Chiofalo MG, Sparaneo A, Chetta M, Franco R, Baorda F, Cinque L, et al. A Novel CDC73 Gene Mutation in an Italian Family With Hyperparathyroidism-Jaw Tumour (HPT-JT) Syndrome. *Cell Oncol (Dordr)* (2014) 37(4):281–8. doi: 10.1007/s13402-014-0187-3
60. Rodrigo JP, Hernandez-Prera JC, Randolph GW, Zafereo ME, Hartl DM, Silver CE, et al. Parathyroid Cancer: An Update. *Cancer Treat Rev* (2020) 86:102012. doi: 10.1016/j.ctrv.2020.102012
61. McClenaghan F, Qureshi YA. Parathyroid Cancer. *Gland Surg* (2015) 4 (4):329–38. doi: 10.3978/j.issn.2227-684X.2015.05.09
62. Schulte KM, Talat N, Galata G, Gilbert J, Miell J, Hofbauer LC, et al. Oncologic Resection Achieving R0 Margins Improves Disease-Free Survival in Parathyroid Cancer. *Ann Surg Oncol* (2014) 21(6):1891–7. doi: 10.1245/s10434-014-3530-z
63. Zhou L, Huang Y, Zeng W, Chen S, Zhou W, Wang M, et al. Surgical Disparities of Parathyroid Carcinoma: Long-Term Outcomes and Deep Excavation Based on a Large Database. *J Oncol* (2021) 2021:8898926. doi: 10.1155/2021/8898926
64. Limberg J, Stefanova D, Ullmann TM, Thiesmeyer JW, Bains S, Beninato T, et al. The Use and Benefit of Adjuvant Radiotherapy in Parathyroid Carcinoma: A National Cancer Database Analysis. *Ann Surg Oncol* (2021) 28(1):502–11. doi: 10.1245/s10434-020-08825-8
65. Sharretts JM, Kebebew E, Simonds WF. Parathyroid Cancer. *Semin Oncol* (2010) 37(6):580–90. doi: 10.1053/j.seminoncol.2010.10.013
66. Pichler R, Compérat E, Klatte T, Pichler M, Loidl W, Lusuardi L, et al. Renal Cell Carcinoma With Sarcomatoid Features: Finally New Therapeutic Hope? *Cancers (Basel)* (2019) 11(3):422. doi: 10.3390/cancers11030422
67. Li X, Wu D, Liu H, Chen J. Pulmonary Sarcomatoid Carcinoma: Progress, Treatment and Expectations. *Ther Adv Med Oncol* (2020) 12:17588359 20950207. doi: 10.1177/1758835920950207
68. Asare EA, Sturgeon C, Winchester DJ, Liu L, Palis B, Perrier ND, et al. Parathyroid Carcinoma: An Update on Treatment Outcomes and Prognostic Factors From the National Cancer Data Base (NCDB). *Ann Surg Oncol* (2015) 22(12):3990–5. doi: 10.1245/s10434-015-4672-3

**Conflict of Interest:** The authors declare that the research was conducted in the absence of any commercial or financial relationships that could be construed as a potential conflict of interest.

**Publisher's Note:** All claims expressed in this article are solely those of the authors and do not necessarily represent those of their affiliated organizations, or those of the publisher, the editors and the reviewers. Any product that may be evaluated in this article, or claim that may be made by its manufacturer, is not guaranteed or endorsed by the publisher.

frontiers in Endocrinology

CASE REPORT
published: 21 December 2021
doi: 10.3389/fendo.2021.784889

# A Silent Corticotroph Pituitary Carcinoma: Lessons From an Exceptional Case Report

*Pablo Remón-Ruiz[1]*, Eva Venegas-Moreno[1], Elena Dios-Fuentes[1], Juan Manuel Canelo Moreno[1], Ignacio Fernandez Peña[2], Miriam Alonso Garcia[3], Miguel Angel Japón-Rodriguez[4], Florinda Roldán[5], Elena Fajardo[5], Ariel Kaen[6], Eugenio Cardenas Ruiz-Valdepeñas[6], David Cano[1] and Alfonso Soto-Moreno[1]*

[1] Unidad de Gestión Clínica de Endocrinología y Nutrición, Instituto de Biomedicina de Sevilla (IBiS), Virgen del Rocio University Hospital/Centro Superior de Investigaciones Científicas (CSIC)/University of Seville, Seville, Spain, [2] Unidad de Gestión Clínica de Endocrinología y Nutrición, Virgen de Valme University Hospital, Seville, Spain, [3] Unidad de Gestión Clínica de Oncología médica, Oncología Radioterápica y Radiofísica Hospitalaria, Virgen del Rocio University Hospital, Seville, Spain, [4] Unidad de Gestión Clínica de Anatomía Patológica, Virgen del Rocio University Hospital, Seville, Spain, [5] Unidad de Gestión de Radiodiagnóstico, Virgen del Rocio University Hospital, Seville, Spain, [6] Unidad de Gestión Clínica de Neurocirugía, Virgen del Rocío University Hospital, Seville, Spain

OPEN ACCESS

**Edited by:**
*Antongiulio Faggiano, Sapienza University of Rome, Italy*

**Reviewed by:**
*Jacqueline Trouillas, Université Claude Bernard Lyon 1, France*
*Betina Biagetti, Vall d'Hebron University Hospital, Spain*

***Correspondence:**
*Pablo Remón-Ruiz*
*pjremonruiz@gmail.com*
*orcid.org/0000-0002-4551-8159*

**Specialty section:**
*This article was submitted to Cancer Endocrinology, a section of the journal Frontiers in Endocrinology*

**Received:** *28 September 2021*
**Accepted:** *30 November 2021*
**Published:** *21 December 2021*

**Citation:**
*Remón-Ruiz P, Venegas-Moreno E, Dios-Fuentes E, Moreno JMC, Fernandez Peña I, Garcia MA, Japón-Rodriguez MA, Roldán F, Fajardo E, Kaen A, Ruiz-Valdepeñas EC, Cano D and Soto-Moreno A (2021) A Silent Corticotroph Pituitary Carcinoma: Lessons From an Exceptional Case Report. Front. Endocrinol. 12:784889. doi: 10.3389/fendo.2021.784889*

Nowadays, neither imaging nor pathology evaluation can accurately predict the aggressiveness or treatment resistance of pituitary tumors at diagnosis. However, histological examination can provide useful information that might alert clinicians about the nature of pituitary tumors. Here, we describe our experience with a silent corticothoph tumor with unusual pathology, aggressive local invasion and metastatic dissemination during follow-up. We present a 61-year-old man with third cranial nerve palsy at presentation due to invasive pituitary tumor. Subtotal surgical approach was performed with a diagnosis of silent corticotroph tumor but with unusual histological features (nuclear atypia, frequent multinucleation and mitotic figures, and Ki-67 labeling index up to 70%). After a rapid regrowth, a second surgical intervention achieved successful debulking. Temozolomide treatment followed by stereotactic fractionated radiotherapy associated with temozolomide successfully managed the primary tumor. However, sacral metastasis showed up 6 months after radiotherapy treatment. Due to aggressive distant behavior, a carboplatine-etoposide scheme was decided but the patient died of urinary sepsis 31 months after the first symptoms. Our case report shows how the presentation of a pituitary tumor with aggressive features should raise a suspicion of malignancy and the need of follow up by multidisciplinary team with experience in its management. Metastases may occur even if the primary tumor is well controlled.

**Keywords: pituitary tumor, silent corticothoph tumor, pituitary carcinoma, radiotherapy, temozolomide**

**Abbreviations:** MRI, Magnetic resonance imaging; ACTH, adrenocorticotropic hormone; CT, Computed tomography; ESE, European Society of Endocrinology.

## INTRODUCTION

Most pituitary tumors are benign although they often invade surrounding structures. However, pituitary carcinomas are extremely rare accounting for only 0.1-0.2% of all pituitary tumors. This prevalence may be likely underestimated due to the challenge in diagnosing pituitary carcinoma (1). As defined by the World Health Organization, pituitary carcinomas are tumors of pituitary origin that have cerebrospinal and/or systemic metastases. Importantly, there are no histological features that can help to discriminate between pituitary carcinoma and non-metastasic pituitary tumors (2).

Literature has changed the landscape of aggressive, atypical pituitary tumors and pituitary carcinomas. The 2017 WHO classification of tumors of the pituitary gland removed the term atypical and set a number of histopathological characteristics with a high probability of recurrence (such as elevated proliferative activity or some subtypes of pituitary tumors) without a defined cut-off for Ki-67, mitotic count or p53 immunoreactivity. Thus, the description and definition of risk characteristics are highly relevant but without a separate denomination. Raverot et al. argued for a clinicopathological classification that includes aggressiveness and invasiveness, with aggressive and invasive tumors being more prone to metastatic dissemination (up to 10% of these cases) (3).

Pituitary carcinomas carry a poor prognosis with a median survival time of 1-2.6 years depending on whether systemic metastasis is found. A recent study has reported overall survival rates for pituitary carcinoma of 57.1% and 28.6% at 1 and 5 years, respectively (4). Treatment of pituitary carcinoma usually involves a multimodal therapy approach combining surgery, radiation and medical therapy. However, due to their rarity, there is a lack of reliable information to establish a standard treatment (3).

Here, we describe the multidisciplinary team experience in managing the only case of pituitary carcinoma diagnosed in our reference center over the span of 12 years. We discuss the diagnosis and treatment of this patient and review the recent literature about pituitary carcinoma.

## CASE DESCRIPTION

A 61-year-old man presented in the emergency room in 2015 complaining of headache. Physical examination revealed third-cranial nerve palsy on the left side and bitemporal hemianopsia. The patient had a history of hypertension, type 2 Diabetes Mellitus and referred loss of libido. No signs or symptoms of hormone hyperproduction were noticed, Cushing disease was ruled out by clinical signs but not by other laboratory testing such as free urinary cortisol or suppression test due to scarce pretest clinical probability. There was not relevant family history. Computed tomography imaging revealed a sellar mass with erosion of the sphenoid bone and invasion into the cavernous sinus regions and extension into the hypothalamus. A subsequent magnetic resonance imaging (MRI) scan of the brain region confirmed a 25-mm pituitary mass lesion extending into both left and right cavernous sinuses (Knosp grade 3) (**Figures 1A, B**). This lesion showed isointensity and hyperintensity on T1- and T2-weighted MRI, respectively. Laboratory test results revealed central hypogonadism and hypothyroidism and prolactin levels of 292 μUI/mL.

Endoscopic endonasal transsphenoidal surgery was performed and subtotal resection was achieved. Postoperative MRI (48 hours after surgery) revealed a tumor remnant (20x7x20 mm) (**Figures 2A, B**). The patient developed permanent postoperative diabetes insipidus but third-cranial nerve palsy improved and was discharged on hormone replacement therapy with oral desmopresine (0.1 mg twice a day), hydrocortisone (20 mg/day divided three times a day) and levothyroxine (50 mcg once a day). Hydrocortisone was initiated after hypotension and hypoglycemia after surgery, hormonal determination after surgery is shown in **Table 1**.

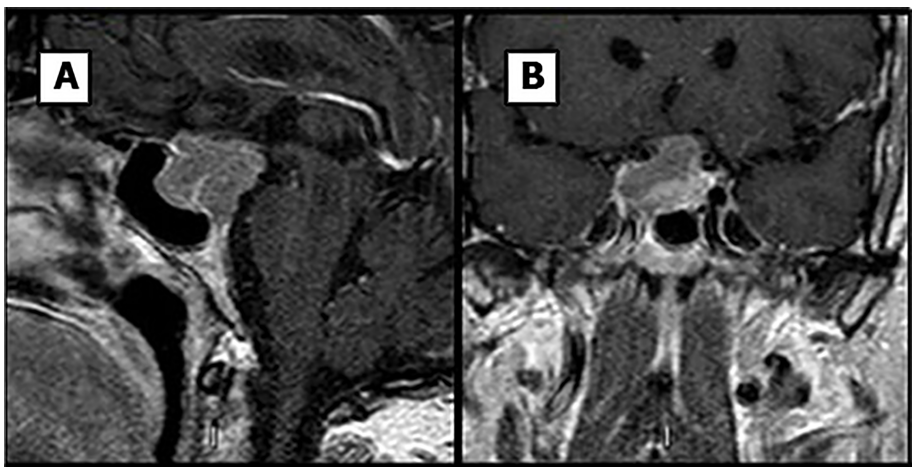


**FIGURE 1** | MR images previous to first surgery. Sagital **(A)** and coronal **(B)** T1-weighted images.

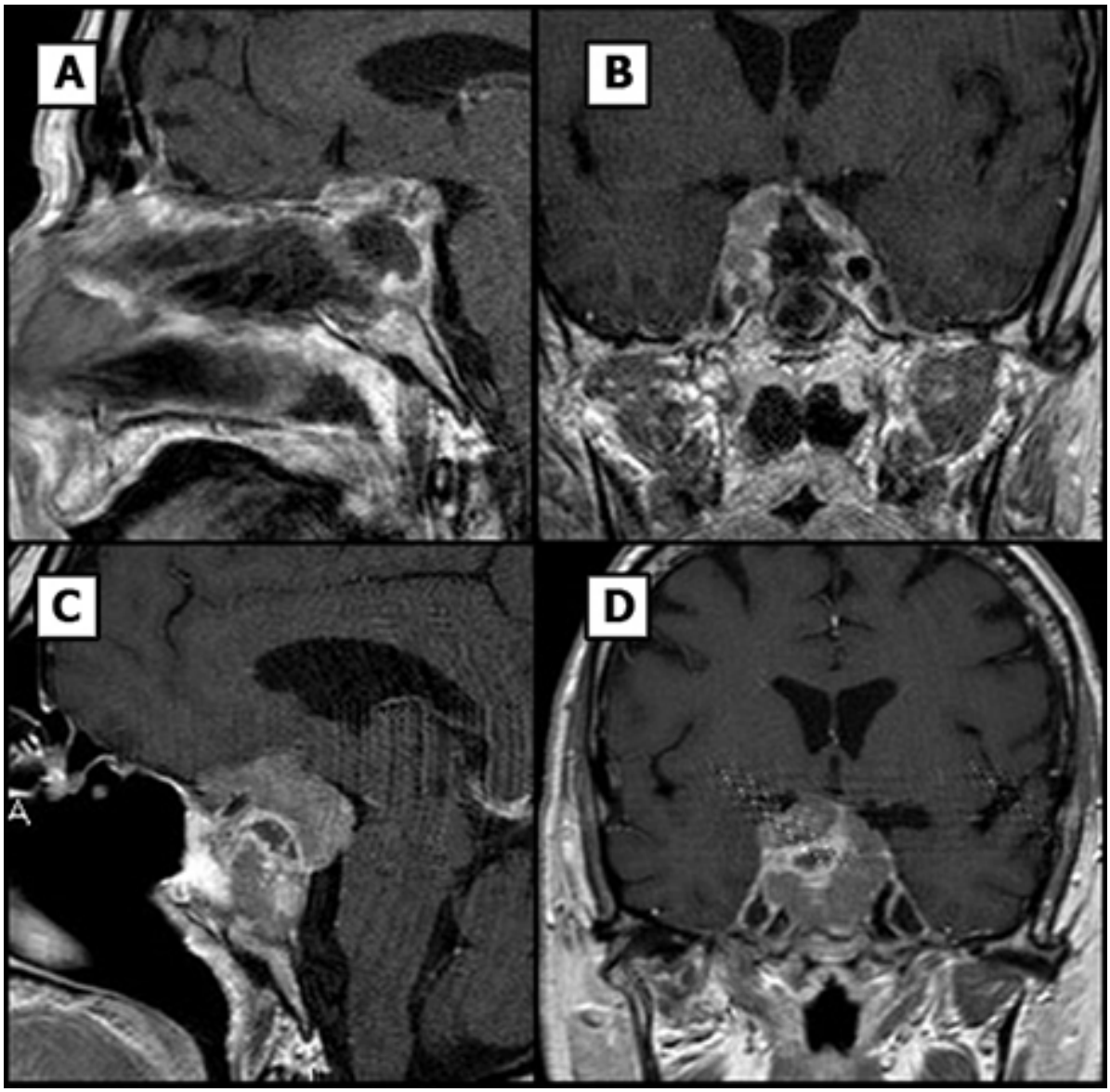


**FIGURE 2** | Pituitary MR images. **(A, B)** Sagital and coronal T1-weighted postsurgical images. **(C, D)** Sagital and coronal T1-weighted images, tumor rest growing can be noticed from small capsular rest to 20 mm invasive tumor.

Two months after surgery, the patient presented in the emergency room with acute headache, worsening of third-cranial nerve palsy and visual loss. Computed tomography imaging surprisingly showed regrowth of the pituitary mass with a maximum diameter of 36 mm, erosion of the sphenoid bone and invasion of the sinus (**Figures 2C, D**). Histological examination of the previous surgery showed a solid and papillary neoplasm composed of slightly basophilic cells (**Figures 3A-C**). Nuclear atypia, multinucleation and mitotic figures were frequent (bigger than 2/10 HPF but not specifically quantified in the report). These cells were positive for ACTH and negative for other pituitary hormones. Ki-67 labeling index was 50% overall but higher (50-70%) in many areas of the tumor, a feature that was alerted in the pathology report. Thus, was classified as invasive, aggressive silent corticotroph tumor with high proliferation index (Grade 2b suspected of malignancy according to Trouillas et al. classification) (5).

Based on the histological findings and rapid progression of the tumor, our multidisciplinary team decided to perform a second surgery and administer postoperative chemotherapy adjuvant treatment with Temozolomide. The patient underwent only partial resection of the tumor due to extensive invasion of the sphenoid bone. A 13-mm tumor remnant could be observed postsurgically. No operative complications were

**TABLE 1** | Hormonal laboratory determination 24 hours after first pituitary surgery.

| | |
|---|---|
| Cortisol* | 307 nmol/L* |
| FSH | 0,9 UI/L |
| LH | 0,4 UI/L |
| Testosterone | 0,1 nmol/L |
| Prolactin | 4 µUI/mL |
| GH | <0,05 ng/mL |
| IGF1 | 149 ng/mL |

**Determination of cortisol after iniciation of high dose of hydrocortisone due to clinical signs of hypocorticism.*

developed. Although no specific symptoms were noted, a screening for metastasis was performed prior to chemotherapy. Computed tomography (CT) imaging of thorax and abdomen and MRI of the spine revealed no metastatic lesions.

Temozolomide treatment was initiated 16.14 weeks after surgery at a dose of 200 mg/m$^2$/day for 5 of every 28 days and was well tolerated by the patient. After four cycles, a MRI was performed and revealed size stabilization of the size of the lesion. This led our multidisciplinary team to decide to additionally treat the patient with fractionated stereotactic radiation therapy. Thus, after the eighth temozolomide cycle treatment and 13 months after the initial diagnosis, radiation therapy was administered at a total dose of 50 Gray in 28 fractions and temozolomide dose was switched to 75 mg/m$^2$/day. MRI was performed three months after starting radiation therapy that did not show growth of the tumor remnant. CT of the thorax and abdomen was negative for metastatic disease. Six months after the start of the radiation therapy, the imaging tests were repeated, and the tumor lesion remained stable and campimetric improvement was also achieved. However, the CT scan now showed a mass at S1-S3 level (**Figure 4A**) compatible with metastasis. A biopsy of the sacral region was obtained. Histological examination showed a solid and papillary neoplasm positive for ACTH, consistent with metastasis of the primary pituitary tumor (**Figures 4B, C**). In this specimen nuclear atypia was pronounced with the presence of numerous giant tumor cells. Ki67 labeling index was 70-80%. Sacrectomy was not considered due to the extensive invasion of the metastatic lesion and temozolomide treatment at a dose of 200 mg/m$^2$/day was restarted. Despite restarting temozolomide, the patient developed severe bilateral lower extremity weakness and the chemotherapy treatment was changed to carboplatin AUC 5 and etoposide 100 mg/m$^2$ three days administered every 21 days. After one cycle of treatment the patient experienced febrile neutropenia likely due to an urinary tract infection. Due to the poor patient's general condition, radiation therapy of the sacral region was not performed. Unfortunately, and despite aggressive antibiotic treatment, the patient died 124.4 weeks after the first surgery. A clinical timeline is shown in **Figure 5**.

## DISCUSSION

The prevalence of incidentally found pituitary tumors in the general population is relatively high. Most of them are benign adenohypophyseal tumors commonly named as pituitary adenomas but a little unknown percentage are aggressive, invasive, resistant or even metastatic tumors. Nowadays, only proven metastatic tumors are carcinomas but a growing body of evidence show that we may have to reconsider some non-metastatic pituitary tumors as tumors with malignant potential (6). We report an additional case of pituitary carcinoma that initially presented as an aggressive pituitary tumor with a rapid metastatic dissemination despite an adequate chemotherapy treatment and radiotherapy of primary lesion. This exceptional case highlights two difficult aspects of aggressive tumors: the diagnosis of malignancy and the management of these aggressive tumors.

Despite intensive research on the subject, predicting an aggressive behavior of pituitary tumors remains an unmet clinical need. Currently, there are not clinical, radiological, surgical and pathological markers of malignancy, except the metastasis that is the reason why until now only the tumors with metastasis are considered as malignant and named "carcinoma". However, in our patient some unusual signs may suggest the malignancy of the primary tumor which was clinically an aggressive tumor.

First of all, initial clinical symptom was third-cranial-nerve palsy which is actually a clinical manifestation of cavernous sinus invasion proven by RMI.

Secondly, aggressiveness and prompt regrowth after the first surgery. It only took two months for the tumor to grow to a similar size as before the first surgery, triggering third-cranial-nerve palsy once more.

Finally, the pathology report gives several clues about the potential inner nature of our tumor. Corticotroph tumor, especially the silent one, is the tumor type the most frequent carcinoma with the lactotroph one (7). In the 2017 WHO classification for pituitary tumors, silent corticotroph tumor is a special subtype a with high probability of recurrence and more aggressive behavior (2). All this, together with the elevated Ki-67 labeling index (≥10%) prompted us to perform screening for metastasis. The use of Ki-67 as a marker for aggressive behavior in pituitary tumors has long been suggested but no clear consensus exists on the cut-off values that can distinguish between pituitary carcinoma and benign tumors (8, 9). Nonetheless, a particularly high Ki-67 labeling index may be suggestive of malignant potential, as described in several reports (10, 11). In agreement with this notion, the observed Ki-67 labeling index in our patient was extremely high compared to most published data on pituitary tumors, and more specifically, pituitary carcinomas (11). A Ki-67 index ≥10% is found in aggressive pituitary tumors as well as pituitary carcinomas and this may be because many aggressive tumors are, in fact, malignant (6).

As is noted by Trouillas et al, although probably the vast majority of pituitary tumors will have a benign behavior, there is a need for an integrative classification which allows to identify malignant potential in order to improve clinical results with an early diagnosis of complications. Trouillas et al. proposed a five grade clinicopathological classification of pituitary endocrine tumors which included a tumor grade based on invasive and proliferative characteristics. So, invasive and proliferative tumors are classified as Grade 2b with a poor prognosis and an increased probability of progression. These tumors could be considered as

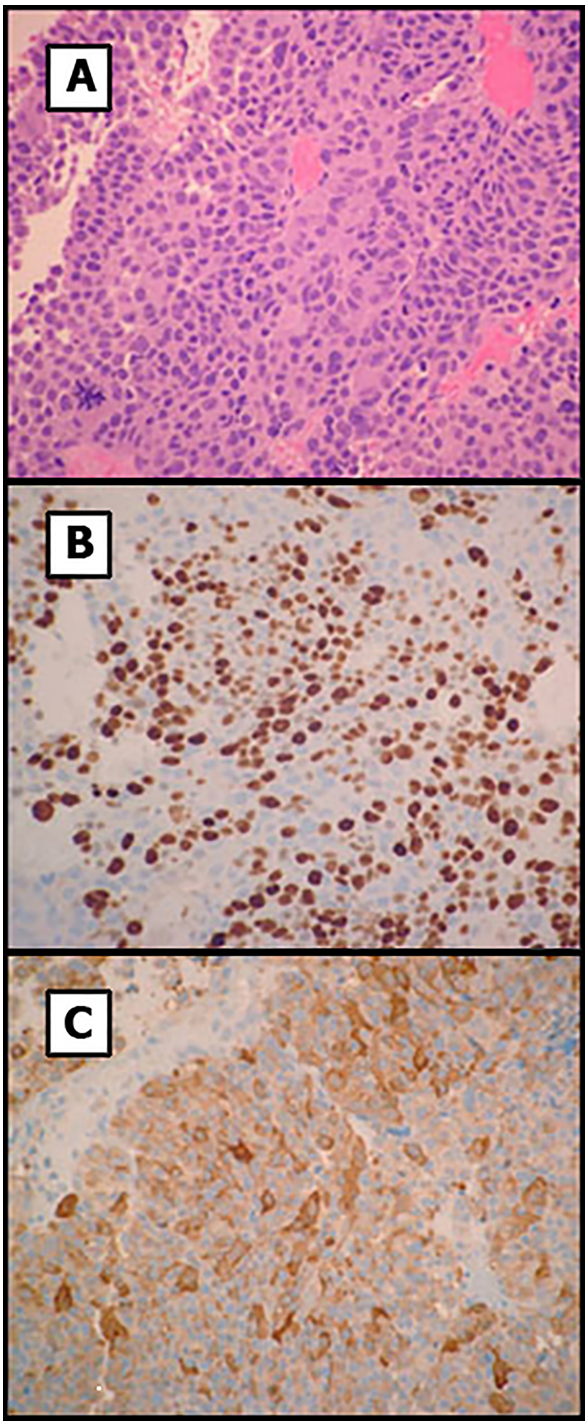


**FIGURE 3** | Histology of the pituitary tumor. **(A)** Primary tumor showed solid and papillary proliferation of basophilic cells with increased nuclear atypia and mitoses. **(B)** Ki-67 labeling showed areas with elevated proliferation index. **(C)** Tumor cells were positive for ACTH. Original magnification x200.

suspected of malignancy as 6/8 carcinomas from the original series were classified as Grade 2b at the initial surgery and with an identification of metastasis during follow-up in 10% of the initial Grade 2b tumors (3, 5).

Current recommendations in metastasis screening refer structural and/or functional imaging studies should be considered in aggressive tumors in the evidence of discordant biochemical and radiological findings in the absence of site-

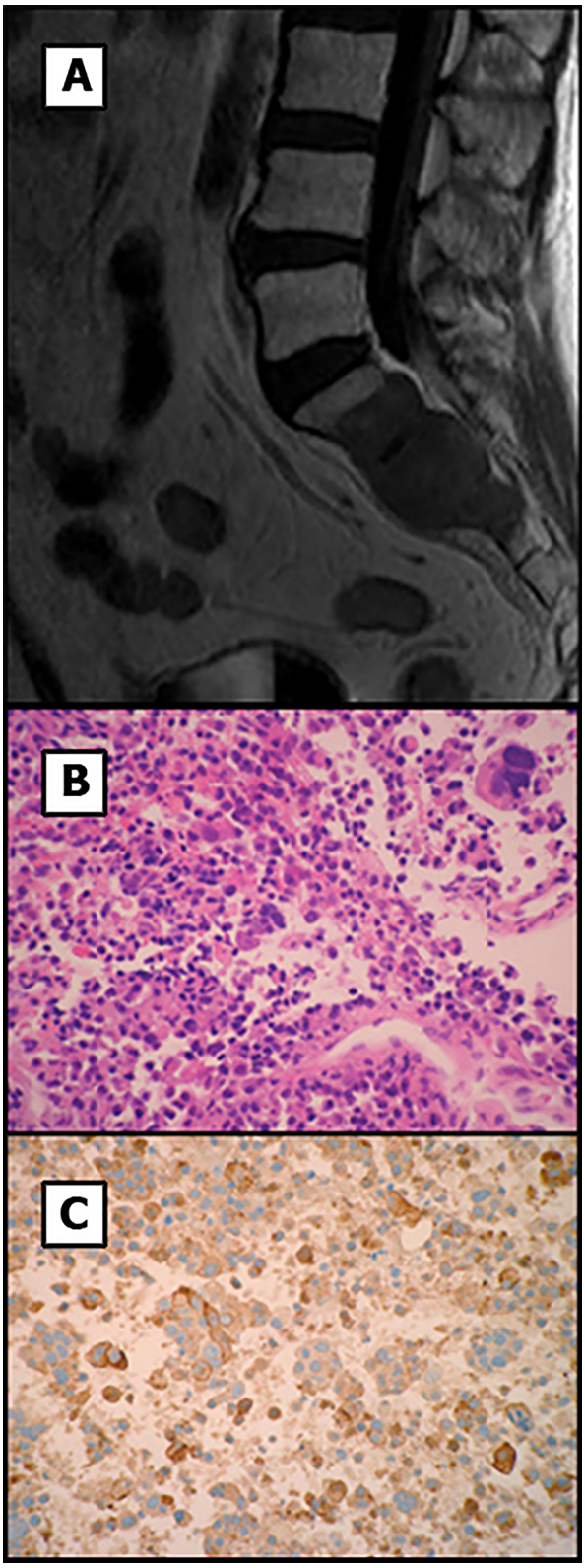


**FIGURE 4** | MR image and histology of the sacral mass. **(A)** T1-weighted MR image shows a highly invasive sacral metastasis. **(B)** Tumor metastasis showed solid and papillary proliferation of atypical cells including numerous giant multinucleated cells. **(C)** Tumor cells were positive for ACTH. Original magnification x200.

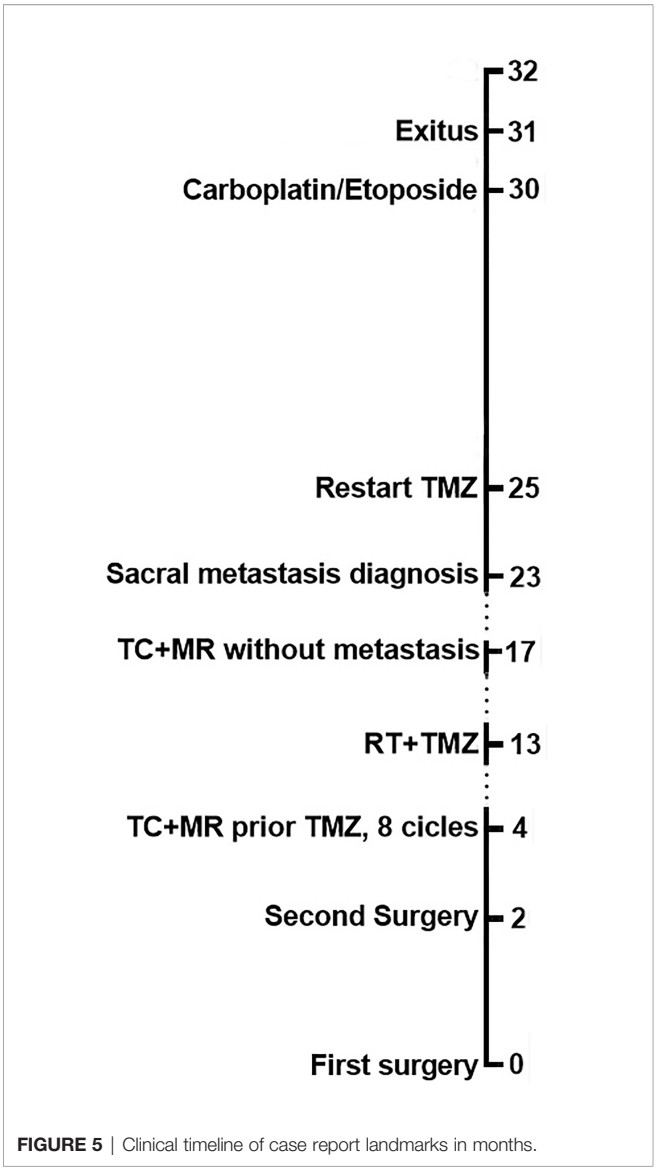


**FIGURE 5** | Clinical timeline of case report landmarks in months.

specific symptoms. Due to previously analyzed tumor characteristics, we considered our pituitary tumor as suspect of malignancy (3) from the second surgery with initial metastasis screening before first cycle of temozolomide and periodical screening after that. We decided to perform thorax and abdomen CT and spine MRI rather than 18F-FDG PET/CT. Up to our knowledge, there is no enough evidence on the best study for screening of pituitary metastasis of pituitary carcinoma. 18F-FDG PET/CT could be more sensitive to small metastasis, but in our case and due to local aggressiveness we thought both studies could give similar sensitivity but with higher specificity.

The treatment of aggressive pituitary tumors and pituitary carcinoma usually combines radiation and medical therapy. First of all, clinical and hormonal presurgical analysis is mandatory in every patient with adenohypophyseal tumors found in RMI because it can lead to adjuvant medical treatment. In prolactinomas, adjuvant medical treatment with dopamine agonist could delay surgical treatment event in giant ones (12). Some subtypes of adenomas have some clinical special features because of the previously mentioned probability of progression and recurrence as lactotroph adenoma in men, sparsely granulated somatotroph adenoma or silent corticotroph adenoa. Until recently, no clear guidelines were available to help clinicians to manage aggressive and malignant pituitary tumors. The European Society of Endocrinology (ESE) published clinical practice guidelines for the management of aggressive pituitary tumors and carcinomas in 2018 (13). The authors acknowledge the limitations of these guidelines since the literature on aggressive pituitary tumors and carcinomas is scarce. However, additional support for the development of the clinical guidelines was obtained from a survey of ESE members specifically designed for that purpose (7). Transcranial or transsphenoidal surgery is the treatment of choice for patients with pituitary tumors. Surgery rarely achieves cure but it can provide relief of symptoms, particularly those associated to mass effect. Tumor recurrence in pituitary carcinoma is very common and additional therapy approaches such as radiation and chemotherapy are thus required. ESE guidelines recommend discussion within a multidisciplinary team regarding additional surgeries prior to consideration of other treatment options. In our patient, even though a diagnosis of carcinoma was not initially confirmed, the aggressive features of the pituitary tumor raised the suspicion of a malignant potential. Thus, we decided to perform an additional surgery and adjuvant chemotherapy to control tumor growth. The alkylating agent temozolomide is the most common chemotherapeutic option for aggressive pituitary tumors and carcinomas (7, 14, 15) and ESE guidelines recommend the use of temozolomide as first-line chemotherapy for aggressive pituitary tumors and carcinomas even though the evidence is based mostly on case reports and small series rather than randomized clinical trials (13). It has been difficult to obtain precise response rates to temozolomide from the literature because of heterogeneity in treatment regimens, and definitions in disease control but it is considered that about half of the patients do not respond to temozolomide treatment (15). Importantly, patients receiving concurrent temozolomide treatment and radiotherapy seem to respond more often (7). ESE guidelines suggest that temozolomide response should be assessed after three cycles of therapy and that treatment can be extended according to their tolerance and clinical response. In our patient, temozolomide treatment was well tolerated and considering that tumor size remained stable we decided to use a lower dose of temozolomide (75 mg/m$^2$) concomitant with radiation therapy, as in the Stupp protocol. However, the identification of metastasis during the follow-up led us to restart temozolomide monotherapy at the highest recommended dose. Temozolomide treatment was largely ineffective though that combined with the rapid progression of the tumor forced us to consider an alternate oncological treatment. Unfortunately, the literature about second and third line treatments for temozolomide-resistant pituitary tumors is scarce and the reported chemotherapeutic agents have been very heterogeneous. Indeed, the recent ESE guidelines were

unable to provide recommendations in this regard. We decided initiated chemotherapy with a combination carboplatin and etoposide [as standard treatment for certain poorly differentiated neuroendocrine tumors (16, 17)] and local radiotherapy treatment for sacral mass later, but the efficiency was limited due to severe complications developed. Indeed other treatments were foreseen, as immunotherapy, mTOR inhibitors and even peptide receptor radionuclide therapy, but according to aggressiveness, histopathological characteristics, refraction to temozolomide and requirements of aggressive treatment, a platine scheme was selected as is contemplated by Raverot et al. in ESE Clinical Practice Guidelines (11, 18). Possible scheme that could be used after the onset of sacral metastasis is capecitabine-TMZ combination (CAPTEM). This combination could enhance TMZ results due to attenuation effect of MGMT DNA repair activity by capecitabine. CAPTEM has been used in different clinical settings with good tolerance and morphological response. Better results have been described when CAPTEM has been used as first line or as second line treatment, particularly in those cases in which TMZ resistance has not been achieved. In TMZ-resistant pituitary tumors, CAPTEM can achieve a partial response in some cases but its efficacy seems to be lower (18).

In conclusion, our case illustrates how the presentation of a pituitary tumor with aggressive features should raise suspicion of malignancy. There remains a need to identify other treatment options for aggressive pituitary tumors and carcinoma.

## DATA AVAILABILITY STATEMENT

The raw data supporting the conclusions of this article will be made available by the authors, without undue reservation.

## ETHICS STATEMENT

Ethical review and approval was not required for the study on human participants in accordance with the local legislation and institutional requirements. The patients/participants provided their written informed consent to participate in this study. Written informed consent was obtained from the individual(s) for the publication of any potentially identifiable images or data included in this article.

## AUTHOR CONTRIBUTIONS

PR-R collected and analyzed the data, and wrote the report. EV-M atended the patient, ED-F atended the patient. JC made literature review. IF atended the patient. MA atended the patient. MJ-R performed the histological examination. FR interpreted MRI image. EF interpreted MRI image. AK performed surgery. ECR-V performed surgery. DC analyzed the data and wrote the report. AS-M coordinated the research, analyzed the data and wrote the report. All authors contributed to the article and approved the submitted version.

## FUNDING

This work was supported by grants from the ISCIII-Subdirección General de Evaluación y Fomento de la Investigación co-funded with Fondos FEDER (PI16/00175 to AS-M and DC) and the Sistema Andaluz de Salud (A-0003-2016 and A-0006-2017 to AS-M, C-0015-2014 and RC-0006-2018 to DC).

## REFERENCES

1. Kaltsas GA, Nomikos P, Kontogeorgos G, Buchfelder M, Grossmanet AB. Diagnosis and Management of Pituitary Carcinomas. *J Clin Endocrinol Metab* (2005) 90:3089–99. doi: 10.1210/jc.2004-2231
2. Lopes MBS. The 2017 World Health Organization Classification of Tumors of the Pituitary Gland: A Summary. *Acta Neuropathol (Berl)* (2017) 134:521–35. doi: 10.1007/s00401-017-1769-8
3. Raverot G, Ilie MD, Lasolle H, Amodru V, Trouillas J, Castinetti F, et al. Aggressive Pituitary Tumours and Pituitary Carcinomas. *Nat Rev Endocrinol* (2021) 17:671–84. doi: 10.1038/s41574-021-00550-w
4. Hansen TM BS Lim M, Balia GL, Burger PC, Salvatori R, Wand G, Quinones-Hinojosa A, et al. Invasive Adenoma and Pituitary Carcinoma: A SEER Database Analysis. *Neurosurg Rev* (2014) 37:279–85. doi: 10.1007/s10143-014-0525-y
5. Trouillas J, Roy P, Sturm N, Dantony E, Cortet-Rudelli C, Viennet G, et al. A New Prognostic Clinicopathological Classification of Pituitary Adenomas: A Multicentric Case-Control Study of 410 Patients With 8 Years Post-Operative Follow-Up. *Acta Neuropathol (Berl)* (2013) 126:123–35. doi: 10.1007/s00401-013-1084-y
6. Trouillas J, Jaffrain-Rea M-L, Vasiljevic A, Dekkers O, Popovic V, Wierinckx A, et al. Are Aggressive Pituitary Tumors and Carcinomas Two Sides of the Same Coin? Pathologists Reply to Clinician's Questions. *Rev Endocr Metab Disord* (2020) 21:243–51. doi: 10.1007/s11154-020-09562-9
7. McCormack A, Dekkers OM, Petersenn S, Popovic V, Trouillas J, Raverot G, et al. Treatment of Aggressive Pituitary Tumours and Carcinomas: Results of a European Society of Endocrinology (ESE) Survey 2016. *Eur J Endocrinol* (2018) 178:265–76. doi: 10.1530/EJE-17-0933
8. Heaney AP. Clinical Review: Pituitary Carcinoma: Difficult Diagnosis and Treatment. *J Clin Endocrinol Metab* (2011) 96:3649–60. doi: 10.1210/jc.2011-2031
9. Asa SL, Ezzat S. Aggressive Pituitary Tumors or Localized Pituitary Carcinomas: Defining Pituitary Tumors. *Expert Rev Endocrinol Metab* (2016) 11:149–62. doi: 10.1586/17446651.2016.1153422
10. Pasquel FJ, Vincentelli C, Brat DJ, Oyesiku NM, Ioachimescu AG. Pituitary Carcinoma *In Situ*. *Endocr Pract Off J Am Coll Endocrinol Am Assoc Clin Endocrinol* (2013) 19:69–73. doi: 10.4158/EP12351.CR
11. Dudziak K, Honegger J, Bornemann A, Horger M, Müssig K. Pituitary Carcinoma With Malignant Growth From First Presentation and Fulminant Clinical Course–Case Report and Review of the Literature. *J Clin Endocrinol Metab* (2011) 96:2665–9. doi: 10.1210/jc.2011-1166
12. Shimon I. Giant Prolactinomas. *Neuroendocrinology* (2019) 109:51–6. doi: 10.1159/000495184
13. Raverot G, Burman P, McCormack A, Heaney A, Petersenn S, Popovic V, et al. European Society of Endocrinology Clinical Practice Guidelines for the Management of Aggressive Pituitary Tumours and Carcinomas. *Eur J Endocrinol* (2018) 178:1–24. doi: 10.1530/EJE-17-0796
14. Losa M, Bogazzi F, Cannavo S, Ceccato F, Curtò L, De Marinis L, et al. Temozolomide Therapy in Patients With Aggressive Pituitary Adenomas or Carcinomas. *J Neurooncol* (2016) 126:519–25. doi: 10.1007/s11060-015-1991-y
15. Halevy C, Whitelaw BC. How Effective Is Temozolomide for Treating Pituitary Tumours and When Should It be Used? *Pituitary* (2017) 20:261–6. doi: 10.1007/s11102-016-0745-y

16. Pulvirenti A, Raj N, Cingarlini S, Pea A, Tang LH, Luchini C, et al. Platinum-Based Treatment for Well- and Poorly Differentiated Pancreatic Neuroendocrine Neoplasms. *Pancreas* (2021) 50:138–46. doi: 10.1097/MPA.0000000000001740
17. Kunz PL, Reidy-Lagunes D, Anthony LB, Bertino EM, Brendtro K, Chan JA, et al. Consensus Guidelines for the Management and Treatment of Neuroendocrine Tumors. *Pancreas* (2013) 42:557–77. doi: 10.1097/MPA.0b013e31828e34a4
18. Nakano-Tateno T, Lau KJ, Wang J, McMahon C, Kawakami Y, Tateno T, et al. Multimodal Non-Surgical Treatments of Aggressive Pituitary Tumors. *Front Endocrinol* (2021) 12:624686. doi: 10.3389/fendo.2021.624686

**Conflict of Interest:** The authors declare that the research was conducted in the absence of any commercial or financial relationships that could be construed as a potential conflict of interest.

frontiers in Endocrinology

CASE REPORT
published: 03 February 2022
doi: 10.3389/fendo.2021.769450

# Adrenal Hemorrhage in a Cortisol-Secreting Adenoma Caused by Antiphospholipid Syndrome Revealed by Clinical and Pathological Investigations: A Case Report

*Kentaro Ochi[1†], Ichiro Abe[1,2*†], Yuto Yamazaki[3†], Mai Nagata[1], Yuki Senda[1], Kaori Takeshita[1], Midori Koga[1], Yuka Yamao[1], Toru Shigeoka[1], Tadachika Kudo[1], Yuichiro Fukuhara[4], Shigero Miyajima[4], Hiroshi Taira[4], Shoji Haraoka[5], Tatsu Ishii[4], Yuichi Takashi[1], Alfred K. Lam[2], Hironobu Sasano[3] and Kunihisa Kobayashi[1]*

[1] Department of Endocrinology and Diabetes Mellitus, Fukuoka University Chikushi Hospital, Chikushino, Japan, [2] School of Medicine and Dentistry, Griffith University, Gold Coast, QLD, Australia, [3] Department of Pathology, Tohoku University Graduate School of Medicine, Sendai, Japan, [4] Department of Urology, Fukuoka University Chikushi Hospital, Chikushino, Japan, [5] Department of Pathology, Fukuoka University Chikushi Hospital, Chikushino, Japan

Due to its rarity, adrenal hemorrhage is difficult to diagnose, and its precise etiology has remained unknown. One of the pivotal mechanisms of adrenal hemorrhage is the thrombosis of the adrenal vein, which could be due to thrombophilia. However, detailed pathological evaluation of resected adrenal glands is usually required for definitive diagnosis. Here, we report a case of a cortisol-secreting adenoma with concomitant foci of hemorrhage due to antiphospholipid syndrome diagnosed both clinically and pathologically. In addition, the tumor in this case was pathologically diagnosed as cortisol-secreting adenoma, although the patient did not necessarily fulfill the clinical diagnostic criteria of full-blown Cushing or sub-clinical Cushing syndrome during the clinical course, which also did highlight the importance of detailed histopathological investigations of resected adrenocortical lesions.

**Keywords: adrenal hemorrhage, cortisol-secreting adenoma, antiphospholipid syndrome, thrombosis, thrombophilia**

OPEN ACCESS

***Edited by:***
*Barbara Altieri, University Hospital of Wuerzburg, Germany*

***Reviewed by:***
*Ashley Grossman, Queen Mary University of London, United Kingdom*
*Tao Wang, Sichuan University, China*
*Duarte L. Pignatelli, Centro Hospitalar Universitário de São João, Portugal*

****Correspondence:***
*Ichiro Abe*
*abe1ro@fukuoka-u.ac.jp*
*orcid.org/0000-0002-7545-9751*

*†These authors have contributed equally to this work*

***Specialty section:***
*This article was submitted to Cancer Endocrinology, a section of the journal Frontiers in Endocrinology*

***Received:*** *02 September 2021*
***Accepted:*** *07 December 2021*
***Published:*** *03 February 2022*

***Citation:***
*Ochi K, Abe I, Yamazaki Y, Nagata M, Senda Y, Takeshita K, Koga M, Yamao Y, Shigeoka T, Kudo T, Fukuhara Y, Miyajima S, Taira H, Haraoka S, Ishii T, Takashi Y, Lam AK, Sasano H and Kobayashi K (2022) Adrenal Hemorrhage in a Cortisol-Secreting Adenoma Caused by Antiphospholipid Syndrome Revealed by Clinical and Pathological Investigations: A Case Report. Front. Endocrinol. 12:769450. doi: 10.3389/fendo.2021.769450*

## INTRODUCTION

Adrenal hemorrhage is rare and caused by various etiologies (1, 2). Systemic studies demonstrated that abdominal trauma, infections, surgery, angiography, and adrenal venous thrombosis could cause adrenal hemorrhage (1–6). As such, it is difficult to diagnose and determine its etiology solely through clinical investigations. In addition, only a few cases have been reported on their pathological findings. In addition, histopathology of adrenal hemorrhage in adrenocortical adenoma has not been described in the literature. Herein, we report the first case of adrenal hemorrhage in a cortisol-secreting adenoma due to thrombophilia by antiphospholipid syndrome.

## CASE PRESENTATION

### Clinical Summary

A 67-year-old woman was incidentally diagnosed with a nodular lesion in her right adrenal gland (25 × 29 mm) by non-enhanced abdominal computed tomography (CT) (**Figure 1A**). She was referred to our hospital and was admitted for further endocrinological examination. Her body mass index was 26.0 kg/m$^2$, and she did not have any clinical findings, suggestive of Cushing's syndrome. Her blood pressure was within normal limits (109/51 mmHg). In addition, she did not have hyperlipidemia [low-density lipoprotein (LDL)-cholesterol, 134 mg/dL; high-density lipoprotein (HDL)-cholesterol, 58 mg/dL; triglyceride 79 mg/dL). Her HbA1c was 5.5%. Results of those laboratory findings were almost within the normal range, but her potassium level was slightly low (3.7 mmol/L). She had never received any anticoagulant therapy and medication for hypertension, hyperlipidemia, and diabetes mellitus in her past history. In the endocrine evaluation, her morning adrenocorticotropic hormone (ACTH) level was relatively low (5.0 pg/mL), while her cortisol level was within the normal range (12.60 μg/dL). Results of 1-mg dexamethasone suppression test demonstrated serum cortisol suppression (0.89 μg/dL), which was lower than 1.8 μg/dL. Her nocturnal serum cortisol levels (taken at 21 pm after 30 min resting) were not necessarily high (2.68 μg/dL), which was lower than 5.0 μg/dL. Dehydroepiandrosterone sulfate level was within normal limits (28.0 μg/dL; normal range, 12–133 μg/dL). These results did not necessarily meet the clinical diagnostic criteria of full-brown Cushing' syndrome (CS) and subclinical Cushing's syndrome (SCS) (7). Her plasma renin activity was low (0.2 ng/mL/hr), while her plasma aldosterone concentration was not necessarily high (80.8 pg/mL; normal range, 4.0–82.1 pg/mL). The ratio of plasma aldosterone concentration/plasma renin activity (ARR) was 404. Results of the upright furosemide-loading test met the diagnostic criteria of primary aldosteronism, while those of the captopril-challenge test and the saline-loading test were within the normal range (**Table 1**). These results above were not conclusive of the clinical diagnosis of primary aldosteronism (7, 8). The plasma/urinary catecholamine and urinary metanephrines values were within the normal range. However, the simultaneous presence of autonomous cortisol secretion and primary aldosteronism could not completely be ruled out in this case. Therefore, the patient was carefully surveyed following her

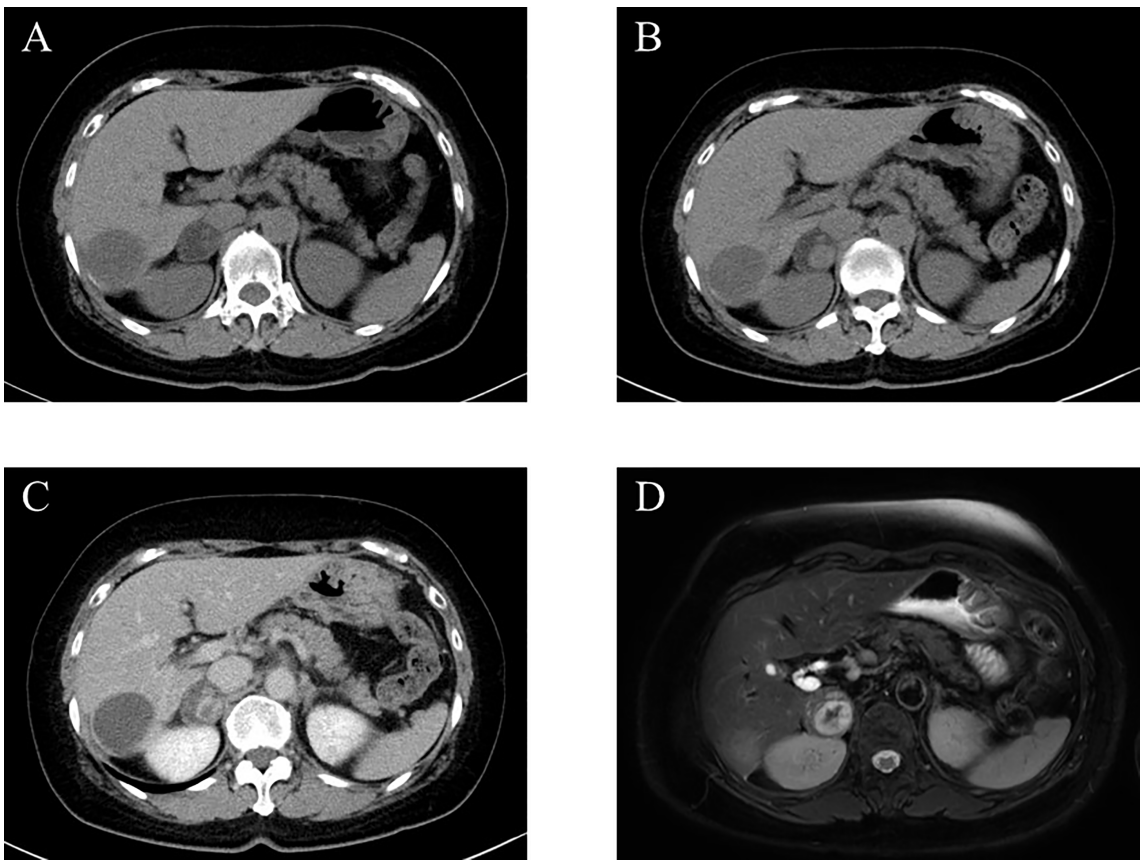


**FIGURE 1** | Imaging analysis. **(A)** Non-enhanced computed tomography (CT) at the first admission. **(B, C)** Non-enhanced **(B)** and enhanced **(C)** CT 3 years after the first admission. **(D)** T2-weighted magnetic resonance imaging (MRI) at the second admission.

**TABLE 1** | Summary of endocrine disorders of the patient.

| | | 1st admission | Preoperation | 3 months after operation | The diagnostic criterion of CS/SCS |
|---|---|---|---|---|---|
| presence or absence of the physical symptom of Cushing's syndrome | | Absence | Absence | Absence | CS: presence/SCS: absence |
| Morning plasma ACTH level (pg/mL) | | 5.0 | 8.7 | 25.8 | CS: <5.0 pg/mL/SCS: <10.0 pg/mL |
| Morning serum cortisol level (μg/dL) | | 12.60 | 9.01 | 5.62 | CS: normal or high (> 8 μg/dl)/SCS: normal (8–18 μg/dL) |
| Nocturnal serum cortisol level (μg/dL) | | 2.68 | 3.84 | N.A. | CS: <7.5 μg/dL/SCS: < 5.0 μg/dL |
| Serum cortisol level on 1-mg dexamethasone suppression test (μg/dL) | | 0.89 | 1.38 | 0.69 | CS: <5.0 pg/mL/SCS: <1.8 pg/mL |
| Dehydroepiandrosterone sulphate level (μg/dL) | | 28 | 15 | 18 | CS and SCS: < 12 μg/dL (considering patient's sex and age) |
| | | **1st admission** | **Preoperation** | **3 months after operation** | **The diagnostic criterion of primary aldosteronism** |
| Baseline ARR | | 404 | 381 | 369 | ARR > 200 |
| Captopril-challenge tests | ARR (60 min) | 56 | 189 | 199 | ARR (60 or 90 min) > 200 |
| | ARR (90 min) | 41 | 248 | 182 | |
| upright furosemide-loading tests | plasma renin activity (120 min) (ng/mL/hr) | 0.9 | 0.9 | 1.2 | Plasma renin activity (120 min) < 2.0 ng/mL/hr |
| Saline-loading test | Plasma aldosterone (240 min) (pg/mL) | 11.1 | <10.0 | 21.4 | Plasma aldosterone (240 min) > 60 pg/mL |

*CS, Cushing's syndrome; SCS, subclinical Cushing's syndrome; N.A, not assessed; ARR, the ratio of plasma aldosterone concentration/plasma renin activity.*

first admission. Three years after her admission, abdominal non-enhanced and enhanced CT demonstrated that the right adrenal tumor had enlarged (35 × 40 mm) and became heterogeneous (**Figures 1B, C**). Therefore, she was readmitted for further endocrinological examination.

Her body mass index was 26.6 kg/m$^2$, and she did not have any clinical findings suggestive of Cushing's syndrome, same as the first admission. She remained normotensive (106/62 mmHg) and without hyperlipidemia and diabetes mellitus. Her potassium level was 3.6 mmol/L. In the endocrine evaluation, her morning ACTH level was still low (8.7 pg/mL), but the cortisol level was within the normal range (9.01 μg/dL). Results of 1-mg dexamethasone suppression test at this admission demonstrated the serum cortisol value higher than that in her first admission (1.38 μg/dL). Besides, her nocturnal serum cortisol level (taken at 21 pm after 30 min resting) was slightly high (3.84 μg/dL). Meanwhile, dehydroepiandrosterone sulfate level was relatively low (15.0 μg/dL). In addition, $^{131}$I-adosterol adrenal scintigraphy showed high uptake of adosterol in the tumor on the right adrenal gland and suppressed uptake in the left adrenal gland. These results indicated that the tumor could be a cortisol-secreting adrenocortical adenoma despite having insufficient diagnostic criteria of SCS. Her plasma renin activity was low (0.2 ng/mL/hr), and her plasma aldosterone concentration was not high (76.2 pg/mL), with an ARR of 381. Results of the captopril-challenge tests and upright furosemide-loading tests satisfied the diagnostic criteria of primary aldosteronism. Results of the saline-loading test were within normal range, same as the first admission (**Table 1**). Overall, the patient could have primary aldosteronism.

Abdominal magnetic resonance imaging (MRI) was performed for the patient and showed a high-intensity region inside the tumor, suspected to be adrenal hemorrhage, despite having no abdominal pain (**Figure 1D**). In addition, she had a history of repeated miscarriage and was positive for anticardiolipin antibody (21.0 U/mL). Based on those findings above, antiphospholipid syndrome was clinically diagnosed.

Considering the tumor enlargement and the clinical necessity of anticoagulant therapy, a laparoscopic resection was performed on the right adrenal tumor. A laparoscopic resection was on the right adrenal tumor. After the operation, she was placed in hydrocortisone replacement therapy. However, her cortisol level remained low (1.14 μg/dL) 14 days after the operation. Three months after the operation, her ACTH and cortisol levels were 25.8 pg/mL and 5.62 μg/dL, respectively. In addition, results of 1-mg dexamethasone suppression test adequately demonstrated cortisol suppression (0.69 μg/dL), and dehydroepiandrosterone sulfate level increased (18.0 μg/dL) (**Table 1**). Therefore, the replacement of hydrocortisone was tentatively terminated at that time. Six months after operation, her ACTH and cortisol levels became normal (33.5 pg/mL and 10.1 μg/dL, respectively). However, there were no changes of ARR and results of the upright furosemide-loading test before and 3 months after operation. The captopril challenge test demonstrated that there were only slight but not significant differences of ARR between before and 3 months after operation (**Table 1**). Therefore, the possibility of primary aldosteronism of the right adrenocortical tumor could be excluded, and the culprit lesion of primary aldosteronism could exist in the left adrenal gland. Regarding the treatment of her antiphospholipid syndrome, anticoagulant therapy was started after operation. She had no symptoms of thrombopenia and hemorrhage in the other organs after the start of anticoagulant therapy.

## Pathological Findings

Macroscopically, a well-circumscribed yellow nodule of the adrenal gland was detected in the resected specimen (**Figure 2A**).

Microscopically, the nodule is composed of large polygonal tumor cells with abundant foamy clear cytoplasm and focally small compact cells composed of eosinophilic cytoplasm arranged in nests, cords, and trabeculae. Mitotic figures were not detected, and the Ki-67 labeling index was <2% in the tumor. The criteria of Weiss (1/9: clear cells in the cytoplasm were only detected) revealed that the tumor was an adrenocortical adenoma (9). In addition, fresh hemorrhage and organizing hematoma were histologically detected within the adenoma above. Fibrin thrombus was formed in the small vessels in the tumor. CD31-positive endothelial cells encroached the thrombus above and recanalization in the blood vessels inside the tumor. Any histological findings of infarction and inflammatory infiltration suggesting vasculitis or infection were not detected. In addition, hyalinized degenerative changes were also detected in the small vessel walls within the adenoma. These findings above were all consistent with the possibility of intratumoral hemorrhage and thrombosis mainly caused by antiphospholipid syndrome (**Figures 2B–D** and **3A, B**).

The tumor cells were immunohistochemically positive for steroidogenic enzymes illustrated in the figures, including DHEA-ST and 3BHSD1 (**Figures 3C–L**). On the other hand, adrenocortical atrophy was not detected, but DHEA-ST immunoreactivity was diminished in the concomitant adrenocortical cells, consistent with the clinical findings that this tumor had slightly elevated autonomous secretion of cortisol (**Figures 3M, N**).

In contrast, CYP11B2-positive cells were not detected in the tumor and adjacent non-neoplastic adrenal tissue. In addition, paradoxical hyperplasia of the zona glomerulosa was not detected (**Figures 3O, P**). These findings all indicated that the tumor produced cortisol. No aldosterone-secreting cells causing primary aldosteronism were identified in the tumor and non-neoplastic adrenal tissues, which was consistent with results of clinical investigations.

## DISCUSSION AND CONCLUSION

One of the major causes of adrenal hemorrhage is thrombosis of the adrenal vein, resulting in occlusion, swelling, and rupture of the adrenal vein (1, 2). Antiphospholipid syndrome is an autoimmune disease and clinically associated with hypercoagulability, which results in thrombophilia through auto-antibodies against the heterologous groups of phospholipids (10). These antibodies also caused arterial/venous thrombosis in various organs. Therefore, antiphospholipid syndrome can account for adrenal hemorrhage of this case through development of adrenal venous thromosis.

When diagnosing adrenal hemorrhage, imaging, such as abdominal CT, MRI, $^{131}$I-adosterol adrenal scintigraphy, has been generally recommended to evaluate its morphological features (11). In our case, adrenal incidentaloma was suspected by abdominal CT, abdominal MRI, and $^{131}$I-adosterol adrenal

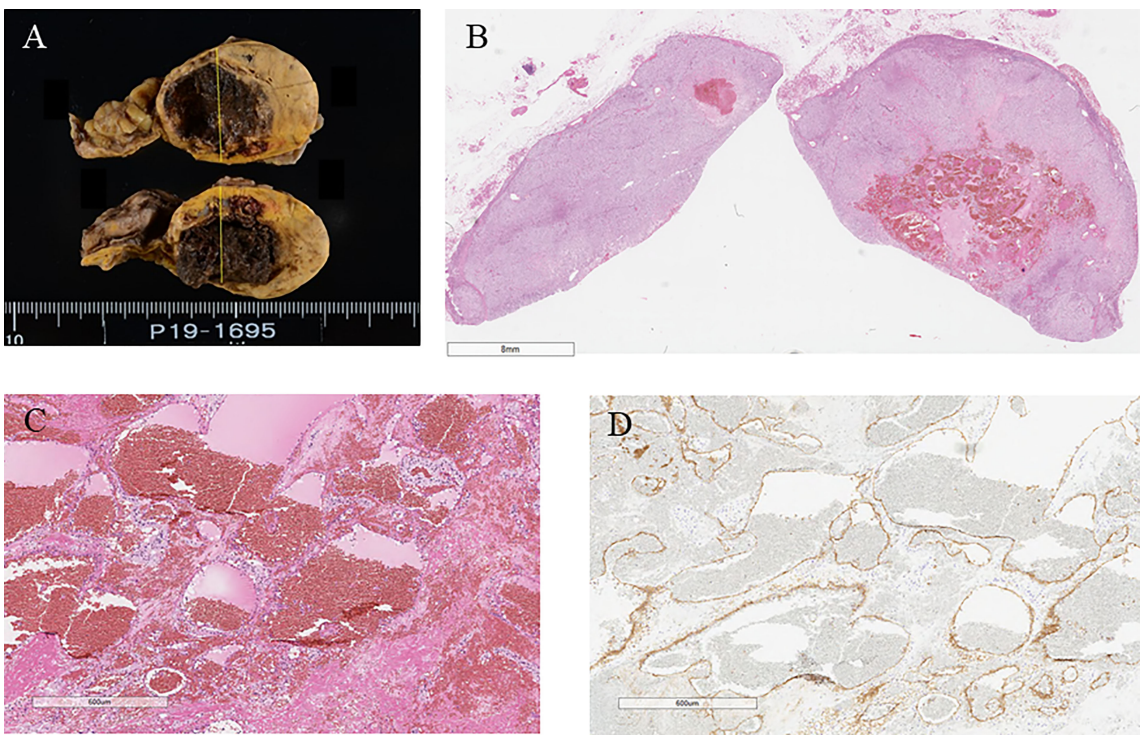


**FIGURE 2** | **(A)** Surgical specimen showing hemorrhage in the adrenal tumor. **(B)** Hematoxylin and eosin-stained tumor section showing hemorrhage in the tumor. **(C)** Hematoxylin and eosin-stained section on high magnification showing hemorrhage without vasculitis and ominous findings of infection (40×). **(D)** CD31 immunostaining (40×).

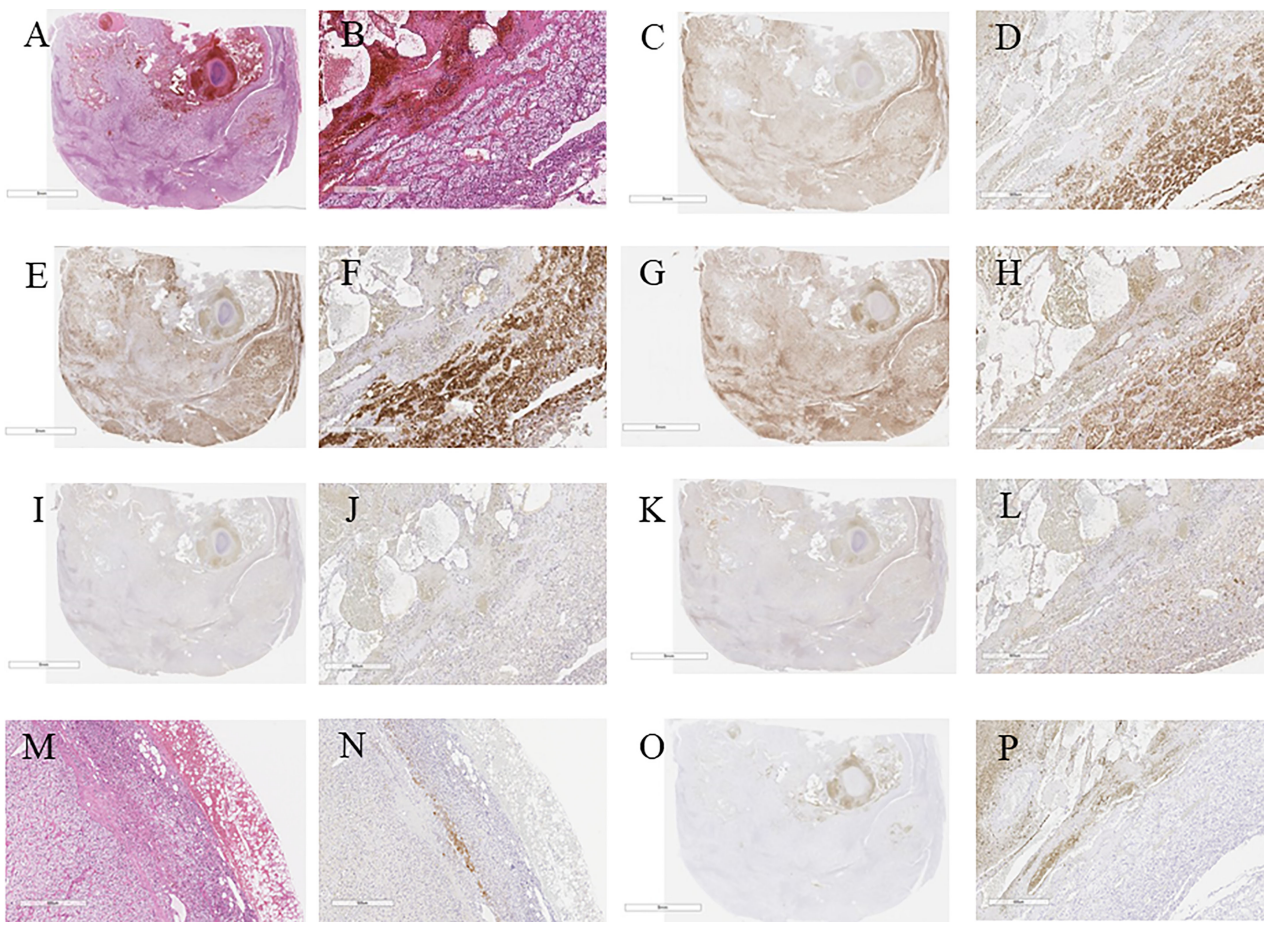


**FIGURE 3** | **(A)** Hematoxylin and eosin immunostaning. **(B)** Hematoxylin and eosin-stained tumor section on high magnification showing cortical adenoma (40×). **(C)** c17 immunostaining. **(D)** c17-stained tumor section on high magnification (40×). **(E)** HSD3B2 immunostaining. **(F)** HSDB2-stained tumor section on high magnification (40×). **(G)** CYP11B1 immunostaining. **(H)** CYP11B1-stained tumor section on high magnification (40×). **(I)** HSDB1 immunostaining. **(J)** HSDB1-stained tumor section on high magnification (40×). **(K)** DHEA-ST immunostaining. **(L)** DHEA-ST-stained tumor section on high magnification (40×). **(M)** Hematoxylin and eosin-stained concomitant adrenal tissue on high magnification (40×). **(N)** High magnification of DHEA-ST-stained concomitant adrenal tissue on high magnification (40×). **(O)** CYP11B2 immunostaining. **(P)** CYP11B2-stained tumor section on high magnification (40×).

scintigraphy. Abdominal CT and MRI revealed the intratumoral heterogeneity inside the tumor, which eventually turned out to be due to adrenal hemorrhage. Nevertheless, the patient did not complain of any abdominal pain. As for the $^{131}$I-adosterol adrenal scintigraphy, an adrenal gland with hemorrhage was reported to commonly demonstrate dissipation or decreased adosterol accumulation because of the impaired cortisol secretion. However, in our case, the adosterol accumulation on the right adrenal gland was markedly detected, while it was diminished on the left adrenal gland. In addition, her cortisol level became lower after tumor extirpation. Therefore, we considered the possibility that the right adrenal tumor could harbor autonomous cortisol secretion despite the fact that preoperative laboratory data was not necessarily diagnostic of full-brown CS and SCS.

The treatment of adrenal hemorrhage is not standardized because the clinical phenotypes varied (2). Izabela et al. demonstrated that patients with a shrinking tumor should not be the candidates for surgery (12). This is because some cases of the adrenal hemorrhage spontaneously reabsorb and recover from the hematoma, which makes follow-up imaging revaluation, such as abdominal MRI or CT, clinically justified. However, when the tumor enlarges, as in our present case, adrenalectomy may be warranted due to the potential of rupture. In addition, the case in our study had concomitant antiphospholipid syndrome. Espinosa et al. reported that patients having antiphospholipid antibody treated with anticoagulation therapy had a better prognosis than those without because antiphospholipid syndrome causes noninflammatory thrombotic microangiopathy in multiple organs (13). Satta et al. demonstrated a case in which adrenal insufficiency was the first clinical symptom of antiphospholipid syndrome and represented deep vein thrombosis 7 months after the diagnose of adrenal insufficiency (14). However, anticoagulation therapy has also been reported to cause adrenal haemorrhage (6). For instance,

McCroskey et al. reported patients with antiphospholipid syndrome who developed adrenal hemorrhage after anticoagulation therapy (15). Hence, appropriate anticoagulant therapy should be required for patients with antiphospholipid syndrome.

In our present case, we removed the right adrenal gland because of its enlargement and internal hemorrhage, possibly caused by the cortisol-secreting adenoma. Anticoagulation therapy was safely initiated after tumor extirpation, which improved her condition. There were no clinical evidence of thrombosis development in any of the organs for 3 years after the surgery. Therefore, acute adrenal insufficiency should be considered, particularly in bilateral adrenal hemorrhage (1, 2, 16–18). In addition, unilateral adrenal hemorrhage could also lead to adrenal insufficiency (19). In our present case, adrenal insufficiency due to adrenal hemorrhage did not occur preoperatively. However, postoperative adrenal insufficiency was expected because of the diminished adosterol accumulation in the left adrenal gland when performing preoperative $^{131}$I-adosterol adrenal scintigraphy. We carefully administered hydrocortisone postoperatively, and the patient did not experience any episodes of adrenal insufficiency. These findings indicated that $^{131}$I-adosterol adrenal scintigraphy should be performed preoperatively in similar cases to further evaluate for adrenal insufficiency due to adrenal hemorrhage and excessive cortisol secretion by the tumor.

The pathological findings also indicated that the tumor was a cortisol-secreting adenoma, although the laboratory data did not fulfill the clinical criteria of full-brown CS or SCS (7). Results of the careful pathological investigation of the resected adrenal specimens may explain this discrepancy. Few adrenocortical cells were positive for DHEA-ST, indicating that the amount of cortisol secreted from this tumor was not necessarily sufficient to suppress hypothalamo-pituitary-adrenal axis. In addition, immunoprofiles of steroidogenic enzymes in our present case were also consistent with results of previously reported studies, which could be consistent with the presence of autonomous cortisol secretion (20, 21). On the other hand, there was no evidence of aldosterone-secreting cells in the adrenal tumor and extirpated concomitant adrenal tissue, which was consistent with results of pre- and postoperative endocrinological investigations. The culprit lesion in the left adrenal gland was expected to cause primary aldosteronism, despite the absence of masses on imaging, but it awaits further investigations for clarification.

Two cases of adrenal hemorrhage that occurred in patients with cortisol-secreting adenoma have been reported in the literature (22, 23). However, there have been no previous reports of adrenal hemorrhage from thrombophilia due to antiphospholipid syndrome in cortisol-secreting adenoma. In our present case, hemorrhage in the tumor possibly caused by antiphospholipid syndrome was accurately diagnosed through both pathological and clinical investigations. Antiphospholipid syndrome was reported to represent 1–5% in the general population (24). Taking the prevalence of antiphospholipid syndrome into consideration, adrenal hemorrhage due to antiphospholipid syndrome should exist to some extent as the previous reports indicated (6, 13–15). In addition, there could be adrenal hemorrhage in patients with cortisol-secreting adenoma due to antiphospholipid syndrome like our present case. Hence, this case could provide important information as to the proper diagnosis and therapy toward similar cases in future. In addition, appropriate anticoagulant therapy for patients with antiphospholipid syndrome could possibly avoid adrenal hemorrhage, but it awaits further investigations for clarification.

In summary, we reported the first case showing adrenal hemorrhage in a cortisol-secreting adenoma due to thrombophilia secondary to antiphospholipid syndrome. The lesion was diagnosed clinically and pathologically, following the diagnosis of adrenal incidentaloma and subsequent adrenalectomy. Even though the adrenal incidentaloma is diagnosed as a non-functional tumor based on specific endocrinological criteria, periodic follow-up must be performed, particularly in the cases with slight endocrine abnormalities. Our present case also highlighted the importance of histopathological evaluation of resected adrenal glands to accurately diagnose the unusual clinical and/or radiological changes detected in the adrenal.

## DATA AVAILABILITY STATEMENT

The original contributions presented in the study are included in the article. Further inquiries can be directed to the corresponding author.

## ETHICS STATEMENT

Ethical review and approval was not required for the study on human participants in accordance with the local legislation and institutional requirements. The patients/participants provided their written informed consent to participate in this study. Written informed consent was obtained from the individual(s) for the publication of any potentially identifiable images or data included in this article.

## AUTHOR CONTRIBUTIONS

KO and IA originally drafted this manuscript and prepared the figures. KO, IA, MY, YS, KT, MK, YukY, TS, TK, YT, and KK performed the clinical investigations. YutY, SH, and HS performed the pathological investigations. YF, SM, HT, and TI performed the experiments. AL, HS, and KK reviewed the manuscript. All authors contributed to the article and approved the submitted version.

## ACKNOWLEDGMENTS

We thank Ms. Yumi Iriguchi for her secretarial assistance.

## REFERENCES


1. Simon DR, Palese MA. Clinical Update on the Management of AdrenalHemorrhage. *Curr Urol* (2009) 10:78–83. doi: 10.1007/s11934-009-0014-y
2. Karwacka IM, Obołończyk Ł, Sworczak K. Adrenal Hemorrhage: A Single Center Experience and Literature Review. *Adv Clin Exp Med* (2018) 27:681–7. doi: 10.17219/acem/68897
3. Jimidar N, Ysebaert D, Twickler M, Spinhoven M, Dams K, Jorens PG. Bilateral Adrenal Hemorrhage After a High Energetic Trauma: A Case Report and Review of Current Literature. *Acta Chir Belg* (2020) 120:131–5. doi: 10.1080/00015458.2018.1515339
4. Frankel M, Feldman I, Levine M, Frank Y, Bogot NR, Benjaminov O, et al. Bilateral Adrenal Hemorrhage in Coronavirus Disease 2019 Patient: A Case Report. *J Clin Endocrinol Metab* (2020) 105:dgaa487. doi: 10.1210/clinem/dgaa487
5. Guarner J, Paddock CD, Bartlett J, Zaki SR. Adrenal Gland Hemorrhage in Patients With Fatal Bacterial Infections. *Mod Pathol* (2008) 21:1113–20. doi: 10.1038/modpathol.2008.98
6. Saleem N, Khan M, Parveen S, Balavenkatraman A. Bilateral Adrenal Hemorrhage: A Cause of Haemodynamic Collapse in Heparin-Induced Thrombocytopaenia. *BMJ Case Rep* (2016) 2016:bcr2016214679. doi: 10.1136/bcr-2016-214679
7. Abe I, Sugimoto K, Miyajima T, Ide T, Minezaki M, Takeshita K, Tamura N, et al. Clinical Investigation of Adrenal Incidentalomas in Japanese Patients of the Fukuoka Region With Updated Diagnostic Criteria for Sub-Clinical Cushing's Syndrome. *Intern Med* (2018) 57:2467–72. doi: 10.2169/internalmedicine.0550-17
8. Nishikawa T, Omura M, Satoh F, Shibata H, Takahashi K, Tamura N, et al. Guidelines for the Diagnosis and Treatment of Primary Aldosteronism–the Japan EndocrineSociety 2009. *Endocr J* (2011) 58:711–21. doi: 10.1507/endocrj.ej11-0133
9. Lam AK. Update on Adrenal Tumours in 2017 World Health Organization (WHO) of Endocrine Tumours. *Endocr Pathol* (2017) 28:213–27. doi: 10.1007/s12022-017-9484-5
10. Kolinioti A, Tsimaras M, Stravodimos G, Komporozos V. Acute Adrenal Insufficiency Due to Adrenal Hemorrhage Complicating Colorectal Surgery: Report of Two Cases and Correlation With the Antiphospholipid Antibody Syndrome. *Int J Surg Case Rep* (2018) 51:90–4. doi: 10.1016/j.ijscr.2018.07.034
11. Vella A, Nippoldt TB, Morris JC3rd. Adrenal Hemorrhage: A 25-Year Experience at the Mayo Clinic. *Mayo Clin Proc* (2001) 76:161–8. doi: 10.1016/S0025-6196(11)63123-6
12. Karwacka IM, Obołończyk Ł, Sworczak K. Adrenal Hemorrhage: A Single Center Experience and Literature Review. *Adv Clin Exp Med* (2018) 27:681–7. doi: 10.17219/acem/68897
13. Espinosa G, Santos E, Cervera R, Piette JC, de la Red G, Gil V, et al. Adrenal Involvement in the Antiphospholipid Syndrome: Clinical and Immunologic Characteristics of 86 Patients. *Medicine* (2003) 82:106–18. doi: 10.1097/00005792-200303000-00005
14. Satta MA, Corsello SM, Della Casa S, Rota CA, Pirozzi B, Colasanti S, et al. Adrenal Insufficiency as the First Clinical Manifestation of the Primary Antiphospholipid Antibody Syndrome. *Clin Endocrinol (Oxf)* (2000) 52:123–6. doi: 10.1046/j.1365-2265.2000.00903.x
15. McCroskey RD, Phillips A, Mott F, Williams EC. Antiphospholipid Antibodies and Adrenal Hemorrhage. *Am J Hematol* (1991) 36:60–2. doi: 10.1002/ajh.2830360113
16. Ramon I, Mathian A, Bachelot A, Hervier B, Haroche J, Boutin-Le Thi Huong D, et al. Primary Adrenal Insufficiency Due to Bilateral Adrenal Hemorrhage-Adrenal Infarction in the Antiphospholipid Syndrome: Long-Term Outcome of 16 Patients. *J Clin Endocrinol Metab* (2013) 98:3179–89. doi: 10.1210/jc.2012-4300
17. Siu SC, Kitzman DW, Sheedy PF2nd, Northcutt RC. Adrenal Insufficiency From Bilateral Adrenal Hemorrhage. *Mayo Clin Proc* (1990) 65:664–70. doi: 10.1016/s0025-6196(12)65129-5
18. Fakih H, Beel BC, Shychuk A, Ataya A. Bilateral Adrenal Hemorrhage. *Intens Care Med* (2017) 43:447–8. doi: 10.1007/s00134-016-4587-x
19. Ly BA, Quintero L. Adrenal Insufficiency From Unilateral Adrenal Hemorrhage in a Patient on Rivaroxaban Thromboprophylaxis. *AACE Clin Case Rep* (2019) 5:e70–2. doi: 10.4158/ACCR-2018-0340
20. Sasano H, Suzuki T, Nagura H, Nishikawa T. Steroidogenesis in Human Adrenocortical Carcinoma: Biochemical Activities, Immunohistochemistry, and *In Situ* Hybridization of Steroidogenic Enzymes and Histopathologic Study in Nine Cases. *Hum Pathol* (1993) 24:397–404. doi: 10.1016/0046-8177(93)90088-X
21. Pereira SS, Costa MM, Gomez-Sanchez CE, Monteiro MP, Pignatelli D. Incomplete Pattern of Steroidogenic Protein Expression in Functioning Adrenocortical Carcinomas. *Biomedicines* (2020) 8:256. doi: 10.3390/biomedicines8080256
22. Saito T, Kurumada S, Kawakami Y, Go H, Uchiyama T, Ueki K. Spontaneous Hemorrhage of an Adrenal Cortical Adenoma Causing Cushing's Syndrome. *Urol Int* (1996) 56:105–6. doi: 10.1159/000282821
23. Redman JF, Faas FH. Acute Unilateral Adrenal Hemorrhage Following ACTH Administration in a Patient With Cushing's Syndrome. *Am J Med* (1976) 61:533–6. doi: 10.1016/0002-9343(76)90333-8
24. Oliveira DC, Correia A, Oliveira C. The Issue of the Antiphospholipid Antibody Syndrome. *J Clin Med Res* (2020) 12:286–92. doi: 10.14740/jocmr4154


**Conflict of Interest:** The authors declare that the research was conducted in the absence of any commercial or financial relationships that could be construed as a potential conflict of interest.

frontiers in Endocrinology

ORIGINAL RESEARCH
published: 24 February 2022
doi: 10.3389/fendo.2022.762589

# Recent Trends in the Incidence of Clear Cell Adenocarcinoma and Survival Outcomes: A SEER Analysis

*Yadong Guo[1,2†], Anil Shrestha[3†], Niraj Maskey[1,2†], Xiaohui Dong[4†], Zongtai Zheng[1,2], Fuhan Yang[1,2], Ruiliang Wang[1,2], Wenchao Ma[1,2], Ji Liu[1,2], Cheng Li[1,2], Wentao Zhang[1,2], Shiyu Mao[1,2], Aihong Zhang[5*], Shenghua Liu[1,2*] and Xudong Yao[1,2*]*

[1] Department of Urology, Shanghai Tenth People's Hospital, Tongji University, Shanghai, China, [2] Urologic Cancer Institute, Tongji University School of Medicine, Shanghai, China, [3] Department of Urology, National Academy of Medical Sciences, Bir Hospital, Kathmandu, Nepal, [4] Department of General Medical, Shanghai Fourth People's Hospital, Tongji University, Shanghai, China, [5] Department of Medical Statistics, Tongji University School of Medicine, Shanghai, China

**Background:** Clear cell adenocarcinoma (CCA) is considered a relatively rare tumor with a glycogen-rich phenotype. The prognosis of CCA patients is unclear. In this study, recent trends in the epidemiological and prognostic factors of CCA were comprehensively investigated.

**Methods:** Patients with CCA from years 2000 to 2016 were identified from the Surveillance, Epidemiological, and End Results (SEER) database. Relevant population data were used to analyze the rates age-adjusted incidence, age-standardized 3-year and 5-year relative survivals, and overall survival (OS).

**Results:** The age-adjusted incidence of CCA increased 2.7-fold from the year 2000 (3.3/100,000) to 2016 (8.8/100,000). This increase occurred across all ages, races, stages, and grades. Of all these subgroups, the increase was largest in the grade IV group. The age-standardized 3-year and 5-year relative survivals increased during this study period, rising by 9.1% and 9.5% from 2000 to 2011, respectively. Among all the stages and grades, the relative survival increase was greatest in the grade IV group. According to multivariate analysis of all CCA patients, predictors of OS were: age, gender, year of diagnosis, marital status, race, grade, stage, and primary tumor site ($P < 0.001$). The OS of all CCA patients during the period 2008 to 2016 was significantly higher than that from 2000 to 2007 ($P < 0.001$).

**Conclusions:** The incidence of CCA and survival of these patients improved over time. In particular, the highest increases were reported for grade IV CCA, which may be due to an earlier diagnosis and improved treatment.

**Keywords: clear cell adenocarcinoma, SEER database, incidence, survival, glycogen-rich phenotype**

OPEN ACCESS

***Edited by:***
*Antongiulio Faggiano, Sapienza University of Rome, Italy*

***Reviewed by:***
*Vincenzo Marotta, AOU S. Giovanni di Dio e Ruggi D'Aragona, Italy*
*Dianwen Song, Shanghai General Hospital, China*

***Correspondence:**
*Aihong Zhang*
*zhangah@tongji.edu.cn*
*Shenghua Liu*
*liushenghuafy@163.com*
*Xudong Yao*
*yaoxudong1967@163.com*

*†These authors have contributed equally to this work*

***Specialty section:***
*This article was submitted to Cancer Endocrinology, a section of the journal Frontiers in Endocrinology*

***Received:*** *22 August 2021*
***Accepted:*** *14 January 2022*
***Published:*** *24 February 2022*

***Citation:***
*Guo Y, Shrestha A, Maskey N, Dong X, Zheng Z, Yang F, Wang R, Ma W, Liu J, Li C, Zhang W, Mao S, Zhang A, Liu S and Yao X (2022) Recent Trends in the Incidence of Clear Cell Adenocarcinoma and Survival Outcomes: A SEER Analysis. Front. Endocrinol. 13:762589. doi: 10.3389/fendo.2022.762589*

## BACKGROUND

Clear cell carcinoma (CCA) consists of a series of malignant tumors, likely caused by abnormal deposition of glycogen (1). Glycogen is a branched-chain polysaccharide composed of glucose that is necessary to maintain homeostasis of normal cell metabolism, but can promote tumor growth, especially under adverse conditions (2–4). Studies have shown that hypoxia within the centers of solid tumors leads to an increase in glycogen storage, allowing adaptation to low oxygen levels and lack of nutrients. The possible mechanism involves hypoxia-inducible factor 1α (HIF-1α)-mediated signaling pathways (4, 5). Therefore, the regulation of glycogen synthesis and degradation is crucial for cellular homeostasis. In recent years, more and more studies have emphasized that reprogramming of glycogen metabolism affects the occurrence and progression of malignant tumors; hence, it has become a recognized feature of tumor cells (6, 7). Although a few drugs targeting glycogen metabolism are currently being tested as a component of comprehensive treatment for tumors, they have not yet been approved for clinical application (8, 9).

There is evidence that CCA shows striking similarities in the gene expression profiles of various organs (10). In addition, histological staining of CCA tumors shows "clear cells" with a transparent and oval appearance that are rich in cytoplasmic glycogen. Since CAA has no obvious symptoms, its diagnosis is based on histopathological identification of these characteristics. Previous research also suggests a link between glycogen-rich tumors and tumor aggressiveness, and CCA of the kidney, ovary, and bladder have a poor prognosis and are resistant to treatment (11–14). In addition, although studies have described the effect of CCA on the prognosis of some cancer patients, the epidemiology and survival of CCA patients in the general population have not been well described. Therefore, in this study, we attempted to perform the most complete analysis of the incidence, patient demographics, and prognostic factors of CCA using data from the Surveillance, Epidemiological, and End Results (SEER) program.

## METHODS

### Database and Patient Selection

The SEER program is the definitive source of cancer incidence and survival data collected by the National Cancer Institute, covering approximately 34.6% of the US population. Our study used the SEER 18 database and identified all malignancies that were diagnosed as CCA between 1 January 2000 and 31 December 2016: kidney and renal pelvis (KRP); ovary; cervix and corpus uteri; lung and bronchus; urinary bladder; vagina; pancreas; breast; peritoneum, omentum, and mesentery (POM); prostate; and liver. The CD-O-3 histology code was used to identify CCA. This code corresponds to the following clinical/histological diagnoses: 8310/2, 8310/3, and 8313/3. The following information was collected from the database: primary tumor site; ICD-O-3 histology; age at diagnosis; gender; marital status; race; grade; tumor stage in 2000; and sites of metastasis at diagnosis (bone, brain, liver, and lung from years 2010 to 2016). Studies with a lack of survival data or fewer than 50 CCA solid tumors were excluded. The final cohort included 104,206 patients.

**Abbreviations:** CCA, clear cell adenocarcinoma; HR, hazard ratio; KRP, kidney and renal pelvis; OS, overall survival; POM, peritoneum, omentum, and mesentery; SEER, Surveillance, Epidemiological, and End Results.

### Statistical Analysis

SEER*Stat software (version 8.3.6, National Cancer Institute Surveillance Research Program) was used to calculate the age-adjusted incidence and age-standardized relative survival. Incidence and relative survival were standardized to the 2000 United States general population.

All statistical analyses were performed using IBM SPSS v25.0 software (International Business Machines, Armonk, NY, USA). The data were analyzed to produce figure using Microsoft Excel software. Differences in demographic and clinical characteristics of different primary tumor sites were determined using Pearson's chi-squared test. Overall survival (OS) was generated using the Kaplan-Meier curves and the difference in survival between groups was assessed using a log-rank test. A multivariate Cox proportional hazards regression model was used to estimate the 3-year, 5-year, and OS for all patients, respectively. Two-tailed $P$ values < 0.05 were considered statistically significant.

## RESULTS

### Annual Incidence of CCA

To assess the recent trends in CCA incidence, we identified all CCA cases from 2000 to 2016 in the SEER database. As shown in **Figure 1A**, the incidence of age-adjusted CCA was 3.3 per 100,000 persons in 2000, and increased to 8.8 per 100,000 persons in 2016; for comparison, the annual age-adjusted incidence of all malignancies is also depicted.

In addition, we divided all CCA cases into different subgroups based on the age and race of the patient as well as grade and stage of the tumor. First, the age-specific incidence was calculated for three age groups: <60 years, 60–69 years, and >70 years. As shown in **Figure 1B**, the incidence of CCA increased dramatically from 2000 to 2016 in patients aged <60 years, with nearly a 3-fold rise to 4.7 per 100,000 persons; among those aged 60–69 years or >70 years, there was a more modest increase of 2.5-fold.

Among the tumor grade groups, the most dramatic rise in incidence was described in patients with grade IV CCA (from 0.1 per 100,000 persons in 2000, to 0.7 per 100,000 persons in 2016; **Figure 1C**). Among the tumor stage groups, the incidence of localized CCA increased the most relative to regional or distant (from 2 per 100,000 persons in 2000 to 6.2 per 100,000 persons in 2016; **Figure 1D**). Among the ethnic groups, the incidence of CCA increased the most in Caucasians (from 2.1 per 100,000 persons in 2000 to 8.4 per 100,000 persons in 2016; **Figure 1E**).

Overall, according to the SEER 18 data, the incidence of CCA cases diagnosed increased statistically significantly from 2000 to 2016 (annual percent change (APC): 4.6, 95% confidence interval (CI) [3.4, 5.7], $P < 0.05$).

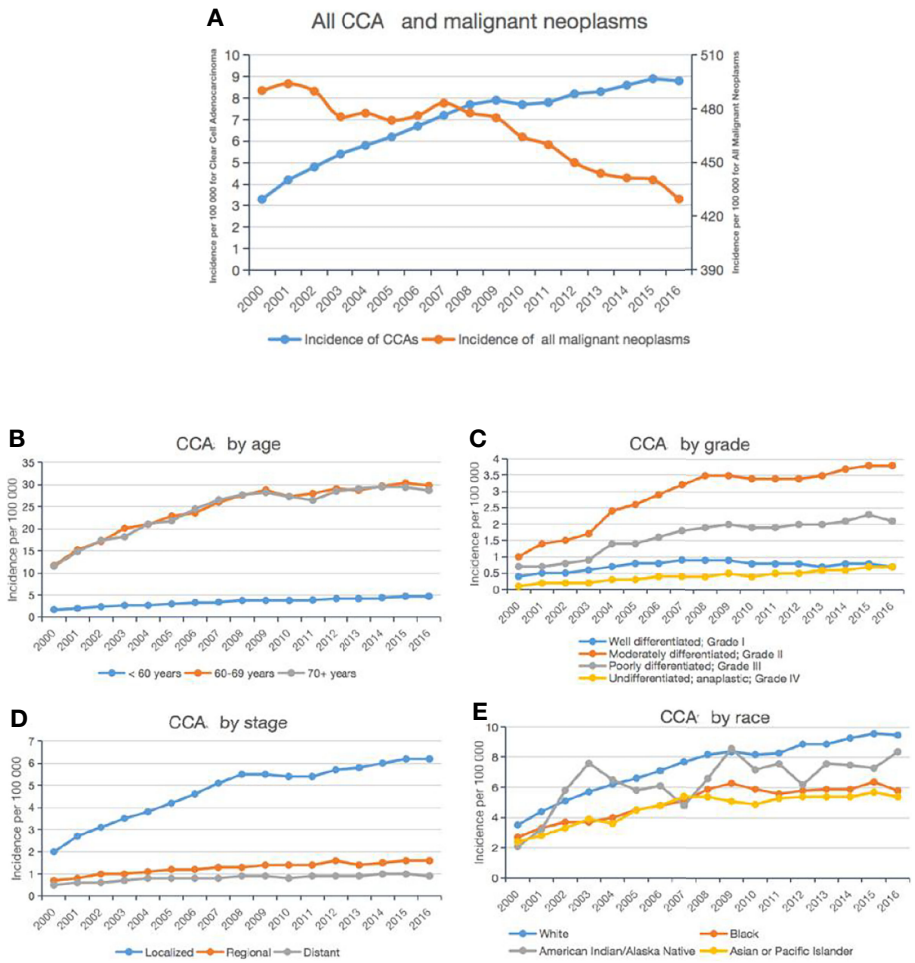


**FIGURE 1** | Incidence trends of CCA from 2000 to 2016. Annual age-adjusted incidence of all CCA cases and all malignant neoplasms **(A)**. Annual age-adjusted incidence of CCA by age group **(B)**, stage **(C)**, grade **(D)**, and ethnicity **(E)**.

## Patient Characteristics

To compare the demographic and clinical characteristics of CCA at the different primary tumor sites, we analyzed 104,206 CCA patients identified in the SEER database (**Table 1**). We found that the median age of these patients at diagnosis was 62 years (range: 53–71 y), and the median OS was 46 months (range: 17–91 mo). Comparing the different primary tumor sites, the lowest median age at diagnosis (56 y) was that of patients with ovarian CCA, and the highest (71 years) was for patients with bladder CCA.

The primary tumor site in these patients was significantly associated with the age at diagnosis ($P < 0.001$; **Table 1**). Patients aged ≥61 years were more likely to develop primary CCA of the KRP, corpus and cervix uteri, lungs, bladder, pancreas, prostate, or liver; while patients aged 31-60 years were more likely to have CCA of the POM. Moreover, the tumor grade was significantly different between the various primary tumor sites ($P < 0.001$; **Table 1**): patients with grade II tumors were more likely to have CCA of the KRP; while patients with grade III tumors were more likely to have CCA of the corpus and cervix uteri, lungs, breast, or prostate.

The tumor stage was significantly different between the various primary tumor sites ($P = 0.001$; **Table 1**): localized CCA was more likely to be in the KRP, ovary, cervix uteri, breast, prostate, or liver; while distant CCA was more likely to be in the lungs or pancreas. In addition, we determined that the metastatic sites differed depending on the type of CCA. Patients with CCA of the KRP, cervix uteri, or vagina were most likely to have lung metastases; patients with CCA of the ovary, bladder, or pancreas were more prone to have liver metastases; and patients with CCA of the lung, breast, or prostate were tended to have bone metastases (**Figure 2**).

## Survival

We identified the latest trends in the survival of all CCA cases from 2000 to 2011 in the SEER database, relative to the general population. As shown in **Figure 3A**, the age-standardized 3-year and 5-year relative survivals increased from 2000 to 2011, rising by 9.1% and 9.5%, respectively. Specifically, when we examined the CCA cases by grade (**Figures 3B, C**), we found that the age-

**TABLE 1 |** Descriptive demographic and clinical characteristics of patients with CCA according to primary tumor site*.

| Covariate | Total | KRP | Ovary | Corpus Uteri | Lung | Cervix Uteri | Bladder | Vagina | Pancreas | Breast | POM | Prostate | Liver | P value |
|---|---|---|---|---|---|---|---|---|---|---|---|---|---|---|
| **n** | 104206 | 94882 | 4750 | 2557 | 914 | 496 | 133 | 112 | 92 | 89 | 68 | 59 | 54 | |
| **Age (%)** | | | | | | | | | | | | | | <0.001 |
| ≤30 | 926 (0.9) | 843 (0.9) | 26 (0.5) | 4 (0.2) | 1 (0.1) | 46 (9.3) | 2 (1.5) | 4 (3.6) | 0 (0.0) | 0 (0.0) | 0 (0.0) | 0 (0.0) | 0 (0.0) | |
| 31-60 | 46677 (44.8) | 42269 (44.5) | 3102 (65.3) | 590 (23.1) | 265 (29.0) | 233 (47.0) | 37 (27.8) | 48 (42.9) | 25 (27.2) | 46 (51.7) | 36 (52.9) | 14 (23.7) | 12 (22.2) | |
| ≥61 | 56603 (54.3) | 51770 (54.6) | 1622 (34.1) | 1963 (76.8) | 648 (70.9) | 217 (43.8) | 94 (70.7) | 60 (53.6) | 67 (72.8) | 43 (48.3) | 32 (47.1) | 45 (76.3) | 42 (77.8) | |
| **Gender, n (%)** | | | | | | | | | | | | | | <0.001 |
| Male | 59587 (57.2) | 58935 (62.1) | 0 (0.0) | 0 (0.0) | 452 (49.5) | 0 (0.0) | 60 (45.1) | 0 (0.0) | 49 (53.3) | 1 (1.1) | 0 (0.0) | 59 (100.0) | 31 (57.2) | |
| Female | 44619 (42.8) | 35947 (37.9) | 4750 (100.0) | 2557 (100.0) | 462 (50.5) | 496 (100.0) | 73 (54.9) | 112 (100.0) | 43 (46.7) | 88 (98.9) | 68 (100.0) | 0 (0.0) | 23 (42.6) | |
| **Year of diagnosis, n (%)** | | | | | | | | | | | | | | <0.001 |
| 2000–2007 | 34615 (33.2) | 30439 (32.1) | 2043 (43.0) | 1017 (39.8) | 543 (59.4) | 228 (46.0) | 59 (44.4) | 57 (50.9) | 46 (50.0) | 57 (50.9) | 37 (54.4) | 50 (84.7) | 39 (72.2) | |
| 2008–2016 | 69591 (66.8) | 64443 (67.9) | 2707 (57.0) | 1540 (60.2) | 371 (40.6) | 268 (54.0) | 74 (55.6) | 55 (49.1) | 46 (50.0) | 32 (49.1) | 31 (45.6) | 9 (15.3) | 15 (27.8) | |
| **Marital (%)** | | | | | | | | | | | | | | <0.001 |
| Married | 64284 (61.7) | 59559 (62.8) | 2557 (53.8) | 1160 (45.4) | 490 (53.6) | 208 (41.9) | 49 (36.8) | 55 (49.1) | 55 (59.8) | 42 (47.2) | 37 (54.4) | 41 (69.5) | 31 (57.4) | |
| Widowed/Divorced | 20294 (19.5) | 17936 (18.9) | 877 (18.5) | 913 (35.7) | 270 (29.5) | 127 (25.6) | 49 (36.8) | 31 (27.7) | 25 (27.2) | 25 (28.1) | 20 (29.4) | 7 (11.9) | 14 (25.9) | |
| Single | 14864 (14.3) | 13041 (13.7) | 1126 (23.7) | 348 (13.6) | 126 (13.8) | 136 (27.4) | 19 (14.3) | 18 (16.1) | 10 (10.9) | 17 (19.1) | 8 (11.8) | 7 (11.9) | 8 (14.8) | |
| Unknown | 4764 (4.6) | 4346 (4.6) | 190 (4.0) | 136 (5.3) | 28 (3.1) | 25 (5.0) | 16 (12.0) | 8 (7.1) | 2 (2.2) | 5 (5.6) | 3 (4.4) | 4 (6.8) | 1 (1.9) | |
| **Race, n(%)** | | | | | | | | | | | | | | <0.001 |
| White | 88231 (84.7) | 80971 (85.3) | 3709 (78.1) | 1902 (74.4) | 785 (85.9) | 396 (79.8) | 108 (81.2) | 76 (67.9) | 81 (88.0) | 69 (77.5) | 53 (77.9) | 47 (79.7) | 34 (63.0) | |
| Black | 7693 (7.4) | 6869 (7.2) | 194 (4.1) | 410 (16.0) | 88 (9.6) | 51 (10.3) | 21 (15.8) | 21 (18.8) | 6 (6.5) | 9 (10.1) | 6 (8.8) | 10 (16.9) | 8 (14.8) | |
| Other | 7633 (7.3) | 6427 (6.8) | 832 (17.5) | 232 (9.1) | 39 (4.3) | 48 (9.7) | 4 (3.0) | 14 (12.5) | 5 (5.4) | 10 (11.2) | 9 (13.2) | 1 (1.7) | 12 (22.2) | |
| Unknown | 649 (0.6) | 615 (0.6) | 15 (0.3) | 13 (0.5) | 2 (0.2) | 1 (0.2) | 0 (0.0) | 1 (0.9) | 0 (0.0) | 1 (1.1) | 0 (0.0) | 1 (1.7) | 0 (0.0) | |
| **Grading, n (%)** | | | | | | | | | | | | | | <0.001 |
| I | 10823 (10.4) | 10666 (11.2) | 53 (1.1) | 42 (1.6) | 33 (3.6) | 13 (2.6) | 0 (0.0) | 1 (0.9) | 4 (4.3) | 1 (1.1) | 1 (1.5) | 2 (3.4) | 7 (13.0) | |
| II | 43452 (41.7) | 42604 (44.9) | 397 (8.4) | 149 (5.8) | 164 (17.9) | 47 (9.5) | 7 (5.3) | 8 (7.1) | 14(15.2) | 34 (38.2) | 2 (2.9) | 18 (30.5) | 8 (14.8) | |
| III | 24787 (23.8) | 21250 (22.4) | 1613 (34.0) | 1199 (46.9) | 349 (38.2) | 191 (38.5) | 36 (27.1) | 26 (23.2) | 19 (20.7) | 40 (44.9) | 23 (33.8) | 32 (54.2) | 9 (16.7) | |
| IV | 6457 (6.2) | 5019 (5.3) | 806 (17.0) | 456 (17.8) | 31 (3.4) | 79 (15.9) | 40 (30.1) | 13 (11.6) | 0 (0.0) | 2 (2.2) | 9 (13.2) | 2 (3.4) | 0 (0.0) | |
| Unknown | 18687 (17.9) | 15343 (16.2) | 1881 (39.6) | 711 (27.8) | 337 (36.9) | 166 (33.5) | 50 (37.6) | 64 (57.1) | 55 (59.8) | 12 (13.5) | 33 (48.5) | 5 (8.5) | 30 (55.6) | |
| **Stage, n (%)** | | | | | | | | | | | | | | 0.001 |
| Local | 71561 (68.7) | 68150 (71.8) | 1655 (34.8) | 1075 (42.0) | 273 (29.9) | 210 (42.3) | 75 (56.4) | 0 (0.0) | 5 (5.4) | 59 (66.3) | 0 (0.0) | 36 (61.0) | 23 (42.6) | |
| Regional | 19183 (18.4) | 15925 (16.8) | 1756 (37.0) | 925 (36.2) | 284 (31.1) | 196 (39.5) | 24 (18.0) | 0 (0.0) | 30 (32.6) | 23 (25.8) | 0 (0.0) | 10 (16.9) | 10 (18.5) | |
| Distant | 12257 (11.8) | 9990 (10.5) | 1288 (27.1) | 457 (17.9) | 339 (37.1) | 78 (15.7) | 23 (17.3) | 0 (0.0) | 53 (57.6) | 6 (6.7) | 0 (0.0) | 11 (18.6) | 12 (22.2) | |
| Unknown | 1205 (1.2) | 817 (0.9) | 51 (1.1) | 100 (3.9) | 18 (2.0) | 12 (2.4) | 11 (8.3) | 112 (100.0) | 4 (4.3) | 1 (1.1) | 68 (100.0) | 2 (3.4) | 9 (16.7) | |

**Reported as n (%), unless indicated otherwise.*

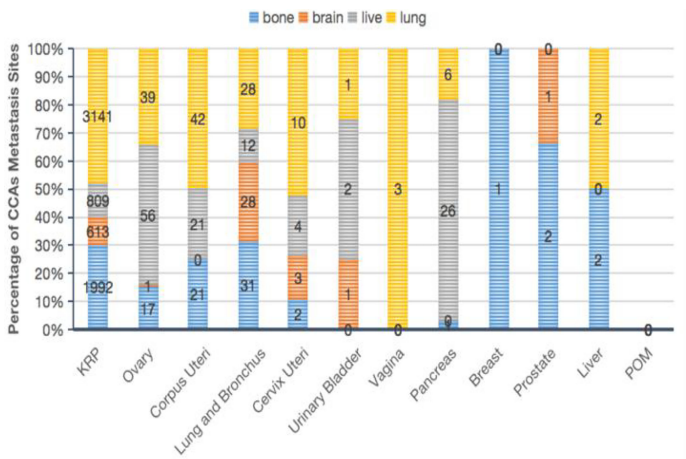


**FIGURE 2** | Characteristics of CCA patients according to the primary tumor site. Proportion of metastatic sites in the bone, brain, liver, or lung (B).

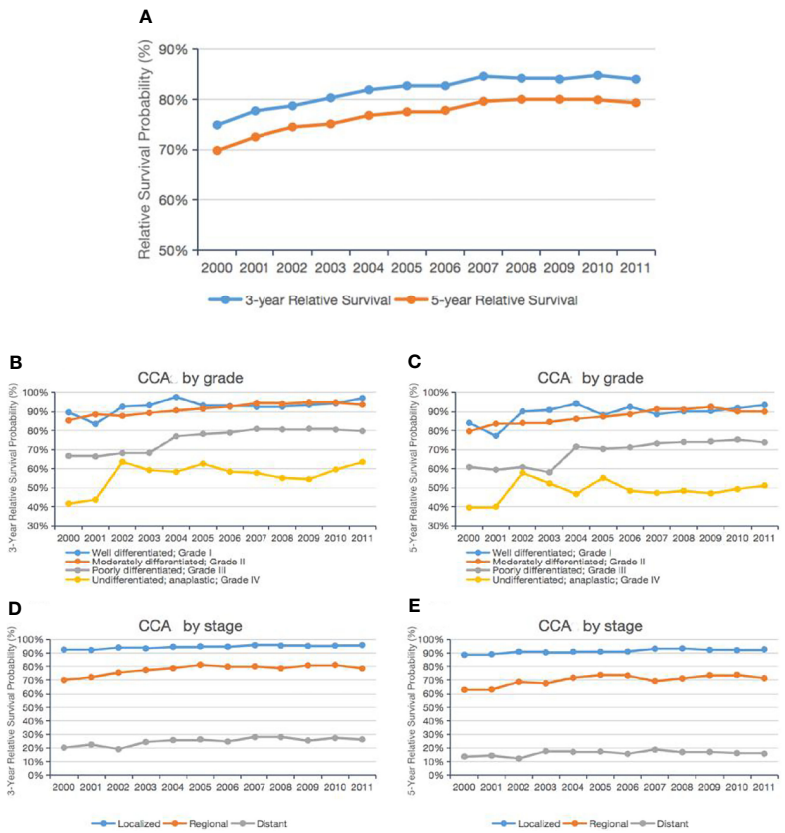


**FIGURE 3** | Trends in the 3-year and 5-year relative survival probabilities of CCA patients from 2000 to 2011. Trends in the 3-year and 5-year relative survival probabilities of all CCA patients **(A)**. Trends in the 3-year and 5-year relative survival probabilities of CCA patients by grade **(B, C)** and stage **(D, E)**.

standardized 3-year and 5-year relative survivals of patients with grade I CCA increased from 89.6% and 84.0% in 2000 to 98.1% and 96.0% in 2011, respectively. Meanwhile, the age-standardized 3-year and 5-year relative survivals of patients with grade II CCA slightly improved from 85.4% and 79.7% in 2000 to 93.6% and 90.0% in 2011, respectively.

Those with grade III–IV CCA showed an even greater improvement: the 3-year and 5-year relative survivals of grade

III patients increased from 66.7% and 41.6% in 2000 to 79.8% and 63.5% in 2011, respectively. The 3-year and 5-year relative survivals of the grade IV patients increased from 60.9% and 39.6% in 2000 to 73.8% and 51.1% in 2011. When we examined the age-standardized 3-year and 5-year relative survivals by tumor stage, we found that the relative survival of patients with localized, regional, or distant tumors had improved slightly over time (**Figures 3D, E**).

The age-standardized 3-year and 5-year survivals of the CCA patients relative to the general population and according to the primary tumor site were analyzed (**Figure 4A**). The largest change in 3-year to 5-year survival was for CCA of the POM (46.8% to 32.2%) or prostate (72.3% to 59.2%), and the smallest change was for CCA of the pancreas (11.4% to 8.3%) or KRP (85.6% to 81.1%). We examined the known 3-year and 5-year relative survivals of CCA of different primary tumor sites according to the tumor stage (**Figures 4B, C**). The best 5-year relative survival for regional and distant tumors was for patients with ovarian CCA.

We performed a multivariate analysis and calculated the hazard ratio for OS (**Table 2**). Age, gender, year of diagnosis, marital status, ethnicity, grade, stage, and primary tumor site

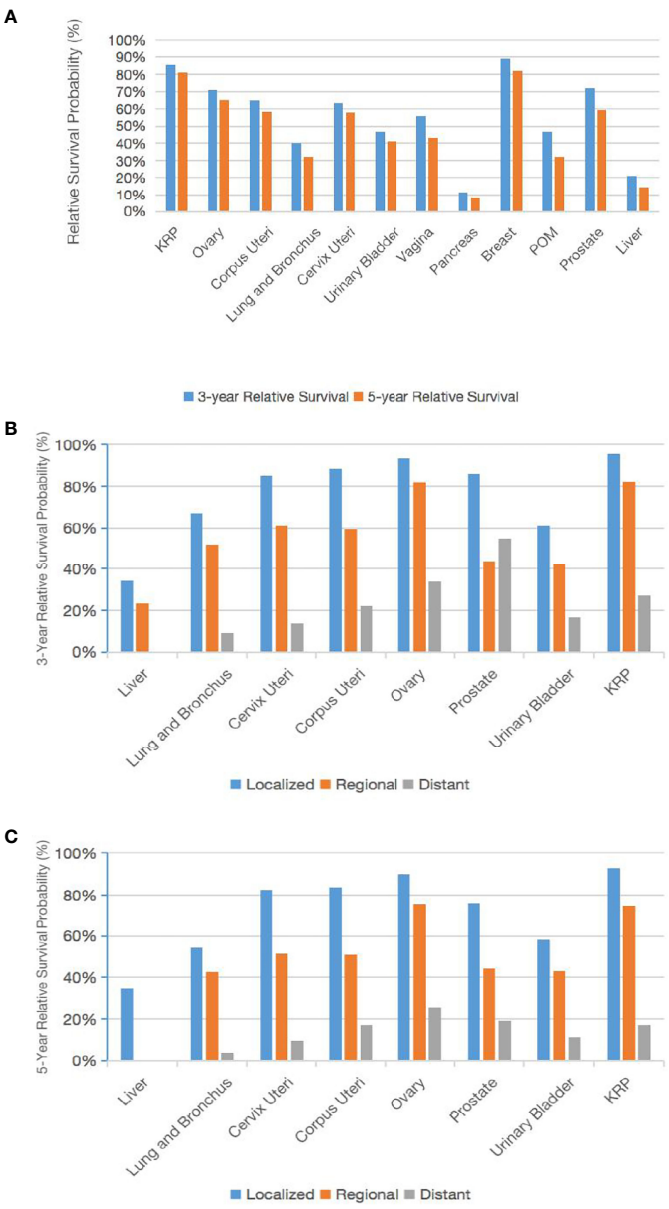


**FIGURE 4** | Trends in the 3-year and 5-year relative survival probabilities according to the primary tumor site. Trends in the 3-year and 5-year relative survival probabilities of patients with CCA at various primary tumor sites **(A)**. Trends in the 3-year and 5-year relative survival probabilities by stage **(B, C)**.

**TABLE 2 |** Multivariate survival analysis of patients with CCA receiving diagnoses from 2000 to 2016.

| Covariate | Overall Survival | | 3-Year Survival | | 5-Year Survival | |
|---|---|---|---|---|---|---|
| | HR | P value | HR | P value | HR | P value |
| **Age,y** | | <0.001 | | <0.001 | | <0.001 |
| ≤30 | 1.00 (ref.) | | 1.00 (ref.) | | 1.00 (ref.) | |
| 31-60 | 2.76 (2.16-3.52) | <0.001 | 1.66 (1.23-2.23) | 0.001 | 1.94 (1.48-2.55) | <0.001 |
| ≥61 | 5.63 (4.41-7.19) | <0.001 | 2.34 (1.74-3.15) | <0.001 | 2.86 (2.18-3.75) | <0.001 |
| **Gender** | | | | | | |
| Male | 1.00 (ref.) | | 1.00 (ref.) | | 1.00 (ref.) | |
| Female | 0.85 (0.83-0.87) | <0.001 | 0.94 (0.91-0.97) | <0.001 | 0.90 (0.88-0.93) | <0.001 |
| **Year of diagnosis** | | | | | | |
| 2000–2007 | 1.00 (ref.) | | 1.00 (ref.) | | 1.00 (ref.) | |
| 2008–2016 | 0.87 (0.85-0.89) | <0.001 | 0.42 (0.41-0.44) | <0.001 | 0.37 (0.36-0.38) | <0.001 |
| **Marital** | | <0.001 | | <0.001 | | <0.001 |
| Married | 1.00 (ref.) | | 1.00 (ref.) | | 1.00 (ref.) | |
| Widowed/Divorced | 1.44 (1.40-1.48) | <0.001 | 1.28 (1.23-1.32) | <0.001 | 1.28 (1.25-1.33) | <0.001 |
| Single | 1.26 (1.22-1.30) | <0.001 | 1.15 (1.10-1.20) | <0.001 | 1.18 (1.14-1.23) | <0.001 |
| Unknown | 0.99 (0.93-1.05) | 0.619 | 0.97 (0.90-1.05) | 0.483 | 0.93 (0.87-0.99) | 0.032 |
| **Race** | | <0.001 | | <0.001 | | <0.001 |
| White | 1.00 (ref.) | | 1.00 (ref.) | | 1.00 (ref.) | |
| Black | 1.20 (1.15-1.25) | <0.001 | 1.20 (1.14-1.26) | <0.001 | 1.18 (1.13-1.24) | <0.001 |
| Other | 0.91 (0.87-0.95) | <0.001 | 1.00 (0.94-1.06) | 0.909 | 0.96 (0.92-1.02) | 0.163 |
| Unknown | 0.26 (0.18-0.36) | <0.001 | 0.27 (0.18-0.42) | <0.001 | 0.31 (0.22-0.46) | <0.001 |
| **Grading** | | <0.001 | | <0.001 | | <0.001 |
| I | 1.00 (ref.) | | 1.00 (ref.) | | 1.00 (ref.) | |
| II | 0.96 (0.92-1.00) | 0.059 | 0.84 (0.79-0.90) | <0.001 | 0.88 (0.83-0.93) | <0.001 |
| III | 1.21 (1.16-1.26) | <0.001 | 1.04 (0.97-1.11) | 0.317 | 1.08 (1.02-1.24) | 0.012 |
| IV | 1.68 (1.59-1.77) | <0.001 | 1.37 (1.27-1.48) | <0.001 | 1.48 (1.39-1.58) | <0.001 |
| Unknown | 1.48 (1.41-1.55) | <0.001 | 1.35 (1.26-1.44) | <0.001 | 1.41 (1.33-1.49) | <0.001 |
| **Stage** | | <0.001 | | <0.001 | | <0.001 |
| Local | 1.00 (ref.) | | 1.00 (ref.) | | 1.00 (ref.) | |
| Regional | 1.91 (1.86-1.97) | <0.001 | 1.64 (1.57-1.71) | <0.001 | 1.66 (1.60-1.72) | <0.001 |
| Distant | 8.29 (8.06-8.53) | <0.001 | 3.92 (3.78-4.07) | <0.001 | 4.49 (4.34-4.64) | <0.001 |
| Unknown | 2.90 (2.66-3.16) | <0.001 | 2.56 (2.30-2.83) | <0.001 | 2.33 (2.12-2.56) | <0.001 |
| **Site** | | <0.001 | | | | |
| KRP | 1.00 (ref.) | | 1.00 (ref.) | | 1.00 (ref.) | |
| Ovary | 0.75 (0.71-0.79) | <0.001 | 0.87 (0.82-0.93) | <0.001 | 0.90 (0.85-0.96) | 0.001 |
| Corpus Uteri | 1.16 (1.09-1.23) | <0.001 | 1.10 (1.02-1.18) | 0.01 | 1.22 (1.25-1.31) | <0.001 |
| Lung | 2.10 (1.95-2.26) | <0.001 | 1.55 (1.42-1.70) | <0.001 | 1.78 (1.64-1.93) | <0.001 |
| Cervix Uteri | 1.29 (1.13-1.48) | <0.001 | 1.10 (0.94-1.28) | 0.229 | 1.46 (1.26-1.68) | <0.001 |
| Bladder | 1.64 (1.32-2.03) | <0.001 | 1.34 (1.06-1.69) | 0.016 | 1.69 (1.35-2.12) | <0.001 |
| Vagina | 1.04 (0.80-1.35) | 0.762 | 0.83 (0.61-1.12) | 0.227 | 0.96 (0.73-1.26) | 0.762 |
| Pancreas | 3.70 (2.99-4.59) | <0.001 | 2.77 (2.22-3.45) | <0.001 | 3.56 (2.86-4.43) | <0.001 |
| Breast | 1.00 (0.71-2.41) | 0.992 | 1.14 (0.65-2.01) | 0.65 | 1.16 (0.76-1.78) | 0.493 |
| POM | 1.77 (1.33-2.36) | <0.001 | 0.96 (0.68-1.35) | 0.804 | 0.90 (0.67-1.22) | 0.502 |
| Prostate | 0.94 (0.68-1.30) | 0.728 | 0.89 (0.55-1.43) | 0.624 | 0.72 (0.48-1.07) | 0.102 |
| Liver | 4.89 (3.71-6.44) | <0.001 | 2.12 (158-2.86) | <0.001 | 2.46 (1.84-3.28) | <0.001 |

were all significantly associated with OS. We found that women (HR, 0.85; 95% CI, 0.83–0.87) had a better OS than men, and patients with grade III (HR, 1.21; 95% CI, 1.16–1.26) or grade IV (HR, 1.68; 95% CI, 1.59–1.77) CCA had a worse OS than did those with grade I CCA. However, the OS was not statistically different between grade II and grade I CCA. After adjusting for other variables, regional CCA (HR, 1.91; 95% CI, 1.86–1.97) and distant CCA had a shorter median survival time compared with localized and regional CCA (14mo VS 193,103 mo, respectively). Compared with CCA of the KRP, patients with CCA of the liver had the worst OS (HR, 4.89; 95% CI, 3.71–6.44), those with CCA of the pancreas had the second worst OS (HR, 3.70; 95% CI, 2.99–4.59), and those with CCA of the ovary had the best OS (HR, 0.75; 95% CI, 0.71–0.79).

We analyzed the latest trends of the OS during 2000–2007 and 2008–2016. Compared with 2000–2007, the risk of death in CCA diagnosed in 2008–2016 was less by 13% (HR, 0.87; 95% CI, 0.85–0.89). We calculated the 3-year and 5-year hazard ratios through multivariate analysis, and the patients with grade II CCA had better 3-year (HR, 0.84; 95% CI, 0.79–0.90) and 5-year (HR, 0.88; 95% CI, 0.83–0.93) survivals than did those patients with grade I CCA. All of the above comparisons are significant ($P < 0.001$).

Furthermore, the Kaplan-Meier curve and median OS were analyze for age, gender, year of diagnosis, marital status, race, grade, stage, and primary tumor site. The results were consistent with multivariate cox regression analysis. Specifically, the population with Widowed/Divorced had the worst prognosis, with the median OS of only 98 months (**Figure 5D**). CCA

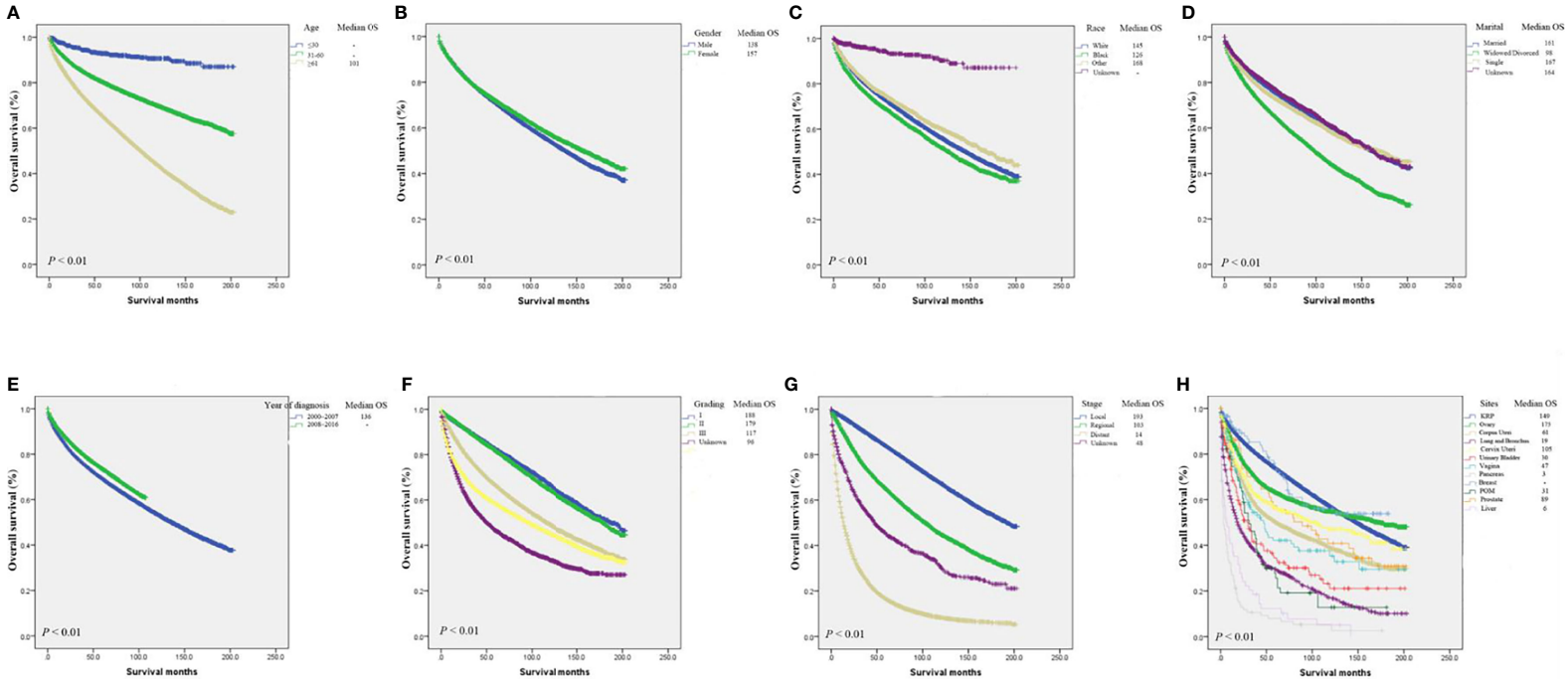


**FIGURE 5** | Kaplan-Meier analysis of survival by age **(A)**, gender **(B)**, race **(C)**, marital status **(D)**, year of diagnosis **(E)**, grade **(F)**, stage **(G)**, primary tumor site **(H)**.

patients with distant-stage had a median OS of only 14 months, compared with 193 and 103 months for localized and regional, respectively. The median OS was best for breast cancer CCA (not achieving median OS) and ovarian cancer CCA (175 mo) (**Figure 5G**), while the median OS was worst for pancreas (3 mo) and liver (6 months). All of these differences in OS were significant ($P < 0.001$; **Figures 5A–H**).

## DISCUSSION

In this study, we used the SEER database to report the largest number of CCA cases for the first time, focusing on incidence, demographic characteristics, and prognostic factors. We found that the age-adjusted incidence of CCA increased from 3.3 per 100,000 persons in 2000 to 8.8 per 100,000 persons in 2016, which is a 2.7-fold increase. This increase may be due in part to factors such as increased early diagnosis of these tumors and insurance coverage (15–17). The survival of CCA patients also increased significantly over time, reflecting that comprehensive treatment based on surgery has improved for CCA patients in recent years (18–20).

Although the incidence increased across all ages, grades, stages, and races during this period, the incidence increased the most for grade IV CCA, then localized stage; and American Indians and Alaskan Natives among races. However, it is unclear whether these differences are due to underlying dietary habits, environmental factors, biological factors, or health care models. Furthermore, CCA is associated with variables such as older age, white, male, grade II and local stage. CCA also occurs most frequently in the kidneys and ovaries. Patients with kidney or ovarian CCA are more likely to have metastasis to the lungs and liver compared with other solid CCAs, respectively, a finding consistent with previous reports (21, 22).

In addition, we analyzed the relative survival of patients with all grades and stages of CCA and found that survival over time increased the most in patients with grade IV CCA. One possible explanation is that surgery-based comprehensive treatment models for high-grade CCA have improved in recent years (23, 24). The results of the multivariate survival analysis showed that age, gender, year of diagnosis, marital status, ethnicity, disease stage, grade, and primary tumor site are important predictors of the OS of CCA patients. We also found that the most useful predictor of prognosis in patients with CCA is probably the primary tumor site. Therefore, the results of our research above can be used as a practical guide for clinicians.

Previous studies have shown that CCA is formed by the abnormal accumulation of glycogen. The prognosis is poor for patients with CCA of the kidney, uterus, ovary, bladder, or breast (11, 13, 25, 26). The present research showed that compared with CCA of the kidney, CCA of the liver and pancreas has a relatively worse OS, while CCA of the ovary has a better prognosis.

The poor prognosis of CCA patients may be due to several biomolecular mechanisms. Glycogen metabolism has recently been recognized as an important pathway for metabolic reprogramming in cancer cells. Others have reported that tumorigenesis and progression inhibit hypoglycemic glycogen metabolism and thereby inhibit active oxygen levels and p53-dependent cell senescence (14). Furthermore, tumor cells can mobilize glycogen to promote glycolysis and increase cancer cell proliferation, invasion, and metastasis through various signaling pathways such as p38α mitogen-activated protein kinase and mammalian target of rapamycin (27, 28).

Abnormal glycogen accumulation can serve as an important energy supply that compensate for nutritional deficiencies in the tumor microenvironment (2). Therefore, targeting glucose metabolism is considered an important approach for cancer treatment (4, 8). However, there is currently no effective treatment for CCA. A deep understanding of cancer glycogen metabolism is needed to identify novel targeted treatments for these glycogen-rich cancers, to serve as options to surgery for comprehensive treatment.

There are some limitations to our research. First, this study was retrospective and had an inherent selection bias. Second, our study did not include factors such as the quality of surgery and systemic treatments, which may confound the results. Finally, the SEER database does not capture a number of possible prognostic indicators such as insurance status, eating habits, and environmental factors, which may also influence treatment decisions and survival outcomes.

## CONCLUSIONS

In this large-scale study, we evaluated the incidence of CCA as well as the demographics and survival of CCA patients. Over time, the incidence of CCA and patient survival increased. In particular, the highest increases were reported for grade IV CCA compared with all subgroups, which may be due to increased diagnosis of the disease and improved treatment. Our research will help clinicians fully understand the natural history and progression of these glycogen-rich tumors as well as provide a theoretical basis for identifying novel targeted therapies.

## DATA AVAILABILITY STATEMENT

The original contributions presented in the study are included in the article/**Supplementary Material**. Further inquiries can be directed to the corresponding authors.

## AUTHOR CONTRIBUTIONS

Conceptualization, YG and XY. Data curation, AS and XD. Formal analysis, NM, AZ, and XD. Funding acquisition, XY.

Investigation, SM. Methodology, RW and AZ. Project administration, YG and XY. Resources, WM. Software, YG. Supervision, CL. Validation, JL and WZ. Visualization, ZZ and WZ. Writing – review & editing, YG and XY. All authors have read and approved the manuscript.

## FUNDING

This work was supported in part by grants from the Shanghai Science Committee Foundation (#19411967700).

## ACKNOWLEDGMENTS

Our research has been presented the presentation of the manuscript in research square.

## SUPPLEMENTARY MATERIAL

The Supplementary Material for this article can be found online at: https://www.frontiersin.org/articles/10.3389/fendo.2022.762589/full#supplementary-material

## REFERENCES


1. Zou Y, Palte M, Deik A, Li H, Eaton J, Wang W, et al. A GPX4-Dependent Cancer Cell State Underlies the Clear-Cell Morphology and Confers Sensitivity to Ferroptosis. *Nat Commun* (2019) 10(1):1617. doi: 10.1038/s41467-019-09277-9
2. Hsu PP, Sabatini DM. Cancer Cell Metabolism: Warburg and Beyond. *Cell* (2008) 134(5):703–7. doi: 10.1016/j.cell.2008.08.021
3. Maruggi M, Layng F, Lemos R, Garcia G, James B, Sevilla M, et al. Absence of HIF1A Leads to Glycogen Accumulation and an Inflammatory Response That Enables Pancreatic Tumor Growth. *Cancer Res* (2019) 79(22):5839–48. doi: 10.1158/0008-5472.CAN-18-2994
4. Denko NC. Hypoxia, HIF1 and Glucose Metabolism in the Solid Tumour. *Nat Rev Cancer* (2008) 8(9):705–13. doi: 10.1038/nrc2468
5. Pescador N, Villar D, Cifuentes D, Garcia-Rocha M, Ortiz-Barahona A, Vazquez S, et al. Hypoxia Promotes Glycogen Accumulation Through Hypoxia Inducible Factor (HIF)-Mediated Induction of Glycogen Synthase 1. *PloS One* (2010) 5(3):e9644. doi: 10.1371/journal.pone.0009644
6. Koppenol W, Bounds P, Dang C. Otto Warburg's Contributions to Current Concepts of Cancer Metabolism. *Nat Rev Cancer* (2011) 11(5):325–37. doi: 10.1038/nrc3038
7. Zois C, Favaro E, Harris A. Glycogen Metabolism in Cancer. *Biochem Pharmacol* (2014) 92(1):3–11. doi: 10.1016/j.bcp.2014.09.001
8. Zois CE, Harris AL. Glycogen Metabolism Has a Key Role in the Cancer Microenvironment and Provides New Targets for Cancer Therapy. *J Mol Med (Berl)* (2016) 94(2):137–54. doi: 10.1007/s00109-015-1377-9
9. Vernieri C, Casola S, Foiani M, Pietrantonio F, de Braud F, Longo V. Targeting Cancer Metabolism: Dietary and Pharmacologic Interventions. *Cancer Discov* (2016) 6(12):1315–33. doi: 10.1158/2159-8290.CD-16-0615
10. Zorn K, Bonome T, Gangi L, Chandramouli G, Awtrey C, Gardner G, et al. Gene Expression Profiles of Serous, Endometrioid, and Clear Cell Subtypes of Ovarian and Endometrial Cancer. *Clin Cancer Res an Off J Am Assoc Cancer Res* (2005) 11(18):6422–30. doi: 10.1158/1078-0432.CCR-05-0508
11. Cheville J, Lohse C, Zincke H, Weaver A, Blute M. Comparisons of Outcome and Prognostic Features Among Histologic Subtypes of Renal Cell Carcinoma. *Am J Surg Pathol* (2003) 27(5):612–24. doi: 10.1097/00000478-200305000-00005
12. Sugiyama T, Kamura T, Kigawa J, Terakawa N, Kikuchi Y, Kita T, et al. Clinical Characteristics of Clear Cell Carcinoma of the Ovary: A Distinct Histologic Type With Poor Prognosis and Resistance to Platinum-Based Chemotherapy. *Cancer* (2000) 88(11):2584–9. doi: 10.1002/1097-0142(20000601)88:11<2584::AID-CNCR22>3.0.CO;2-5
13. Zhou Z, Kinslow C, Wang P, Huang B, Cheng S, Deutsch I, et al. Clear Cell Adenocarcinoma of the Urinary Bladder Is a Glycogen-Rich Tumor With Poorer Prognosis. *J Clin Med* (2020) 9(1):138. doi: 10.3390/jcm9010138
14. Favaro E, Bensaad K, Chong M, Tennant D, Ferguson D, Snell C, et al. Glucose Utilization via Glycogen Phosphorylase Sustains Proliferation and Prevents Premature Senescence in Cancer Cells. *Cell Metab* (2012) 16(6):751–64. doi: 10.1016/j.cmet.2012.10.017
15. Altekruse S, Das A, Cho H, Petkov V, Yu M. Do US Thyroid Cancer Incidence Rates Increase With Socioeconomic Status Among People With Health Insurance? An Observational Study Using SEER Population-Based Data. *BMJ Open* (2015) 5(12):e009843. doi: 10.1136/bmjopen-2015-009843
16. Mann S, Saxena R. Differential Diagnosis of Epithelioid and Clear Cell Tumors in the Liver. *Semin Diagn Pathol* (2017) 34(2):183–91. doi: 10.1053/j.semdp.2016.12.014
17. Cochrane D, Tessier-Cloutier B, Lawrence K, Nazeran T, Karnezis A, Salamanca C, et al. Clear Cell and Endometrioid Carcinomas: Are Their Differences Attributable to Distinct Cells of Origin? *J Pathol* (2017) 243(1):26–36. doi: 10.1002/path.4934
18. Dudek A, Liu L, Gupta S, Logan T, Singer E, Joshi M, et al. Phase Ib/II Clinical Trial of Pembrolizumab With Bevacizumab for Metastatic Renal Cell Carcinoma: BTCRC-GU14-003. *J Clin Oncol Off J Am Soc Clin Oncol* (2020) 38:JCO1902394. doi: 10.1200/JCO.19.02394
19. Oseledchyk A, Leitao M, Konner J, O'Cearbhaill R, Zamarin D, Sonoda Y, et al. Adjuvant Chemotherapy in Patients With Stage I Endometrioid or Clear Cell Ovarian Cancer in the Platinum Era: A Surveillance, Epidemiology, and End Results Cohort Study, 2000-2013. *Ann Oncol Off J Eur Soc Med Oncol* (2017) 28(12):2985–93. doi: 10.1093/annonc/mdx525
20. Bex A, Albiges L, Ljungberg B, Bensalah K, Dabestani S, Giles R, et al. Updated European Association of Urology Guidelines for Cytoreductive Nephrectomy in Patients With Synchronous Metastatic Clear-Cell Renal Cell Carcinoma. *Eur Urol* (2018) 74(6):805–9. doi: 10.1016/j.eururo.2018.08.008
21. Guo Q, Zhang C, Guo X, Tao F, Xu Y, Feng G, et al. Incidence of Bone Metastasis and Factors Contributing to Its Development and Prognosis in Newly Diagnosed Renal Cell Carcinoma: A Population-Based Study. *Cancer Manage Res* (2018) 10:2935–44. doi: 10.2147/CMAR.S170083
22. Deng K, Yang C, Tan Q, Song W, Lu M, Zhao W, et al. Sites of Distant Metastases and Overall Survival in Ovarian Cancer: A Study of 1481 Patients. *Gynecol Oncol* (2018) 150(3):460–5. doi: 10.1016/j.ygyno.2018.06.022
23. Franzese C, Franceschini D, Di Brina L, D'Agostino G, Navarria P, Comito T, et al. Role of Stereotactic Body Radiation Therapy for the Management of Oligometastatic Renal Cell Carcinoma. *J Urol* (2019) 201(1):70–5. doi: 10.1016/j.juro.2018.08.049
24. Stenman M, Sinclair G, Paavola P, Wersäll P, Harmenberg U, Lindskog M. Overall Survival After Stereotactic Radiotherapy or Surgical Metastasectomy in Oligometastatic Renal Cell Carcinoma Patients Treated at Two Swedish Centres 2005-2014. *Radiother Oncol J Eur Soc Ther Radiol Oncol* (2018) 127(3):501–6. doi: 10.1016/j.radonc.2018.04.028
25. Gadducci A, Cosio S, Spirito N, Cionini L. Clear Cell Carcinoma of the Endometrium: A Biological and Clinical Enigma. *Anticancer Res* (2010) 30(4):1327–34.
26. Zhou Z, Kinslow C, Hibshoosh H, Guo H, Cheng S, He C, et al. Clinical Features, Survival and Prognostic Factors of Glycogen-Rich Clear Cell Carcinoma (GRCC) of the Breast in the U.S. Population. *J Clin Med* (2019) 8(2):246. doi: 10.3390/jcm8020246
27. Curtis M, Kenny H, Ashcroft B, Mukherjee A, Johnson A, Zhang Y, et al. Fibroblasts Mobilize Tumor Cell Glycogen to Promote Proliferation and Metastasis. *Cell Metab* (2019) 29(1):141–55.e9. doi: 10.1016/j.cmet.2018.08.007
28. Koo J, Yue P, Gal A, Khuri F, Sun S. Maintaining Glycogen Synthase Kinase-3 Activity Is Critical for mTOR Kinase Inhibitors to Inhibit Cancer Cell Growth. *Cancer Res* (2014) 74(9):2555–68. doi: 10.1158/0008-5472.CAN-13-2946


**Conflict of Interest:** The authors declare that the research was conducted in the absence of any commercial or financial relationships that could be construed as a potential conflict of interest.

the publisher, the editors and the reviewers. Any product that may be evaluated in this article, or claim that may be made by its manufacturer, is not guaranteed or endorsed by the publisher.

frontiers in Endocrinology

REVIEW
published: 28 March 2022
doi: 10.3389/fendo.2022.855326

# Tailored Approach in Adrenal Surgery: Retroperitoneoscopic Partial Adrenalectomy

*Pier Francesco Alesina*[1*†], *Polina Knyazeva*[2†], *Jakob Hinrichs*[2] *and Martin K. Walz*[2]

[1] Clinic for Endocrine Surgery, Helios Universitätsklinikum Wuppertal, Wuppertal, Germany, [2] Department of Surgery and Centre of Minimally Invasive Surgery, Evang. Kliniken Essen-Mitte, Essen, Germany

The interest on partial adrenalectomy has steadily increased over the past twenty years. Adrenal pathologies are mostly benign, making an organ-preserving procedure attractive for many patients. The introduction of minimally invasive techniques played probably an important role in this process because they transformed a complex surgical procedure, related to the difficult access to the retroperitoneal space, into a simple operation improving the accessibility to this organ. In this review we summarize the role of partial retroperitoneoscopic adrenalectomy over the years and the current indications and technique.

**Keywords: adrenalectomy, partial adrenalectomy, minimally invasive, adrenal surgery, conn, pheochromocytoma, cushing adenoma**

OPEN ACCESS

***Edited by:***
*Barbara Altieri,*
*University Hospital of Wuerzburg, Germany*

***Reviewed by:***
*Fabio Medas,*
*University of Cagliari, Italy*
*Rosaria Maddalena Ruggeri,*
*University of Messina, Italy*

****Correspondence:***
*Pier Francesco Alesina*
*pieroalesina@libero.it*
*orcid.org/0000-0002-8508-9934*

*†These authors share first authorship*

***Specialty section:***
*This article was submitted to Cancer Endocrinology, a section of the journal Frontiers in Endocrinology*

***Received:*** *15 January 2022*
***Accepted:*** *24 February 2022*
***Published:*** *28 March 2022*

***Citation:***
*Alesina PF, Knyazeva P, Hinrichs J and Walz MK (2022) Tailored Approach in Adrenal Surgery: Retroperitoneoscopic Partial Adrenalectomy. Front. Endocrinol. 13:855326. doi: 10.3389/fendo.2022.855326*

## INTRODUCTION

The first description of experimental partial adrenalectomy is attributable to Frederick Gates. In 1918, he investigated the potential role of the adrenal glands in antibody formation (in guinea pigs) and found out that these glands are not an essential part in immunity processes. Moreover, they observed that the removal of three-quarters to seven-eighths of the adrenal tissue does not cause adrenal insufficiency (1). The first description of partial adrenalectomy in humans was published in 1934 based on the hypothesis that medullary adrenal hyperplasia is responsible for severe arterial hypertension and bilateral partial adrenalectomy might be its therapy (2). The operation that consisted in the removal of two-third to three-fourth of each adrenal was performed in two stages from the back through a "so-called" kidney incision under spinal anesthesia. This report includes 8 cases with no mortality or severe complications. The first report of partial adrenalectomy for bilateral adrenal tumors was published in 1982 but the operation was performed in 1965 (3). A 13-year-old boy underwent total adrenalectomy on the right side and partial on the left side for bilateral pheochromocytoma. For two days after surgery the patient received diminishing doses of cortisol and 6 days postoperatively 5 mg prednisone was given twice a day orally. The substitution therapy was discontinued after 4 months and a computer tomography scan 15 years later proved the adrenal remnant without tumor recurrence. In 1983, Irvin and colleagues, and in 1984 van Heerden and coworkers reported on partial adrenalectomy in bilateral pheochromocytomas each in 3 patients (4, 5). Irvin described a family of a father and two daughters with bilateral pheochromocytomas who had been recurrence-free for 3–8 years after partial adrenalectomy. The Mayo group mentioned "enucleation" of bilateral pheochromocytomas in two patients in the early 1950s and a third case of an airline pilot (5) published more in detail as a case report in 1985 (6). By successful function-

preserving adrenalectomy on both sides the latter patient could continue his professional career. As none of these patients—mainly with hereditary diseases—developed a tumor recurrence, the concept of partial adrenalectomy seemed to be a real alternative to life-long corticoid replacement with high risks of Addisionian crisis and death (7, 8) and became an alternative strategy for selected patients in adrenal surgery. The first reports of minimally invasive partial adrenalectomy were published by us in 1996 (9). In 5 cases (2 Conn's adenomas, 3 non-functioning tumors) the retroperitoneoscopic approach was used.

## MATERIAL AND METHODS

A literature search (Medline database) with the keywords "partial adrenalectomy" and/or "cortical-sparing adrenalectomy" and "retroperitoneoscopic partial adrenalectomy" has been performed and the data were analyzed. The present review and the search from the literature focused specifically on the retroperitoneoscopic technique. Papers with >10 reported cases have been included while smaller series and case reports were not considered for the present analysis. Additionally, all the data presented have been extracted from our previous publications with a specific focus on partial adrenalectomy performed by the retroperitoneoscopic approach (10–16). **Table 1** summarizes the results of the studies presented in this review.

## THE SURGICAL TECHNIQUE

The first description of an experimental retroperitoneal endoscopic adrenalectomy was published in 1993 by Brunt et al. (22). The authors performed the procedure in a domestic swine model using insufflation of the retroperitoneal space with carbon dioxide and concluded that the posterior route could have been potentially suitable to the treatment of adrenal lesions. In 1994 and 1995 retroperitoneal adrenalectomy in humans has been described in Japan, New Zeeland, Sweden, Italy, Germany and Turkey (23–28) including our own paper (29). Some used the lateral approach (23–25, 27), others the posterior access (26–29). The latter is more accepted today with the patient in the prone, half-jackknife position. On our own hands a rectangular pillow is used that allows the abdominal wall to hang through ventrally (**Figure 1**). Alternatively, a roll may be positioned below the chest and the pelvis. The angle of the hip joint should be around 90°. This position creates an optimal space between the ribs and the iliac crest. A 1.5 to 2 cm skin incision is performed at the level of the 12th rib and the retroperitoneal space is reached by blunt and sharp dissection with scissors. A finger is inserted into the retroperitoneum in order to position a 5 mm port inserted just below the tip of the 11th rib under digital control. A blunt trocar with an inflatable balloon and an adjustable sleeve (Medtronic, Minneapolis, USA, ®) is introduced into the initial incision site and blocked. Under $CO_2$ insufflation pressure of 20–30 mmHg a working space is created by opening Gerota's facia and pushing all retroperitoneal fatty tissue ventrally. By this maneuver the region around the kidney and the adrenal gland are visualized. A third trocar (5 or 10 mm in diameter) is inserted under visual control paying attention to avoid the subcostal nerve running parallel to the 12th rib. The final position of the trocar is demonstrated in **Figure 2**. The dissection starts on the upper pole of the kidney that is freed from the adhesions to the retroperitoneal fatty tissue. The kidney is gently retracted caudally and medially to expose the lower pole of the adrenal gland. The dissection is then

**TABLE 1** | Retroperitoneoscopic partial adrenalectomy.

| Author | Year | Disease | No. of Patients | No. of partial adrenalectomies | Follow-up (months) | Comments |
|---|---|---|---|---|---|---|
| Walz et al. (10) | 2006 | Pheochromocytoma | 127 | 57 | 45 | In 21 of 22 patients with bilateral adrenal pheochromocytomas, partial adrenalectomy was performed at least on one side |
| Alesina et al. (14) | 2012 | Pheochromocytoma | 66 | 89 | 48 | The study included only patients with bilateral disease |
| Walz et al. (16) | 2018 | Pheochromocytoma | 31 | 31 | 109 | children and adolescents between 7 and 20 years old, 18 had unilateral and 13 bilateral disease |
| Sasagawa et al. (17) | 2003 | Conn's syndrome | 47 | 13 | Not reported | All patients with functional cortical adenoma and pheochromocytoma showed normal adrenal function after the operation |
| Walz et al. (12) | 2008 | Conn's syndrome | 183 | 47 | 59 | No difference in the rate of blood pressure improvement was found in patients with partial adrenalectomy versus those with total adrenalectomy |
| Fu et al. (18) | 2011 | Conn's syndrome | 212 | 104 | 96 | Patients in the partial adrenalectomy group showed similar improvement in hypertension compared to total adrenalectomy (n = 108) |
| Alesina et al. (13) | 2010 | Cushing's syndrome | 170 | 44 | 71 | No recurrence |
| Lowery at al (15). | 2017 | Cushing's syndrome | 42 | 35 | 40 | Only patients with bilateral disease were included; remission rate 92% |
| He et al. (19) | 2012 | Cushing's syndrome | 93 | 87 | Length not indicated | Recurrent or persistent hypercortisolism was observed after surgery in one patient |
| Xu et al. (20) | 2015 | Non-functioning adenomas, concomitant hypertension | 75 | 69 | 24 | Hypertension cured in 35% of the patients and improved in 31%, no recurrence |
| Zhang et al. (21) | 2007 | Cysts | 14 | 14 | 12 | Nine cases of cyst decortication and five cases of partial adrenalectomy; no recurrence |


**FIGURE 1** | Patient's position.

continued medially from caudal to cranial. On the right side the vena cava is visualized and the retrocaval dissection is performed until the adrenal vein is reached; on the left side the adrenal vein is isolated medially when completing the dissection of the lower pole of the adrenal. The cranial dissection represents the last step of the procedure. Total adrenalectomy is usually performed as an "en-bloc" resection of the gland and retroperitoneal fatty tissue and needs to be modified in partial adrenalectomy. Preconditions for successful function-preserving adrenal surgery are special knowledges in anatomy and surgical technique. Adrenal glands are perfused from medial, inferior, and cranial but not from lateral. By this, adrenal tissue can be dissected in any direction preserving at least one direction of perfusion. The preservation of the main vein is not mandatory. Planning of cortical-sparing procedures is based on a detailed analysis of preoperative imaging in order to understand position and size of the tumor within the gland. Intraoperative ultrasound may facilitate the identification of neoplasias, especially in obese patients. For tumors located at the upper pole of the gland, the dissection of the lower pole should be avoided and vice versa

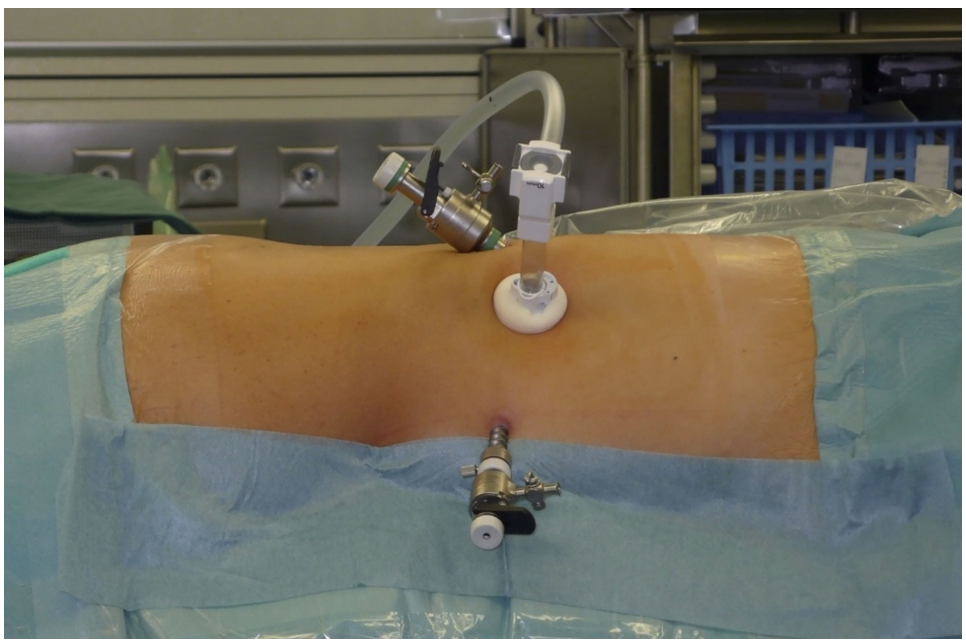

**FIGURE 2** | Trocar's position.

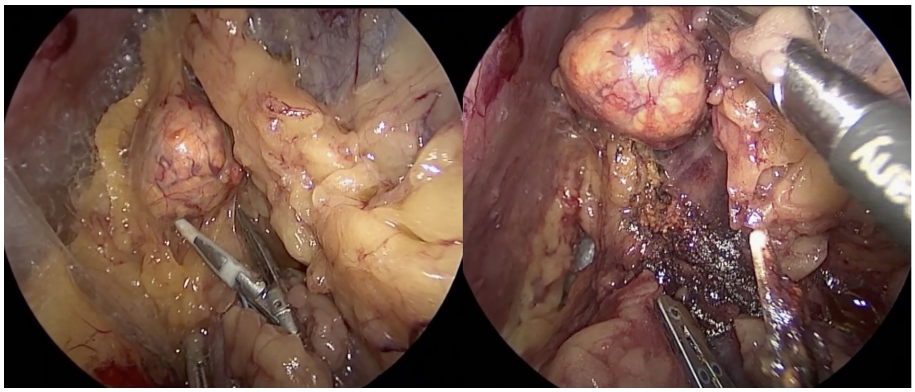

**FIGURE 3** | Tumor located on the upper pole on the right side: the dissection of the lower part of the adrenal gland is avoided.

(**Figure 3**). The division of the adrenal tissue can be performed by any energy device and residual bleeding from the remnant that can be easily controlled by standard coagulation instruments (**Figure 4**).

In recent years indocyanine green (ICG) fluorescence has been used to visualize viability of adrenal remnant after resection. The first report was published in 2013 by Manny and colleagues in three patients during robotic adrenalectomy (30). In the setting of a collaboration with the Institute for Research Against Cancer of the Digestive System (IRCAD) in Strasbourg we analyzed the behavior of the adrenal tissue in a porcine model and found out that fluorescence imaging can provide real-time guidance during minimally invasive adrenal surgery. Prior to dissection, it allows to easily discriminate the adrenal gland from surrounding retroperitoneal structures. After adrenal gland division, ICG injection associated with a computer-assisted quantitative analysis helps to distinguish between well-perfused and ischemic segments (31). These findings have been confirmed in some studies analyzing different adrenal pathologies in the humans (32, 33). Fluorescence guidance can be also useful to estimate more precisely the volume of the adrenal remnant. This is

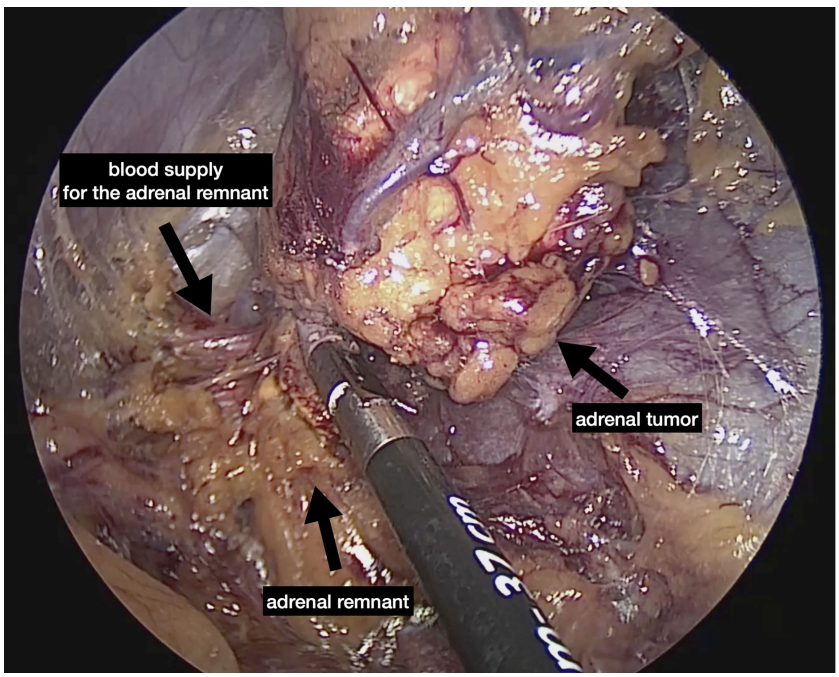


**FIGURE 4** | Division of the gland performed by bipolar instrument.

particularly important in patients submitted to bilateral surgery to decide about the necessity of corticosteroids substitution. It is well-known that preservation of 15 to 30% of one gland is necessary to avoid a substitution therapy (34). Brauckhoff et al. studied 10 patients with bilateral adrenal tumors which underwent measurement of plasma adrenocorticotropic hormone (ACTH), serum cortisol, and maximal cortisol liberation with an ACTH test after subtotal bilateral adrenalectomy, which left 15 to 30% of adrenal tissue in situ. In the early postoperative period, all patients had normal basal serum cortisol levels, despite in 6 patients a pathologic ACTH test result was observed. During follow-up all patients were found to have a normal ACTH test result. None of the patients required long-term steroid supplementation. This is confirmed by our experience on 66 patients operated for bilateral pheochromocytomas (14). All patients with preservation of less than 15% of adrenal tissue ultimately became steroid-dependent.

## Pheochromocytoma

Partial adrenalectomy should always be considered in the case of pheocromocytoma. The risk of developing bilateral tumors is much higher than historically assumed, as part of the well-known 10%-rule for pheochromocytoma. This is particularly true when considering that familial diseases account nowadays for almost 40% of the cases (35). The main consequence of performing adrenal preservation, especially in hereditary pheochromocytoma, is the possible development of recurrent disease that needs to be weighed against avoidance of a lifelong steroid therapy. Nevertheless, a clear distinction between ipsilateral and contralateral recurrence should be made, as only ipsilateral recurrence can be avoided if total instead of partial adrenalectomy is undertaken. Older studies based on open partial adrenalectomy reported recurrence in up to 20% (35), whereas recent papers using minimally invasive techniques describe lower recurrence rates of less than 10%. Data of the European-American-Asian-Bilateral-Pheochromocytoma-Registry including a total of 625 patients with bilateral tumors show that partial adrenalectomy was performed for smaller tumors compared to total adrenalectomy (3 vs. 3.5 cm) and more often since 2010 (36). This seems to be related to the increased use of minimally invasive techniques which allow a more precise dissection. Recurrent ipsilateral pheochromocytoma developed in 35 of 625 patients (5.6%); 33 out of 248 patients (13%) after partial adrenalectomy and 2 out of 301 (0.6%) after total adrenalectomy. Moreover, metastatic pheochromocytoma was diagnosed in 8 of 625 patients (1.3%). Our group published the results of partial adrenalectomy for pheochromocytoma in 2006 (10). In this series 94 unilateral and 12 bilateral tumors were removed by the posterior approach. Fifty-seven partial adrenalectomies had been performed. There was neither mortality nor conversion to open surgery. A bleeding occurred after left-sided resection in a patient with bilateral pheochromocytomas. This patient required transfusion of 4 units of blood and retroperitoneoscopy to remove the hematoma on the first postoperative day. After a mean follow-up of 45 ± 33 months no recurrence was observed. Later on, we reported the results in the subgroup of children and adolescents between the age of 7 and 20 years (16). There were 35 retroperitoneoscopic and two combined laparoscopic–retroperitoneoscopic operations. Thirty-one partial adrenalectomies have been performed. None of the bilateral pheochromocytoma patients needed corticoid supplementation following partial adrenalectomy. After a mean follow-up of 9.1 ± 4.6 years, 2 patients affected by von Hippel–Lindau disease developed an ipsilateral recurrent after 16 and 22 months, respectively. These tumors were removed by redo surgery by the retroperitoneoscopic approach.

According to the data available, the risks of recurrence and malignancy are low and justify, in our opinion, the use of partial adrenalectomy in most cases. Moreover, redo surgery by the posterior retroperitoneoscopic approach is almost always feasible independent of the surgical access of the first operation (11). Partial adrenalectomy can achieve lifelong steroid independency in most of the patients affected by bilateral tumors. We published the results of surgery on a group of 66 patients treated for bilateral disease (14). Fifty-seven patients (88%) were affected by genetic diseases. In 32 cases surgery was synchronously performed on both sides, in 34 cases unilateral adrenalectomy followed previous surgery on the contralateral side. A cortical-sparing resection was possible in 89 procedures resulting in a corticoid-free postoperative course in 60 patients (91%). A postoperative corticosteroid substitution therapy was necessary in six patients. After a median follow-up period of 48 months, one patient showed a persistent disease and needed reoperation, none developed a recurrent disease. Partial adrenalectomy is suggested also from the Endocrine Society guidelines (37) at least for patients with hereditary pheochromocytoma, with small tumors who have already undergone a contralateral complete adrenalectomy. The recommendation is based on the low risk of recurrence reported (7% over 3 years, and 10–15% over 10 years) and the high probability of steroid-independency (78–90%).

## Conn's Syndrome

Preliminary results of partial adrenalectomy for hyperaldosteronism performed by the retroperitoneoscopic route have been reported by our group in 1998 (38). Between 1994 and 1997, 11 out of 22 patients which underwent cortical-sparing surgery were affected by Conn's adenomas. These tumors are generally small and have a negligible risk of malignancy, therefore partial adrenalectomy seems to be a good alternative to total adrenalectomy. In 2003 Sasagawa and colleagues reported the results of partial adrenalectomy performed in 47 cases including 13 cases of Conn's adenomas (17). There was one conversion to open surgery because of bleeding (2%). The authors described as intraoperative complications three (6.4%) adrenal bleedings, two (4.3%) pneumothoraces, one (2.1%) massive hemorrhage (more than 1,000 ml) and one (2.1%) injury of the renal vein. In 2008 we reported the results of partial adrenalectomy in 47 patients which represented 26% of those operated for Conn's syndrome at our Institution between August 1994 and January 2007 (12). After a mean follow-up of almost 5 years, completed for 160 patients (87%), the rate of patients with improvement of hypertension was similar following partial (n = 37) and total adrenalectomy (n = 123): (92% vs. 85%, p = 0.41). Our results

are confirmed by a prospective randomized study performed on 212 patients (108 and 104 who underwent total and partial adrenalectomy, respectively) (18). Intraoperative blood loss in the partial adrenalectomy group was significantly higher than in the total adrenalectomy group ($p < 0.05$) but no patient needed blood transfusion. Patients in both groups showed improvement in hypertension, and in all aldosterone returned to normal.

Opponents of cortical-sparing surgery are concerned about the possible presence of multiple nodules or adrenal hyperplasia in the tumor-carrying gland. The decision to perform partial adrenalectomy should be weighed against the risk of leaving a remnant with pathological tissue. In our series from the 2008 histologic examination revealed solitary adenomas in 127 patients and nodular hyperplasia in 56. Patients with an adenoma were significantly younger than those with nodular hyperplasia ($47.8 \pm 13.1$ vs. $53.8 \pm 10.9$ years, $p < 0.05$). Suitable candidates for cortical-sparing surgery are particularly young patients (<45 years old) with a clearly visible nodule on preoperative imaging. In most of the series reported in the literature the cure rate of cortical-sparing surgery is even better than after total adrenalectomy probably because of this selection bias (39). Moreover, a recent German multicentric study showed that both, postoperative hypocortisolism (11.5% vs 25.0% after partial and total adrenalectomy, respectively; $p < 0.001$) and postoperative hypoglycemia (2.6% vs 7.1%; $p = 0.039$) occurred more frequently after total adrenalectomy. No recurrence was encountered in both groups (40).

## CUSHING'S SYNDROME

The first report on partial adrenalectomy for hypercortisolism has been published in 1934 by Walters (41). In this study ACTH-dependent and independent cases are included and a total number of 46 partial adrenalectomies with a mortality rate of 15% is reported. Certainly, partial adrenalectomy is nowadays not an option for ACTH-depending Cushing's syndrome, as recurrences are obligatory. In cases of ACTH-independent hypercortisolism caused by adrenal adenomas or bilateral macronodular hyperplasia cortical-sparing surgery can be considered. In 2010 we published the results of retroperitoneoscopic adrenalectomy for clinical and subclinical Cushing's syndrome. In this series 157 patients suffered from unilateral adrenal disease and 13 patients from bilateral macronodular hyperplasia. There were 44 partial adrenalectomies performed with no ipsilateral recurrence after a mean follow-up of 70.9 months (13). There are three different strategies in case of bilateral hyperplasia causing hypercortisolism: bilateral total adrenalectomy, unilateral adrenalectomy guided by the size of the glands or result of adrenal venous sampling, bilateral surgery including cortical-sparing adrenalectomy at least on one side. Unilateral surgery and bilateral surgery with partial adrenalectomy can both avoid substitution therapy. We reported the results of bilateral surgery on 42 patients with clinical or subclinical Cushing's syndrome (15). Thirty-nine out 42 patients were treated by cortical-sparing surgery, namely, unilateral resection (n = 3), unilateral adrenalectomy (n = 15), bilateral resection (n = 9), adrenalectomy and contralateral resection (n = 14). After median follow-up of 40 months the remission rate was 92%; 11 patients required ongoing steroid supplementation. There were three biochemical recurrences after unilateral surgery (two underwent contralateral resection); two patients with new/progressive radiological nodularity were biochemically eucortisolaemic at the time of last follow-up. He and colleagues reported on the results of adrenal-sparing surgery in 87 cases (31 performed by open surgery, 56 by retroperitoneal laparoscopy) (19). The cure rate was 97.8%; recurrent or persistent hypercortisolism was observed after surgery in one patient in which total adrenalectomy was performed. Despite the increasing evidence published in the literature, partial adrenalectomy is still not recommended for patients with hypercortisolism in any of the published guidelines. Nevertheless, the evidence from the literature allow to consider it especially for tumors smaller than 4 cm which harbor a negligible risk of malignancy.

## NON-FUNCTIONING TUMORS

Adrenal non-functioning incidentalomas have a 2 to 5% chance of malignancy. The likelihood of a benign adrenal tumor is higher in the group of adrenal incidentalomas ≤6 cm (42). A study from Xu et al. analyzed the effect of adrenal surgery on blood pressure in patients with non-functioning adrenal adenoma and concomitant hypertension (20). After a complete endocrinological evaluation confirming the hormonal inactivity of the tumor 77 out 186 patients underwent surgery according to the diameter of the tumor (>4cm) or preference of the patient. Retroperitoneoscopic partial adrenalectomy was performed in 69 patients, and six patients underwent retroperitoneoscopic total adrenalectomy while two patients had open total adrenalectomy. After two years of follow-up 27 patients (35%) in the surgery group were cured from hypertension, whereas 24 (31%) improved, and 26 (34%) remained refractory when compared with the control group. Therefore, the authors conclude that early partial adrenalectomy can play a role in patients with incidentalomas and concomitant hypertension. Preoperative imaging could determine the risk for malignancy and define the indication for surgery which is based on the size of the tumor. As surgery is usually performed to exclude malignancy, partial adrenalectomy is not routinely recommended for those patients. Moreover, cortical-sparing surgery is mostly not feasible for tumors larger than 6 cm because of the absence of normal adrenal tissue. Conversely, it could be performed in individually selected cases for tumors between 4 and 6 cm with a low malignant potential and in case of bilateral tumors. Adrenal symptomatic cysts requiring resection are an ideal indication for partial adrenalectomy. The largest series of cortical-sparing surgery for adrenal cysts has been published by Zhang et al. (21) which performed a cortical-sparing

procedure in 14 cases. The retroperitoneoscopic resection was performed with the patients in the lateral decubitus.

## METASTASIS

Partial adrenalectomy is not a standard procedure for adrenal metastasis. It can be indicated in selected cases in patients after previous adrenalectomy on the contralateral side or in case of bilateral metastasis. Few case reports have been published mostly on adrenal metastasis from renal cell carcinoma (43–45).

## CONCLUSIONS

Over the last twenty years partial adrenalectomy has become the preferred operation for patients with bilateral pheochromocytoma and patients with metachronous tumors after previous total adrenalectomy on the contralateral side. Moreover, it is a recognized option in case of unilateral pheochromocytoma and Conn's adenoma. The role of cortical-sparing surgery is uncertain for patients with Cushing's syndrome and incidentaloma, as there are only few studies in the literature investigating the long-term results of partial adrenalectomy in this subgroup of patients.

## AUTHOR CONTRIBUTIONS

PFA and PK wrote the manuscript. JH contributed to the discussion. MKW participated in the design of this study and edited the manuscript. All authors listed have made a substantial, direct, and intellectual contribution to the work and approved it for publication.

## REFERENCES


1. Gates FL. Antibody Production After Partial Adrenalectomy in Guinea Pigs. *J Exp Med* (1918) 27(6):725–38. doi: 10.1084/jem.27.6.725
2. Decourcy JL. Subtotal Bilateral Adrenalectomy for Hyperadrenalism (Essential Hypertension). *Ann Surg* (1934) 100(2):310–8. doi: 10.1097/00000658-193408000-00006
3. Giordano WC. Preservation of Adrenocortical Function During Surgery for Bilateral Pheochromocytoma. *J Urol* (1982) 127(1):100–2. doi: 10.1016/s0022-5347(17)53627-7
4. Irvin GL3rd, Fishman LM, Sher JA. Familial Pheochromocytoma. *Surgery* (1983) 94(6):938–40.
5. van Heerden JA, Sizemore GW, Carney JA, Grant CS, ReMine WH, Sheps SG. Surgical Management of the Adrenal Glands in the Multiple Endocrine Neoplasia Type II Syndrome. *World J Surg* (1984) 8(4):612–21. doi: 10.1007/BF01654950
6. van Heerden JA, Sizemore GW, Carney JA, Brennan MD, Sheps SG. Bilateral Subtotal Adrenal Resection for Bilateral Pheochromocytomas in Multiple Endocrine Neoplasia, Type IIa: A Case Report. *Surgery* (1985) 98 (2):363–6.
7. Lairmore TC, Ball DW, Baylin SB, Wells SA Jr. Management of Pheochromocytomas in Patients With Multiple Endocrine Neoplasia Type 2 Syndromes. *Ann Surg* (1993) 217(6):595–603. doi: 10.1097/00000658-199306000-00001
8. Seyam R, Khalil MI, Kamel MH, Altaweel WM, Davis R, Bissada NK. Organ-Sparing Procedures in GU Cancer: Part 1-Organ-Sparing Procedures in Renal and Adrenal Tumors: A Systematic Review. *Int Urol Nephrol* (2019) 51 (3):377–93. doi: 10.1007/s11255-018-02070-5
9. Walz MK, Peitgen K, Hoermann R, Giebler RM, Mann K, Eigler FW. Posterior Retroperitoneoscopy as a New Minimally Invasive Approach for Adrenalectomy: Results of 30 Adrenalectomies in 27 Patients. *World J Surg* (1996) 20(7):769–74. doi: 10.1007/s002689900117
10. Walz MK, Alesina PF, Wenger FA, Koch JA, Neumann HP, Petersenn S, et al. Laparoscopic and Retroperitoneoscopic Treatment of Pheochromocytomas and Retroperitoneal Paragangliomas: Results of 161 Tumors in 126 Patients. *World J Surg* (2006) 30(5):899–908. doi: 10.1007/s00268-005-0373-6
11. Walz MK, Alesina PF, Wenger FA, Deligiannis A, Szuczik E, Petersenn S, et al. Posterior Retroperitoneoscopic Adrenalectomy–Results of 560 Procedures in 520 Patients. *Surgery* (2006) 140(6):943–8; discussion 948-50. doi: 10.1016/j.surg.2006.07.039
12. Walz MK, Gwosdz R, Levin SL, Alesina PF, Suttorp A-C, Metz KA, et al. Retroperitoneoscopic Adrenalectomy in Conn's Syndrome Caused by Adrenal Adenomas or Nodular Hyperplasia. *World J Surg* (2008) 32(5):847–53. doi: 10.1007/s00268-008-9513-0
13. Alesina PF, Hommeltenberg S, Meier B, Petersenn S, Lahner H, Schmid KW, et al. Posterior Retroperitoneoscopic Adrenalectomy for Clinical and Subclinical Cushing's Syndrome. *World J Surg* (2010) 34(6):1391–7. doi: 10.1007/s00268-010-0453-0
14. Alesina PF, Hinrichs J, Meier B, Schmid KW, Neumann HP, Walz MK. Minimally Invasive Cortical-Sparing Surgery for Bilateral Pheochromocytomas. *Langenbecks Arch Surg* (2012) 397(2):233–8. doi: 10.1007/s00423-011-0851-2
15. Lowery AJ, Seeliger B, Alesina PF, Walz MK. Posterior Retroperitoneoscopic Adrenal Surgery for Clinical and Subclinical Cushing's Syndrome in Patients With Bilateral Adrenal Disease. *Langenbecks Arch Surg* (2017) 402(5):775–85. doi: 10.1007/s00423-017-1569-6
16. Walz MK, Iova LD, Deimel J, Neumann HPH, Bausch B, Zschiedrich S, et al. Minimally Invasive Surgery (MIS) in Children and Adolescents With Pheochromocytomas and Retroperitoneal Paragangliomas: Experiences in 42 Patients. *World J Surg* (2018) 42(4):1024–30. doi: 10.1007/s00268-018-4488-y
17. Sasagawa I, Suzuki Y, Itoh K, Izumi T, Miura M, Suzuki H, et al. Posterior Retroperitoneoscopic Partial Adrenalectomy: Clinical Experience in 47 Procedures. *Eur Urol* (2003) 43(4):381–5. doi: 10.1016/s0302-2838(03)00087-3
18. Fu B, Zhang X, Wang GX, Lang B, Ma X, Li HZ, et al. Long-Term Results of a Prospective, Randomized Trial Comparing Retroperitoneoscopic Partial Versus Total Adrenalectomy for Aldosterone Producing Adenoma. *J Urol* (2011) 185(5):1578–82. doi: 10.1016/j.juro.2010.12.051
19. He HC, Dai J, Shen ZJ, Zhu Y, Sun FK, Shao Y, et al. Retroperitoneal Adrenal-Sparing Surgery for the Treatment of Cushing's Syndrome Caused by Adrenocortical Adenoma: 8-Year Experience With 87 Patients. *World J Surg* (2012) 36(5):1182–8. doi: 10.1007/s00268-012-1509-0
20. Xu T, Xia L, Wang X, Zhang X, Zhong S, Qin L, et al. Effectiveness of Partial Adrenalectomy for Concomitant Hypertension in Patients With Nonfunctional Adrenal Adenoma. *Int Urol Nephrol* (2015) 47(1):59–67. doi: 10.1007/s11255-014-0841-8
21. Zhang X, Zheng T, Ma X, Li HZ, Fu B, Lang B, et al. Retroperitoneoscopic Surgery for Adrenal Cysts: A Single-Center Experience of 14 Cases. *J Endourol* (2007) 21(2):177–9. doi: 10.1089/end.2006.0201
22. Brunt LM, Molmenti EP, Kerbl K, Soper NJ, Stone AM, Clayman RV. Retroperitoneal Endoscopic Adrenalectomy: An Experimental Study. *Surg Laparosc Endosc* (1993) 3:300–6.
23. Uchida M, Imaide Y, Yoneda K, Uehara H, Ukimura O, Itoh Y, et al. Endoscopic Adrenalectomy by Retroperitoneal Approach for Primary Aldosteronism. *Hinyokika Kiyo* (1994) 40:43–6.
24. Whittle DE, Schroeder D, Purchas SH, Sivakumaran P, Conaglen JV, et al. Laparoscopic Retroperitoneal Left Adrenalectomy in a Patient With Cushing's Syndrome. *Aust N Z J Surg* (1994) 64:375–6. doi: 10.1111/j.1445-2197.1994.tb02227.x

25. Johansson K, Anderberg B. Asberg B Endoscopic Retroperitoneal Adrenalectomy. A Technique Useful for Surgery of Minor Tumors]. *Lakartidningen* (1994) 91:3278,3281.
26. Mandressi A, Buizza C, Antonelli D, Chisena S, Servadio G. Retroperitoneoscopy. *Ann Urol (Paris)* (1995) 29(2):91–6.
27. Heintz A, Junginger T. Die Endoskopische, Extraperitoneale Adrenalektomie [Endoscopic, Extraperitoneal Adrenalectomy]. *Chirurg* (1994) 65(12):1140–2.
28. Mercan S, Seven R, Ozarmagan S, Tezelman S. Endoscopic Retroperitoneal Adrenalectomy. *Surgery* (1995) 118(6):1071–5; discussion 1075-6. doi: 10.1016/s0039-6060(05)80116-3
29. Walz MK, Peitgen K, Krause U, Eigler FW. Die Dorsale Retroperitoneoskopische Adrenalektomie–eine Neue Operative Technik [Dorsal Retroperitoneoscopic Adrenalectomy–A New Surgical Technique]. *Zentralblatt für Chirurgie* (1995) 120(1):53–8.
30. Manny TB, Pompeo AS, Hemal AK. Robotic Partial Adrenalectomy Using Indocyanine Green Dye With Near-Infrared Imaging: The Initial Clinical Experience. *Urology* (2013) 82(3):738–42. doi: 10.1016/j.urology.2013.03.074
31. Seeliger B, Walz MK, Alesina PF, Agnus V, Pop R, Barberio M, et al. Fluorescence-Enabled Assessment of Adrenal Gland Localization and Perfusion in Posterior Retroperitoneoscopic Adrenal Surgery in a Preclinical Model. *Surg Endosc* (2020) 34(3):1401–11. doi: 10.1007/s00464-019-06997-3
32. Kahramangil B, Kose E, Berber E. Characterization of Fluorescence Patterns Exhibited by Different Adrenal Tumors: Determining the Indications for Indocyanine Green Use in Adrenalectomy. *Surgery* (2018) 164(5):972–7. doi: 10.1016/j.surg.2018.06.012
33. Lerchenberger M, Gündogar U, Al Arabi N, Gallwas JKS, Stepp H, Hallfeldt KKJ, et al. Indocyanine Green Fluorescence Imaging During Partial Adrenalectomy. *Surg Endosc* (2020) 34(5):2050–5. doi: 10.1007/s00464-019-06985-7
34. Brauckhoff M, Gimm O, Thanh PN, Bär A, Ukkat J, Brauckhoff K, et al. Critical Size of Residual Adrenal Tissue and Recovery From Impaired Early Postoperative Adrenocortical Function After Subtotal Bilateral Adrenalectomy. *Surgery* (2003) 134(6):1020–7; discussion 1027-8. doi: 10.1016/j.surg.2003.08.005
35. Castinetti F, Taieb D, Henry JF, Walz M, Guerin C, Brue T, et al. MANAGEMENT OF ENDOCRINE DISEASE: Outcome of Adrenal Sparing Surgery in Heritable Pheochromocytoma. *Eur J Endocrinol* (2016) 174(1):R9–18. doi: 10.1530/EJE-15-0549
36. Neumann HPH, Tsoy U, Bancos I, Amodru V, Walz MK, Tirosh A, et al. Comparison of Pheochromocytoma-Specific Morbidity and Mortality Among Adults With Bilateral Pheochromocytomas Undergoing Total Adrenalectomy vs Cortical-Sparing Adrenalectomy. *JAMA Netw Open* (2019) 2(8):e198898. doi: 10.1001/jamanetworkopen.2019.8898
37. Lenders JW, Duh QY, Eisenhofer G, Gimenez-Roqueplo AP, Grebe SK, Murad MH, et al. Pheochromocytoma and Paraganglioma: An Endocrine Society Clinical Practice Guideline. *J Clin Endocrinol Metab* (2014) 99 (6):1915–42. doi: 10.1210/jc.2014-1498
38. Walz MK, Peitgen K, Saller B, Giebler RM, Lederbogen S, Nimtz K, et al. Subtotal Adrenalectomy by the Posterior Retroperitoneoscopic Approach. *World J Surg* (1998) 22(6):621–6; discussion 626-7. doi: 10.1007/s002689900444
39. Chen SF, Chueh SC, Wang SM, Wu VC, Pu YS, Wu KD, et al. Clinical Outcomes in Patients Undergoing Laparoscopic Adrenalectomy for Unilateral Aldosterone Producing Adenoma: Partial Versus Total Adrenalectomy. *J Endourol* (2014) 28(9):1103–6. doi: 10.1089/end.2014.0102
40. Billmann F, Billeter A, Thomusch O, Keck T, El Shishtawi S, Langan EA, et al. Minimally Invasive Partial Versus Total Adrenalectomy for Unilateral Primary Hyperaldosteronism-a Retrospective, Multicenter Matched-Pair Analysis Using the New International Consensus on Outcome Measures. *Surgery* (2021) 169(6):1361–70. doi: 10.1016/j.surg.2020.09.005
41. Walters W. Subtotal Adrenalectomy for Cushing's Syndrome. *AMA Arch Surg* (1953) 66(2):244–52. doi: 10.1001/archsurg.1953.01260030257015
42. Fassnacht M, Arlt W, Bancos I, Dralle H, Newell-Price J, Sahdev A, et al. Management of Adrenal Incidentalomas: European Society of Endocrinology Clinical Practice Guideline in Collaboration With the European Network for the Study of Adrenal Tumors. *Eur J Endocrinol* (2016) 175(2):G1–G34. doi: 10.1530/EJE-16-0467
43. Kumar A, Hyams ES, Stifelman MD. Robot-Assisted Partial Adrenalectomy for Isolated Adrenal Metastasis. *J Endourol* (2009) 23(4):651–4. doi: 10.1089/end.2008.0440
44. Kaneko G, Katsui M, Orikasa H, Hattori S, Hara S. Retroperitoneoscopic Partial Adrenalectomy for Metachronous Renal Cell Carcinoma Metastasis to Solitary Adrenal Gland. *Int Cancer Conf J* (2019) 9(1):1–4. doi: 10.1007/s13691-019-00383-5
45. Schomer NS, Mohler JL. Partial Adrenalectomy for Renal Cell Carcinoma With Bilateral Adrenal Metastases. *J Urol* (1995) 153(4):1196–8. doi: 10.1016/S0022-5347(01)67550-5


**Conflict of Interest:** The authors declare that the research was conducted in the absence of any commercial or financial relationships that could be construed as a potential conflict of interest.

frontiers | Frontiers in Endocrinology

CASE REPORT
published: 13 April 2022
doi: 10.3389/fendo.2022.857504

# Case Report: Giant Paraganglioma of the Skull Base With Two Somatic Mutations in *SDHB* and *PTEN* Genes

*Ailsa Maria Main[1,2], Götz Benndorf[3,4], Ulla Feldt-Rasmussen[1,2], Kåre Fugleholm[5], Thomas Kistorp[6], Anand C. Loya[2,7], Lars Poulsgaard[5], Åse Krogh Rasmussen[1], Maria Rossing[8], Christine Sølling[9] and Marianne Christina Klose[1]**

[1] Department of Medical Endocrinology and Metabolism, Rigshospitalet, Copenhagen University Hospital, Copenhagen, Denmark, [2] Faculty of Health and Medical Sciences, University of Copenhagen, Copenhagen, Denmark, [3] Department of Radiology, Copenhagen University Hospital, Copenhagen, Denmark, [4] Department of Radiology, Baylor College of Medicine, Houston, TX, United States, [5] Department of Neurosurgery, Copenhagen University Hospital, Copenhagen, Denmark, [6] Department of Anaesthesiology, Copenhagen University, Copenhagen, Denmark, [7] Department of Pathology, Copenhagen University Hospital, Copenhagen, Denmark, [8] Center for Genomic Medicine, Rigshospitalet, Copenhagen, Denmark, [9] Department of Neuroanaesthesiology, Copenhagen University Hospital, Copenhagen, Denmark

OPEN ACCESS

**Edited by:**
*Enzo Lalli, UMR7275 Institut de Pharmacologie Moléculaire et Cellulaire (IPMC), France*

**Reviewed by:**
*Carl Christofer Juhlin, Karolinska Institutet (KI), Sweden*
*Jacques Lenders, Retired, Nijmegen, Netherlands*

***Correspondence:**
*Marianne Christina Klose*
*Marianne.christina.klose.01@regionh.dk*

**Specialty section:**
*This article was submitted to Cancer Endocrinology, a section of the journal Frontiers in Endocrinology*

**Received:** *18 January 2022*
**Accepted:** *18 March 2022*
**Published:** *13 April 2022*

**Citation:**
*Main AM, Benndorf G, Feldt-Rasmussen U, Fugleholm K, Kistorp T, Loya AC, Poulsgaard L, Rasmussen ÅK, Rossing M, Sølling C and Klose MC (2022) Case Report: Giant Paraganglioma of the Skull Base With Two Somatic Mutations in SDHB and PTEN Genes. Front. Endocrinol. 13:857504. doi: 10.3389/fendo.2022.857504*

Head and neck paragangliomas (HNPGLs) are neuroendocrine tumors. They arise from the parasympathetic ganglia and can be either sporadic or due to hereditary syndromes (up to 40%). Most HNPGLs do not produce significant amounts of catecholamines. We report a case of a giant paraganglioma of the skull base with an unusually severe presentation secondary to excessive release of norepinephrine, with a good outcome considering the severity of disease. A 39-year-old Caucasian woman with no prior medical history was found unconscious and emaciated in her home. In the intensive care unit (ICU) the patient was treated for multi-organ failure with multiple complications and difficulties in stabilizing her blood pressure with values up to 246/146 mmHg. She was hospitalized in the ICU for 72 days and on the 31$^{st}$ day clinical assessment revealed jugular foramen syndrome and paralysis of the right n. facialis. A brain MRI confirmed a right-sided tumor of the skull base of 93.553 cm$^3$. Blood tests showed high amounts of normetanephrine (35.1-45.4 nmol/L, ref <1.09 nmol/L) and a tumor biopsy confirmed the diagnosis of a paraganglioma. Phenoxybenzamine and Labetalol were used in high doses ((Dibenyline®, 90 mg x 3 daily) and labetalol (Trandate®, 200 + 300 + 300 mg daily) to stabilize blood pressure. The patient underwent two tumor embolization procedures before total tumor resection on day 243. Normetanephrine and blood pressure normalized after surgery (0.77 nmol/L, ref: < 1.09 nmol/L). The damage to the cranial nerve was permanent. Our patient was comprehensively examined for germline predisposition to PPGLs, however we did not identify any causal aberrations. A somatic deletion and loss of heterozygosity (LOH) of the short arm (p) of chromosome 1 (including *SDHB*) and p of chromosome 11 was found. Analysis showed an *SDHB* (c.565T>G, p.C189G) and *PTEN* (c.834C>G, p.F278L) missense mutation in tumor DNA. The patient made a remarkable recovery except for neurological deficits after intensive multidisciplinary treatment and rehabilitation. This case demonstrates the necessity for an early tertiary center approach with a

multidisciplinary expert team and highlights the efficacy of the correct treatment with alpha-blockade.

**Keywords: paragangliogliomа, catecholamine, neuroendochrine tumor, *SDHB* gene, alpha blockade, multidisciplinary approach, rehabilitation, Head and neck paraganglioma (HNPGL)**

## INTRODUCTION

HNPGLs (head and neck paragangliomas) are neuroendocrine tumors. They arise from the parasympathetic ganglia and can be either sporadic or due to hereditary syndromes (up to 40%). Most HNPGLs do not produce significant amounts of catecholamines (1). Often, HNPGLs are detected in late stages due to compression or infiltration of cranial structures (1).

We report a case of a paraganglioma of the skull base with an unusually severe presentation secondary to excessive release of norepinephrine, with a good outcome considering the severity of disease after an intensive multidisciplinary approach for more than a year. Remarkably, we identified two somatic missense variants in *SDHB* (succinate dehydrogenase gene B) and *PTEN* (phosphatase and tensin homolog), respectively.

## CASE DESCRIPTION

### Regional Medical Center

A 39-year-old Caucasian woman with no prior medical history was found unresponsive by her parents in their home with a Glasgow Coma Scale (GCS) of 3. She had a respiratory rate of 5-7 per minute, hypotension, and immeasurably low blood glucose concentrations. Following a total of 500 mL 100 mg/mL intravenous glucose solution, she was admitted to the local hospital. On admission to the ICU, she had a GCS of 10, a respiratory rate of 15 per minute, blood pressure of 89/64 mmHg, pulse 94 bpm, peripheral oxygen saturation of 97%, and body temperature (ear) of 34,9° Celsius. The abdomen was swollen and tense, the skin was pale, and the extremities were bluish and marbled. Neurological examination revealed lagophthalmos on the right side and a right-sided central facial nerve palsy. No cardiac or pulmonary murmurs were present on auscultation. Cardiac ultrasonography revealed left ventricle failure with an ejection fraction of 10%. The patient had multiple chronic ulcers on her feet and lower legs, including decubitus on both heels and lower back (**Figure 2**). The patient was emaciated (38 kg, BMI: 14.8 kg/m$^2$), oedematous and had severe constipation.

The paramedics described that the patient's home showed signs of profound social deprivation with unsanitary living conditions. According to the family, she had developed a slurred speech and had been eating less than usual (mainly corn starch porridge) over the course of 2-3 months.

After the initial life-saving treatments for multi-organ failure (**Table 1**), the initial hypotension was replaced by refractory life-threatening hypertension with blood pressure spikes up to 246/146 mmHg despite treatment with carvedilol 12,5 mg x 2, ramipril 5 mg x 2, and methyldopa 500 mg x 4.

Respiratory distress, and hypercapnia, as well as bilateral pleural effusion ensued, necessitating intubation for 49 days and pleural drainage. Further necrotic sores evolved on her toes and fingertips. This was initially thought to be due to sepsis and DIC and amputation was considered. Aggressive treatment with antibiotics, surgical revision, and bandaging was carried out.

The patient also had stomach pain due to coprostasis, which was difficult to treat with normal laxatives.

On the 7$^{th}$ day in the ICU, an occupational therapist described right-sided facial nerve palsy, lagophthalmos of the right eye, her uvula was pulled to the left, and she had soft palate dysfunction. Right-sided jugular foramen syndrome (paresis of the glossopharyngeal, vagal, hypoglossal, and accessory nerves) as well as a right-sided facial nerve palsy were diagnosed on day 31 following an ENT assessment.

A brain CT was performed at admission to rule out intracranial bleeding. Unfortunately, due to movement artifacts, the skull base could not be evaluated in this CT and a new brain CT was not prioritized as intracranial bleeding had been ruled out. Due to the central facial nerve palsy diagnosed on day 31 repeat CT scanning as well as magnetic resonance (MR) imaging were performed, revealing a giant (93.553cm$^3$) tumor of the skull base located both intra- and extracranially (**Figure 2**). Subsequent $^{18}$F-FDG PET/CT imaging revealed a high FDG uptake confined to the tumor. A tumor biopsy was performed to determine the type of tumor. This showed a classic paraganglioma with a Ki-67 index of 4%. Plasma metanephrines were measured after the pathology results and showed very high concentrations of normetanephrine (35.1-45.4 nmol/L, ref <1.09 nmol/L), confirming the clinical suspicion of a catecholamine secreting paraganglioma. Chromogranin A measured on day 40 was 242 uL/L (ref: <102 uL/L).

### Tertiary Medical Center

The patient spent 72 days in the local ICU before being admitted to a tertiary referral center under a multidisciplinary team. $^{123}$MIBG-scintigraphy showed no uptake in the tumor or elsewhere and alpha-blockade treatment was initiated. $^{18}$Ga-Dotatoc PET-CT showed localized grade 2 uptake in the tumor with no radiological signs of metastatic disease in the thorax or abdomen. Alpha-blockade treatment was gradually increased, according to daily orthostatic blood pressure measurements, to high doses of phenoxybenzamine (Dibenyline®, 90 mg x 3 daily) and labetalol (Trandate®, 200 + 300 + 300 mg daily). The goal was to stabilize the blood pressure and improve the general physical state before the first tumor embolization treatment. Upon alpha blockade and blood pressure stabilization the patient

**TABLE 1** | Initial life-saving treatments for multi-organ failure.

| Day | ICU diagnosis | Intervention |
|---|---|---|
| 1 | GCS 3on site, GCS 10 upon arrival to the ICU | CT cerebrum showing no signs of apoplexia. Basis cranii could not be evaluated due to poor imaging (artefacts due to movements) |
| 1 | Hypotension (blood pressure 89/64 mmHg) | Bolus IV fluids; 1000 mL Ringer Acetate, 100 mL human albumin, 500 mL isotonic NaCl. |
| 1 | Hypoglycaemia (blood glucose levels unmeasurably low) | 500 mL 100 mg/mL glucose |
| 1 | Left ventricle failure (LVEF max 10%) | Dobutamin and norepinephrine infusions |
| 1 | Suspicion of vasculitis | 75-100 mg Prednisolone daily<br>Blood samples: erythrocyte sedimentation rate, immunoglobulins, anti-ANA, ANCA, ACE, beta-2-glycoprotein, HgA1c |
| 1 | ATN (Creatinine 160 um/L, eGFR 33 ml/min, Carbamide 52 mmol/l) | Haemodialysis |
| 1 | Malnourishment (BMI 14.8 kg/m$^2$) | Nasogastric tube<br>Thiamin, vitamin B complex, vitamin C, selenium, zinc<br>Daily blood samples for refeeding syndrome |
| 1 | Suspicion of septic shock | High-dose IV antibiotics according to local protocol (meropenem, clindamycin, ciprofloxacin) |
| 1 | Suspicion of Addison's crisis | Hydrocortisone 100 mg IV as bolus<br>Hydrocortisone 200 mg IV over 24 hours |
| 2 | Blood pressure spikes up to 246/146 mmHg | Carvedilol 12.5 mg x 2, ramipril 5 mg x 2, methyldopa 500 mg x 4 |
| 2 | DIC<br>Thrombocytopenia (thrombocytes 17, ref: 145-390 x 10$^9$/L) | Antithrombin III, dalteparin |
| 3 | Coprostasis | Movicol (macrogol 3350 og elektrolytter), Klyx (docusat sorbitol) |
| 4 | Respiratory distress and hypercapnia | Tracheostomy and respirator treatment for a total of 49 days |
| 4 and 15 | Bilateral pleural exudates | Pleurocentesis |
| 5 | Chronic ulcers and decubitus | IV antibiotics, surgical revision, bandaging |

*ANA, antinuclear antibodies; ANCA, antineutrophil cytoplasmic antibodies; ATN, acute tubular necrosis; Anti-ACE, anti-angiotensin converting enzyme antibodies; DIC, disseminated intravascular coagulation; eGFR, estimated glomerular filtration rate; GCS, Glasgow Coma Scale; HgA1c, hemoglobin A1c; IV, intravenous; LVEF, left ventricular ejection fraction; SAG-M, Saline-Adenine-Glucose-Mannitol.*

gained weight (**Figure 1**), and the chronic sores and necrotic fingertips and toes started to heal (**Figure 2**).

The patient's nutrient intake was closely regulated by a dietician to help her gain weight together with close monitoring of blood samples to avoid refeeding syndrome. Together with physio- and occupational therapists, ADL (activities of daily living) functions were assessed and trained intensively. After approximately 2 months of alpha-blockade treatment the patient was able to swallow bread crusts, not just liquids and soft foods (see **Figure 1**).

Finally, the patient was physically strong enough and the first tumor embolization was performed on day 150. Tumor branches

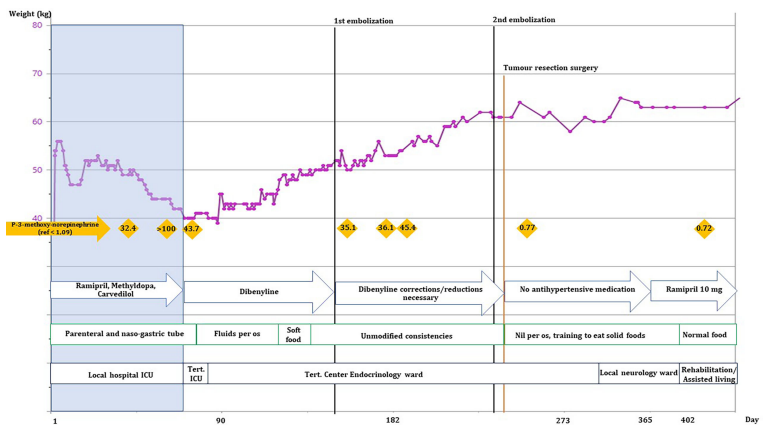


**FIGURE 1** | Development of the patient's weight (kg), normetanephrine levels, antihypertensive medicine, nutritional intake, and physical location over the first 365 days of hospitalization. Black lines: embolization procedures, orange line: tumor resection surgery, orange rhombes: plasma-3-methoxy-norepinephrine levels (nmol/L), blue arrows: changes in blood pressure medications, green blocks: changes in the patient's ability to drink/eat. She was at no point able to sustain nutrient intake without supplemental nutrition by naso-gastric tube. Black boxes show the patient's location.


**FIGURE 2** | Before and after; MRI scans, pictures of scores, and DSAs. MRI (magnetic resonance imaging) scans before and after tumor resection, clinical pictures of sores on right foot and left hand at admission and at end of hospitalization, and DSA (Digital Subtraction Angiography) images before and after embolization.

of the ascending pharyngeal artery were embolized with Embospheres and an anastomosis was coiled. This reduced the anterior spinal artery supply to about 60-70%. Between the first and the second tumor embolization the patient's antihypertensive medication was adjusted to phenoxybenzamine 70 + 80 + 80 mg daily and labetalol 300mg x 3 daily. Before the second embolization on day 238 an MRI scan showed tumor growth since the first embolization (6 x 5.4 x 5.5 cm). The right internal carotid artery was coiled, and the anterior tumor compartment was subsequently embolized. Complete embolization of all the arterial tumor supply was not achieved.

In relation to the surgical procedures the patient was categorized as an ASA (American Society of Anesthesiologists) score of 4, indicating an immediately life-threatening condition. Preparations in the form of an arterial line for continuous blood pressure monitoring and large bore central venous catheter was inserted as moderate to severe blood loss was expected.

Phenoxybenzamine and labetalol were discontinued on the day of the craniotomy on day 243 when the tumor was resected by a total petrosectomy. Infusions with adenosine and magnesium-sulphate were started at the induction of anesthesia. Intravenous norepinephrine was infused intermittently to maintain mean arterial blood pressure (MAP) between 70-100 mmHg. In relation to the petrosectomy a defect in the dura in the posterior fossa was repaired with pericranium. Fat tissue from the abdomen was harvested to fill the petrous bone defect and the defect was restored by a titanium cranioplasty. The procedure lasted close to seven hours and the hemorrhage volume (estimated at 5100 ml) was replaced with packed red blood cells, plasma, and platelets in accordance with local guidelines and thromboelastographic testing of coagulation. Respiratory and circulatory stability was achieved during all three procedures in general anesthesia. Infusions with adenosine, magnesium and norepinephrine were adjusted frequently in the 2 days after surgery to keep a MAP above 80 and systolic blood pressure below 180 mmHg.

Normetanephrine normalized after surgery (0.77 nmol/L, ref: < 1.09 nmol/L) and her blood pressure normalized (approx. 130/80 mmHg) without antihypertensive drugs. The damage to the cranial nerves (n. glossopharyngeus, n. vagus, n. hypoglossus, n. accessories, and n. facialis) was permanent.

### Pathology, Genetic Analysis, and Diagnosis

The tumor cells stained positive for synaptophysin, chromogranin, and S-100 along with SOX10 highlighted haphazardly distributed sustentacular cells. SDHA immunostaining was strongly positive, however *SDHB* was faint and thus difficult to conclude upon. The pathology analysis of the excised tumor itself showed the same histopathological patterns. Also, staining revealed loss of *PTEN* staining and alpha-inhibin staining was focally and weekly positive in tumor cells.

Molecular analysis including sequencing on tumor DNA revealed an *SDHB* (c.565T>G, p.C189G) and *PTEN* (c.834C>G, p.F278L) missense mutation. An SNP-array of tumor DNA showed loss of heterozygosity of p.1 (including *SDHB*) and p.11 in tumor tissue. Germline DNA was sequenced in parallel and the initial gene panel analysis did not show any variants in *FH, MAX, MEN1, NF1, RET, SDHX, THEM127* or *VHL*. Subsequent whole genome sequencing on germline DNA did not reveal any genetic etiology of the disease.

## Follow-Up and Outcome

The patient was transferred to a local neurology ward on day 292. The primary focus was to improve Activity of Daily Life with physio- and occupational therapists and after a total of 402 days in hospital she was transferred to a rehabilitation facility. She has been fitted with a Montgomery prosthesis to help her weak voice and may in future regain the ability to eat normal foods. Follow-up MRI three months post-surgery showed no signs of tumor remnant or regrowth. Future lifelong follow-up is planned according to international guidelines for pheochromocytomas and paragangliomas (PPGLs) (2).

## DISCUSSION

This case of a giant paraganglioma of the skull base with an unusually severe presentation secondary to excessive release of

norepinephrine highlights how the correct diagnosis, treatment, and the use of a multi-disciplinary approach can result in a relatively good outcome.

Our patient presented with a multi-organ crisis which is a rare presentation in PPGLs. She developed pulmonary exudates, acute renal failure and DIC. The symptoms were at first confused with sepsis, which has also previously been reported in other severe cases (3). PPGLs can present with life-threatening cardiovascular manifestations (3, 4). In our case the cardiogenic shock was most likely associated with severe hypotension on the basis of pump failure due to a severe left ventricular dysfunction, which has previously been reported in a substantial number of patients with PPGLs (4, 5).

HNPGLs that secrete catecholamines give rise to hypertension and in our case the norepinephrine-mediated alpha receptor stimulation resulted in vasoconstriction and hypertension (6) but also episodes of orthostatic hypotension. It has previously been reported that norepinephrine can cause orthostatic hypotension. The mechanisms behind this could be an impaired vasoconstrictor response due to downregulation and desensitization of the alpha-adrenergic receptors and feedback inhibition of sympathoneuronal norepinephrine release either by sympathoinhibition or as a result of stimulation of presynaptic alpha2-adrenergic receptors (3, 7). It is however difficult to discern whether the patients cachectic state could also have contributed to or be the reason for the orthostatic hypotension.

Our patient also suffered from peripheral ischemia with necrosis due to extreme vasoconstriction caused by hypercatecholaminaemia which has previously been reported in other patients with extremely high concentrations of normetanephrine (6).

Together with long term immobilization the excess amount of catecholamines could explain the coprostasis. Norepinephrine inhibits the plexus of the enteric nervous system which will inhibit bowl movements, gastrointestinal secretions and blood flow. Also, norepinephrine inhibits the presynaptic release of acetylcholine which stimulates normal bowel functions (8). This can explain why it was so difficult to treat the constipation, which is a rare but previously described complications in PPGLs (8).

The question is still how the patient managed to develop such a severe disease with pronounced disease manifestations due to many months of tumor pressure and elevated catecholamine levels. In our case the suspicion is that the predominant cause is severe social deprivation, but it has not been possible to obtain more detailed information about the patient's life or physical health in the time leading up to admission. After admission to the local ICU it took more than a month before the tumor was discovered as the underlying cause. Unfortunately, the tumor was not diagnosed at the initial CT scan on the day of admission due to artefacts on the scan performed mainly to rule out intracranial hemorrhage. The right facial nerve palsy, the lagophthalmos of the right eye and other signs of foramen jugulare syndrome were described both at admission and on day 7 following her admission. It is unclear why this was not followed up immediately but first on day 31 at the ENT assessment. The symptoms may have been overlooked due to the multiple other life-threatening symptoms. Had the central nerve palsy been diagnosed properly at an earlier stage a repeat CT of the brain would have revealed the tumor at the skull base.

The differential diagnosis of a HNPGL had not been considered prior to the biopsy, and the patient thus underwent a tumor biopsy due to suspicion of a malignant brain tumor. Had a HNPGL been considered as differential diagnosis, then the appropriate succession of events would have been to measure the catecholamines prior to taking the biopsy to ensure relevant alpha-blockade treatment to minimize the risk for the patient (9). This would also have provided the possibility of measuring the dopamine metabolite 3-methoxytyramine which is a very strong and relevant predictor of metastases development (10) in a patient with a somatic *SDHB* mutation.

After the initial CT and MRI scan our patient underwent $^{18}$Ga-Dotatoc PET-CT which is first choice in HNPGL detection (9, 11).

The patient's poor physical state protracted the progress and it took many months to get her physically strong enough to undergo the tumor resection. The correct tumor diagnosis proved detrimental to improving the patient's physical strength as this clearly required the correct treatment with alpha-blockade. In our case the patient's weight stabilized just after the alpha-blockade treatment was initialized (**Figure 1**). Subsequently she gained weight at a steady rate and was back to her normal weight (approximately 60 kg, BMI: 23.4 kg/m$^2$) on day 214. The initial weight stabilization and weight gain could be attributed to the alpha-blockade treatment as the excess catecholamines are known to increase metabolism in patients, resulting in weight loss (12, 13). After approximately 2 months of alpha-blockade the patient regained the ability to swallow more solid foods which likely contributed to her further weight gain. It has previously been shown in a study on rats that catecholamines can inhibit the swallowing reflex (14).

Patients with catecholamine producing PPGLs have an increased risk of developing diabetes (13). This is mainly caused by high levels of circulating catecholamines leading to compromised insulin secretion from the pancreatic β-cells, decreased glucose uptake, and increased insulin resistance (15). Perhaps, did not occur in our patient (HbA1c 38-40 nnmol/mol (ref <48 nmol/mol)) because of her emaciated state and lack of food intake at admission where she was severely hypoglycemic due to her cachectic and catabolic condition. One could also speculate, that the reason for her not developing diabetes during her hospital stay was because of the alpha-blockade treatment.

A previous case report from 2011 concluded, that multidisciplinary approach is necessary when treating large secreting intracranial paragangliomas. Mainly, the use of pre-operative embolization decreases the risk of surgical hemorrhage before complete surgical resection which is the optimal treatment as a curative aim (16). The embolization approach has also been used in other casuistic cases (17) and a systematic review and meta-analysis concluded that embolization of carotid body tumors prior to surgery reduced blood loss during surgery (18).

Our patient was comprehensively examined for germline predisposition to pheochromocytomas and paragangliomas, however we did not identify any causal aberrations. Rare cases

of sporadic paragangliomas due to somatic variants of *SDHB* have been reported (19–21). Pathology immunohistochemistry analysis showed loss of *PTEN* expression in tumor tissue, underlining the influence of the *PTEN* missense mutation. Our case is the first to report highlight the possible significance of *PTEN* mutations in PPGLs. *PTEN* is one of the most frequently somatically mutated genes in cancer (22–24) and has been reported in brain tumours, lung cancer, prostate cancer, endometrial cancer breast cancer and pancreatic cancer (22). Furthermore, a quarter of thyroid adenomas and several sporadic malignant thyroid cancers were found to have *PTEN* LOH (22).

The somatic *PTEN* variant (c.834C>G, p.F278L) has previously been reported, but not in PPGLs (25). The *SDHB* variant (c.565T>G, p.C189G) has not previously been reported and neither variant is annotated in dbSNP (https://www.ncbi.nlm.nih.gov/snp/), ClinVar (https://www.ncbi.nlm.nih.gov/clinvar/), or in GnomAD (https://gnomad.broadinstitute.org/). *PTEN* mutations have not been found in human PPGLs but LOH at the *PTEN* loci has previously been reported in 2% (26) to 16% of examined tumors (27) Furthermore it has been shown in studies on mice that *PTEN* mutations can cause development of malignant PPGLs (27) and the loss of *PTEN* expression has therefore been associated with the progression of these tumors.

Alpha-inhibin immunohistochemistry was focally and weekly positive in tumor tissue. The expression of alpha-inhibin has been suggested as a screening tool for pseudo-hypoxic paragangliomas (Cluster 1 disease including *SDHB*-related disease) (28). Although alpha-inhibin cannot stand alone as a diagnostic tool for *SDHx*-related disease (28) it may contribute in cases where the *SDHB* expression is difficult to conclude on as in our case.

*SDHB* mutations in general are strongly associated with recurrence (29). Furthermore, as per the newest WHO guidelines, paragangliomas are not differentiated into benign or malignant as these tumors are all potentially malignant and should have follow-up according to guidelines (30).

The TIER classification system is a proposed alternative for classifying somatic variants (31). Even though we suspect that this variant of *SDHB* could be pathogenic we have not been able to classify it as more than a TIER III class variant (Variant of Unknown Significance) based on the lack of functional studies. Based on our current knowledge it is therefore not possible to predict the future clinical outcome for our patient and she will be followed with lifelong clinical screenings.

In conclusion we describe a case with an unusually severe presentation of a giant skull base PPGL with a relatively good outcome under the given circumstances. This case demonstrates the necessity for an early tertiary center approach with multidisciplinary expert teams. Furthermore, it highlights the efficacy of the correct treatment with alpha-blockade sooner rather than later. The condition is treatable but can be fatal and have serious long-term consequences for the patients. There is need for a more extensive knowledge on how to follow up on patients with PPGLs based on genetic, pathological, and clinical symptoms in the individual patient.

## DATA AVAILABILITY STATEMENT

The original contributions presented in the study are included in the article/supplementary material. Further inquiries can be directed to the corresponding author.

## ETHICS STATEMENT

Written informed consent was obtained from the individual(s) for the publication of any potentially identifiable images or data included in this article.

## AUTHOR CONTRIBUTIONS

AM: first author, data collection, manuscript writing, and manuscript editing. GB: expert on tumor embolization procedure, manuscript proofreading, and writing section on embolization procedure. UF-R: expert in treatment of catecholamine producing tumors pre-op, writing section on endocrine treatment, and manuscript proofreading. KF: expert in neurosurgery, manuscript proofreading, and writing on section on perioperative procedure. TK: expert in anesthesiology and writing on section on section on perioperative procedure. AL: expert in pathology and writing section on pathology findings. LP: expert in neurosurgery and writing on section on neuroimaging. ÅR: expert in treatment of catecholamine producing tumors pre-op, writing section on endocrine treatment, and manuscript proofreading. MR: expert in genetic analysis and writing section on genetic analysis finding. CS: expert in anesthesiology and writing on section on perioperative procedure. MK: expert in treatment of catecholamine producing tumors pre-op, writing section on endocrine treatment, and manuscript proofreading. All authors contributed to the article and approved the submitted version.

## FUNDING

UF-R's research salary is sponsored by The Kirsten and Freddy Johansen's Fund.

## REFERENCES

1. Lenders JWM, Kerstens MN, Amar L, Prejbisz A, Robledo M, Taieb D, et al. Genetics, Diagnosis, Management and Future Directions of Research of Phaeochromocytoma and Paraganglioma: A Position Statement and Consensus of the Working Group on Endocrine Hypertension of the European Society of Hypertension. *J Hypertens* (2020) 38(8):1443–56. doi: 10.1097/HJH.0000000000002438
2. Plouin PF, Amar L, Dekkers OM, Fassnacht M, Gimenez-Roqueplo AP, Lenders JW, et al. European Society of Endocrinology Clinical Practice Guideline for Long-Term Follow-Up of Patients Operated on for a

Phaeochromocytoma or a Paraganglioma. *Eur J Endocrinol/European Fed Endocrine Societies* (2016) 174(5):G1–G10. doi: 10.1530/eje-16-0033
3. Prejbisz A, Lenders JW, Eisenhofer G, Januszewicz A. Cardiovascular Manifestations of Phaeochromocytoma. *J Hypertens* (2011) 29(11):2049–60. doi: 10.1097/HJH.0b013e32834a4ce9
4. Riester A, Weismann D, Quinkler M, Lichtenauer UD, Sommerey S, Halbritter R, et al. Life-Threatening Events in Patients With Pheochromocytoma. *Eur J Endocrinol/European Fed Endocrine Societies* (2015) 173(6):757–64. doi: 10.1530/eje-15-0483
5. Falhammar H, Kjellman M, Calissendorff J. Initial Clinical Presentation and Spectrum of Pheochromocytoma: A Study of 94 Cases From a Single Center. *Endocr Connect* (2018) 7(1):186–92. doi: 10.1530/EC-17-0321
6. YH S, Falhammar H. Cardiovascular Manifestations and Complications of Pheochromocytomas and Paragangliomas. *J Clin Med* (2020) 9(8). doi: 10.3390/jcm9082435
7. Streeten DH, Anderson GHJr. Mechanisms of Orthostatic Hypotension and Tachycardia in Patients With Pheochromocytoma. *Am J Hypertens* (1996) 9 (8):760–9. doi: 10.1016/0895-7061(96)00057-x
8. Osinga TE, Kerstens MN, van der Klauw MM, Koornstra JJ, Wolffenbuttel BH, Links TP, et al. Intestinal Pseudo-Obstruction as a Complication of Paragangliomas: Case Report and Literature Review. *Neth J Med* (2013) 71 (10):512–7.
9. Lenders JW, Duh QY, Eisenhofer G, Gimenez-Roqueplo AP, Grebe SK, Murad MH, et al. Pheochromocytoma and Paraganglioma: An Endocrine Society Clinical Practice Guideline. *J Clin Endocrinol Metab* (2014) 99 (6):1915–42. doi: 10.1210/jc.2014-1498
10. van Berkel A, Lenders JW, Timmers HJ. Diagnosis of Endocrine Disease: Biochemical Diagnosis of Phaeochromocytoma and Paraganglioma. *Eur J Endocrinol/European Fed Endocrine Societies* (2014) 170(3):R109–19. doi: 10.1530/eje-13-0882
11. Kong G, Schenberg T, Yates CJ, Trainer A, Sachithanandan N, Iravani A, et al. The Role of 68Ga-DOTA-Octreotate PET/CT in Follow-Up of SDH-Associated Pheochromocytoma and Paraganglioma. *J Clin Endocrinol Metab* (2019) 104(11):5091–9. doi: 10.1210/jc.2019-00018
12. An Y, Reimann M, Masjkur J, Langton K, Peitzsch M, Deutschbein T, et al. Adrenomedullary Function, Obesity and Permissive Influences of Catecholamines on Body Mass in Patients With Chromaffin Cell Tumours. *Int J Obes (Lond)* (2019) 43(2):263–75. doi: 10.1038/s41366-018-0054-9
13. Krumeich LN, Cucchiara AJ, Nathanson KL, Kelz RR, Fishbein L, Fraker DL, et al. Correlation Between Plasma Catecholamines, Weight, and Diabetes in Pheochromocytoma and Paraganglioma. *J Clin Endocrinol Metab* (2021) 106 (10):e4028–38. doi: 10.1210/clinem/dgab401
14. Kessler JP, Jean A. Effect of Catecholamines on the Swallowing Reflex After Pressure Microinjections Into the Lateral Solitary Complex of the Medulla Oblongata. *Brain Res* (1986) 386(1-2):69–77. doi: 10.1016/0006-8993(86) 90142-3
15. Mesmar B, Poola-Kella S, Malek R. The Physiology Behind Diabetes Mellitus In Patients With Pheochromocytoma: A Review Of The Literature. *Endocr Pract* (2017) 23(8):999–1005. doi: 10.4158/ep171914.Ra
16. Graillon T, Fuentes S, Régis J, Metellus P, Brunel H, Roche PH, et al. Multidisciplinary Management of Giant Functional Petrous Bone Paraganglioma. *Acta Neurochir (Wien)* (2011) 153(1):85–9. doi: 10.1007/s00701-010-0818-z
17. Jha N, Crockett MT, Bala A, McAuliffe W. Preoperative Embolisation of a Hypervascular, Calvarial Paraganglioma Metastasis *via* a Combined Percutaneous and Transophthalmic Arterial Approach. *BMJ Case Rep* (2018). doi: 10.1136/bcr-2018-227640
18. Texakalidis P, Charisis N, Giannopoulos S, Xenos D, Rangel-Castilla L, Tassiopoulos AK, et al. Role of Preoperative Embolization in Carotid Body Tumor Surgery: A Systematic Review and Meta-Analysis. *World Neurosurg* (2019) 129:503–13 e2. doi: 10.1016/j.wneu.2019.05.209
19. van Nederveen FH, Korpershoek E, Lenders JW, de Krijger RR, Dinjens WN. Somatic SDHB Mutation in an Extraadrenal Pheochromocytoma. *N Engl J Med* (2007) 357(3):306–8. doi: 10.1056/NEJMc070010
20. Koopman K, Gaal J, de Krijger RR. Pheochromocytomas and Paragangliomas: New Developments With Regard to Classification, Genetics, and Cell of Origin. *Cancers (Basel)* (2019) 11(8). doi: 10.3390/cancers11081070
21. Yamazaki Y, Gao X, Pecori A, Nakamura Y, Tezuka Y, Omata K, et al. Recent Advances in Histopathological and Molecular Diagnosis in Pheochromocytoma and Paraganglioma: Challenges for Predicting Metastasis in Individual Patients. *Front Endocrinol (Lausanne)* (2020) 11:587769. doi: 10.3389/fendo.2020.587769
22. Ngeow J, Eng C. PTEN in Hereditary and Sporadic Cancer. *Cold Spring Harb Perspect Med* (2020) 10(4). doi: 10.1101/cshperspect.a036087
23. Hollander MC, Blumenthal GM, Dennis PA. PTEN Loss in the Continuum of Common Cancers, Rare Syndromes and Mouse Models. *Nat Rev Cancer* (2011) 11(4):289–301. doi: 10.1038/nrc3037
24. Simpson L, Parsons R. PTEN: Life as a Tumor Suppressor. *Exp Cell Res* (2001) 264(1):29–41. doi: 10.1006/excr.2000.5130
25. . Available at: https://cancer.sanger.ac.uk/cosmic/mutation/overview?id=113801764 (Accessed [3rd March 2022]).
26. Bratslavsky G, Sokol ES, Daneshvar M, Necchi A, Shapiro O, Jacob J, et al. Clinically Advanced Pheochromocytomas and Paragangliomas: A Comprehensive Genomic Profiling Study. *Cancers (Basel)* (2021) 13(13). doi: 10.3390/cancers13133312
27. Fishbein L, Nathanson KL. Pheochromocytoma and Paraganglioma: Understanding the Complexities of the Genetic Background. *Cancer Genet* (2012) 205(1-2):1–11. doi: 10.1016/j.cancergen.2012.01.009
28. Mete O, Pakbaz S, Lerario AM, Giordano TJ, Asa SL. Significance of Alpha-Inhibin Expression in Pheochromocytomas and Paragangliomas. *Am J Surg Pathol* (2021) 45(9):1264–73. doi: 10.1097/pas.0000000000001715
29. Gimenez-Roqueplo AP, Favier J, Rustin P, Rieubland C, Crespin M, Nau V, et al. Mutations in the SDHB Gene are Associated With Extra-Adrenal and/or Malignant Phaeochromocytomas. *Cancer Res* (2003) 63(17):5615–21.
30. Lloyd RV, Osamura RY, Klöppel G, Rosai J. *WHO Classification of Tumours of Endocrine Organs*. France: International Agency for Research on Cancer (2017).
31. Li MM, Datto M, Duncavage EJ, Kulkarni S, Lindeman NI, Roy S, et al. Standards and Guidelines for the Interpretation and Reporting of Sequence Variants in Cancer: A Joint Consensus Recommendation of the Association for Molecular Pathology, American Society of Clinical Oncology, and College of American Pathologists. *J Mol Diagn* (2017) 19(1):4–23. doi: 10.1016/j.jmoldx.2016.10.002

**Conflict of Interest:** The authors declare that the research was conducted in the absence of any commercial or financial relationships that could be construed as a potential conflict of interest.

# Advantages of publishing in Frontiers

**OPEN ACCESS**
Articles are free to read for greatest visibility and readership

**FAST PUBLICATION**
Around 90 days from submission to decision

**HIGH QUALITY PEER-REVIEW**
Rigorous, collaborative, and constructive peer-review

**TRANSPARENT PEER-REVIEW**
Editors and reviewers acknowledged by name on published articles

**Frontiers**
Avenue du Tribunal-Fédéral 34
1005 Lausanne | Switzerland

**Visit us:** www.frontiersin.org
**Contact us:** frontiersin.org/about/contact

**REPRODUCIBILITY OF RESEARCH**
Support open data and methods to enhance research reproducibility

**DIGITAL PUBLISHING**
Articles designed for optimal readership across devices

**FOLLOW US**
@frontiersin

**IMPACT METRICS**
Advanced article metrics track visibility across digital media

**EXTENSIVE PROMOTION**
Marketing and promotion of impactful research

**LOOP RESEARCH NETWORK**
Our network increases your article's readership